WORLD METEOROLOGICAL ORGANIZATION

INSTRUMENTS AND OBSERVING METHODS

REPORT No. 74

PAPERS PRESENTED at the WMO TECHNICAL CONFERENCE ON METEOROLOGICAL AND ENVIRONMENTAL INSTRUMENTS AND METHODS OF OBSERVATION

(TECO-2000)

Beijing, China, 23 - 27 October 2000

WMO/TD - No. 1028

2000

NOTE

The designations employed and the presentation of material in this publication do not imply the expression of any opinion whatsoever on the part of the Secretariat of the World Meteorological Organization concerning the legal status of any country, territory, city or area, or of its authorities, or concerning the delimitation of its frontiers or boundaries.

This report has been produced without editorial revision by the WMO Secretariat. It is not an official WMO publication and its distribution in this form does not imply endorsement by the Organization of the ideas expressed.

FOREWORD

The concept of this *WMO Technical Conference on Meteorological and Environmental Instruments and Methods of Observation* (TECO-2000) arose from a proposal of the twelfth session of the Commission for Instruments and Methods of Observation (CIMO-XII). The fifty-first session of the WMO Executive Council gave approval in May 1999 and the China Meteorological Administration kindly offered to host the Conference in Beijing from the 23 to 27 of October 2000.

TECO-2000 was held between sessions of CIMO, two years after its twelfth session. An *Exhibition on Meteorological Instruments, Equipment and Services* (METEOREX-2000) was also organized to coincide with TECO-2000 to provide participants with an additional opportunity to view the latest developments in instrumentation by manufacturers from many countries.

An *International Programme Committee* for TECO-2000, composed of R.P. Canterford (Australia), Scientific Director of TECO-2000, Baoxiang Xu (China), J. Kruus (Canada), A. Belhouji (Morocco), J. Nash (UK), and A. Gusev (Russian Federation), was responsible for specifying the themes and contents of sessions as well as for selecting the papers.

With the rapid developments in the technology of meteorological and environmental instruments and sensors, this Conference is ideally timed as we move into the next decade. It has given authors and participants the opportunity to present and discuss the critical changes that are taking place in their work with instruments and methods of observation.

The Conference topics have been designed to reflect these changes and the diversity of the main areas of CIMO activities, as stated in the WMO Instruments and Methods of Observation Programme (IMOP). These fields include surface observation systems, automatic weather stations, intercomparisons, instrument design, solar radiation observations, quality of observations, upper-air observation systems (in-situ and remote), weather radars and lightning detection systems, measurement of atmospheric composition, operation of instruments in harsh conditions, urban meteorology, management of networks and, most importantly, capacity building and technology transfer.

The large range of papers presented under the conference theme and these topics in particular display innovations to improve the quality and homogeneity of observations. These developments are essential to meet the requirements of WMO Programmes and National Meteorological and Hydrological Services.

I wish to express my deep gratitude to the Government of China and to the China Meteorological Administration, to authors of papers, to members of the International Programme Committee, to the Local Organizing Committee, and to the Secretary-General of WMO for their efforts and the resources devoted to planning and holding TECO-2000.

(Dr Ray P. Canterford)
Vice-president of CIMO
Scientific Director of TECO-2000

TABLE OF CONTENTS

0 INTRODUCTORY KEYNOTE PAPER

Major Challenges Facing WMO Member Countries in Operating and Maintaining Meteorological and Environmental Instrument Networks and the Role of CIMO
by Canterford, Ray P. (Australia) **1**

1 MEASUREMENT TECHNOLOGY, PERFORMANCE, AND QUALITY ASSURANCE

1.1 Surface Observation Systems

Keynote Paper

Developments in Instruments for Surface Measurements and Meteorological Observation Techniques
by van der Meulen, Jitze P. (Netherlands)
Chairman of the CIMO Working Group on Surface Measurements **9**

1.1.1 Automatic Weather Stations

1.1.1(1) New Measurements Technologies – A Critical Change to Climate?
by Rudel, Ernest (Austria) **13**

1.1.1(2) RADOME Network
by Grégoire, Pierre (France) **17**

1.1.1(3) Automatic Weather System in Korea Meteorological Administration
by Lee, Chun-Woo; Choi, Chee-Young and Park, Jong-Seo (Rep. of Korea) **21**

1.1.1(4) SIMEPAR Hydrometeorological Data Collection Network
by de Moraes, Luis Tarciso (Brazil) **26**

1.1.1(5) L'automatisation de l'observation météorologique du Maroc (The Automation of Meteorological Observation in Morocco)
by Louaked, Brahim (Morocco) **30**

1.1.1(6) Hong Kong Automatic Weather Station Network in 2000
by Chan, Yuk Kwan (Hong Kong, China) **34**

Poster Presentations

P1.1.1(1) Field-calibrated Method for Automatic Meteorological Station
by LU, Wenhua; ZHU, Lekun and WANG, Jingye (China) **38**

P1.1.1(2) Airport Meteorological Measuring Systems Automation in Slovenia
by Zlebir, Silvo (Slovenia) **42**

P1.1.1(3) Automatic Measuring System for Provision of the Meteorological Data for Djoran Lake Researching
by Alcinova Monevska, Suzana (The former Yugoslav Rep. of Macedonia) **46**

P1.1.1(4) Automatic Weather Stations in India – Recent Trends
by Vashistha, Ramdhan D. and Dikshit, S.K. (India) **50**

1.1.2 Intercomparisons

1.1.2(1) A Comparison of Air Temperature Radiation Screens by Field Experiments and Computational Fluid Dynamics (CFD) Simulations
by Spetalen, Aril; Lofseik, Cecilie and Nordli, Per θyvind (Norway) **54**

1.1.2(2) Effects of Different Screen Designs on Temperature: Field Experiment
by Yeshanew, Abebe (Ethiopia) **58**

1.1.2(3) Temperature Measurements: Some Consideration for the Intercomparison of Radiation Screens
by van der Meulen, Jitze P. (Netherlands) **60**

1.1.2(4) Report on the International Pyrheliometer Comparisons – The Maintenance and Dissemination of the World Radiometric Reference
by Rüedi, Isabelle; Fröhlich, C.; Schmutz, W. and Wehrli, Ch. (Switzerland) **64**

1.1.2(5) Evaluation of the Latest Laser Cloud Base Recorders: 1998-1999
by Muller, Carl C.; Hatton, D.B. and Jones, D.W. (UK) **68**

1.1.2(6) Wind Measurements: Potential Wind Speed Derived from Wind Speed Fluctuations Measurements, and the Representativity of Wind Stations
by van der Meulen, Jitze P. (Netherlands) **72**

Poster Presentation

P1.1.2 Comparaison entre une station météo traditionnelle et une station météo automatique
(Comparison of a Traditional and an Automatic Weather Station)
by Beltrano, Maria Carmen and Perini, Luigi (Italy) **76**

1.1.3 Instrument Design

1.1.3(1) Meteorological Sensors for Fully Automated Surface Observation Systems
by Dibbern, Jochen; Klapheck, Karl-Heinz and Szabó, Imre (Germany) **80**

1.1.3(2) Infra Red Thermal Imaging Cameras as an Observing Tool
by Dewey, Simon; Hatton, D.; Jones; D.W. and Keogh, S.J. (UK) **84**

1.1.3(3) Détermination automatique de l'epaisseur de neige sur les aéroports au moyen d'un système embarqué sur véhicule
(On Board Measurement System for automatic Determination of Snow Thicknesses on Airports)
by Gaumet, Jean-Louis; Zephoris, M. and Zanghi, F. (France) **88**

1.1.3(4) Calibration and Control Methods for Tipping-Bucket Raingauges
by Leroy, Michel (France) ***92***

1.1.3(5) A Procedure to Improve Measurements of Dew Point by Automatic Weather Stations
by Sparks, W.R.; Jones, D.W. and Hatton, D.B. (UK) **96**

Poster Presentations

P1.1.3(1) New Automatic Observation Method of Evaporation – Class "A" Evaporation Pan
by Lee, Bu-Yong; Park, Byoung-Yoon and Woo, Hyung-Taek (Rep. of Korea) **100**

P1.1.3(2) The Application of the Remote Automatic Rainfall Recorder (RARR) in the Surveillance of Urban Rainfall Distribution
by FANG, Guoliang and SHAO, Lingling (China) **104**

1.1.4 Solar Radiation Observations

1.1.4(1) Absolute Calibration of Pyrgeometers: A Proposal for a World Radiometric Reference for Longwave Irradiance Measurements
by Philipona, Rolf and Ohmura, Atsumu (Switzerland) **108**

1.1.4(2) Investigations of Night-time Zero Offsets at Short-wave Broadband Radiometers
by Behrens, Klaus and Dehne, Klaus (Germany) **112**

1.1.4(3) Automatic Indirect Observations of Sunshine Duration
by Nunes, Luis F. and Carvalho, Fernanda (Portugal) **116**

Poster Presentations

P1.1.4(1) A Sensor for the Horizontal Component of Solar Radiation
by van der Hage, Jeroen C.K. (Netherlands) **120**

P1.1.4(2) Performance Evaluation for Pyranometers
by LU, Wenhua and MO, Yueqin (China) **124**

P1.1.4(3) UV and Visible Solar Radiative Fluxes Above Arctic Sea Ice
by Los, Alexander; de Roode, Stefan R. and Duynkerke, Peter G. (Netherlands) **128**

1.1.5 Quality Observations

1.1.5(1) Representativity of Wind Measurements in The Netherlands: A Discussion on Methods of Transforming Observed Values of to the Area Involved
by Benschop, Henk (Netherlands) **132**

1.1.5(2) A Full Model for Correction of Precipitation Measurement Data and a Method and Algorithm for Estimation of Systematic Error Components (submitted in Russian language)
by Konovalov, Dmitry; Golubev, V.S.; Bogdanova, E.G. and Ylin, B.M. (Russian Federation) **136**

1.1.5(3) A Method of Field Calibration of Automatic Weather Stations
by HU, Yufeng and ZHOU, Weixin (China) **140**

1.1.5(4) Corrections of the Wind-induced Error of Tipping-bucket Precipitation Gauges in Switzerland Using Numerical Simulation
by Sevruk, Boris; Roulet, Y.-A. and Nespor, V. (Switzerland) **144**

1.1.5(5) Accredited Calibration Laboratory of the Hydrometeorological Institute of Slovenia
by Zlebir, Silvo (Slovenia) **148**

1.1.5(6) A Simple Tool for Recording Meteorological Instrument Site Exposure
by Hatton, David B. and Parker, M. (UK) **152**

1.1.5(7) Acceleration and Deceleration of a Cup Anemometer in a Wind Tunnel and in Natural Turbulence
by Jones, D.W.; Sparks, W.R. and Hatton, D.B. (UK) **155**

1.2 Upper-air Observation Systems

Keynote Paper

The Composite Upper-air Observing System, a Challenge for the Future Work of CIMO
by Nash, John (UK)
Chairman of the CIMO Working Group on Ground-based Upper-air Observing Systems **159**

1.2.1 In-situ Upper-air Observation Systems

1.2.1(1) The Preliminary Experiment of Deriving Integrated Atmospheric Water Vapor from Ground-based GPS
by XU, Baoxiang; HE, Ping and ZHOU, Xiuji (China) **167**

1.2.1(2) Overview of the NWS Radiosonde System Replacement
by Thomas, Richard D., Jr. and Bower, Carl A., Jr. (USA) **171**

1.2.1(3) The New Phase Array Aerological Radar-MARL
by Ivanov, Alexei; Azarov, A., Kochin, A. and Chistuhin, V. (Russian Federation) **175**

1.2.1(4) New Technology in Upper-air Observations
by Smout, Richard E.; Elms, J.B.; Lyth, D.R. and Nash, J. (UK) **179**

1.2.1(5) The Development of a Recoverable Radiosonde: The Glidersonde Project
by Howard, Ken; Douglas, M.; Renno, N.; Egle, D. and Gallapher, F. (USA) **183**

1.2.1(6) A Robot Plane Meteorological Sound System
by MA, Shuqing; WANG, Gai; PAN, Yi and LIU, Zulun (China) **187**

1.2.1(7) New Radiosonde for Chinese Ground Equipments
by LI, Jiming and FENG, Dali (China) **191**

Poster Presentations

P1.2.1(1) New Stabilised Balloons for GPS Radiosondes
by Barat, Jean (France) **195**

P1.2.1(2) New Instruments for Russian Upper-air Network
By Balagurov, Alexander; Grinchenko, V. and Kats, A. (Russian Federation) **199**

P1.2.1(3) New Radiosondes for Russian Systems of Upper-air Observations (submitted in Russian language)
by Ivanov, Vjacheslav; Essyak, S.P.; Lazarev, V.F.; Volkov, V.L.; Zakharova, G.S. and Bogov, V.T. (Russian Federation) **203**

P1.2.1(4) Radiosonde System for Conducting Upper-air Observation (submitted in Russian language)
by Ivanov, V.E.; Gusev, A.V.; Mironenko, O.V. and Petrov, R.A. (Russian Federation).. **207**

P1.2.1(5) Measures Fines de Vent – A l'aide d'un système de radiosondage équipé d'un GPS 4D *(Fine Wind Measurements Carried out Using a Radiosounding System Equipped with sonde GPS-D)*
by Charpentier, Patrick (France)..... **211**

1.2.2 Remote Upper-air Observation System

1.2.2(1) Operational Experience of a Boundary Layer Wind-profiler Network
by Matkin, Nicola; Oakley, Tim; Turp, Myles and Nash, John (UK) **215**

1.2.2(2) Multiple Beam Statistical Analysis of Wind Profiler Data
by Currier, Philipp and Berthou, T. (France)..... **219**

1.2.2(3) Combined Temperature and Wind Microwave Profiler: Results of Field Testing and Comparison
by Kadygrov, Evgeni N.; Ivanov, A.A. and Viazankin, A.S. (Russian Federation) **222**

1.2.2(4) Automatic Cloud Coverage Determination by Evaluation of Thermal Radiation Differences
by Heyn, Klaus; Schesonka, Ingo and Engel, Stefan (Germany)..... **226**

1.2.2(5) Long Range Sodar – Improving the Resistance of such System to Ambient Acoustic Noise
by Fage, Jean Michel (USA)..... **229**

1.2.2(6) The Observation of Heavy Rainfall Events over China Using TRMM Data
by CHENG, Minghu; HE, H.; MAO, D.; QI, Y.; CUI, Z.; SHI, R. and ZHOU, F. (China)... **231**

1.2.2(7) The Experiments on the Improvement and Application of GPS/PWW Technique in Shanghai Area
by DING, Jincai; WANG, Xiaoya; ZHU, Wenyao and YAN, Haojian (China) **235**

Poster Presentations

P1.2.2(1) Quality Evaluation for the COST 76 European Wind-profiler Network
by Nash, J.; Latham, N.; Oakley, T.; Lyth, D. and Turp, M. (UK) **239**

P1.2.2(2) Distributed Transmitter / Receiver Design for Operational ST Wind Profilers
By Currier, Philipp and Berthou, T. (France) **243**

1.3 Weather Radars and Lightning Detection System

1.3(1) A Lightning Detection and Location Network for New Zealand
by Pannett, Ralph A. and Mipenz, M.E. (New Zealand)..... **246**

1.3(2) The UK Met. Office's Upgraded Lightning Location System
by Nash, John; Hibbert, Eric; Callaghan, Greg; Taylor, Paul; Daly, Noelle; Burness, Richard and West, Graeme (UK)..... **250**

1.3(3) Gestion, efficacité et qualité des réseaux français de détection d'impacts de foudre (Management, Efficiency, and Quality of the French Lightning Detection Network)
by Montariol, Françoise (France)..... **254**

1.3(4) Total Lightning Detection Technology, Application in Weather Nowcasting
by Richard, Philippe (France) **258**

1.3(5) China New Generation Radar
by GE, Runsheng; ZHU, Xiaoyao; JIANG, Haiyan and WANG, Lixuan (China)..... **262**

1.3(6) Le rèseau ARAMIS de radars-précipitations: démarche pour une utilisation quantitative (The ARAMIS Precipitation Radar Network: Towards a Quantitative Utilization)
by Cheze, Jean-Luc (France) **265**

1.3(7) A New Retrieval Technique for Single-Doppler Radar
by JIANG, Haiyan and GE, Runsheng (China) **269**

1.3(8) Preliminary Study of Correction for Precipitation Attenuation for C-band Radar Data
by CHENG, Minghu; SHI, R.; CUI, Z.; QI, Y.; HE, H.; CAI, Z. and XU, H. (China) **273**

1.3(9) Introduction to CINRAD WSR-98D Signal Processor
by HE, Jianxin and WANG, Ping (China) **277**

1.3(10) Employment of an S-Band Vertically Pointing Radar
by Gourley, Jonathan J.; Howard, Kenneth W. and Winston, Herb (USA) **281**

Poster Presentations

P1.3(1) Dual-Polarization and Processor Efficiency Enhancements of the DOE's Millimeter-Wavelength Cloud Radars (MMCR)
by Winston, Herb; Moran, K.P. and Martner, B.E. (USA) **285**

P1.3(2) The Capabilities of Weather Radars to Detect Dust Storms
by Amer, Moustafa A.E. (Egypt) **289**

P1.3(3) Thailand Radar Network
by Dangintawat, Kasidej and Sinuthog, Chooseang (Thailand) **291**

P1.3(4) From NEXRAD WSR-88D to CINRAD WSR-98D
by WANG, Chong Wen (China) **295**

P1.3(5) Radar Complex for Atmosphere Dynamic Characteristics Measurement
by Efremov, Vladimir N. (Republic of Uzbekistan) **299**

P1.3(6) Radar Studies of Thunderstorm Clouds and Lightning Channels (submitted in Russian language)
by Shchukin, Gregory G. and Galperin, S.M. (Russian Federation) **302**

1.4 Measurement of the Atmospheric Composition

Keynote Paper

Atmospheric Composition - A Challenge for the Observations
by Fricke, Wolfgang (Germany) **306**

1.4(1) Measurement of Atmospheric Components by a Ground-based Remote Sensing Method
by WANG, Gengchen; Kong, Qinxin; Liu, Guangren; Gu, Zhifang and Wan, Xiaowei (China); Grechko, E.I. and Fokeeva, E.V. (Russian Federation) **314**

1.4(2) Low-Cost Technologies for Meteorological Monitoring of Atmospheric Pollution (submitted in Russian language)
by Volberg, N.S.; Gurevich, Y.G.; Kuzmina, T.A. and Pavlenko, A.A. (Russian Federation) **318**

Poster Presentation

P1.4 An Automatic Device Based on the Fourier Spectrometer for Measuring the Total CO_2 and CH_4 Content (submitted in Russian language)
by Reshetnikov, Aleksandr Y.; Obraztsov, S.P.; Privalov, V.Y. and Rumiyntsev, D.V. (Russian Federation) **321**

1.5 Instruments and Systems Operated under Harsh Environment Conditions

1.5(1) Operation of Automated Surface Observing Systems in Harsh Climatological Environments
by Gifford, M. Douglas (USA); Pearson, Garry M. (Canada) and Hegg, Kjell (Norway) ... **325**

1.5(2) Exploitation des instruments météoroligiques en milieu tropical (Use of Meteorological Instruments in the Tropical Environment)
by Soumah, Facinet (Rep. of Guinea) **329**

1.5(3) Operational Considerations in Implementing a Network of Automated *Upper*-air Systems in Harsh Environment
by Canterford, Ray P.; Smith, P.R.; Braden, L.J. and Joyce, M.J. (Australia) **332**

Poster Presentations

P1.5(1) Unattended Microwave Remote Sensing System for Winter Clouds Parameters Monitoring
by Koldaev, Arkady V.; Kadygrov, V.E.; Koloskov, A.B.; Miller, E.A. and Mironov, A.F. (Russian Federation) **336**

P1.5(2) Static Windsensor Quatro for Harsh Environment Conditions
by Burgos, Ernesto and Nemeth, Kurt (Germany) **340**

1.6 Urban Meteorology

Keynote Paper

The Requirements of Urban Meteorological Measurements and CIMO's Role
by Vashistha, Ramdhan (India), Co-rapporteur of CIMO on Urban Meteorology **344**

1.6 Automatic Weather Station for Collecting Meteorological Data from Urban Areas
by Vashistha, Ramdha and Srivastav, S.K. (India) **352**

2 MANAGEMENT OF INSTRUMENTS AND TECHNICAL SUPPORT FOR OPERATIONAL MEASUREMENTS

2(1) Developments in a Modern Quality Management System: Observations Quality Control, Network Performance and METADATA Database
by Canterford, Ray P.; Evans, D.K. and Allan, L.C. (Australia) **356**

2(2) New Approach to Development of Calibration Procedures and Decision Support System Realized in Yugoslavia
by Milinkovic, Mladen, B.; Knezevic, Jasmina and Radojevic, Dragan (Yugoslavia) **360**

2(3) Some Aspects of Quality Assurance Process at the Slovak Hydrometeorological Institute
by Ondras, Miroslav and Novanska, Olga (Slovakia) **365**

2(4) USA National Weather Service Radiosonde Upper Air Excellence *Award* Program
by Bower, Carl A., Jr. and Blackmore, William H. (USA) **369**

Poster Presentations

P2(1) Météoroutes: The Walloon Meteorological Observation Programme which Aims at Improving Climatic Forecasts
by Ledent, Thierry (Belgium) **373**

P2(2) A Lifecycle Management System for National Monitoring Networks in Canada
by Pearson, Garry M.; Dockendorff, Dave and Lynch, Darryl (Canada) **377**

P2(3) Nuevas Tecnologias Para la Medicion de Precipitacion y su Impacto Tecnologico (New Technologies for Precipitation Gauging and their Impact)
by Guillen Orellana, Marielba (Venezuela) **381**

P2(4) The Effect of Data Collection Instruments on the Quality of Data: The Case of Ethiopia
by Alemtsehay, Estifanos (Ethiopia) **384**

3 CAPACITY BUILDING AND TECHNOLOGY TRANSFER

3(1) Dévelopment et perspectives de l'enseignement des instruments météorologiques (Development and Perspectives in Meteorological Instruments Teaching)
by Hamza, Abderrahim (Algeria) **387**

3(2) Capacity Building for Instrumentation
by Kruus, Jaan and Angle, Bruce (Canada) **391**

APPENDICES

- List of members of the International Programme Committee for the preparation of TECO-2000
- List of publications in the Instruments and Observing Methods Report series

****

0 INTRODUCTORY KEYNOTE PAPER

MAJOR CHALLENGES FACING WMO MEMBER COUNTRIES IN OPERATING AND MAINTAINING METEOROLOGICAL AND ENVIRONMENTAL INSTRUMENT NETWORKS AND THE ROLE OF CIMO

R.P. Canterford
(Vice President of CIMO)

Australian Bureau of Meteorology
PO Box 1289K Melbourne, Vic. AUSTRALIA
Tel (+613) 9669 4225, Fax (+613) 9669 4168
Email : R.Canterford@bom.gov.au

Abstract

Increasing demands on instrument specialists and network managers is leading to critical change in the way National Meteorological and Hydrological Services (NMHS) are operating meteorological and environmental measurement networks. An analysis is given of the types of changes, including new technologies for instruments, sensors and observing systems, and the demands for cost effective network operations within limited resources. The role of manufacturers and the World Meteorological Organization (WMO) Commission for Instruments and Methods of Observation (CIMO) in supporting NMHS is discussed. A model of increased collaboration between manufacturers and NMHS, supported by various CIMO groups and activities, is presented as the best way to draw on the strengths of all stakeholders in facing the critical change of the next decade. Both the common and contrasting requirements of developed and developing countries in this model are discussed

1. Introduction

The purpose of this paper is to provide an overview of the changing activities and resultant issues facing National Meteorological or Hydrological Services (NMHS) as we move into the next decade. The paper will highlight the role of WMO and CIMO in particular, through the Instruments and Methods of Observation Programme (IMOP).

The theme of this Conference is "Operational Measurement Technologies for the Next Decade – Critical Change or Business as Usual?" This keynote paper will attempt to outline the types of challenges that are facing NMHS. Within this context it will be proposed that "business as usual", which allows for some dynamic change, is not sufficient if networks of modern instruments are to provide accurate homogeneous data for operations and research. A model of increased cooperation between manufacturers and NMHS, assisted through the activities of CIMO, is proposed as the vehicle for critical change.

Instrument specialists and managers of meteorological and environmental observing networks are facing increasing demands in the operation of these networks. These demands can include, but are not restricted to:

i. sustained performance to meet operational requirements for the Global Observing System (GOS);
ii. increased performance to meet WMO programme requirements, such as that required for the Global Climate Observing System (GCOS);
iii. increased pressure to operate efficient networks within limited resources, which can lead to reductions in personnel to operate, inspect and maintain equipment;
iv. increased emphasis on costed network outputs, including performance measures and equipment lifecycles;
v. increased automation of some observations and resulting calibration and quality assurance requirements;
vi. increased sophistication of equipment and inability of some NMHS to operate this without manufacturers' support;
vii. the need to replace obsolete systems which can no longer be maintained;
viii. reliance on long term support of manufacturers and the impact on developing countries;
ix. opportunities presented by new technologies, including increased technical performance for improved observations frequency and homogeneity; and

x. widening technological gap between developed and developing countries.

Many of the above demands and influences occur in most NMHS. CIMO experts, participating in its Working Groups and Expert Meetings from a broad representation of NMHS, have found these are common issues of concern.

This paper will try to address these issues and point out that "business as usual" is not sufficient. NMHS must change in line with new technology and often reducing or limited resources. Furthermore, CIMO should have an increasing role in assisting NMHS adapt to these changes.

2. The Role of Instrument Specialists and Managers in Determining Changes

The fundamental problem with any change of instrumentation is the change in the characteristics of the measurement itself. This can have a marked impact on the homogeneity of the historical record and consequently diminish the value of climate studies based on these records. As technology changes significantly over shorter time periods, this is a major concern to climate researchers and operational data users. However, the changing technology to automated observations can have a positive impact on homogeneity, if good metadata records are maintained.

By the time mandatory overlap periods as recommended by WMO are achieved, further advanced technology can be available. This makes it quite difficult for developed countries - whether to adopt the new technology or sensors; and developing countries - at what stage should they consider the new technology economical and will it be supported for reasonable periods in the future.

Therefore the role of the instrument specialist is changing from one of deep understanding of the characteristics of long established instruments to one of demands to evaluate new sensors and instruments over shorter periods of time. At the same time the technology is becoming more complex and manufacturers often do not release sufficient information for commercial reasons. Furthermore, many NMHS are having difficulty maintaining sufficient qualified and trained instrument specialists and are relying on manufacturers to provide the necessary expertise.

This reduction of instrument specialists in NMHS and increased reliance on manufacturers may appear to be a satisfactory solution, especially for developed countries. However, the relationship between manufacturers and NMHS will have difficulties if a good balance is not achieved. Manufacturers and instrument designers have often relied on NMHS and WMO instrument intercomparisons, initiated and conducted by CIMO, to assist with the development, testing and implementation of equipment into a field environment. NMHS have employed instrument specialists with many years experience and manufacturers have relied on this experience to a great extent. Manufacturers have played a key role in the development of sensors and instruments by keeping pace with changing technology. Obvious examples are automatic weather stations (AWS) and radiosondes using GPS navigation. The close relationship between WMO Members and manufacturers needs to be enhanced for both developing and developed countries. CIMO should continue to play a key role in this cooperation. This will be explored further later in the paper against this background.

Instrument specialists and network managers should be fully aware of this relationship with manufacturers and the benefits and possible pitfalls. They should be aware of the initiatives of CIMO in fostering closer cooperation, and with the increasing access to the Internet making the availability of WMO/CIMO reports much easier. Many of these reports describe detailed instrument intercomparisons involving WMO Member experts and manufacturers.

In addition to the above performance driven changes, instrument specialists and network managers can benefit from changes in technology to achieve cost effective solutions for networks. Indeed, this can often be the most compelling argument for critical change.

3. The Role of CIMO in Facilitating Ongoing Operations and Changes to Instrument Networks

CIMO essentially operates with two key Working Groups, one for surface measurements and one for upper air measurements, plus several Rapporteurs on other observing systems and areas of concern, such as capacity building. These experts are supported by a small Secretariat at WMO headquarters in Geneva. CIMO is responsible for the WMO Instruments and Methods of Observation Programme (IMOP), which it manages through a series of activities as shown in Figure 1.

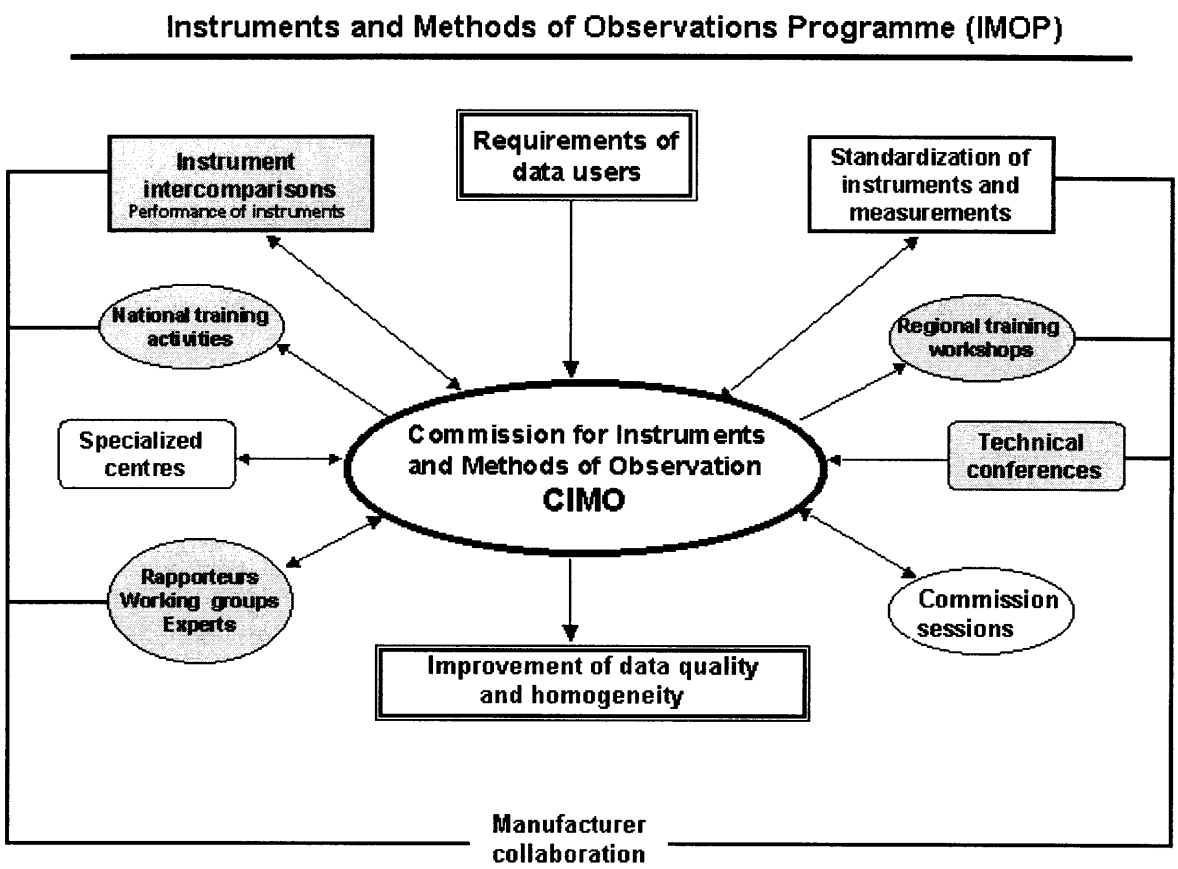

Figure 1: CIMO activities in support of WMO Members maintaining environmental instrument networks and the shaded areas where manufacturer collaboration is important.

Manufacturers are now being encouraged to be involved in most of the CIMO activities shown in Figure 1 to enhance cooperation. CIMO needs to play an increasing role in assisting WMO Members to operate and adopt new observing systems, instruments and sensors. As mentioned earlier, instrumentation technology is changing rapidly and homogeneity of records must be maintained. This involves, as well as instrument overlap periods, greater demands on calibration and maintenance of equipment. In particular, if the equipment is automated, sound quality management procedures must be firmly established. A lack of on-site staff to quality control the data from instruments means there is a shift to reliance on field inspections by staff, often every six months, depending on sensor performance.

Again the demand for accurate metadata records increases as sensors change. An associated problem is the increasing use of algorithms to determine standard atmospheric variables from sensors. Some manufacturers (and sometimes NMHS) are reluctant to publish this information. This can lead to great difficulty for NMHS introducing and maintaining new instruments. Therefore CIMO encourages manufacturers and Members to publish this information.

Further, manufacturers often raise the problem of varying instrument requirements amongst NMHS as a cause of high costs, as they need to accommodate many slightly, or sometimes significantly, different systems. CIMO has an important role in this respect and reports in the WMO "Instruments and Observing Methods" "green stripe"-IOM series assist in providing some uniformity, through expert determination of performance in particular applications. Recent examples include the "Guidance on Automatic Weather Systems and their Implementation" (IOM Report No. 65) and "WMO Wind Instrument Intercomparison" (IOM Report No 62). With increasing developments in electronics and computing technology, the skills of instrument specialist, especially those involved in field inspections or calibration of equipment, are changing rapidly, along with the equipment necessary to perform the instrument maintenance. Van der Meulen (1998) has published several "Instrument Develop Inquiry" studies through CIMO and discusses future requirements for Surface Observations (Van der Meulen, TECO 2000). CIMO, through its efforts to promote global homogeneity of data, along with high quality, sponsors Regional Workshops to train

instrument specialists. CIMO is also enhancing the number and role of Regional Instrument Centres (RICs), which will be discussed later.

Developing countries have additional concerns and problems with the ever-increasing technology of environmental monitoring instruments. As well as the issues of maintaining the homogeneity of data and the increasing dependence on the expertise of manufacturers suffered by developed countries, developing countries will be even more dependent on manufacturers for support. A recent WMO Instruments and Observing Methods Report No. 68 "Guidance Material on the Choice of Meteorological Instruments for Surface Observations Suitable for use in Developing Countries" (Odero, 1998) outlines many of these problems. Often manufacturers provide the support in the early stages of equipment purchases and implementation, but this support can decrease over time. This is critical as we commence the next decade, since sensors and technology change rapidly and manufacturers are keen to keep pace and maintain a competitive edge. Developing countries and developed countries have great difficulty supporting the "older technology" if a manufacturer decides to discontinue a particular sensor or instrument and spare parts and support is withdrawn. This is a question of "what is the economic life cycle of a system?" While keeping pace with technology is good (if it supports the real needs of the NMHS), manufacturers may not be fully aware of the implications for NMHS, who often do not have funds to "upgrade".

Additionally, manufacturers may not be fully aware of the major impact their instrument changes have on the climate record. A good example is the large range of temperature screens produced by manufacturers, especially for new AWS. This has a marked impact on the climate record and creates problems for NMHS. CIMO, though IOM Report No 66, outlines the range, the standards and the requirements of NMHS to maintain their national benchmarks. Of course manufacturers are not entirely to blame in this regard. They are market driven. If the developed countries always go for the latest hi-technology (perhaps to reduce operating costs), then less developed countries suffer from equipment obsolescence as the market distorts. On the other hand, NMHS who are not well advised (by CIMO reports and experts) may buy cheaper but poorly performing systems, perhaps designed for the non-professional consumer market.

The impact on climate studies is obvious in this single item of temperature screens, let alone changes to sensors and their particular calibration and performance. If a global intercomparison is not achievable due to different climatological requirements of screens, IOM Rep No. 66 recommends at least a national or regional intercomparison, temporal overlaps at sites and national intercomparisons of new screens (which may in fact have superior characteristics) with traditional screens. These tests are essential, especially if data are to be normalised across international boundaries.

The above is just one aspect of NMHS meeting the demands listed in Section 1. Manufacturers also have a role in standardising their designs for reasons of production economics, and publishing performance characteristics.

Another recent example of the role of CIMO in addressing the demands placed on NMHS is the "Expert Meeting on Operational Issues for Radiosonde Applications in the Tropics and Sub-tropics" in Oct 1999. It should be highlighted that WMO, through CIMO, has organised several intercomparisons of radiosondes in the last 15 years to determine their performance characteristics; and new GPS based radiosondes require testing, which is planned by CIMO for later this year. Several Member countries have undertaken national trials and provided valuable feedback to the manufacturers. In particular, manufacturers are to be congratulated on meeting the demand for the new GPS radiosondes after the demise of the Omega navigation system. Close cooperation between CIMO experts and manufacturers remains a high priority. The Oct 1999 Expert Meeting highlighted some deficiencies in GPS radiosondes for wind finding and relative humidity measurements. The findings and recommendations of this CIMO Expert Meeting were reported to the full session of the CIMO Working Group on Ground Based Upper Air Observing Systems in New Delhi, India last December. At that particular meeting several manufacturers were represented.

4. New Technologies for Observing Systems

CIMO experts in Member countries are becoming involved in an ever-increasing range of new technologies and observing systems. The role of these systems in the Future Composite Global Observing System (FCGOS) is essential for well-balanced cost effective observing networks. However the same fundamental concepts of data uncertainty, maintainability, calibration and intercomparisons used by instrument specialist over the years must be applied to these new technologies, otherwise homogeneity will not be achievable. The Commission for Basic Systems (CBS) has a fundamental interest in these new

systems and must rely heavily on CIMO experts to ensure the credibility of the environmental data. It is encouraging to note that CBS is taking full account of climate requirements through GCOS, and CIMO can assist greatly in achieving the aims of this important WMO activity. In particular, uniform and routine calibration of instruments against National Standards linked to Regional Standards is fundamental for the integrity of climate data. CIMO's initiative in establishing guidelines (Guide to Meteorological Instruments and Methods of Observation, termed the *CIMO Guide*, WMO No 8) and frameworks for Regional Instrument Centres is therefore important.

As can be seen from the programme of technical papers for this conference, some of the new or updated technologies for observing systems that are being established and maintained by NMHS include:

- AMDAR (Aircraft Meteorological Data Relay) or more specifically the rapidly expanding ACARS (Aircraft Communication Addressing and Reporting System).
- ASAP (Automated Shipboard Aerological Programme)
- Advanced Automatic Weather Stations (AWS), which include sensors for visual parameters etc such as the "Present Weather" variables.
- Advanced radar systems involving Doppler and Dual Polarisation capabilities
- GPS signal monitoring for water vapour and virtual temperature measurements
- New generation radiosondes
- Unmanned Aerial Vehicles (UAV) eg. Glidersonde and Aerosonde
- Satellite based systems such as new sounders, lidars etc
- Atmospheric Profilers
- Lightning Detection networks (especially new networks based on "time of arrival")
- Advanced marine observing platforms beyond drifting buoys to sub-surface floats
- Updated shipboard systems such as AWS.

Many of these systems are being considered for the future composite Global Observing System (CBS OPAG Expert Team, Third Session June 2000) and the upper air component are discussed in a later keynote address (Nash, TECO 2000). CIMO is aware of these changing technologies and its members are often at the forefront of developments in the technology. They are being required to benchmark or calibrate the data from these systems against more conventional data. For example, quality control and assurance measures have been developed for AMDAR data against conventional radiosonde data as well as other aircraft and Numerical Weather Prediction Models.

As another example, advanced AWS sensors such as ceilometers and visibility meters are providing new types of information for both weather forecasting and climate studies. In order to fully utilise these new and more frequent observations, CIMO has encouraged CBS to develop enhanced codes. CIMO organised, in collaboration with CBS, an Expert Meeting on the Requirements and Representation of Data from AWS (Netherlands, 1999) on this important issue. It was attended by experts from all WMO Technical Commissions for the benefit all data users.

It must be emphasised that all current and future observing equipment, procedures and systems must comply with rigorous calibration and traceability against appropriate standards. CIMO and its instrument specialists are endeavouring to achieve this and must have the full support of NMHS - any new observing system will have to include these underlying costs in its operation if it is to provide sustainable reliable homogeneous data. It should be noted that some of these systems (eg. lightning location networks) might be supplied and operated by private firms. This leads to some complications in ensuring appropriate accuracy of data and again close cooperation of WMO experts with manufacturers and suppliers is essential, since the user requirements for the data may conflict.

5. The Role of Manufacturers in supporting Change

The previous Section highlights the increasing diversity and complexity of observing instruments and procedures. Coupled with often reducing resources, NMHS instrument specialists are becoming more dependent on manufacturers/suppliers support. TECO-2000 has adopted an approach of encouraging participation by manufacturers in both the Technical Papers and Panel Sessions. This is in addition to the associated METEOREX display. Manufacturers have welcomed previous cooperative approaches, which is predominantly a feature of CIMO within WMO. This TECO/METEOREX is a further example of adaptation to the critical change facing NMHS. By using this forum to discuss these changes with a wide range of manufacturers, it will hopefully jointly enhance understanding of each other's aims and problems.

It may also be able to allay the concerns of some manufacturers of conventional observing systems and instruments - these will be required for many years to come as a method of benchmarking or anchoring new technologies as they arise, as well as for economic reasons. The need for long-term high quality climate data cannot be overemphasised. Additionally, manufacturers must appreciate the special needs of developing countries in their long-term support. Equipment should not be supplied and then not supported over long time periods. Systems cannot be continually upgraded without support and backward compatibility to earlier systems. It is not responsible, and a waste of resources, to install equipment without adequate provision for support of the system for the duration of its economic life.

Manufacturers must be aware of the continuing decline of "instrument budgets" of NMHS in designing new equipment. NMHS are often faced with dilemmas on whether to upgrade at great cost - cooperation is needed before manufacturers make unilateral decisions to upgrade systems or consumables. Radiosondes are an impressive example of this, since they can have significant implications in annual budgets of NMHS.

Other issues that face instrument specialists when determining future instrument purchases or upgrades include:

- reliability of manufacturers' performance information or specifications,
- compatibility with current systems and
- long term support for spare parts and possible maintenance, training and calibration facilities.

Some manufacturers supply training in their factories prior to purchase and this can highlight potential problems. However, there appears to be a widespread belief that manufacturers could assist NMHS further by providing more reliable and detailed performance specifications and evidence of field trials (possibly conducted in conjunction with a particular NMHS). It is recognised that this already occurs for some instruments by some manufacturers, but it should become more widespread, especially as more complex instruments are released. (Indeed, some system calibration, eg. radiosondes, remote sensing systems, is often beyond the resources of NMHS, and must depend on manufacturers field trials, hopefully in collaboration with CIMO.) Manufacturers should also ensure NMHS are automatically supplied with upgrades of software for the life of the system.CIMO has recently established a CIMO Newsletter, which is delivered to all CIMO members, observers and some 400 manufacturers to improve the flow of information. Indeed, the CIMO president Dr Srivastava recently convened a special meeting with manufacturers of Upper Air Observing Systems to foster cooperation, which was welcomed by the manufacturers (CIMO Newsletter Edition: March 2000).

6. The Role of NMHS and Manufacturers in Capacity Building

A major challenge for the next decade facing WMO Member countries is capacity building for developing countries. WMO activities are highly dependent on the ability of ***all*** Member countries to contribute to global programmes, operations and research activities. This inter-reliance of all Member countries is very clear in the area of meteorological and environmental observations. Examples are the Global Observing System for meteorological operations and numerical weather prediction and the Global Climate Observing System. If developing countries are limited in the provision of accurate routine observations, then all these activities are compromised. CIMO is very much aware of this interdependence and has historically supported developing countries with respect to instrument development. The CIMO Guide (WMO No 8) plus the IOM "green stripe" series are aimed at providing consistency across national boundaries. The dependence on high quality accurate data from developing countries must not be overlooked in the developments of the Future Composite Global Observing System.

CIMO convened an Expert Meeting on Capacity Building last year (Beijing, China, 1999) and several additional initiatives resulted from that meeting. Some of these have already been mentioned, but it is worth noting that the meeting strongly endorsed increased collaboration with manufacturers for more cost effective equipment for developing countries, and involvement by manufacturers in field training prior to installation of equipment. In this regard, 400 manufacturers are circulated letters and newsletters of CIMO activities and requirements. Attendance of manufacturers at workshops and technical conferences, such as METEOREX 98 and 2000 are very important for technology transfer to developing countries. The proposed Instrument Catalogue (CIMO XII, para 4.3.6, 1998) was aimed at assisting developing countries in choosing the correct instrumentation for their environmental and financial conditions.

Regional Instrument Centres are another area in which CIMO is preparing to enhance support for critical change. Additional RICs have recently been established; and there are now 13 available within all WMO Regions. Although these centres get no direct financial support from WMO, they do act as a focal point for calibration of national standards and training of instrument specialists. Recent meetings of CIMO Capacity Building experts (Beijing, China, Sep 1999) recommended manufacturers view these RICs as

special focal points for provision of discontinued equipment, instrument standards and information, and for attendance at training events. As all NMHS should be in contact with their respective RICs, this is an efficient way of spreading technical information and cooperation between WMO Members and manufacturers. Of course, manufacturers are often invited, when feasible, as observers to various Working Group and Expert Meetings as observers.

A recent letter to manufacturers of instruments and equipment by the Secretary-General of WMO sought views from them on the enhanced collaboration mechanisms. As pointed out in that letter, WMO Congress endorsed the continued capacity building efforts of CIMO and this conference, TECO-2000, and the conjointly organised METEOREX 2000, should assist. The letter floated the concept of an Association of Manufacturers of Instruments and Equipment.

CIMO has developed further its own Web site as part of the WMO site. Links to CIMO documents and the IMOP are contained in the page along with the Terms of Reference of CIMO, officials and Working Group Members, Rapporteurs and their TORs. These official positions are elected at Commission Meetings every four years. Currently there are 280 instrument experts nominated by some 140 Member countries and registered as members of CIMO. Of these, 46 experts representing all WMO Regions and other technical commissions are involved in the Working Groups or are Rapporteurs actively supporting CIMO activities. CIMO also has strong links to WMO Regional Associations through the RICs and Rapporteurs on the "Regional Aspects of Instrument Development, Related Training and Capacity Building".

7. Conclusion

This paper has highlighted the joint roles of CIMO, instrument specialists of NMHS and manufacturers, in facing the critical changes of the next decade. Clearly "business as usual", which can allow for some dynamic or pro actively created change, is not sufficient. CIMO in particular, through its NMHS specialists, has certainly adapted to technical change in recent years and will continue to enhance its activities. This is most evident in its contributions to the move to GPS radiosonde technology, Radio Frequency Coordination, GCOS, the revised CIMO Guide, increasing links to manufacturers, extensive intercomparisons of instruments, facilitation of Regional Instrument Centres, its Web site, TECO/METEOREX 1998 and 2000 and valuable technical publications through the IOM Series. These activities are only possible through the active role of instrument specialists. Additional experts are very welcome to contribute to any of these activities.

As discussed in the paper, all instrument specialists are facing major challenges and greater collaboration with manufacturers has been emphasised as one way forward. The advantages and disadvantages of this approach have been highlighted and must be kept in mind by all specialists and network managers.

The role of manufacturers in working with NMHS and CIMO as we move into the next decade, has been highlighted. Through this paper, the TECO-2000 papers that follow, the joint manufacturer/instrument specialist panels and METEOREX-2000, avenues of further cooperation can hopefully be developed.

8. References

- CIMO/CBS Expert Meeting on Requirements and Representation of Data from Automatic Weather Stations, De Bilt, Netherlands, 19-23 April 1999.
- CIMO TECO-98. "WMO Technical Conference on Meteorological and Environmental Instruments and Methods of Observation, Casablanca, Morocco, 13-15 May 1998. IOM No 70.
- CIMO Expert Meeting on Capacity Building Related to Instruments and Methods of Observation, Beijing, China, 23-25 September 1999.
- CIMO Expert Meeting on Operational Issues for Radiosonde Applications in the Tropics and Subtropics, Geneva, 19-22 October 1999.
- CIMO Newsletter: http://www.wmo.ch/web/www/IMOP/Index-Circular-Letters.html
- CBS Open Programme Area Group (OPAG) on Integrated Observing Systems. Expert Team on Observational Data Requirements and Redesign of the Global Observing System. Geneva, 19-23 June 2000.

- Guidance on Automatic Weather Systems and their Implementation:
  Part I Guidance Specifications (Functional) for a General Purpose Automatic Weather Station
  Part II Implementation and User Training Considerations.
  By Observations and Engineering Branch, Australian Bureau of Meteorology, WMO, IOM No 65, 1997.
- Guidance Material on the Choice of Meteorological Instruments for Surface Observations Suitable for Use in Developing Countries. By J. P. Odero. WMO IOM No 68, 1998.
- Guide to Meteorological Instruments and Methods of Observation. (CIMO Guide). Sixth Edition. WMO No 8. 1996.
- Instrument Development Inquiry (Sixth Edition), By J. P. van der Meulen. IOM No 71, 1998.
- Nash, J. "The Composite Upper Air Observing System, a challenge for the future work of CIMO". TECO-2000. Beijing China, Oct. 2000.
- "Recent Changes in Thermometer (Screen) Design and Their Impact". By Barnett et al. IOM No 66, 1998.
- Van der Meulen, J. P. "Future Requirements for Surface Instruments". TECO 2000. Beijing China, Oct. 2000.
- WMO Wind Instrument Intercomparison. By P. Gregoire and G. Oualid. IOM No 62, 1997.

Acknowledgements

The author would like to express his appreciation to Mr. Ralph Pannett (Meteorological Service of New Zealand Ltd) for some valuable suggestions and Mr Klaus Schulze (WMO Secretariat) for additional comments.

1 MEASUREMENT TECHNOLOGY, PERFORMANCE, AND QUALITY ASSURANCE

1.1 Surface Observation Systems

Keynote Paper

Developments in Instruments for Surface Measurements and Meteorological Observation Techniques

Jitze P. van der Meulen
Royal Netherlands Meteorological Institute
Postbus 201, 3730 AE De Bilt, the Netherlands
tel +31 30 2206432, fax +31 30 2210407, e-mail meulenvd@knmi.nl

Introduction

Automatic Weather Stations (AWS) are becoming more and more popular. Quality and reliability of measurements are improved and the need for maintenance is reduced the last decade. As a consequence observations received from these automatic observing locations can meet the operational accuracy limits, stated by WMO. Not only new and improved sensor technologies have stimulated this development, but also the introduction of data acquisition systems, computers and data transmission systems.

Today, developments in the methods of observation are focussed on the technology of optics. Such developments are important for the introduction of new techniques for use as an alternative for visual observations (*e.g.* the very promising Present Weather Systems). Another important development is the introduction of microelectronics in measuring devices. Moreover, the integration of micro-sensors and microprocessors, providing a fully computer controlled digital measuring system has become a major development during the last years.

As a consequence of these developments, the new measuring devices have become a part of a primary measuring system of a weather station. This configuration, however, differs significantly from the traditional observing stations, where the measuring instruments are used as a helping tool for the observer, who was responsible in the first place for the quality of the measurement. This development implies a shift in responsibility as well. Quality control of the performance of an AWS has become more and more a task for the data managers of the stations. Moreover, inspection and maintenance are essential parts of good management of any AWS and will become increasingly important in future.

Instrument development

Within the framework of the Instruments and Methods of Observation Programme, two *Instrument Development Inquiries* were published by WMO during the last years (IDI-5, IDI-6) [ref. 1, 2]. For both inquiries most entries were received for the item *automatic meteorological station*, and it is clearly demonstrated that most effort is put into this special kind of development. Nevertheless the development of new systems to measure the traditional meteorological variables should not be underestimated. Interesting developments are going on to design new devices to measure air temperature, humidity, wind, precipitation, radiation, *etc.* for both surface as upper air measurements.

Some developments are less popular, but still very significant: Both new in-situ sensors (for radio-sondes) and modern remote sensing technology are introduced to improve the measurement of wind, temperature and pressure and the observation of clouds. Of interest is the use of optics in a wide range of methods of observation (*e.g.* visibility, radiation, and precipitation identification by so-called *Present Weather Sensors*). Although the use of optics requires intensive maintenance due to pollution, optics are becoming increasingly popular for the automation of visual observations.

An interesting issue concerning any development is the *motivation* behind it. Both IDI-5 and IDI-6 show that "Improved reliability or accuracy" is the leading motive for development. Nevertheless both "Cost effectiveness" and "Automation of manual observations" are given as major motives as well. Typically, the motive "New type of observation" holds only for a small number of new developed instruments. Consequently, few instruments are developed to measure meteorological parameters using a pure alternative technology.

Regarding the popular development of the AWS it is found that such development is in many cases a combination of a data-acquisition and data-dissemination system and also a set of appropriate sensors

suitable for such a system. Then design of such an AWS always fulfils the concept of one processing system, uniquely coupled to a sensor measuring one meteorological variables, *i.e.* most AWS are not really designed to perform intelligent calculations using data from a set of sensors to present alternative variables. It is worthwhile mentioning this point since it is found to be rather relevant within the framework of automation of visual observations, where the use of complex algorithms is found to be necessary.

Changing needs

In conjunction with the CBS-ext(98) session a technical conference was organised on *integrated upper-air observing*. Although many papers covered different topics, the integration of observing systems or networks in combination with NWP was indicated as a necessary constraint for further developments in terms of observations. In other words, the integral use of synoptical surface measurements, space borne measurements, radar measurements and in-situ upper-air measurements should be organised. Although such statements seem to be rather obvious, the impact on the need for appropriate observations will change. For example, if satellites, like ERS will monitor globally the wind at sea surface, the need for observations of the wind from VOS ships shall reduce. Or, if with the help of satellites cloud coverage is determined, such observation at a ground station may be stopped as well. And also the modern remote sensing technologies (ground or space based) will provide information as input for numerical weather prediction models (NWP) reducing the need for data determined on the classical way. On the other hand the increasing use of improved NWP models will require alternative meteorological parameters in future. In any case, it may be expected that the current classical set of observation parameters, well known from SYNOP and SHIP and well described in the CIMO Guide (WMO-No. 8) will alter into a much more complex configuration of observational parameters.
Today, modern weather forecasting is based in the first place on the results of operational NWP calculations. Not only global models or medium range prediction models will provide information but also limited area NWP models with high resolution in space (5 km) and time (1 H) are becoming very accurate, reliable and therefore popular for the meteorologists. For this purpose new types of information, like geological information is required and observations should be performed more frequently as well (*e.g.* every 10 min or continuously).
Using these high-resolution models, running almost continuously the actual state of the atmosphere is described on a three dimensional manner. By using this source of information a now-casting system is available to provide any user any actual meteorological information. From this point of view the need for the direct deliverance to a user of actual measured data from a weather station will reduce in future because any user may retrieve the more appropriate data from such now-casting system.
With respect to the growing impact of NWP, a significant move in terms of observation requirements can be expected. Today all types of observational data are assimilated into models and the impact of these data depends on appropriate weighting functions. In practice many data is over-redundant, *i.e.* data is available from different types of sources (*e.g.* surface measurements, radar). Moreover the impact of some parameters on NWP is rather limited and used for NWP analyses purposes only. In the near future with now-casting systems, were observations and NWP are highly integrated, a significant shift in the functional requirements for the variables is to be expected. For instance, wind speed may not be measured any more or only at some locations for specific purposes since the integrated system will provide such information by using other data sources.
From this point of view the traditional "continuous improvement of instrument" will not be a leading force in instrument development, but the search for the most appropriate observational parameters for input in a now-casting system.

Automatic observations

As stated already, the push behind instrument development is *cost effectiveness* and *automation of visual observations*. The latter motive can also be interpreted as a goal to reduce costs. In many countries automation of manned stations is going on and it can be expected that primary synoptical stations will become 100% unmanned within the next ten years. Control for maintenance and quality will be performed remotely from a central facility. And also locations where observations for aeronautical purposes are done will be automised and staff will be reduced to a minimum level, due to financial constraints.
For instance, in the Netherlands such a financial constraint was reason to decide to completely automise all synoptical observing stations and to reduce the number of observers at the aeronautical stations. This decision is based on the assumption that with the help of the currently observation technology enough

information can be generated to guarantee that the quality of the forecasting and warning systems shall not reduce noticeably. RSBN station WMO-06260 "De Bilt" will be the first station to be a 100% automatic (unmanned) station presenting the complete $7w_aw_aW_{a1}W_{a2}$ in the SYNOP code. This action was already taken end of May 1999, but after a month this station was reconfigured to be a 100% manned station again. Although a discussion is going on concerning the actual need for 100% automation, the arguments are valid that an adequate forecast system can be operational using automatic observations only. A number of lessons learned from this typical case are:

1. The increased complexity of the use of observational data to compile a SYNOP requires a very reliable and stable computer and data infrastructure. Very small shortcomings, simple errors and short time delays cause a significant degradation of the performance of such a station.
2. Parameters, previously observed by visual means, are measured and calculated using an integral data set from present weather observing systems, radar and lightning networks and ceilometers. On average, these determined data demonstrate a high degree of reliability. However, taking the requirements for severe weather warning systems into account, there are specific circumstances for which these data will have dangerous, misleading impacts. Especially light precipitation and temperatures around 0°C can be such a situation. Slipperiness or iciness caused by light snowfall or undercooled drizzle may result in many injured during the first hour of this phenomenon. Early and adequate warnings are one of the major and important tasks for meteorological services, even if such a situation seldom occurs.
3. The assumption that one-to-one automation of any single observational variable is enough is incorrect. Although the observational parameters are to be presented in the FM-12 SYNOP code, it was found that fulfilling this requirement only is far too simple. Note that many conclusions drawn by the WMO Expert Meeting on Requirements and Representation of Data from AWS (de Bilt, Netherlands, 1999) are in line with this statement. It is recommended to use the BUFR/CREX code world wide in the near future to disseminate more appropriate observation information.

Future Developments

All various methods of observations with in-situ sensor technology or by remote sensing, surface, space and airborne measurements provide the meteorological community with a gigantic amount of information. Taking this situation into account the need for human observations will reduce more and more and with no remarkable degradation of the weather forecast.
However, the design of the data flow diagram, the structure of the weather information generator and the data acquisition and dissemination infrastructure will be modified significantly. To understand this, see as an example the diagram below:

Classical concept: One-to-one observations

precipitation gauge	→	local precipitation amount/intensity
precipitation detector	→	local precipitation detection
thermometer	→	air temperature (*e.g.* non freezing)
anemometer	→	local wind speed
observer	→	determination type of precipitation (*e.g.* undercooled drizzle from time to time)
	→	cloud types
	→	cloud amount
	→	other weather phenomena (for $7wwW_1W_2$)

In future a more complex structure with integral use of observational data and dedicated algorithms:

Future: Complex structures
[simple subset to show the determination of some parameters, usually visually observed)

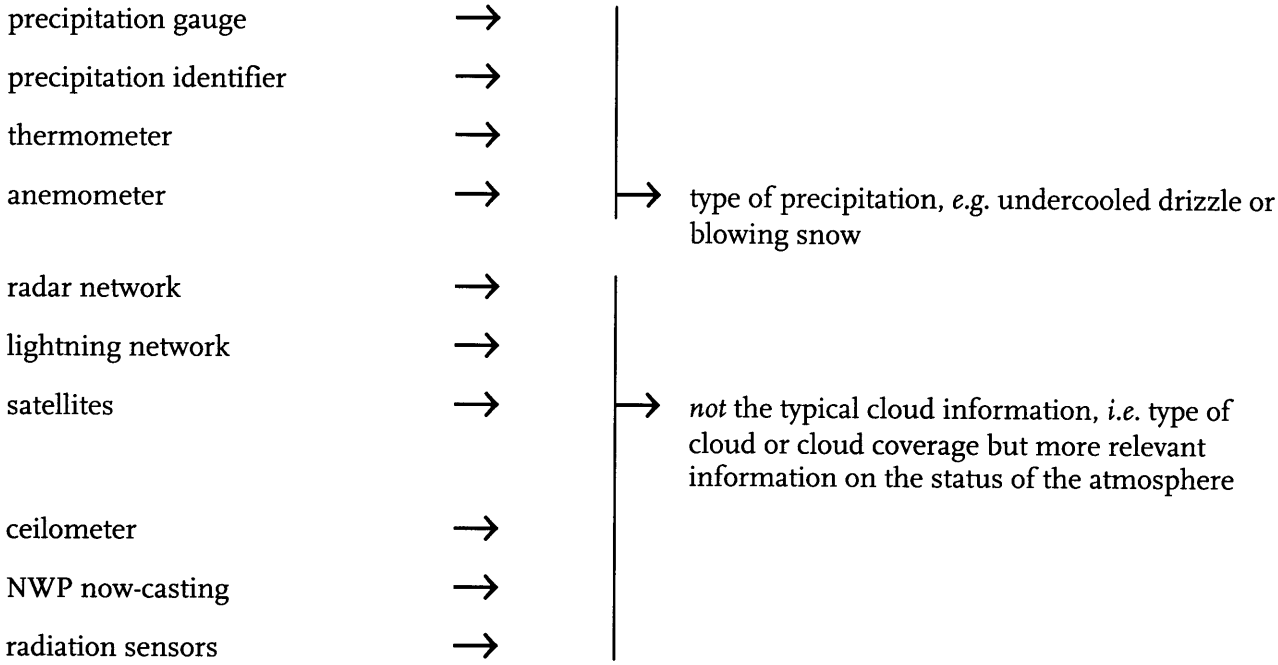

In summary, the information flow can be expressed in the following simple diagram:

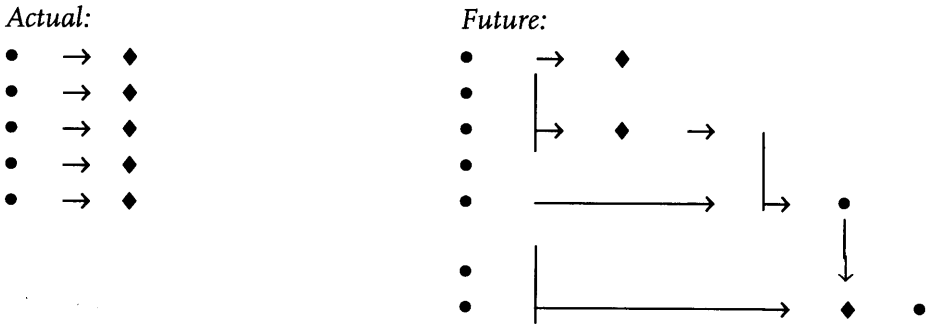

Please note that it is very obvious that such a structure requires a very high degree of reliability and performance of all components. Within the classical concept, the brake down of one single component will not affect the others. Within the new, integral concept simple shortcomings (*e.g.* short time delays) will reduce the performance of the complete system. To moderate this problem the used algorithms should be developed in such a way that brake downs of instruments or systems can be tackled as far as possible but requires a lot of experience for realisation.

Finally

One of the major goals of WMO is the standardisation of observations by taking into account the users' requirements. Within this context the standardisation of integrated observing methods and appropriate algorithms will be a complex and difficult task.
Nevertheless it is an interesting challenge as well.

References:

[1] Van der Meulen, J.P., *Instruments Development Inquiry (fifth edition)*, Instruments and Observing Methods Reports No. 54, WMO/TD-No. 578 (WMO, Geneva, 1993)
[2] Van der Meulen, J.P., *Instruments Development Inquiry (sixth edition)*, Instruments and Observing Methods Reports No. 54, WMO/TD-No. 878 (WMO, Geneva, 1998)

1 MEASUREMENT TECHNOLOGY, PERFORMANCE, AND QUALITY ASSURANCE

1.1 Surface Observation Systems

1.1.1 Automatic Weather Stations

New Measurements Technologies - A Critical Change to Climate ?

Ernest Rudel
Central Institute of Meteorology and Geodynamics, A-1190 Vienna, Hohe Warte 38, Austria
Tel.: +43 1 36026 2201, Fax: +43 1 36026 72, E-mail: ernest.rudel@zamg.ac.at

There was a lot of progress in recent times on measuring and observing meteorological variables by the application of direct and remote surface and space based techniques. Various types of instruments and equipment applied for these observations are already operated in automatic networks either on national or regional levels. The net of AWSs is increasing worldwide.

The demand for automation is increasing with the interlink of economy with weather. In the 1960ies and 70ies the considerable progress of micro processing techniques caused the development of low-cost automatic systems for the recording of meteorological and climatological data. Without going into details we have to distinguish four generations and the real step forward was that most of the tasks of these systems are executed by the software and not only by the hardware. The trend to automation of surface data acquisition systems has started already in the seventies of this century, has risen in the eighties and nineties and can be expected to continue in the next decades worldwide. In about thirty years automated surface weather systems stations will replace conventional weather observing systems at most sites. The future surface observational networks will consist largely of unmanned stations with a temporal resolution of as little as 10 Minutes and a spatial resolution of less than 50 km. There are big advantages to the new systems: Automation of surface weather observations reduces costs, increases area coverage and provides data continuously at frequent intervals and for any observation time. On top of it these systems eliminate the subjectivity inherent in manual observations such as visibility, cloudiness and estimates of the winds. This reflects the requirements of all users of near real time synoptic data. It also reflects the trends to reducing model grid scale and the need for more observations to be available in shorter timescales. But also the users of climatological, hydrological, and agrometeorological applications have a growing advantage of the ongoing installation of AWSs. The digital evaluation of different meteorological elements needed for the different applications in climatology was never as easy as with the outputs of autostations. The initial motivation for the use of AWSs in climatology or agrometeorology was to get more evaluated meteorological information and especially data in hourly frequency. The motivation for a move to automated observations in climatology is primarily financial, because evaluation of analogous registration is expensive. In the past climatologists have estimated daily mean temperature from a range of methods (e.g. averaging maximum and minimum temperatures or averaging all three-hourly temperatures for a day) and nowadays an autostation can provide exact values in a very easy and cheap way. (2)

But the new generation of weather stations cause many changes in sensor design, in observation techniques, in the interrogation time and data processing algorithms and this will inevitably introduce inhomogeneities into the climatic record of sites with a long history of conventional observations. Data measured on the same place and with the same environmental conditions but by different systems usually show slight discrepancies. Due to one of the most important questions of today "Changing Climate?" there should be brought special emphasis on the homogeneity of the meteorological data series. Different guidelines

and standards for archiving data of AWS are used on national levels and in some of the results of time series one can see quite clearly the influence of the changes of measuring and averaging techniques. (3)

Climatic records, at least those which are readily available, are normally mixtures of both apparent and real variations. Factors causing long-term climatic changes which may be influenced by changing the system from a conventional to an automated are the following:

- Changes in observing times
- Changes in averaging methods
- Stations relocation
- Change in design (e.g. screen, aspiration)
- Changes in location height
- Changes in calibration method

The deviations can be divided into systematic and stochastic ones. If the systematic differences are not corrected, inhomogeneities in the climatological series are the consequence. Intercomparisons of different systems over a long period of time(e.g. one or two years) on some representative locations covering different weather conditions are necessary to test the compatibility and to find out correction algorithms.

Several statistical methods are available, which can show whether any bias is included in the data records. Some methods provide also an indication of its location, but the causes cannot be revealed by any statistical methods.

Therefore nearly all the NMHSs which introduced Automated Surface Weather Observing Systems undertake increased efforts to test and evaluate new algorithms for auto-stations which ensure a kind of Climate Data Continuity.

Climatologists should have more than a passive interest in the future development of AWSs. As well as making clear what "historical" observations are required to maintain continuity and homogeneity of the climate record, climatologists should look for opportunities for obtaining more relevant data to their needs. Finally, although it is acknowledged that the needs of climate are generally more stringent than the demands of other stakeholder groups, they are also generally less complex given that the priority surface climate data needs have changed little over the century. Following the ten principles for long-term climate monitoring will undoubtedly have benefits for the broader organization in the long-run. (1, 2)

The AWSs must be developed in close connection with all users of the meteorological community (forecast meteorologists, climatologists, agrometeorologists, environmental meteorologists).

To reach these aims it is clear that responsibility for providing and using data has to be shared between the data collector and the data user.

Recommendations for the data collector:

We must distinguish if an AWS replaces a standard ordinary staffed meteorological station or if it is installed on a new site. But in any case there is a strong demand for

- The total system of the AWS, its accuracy and resolution should be in accordance with WMO requirements

- There must be established standard procedures for collecting overlapping measurements for all significant changes made in instrumentation and observing practices.
- There must exist detailed documentations of the construction of the data set from the measurements.
- The list of variables for AWS measurements has to be continually reviewed and updated based on the developments in new technology and new software .
- The configuration of the AWS must be in this way that the accuracy of the output data set must be nearly identical to the accuracy to the output of an ordinary staffed meteorological station.
- If the sensor performance of the AWS' allows only a less accuracy the ordinary measurement should still be carried out as long as possible.
- Influences on the climate record of changes in ordinary staffed stations to AWS must be known prior to implementing such changes.
- Comparison observations and measurements should be carried out and there should be no compromising of the homogeneity of time series.
- AWS should be fully tested in the field for a carefully selected number of stations. This should span at least one year with comparison data collected for two stations, and possibly even longer for climate parameters with high interannual variability.
- Document all the procedures and comparisons in a technical or research report.

Recommendations for the data user:

The users of meteorological data have to look after the metadata , because only the knowledge about the description of the instruments, the calibration methods, the observation reporting practices, the sites and the changes of sites and the data archiving policy can give full information about their continuity and homogeneity. If a site was changed from an ordinary staffed meteorological station to an AWS the user should look after:

- The documentation of the construction of the data sets.
- The documentation of the comparison of the observations and measurements.
- Implement continuity and homogeneity tests on the data series.
- Work close together and have feedback with instrument engineers, station network operators and climate data managers.

CONCLUSIONS

In view of the proliferation of automatic weather stations (AWSs),there must be given adequate attention to the archiving and future use of such data for climate change detection and climate variability studies on global and regional scales.

The measurements produced by automated surface stations necessitate a change of climate data. In the period 1961-1990 these inhomogeneities might have played still no large role. For the Standard Normals of the next period 1991 - 2020 the majority of climate data will be produced by AWS and therefore the homogeneity of the time series has to be carefully handled. There is needed a concerted effort to address the climate observation/data problems and opportunities associated with the planning, implementation and operation of these networks. Following the successful example of the joint CBS/CCl/GCOS efforts to establish the GCOS Surface Network, a similar joint approach through CCl (Working Group on Climate

Data), CBS (Expert Team on Requirements and Representation of Data from Automatic Weather Stations), CIMO (Working Group on Surface Observations) and GCOS (Atmosphere Observation Panel on Climate) should be started.

The next generation of automatic meteorological measurements will not introduce a critical change to climate if the following ten rules are esteemed:

1. In cases where an AWS replaces a manual observing system that has been in operation for a long time, a sufficient overlap in observation systems to facilitate maintaining the homogeneity of the historical record must be assured:
2. Maintain accurate metadata for AWS installations:
3. Maintain the homogeneity of climate data sets that include AWS data;
4. Standardize procedures for quality assurance and processing of data from AWSs;
5. Define more precisely the existing and future requirements of users of climate data and give them consideration in developing statements of requirement for observations to be done automatically by AWSs;
6. Train climate users in the most effective use of AWS data and engage them in future AWS developments;
7. As users of data from AWSs, climatologists are urged to be more proactive in future AWS developments, including incorporation of AWSs into composite observing systems;
8. Develop specifications for a standardized climate AWS, which would record a basic set of climate parameters such as temperature, precipitation, pressure and wind. Particular attention should be paid to ensure extreme values are accurately and consistently recorded in a way that can be accurately related to older, manually-observed, data;
9. Automated and standardized water vapour measurements should be included in AWS parameters due to the significance of this parameter in climate change studies;
10. There should be close collaboration with the CCl, CIMO and GCOS in the development of climate specifications for AWSs;

REFERENCES

1. Karl T. R., Derr, V. E., Easterling, D. R., Folland, C. K., Hofmann, D. J., Levitus, S., Nicholls, N., Parker, D. E. and Withee, G.W.1995: Critical issues for long-term climate monitoring. Climate Change, 31.185-221
2. Plummer, N., Collins, D., Trewin, B. and Della-Marta, P. 1999: Automatic weather Stations in Australia – A Climate Perspective. Proceedings of the ICEAWS99, in Vienna, 27-29 September 99, Austria
3. Rudel, E.1997: Report and review about data processing and quality control procedures involved in the conversion of manually operated stations to automatically operated stations. World Climate Programme: Data and Monitoring No.31, WMO-TD No.833

RADOME NETWORK

P.Grégoire
Météo-France, Direction des Systèmes d'Observation, BP202 78195 Trappes, France
Pierre.gregoire@meteo.fr

The old network of Météo-France

Few years ago, the surface observation network of Météo-France was composed of different networks :

- The national synoptic network (RSBR and RSNC) with Météo-France staff.
- Regional networks of Automatic Weather Stations (AWS) by the 7 Regional centres of Météo-France, with the particularity that few stations belong to Météo-France, the networks being paid by regional authorities.
- The " climatologic " network.

Météo-France has developed forecast and climatological products based on the synoptic and regional networks. The perenity and quality of the regional networks being not controlled by Météo-France, the situation had to be clarified. Recently Météo-France decided to gather them in a new network.

The new surface observation network of Météo-France : RADOME

Radome is the new surface observation network that is created, fully supported and managed by Météo-France. Today this network is composed of (mother country and overseas) :

43 + 34 (mother country) (overseas) stations RSBR,
118 + 8 stations RSNC,
364 + 25 automatic weather stations.

The main goals of this network is forecast and climatology

A new approach for the observation network

In view of improving the quality and availability of data, a new approach for the whole network was reinforced. Many actions were taken like :

- The choice of the different sites was optimised in order to guarantee the quality of measurements.
- A new generation of AWS was developed with new functionality and different supports of communication. A standardisation of sensor and data processing was achieved.
- A new circulation of data was carried out : it integrates a new quality control of data and the delay of disposal for all customers is guaranteed below 10 minutes.
- Operations of preventive maintenance, supervision in real time of the AWS will allow to improve the data quality control.

The new automatic weather station

This automatic weather station was specially developed for uninhabited sites. Today it measures :

- In the basic version : wind speed and direction, air temperature and humidity, precipitation.
- In the extended version : all the parameters mentioned above plus global radiation and two additional temperatures (soil) defined by the user.
- In the next future, it will also be able to measure pressure, visibility and clouds height.

Compared to the old automatic weather stations, it offers new possibilities :

- It stores data in UTC (one, six minutes and one-hour steps) or True Solar Time (one hour) files.
- It supervises instantaneous and mean wind speed, the amount of precipitation and trigger warnings when values overstep the bounds. The user define many kind of related actions : writes the data in a file, sends a message to the network supervisor or modifies the periodicity of message transmissions.
- It gives to the user the possibility to choose which data to transmit and when.
- It creates a new file which contain hours (one second resolution) of each impulse of the rain gage tipping bucket.

- It processes information about the status of the sensors, the acquisition system and the transmission network. They are important indicators that allow managing maintenance actions.

Concerning the technology, the structure of the AWS was modified :

The acquisition system

A CAN field bus (Controller Area Network) is used because it is easy to deploy, to use and very reliable. Each sensor is connected to the bus by an interface, which integrate acquisition and processing resources. This structure improve the quality of measurements :

. The acquisition system is installed closer to the sensor : it's important for very low signals like radiation measurements.
. Each data is checked by different filters implemented in the interface : only reliable values are transmitted to the user.
. Using the measurements and the results of the different filters, the microprocessor can give information related to the different parts of the measuring system.
. Finally, it is easy to test in the field the data acquisition system.

Information are sent on the field bus by using a documented code (named BUFS : quite identical to BUFR). This code is developed by Météo-France but all specifications will be public and published. The main goal is to encourage manufacturers to develop sensors or interfaces using these specifications.

Communications

Several communication supports can be used : the Public Telephone Network, GSM data and Inmarsat mini M. This allows to communicate for all the sites in our mother country and overseas.
The communication protocol, also developed by Météo-France, allows communications with bi-directional but not necessary interactive supports (like Inmarsat C). This protocol is public.

The AWS can be powered by :
- Solar panels
- By main power. In this case one power module supplies heating energy for the wind sensors and the rain gauge and for ventilating the glass of the pyranometer.

Actually, an experimental network of 25 stations of this new AWS, with different acquisition configurations, power supply and communication modems are under test at the main quarters of the Observation Service (DSO) in Trappes. In the next future about 200 stations will be installed.

The concentrator

It carries out the following actions :
- It programs the working of the AWS by the means of different profiles :

The station profile contents the area code, the geographic information, etc. of AWS.
The acquisition profile indicates the different sensors used with their acquisition parameters.
The exploitation profile gives the kind of data and the hours of periodic transmissions.
The warning profile allows to define the alert thresholds for the different parameters and the corresponding actions.
All this profiles are stored in a database.
- It supervises all the dialogs between the AWS and the modem pool. Row data are stored and different processes analyse data in order to extract quality information.
- It distributes coded data (using BUFR code) :
  - To different services of Météo-France by means of satellite broadcast. The delay of disposal is about 10 minutes after the measurements.
  - To other users by modems (FTP protocol)
- It supervises the network. Configurations and daily quality controls of AWS are available to the Météo-France staff by the mean of the Intramet network. All person using a navigator can access the information.
- It displays the results of the different messages sent by the AWS.

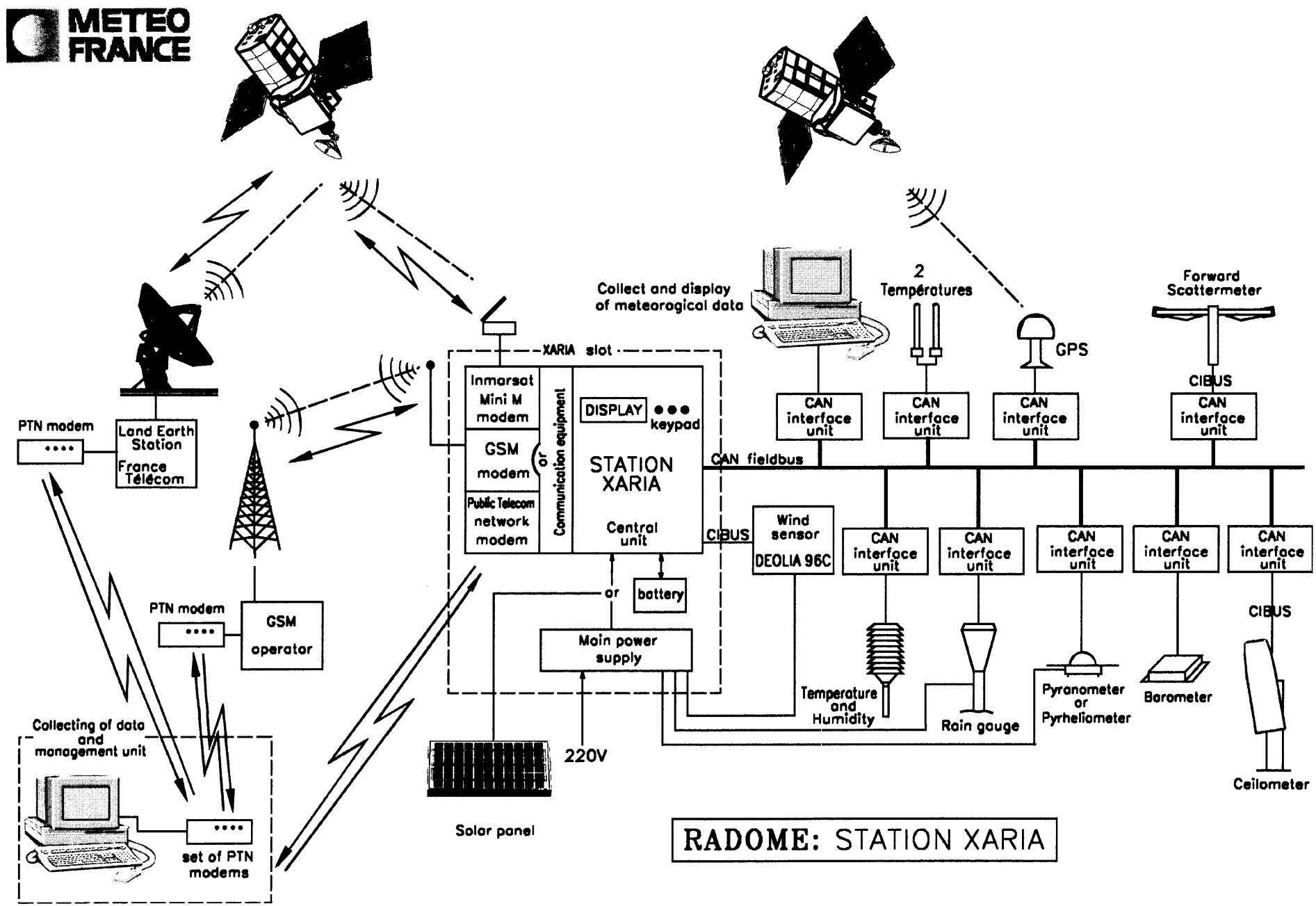

RADOME: STATION XARIA

METEO FRANCE

OVERVIEW OF DATA COLLECTION AND MANAGEMENT OF THE RADOME NETWORK

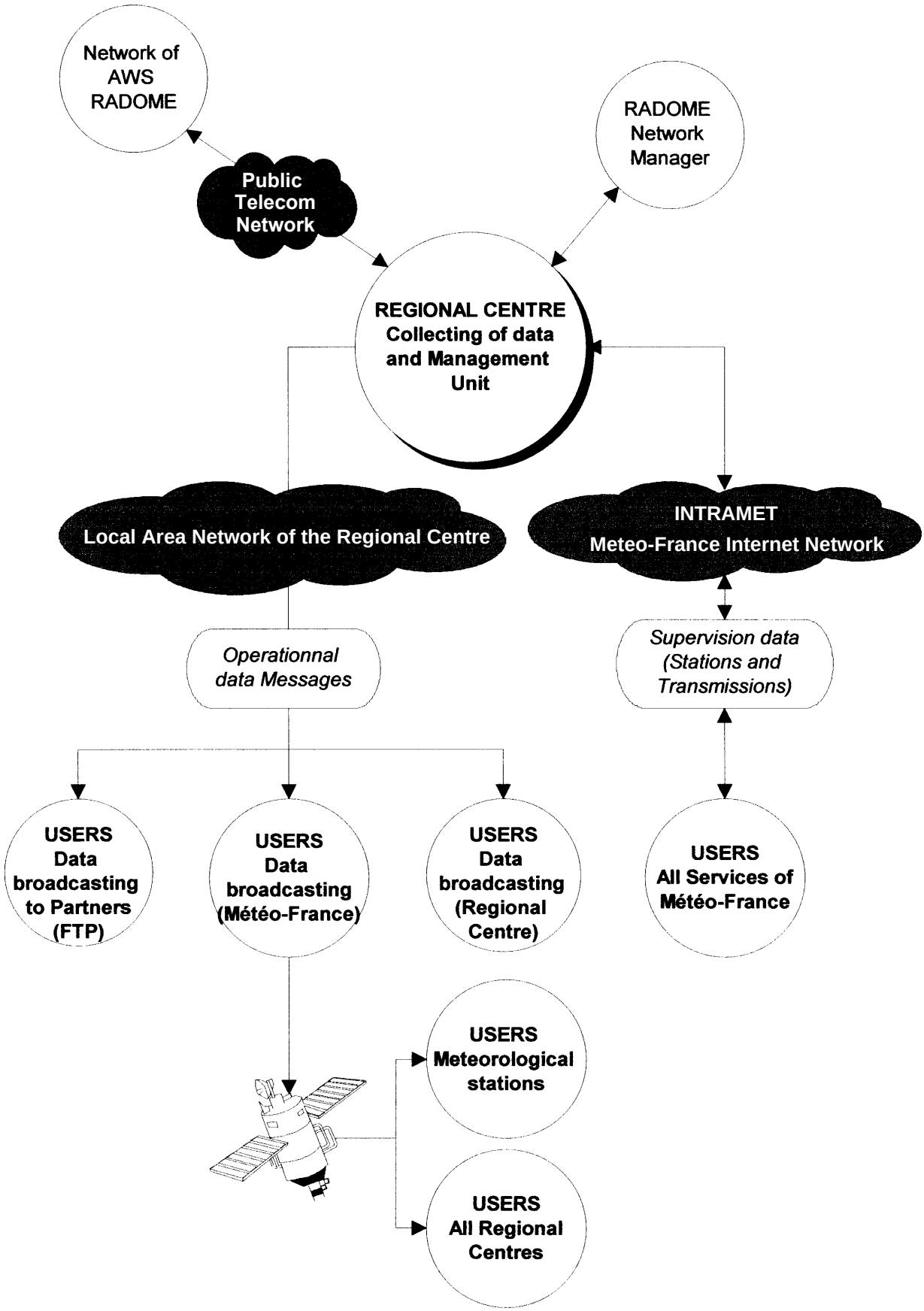

Automatic Weather System in Korea Meteorological Administration

Chun-Woo Lee, Chee-Young Choi, Jong-Seo Park
Korea Meteorological Administration
460-18 Shindaebang-dong, Dongjak-gu, Seoul, Republic of Korea
Tel. 82-2-841-5106, Fax. 82-2-836-6753
cwlee@kma.go.kr

1. Introduction

Two kinds of Automated Weather System (AWS) had been installed in Korea. The one is Local Weather Monitoring System which is a network of densely distributed unmanned automated weather stations. The purpose of the system is early detection of severe weather phenomena such as heavy rainfall and local storms.

The other is the Automated Surface Observation System (ASOS) which had been installed at manned stations to reduce routine work of staffs.

The implementation project of the Local Weather Monitoring System was started from 1990 and completed in 1996. And the ASOS system was started from 1995 and completed in 1999. At present times both of them are successfully operated.

2. Local Weather Monitoring System

1) History

At the beginning 15 AWS was installed in 1988 for the purpose of weather support for the Seoul Olympic Game. After that KMA made a plan to implemente dense AWS network national widely for nowcasting, and then the first 80 AWS was installed in 1990. From the time KMA has increased the number of AWS year by year. Finally, the network came to have 400 AWSs in 1994.

In the first phase, the data transmission was made using dial-up technology. Normally, AWS data was acquired hourly, but when severe weather expected, forecasters could call data more frequently, i.e. every 10 minutes for a limited area under examination.

There are something inadequate in the dial-up calling system for nowcasting, especially when severe weather is appeared, collection rate is notably decreased. So, in 1996 KMA changed the method of data acquisition from dial up calling to continuous connected leased line.

In last year KMA added 20 AWS for the area of islands and mountains. The present total number of AWS is 420, which provides average spacing of 15~20 km interval.

2) Sensors

The AWS is composed of sensors, datalogger. power supply, LED display and tower. The sensors are wind direction, wind speed, air temperature, precipitation amounts, and precipitation detection. Vane type sensor is used to measure wind. Wind direction and wind speed are convert

into 8bit gray code signal by a photo-encoder and optical pulses through a slit, respectively.

A 4-wire platinum resistance probe(pt-100) is used to measure air temperature. To reduce the time constant, thin metal tube is used to protect platinum sensor and the tube is housed in a shelter ventilated at 5 m/s.

Precipitation Amount is measured in the unit of 0.5mm with a tipping bucket type rain gauge with a collection funnel 200mm in diameter. Presence of a precipitation phenomenon is determined by a droplet detector that detects resistance changes caused by rain drops.

The software of data logger is designed to do the function of sampling, signal conditioning, averaging, accumulating, data generating, data transmission and status checking.

3) Local Acquisition Unit

In order to collect AWS data, KMA introduced the Local Acquisition Unit(LAU) at 68 meteorological offices nation-widely. The LAU receives data from neighboring AWSs (average 6, actually 1 to 30) every 1 minute. The data are transmitted to a main computer system for data processing and presentation.

LAU consists of Main Processing Module(MPM) for data quality control and time synchronizing, Memory Module for buffering the data, Communication Processing Module(CPM), Remote Control Processing Module(RCM), Key Pad and multi communication modem ports. The multi communication modem ports can be extended up to 64 ports. Weather information and sensor status data from each of the sensors is collected by LAU and transmitted to the main computer system.

The data communication mode between AWS and LAU is free run and the speed is 2400 bps on a dedicated line. And from LAU to the main computer, TCP/IP protocol is used through communication trunk line. The telecommunication trunk line is T1 (1.544 Mbps) and E1 (2.048 Mbps) grade high speed lines which can cover all communication needs in KMA, such as data, fax, picture/ voice for remote conference, telephone.

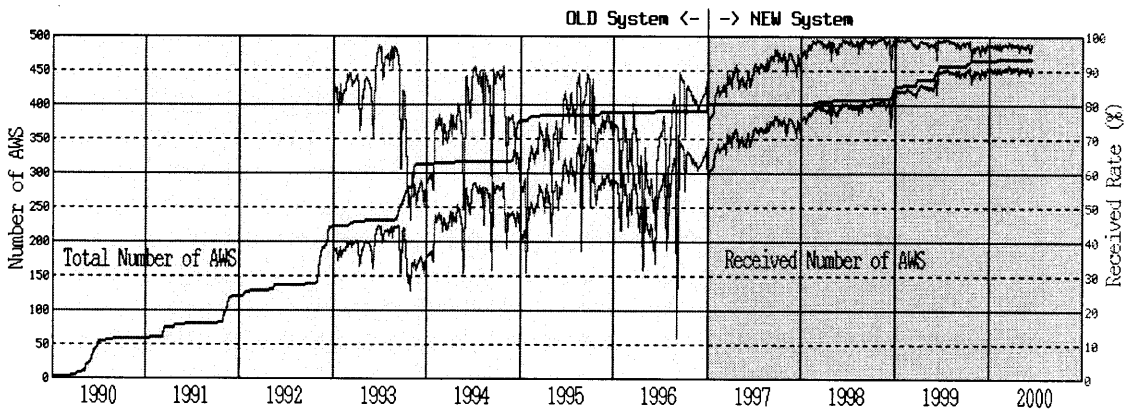

Fig. 1 Time series of collection rate. As time goes by, collection rate is increased.

Data collection rate is automatically checked in real time basis. Average of daily collection rate is recorded more than 96%. The figure 1 shows collection rate changes year by year. After 1997 collection rate is raised significantly. This is caused by replacement public communication line with dedicated line.

4) Application

There are workstations at each meteorological office to display the products of AWS observation. From the workstations, forecasters and observers can obtain not only numeric data but also graphical presentation, such as colored map of; temperature, rainfall and wind vector.

for selectable interval, with zooming and animation capability.

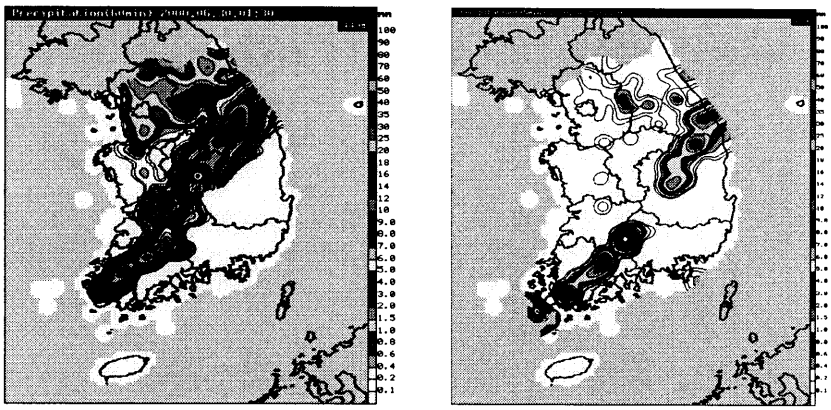

Fig. 2 This is shown 6 hour(left) and 15 hour(right) precipitation distributions in Jun 30 2000.

3. Automated Surface Observation System

1) History

The second phase of AWS implementation project for manned station was started in 1995. The new ASOS was installed at 8 sites in test mode. During the test mode, many of examinations including field test of sensors, meteorological message transmitting to host computer had been carried on each sites in real time basis. These system has the sensor such as visibility & present sesor(WIVIS) manufactured by SCTI. Considering the cost effectiveness, the WIVIS sensor was excluded from the ASOS system since 1998. Now 39 new ASOS systems were installed in manned synoptic stations.

2) Sensors

observation elements of ASOS system are air temperature, pressure, precipitation, humidity, wind speed and direction, global radiation, sunshine duration, precipitation detection, grass temperature, surface temperature. All sensors conform to the sixth edition of Guide to Meteorological Instruments and Methods of Observation(WMO-No.8).

Rainfall amount is measured with two tipping bucket type rain guage (0.1mm and 0.5mm) at the same time. Specification is similar to that of Local Weather Monitoring System. RM-Ypong windvane Model 0516 is used for measuring wind speed and direction, and a three cup anemometer is for measuring wind run. Temperature sensor is just equal to that of Local Weather Monitoring System. Humidity sensor is Vaisala instrument Model HMP45D. The accuracy is ±2% in the range from 0.8 % to 100%. Solar radiation sensor is Kipp & Zonen instrument Model CM21 secondary

standard pyranometer. The sensitivity is 7~17μV/Wm^{-2}. Sunshine duration sensor is a EKO, Inc. Model MS-091 sunshine duration meter. When the direct solar radiation is exeeded 0.12 kW/m^2, the sunshine duration is calculated by accumulator. There are some platinum temperature sensors to measure grass minimum temperature and soil surface temperature.

3) Automation for Observational Work of Human Observer

ASOS system consists of two distinct subsystem, an indoor equipment group comprised of the data logging and processing unit with its displays and 2 personal computer, and an outdoor equipment group consisting of sensors and their signal processing unit (Fig. 3). Observing elements are air temperature, pressure, precipitation, humidity, wind speed and direction, global radiation, sunshine duration, precipitation detection, grass minimum temperature, soil surface temperature. The dewpoint temperature and vapor pressure, are obtained by processing the basic values over the required time period.

The following design concept and feature apply to ASOS system;

- ☐ The system automatically make "observation" previously only available from humans.
- ☐ The extreme and averaging value and their observing time made by algorithm and software.
- ☐ Sensor selection has been performed through an analytical approach that took performance, specification compliance, acquisition cost, reliability. and maintainability into account.
- ☐ Software allow the observer to view the measurements on screen in the form of alphanumeric type and simple graph.
- ☐ After the quality control has been done, the PC for observers archives the data into ASOS database and CD-ROM.
- ☐ Automation of routine work such as making daily and monthly summaries is possible.

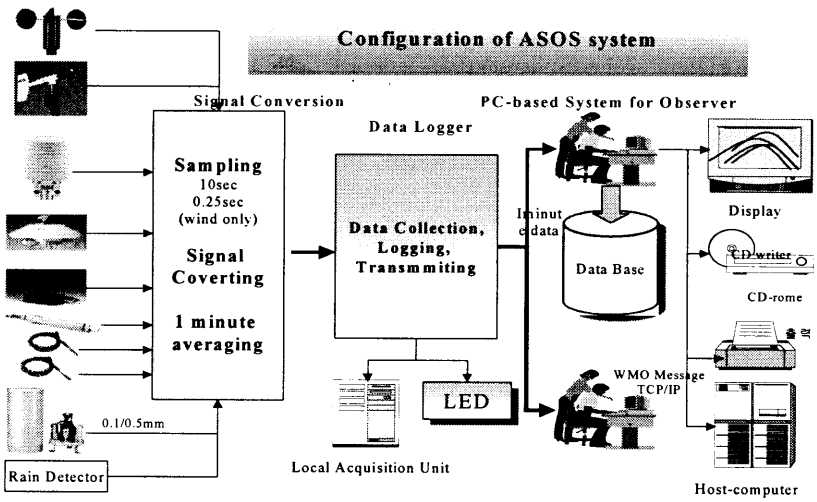

Fig. 3. Configuration of Automated Surface Observation System and it's data flow

The ASOSs are making continuous measurement of atmosphere and reporting the result. Two types of reporting are made. The synoptic reports are made each hour with 10 minutes average

and also current status is presented with 1 minute average. All elements except wind is measured every 10 second. Sampling rate of wind is 0.25 second because wind-gust based on 0.25 second readings. Raw data obtained by ASOS is collected by data logger and transmitted to main processing PC for observer. Main processing PC checks raw data to assure data quality, make WMO message, and composite display of all element for comprehensive understanding the rapidly changing weather (Fig. 4).

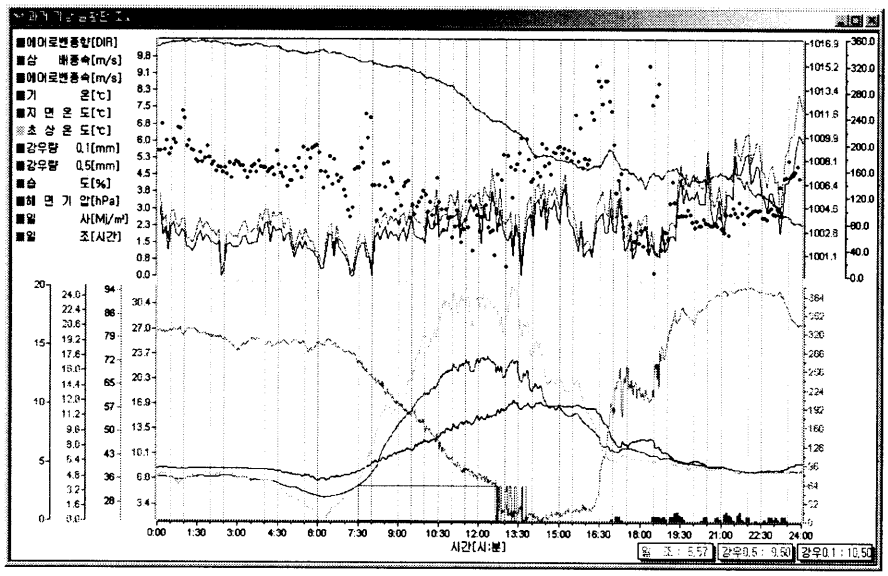

Fig. 4. Composite display of various meteorological valuables such as pressure, temperature, precipitation, and sunshine duration.

4. Conclusion and Future Plan

The AWS network of KMA has been found very useful for nowcasting and severe weather warning. Especially Local Weather Monitoring System information is well utilized in KMA as well as related organization such as National Institute for Disaster Prevention, Ministry of Government Administration and Home Affairs.

The ASOS system are being deployed all manned station, and the system removes most observational burden for observers. Therefore it is able to reduce personnels creating observation, so more trained personnels can be better used to assist the forecast and warning program and provide more effective services to the public. And KMA also has a plan to increase the number of ASOS for automation of small weather offices hiring only a few personnels.

SIMEPAR HYDROMETEOROLOGICAL DATA COLLECTION NETWORK

Luís Tarciso de Moraes
Sistema Meteorológico do Paraná – SIMEPAR, Brasil
Parana State Meteorological System
Caixa Postal 19100 - CEP 81531-990, CURITIBA - PR, Brazil
Tel: (+55 41) 366 2020 Fax: (+55 41) 366 2122 E-mail: luis@simepar.br

1. Introduction

The Paraná State Meteorological System – SIMEPAR, established in 1994 to supply the increasing demands for meteorological and hydrological information, has defined its sub-systems after an extensive research involving potential users and is now operating a Doppler S-band Radar, a Lightning Location and Detection System, a Satellite Imagery and a Hydrometeorological Data Collection Network.

Designed and implemented aiming to explore the benefits that a reliable meteorological and hydrological data collection and information system can bring, the SIMEPAR Hydrometeorological Data Collection Network has completed three operational years achieving and exceeding the expected results specially considering those related to end users new applications, interaction and feedback.

The paper describes the gathered experience while operating and maintaining the network, associated with the calibration lab implementation, data quality control and software development conducted mainly to improve the system reliability. The network was planned to reach 170 stations, being composed now of 35 met and 34 hydro stations transmitting through the GOES satellite to a Central Station consisting of a Satellite Receiver, an Oracle Database and associated in house developed UNIX based ingestion, visualization and supervision software.

2. Strategy

By submitting the system pre-specs for the potential users and suppliers and promoting an open discussion the final specification incorporated the constructive criticisms and suggestions from both sides.

Previous reports of some isolated and non-successful telemetry attempts, specially in hydrology, and the necessity of monitoring remote areas where telephone and radio communication were considered technically unfeasible and/or very expensive along with satellite telemetry features and possibilities played an important role while choosing which telemetry would be most suitable for the network. Availability and performance versus maintenance costs experience has proved satellite to be the best choice so far.

The network density will gradually increase starting with an average distance of 75 km between stations up to 40 km upon system completion. After an international competition Sutron Co. has integrated and supplied the complete system, providing also the factory and on-site training considered very important to enable SIMEPAR staff to conduct installation, operation and maintenance.

Because self-support was considered strategic, opposed to the idea of externally contract the network operation and maintenance, SIMEPAR has decided to develop technician skills and take full control over the system and the plans started with a extensive training

program and implementation of a repair facility, going up to electronic board repair and component replacement.

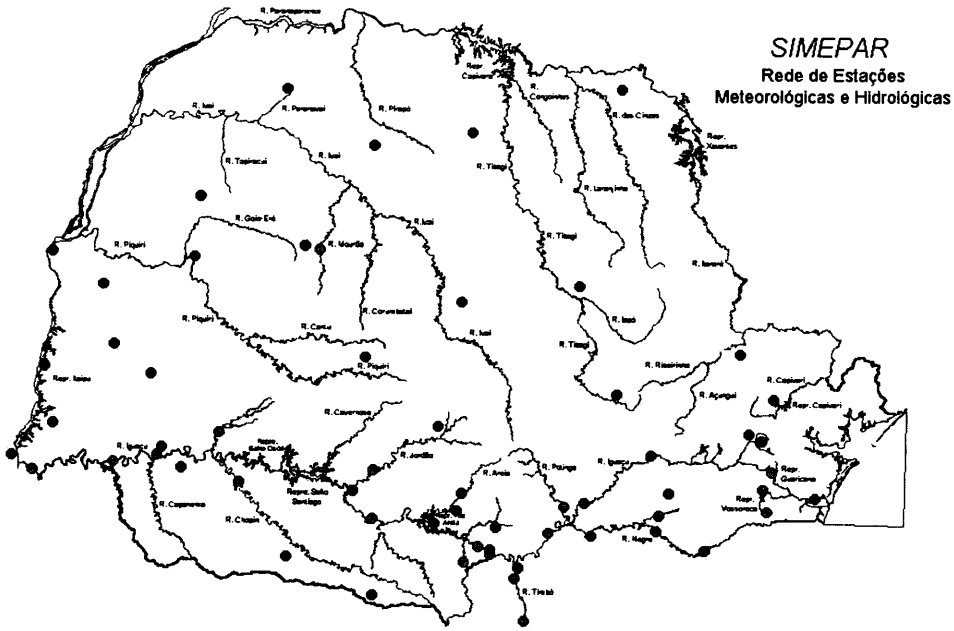

Fig 1. SIMEPAR Hydrometeorological Data Collection Network

3. Installation, Operation and Maintenance

For the initial installation phase the chosen sites were, in the majority, located in the same area of existing conventional stations allowing regular data comparison used for preliminary sensor validation. Data discrepancies were monitored and evaluated to find out if related to measurement techniques or exposure.

The meteorological stations incorporate sensors of air temperature, relative humidity, atmospheric pressure, wind speed and direction, solar radiation and rainfall while the hydrological water level and rainfall. The data collection modules process and log hourly values including average, maximum, minimum and accumulation, preparing the messages for transmissions that occurs every three hours, the hydrological stations have also the alarm transmission capability trigged when a predefined sensor value is exceeded.

For preventing data losses, a total of 128 Kbytes of memory is present in each station and discards oldest values when full, assuring at least 6 months of data storage. Data is downloaded systematically in every maintenance visit through faster PCMCIA card or notebook, serving for a database consistency program while reaching the Central Station.

Preventive maintenance aim to carry out a periodic revision on the station equipment, consisting basically of a check-list revision guidance items to be verified and activities conducted by the responsible technician that includes site conditions overview, equipment and sensors outlook, time expired consumables replacement and sensor values comparison against portable test field equipment. Preventive maintenance are generally carried out every 6 months, although learning from the experience, some sites were

selected according to the local conditions to be visited in a shorter interval that can be as frequent as 3 months.

Corrective Maintenance is executed based on the transmission failures or data incoherence and are normally alerted by the quality control and system supervision program that are fully integrated to the database. Some system follow-up parameters are also transmitted being quite useful in defining the need for site travels like battery voltage and charging status.

4. Central Station

Based on the operational characteristics of the network and special requisites of funcionalities and robustness not available commercially, SIMEPAR conducted a research program and implemented a UNIX based software responsible for the data ingestion, decoding, processing and the interactions among the database, visualization and supervision modules.

Central Station Data Ingestion and Storage is a group of programs designed to complement each other and perform the tasks of receive, process and insert data from the telemetric station. The programs normally work in a sequence but they can be used apart allowing complete control of each task whenever it is necessary.

Data Ingestion is the front-end acquisition program responsible for collecting data entering from the different sources and is flexible enough to collect data from satellite, Internet, leased or public telephone lines coming on fixed schedules or randomly, one of its basic functions will be prepare the message for decoding, identifying the station code, the message type and data included.

Station setups are defined according to principal types and stored as templates that can be used while adding new stations with the same sensors and procedures or work saving in case of editing existing stations are necessary. Station set-up stored in CS should match the existing at the stations, confrontation is made through the Supervision Console

To compose the CS database Oracle8i was used not only because of the large proved worldwide acceptance being the mostly used Client/Server and Web development architecture but also due to important features other than robustness like:

- Relational and object oriented
- On-line back-up and recovery
- Multimedia (text, sound, video and image) Support
- Binary objects and binary indexes

Database have the main function of storing incoming meteorological and hydrological data originated from the telemetric stations and events generated but is not restricted to any type of data, as a matter of fact Database can accept data from a wide variety of sources, customize and process specific data groups delivering for the visualization subsystem or network distribution.

The database structure is composed of tables assigned and sized to the different data, tables may be assigned according to pre-defined parameters for entering data. Data ingestion in the database can be fully controlled also and defined by parameters value

limits, type and source allowing the manager to specify exactly which type of data can be discarded.

Retrieving data can be done either by customized displays behind virtual tables where regular data and events are stored and presented according to the user definition or through SQL commands that provides easy and fast access to the full content of the database considering events, parameters and data.

5. Supervision and Visualization

Subsystem responsible for the data presentation and all user-friendly interaction, alarms, reports and events generated. Totally based on graphical interfaces with network/database events error handling attributes implemented, allow interactive use to emit commands and parameters configuration. Data presentation program access all information stored in the database and can display simultaneously all data and events from a given station, make graphs, plots and includes statistical computation such as max/min, average and standard deviation.

By implementing a Data Quality Control Program that checks every single data acquired giving flags according to climatological limits, rate of change, persistency or neighbourhood regions, it was possible to monitor and knowledge the database reliability. Quality control requires continuos follow-up and fine-tuning adjustments are made every time suspicious or non-valid flag is considered valid.

6. Calibration Laboratory

Complementing the system and aiming to assure data quality, a Calibration Lab was also implemented as part of a cooperation program with INMET (Instituto Nacional de Meteorologia), consisting of a complete infrastructure capable of evaluate, compare and calibrate meteorological and hydrological sensors like temperature, relative humidity, atmospheric pressure, water level and rain gauges.

Automation was the key word for the Calibration Lab design, in such a way that a signal condition module coupled with data acquisition software allows simultaneous calibration of up to 15 sensors with report generation. Sensors are returned, repaired and calibrated based on the certificate expiration or drifts.

Reference:

WMO Nº8 Guide to Meteorological Instruments and Methods of Observation

****

L'AUTOMATISATION DE L'OBSERVATION METEOROLOGIQUE DU MAROC

Brahim LOUAKED
Direction de la Météorologie Nationale Marocaine
Aéroport-Anfa Casablanca Maroc
Tél 212 2 91111 37 FAX 90 85 93 E.mail: louaked @ hot mail.com

INTRODUCTION

Les premières observations automatiques datent de plus de 30 ans. En effet, la première station météorologique automatique a été installée à l'aéroport de CASABLANCA-ANFA en 1964. Cette génération de station très encombrante, consommatrice de courant, fût abondannée après 5 ans d'exploitation car peu fiable et très coûteuse à l'entretien.

La deuxième tentative d'automatisation fut consacrée à la mesure de la visibilité et du plafond nuageux. Quatre stations météorologiques d'aéroports furent équipées de visibilimètres et télémètres de nuages. Après une période d'essai, les résultats furent validités. Les visibilimètres et les télémètres de nuages ont été mis en exploitation mais comme équipements d'appoint, la référence reste cependant l'observation humaine.

PRESENTATION DU RESEAU NATIONAL D'OBSERVATION DE BASE

Quatre régions météorologiques pilotes exploitent actuellement le réseau national d'observation de base, voir tableau récapitulatif.

Ce réseau constitué de quarante cinq stations synoptiques de surface, 700 stations climatologiques et 558 postes pluviométriques, est appelé à se développer pour pouvoir satisfaire les besoins exprimés par les divers secteurs socio-économiques sensibles à l'assistance météorologique.

TABLEAU RECAPITULATIF DU RESEAU D'OBSERVATION

Régions Météorologiques	Stations Synoptiques	Stations Climatologiques	Postes Pluviométriques
NORD	8 dont 2 automatiques	120 dont 8 automatiques	88
NORD-EST	11	214 dont 5 automatiques	180
CENTRE	14 dont 2 automatiques	277 dont 8 automatiques	213
SUD	12 dont 1 automatique	95 dont 7 automatiques	77

A- RESEAU DE STATIONS CLIMATOLOGIQUES AUTOMATIQUES (SCA)

Le réseau de SCA couvre une partie non négligeable du ROYAUME, mais la maille reste assez large.

Pour avoir une représentativité globale de la climatologie du pays, la stratégie adoptée consiste à équiper l'ensemble du territoire ne serait-ce que par quatre ou cinq points de mesures automatiques par région.

Les données des paramètres pression, humidité, température, précipitation, rayonnement, vent, collectées par les SCA sont exploitées in-situ et acheminées automatiquement via une liaison commutée vers un calculateur concentrateur installé à CASABLANCA.

B- STATIONS METEOROLOGIQUES AUTOMATIQUES D'AEROPORT (SMAA) (fig. 1 et 2)

Les principaux aéroports du Royaume du Maroc sont équipés de SMAA ou sont sur le point de l'être.

Les SMAA équipant ces principaux aéroports, sont architecturées autour d'une unité d'acquisition intégrant un microprocesseur faible consommation et se composent de :

- un calculateur d'observation central installé à la tour d'observation météorologique,
- des postes de visualisation installés à la salle de prévisions et à la tour de contrôle,
- d'enregistreurs et d'indicateurs installés à la salle d'observation et tour de contrôle,
- une unité de prétraitement installée près de la piste,
- de différents capteurs installés près du seuil de piste.

B-1.- Le calculateur central d'observation gère un environnement comprenant :

- Un réseau de collecte de données
- Un réseau de distribution de données sous forme numérique vers les postes de visualisation
- Un réseau de télécommunications, liaison RTC/LS
- Une ou deux imprimantes pour l'édition des documents papier

B.2.- Le logiciel assure les fonctions suivantes :

- Acquisition des données, visualisation de l'image site rafraîchie par les données minute et 6 minutes
- Supervision des données capteur
- Aide à la saisie du tour d'horizon
- Codage des messages METAR, SYNOP, SPECI, CLIMAT avec détection des conditions de codage SPECI
- Transmissions des messages
- Configuration des capteurs raccordés à la SMAA avec possibilité de sélection/substitution.

B.3.- Postes de visualisation :

La visualisation des données collectées par les SMAA est réalisée à partir d'ordinateurs classiques (PC)

Les PC sont installés à la salle de prévisions et à la tour de contrôle. Les utilisateurs ont ainsi à leur disposition plusieurs pages. La page principale renseigne les données:

- QNH, QFE et tendance.
- La direction et force du vent
- La température de l'air et du point de rosée
- La hauteur de la base des nuages
- La portée visuelle de piste

Les autres pages sont réservées à la supervision, la configuration des capteurs et au paramétrage.

B.4.- Enregistreurs indicateurs

Les enregistreurs indicateurs reçoivent les données via la voie secours et visualisent les paramètres représentatifs du vecteur vent.

C- CARACTERISTIQUES TECHNIQUES DES SMAA

C.1.- Calculateurs : Pour s'assurer un fonctionnement permanent, la DMN a organisé les SMAA autour d'une configuration de calculateurs normal/secours destinés à gérer les différents capteurs du système.

Les calculateurs sont structurés autour d'un processeur central du type Pentium III 500 MHz, fonctionnant sous environnement WINDOWS NT, disque dur de 8,4 Go ext, lecteur de disquettes 3" ½, CD ROM 48X, Carte réseau 10/100 Mbs.

C.2.- Postes de visualisation : Les postes de visualisation sont des ordinateurs de bureau ayant les mêmes performances que celles des calculateurs d'observation.

Chaque ordinateur est équipé d'un modem multipoints avec sa connectique, ainsi qu'une carte multifonction avec microprocesseur 32 bits assurant un fonctionnement en mode automate programmé avec REPROM pour programme et système d'exploitation.

C.3.- Capteurs : Les capteurs mis en œuvre sont les suivants: capteur pression, capteur température de l'air , capteur température point de rosée, capteur humidité relative, capteur anémomètrique, capteur girouette, capteur pluviométrique, capteur pour la mesure du rayonnement global, un télémètre de nuage et un transmissomètre .

C.4.- Voies secours : Les données des capteurs anémomètre et girouette sont acheminées vers la station pour diffusion et archivage sur une voie de secours indépendante vers les indicateurs de tableau. Cette solution permet ainsi une disponibilité en cas de problème sur la voie automatique.

C.5.- Paramètres de sorties : En conformité avec les recommandations de l'OMM, les paramètres de sorties délivrés par la SMAA sont les données aéronautiques , synoptiques et climatologiques .

C.6.- Observations manuelles : Données représentatives de la visibilité, des nuages, du temps présent et passé, des séquences pluvieuses, de l'état du sol, de l'évaporation, des phénomènes spéciaux et des phénomènes aéronautiques.

D.- ALARMES

Le système est muni d'un dispositif de vérification permanent de l'ensemble des capteurs aboutissant directement à l'unité centrale. Ce système a pour rôle essentiel de déclencher une alarme sonore et/ou visuelle lorsqu'une aggravation d'une ou plusieurs conditions météorologiques se produit et notamment :

a) lorsqu'il y a une variation du vent
b) Lorsque la visibilité atteint des seuils prédéterminés.
c) lorsque la base des nuages atteint une hauteur critique prédéterminée.
d) lorsque les précipitations sont accompagnées de neige, de grêle, pluie mêlées et/ou orage.

Une donnée est déclarée en alerte lorsque sa valeur dépasse un seuil fixé par l'opérateur.

E.- INSTALLATION :

Quelque soit le type de station automatique une étude du site d'implantation est réalisée par l'équipe d'installation et maintenance.

Pour les sites devant accueillir les stations climatologiques, l'étude prend en compte la représentative du site, son état et son voisinage immédiat (sécurité), l'accessibilité, la disponibilité du réseau électrique et des moyens de télécommunications.

Pour les SMAA, l'étude se concentre sur les normes de sécurité près des pistes d'envol et les problèmes que pose la cohabitation entre les équipements météorologiques avec ceux de l'aéronautique.

F.- MAINTENANCE

La maintenance des systèmes automatisés est assurée par les techniciens de maintenance de la DMN selon un programme de maintenance préventive.

Ce programme défini les actions de maintenance hebdomadaire, mensuel et trimestriel.

Ainsi les techniciens de maintenance affectés aux régions météorologiques sont chargés de la maintenance préventive et des deux premiers degrés d'intervention en ce qui concerne la maintenance corrective.

La maintenance centrale est responsable du troisième degré et de la remise à neuf des équipements.

Un programme de télémaintenance est en cours d'essai.

Il y a lieu de signaler que pendant les deux premières années qui suivent l'acquisition des équipements, la maintenance préventive et curative (s'il y a lieu) est assurée par le fournisseur assisté par les techniciens de la DMN. Lors des missions de maintenance préventive, le fournisseur procède à une formation complémentaire au profit des techniciens de maintenance.

G.- PERSPECTIVES D'AVENIR

L'action prioritaire du plan 2000-2004 est l'automatisation de la mesure météorologique des réseaux d'observations météorologiques et climatologiques afin de répondre à une demande croissante en données fiables et de haute qualité à l'exécution des tâches opérationnelles et à la réalisation d'applications météorologiques répondant à des préoccupations nationales dans les domaines stratégiques pour le pays à savoir :

- les ressources en eau (optimisation et rationalisation)
- L'agriculture (rendement des cultures, programme de lutte contre la sécheresse)
- Programme de lutte contre la désertification
- Les systèmes d'alerte précoce et de surveillance des phénomènes extrêmes.

Ce plan 2000-2004 vise d'une part à renforcer le réseau d'observation de surface en le dotant de stations météorologiques automatiques en mesure de fournir des données de qualité et d'autre part à mettre l'accent sur une politique de formation du personnel d'exploitation et de maintenance.

H.- CONCLUSION

Les stations automatiques installées dans les aéroports représentent un moyen d'observation moderne qui a été bien apprécié par les contrôleurs aériens, les protectionnistes et les observateurs. Les premiers résultats obtenus sont satisfaisants, le taux de disponibilité de données avoisine les 98%.

L'automatisation de l'observation permet d'obtenir des relevés de données météorologiques de qualité, à intervalles réguliers ne nécessitant plus d'interventions humaines. L'observateur peut alors se consacrer exclusivement à l'analyse des données qui lui sont présentées sur les différents postes de visualisation et l'étude des phénomènes météorologiques.

REFERENCES

- Plan de développement de la DMN (A. DIOURI)
- Système intégré d'observation d'aérodrome SIOMA/AURIA

AUTOMATISATION DE L'OBSERVATION METEOROLOGIQUE
AEROPORT DE TANGER

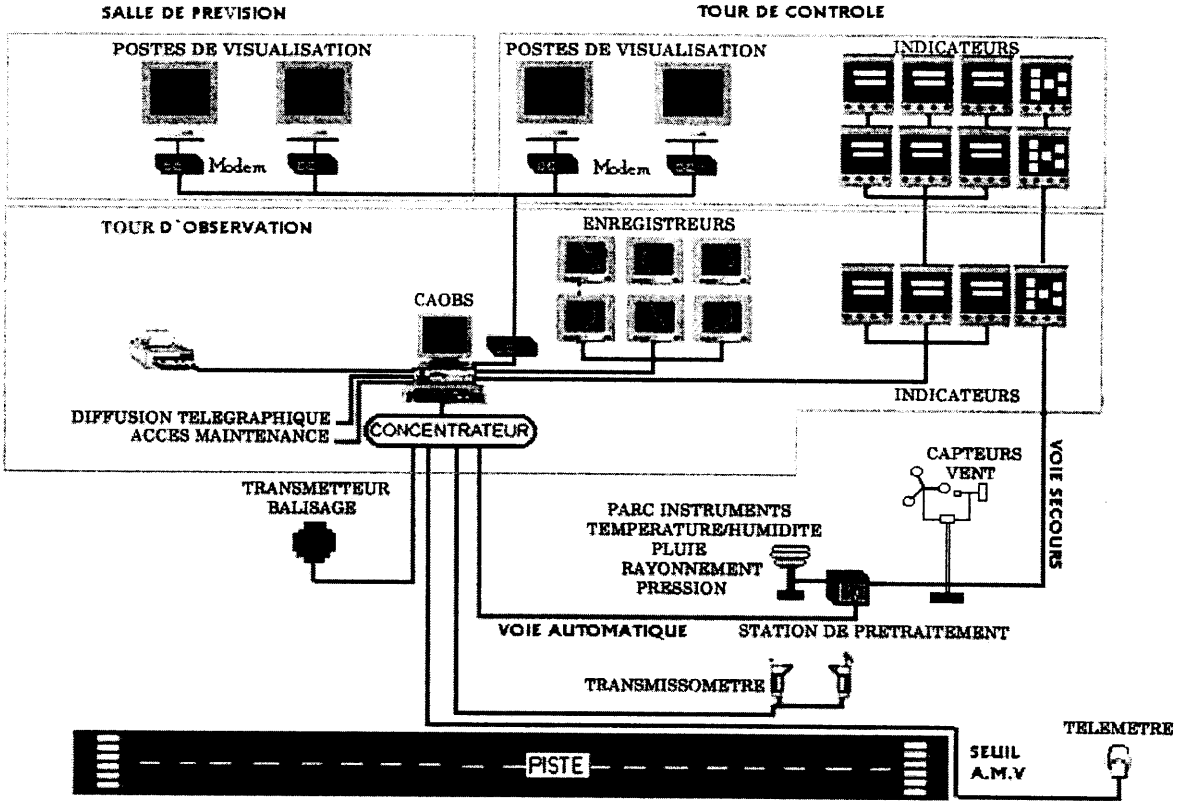

FIG 1

AUTOMATISATION DE L'OBSERVATION METEOROLOGIQUE

SYNOPTIQUE GENERAL DE L'AEROPORT DE TANGER

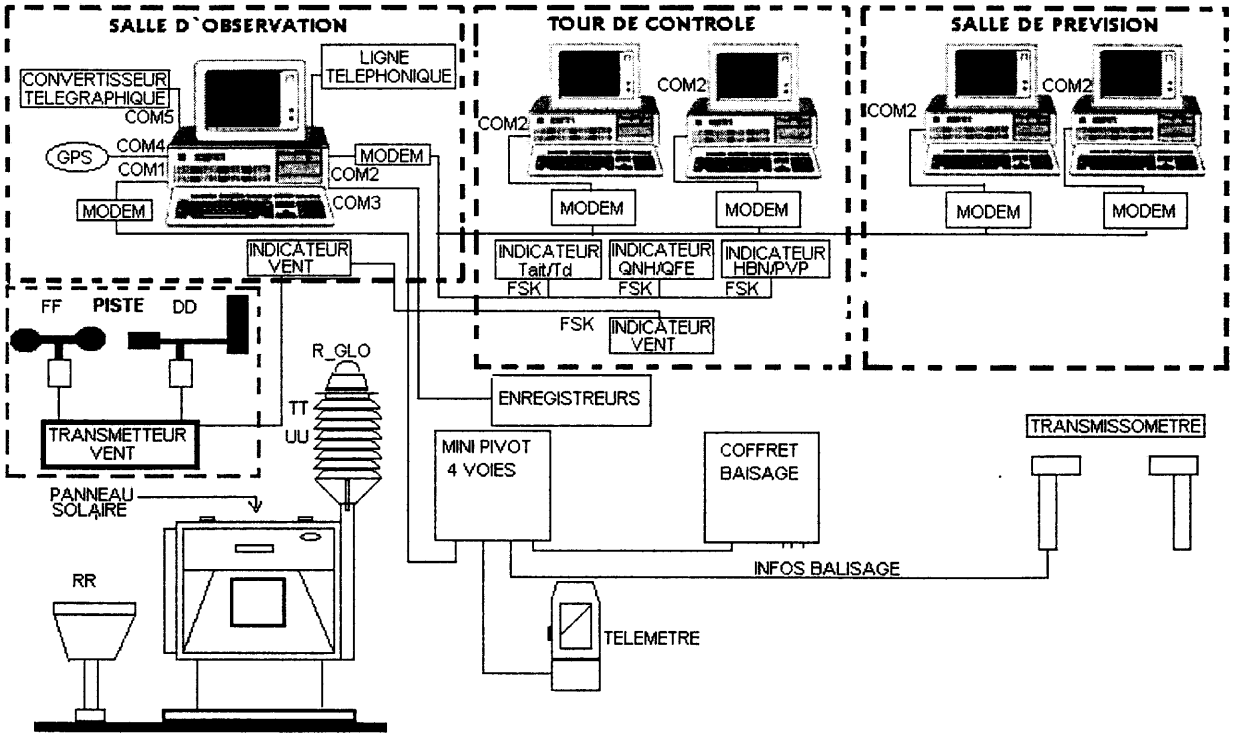

FIG 2

Hong Kong Automatic Weather Station Network in 2000

Y.K. Chan
Hong Kong Observatory
134A, Nathan Road, Kowloon, Hong Kong, China
Tel.: (852) 2926 8343 Fax: (852) 2311 9448
Email: ykchan@mail.gcn.gov.hk

1. Introduction

The Hong Kong Observatory (HKO) started in 1983 the development of a network of automatic weather stations (AWS) to acquire timely surface observations for use in meteorological applications.

Over the years, the HKO has made use of the latest technology to enhance the AWS. At the same time, the coverage of the network has expanded steadily to provide comprehensive meteorological information on regional variations over Hong Kong in real time. The information would help to improve the accuracy of weather forecasts and to ensure the issuance of timely warnings to minimize the loss of life and damage to property due to severe weather.

2. The Hong Kong Automatic Weather Station (AWS) Network

2.1 The Network

The Hong Kong Automatic Weather Station Network consists of groups of field stations linked to their corresponding central stations. At present, a total of 69 field stations are in operation within Hong Kong Special Administrative Region and four over the Pearl River Estuary (established in collaboration with the Guangdong Meteorological Bureau). The locations of the field stations over Hong Kong are shown in Figure 1. The network expanded from the first generation installed in 1984, with one central and three field stations.

The four Pearl River Estuary stations and 27 of the local stations measure wind, air temperature, humidity, pressure and rainfall, while the remaining 42 local ones collect data on either wind or rainfall. Among the latter, two stations measure the wind at different heights in the lower atmosphere by a wind profiler. Among the former, one station (at Waglan, a small island due south to Hong Kong) provides information on the weather conditions and visibility by means of a remote controlled video camera, while the other (at King's Park) measures total global solar radiation. The data from field stations are transmitted in real time to their respective central station via telephone lines or UHF radio links.

The dense AWS network is indispensable in monitoring severe weather systems such as tropical cyclones and rainstorms in the vicinity of Hong Kong. Without these stations, it would have been much more difficult to identify the formation of a tropical cyclone on 18 June 2000 at a close distance of 35 km south-southwest of HKO Headquarters. The tropical cyclone was the first one in 2000 passing over Hong Kong and necessitated the hoisting of warning signal. Throughout its passage, the dense AWS network enables the precise location of its centre and the accurate estimation of its maximum winds.

The two wind profiler stations and a group of anemometer stations around the Hong Kong International Airport and in exposed areas provide the necessary wind data for the Windshear and Turbulence Warning System. The System detects terrain-induced low-level windshear and turbulence for the generation of windshear and turbulence alerts. These warnings are relayed to pilots of approaching and departing aircraft so that they are able to respond appropriately during landings and take-offs by having a better grasp of the weather situation around the Airport.

2.2 System Design

The first AWS network was designed to run on city power with data transmitted from the field stations to the central station via dedicated telephone lines. Without city power on remote sites, the second generation AWS network was designed to have very low power rating, enabling the field station to operate on solar power alone. The solar power supply system installed is capable of charging up batteries for at least 15 day's continuous operation under overcast sky. Records of continuous operation exist for a period of three months under mostly overcast sky. The re-designed circuit also included a radio transmitter for data transmission.

A schematic diagram of the AWS design is shown in Figure 2. The field unit is designed to use low power, high speed CMOS components to minimize power consumption. It consists of a sensor suite, an analog to digital circuit, a CPU, and a serial input/output circuit. Up to 12 sensors can be connected to the data processing unit at each station. The analog output from the sensor is a voltage from 0 to 5 V. The CPU, base on a 80C320 microprocessor, controls the sampling of these analog signals at a rate of 1 sample/channel/second. The analog signals are digitized into 12-bit binary data by an analog to digital converter. The data are then serialized and transmitted with station name and date/time information through a serial input/output circuit to the central station at HKO Headquarters. The serial input/output component consists of four RS-232C serial ports and a single chip modem that can interface with either a telephone line or a UHF transmitter.

The central station consists of a PC and a modem for communication over telephone data lines. With software written in C, the central station polls each field station in turn at least once in a minute to collect real time minute-by-minute data. Every report from the field stations will be

quality checked once received at the central station. The field reports are then re-compiled into a composite report which is sent to the main computer at HKO Headquarters. The composite report is also sent to the Central Forecasting Office at HKO Headquarters for display on a video terminal. On the 00th and 30th minutes of every hour, the data are dumped onto a line printer for temporary archive. When the communication between the field unit and the central station fails such as malfunction of telephone line, the unsent data reports will be stored in the memory of the field unit. These unsent reports are re-transmitted automatically to the central station in the form of backlog data when communications resume normal. The system clock of each field station is synchronized with the central station clock to within one minute every day. This ensures that all time critical elements such as daily maximum/minimum temperatures are correctly registered and the backlog data are written into the correct memory location in the main computer.

2.3 Sustainable development

The world is becoming more and more environmentally conscious. To ensure that the expansion of the AWS network is a sustainable development, the HKO has introduced environmental-friendly power supply for its field stations. To date, ten stations (including the four Pearl Estuary stations) are powered by solar panels. The solar power supply systems are more reliable than city power at some locations, and are thus used even at locations with city power.

The HKO has also turned to wind power as an alternative source of energy. The wind power supply system generates electricity by a turbine with three rotating blades each about one metre long. It is capable of producing sufficient power under moderate winds to meet the needs of the stations. To date, two stations using wind power have been introduced and a few more are being planned on remote islands and hilltops. Apart from being environmental friendly, the wind power supply system only requires minor civil work for its installation. It is reliable as the wind turbine has built-in self-protection mechanism and is designed to withstand high winds. Its low failure rate substantially reduces the number of maintenance visits.

3. Future development

The HKO is planning to develop a new generation of AWS network with the concept of remote diagnosis and limited-scope automatic rectification in mind. The maintenance staff will be able to interrogate with the field stations and conduct remote diagnosis of the system when problems arise. The cause of the failure will then be identified remotely and the efforts spent during the on-site maintenance will thus be minimized. The new generation of AWS network will also have ruggedized design to minimize maintenance with the target of needing only one or two routine maintenance services annually.

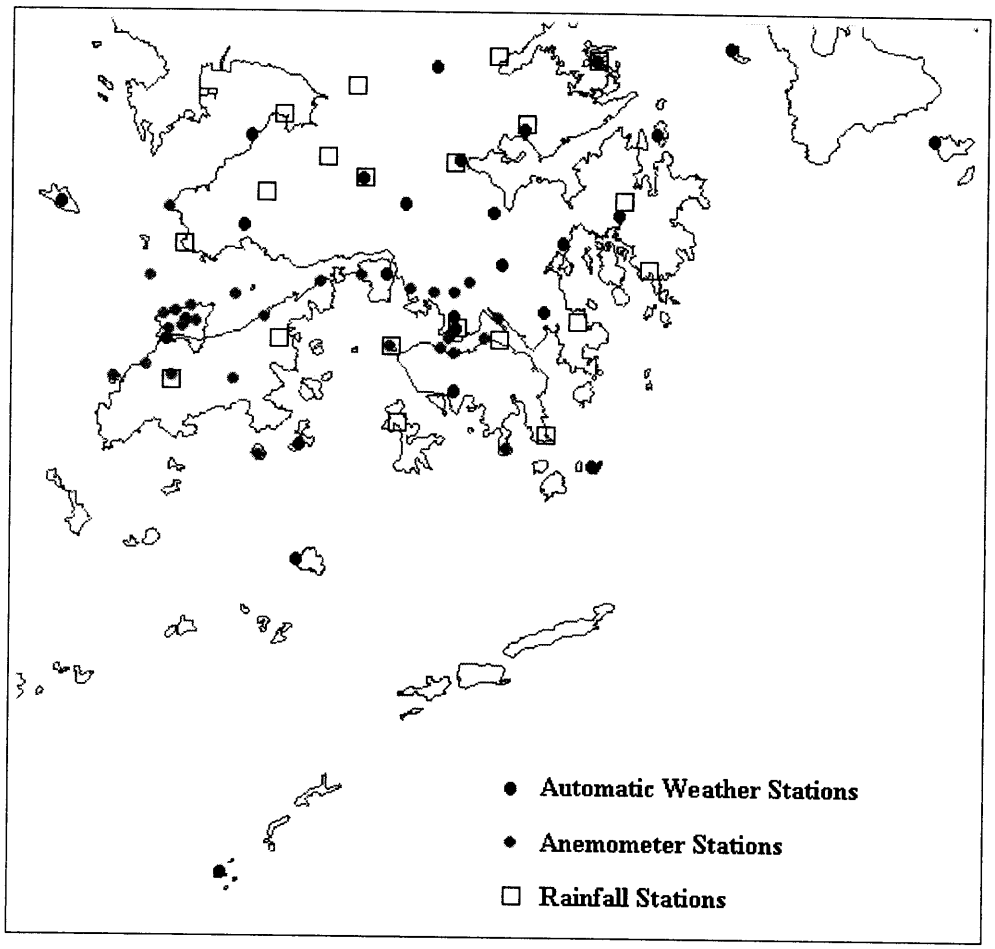

Figure 1 LOCATIONS OF AUTOMATIC WEATHER STATIONS, ANEMOMETER STATIONS AND RAINFALL STATIONS IN HONG KONG

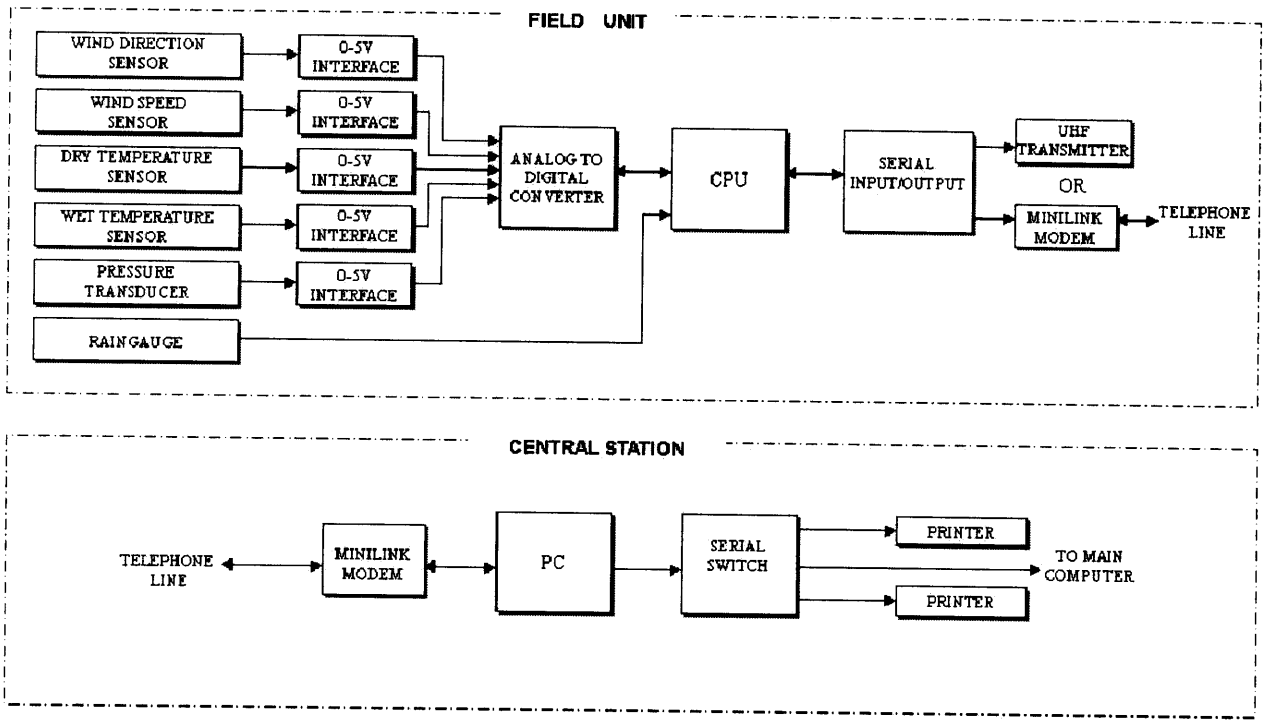

Figure 2 SCHEMATIC DIAGRAM OF THE AUTOMATIC WEATHER STATION DESIGN

Field-Calibrated Method for Automatic Meteorological Station

Lu Wenhua Zhu Lekun and Wang Jingye
Chinese Academy of Meteorological Sciences.
46 Baishiqiao Road, Beijing 100081, China
Tel/Fax: 86-10-68406866 E-mail: Lwh@cams.cma.gov.cn

1. Introduction

Automatic meteorological station belongs to automatic observing instrument with many parameters. It is different from conventional meteorological instrument. In order to ensure normal operation and the accuracy 、 stability for measuring results, it is should be calibrated periodically.

The field calibration for automatic meteorological station is that standard instrument and related device were transported to site, compared with automatic meteorological station. According to comparison result, decide to adjust base point value of various sensors or not.

2. Standard Instrument and Device

2.1 Pressure

Standard digital pressure gauge (measuring range: 400～1100hPa; uncertainty: 0.02%FS).

Pressure regulator (pressure adjusting range 0.1~0.4MPa).

2.2 Temperature

Digital platinum thermometer (measuring range – 60 ～ +80℃; uncertainty: 0.06℃).

Portable temperature calibration chamber (operating range: –30 ～ +20℃; homogeneity of control temperature : ±0.05℃).

2.3 Humidity

Secondary standard digital psychrometer (measuring range: 10% ～ 95%RH; uncertainty: better than 2%RH).

Humidity calibrator with saturated salt solution (humidity point generated: 33%RH, 75%RH 97%RH; uncertainty calibrated: better than 2%RH).

2.4 Precipitation

10 mm standard measuring glass (uncertainty: 0.1mm).

2.5 Wind Direction

Standard measuring plate (0 ～ 360°), calibrating device for starting speed

2.6 Wind Speed

Wind speed calibrator(measuring range: 0.4～60m/s) ;calibrating device for starting speed.

2.7 Radiation and Sunshine

Standard radiometer (pyrheliometer: uncertainty 1%; pyranometer: uncertainty 2%; net pyrradiometer: uncertainty 10%) and automatic solar tracker.

2.8 Evaporation

Standard pattern plate(10mm, 20mm, 50mm, 100mm).

3. Calibration Method

The following is field calibration method for automatic meteorological station

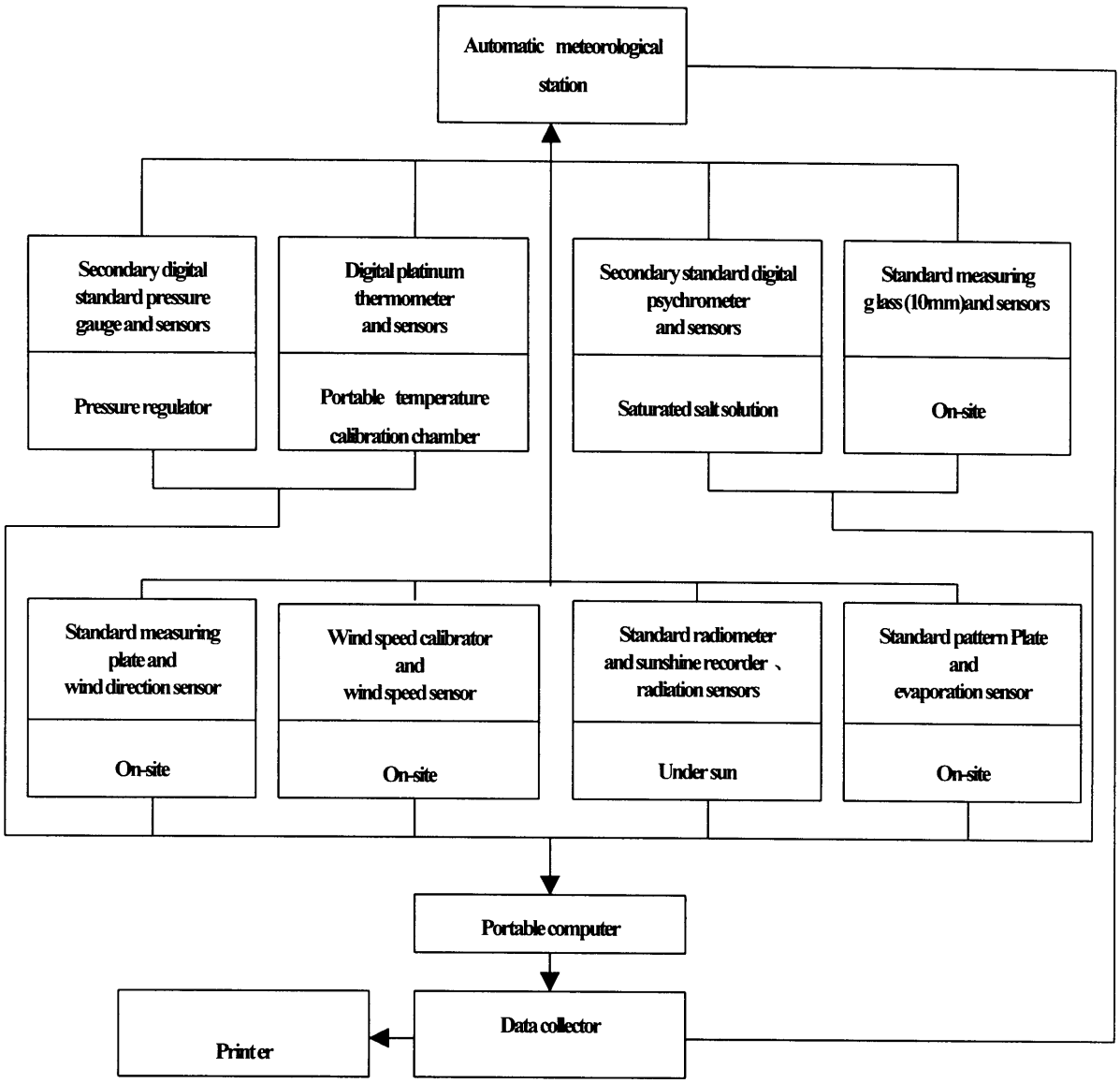

Field calibration diagram for automatic meteorological station

3.1 Pressure

At first , by mean of pressure regulator, link up standard Digital pressure gauge and sensor calibrated, check up airtight (not more than 0.3hPa/10min) .

According to average pressure value of using place of automatic meteorological station, select calibrating pressure point, which is three pressure point (average pressure point; more than and less than 50 hPa for average pressure point).

On per setting point, carry out two circle test, indication value of sensor calibrated minus indication value of standard instrument is measuring error. Finally , Calculate total average value of

measuring error value of three pressure point. If total average value exceed allowable error value, the base point value of sensor is adjusted.

3.2 Temperature

Calibration temperature point is at +20 ℃; 0℃; –20℃, calibration of 0℃Temperature point was carried out in the freezing point device. Other temperature point's calibration (+20℃; –20℃) was carried out in the portable temperature calibration chamber. At first, insert the sensor of standard instrument and sensor calibrated into the freezing point device, after stabilizing, read out indication value of standard instrument and sensor calibrated. At per temperature point, read out indication value of standard instrument and temperature sensor, four times temperature value is read out continuously in one minute, the average value for four times measuring value of standard instrument plus correction value is equal to standard value (relative truth value). The average value of four times measuring value minus standard value is equal to measuring error on this temperature point. Measuring error of various temperature point is calculated, If average value of measuring error exceed permissible error value, its basic point value must be adjusted into within allowing range.

3.3 Humidity

By means of saturated salt solution ($MgC1_2$; NaC1; K_2SO_2), three humidity point (33%RH; 75%RH; 97%RH) are generated. Before calibration, put sensors of standard instrument and calibrated sensor into humidity calibrator with saturated salt solution. After ten minutes, start to calibrated it. The measuring value of sensor calibrated subtract measuring value for standard hygrometer is measuring error(once),calculate measuring error of various humidity point and average value of measuring error of difference humidity point. If average value of all measuring error for difference humidity point exceed permitting value, the basic point of sensor is adjusted. within allowing range.

3.4 Wind direction

Using standard measuring plate as standard instrument, the accuracy of wind direction sensor is calibrated in accordance with all direction (360°)

3.5 Wind speed

Using wind speed calibrator as field calibration standard instrument, before calibration, wind speed calibrator must be compared in the wind tunnel. Through comparing, get the relationship between wind speed and rotation speed. Under field environmental condition, the wind speed calibrator is compared with wind speed sensor for automatic meteorological station (calibration point: 5, 10, 20, 30, 40, 50, 60m/s). Calculate linear regression equation ($V= a + bV'$)and error for linear regression equation ($\Delta V = a + (b-1)V'$) of the sensor calibrated. When wind speed error exceed allowable value, wind speed sensor must be washed or replaced.

3.6 Radiation and Sunshine

Under a sunny day, standard radiation instrument compare with radiation sensor calibrated for three to four hours. It takes two minutes for collecting one data.

Using pyrheliometer with automatic solar tracker as a standard instrument, by connecting

with an appropriate indicator of recorder, sunshine sensor is calibrated. According to calibration results, adjust it's threshold value or not.

3.7 Evaporation

Put standard pattern plate into evaporation barrel, simulate altitude of water level, (calibration point is at 0mm; 10mm; 20mm; 50mm; 100mm).We use this method to calibrate the evaporation sensor.

3.8 Precipitation

Using standard measuring glass, pour water into tipping – bucket rain gauge. Record three times measuring value of tipping–bucket rain gauge, using the average value of three times measuring value minus average value of three times output value of standard measuring glass is measuring error. Using maximum value of measuring error is as evaluation.

REFERENCES

WMO. Guide to Meteorological Instruments and Methods of Observation. Six Edition.WMO No.8.1996.

AIRPORT METEOROLOGICAL MEASURING SYSTEMS AUTOMATION IN SLOVENIA

Silvo Žlebir
Hydrometeorological Institute of Slovenia
Vojkova 1/b, 1000 Ljubljana, Slovenia
Tel.: +386 1 478 4306, E-mail: silvo.zlebir@rzs-hm.si

Introduction

Accurate and reliable determination of meteorological conditions on airports is very important for safety of the air traffic. Airplanes can take-off and land only when these operations are completely safe, having in mind respective degree of equipping of the airport, also meteorological. Consequently, also the quantity of the traffic and economics of the airport is weather dependent.

During last few years, meteorological measuring systems for international airports in Slovenia were automated and renewed. In 1999, Ljubljana Brnik airport started to operate according to the ICAO category CAT III rules, which is the highest ICAO category, enabling functioning of the airport in worst meteorological conditions. For the case of Ljubljana Brnik airport, the decision height is not lower than 15m and RVR is over 200m. Other two Slovenian international airports, Maribor and Porotorož, operate under CAT I rules. Automatic meteorological measurement systems were implemented on these airports. Visibility meters, anemometers, ceilometers, automatic weather stations and software for acquisition, archiving and visualization of the measured data are the most important elements of each system. Automatic generation of meteorological messages and reports is also implemented. When projecting the systems, quality assurance and reliability of the systems were very important items. Systems on the three Slovenian international airports differ by elements of the equipment which are required for different ICAO airport categories. Configuration of the measuring systems is otherwise similar.
Project of modernization of the meteorological equipment on airports was led by the Hydrometeorological Institute of Slovenia. Two main equipment producers were involved in project, Finnish Vaisala Oy and Slovenian AMES d.o.o.

Configuration of the Slovenian meteorological airport systems

Automatic measuring systems are composed of meteorological instruments, communication computer and central computer for evaluation, presentation, local archiving of measured data and automatic generation of meteorological reports. PC's with appropriate software, which serve as on-line data presentation display in Airport tower control and in Airport approach, are also treated as part of the systems. Basic guidance, when projecting automatic measuring systems at the Hydrometeorological Institute of Slovenia, were recommendations and requirements of the ICAO and the WMO[1,2,3]. All these requirements are fulfilled, including measurement uncertainties, sampling rates and presentation of measured data. CAT III on Ljubljana airport is enabled by double base RVR system. Automatic systems mitigate the work of meteorologist and observers on airports.

Configuration of the meteorological system on Ljubljana airport is schematically shown on Picture 1. Different measuring instruments and subsystems, computers and display terminals and their linkage to the whole system is shown. System is the largest among the three, differences being in some types and number of instruments and sensors included.

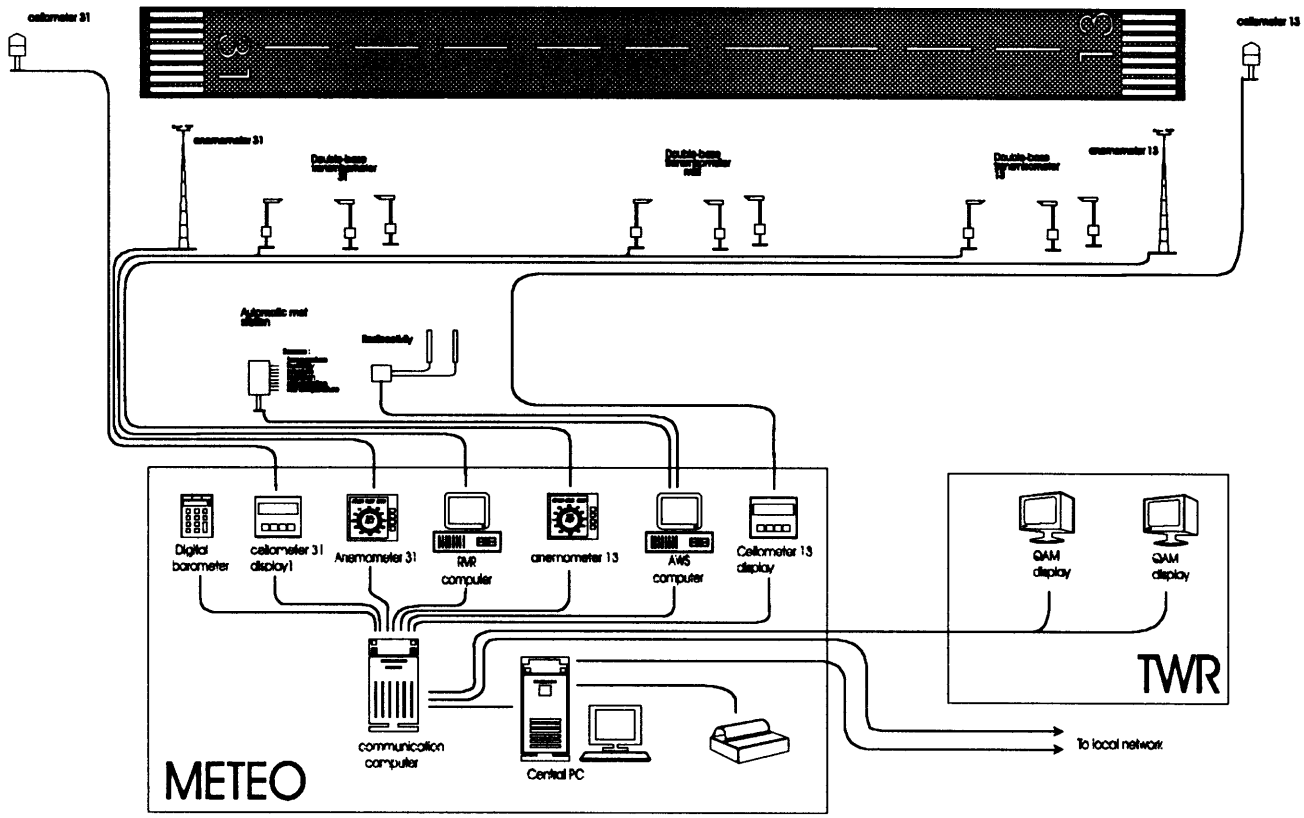

Picture 1

Sensors and measuring instruments are located on adequate sites near the airport runway. Ceilometer, which measures cloud height with the aid of back scattering of laser beam, is in the line of runway, at the very end of the airport. In CAT III system, two ceilometers are used on both runway ends, while in CAT I systems of Maribor and Portorož, only one ceilometer is used. Two independent wind measuring systems are also used on Ljubljana airport, while one on Portorož and Maribor airports, respectively. Basic differences among the three systems are in visibility meters. On Ljubljana airport, three double-base (15m and 75m) transmisometers are used, while one single base transmisometer is used on Maribor airport and forward-scatter visibility meter is used on Portorož coastal airport. Shorter measuring base, used on Ljubljana airport, enables accurate and reliable measuring of visibility in worst visibility conditions. All three airport systems include automatic meteorological station with a set of sensors for measurement of air and soil temperature, humidity, global and diffused solar radiation and precipitation quantity. All field instruments are linked to corresponding display units or, in the case of transmisometers, to RVR computer, which are located in the airport met office. On one airport, optical lines are used for linking. Precision electronic barometer is installed in met office of each airport. All instantly measured data from instruments or corresponding display units are collected continuously via front-end communication computer on the central PC unit of each system. Program applications on central PC serves for instant and average data control, data archiving and data presentation. Different data presentation modes are possible. The basic one is so-called QAM presentation mode, which shows instant measured and calculated data of wind, MOR, RVR, cloud base height, air-temperature, dew temperature, QNH and QFE. Special application was developed, which enables automatic generation of SYNOP (hourly) and METAR (half-hourly) reports, using the data from measuring systems. Observer can add his own meteorological observations to these data to complete the

report: actual weather, cloud types, special warnings etc. As central PC of the system is virtually connected to the local network of the Hydrometeorological Institute, reports are distributed and sent into international exchange. On the other hand, instant QAM data are continuously distributed to display terminals, which are actually PCs, located in airport air traffic control tower and in approach control. Data shown on these terminals are used in operational work of airport navigation services and control.

Reliability and quality assurance of measured data

When designing automatic measuring systems on Slovenian airports, special care was devoted to the reliability. Also software application programs include some reliability tasks. Systems are powered by uninterrupted power supplies. In case of cutout of central PC of the system or some communication lines, each measuring unit functions as a completely autonomous instrument with its own display unit.

As measured data are directly employed in air-traffic, its quality is very important. Working procedures in case of bad weather conditions (low visibility and low cloud base) are defined in special manual. Measurement uncertainties for all instruments and sensors are analysed to comply the recommendations of the ICAO and WMO. Maintenance of the equipment is performed by the qualified group from Hydrometeorological Institute of Slovenia. Instrumentation and its maintenance is a subject of inspection and control from the side of air-traffic supervision body. Measuring instruments are regularly calibrated by the calibration laboratory of the Hydrometeorological nstitute of Slovenia, which is accredited according to the international standard ISO17025/EN45001. Calibration intervals, defined according to the recommendations of WMO, are regulated in special document and strictly followed

Conclusions

Among the three airport meteorological measuring systems in Slovenia, the one on Ljubljana airport is now in use for the longest time. It was partly installed in 1994 and then finished in 1997. Operators of the system have got enough experiences and some statistical analyses have already been done for this system's working period. Detailed statistical analysis about visibility and cloud base height conditions on this airport has also been done[4]. Results of this analysis, among others, were used in justifying the upgrading of the airport into CAT III category.
Some results of the statistical analysis of visibility and cloud base conditions on Ljubljana airport are shown in Table 1, where number of days of low visibility during years 1994-1997 for conditions of different corresponding ICAO categories are given. Low visibility and cloud base height (decision height) conditions are subdivided into four categories according to the ICAO.

Year	CAT I	CAT II	CAT IIIA	CAT IIIB
1994	44	65	67	14
1995	54	81	80	29
1996	77	84	80	64
1997	75	88	85	38
Average	62	79	78	36

Table 1

Table gives good picture of visibility conditions on Ljubljana airport. Number of days with visibility according to CAT II and CAT IIIA is higher than that of CAT II. Generally speaking, when there is a fog on the airport, it is relatively dense.

On the base of further statistical analysis of low visibility conditions on Ljubljana Airport, following conclusions can be given:

- Low visibility conditions appear on average in about 100 days per year, with a total duration of approximately 600 hours per year
- Duration of each low visibility occurrence is on average 6 hours; conditions for CAT III (A or B) operations last on average approximately 2.5 hours
- Conditions for CAT III occur in wintertime over the whole day, in summertime mainly during the second half of the night.

References

(1) Meteorological Service for International Air Navigation - Annex 3 to the Convention on International Civil Aviation; International Civil Aviation Organization, 11th edition, July 1992

(2) Guide on Meteorological Observation and Information Distribution Systems at Aerodromes; World Meteorological Organization - No.731

(3) Runway Visual Range Observing and Reporting Practices; ICAO Circular 113 - AN/85

(4) A. Hrabar: Study on Low Visibility Conditions on Runway RWY31 of the Ljubljana airport, Hydrometeorological Institute of Slovenia, Ljubljana, February 1998

(5) S. Žlebir, M. Ferlan, M. Miholič: Meteorological Measurements on Ljubljana-Brnik Airport in Conditions of CAT III, 1st Congress TRANSPORT TRAFFIC LOGISTICS, Maribor, October 1998

AUTOMATIC MEASURING SYSTEM FOR PROVISION OF THE METEOROLOGICAL DATA FOR DOJRAN LAKE RESEARCHING

Suzana Alcinova Monevska
Republic Hydrometeorological Institute-Skopje
Skupi.bb, 91 000 Skopje, Republic of Macedonia
smonevska@meteo.gov.mk

INTRODUCTION

The intensive progress of science and technology during the last decades enabled a beginning of a process of automatization of the conventional meteorological measurements in the Republic of Macedonia basic meteorological network. Automatic measuring systems (AMS) with various working programs, configurations of sensors and manufacturers have been installed at measuring sites in Skopje-Zajcev Rid, Kavadarci and Star Dojran and they operate jointly with conventional meteorological measurements.

Basic reason for installation of the AMS in Star Dojran was the first phase realization of the Research Project for Dojran Lake protection, approved and financed by the **UNESCO**, which comprised provision of the main meteorological parameters necessary for water balance estimation. The Project Leader- Faculty for civil engineering, jointly with the Republic Hydrometeorological Institute committed themselves to carry out measurements and evaluation of meteorological parameters and creation of data base that will be used for further research.

The supplied AMS from a German manufacturer of meteorological and hydrological equipment was installed on a representative site, and starting from 1996 until today has registered a huge amount of meteorological data.

Dojran Lake is one of the three natural lakes in Macedonia, which is notable by its specific biodiversity and climate conditions. It is situated on the south border line of Republic of Macedonia and Greece, with a surface area of 41 km^2 (63% belongs to Macedonia and 37% to Greece). The lake has elliptic form with total accumulated water amount of 262 mil m^3 and average depth of 10 m. It is very popular tourist resort and fishery region, unique by the method of fishing with birds' assistance.

During the last period of prolonged dryness and intensive and uncontrolled antropogenic influence, the lake suffered enormous decrease of the water level. The Hydrological Department at the Republic Hydrometeorological Institute, responsible for operational monitoring of the hydrological parameters had been recording the oscillation of the water level since 1951.

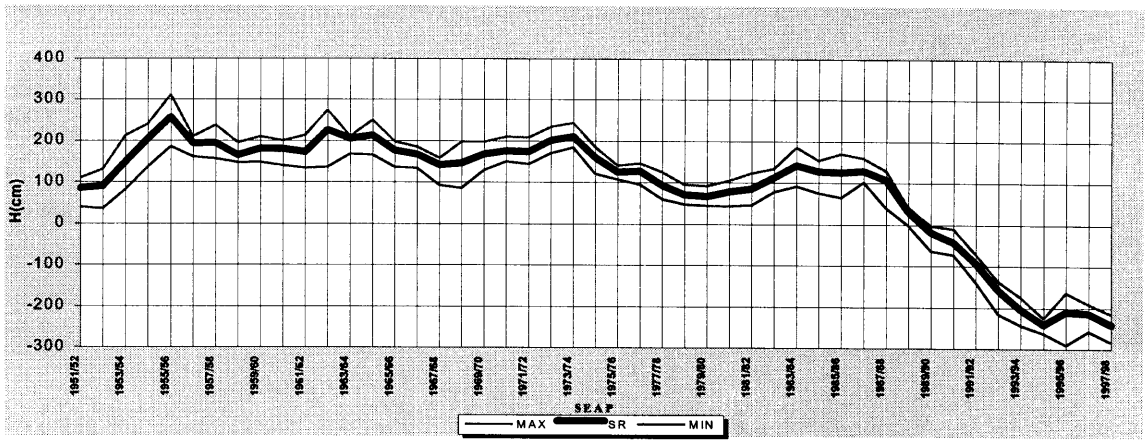

Fig.1 - Water level decrease started in 1987

CONFIGURATION AND AMS OPERATION

The entire automatic measuring system is design to provide simple, quality and exact measurements of the necessary meteorological data. The system is modern, universal and economical type of a meteorological equipment with a possibility for future upgrade in order to register the hydrological parameters, as well.

The internal memory capacity (ring memory) is 128 to 512 kB, which respond to 60 000 - 250 000 registered values. Each channel (possible 16 channels) has an option for time-interval set up from 1 second up to 1 month. The standard program at S.Dojran AMS records and stores hourly average and extreme values, so the needed storage per sensor per day is 600 bytes.

Depending of the measurement time and values there are various modes of measurements and the system has a possibility for automatic sensor calibration, as well.

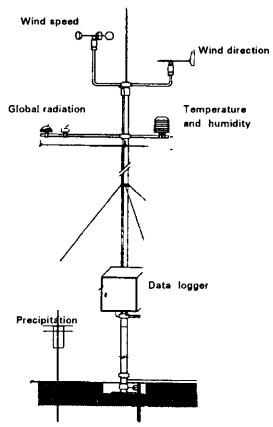

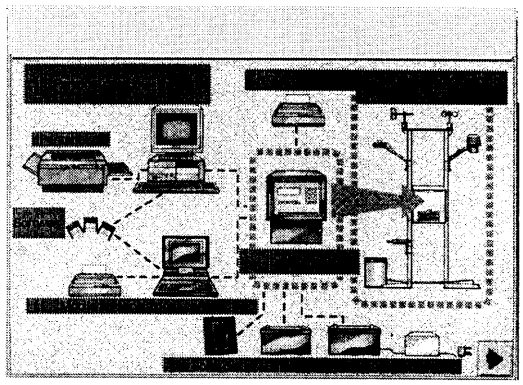

Fig. 2,3 - Installed sensors and the system for automatic meteorological measurements

There are several options for configuration of measurement parameters and transfer of the already recorded values from the central data-logging unit. The settings of sensors and readings of the data can be done with a mobile personal computer (laptop) or with replaceable memory cards. The stored data later are transferred with a reading unit and evaluated with a PC software. A remote communication using a modem is planned for near future, together with the upgrade of the AMS with a transmission system.

The present AMS is consisted of: data logging unit, sensors (air pressure, temperature, humidity, wind speed and direction, precipitation and radiation), operation software and software for multy parameter valorization, reading unit and memory cards.

Registrations from the installed sensors are memorized in a way and time intervals set up from the central unit with the operative software. In the beginning reading of the stored data was carried out once in 40-50 days with a mobile computer, and recently the registrations are stored on a memory card, which are later evaluated at the Republic Hydrometeorological Institute.

EXAMPLES OF MEASUREMENTS AND OPTIONS FOR DISPLAY

The data of the air temperature and humidity are set to be memorized in every full hour, wind speed and direction in an interval of 10 minutes, and the sensor for the precipitation registration records every 0.1 mm rain. The measurements have begun in June 1996 and until now a solid data base has been created.

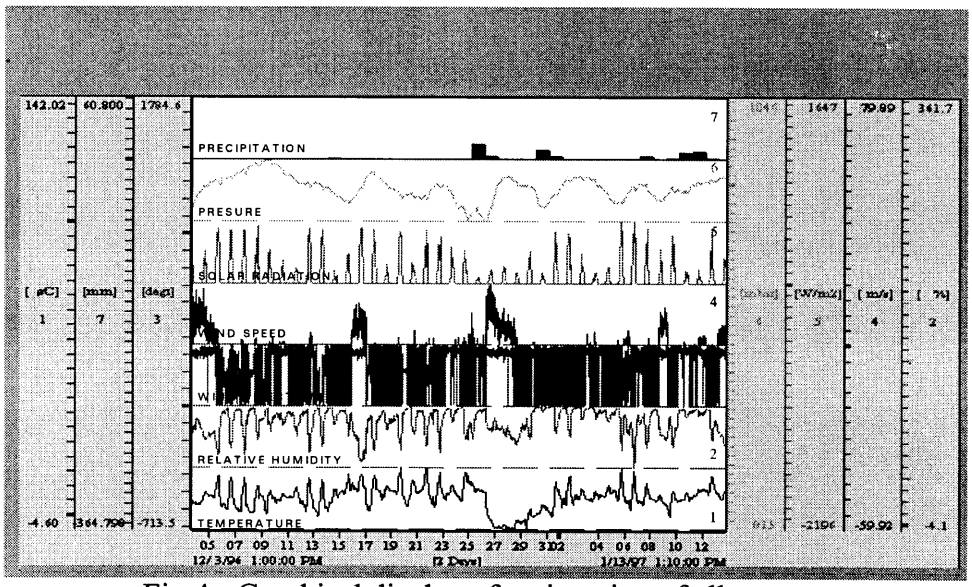

Fig.4 - Graphical display of registration of all sensors

The validation of the stored data is carried out with the multy parameter software package, which provide many options for tabular and graphic presentation of the measured values.

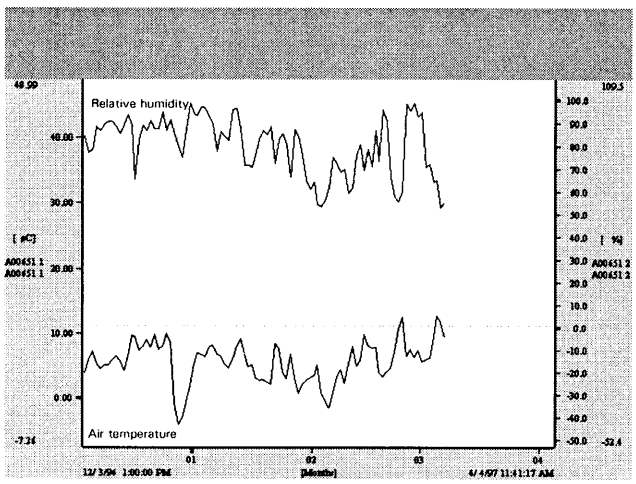

Fig. 5 - Graphical display of the air temperature and humidity for a three month period

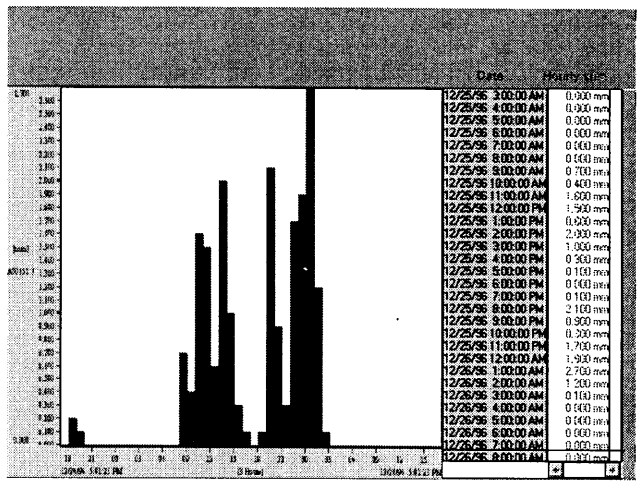

Fig. 6 - Graphical and tabular display of the hourly measurements of the precipitation sum

Beside the tabular and graphic presentation of all data, the analyze of each meteorological parameter can be done individually as well. There is also a possibility for complex analyze of two or more meteorological parameters. Also, the evaluation period can be enhanced from minute intervals to daily, monthly or annual period.

CONCLUSION

The automatic measuring system installed in Star Dojran with its five years of operation has created the necessary data base of relevant meteorological data for water balance components research, primary of the surface water evaporation estimation using complex empirical methods (Penman or other).

The installed system has a possibility for simple and economical upgrade, not only regarding the installation of additional sensors for automatic measurements of water level and temperature, but the improvement of the communication method and establishment of a real-time meteorological monitoring, as well.

Also, comparison of the AMS measurements with the classic method of meteorological measurement from the existing conventional meteorological instrumentarium on the nearby site will provide contribution toward the research of the compatibility of different methods of observation in the Macedonian meteorological network.

We look forward that the activities in the future period (including establishment of additional pluviometric sites along the coast line of the Dojran Lake, improvement and continuance of the AMS operation, etc.) will provide valuable information for time and space distribution of the meteorological parameters relevant for Dojran Lake ecological problem solution.

REFERENCES

1. WMO, 1996: Guide to Meteorological Instruments and Methods of Observation, 6th edn, WMO-No.8, World Meteorological Organization, Geneva
2. Observation & Engineering Branch, Australian Bureau of Meteorology, 1997: Guidance on Automatic Weather Systems and Their Implementation, WMO/TD-No.862
3. J.Ehinger, 1993: Siting and Exposure of Meteorological Instruments, WMO/TD-No.589
4. ZAMG Austria, 1995: Papers Presented at the International Workshop on Experiences with the Automatic Weather stations on Operational Use within National Weather Services, WMO/TD-No.670

AUTOMATIC WEATHER STATIONS IN INDIA – RECENT TRENDS

R.D. Vashistha and S.K. Dikshit
India Meteorological Department, Pune - 411 005, India

Introduction:

New developments in sensing, logging and communication technology have given new opportunity to a weatherman in using automated system with more confidence and reliability. In India the concept of automation in collection of meteorological data was evolved in early eighties and since then there has been a continuous progress, though slow, in this field. At present Meteorological Department has been operating 100 Automatic Weather Station in remote and inaccessible places, spread all over India. India's Geostationary Satellite INSAT is utilized for up linking AWS field site at a frequency of 402.75 MHz. The satellite's transponder (DRT) retransmits the data to a Central Receiving Station at a downlink frequency of 4038.1 MHz (extended C-band). The AWS data is processed, quality checked and disseminated to the user agencies over GTS (Global Telecommunication Service). Operation of these systems in India has passed through several critical phases with a number of problems, both in design limitations, field maintenance problems as well as infrastructure. Nevertheless, the field experience has given invaluable experience.

The Automatic Weather Stations presently installed in some of the sites in Indian network have the following salient features:

- The systems are compact, portable and operate on a single 12V maintenance free battery put on float charge using a solar panel.
- System has a synthesized UHF transmitter and could be adjusted to any required frequency in the band 402.65 to 402.85 MHz.
- It has RS-232 Port for retrieving the data on PC. The system setup and Basic programs could also be adjusted through a notebook PC in remote field sites.
- System has facility for averaging any meteorological parameter like wind speed and direction for a required duration of 3 minutes, 10 minutes etc.
- The AWS can log the data at predefined intervals of different parameters for a duration of six to eight months and could be retrieved using a Laptop or a PCMCIA card.
- The system has a multipurpose crossed Yagi antenna which could be used for LHCP (Left Hand Circular Polarisation) or RHCP (Right Hand Circular Polarisation).
- The AWS could be hooked up through Telephone Modem for retrieving the data from a Central station. Fig 1 and adjoinging table gives the schematic of A.W.S and the list of sensors utilized

- **. Data Comparison between AWS and Manual Observatories:**

A few AWS stations have been deployed for monitoring the quality of their data vis-à-vis co-located manual observatories. Table 1-3 gives a statistical analysis of AWS data vis-à-vis. observatory data. From Table-1 and Table-2 it is noted that the main sampling characteristics of temperature and pressure obtained with AWS and manual observatory have similar statistical behavior at Pune (India). From table-3 it is noted that the instrument bias is about 0.33°C for temperature at 3UTC and –0.37°C at 12UTC. The instrument bias is –0.52hPa for 3UTC and –0.25hPa at 12UTC for atmospheric pressure at Pune site. The WMO specified accuracy limits for automatic weather systems are ±0.5°C for temperature and ±0.5hPa for pressure (WMO 1996-CIMO guide). The observed differences in the present analysis are within the WMO specified accuracy limits. While comparing the data from an automatic weather station with the manual observatory data, two important factors are very vital. Firstly the observations from a manual observatory do not correspond to full hour UTC, the observations are recorded by an observer at

least 10-15 minutes earlier. This time difference could lead to a significant difference in temperature values as compared to automated observations which are sampled exactly at full hour UTC. Secondly the observer records the temperature observations by opening the thermometer screen which could lead to significant difference in temperature values as compared to automated observations where thermometer screen is not opened and the whole process of sampling of values is automatic.

Conclusion:

The introduction of state-of-the-art AWS system at a few locations in India has given a new confidence to the weatherman in collecting reliable and uninterrupted meteorological data in real time for disaster warning and mitigation. With the availability of sophisticated sensors and improved communication facilities, the AWS systems will provide accurate and timely surface meteorological data for coming years. While the process of automation has the advantages highlighted in the preceeding paragraphs, there is a need to create confidence among the users for accepting the end products of an automatic observing system. The technological complexities of automation has created reluctance among the users to introduce these systems in their network very rapidly. The experts who work in the field of automation have greater responsibility to ensure that the process of automation is made simpler so that the available manpower in meteorological services world over could be effectively utilized for using and maintaining the Automatic Weather Station.

REFERENCES

1. Datar S.V., A.N. Kutty and R.D. Vashistha — "Automatic Collection of Surface Meteorological Data via Satellites, IETE Symposium, November.
2. S.V.Datar, S. Krishnaiah and R.D. Vashistha, — Automatic Transmission of Surface Meteorological Data from Remote Stations via Satellite, Journal of IETE Vol. 29, No.8, 1983, pp.403-412.
3. Mishra D.K. and S.N. Srivastava — Communication of Environmental Data through Satellites, Vayu Mandal, 12, 2 (1982)
4. Ranju Madan, M.K. Gupta and R.D. Vashistha — Automation in measurements of surface meteorological parameters, TROPMET-95 Symposium on "Advanced Technologies in Meteorology".
5. Fraik W. Gallagher III — The next generation of sensors of ASOS, Fourth WMO Technical Conference on Instruments and Method of Observation (TECIMO-IV)
6. Vashistha, R.D., M.S. Rawat and R. Pratap — Field Experiences in Unmanned Meteorological Data Collection. WMO Technical Conference on Instruments and Method of Observation (TECO-94).
7. Luis Fillpe, A.C. Nunes, — Comparison of Daily maximum air temperature data series observed by Classical and Automatic Meteorological Systems, WMO Technical Conference on Instruments and Method of Observation (TECO-98).
8. WMO 1996 — Guide to Meteorological Instruments and Methods of observation, 6th Edition, WMO, No.8, 1996.
9. WMO 1998 — Instrument and observing method, Report No. 68.

****

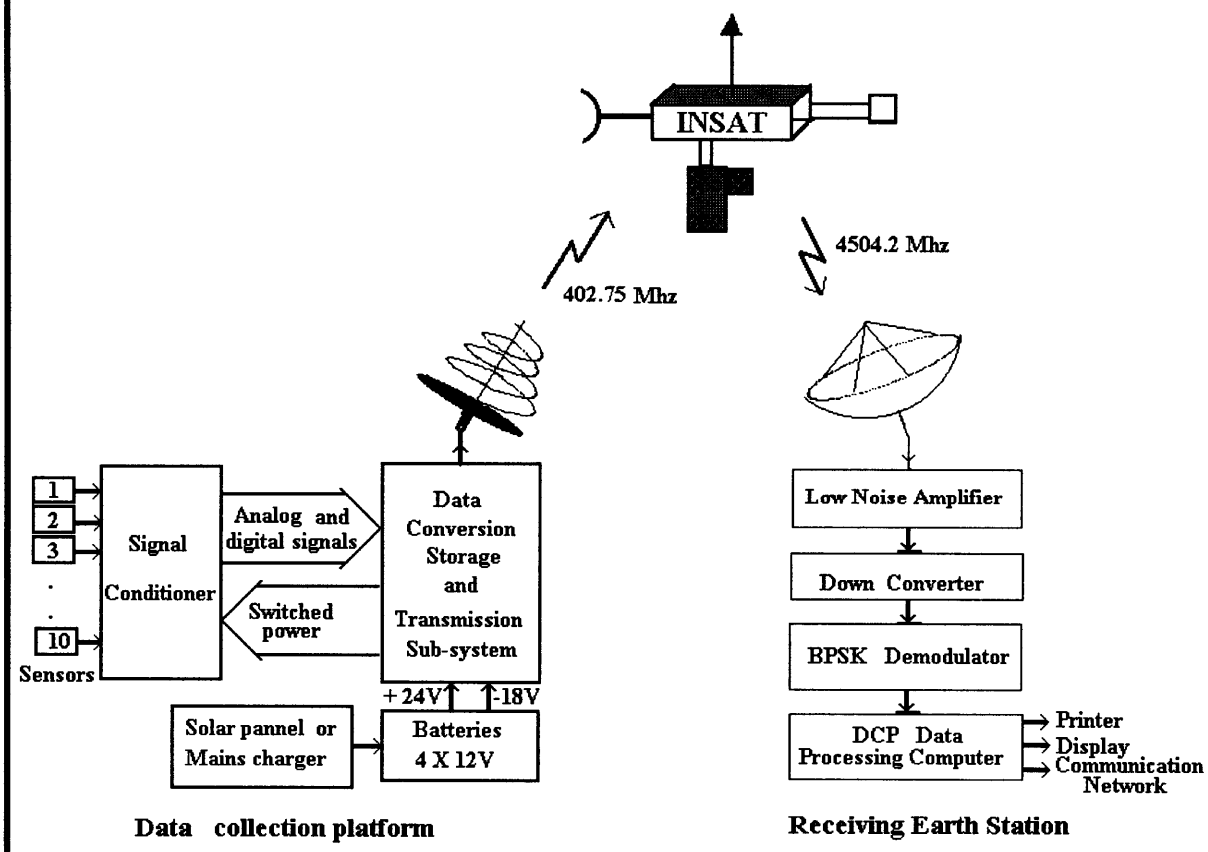

Fig. 1 INSAT DATA COLLECTION SYSTEM

Parameter	Sensor Used	Range	Sensor accuracy	Overall accuracy
Temperature	Thermistor	0-50°C (or-20 to +30°C)	0.20°C	1.0°C
Wind speed	Cup Generator Anemometer	0-100 knots	1 knot	2 knots
Wind direction	Potentiometric Windvane	0-360°	1°	10°
Pressure	Aneroid	0-100 hPa above a fixed datum	0.3 hPa	1 hPa
Relative Humidity	Humicap	0 - 100%	5%	10%
Rainfall	Tipping Bucket Raingauge	0 - 1023 mm	1 mm	10%

TABLE 1: SAMPLING CHARACTERISTICS OF 3 GMT DATA AT PUNE (INDIA) NOV 98 TO JUN 1999

SERIES	PARAMETER	OBS. SYS	MEAN	MEDIAN	MIN	MAX	PC25	PC75	S.D.	KURT	SKEW
PUNE	DB TEM. (°C)	AWS	22.4	24.0	11.0	28.9	19.8	25.9	4.48	-0.14	-0.95
		OBS	22.1	23.6	10.1	29.1	19.2	25.8	4.65	-0.08	-0.95
PUNE	S.L.P (hPa)	AWS	947.2	947.3	937.8	954.2	944.5	950.6	3.8	-0.83	-0.14
		OBS	947.8	947.6	939.8	954.8	945.0	950.9	3.68	-0.97	-0.1

TABLE 2: SAMPLING CHARACTERISTICS OF 12 GMT DATA AT, PUNE(INDIA) PERIOD NOV 98 TO JUN 1999

SERIES	PARAMETER	OBS SYS	MEAN	MEDIAN	MIN	MAX	PC25	PC75	S.D.	KURT	SKEW
PUNE	DB TEM. (°C)	AWS	29.4	28.6	20.2	37.8	26.0	32.7	4.03	-1.05	0.30
		OB.	29.7	28.8	23.0	37.8	26.4	33.4	4.11	-1.12	0.31
PUNE	S.L.P (hPa)	AWS	944.5	943.9	937.5	952.0	941.8	947.8	3.59	-0.09	0.22
		OBS	944.8	944.0	938.2	951.9	942.4	947.8	3.32	-0.96	0.28

TABLE-3 SAMPLING CHARACTERISTICS OF AWS – OBS. DIFFERENCE SERIES AT PUNE(INDIA)

SERIES	PARAMETER	TIME	MEAN	MEDIAN	MODE	S.D
PUNE –(AWS -OBS)	DB TEM. (°C)	03	0.33	0.2	0.2	0.63
		12	-0.37	-0.4	-0.5	0.57
PUNE (AWS -OBS)	S.L.P. (hPa)	03	-0.52	-0.7	-0.6	0.33
		12	-0.25	-0.2	-0.4	0.46

****

1 MEASUREMENT TECHNOLOGY, PERFORMANCE, AND QUALITY ASSURANCE

1.1 Surface Observation Systems

1.1.2 Intercomparisons

A comparison of air temperature radiation screens by field experiments and Computational Fluid Dynamics (CFD) simulations

Aril Spetalen[1] , Cecilie Lofseik[2] and Per Øyvind Nordli[1]

[1)]Norwegian Meteorological Institute (DNMI), Observation Division, PO Box 43 Blindern, N-0313 OSLO, Norway.
Tel: +47 22 96 30 00, Fax: +47 22 96 30 50, email: aril.spetalen@dnmi.no
[2)]Aker Engineering, Oslo, Norway

Introduction

For the purpose of climatological research, it is necessary to use measurements generated by different observing systems. Climate changes caused by anthropogenic effects may be of a magnitude of some tenths of a degree centigrade, i.e. of the same magnitude as effects on temperature caused by different screening of the thermometers or sensors. It is therefore crucial to be able to distinguish between real climate changes and the virtual ones caused by the changes of observation techniques and thermometer screening . The major changes that have taken place in the network of the Norwegian Meteorological Institute (DNMI) is about to be examined in a test field of fairly unobstructed grass just outside the DNMI head centre. The project runs from 1 February 2000 to 31. March 2001.

Among the new screening principles is the use of a fan for artificially controlled ventilation, but this principle has not yet come to use in the Norwegian station network. However, Platinum Resistance Thermometers (PRT) in small circular thermometer screens were introduced at automatic stations as early as in the 1970s. Another major change in the network occurred some 60 years ago, when wall mounted "cages" were replaced by free standing screens. The effects of this change are among the poorest documented changes in the history of the Norwegian network, and are the main motivation for this test [Nordli], [Langlo]. Mr. Nordli is the leader of this comparison project.

The results will hopefully increase the value of the oldest measurement series. The use of modern sensor technology enables us to investigate the properties of historical thermometer screens easier and more accurately.

Experimental setup A: Field test setup

Screens investigated

There are 4 principally different types of screens represented in the experiment.

The 1st type is the single louvered screen mounted on a wall or window. These dominated the Norwegian station network from 1866 until the 1930s. The wall screen model "Dombås" is made of steel, with a louvered front door and yellow painting. The oldest screen tested, a window screen model "Bergen", is made of wood and has no door, because it's mounted in front of a window, designed for reading through the window glass.

The 2nd type is the classical free standing screen. This type came into widely use throughout the 1930s, and have been designed in different models. The currently used model is the "MI-46", a screen that resembles the double louvered Stevenson type. This MI-46 model is still the dominating screen in the DNMI station network.

The 3rd type is the small cylindrical screen designed for Platinum Resistance Thermometers (PRT), of which 3 models are represented. These are the "MI-74" (with or without hygrometer), a model manufactured by "Young"®, and a model manufactured by "Vaisala"®. The MI-74 differs from the others by its double rings inspirited by the double louvers of the Stevenson screen.

One artificially ventilated screen is tested, the Paroscientific® "Met 3A". This screen is a combined pressure, humidity and temperature sensor. The radiation screen is rather small, made of aluminium and ventilated by an electrical fan.

In order to investigate the differences of the response times of mercury thermometers and PRTs, we have built a mercury dewar surrounding one PRT placed in the Dombås screen.

Choice of Reference

As reference, we have chosen the model, which is the dominating screen at DNMI – the MI-46. This screen is a classical wooden, Stevenson type, double louvered screen.

The main advantage using this screen as reference is the fact, that it is represented in two historical screen changes at DNMI. It was the new model when introduced in 1946, and it is the one being replaced by MI-74 now. The screen has also been thoroughly tested [Langlo].

System Overview

The measurement system consists of an ordinary PC collecting data from 3 different units. These units are

- A data logger (Vaisala® QLC 50) collecting the non-temperature parameters
- A Met 3A aspirated thermometer screen (Paroscientific®), that also reports pressure and humidity
- A switch & Digital MultiMeter (DMM) (Hewlett Packard® 34970A) measuring all Pt 100 PRTs 12 times per minute.

The calculation and storing of data is done by a CVI ® program in the PC. The complete system is outlined in figure 1.

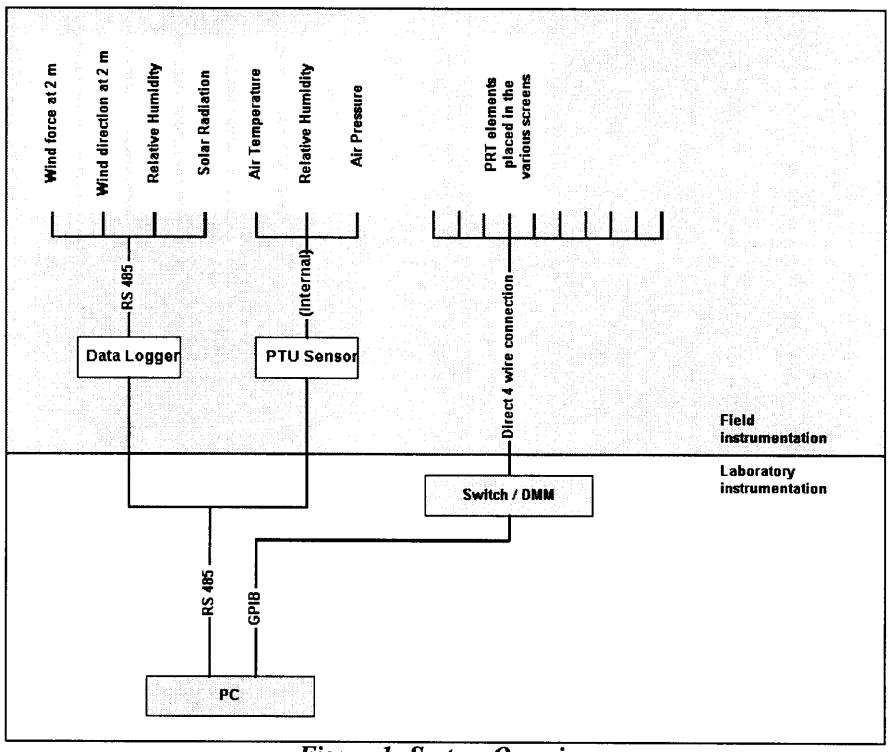

Figure 1: System Overview

Temperature measurement

All radiation screens are equipped with Pt 100 elements of IEC-751 Class A. They have been calibrated in our (DNMI) temperature laboratory, and the uncertainty is better than ± 0.1 ° C in the actual measurement range. An exception is the Met 3A, which has a specially designed Pt 1000 element, which cannot be removed from the housing, and therefore not calibrated separately. The Pt 100 elements are connected directly to the switch by 4 wires and measured 12 times per minute. One minute mean values (n=12) for all temperature measurements are stored as well as the hourly extremes.

Regarding thermometers, WMO suggests a "...time constant, defined by the time required by the thermometer to register 63.2 % of a step change in air temperature, should be between 30 and 60 seconds in a wind speed of 5 m/s. The time constant is roughly inversely proportional to the square root of the wind speed" [WMO]. The wind readings recorded at the radiation screen level (2 m above ground), have not so far exceeded 3 m/s, not even at times when the wind force recorded by the Oslo AWS was far higher. Although this will give a slower response, the exposure area is not in conflict with the WMO suggestions. Also, any occasions of the well-known problem with overheating on quiet sunny days will be easily detected.

Exposure and additional Parameters

The exposure area is planned according to the suggestions made for a preliminar ISO screen comparison test method. Some screens are represented by 2 equivalent units. The relative humidity, wind force and direction at 2 m level, and total radiation is measured. The screens are placed in a grass covered area with individual distances of about 2 m.

Additional Parameters (wind, humidity, radiation, pressure) are measured and stored in the data logger. The logger calculates the mean values internally, and these are transferred and written by the computer program once per minute.

The Met 3A data are read synchronously with the others; that is, temperature 12 times per minute, pressure and humidity once per minute.

Experimental setup B: Computational Fluid Dynamics (CFD) simulations

The CFD program Fluent™ has been used for simulating some of the scenarios observed in the field test. Fluent is a commercially available computer program for modelling fluid flow, heat transfer and chemical reactions.

Geometrical models of MI 74 and Met 3A have been made based on the technical drawings and measures of the screens, see figure 2. For the mechanically ventilated screen, MET 3A, two different ventilation rates have been tested. A fixed overheating has been set as a boundary condition on part of the outer wall and a fixed ambient wind profile with reference speed 2 m/s. Steady state simulations have been run; hence the development in time has not been investigated. The ventilation in the MI 74 screen has been calculated for two ambient wind speeds.

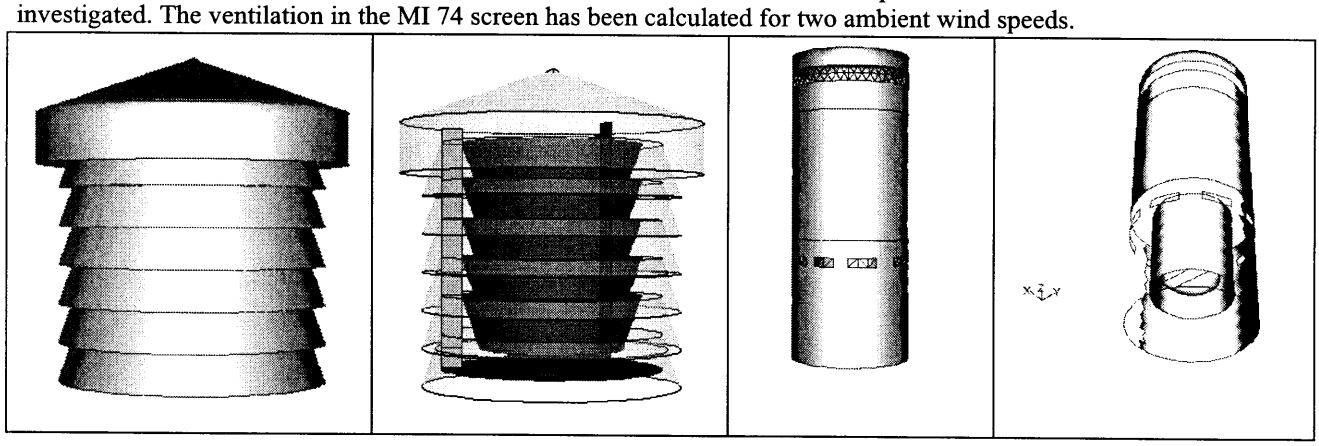

Figure 2: The models of MI 74 and Met 3A used in the simulations

Data Preview – Discussion

The objective of the experiment is to collect measurement data for two years, then perform the statistical work, and make procedures for handling the historical measurement data. However, some tendencies can be seen already at this stage. Figure 3 shows temperature readings and the differences from the Reference on a summer day (1. July 2000). The lower diagram shows that the historical wall and window cages give the highest values. This is typical on summer days. We especially note, that the temperature reading of the mercury "insulated" sensor shows a higher difference from the non-insulated sensor in the same screen when the sensors are exposed to reflected and spread short wave radiation. These screens are without a floor, so that reflected radiation from the ground can easily penetrate into the cage.

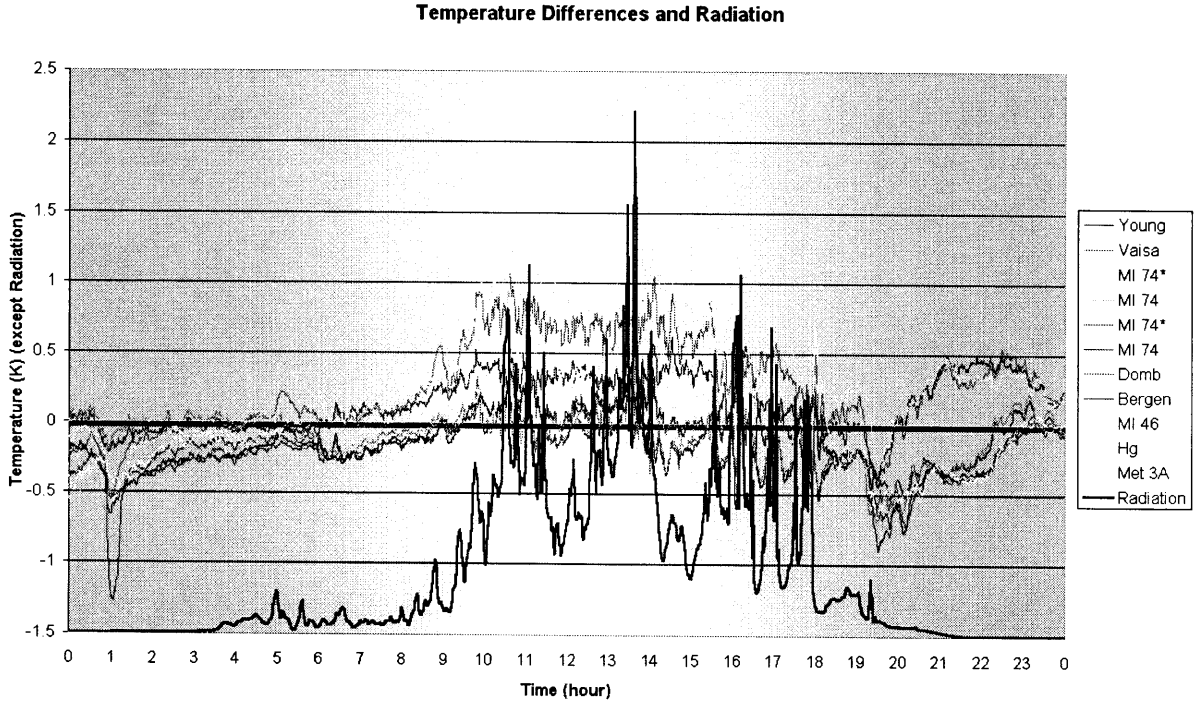

Figure 3: Read Values and Differences from Reference, 1. July 2000

A series of similar field tests has been performed, that may be used as guide line for comparison [Anderson], [Lefebvre], [van der Meulen].

The CFD simulations confirm the measurement dependency of good ventilation. The sensor temperature in the MET 3A screen was observed for a test case were the ambient temperature was set to 8 ° C and the outer wall overheating was 19 ° C. With a ventilation rate corresponding to a velocity of 4.5 m/s past the fan, the sensor temperature is 8.7 ° C. When the velocity was reduced to 2.8 m/s, the sensor temperature estimated was 9.1 °C. Figure 4 shows the path lines that the air is following through the device for these two cases.

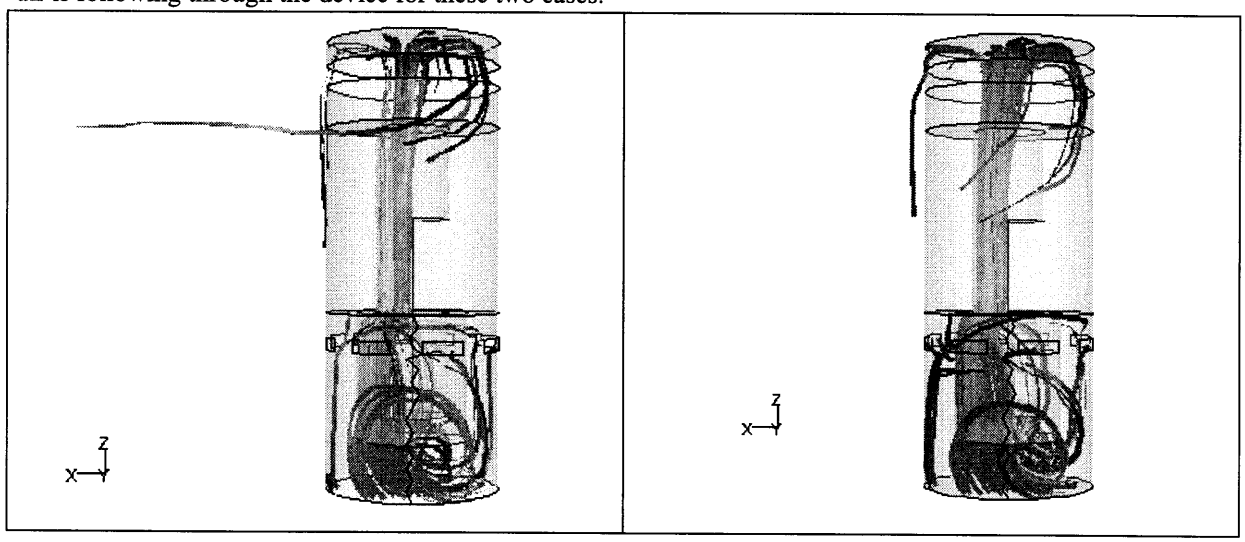

Figure 4: Path lines through Met 3A for the two test cases.

References

[Anderson] "*A field test of thermometer screens*"; by Anderson T, Mattison I; SMHI-RMK nr 62, 1991

[Barnett] *"Recent changes in thermometer design and their impact"*; Barnett A, Hatton DB, Jones DW; WMO/TD – No. 871; 1998; 12 p

[Langlo] *"Investigations on the air temperature observed in various types of norwegian thermometer screens";* by Kåre Langlo; Meteorologiske Annaler bd. 2 nr. 12; 1947; 387-402

[Lefebvre] *"Comparison of meteorological screens for temperature measurement";* by Lefebvre, Guy; TECO-98 Casablanca; 315-318

[Leroy] *"Test methods for comparing the performance of thermometer shields/screens and definiting of important characteristics";* Leroy, M; METEO France; No. SMF 93-137; 1993; 8 sider

[Nordli] *"The Effect of Radiation Screens on Nordic Time Series of Mean Temperature";* by Nordli, Alexandersson, Frich, Førland, Heino, Jónsson, Tuomenvirta, Tveito; International Journal of Climatology 17; 1997; 1667-81

[Sparks] *"The effect of thermometer screen design on the observed temperature";* by Sparks, WR, WMO no. 315; 1972; 106 p.

[van der Meulen] "*A thermometer screen intercomparison*"; by Jitze P. van der Meulen; TECO-98 Casablanca; 319-322

[WMO] *"Guide to Meteorological Instruments and Methods of Observation* " WMO No. 8, 6th ed. § 2.1.3.3

Effects of Different Screen Designs on Temperature: Field Experiment

Abebe Yeshanew, Senior Meteorologist
National Meteorological Services Agency, P.O. Box 1090, Addis Ababa, Ethiopia
Tel.: 251 1 61 57 79, Fax: 251 1 51 70 66, E-mail: a_yeshanew@hotmail.com

1 Introduction

Introduction of different screen designs in national meteorological observing network is a paramount concern in the meteorological community and the World Meteorological Organization. The concern arises from the change that could influence the homogeneity of temperature record and that could lead to false signal of climate change or other signals. Prior to introducing of different screen in the national meteorological observing network, it is imperative to conduct intercomparison experiment to eliminate any heterogeneity in the data base. The purpose of undertaking this type of experiment is to correct the changes introduced in the observation due to the new screen. Besides, to establish the quantitative relationship between the observation taking from the new screen and the old screen to maintain the uniform data set.

The drive for changes in meteorological measurements is based primarily on economical and sustainability.

The objective of this experiment is to find out the quantitative influence of introducing galvanized metal on a wooden screen on temperature.

The experiments to be done will identify influence of galvanized screens on the temperature under calm and windy conditions over different climatic conditions, namely, cold climate, hot climate and mild climate.

2 Motivation of the Experiment

Since some years ago, the National Meteorological Services Agency has modified the wood screen by using on the top a 0.20 mm galvanized sheet metal. One week survey has been done in the Agency (Addis Ababa) to find the effect of the modified screen on temperature prior to the introduction of this screen in the network. However, neither a documented study nor data is available in any form. As a result, it is very difficult to distinguish the effect of new screen on temperature from the old one. Presently, the observed temperature under the new screen is archived in the same file as the old one. This aspect and practice triggered the author of this paper to conduct a comprehensive experiment not only over Addis Ababa Bole but also over Metehar and Debre Brihan Stations.

3 Experiment Sites

To investigate the effect of the modified screen on temperature, three experimental sites with different temperature regimes are selected. The general characteristics of these sites are:

- Addis Ababa Bole is located at latitude of 9.033°N, longitude of 38.75°E and altitude of 2354 metres. On the average, the daily temperature of Addis Ababa Bole ranges

from 14.0°C to 17.6 °C. The average minimum temperatures range 5.5 C to 10.7°C whereas the maximum temperature varies between 20.8°C and 24.7°C.

- Debre Birhan meteorological station is located at latitude of 9.633°N, longitude of 39.50°E and altitude of 2754 metres. The average daily temperature over this station ranges from 11.9°C to 15.1°C. The average minimum temperatures range 4.6°C to 9.8°C whereas the maximum temperature varies between 18.6°C and 21.3°C.
- Metehara meteorological station is located at latitude of 8.867°N, longitude of 39.90°E and altitude of 930 metres. On the average, the daily temperature of Metehara ranges from 21.8°C to 28.5 °C. The average minimum temperatures range 13.3 C to 21.5°C whereas the maximum temperature varies between 24.4°C and 35.6°C.

4 Method

To find out the effect of the modified screen on temperature with respect to the wooden screen, verification methods will be used. The techniques that will be used are the probability of detection (POD), the false alarm ratio (FAR), the per cent error (f), the critical-successindex, the loss function (Fi), bias, mean absolute error (MAE) and root mean square error (Tsonis, 1988;Stanski et al, 1989 and Cheng etal, 1993).

If the temperature measurement difference between the modified screen and the wooden screen is not within the operational accuracy of WMO Commission for Instruments and Methods of Observation(CIMO), then attempt will be done to figure out the quantitative relationship between the two temperature measurements using a coefficient of correlation and regression equation.

5 Results

The experiment will commence in August 2000. The temperature (average temperature, minimum temperature and maximum temperature) measurements will be taken on standard time (00, 03, 06,09, ...).

The results of the experiment will be presented at the WMO Technical Conference on Meteorological and Environmental Instruments and Method of Observation (TECO-2000).

6. References

Cheng, M., R. Brown, and C.G. Collier, 1993: Delineation of precipitation areas using meteosat infrared and visibile data in the region of the United Kingdom. J. Appl. Meteor., 32, 884-898.

Stanski, H.R., L.J. Wilson and W.R. Burrows, 1989: Survey of common verification methods in meteorology. World Weather Watch Technical Report No. 8, WMO/TD No. 358.

Tsonis, A.A., 1988: Single thresholding and rain area delineation from satellite imagery. J. Appl. Meteor., 27, 1302-306.

****

Temperature measurements:
some considerations for the intercomparison of radiation screens

Jitze P. van der Meulen
Royal Netherlands Meteorological Institute
Postbus 201, 3730 AE De Bilt, the Netherlands
tel +31 30 2206432, fax +31 30 2210407, e-mail meulenvd@knmi.nl

Introduction

In a previous paper [1] a brief overview is presented of the thermometer screen intercomparison, carried out for six years at KNMI, De Bilt, Netherlands. Different designs of screens were investigated for this intercomparison. After analysis it was found that most screen agree to a reference on average within approximately 0.2°C (*e.g.* see fig. 1). However daily minimum and maximum temperatures differed

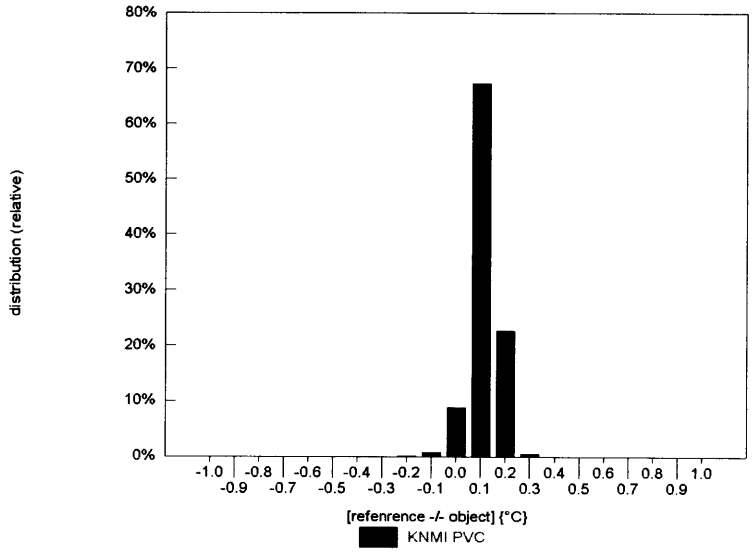

Fig. 1 Distribution of the mutual temperature differences during one day and for two different types of screen.

from screen tot screen for about 0.5 to 1.0°C. Even worse, under particular circumstances large deviations (1°C or more) were found. Although temperature measurements performed in the different screens resulted in agreeable results, it is a serious point for understanding the larger differences, which were found occasionally.

Analysis precautions

As a result of a more detailed analysis it was found that many larger differences are caused by short term fluctuations in and around the shelter, *i.e.* by micro-climatological effects and not caused by the particular design of the screen. Even when the screens were placed very close together, *e.g.* for an intercomparison, such effects may have a serious impact on the analyses. Off course, impacts of radiation, wind, rain, dew-deposition or artificial ventilation should be considered in the first place for any design of a screen. Nevertheless micro-climatological or micro-meteorological effects, mainly small turbulences and other fluctuations have to be taken into consideration when analysing the data set. This statement holds for both the reference screen and the screen to be compared with.

Apart from micro-climatological impacts on the analysis, the daily cycle of the air temperatures measured inside each screen have to be analysed first. Typical effects should be taken apart, *e.g.* at sunrise and sunset the sun may illuminate on a horizontal way the east or west side of a Stevenson screen causing an significant temperature increase. Another example to be noticed on forehand is when there is almost no wind, but with much moisture or condensation. The temperature of the screen will drop below the temperature of the surrounding air (typically at night before sunrise). If such effects are

not taken apart and statistical analysis is performed on *e.g.* daily averages, then any results may be rather disputable.

Typical examples of micro or short term effects.

In the figures 2 to 6 some typical examples are shown. For this purpose a conventional Stevenson screen is used and a "round shaped multi-plate" screen (20cm × 20cm). From the data set of temperature measurements, containing point samples with a time resolution of 15", the mutual difference, *i.e.*

$$\Delta t = t(\text{round shaped screen}) - t(\text{Stevenson screen}),$$

is calculated. Note that the any difference can be caused by one of both screens. Only with the help of sets of screens, with a different design, the particular screen causing such difference can be determined. Figure. 2 shows two daily cycles for air temperature, wind speed and radiation, indicated by day 0307 and 0304. Both days are with sunshine but no rain. Day 0304 is a day with temperatures below 0°C before sunrise and an increase of the wind speed in the morning. Day 0307 is a day with only small temperature variations and a rather stable wind.

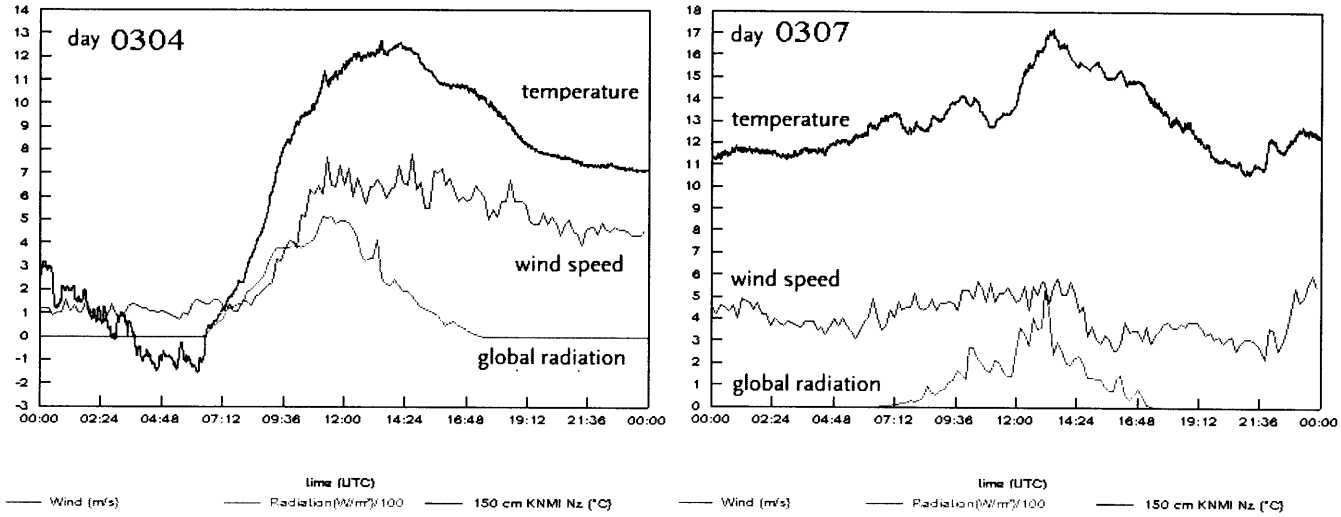

Fig. 2 Air temperature (in °C), wind speed (in m/s) and global radiation (in 100 W/m²) measured on day 0304 and 0307.

Values for Δt as a function of time are shown in fig 3. Obviously the low temperatures after midnight on day 0304 and the lower wind speed may have caused these strong fluctuating differences (Δt refresh interval: 15"). In any case, such night-time behaviour, which is also demonstrated on day 0307, when temperature and wind speed are stable, is quite typical. Especially for day 0304 deposition of moisture may have affected the measurements.

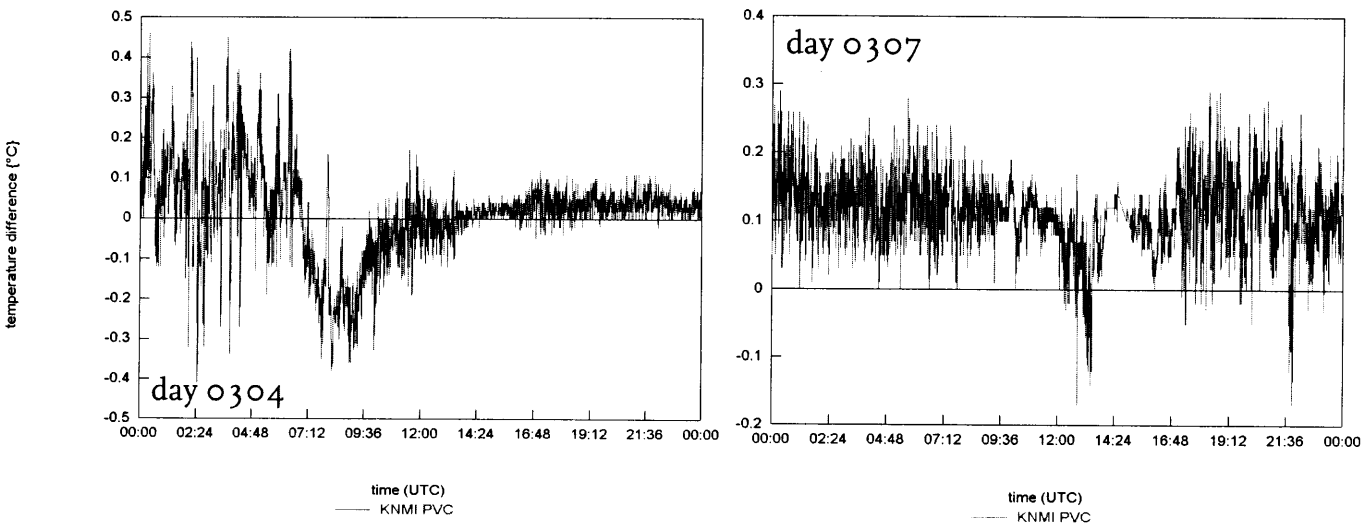

Fig. 3, Δt as a function of time for both days. Notice the fluctuations at night time, especially for day 0403.

Another way to show the relation of air temperature and the measured temperature difference is by presenting a plot of Δt versus air temperature (see fig.4).

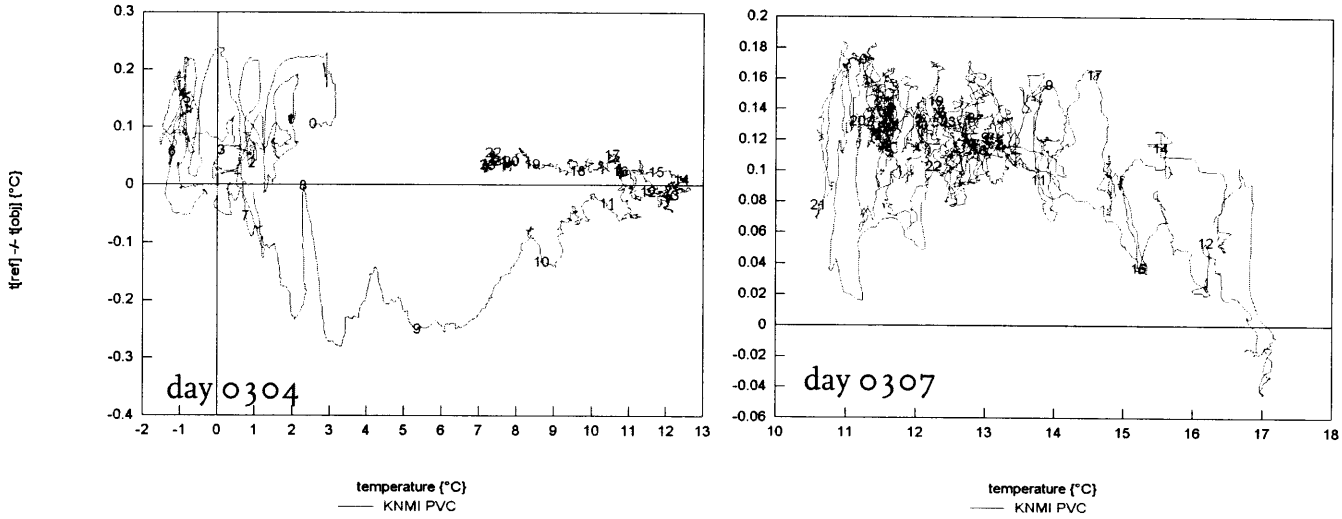

Fig. 4, Δt as a function of temperature for both days (digits are timestamps in H UTC). Notice the typical mutual differences for both days, especially the differences in fluctuation behaviour.

Plotting Δt versus wind speed, we get results as shown by fig. 5. To avoid a very noisy figure wind speed data is averaged first over 10' intervals. Considering day 0307 no significant impact of the wind is observed although it is a sunny day. For day 0304 however strong fluctuations in Δt are observed during night-time.

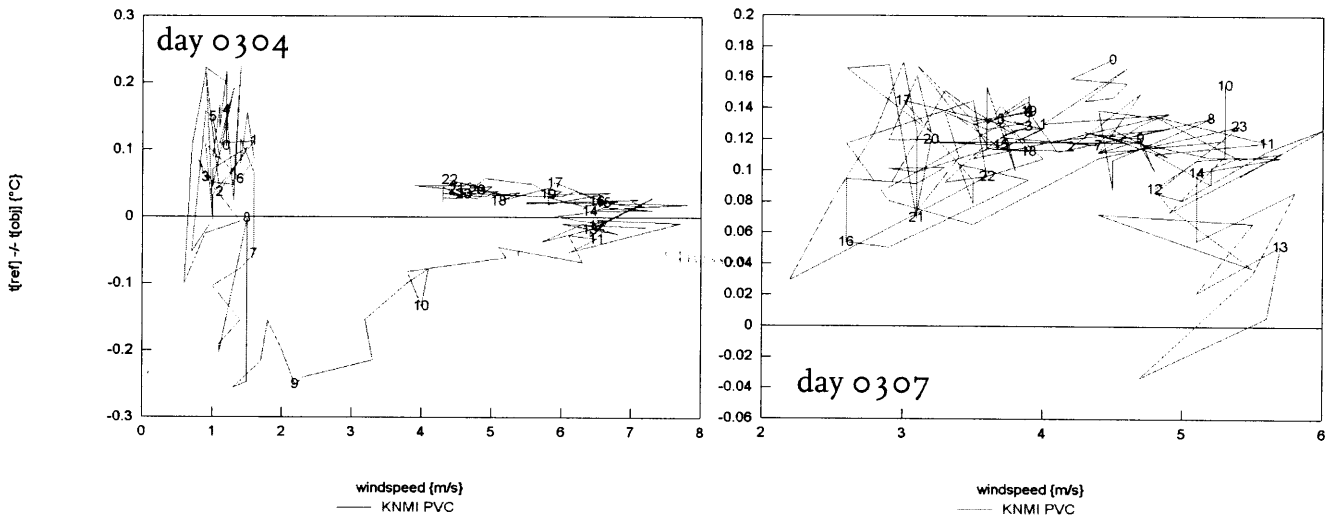

Fig. 5, . Δt as a function of wind speed. Note the large-scale fluctuations during the time before sunrise of day 0304

After all, temperature screens are used mainly to reduce the impact of radiation to the thermometer (or temperature sensor). Therefore to study the impact of the radiation on Δt will be the most interesting topic for an intercomparison. For both days we found results, shown in fig. 6 (10' average value of the global radiation are used). When comparing both figures however, no clear correspondence is found. Obviously differences Δt are not typically caused by radiation impacts only. Considering figs. 5 and 6 for day 0304 a typical combination of radiation with low wind speeds may have caused the larger Δt during the morning hours.

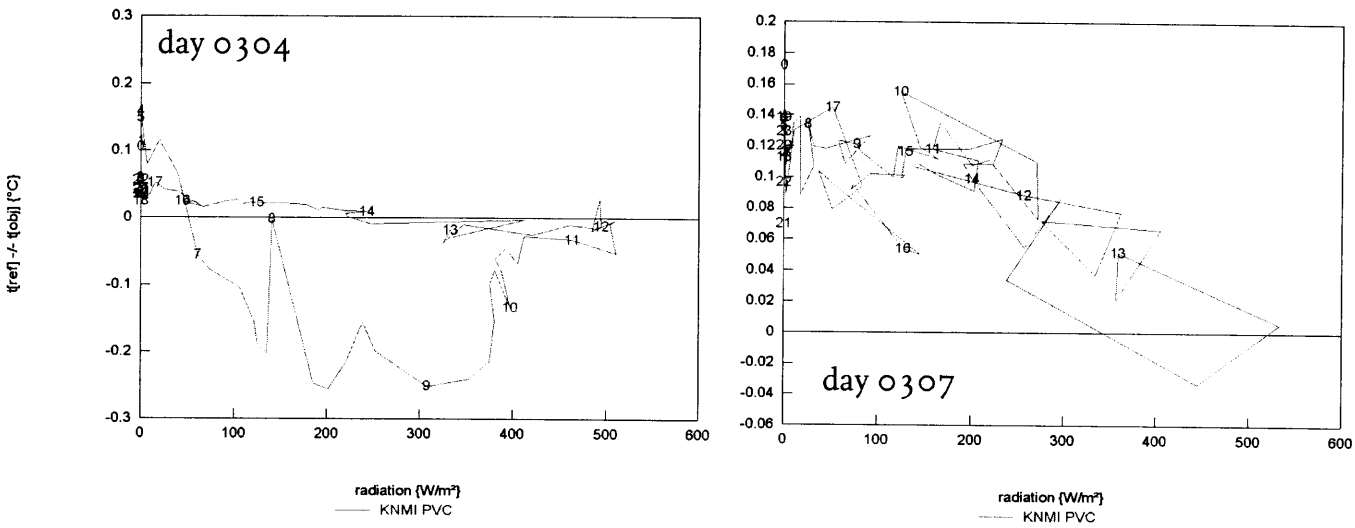

Fig. 6. Δt as a function of global radiation. Note the remarkable large Δt during the morning hours of day 0304 when the wind speed was low and with increasing radiation.

Conclusion

For the analysis of temperature measurements micro and short term effects should be considered first. Comparing different types of screens using statistical analyses of the mutual temperature differences, averaged over a day, month or year, the results will only be meaningful if micro and short-term effects (1 min or less) are taken into account.

References:

[1] Van der Meulen, J.P., in "Papers presented at the WMO Technical Conference on Meteorological and Environmental Instruments and Methods of Observation (TECO-98)" (Casablanca, Morocco, 13-15 May 1998), Instruments and Observing Methods report No. 70 (WMO/TD - No. 877, WMO, Geneva, 1998), pp 319.

Report on the International Pyrheliometer Comparisons —The Maintenance and Dissemination of the World Radiometric Reference†

I. Rüedi, C. Fröhlich, W. Schmutz, Ch. Wehrli
Physikalisch-Meteorologisches Observatorium Davos, Dorfstr. 33, CH-7260 Davos Dorf, Switzerland
Tel: +41-81-417 5111, Fax: +41-81-417 5100

Abstract. We report on the performance of the World Standard Group (WSG) which realizes the World Radiometric Reference (WRR). It is the basis for meteorological radiation measurements and to guarantee their worldwide homogeneity. It is the duty of the World Radiation Center to maintain the WSG in order to ensure the stability of the WRR. The periodic International Pyrheliometer Comparisons taking place at the World Radiation Center of the Physikalisch-Meteorologisches Observatorium Davos have for purpose the worldwide dissemination of the WRR.

1. Introduction

In the past a variety of radiometric scales were used based on the measurement of standard instruments[1]. They did not agree between each other and were sensitive to malfunction of their reference instrument. Actually, the concept of "scale" was wrong because a scale, in SI units [Wm^{-2}], is already defined on the basis of the standard physical unity system.

The development of modern absolute radiometers in the late sixties yielded more reliable measurements. They are electrically-calibrated cavity receivers and consequently need no calibration by comparison with a standard as also suggested by their name. Much better agreements were obtained between different types of absolute radiometers as between traditional instruments. It was consequently possible to realize a new reference for meteorological radiation measurements: the World Radiometric Reference (WRR) which was based on the performance of a group of absolute radiometers[2]. Its uncertainty was estimated to be less than 0.3%. Later, comparisons with cryogenic radiometers showed that the WRR lies within 0.03% of the basic SI Wm^{-2} [3, 4]. The mandatory use of the WRR for reporting meteorological irradiance measurements was introduced by the World Meteorological Organization in 1979 [5].

In order to guarantee the long-term stability of the WRR, a group of absolute radiometers of different types was defined: the World Standard Group (WSG) which is a realization of the WRR. It is the duty of the World Radiation Center (WRC) to maintain the WSG and thus to ensure the stability of the WRR. The purpose of the International Pyrheliometer Comparisons (IPCs) is its dissemination to ensure worldwide homogeneity of meteorological irradiance measurements.

The World Standard Group comprises at the moment 7 instruments: PMO-2, PMO-5, CROM-2L and CROM-3R, PAC3, MK67814, and HF18748. They are periodically evaluated and compared in order to check their stability and proper functioning.

In this article, we discuss the results of previous International Pyrheliometer Comparisons and report on the performance of the WSG over the last 10 years.

2. The IPC

International Pyrheliometer Comparisons were held for the first time in 1959, then in 1964 and from 1970 on every 5 years at the Physikalisch-Meteorologisches Observatorium/ World Radiation Center (PMOD/WRC) in Davos, Switzerland [6]. The last comparisons took place in September/October 1995 and the next comparisons, IPC-IX, will be in September/October 2000. The IPCs are intended for dissemination of the WRR to the Regional Centers which are responsible to further disseminate it to the National Centers. The IPC VII was combined with Regional Pyrheliometer Comparisons of 4 regions.

At the IPC-VIII 62 participants from 15 Regional and 28 National Centers and from 8 Institutions not directly linked to the WMO structures took part in the comparisons. They operated a total of 77 pyrheliometers, 44 of which were already present at the IPC-VII and 33 instruments were

† The IPC-IX will take place just before the TECO-2000 meeting, namely from 25 September 2000 to 13 October 2000 at Davos. Therefore, preliminary results from the IPC-IX will be included in the oral presentation at the TECO-2000.

compared to the WRR for the first time.

Measurements were taken on 10 days of which 8 days provided very good to excellent measurement conditions and were used for the final evaluation. Time on the other days was used for technical preparation, training of the participants and for a symposium on meteorological radiometry.

The measurements are taken in runs lasting 21 minutes with a basic cadence of 90 seconds. Each instrument is operated with its standard equipment which avoids electrical interface problems and mutual interferences. For each instrument the irradiance is obtained with the corresponding evaluation procedure. As during all the IPCs since 1975, the PMO-2 instrument is used as the local reference instrument because it can be operated fast enough to provide an irradiance value every 90 seconds. At the end of its open phase, 8 readings are taken in rapid succession. The standard deviation of these 8 readings is used during the final evaluation as a quality parameter to judge the stability of the radiation during each measurement.

Several criteria are used to select the data for final evaluation. A first criterion eliminates the influence of the local horizon entering the view limiting angle of the instruments, specially for the Ångström-pyrheliometers. A second criterion rejects sequences when the standard deviation of the 8 rapid PMO-2 readings is larger than 0.3 Wm^{-2}. The final criterion applies on each individual instrument: a filter rejects measurements as outliers with a deviation of more than 1% from the mean ratio to WRR of that instrument.

3. Determination of the WRR

The main objective of the periodic Pyrheliometer Comparisons is the dissemination of the World Radiometric Reference (WRR). For the traceability of the WRR from IPC-VII to IPC-VIII four instruments of the WSG were used: PMO-2, PMO-5, CROM-2L and CROM-3R. The remaining three instruments, PAC3, MK67814 and HF18748, had various instrumental problems (flies had entered the cavity of 2 instruments and the electronic control box of the third instrument was deficiant). Therefore, these instruments were not included for the transfer of the WRR but have been recalibrated during the IPC-VIII and thus are again valid members of the WSG.

For the evaluation of the results, the WRR is determined as follows: In a first step the irradiances of all the WSG radiometers are scaled to WRR by their WRR factors[1] either from the IPC-VII (PMO-2, PMO-5, CROM-2L and CROM-3R) or estimated from the results of interim comparisons (PAC3, MK67814 and HF18748). They are listed in the second column of Table 1. For the 255 sequences where all 4 instruments had valid irradiance values their average is used as reference to calculate the ratio of each measured irradiance to that reference. In a second step the mean and standard deviation of these ratios are calculated for all WSG pyrheliometers. They are listed in column 3 and 4 of Table 1. The mean of the ratios for the 4 radiometers tracing the WRR from IPC-VII amounts to 0.999998 with a standard deviation of 0.000222. The mean being very close to one demonstrates the stability of the 4 WSG instruments and the careful maintenance of the WRR.

For the final evaluation of the participants' instruments the ratios of column 3 are used to calculate for each sequence the WRR as the mean irradiance of all WSG pyrheliometers that are available at a given sequence. This means that the final ratios of the WSG instruments as listed in column 5 of Table 1 are slightly different from the ones in column 3. Moreover, to remove outliers from the WSG the following criterion is used: if the standard deviation of the reference irradiance is greater than 5 Wm^{-2} the individual WSG value which causes this deviation is rejected.

Table 1: WRR-factors of the WSG instruments. The first column gives the instrument names, the second their WRR-factors as determined during IPC-VII. The third column gives the ratio to WRR obtained at IPC-VIII using the WRR-factors of IPC-VII and column 4 gives their standard deviation. The last column gives the WRR factors obtained at the IPC-VIII.

Instrument	WRR factor IPC-VII	Ratio to WRR IPC-VIII	Standard deviation	WRR factor IPC-VIII
PMO-2	0.99944	1.00058	0.0015	0.99936
PMO-5	1.00063	0.99909	0.0014	1.00091
CROM-2L	1.00294	0.99706	0.0018	1.00290
CROM-3R	0.99890	1.00137	0.0033	0.99897
PAC3	1.00027	0.99818	0.0014	1.00186
MK67814	1.00094	0.99936	0.0015	1.00068
HF18748	0.99576	1.00402	0.0015	0.99595

The stability of the WRR can be further checked by calculating the average ratio over all pyrheliometers that have also participated in the previous IPC. Taking all instruments (39, including the WSG instruments) the average amounts to 0.999658 with a standard deviation of 0.001334. If instruments with a ratio deviating by more than 0.3% (0.2%) are rejected, the average is 0.999710 (0.999832) with 37 (35) instruments remaining. These results certainly confirm the conclusion from the results of the WSG alone that the WSG instruments have been very stable.

Finally the ratio and its standard deviation to the WRR is determined for each instrument that participated at the IPC and a recommended WRR- or calibration-factor is derived.

[1] The WRR factor is the value by which the instrument's readings (referred to its calibration factor) have to be multiplied in order to obtain the WRR irradiance values.

4. Approval and Dissemination of the Results

Since 1990 the WMO decided to nominate an ad-hoc Working Group from among the participants of the IPC to discuss the WRR factors of the WSG instruments to be used for the final evaluation. The official approval is documented in a CIMO-Recommendation.

5. Stability of the WRR over the years

Figure 1 shows a summary of the WRR-factors for the WSG instruments as obtained during the last 4 IPCs. It shows that in general the instruments are very stable. A few exceptions are observed and can be traced back to some specific problems having occurred to the instruments. The very large jump observed for MK67814 (crosses) between IPC-VI and VII is due to a damage inflicted to the instrument: the aperture was damaged during an attempt to measure it in order to better characterize the instrument!

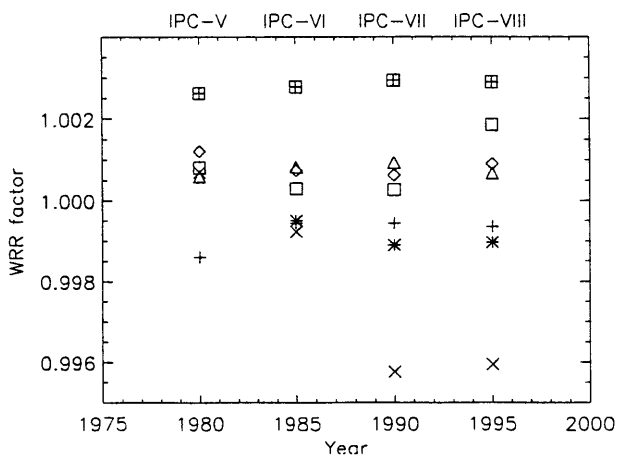

Figure 1: WRR-factors of the WSG instruments obtained during the last 4 IPCs. The plus signs refer to PMO-2, the diamonds to PMO-5, the squares filled with plus signs to CROM-2L, the stars to CROM-3R, the empty squares to PAC3, the triangles to MK67814 and finally, the crosses denote HF18747.

6. From IPC-VII to IPC-IX

Figure 2 shows an overview of the WSG instruments' performances over the last 10 years. For each day on which the WSG instruments were operated, the average deviation of each instrument's reading relative to the WRR is plotted. In each instrument's plot, the horizontal dashed line represents the WRR, defined as explained in Sect. 3. The points plotted light gray on the figure were not taken into account for the determination of the WRR.

This figure shows that at least 4 (PMO-2, PMO-5, CROM-2L and HF18748) of the 7 instruments are performing very well over the whole period.

The lack of points for MK67814 from 1996 to 1999, is due to incorrect operation of the instrument due to a change in the control electronics and a change of personnel. The newly developped electronics had some problems when it operated first in fall 1999. As the most recent measurements show this has been fixed and the results demonstrates that the instrument did not change.

The decaying performance of PAC3, the oldest instrument in the group, is also worrying. Its reason is unfortunately not yet known.

Finally, the large scatter exhibited by CROM-3R is believed to be due to a bad adjustment of its control electronics.

This graphical representation demonstrates the importance of periodically verifying the WSG members in order to insure the stability of the WRR and to detect malfunctions early enough to investigate possible causes. Information on the performance of the WSG members traceable over time is essential, because at the time of the next IPC (25 September to 13 October 2000), only those instrument that have functioned perfectly over the whole period since the previous comparisons may be used to establish the WRR and consequently, the ratio to the WRR for all instruments participating in the comparisons. So, for IPC-IX the following instruments will be used: PMO-2, PMO-5, CROM-2L and HF 18748.

References

1. Fröhlich C.: 1991, Metrologia 28, 111
2. CIMO VII Session: 1978, Annex IV, WMO No. 490, World Meteorological Organization, Geneva
3. Romero J., Fox N. P., Fröhlich C.: 1991, Metrologia 28, 125
4. Romero J., Fox N. P., Fröhlich C.: 1995/96, Metrologia 32, 523
5. Technical Regulations: 1979, No. 49, World Meteorological Organization, Geneva
6. PMOD/WRC International Pyrheliometer Comparison IPC-VIII, Results and Symposium 1996: Swiss Meteorological Institute, Davos & Zurich, Working Report No. 188

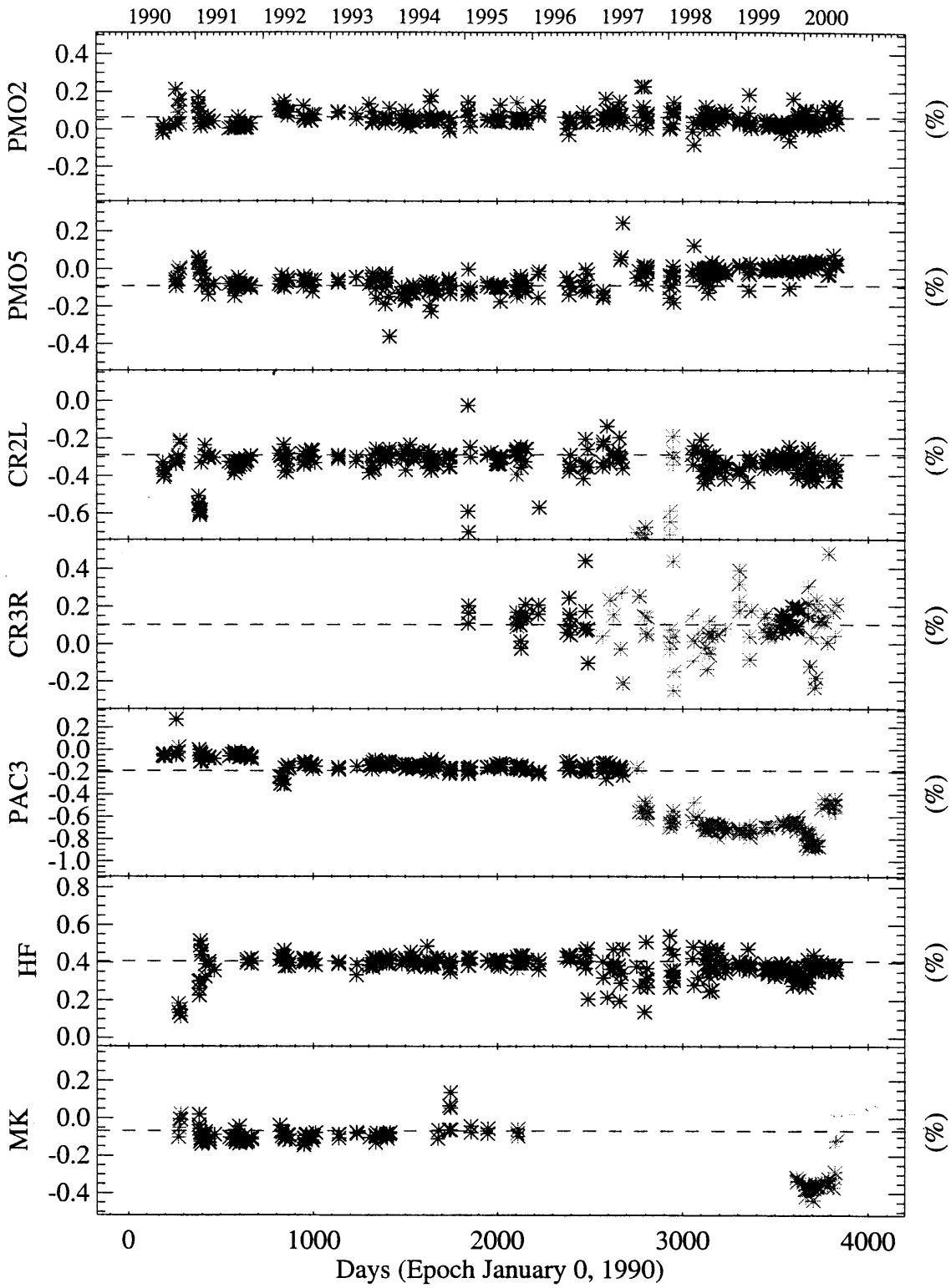

Figure 2: Deviation from the WRR in % for the WSG instruments for the period between 1990 and present. The dark gray points represent the IPCs. For the whole period the WRR was determined using the WRR factors of IPC-VIII. The points plotted light gray were not used for the determination of the WRR. For each day of comparison, the daily average value is plotted.

Evaluation of the latest Laser Cloud Base Recorders 1998 – 1999

C.S. Muller, D.B. Hatton, D.W. Jones
The Met. Office, Beaufort Park, Easthampstead, Wokingham, RG40 3DN. United Kingdom
Tel. +44 (0)1344 855828, Fax. +44 (0)1344 855897, Email. csmuller@meto.gov.uk

Introduction

Laser Cloud Base Recorders (LCBRs), or ceilometers, are now a standard instrument for measuring cloud height both as an aid to observers and as part of the suit of instrument sensors deployed on automatic weather stations. Advances in computing, electronics and optical technologies have resulted in significant developments in capability over what was the norm less than ten years ago such that instruments with a claimed range of 20,000ft or more and 25ft resolution are now readily available from a number of manufacturers.

The Met. Office's standard instrument for cloud height detection is the Belfort 7013 ceilometer. The instrument has the capability of reporting cloud height in excess of 20,000ft, but like all of those that were available 10 years ago, it has deficiencies during some precipitation events. This was resolved at manned observing stations as the detailed backscatter profile could be viewed, and had subtle information that the instruments computer processing was unable to reliably interpret and report. LCBR technology has advanced in the last 10 years. This trial was undertaken between December 1998 to June 1999 to determine the suitability of modern instruments, especially for use at fully automated observing sites.

1. Description of instruments and Experimental Site.

An investigation into the quality of measurements made by the LCBRs currently available on the market was undertaken between December 1998 to June 1999. Seven LCBRs including the Belfort 7013C, Vaisala CT25K, Handar 450C, Impulsphysik LD-25 and LD-40, were deployed in conjunction with a Vaisala Present Weather Sensor (model: FD12P). All of the ceilometers claimed to be able to detect cloud at altitudes in excess of 20,000ft.

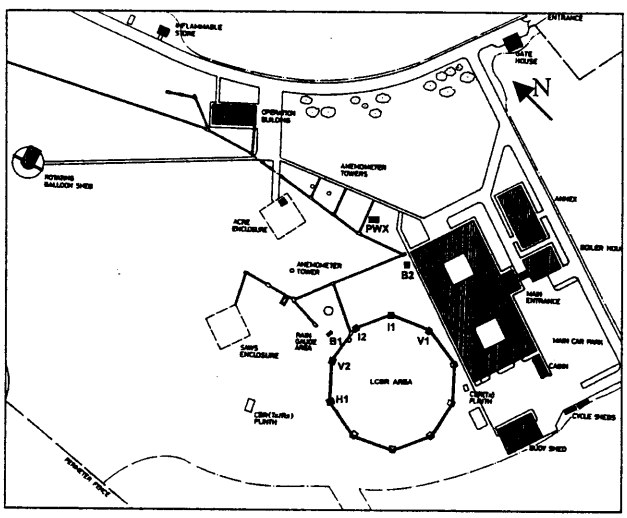

Figure 1: LCBR Deployment Site Plan at Beaufort Park

The location chosen for the intercomparison was The Met. Office's experimental site, Beaufort Park, 4km SW of Bracknell, 80m above mean sea level, using the location established for the WMO ceilometer intercomparison in 1986[1]. Each instrument was positioned around the circumference of a circle, separated by at least 20m from its nearest neighbour in order to avoid optical interference.

2. Experienced Weather

Beaufort Park is not an operational manned observing site. Only a limited number of observations were made, and only during specific meteorological phenomena.

To categorise the performance under different weather conditions the data set was subdivided into different weather types according to the observations recorded using an onsite Vaisala FD12P present weather sensor (PWx). It is recognised that such sensors may differ from a 'clinical observation' made by a local observer[2] but was considered suitable for this analysis.

Table 1 illustrates the breakdown of the weather reports during the trial.

	Hours	%
Fog	37.9	1.3
Mist	711.2	23.7
Snow lt	4.9	0.2
Drizzle lt	77.4	2.6
Drizzle mod	58.7	1.9
Driz hvy	2.5	0.1
Rain lt	118.6	4.0
Rain mod	35.8	1.2
Rain hvy	10.3	0.3
Dry/clear	1942	64.7

Table1: Present Weather reported during the trial period

3. Data Analysis

From the 1 minute logged PWx data, ceilometer observations were divided into the dominant weather conditions, sorted in time order.

As there were few manual cloud height observations made during the study the median LCBR height was used as a basis for the sensor inter-comparison. The median cloud height was calculated when four or more of the LCBRs reported a cloud height for a single measurement period.

Even small differences in the spatial separation of the ceilometers or in the times of measurement, can result in significant variations in cloud base such that direct comparison of minute resolution heights, for example in a scatter plot, would yield unmeaningful results. To overcome this problem a number of analysis techniques were used. One such method is Empirical Quantile-Quantile plotting[3] (EQQ), previously used in the WMO ceilometer intercomparison in 1986[1], (see figure 2).

Other analyses were made when a relatively uniform layer of cloud (e.g. stratocumulus) was in the field of view of the ceilometers. These included assessment of the variation in cloud height reports derived from the root mean square of the differences between LCBR observations. Coefficients of variation were also calculated for the individual sensors.

4. Results

Lack of space precludes an exhaustive description of all the analysis methods used in this paper, and their results. A detailed report is being produced[4] and some of the important findings are presented below.

4.1 Consistency of Measurement

In fine, dry conditions with visibility in excess of 1000m all of the ceilometers were able to detect cloud with equal capability up to an altitude of ~6,000ft as seen by how close the reports are to the median lines in the EQQ plots of figure 2. Significant deviations occur above ~6,000ft for some ceilometers.

Figure 3 demonstrates the relative ability of a selection of instruments to report cloud in different height ranges. The Impulsphysik LD-40 is clearly able to detect a greater proportion of cloud at higher altitudes than either the Belfort 7013C or Vaisala CT25K. This may be a result of this instruments claimed upper range of 43,000ft.

Figure 4 demonstrates that when monitoring the same cloud layer, different makes of instrument can exhibit clear systematic differences in the reported heights. In this example, under clear dry conditions, differences of the order of 150ft were observed for cloud heights between 1,200 and 2,000ft. It is not known whether this difference is maintained over the whole operating range.

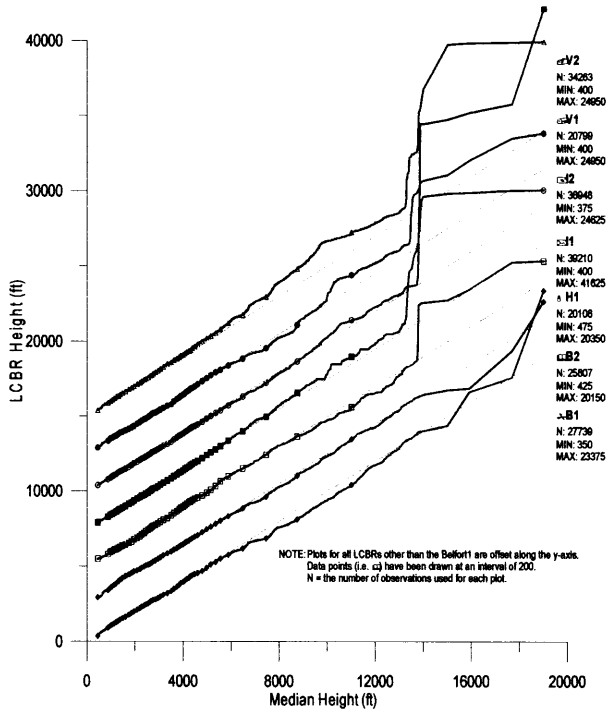

Figure 2: EQQ Plot of level 1 heights from each LCBR, observed in precipitation free conditions between the 19th February - 31st March 1999.

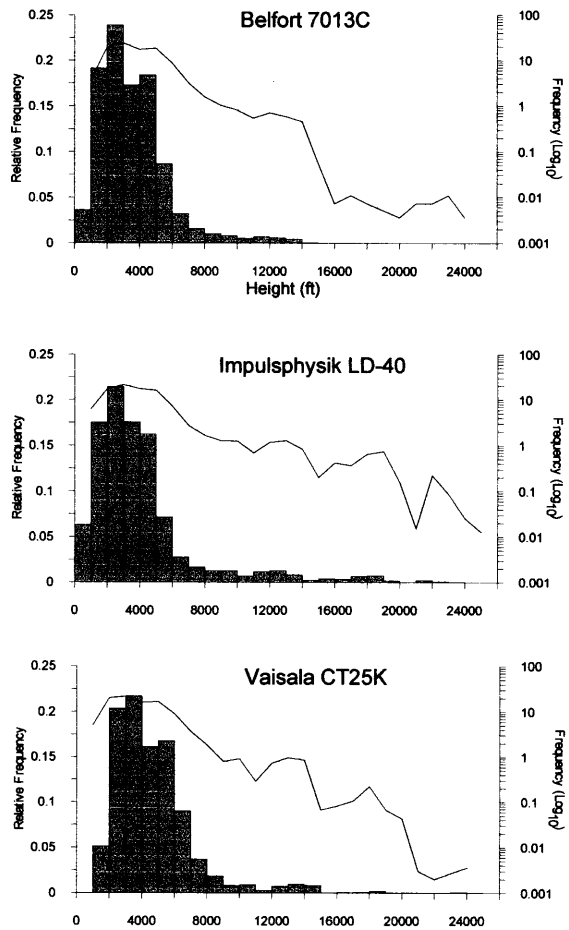

Figure 3: Example histograms of cloud base reports generated by three of the evaluated LCBRs observed in precipitation free conditions between the 19th February - 31st March 1999. The left-hand axis relates to the histogram bar chart, the right to the plotted frequency line.

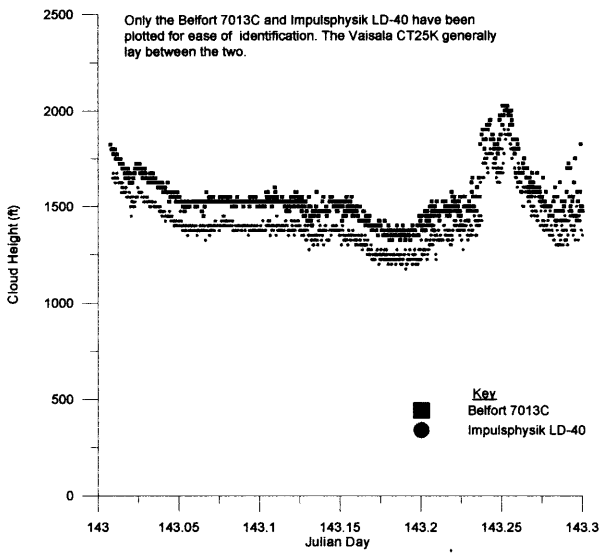

Figure 4: Real Time plot of cloud detected by two of the ceilometers during dry conditions.

No degradation in the quality and accuracy of measurement was observed by any of the instruments over the 6-month period.

4.2 Solar Radiation Effects

To see if solar radiation had any effect upon the LCBRs performance, data was segregated into day and nightime observations. During daylight hours the instruments were sometimes found to have difficulties in reporting cloud at altitudes above 6,000ft. No such limitation was found during nightime hours. Solar radiation may therefore be causing an increase in the signal to noise ratio of the return pulses, limiting cloud detection.

4.3 Precipitation

Some form of precipitation (drizzle, rain or snow) occurred for approximately 10.3% of the deployment period. Accurate cloud reports from ceilometers under these conditions are particularly important both when used as an aid to an observer and when part of a fully automatic observation.

Droplet size and precipitation intensity had a significant effect on the detection characteristics of the LCBRs on trial. Figure 5 illustrates the percentage of reports, which failed to identify a cloud layer under each precipitation category. The correct identification of cloud under these conditions is not uniform. One of the main difficulties with any LCBR trial is to substantiate whether the cloud base height reported is true.

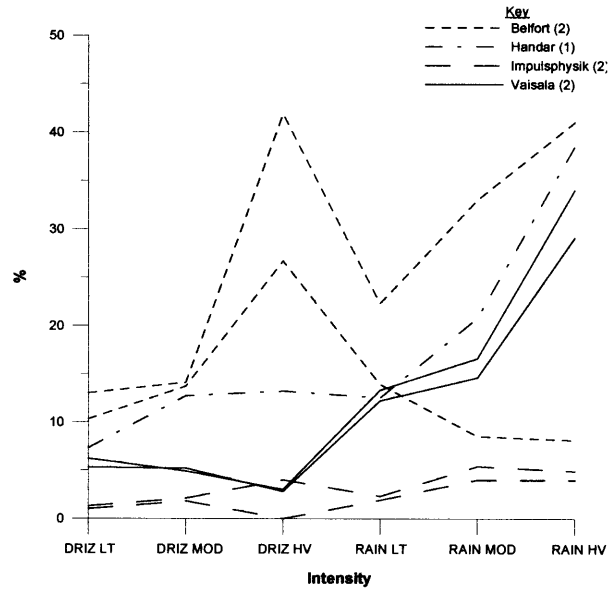

Figure 5: Percentage of reports generated by the ceilometers failing to identify a cloud layer with increasing precipitation intensity

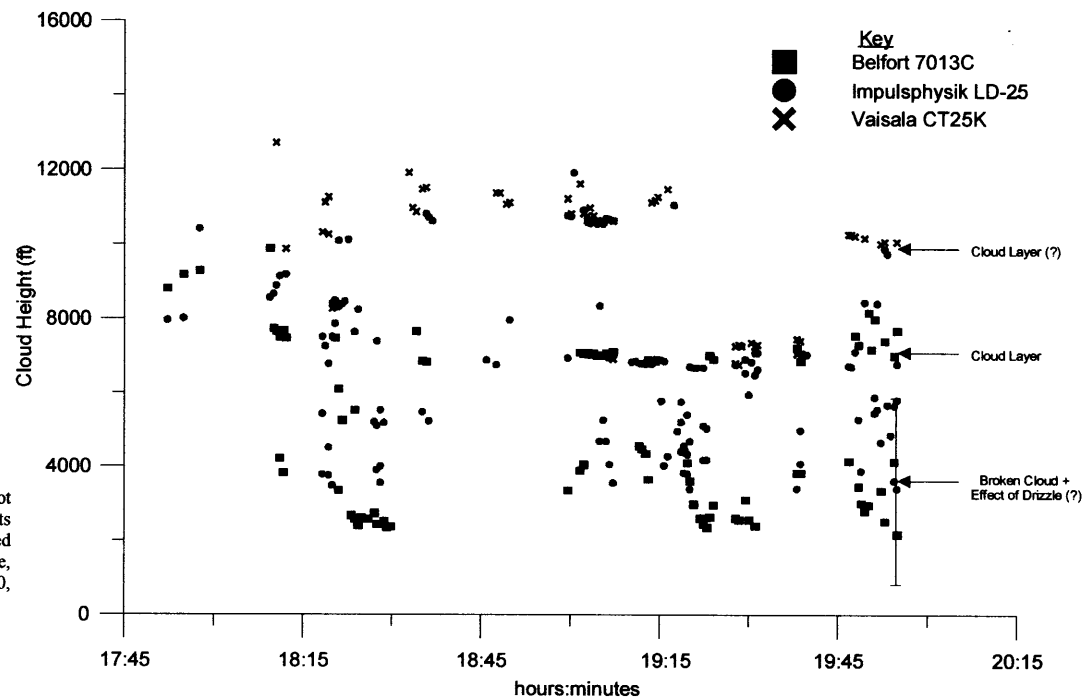

Figure 6: Real Time plot of cloud height reports by three of the studied LCBRs in light drizzle, between 17:45 – 20:10, 11th March 1999

Figure 6 illustrates cloud base observations reported by a Belfort 7013C, Impulsphysik LD-25 and a Vaisala CT25K during a period of light drizzle. The Belfort and Impulsphysik, and on occasion the Vaisala, identified a cloud layer between 7,000–8,000ft. Another cloud layer was identified by the Impulsphysik and Vaisala between 10,000-12,000ft, but was generally missed by the Belfort. However a further cloud layer between 2,000-6,000ft was identified by both the Impulsphysik and Belfort, with the Vaisala tending to report either a vertical visibility value comparable to the Belfort and Impulsphysik's cloud height reports, or sky obscured.

4.4 Visibility

During fog conditions only the Vaisala CT25K correctly identified its presence, reporting a visibility value rather than a cloud height. All of the others reported cloud at an altitude of between 25-300ft. However in general the Vaisala CT25K produced more vertical visibility and sky obscured reports than any of the other ceilometers.

The Belfort 7013C and Vaisala CT25K reported more cloud with increasing horizontal visibility when compared to the other ceilometers, suggesting that the detection capabilities of these instruments are linked to atmospheric clarity.

5. Discussion

Cloud base height is inherently difficult to measure; together with the human observer, ceilometers are the primary instrument for measuring cloud base height. Consistency of measurement is vital in providing accurate observations, particularly for aviation safety. This trial has identified that the heights of the clouds reported by LCBRs differ between the make and model. Differences in the order of 150ft (as reported in paragraph 4.1), whilst not important for high cloud, may be significant for very low clouds.

It is clear from comparison with previous studies[1] that the use of advanced signal and data processing techniques has resulted in some improvements in the ability of LCBRs to detect cloud during periods of precipitation. However, this report shows that deficiencies still exist, and the ability of ceilometers to detect a cloud layer can be severely diminished in periods of precipitation.

The investigation was made more difficult by the lack of human observations, relying instead on an automatic instrument known to have certain limitations. Future studies may benefit from the use of ground based cloud images and a combination of meteorological observing sources (human and automatic). However it must be recognised that creating the ideal data set can be expensive in terms of trial set-up and subsequent analysis.

6. Conclusions

With today's need to provide more frequent cheaper observations automatically, meteorological sensors need to be accurate, reliable, and provide high quality data in all conditions.

The current state of the art ceilometers have improved since the introduction of the Belfort 7013C into The Met. Office's observing network. However, it is clear that there remain considerable differences between instrument types, and as yet none perform perfectly.

It is also apparent that while manufacturers quote an instrument range for example "0 to 25000ft", there are many occasions when conditions preclude accurate measurement over the whole of this range.

Precipitation and other meteorological phenomena still affect cloud base determination, even those made by the current 'state of the art' LCBRs.

7. References

1. Jones, D.W / Ouldridge, M / Painting, D.J (1988) "WMO International Ceilometer Intercomparison" WMO Instruments and Observing Methods, Report No. 32

2. Leroy, M (1998) "PREWIC, The WMO Intercomparison for Present Weather Sensors" Instruments and Observing Methods, Report No. 70, TECO-98. 19-21pp

3. Murphy, A / Katz, R (1985) "Probability, Statistics and Decisions Making in the Atmospheric Sciences", Westview Press, Boulder, Colo. pp547

4. Muller, C.S (2000) "Results of the Laser Cloud Base Recorder Intercomparison", Internal Technical Report - in preparation

Wind measurements:
potential wind speed derived from wind speed fluctuations measurements, and the representativety of wind stations

Jitze P. van der Meulen
Royal Netherlands Meteorological Institute
Postbus 201, 3730 AE De Bilt, the Netherlands
tel +31 30 2206432, fax +31 30 2210407, e-mail meulenvd@knmi.nl

Introduction

In a previous paper [1] the use of the measured standard deviation of the wind speed to determine and reduce artificial wind gusts is presented. With the help of both the calculated average wind speed U and its standard deviation σ_U and by taking an averaging interval of 10 minutes, the actual wind speed u can be transformed into the *normalised* wind speed u_n,

$$u_n = (u - U)/\sigma_U \qquad (\sigma_U > 0). \qquad (1)$$

In the figs. 1 and 2 it is clearly demonstrated that u_n is independent of u: Significant changes in the wind speed have no remarkable impact on the structure of u_n. In fact u_n is mainly affected by the wind speed fluctuations.

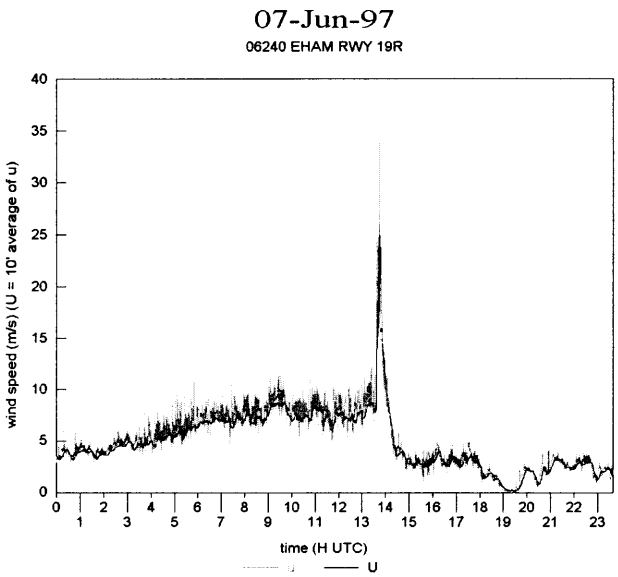

Fig. 1 Measured wind speed (m/s) as a function of time

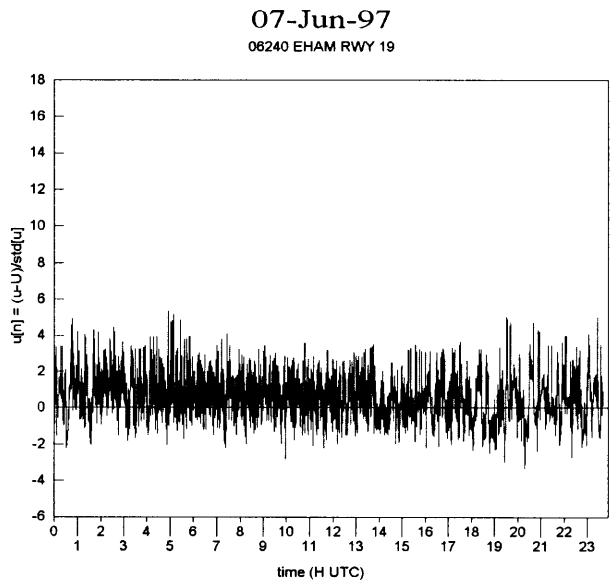

Fig. 2, Determined u_n as a function of time

For the appropriate use of wind speed in meteorology the determination of the potential wind is important [4]. Stated in the CIMO Guide [2] and explained by Wieringa [3] and Beljaars [4], the potential wind speed U_p can be calculated by taking into account he terrain roughness length or with a multiplication factor F, called the *exposure correction factor* (or shelter factor). This reduction factor varies from about 0.9 for a very open terrain to 1.2 for very rough terrain. A method to derive such a factor is described by Benschop [5]. Notice that Benschop demonstrates that F is wind direction dependent, especially for locations close to forests and buildings. As a consequence the potential wind has to be determined as a function of the wind direction as well.

The method to derive this factor is traditionally based on statistical analysis of wind speeds averaged over one hour and the maximum wind speed (gust) observed during that hour (see [5]). In fact, however, this method itself is derived from a relation of U_p with U and σ_U. Therefore, direct

measurements of 10' average values of the wind speed (U) and its 10' standard deviation (σ_U) should produce such a factor as well.

Exposure correction factor F

For the determination of the exposure correction factor F a logarithmic wind profile is assumed [2, 3, 4], *i.e.*

$$U_1/U_2 = \ln(z_1/z_o) \,/\, \ln(z_2/z_o), \qquad (2)$$

where U_x represents the wind speed at height z_x and where z_o is the roughness length of the terrain (see Wieringa [6] for an overview of the use of z_o). From this relation a linear relation between the wind speed U and the potential wind speed U_p, U_p can be derived, *i.e.*

$$U_p = F \cdot U \qquad (3)$$

Assuming a blending height z_b=60m and taking the defined standard for a WMO wind station (*cf* CIMO Guide [2]), where z=10m and z_o=0.03m ("Open terrain") as reference for U_p, it can be demonstrated by using (2) that:

$$F = 0.76427 \,(\, \ln(60/z_o) \,/\, \ln(z_x/z_o)\,) \qquad (4)$$

Beljaars [4] has indicated the relation between z_x/z_o and σ_U/U, which can be derived from measurements of the turbulence of the wind speed, *i.e.*:

$$\sigma_U/U = 1 \,/\, \ln(z_x/z_o) \qquad (5)$$

Note that both relations (3) and (5) should only be used for $20z_o<z_x<100$m and with averaging intervals of 10 min. Moreover, these relations will only have any physical significance for wind speeds of about 5 m/s or above. From the mathematical point of view it is rather obvious that both U and σ_U should be far from zero. By taking relation (5), the exposure correction factor F can be derived in terms of σ_U/U from eq. (4), *i.e.*

$$F = 0.76427 \,(\, 1 + 1.79176 \cdot \sigma_U/U\,) \qquad (6)$$

Measurements of σ_U/U and the determination of F

In the national meteorological network in the Netherlands use is made of a standard automatic wind measuring system. With this system wind speed and direction are measured continuously and apart from the actual values, also the 10' averages and standard deviations are presented every 12". Values of both σ_U and U are calculated from sequential 3" samples of u, the actual wind speed. Figure 2 is an example for which use is made of u, U and σ_U to show u_n.

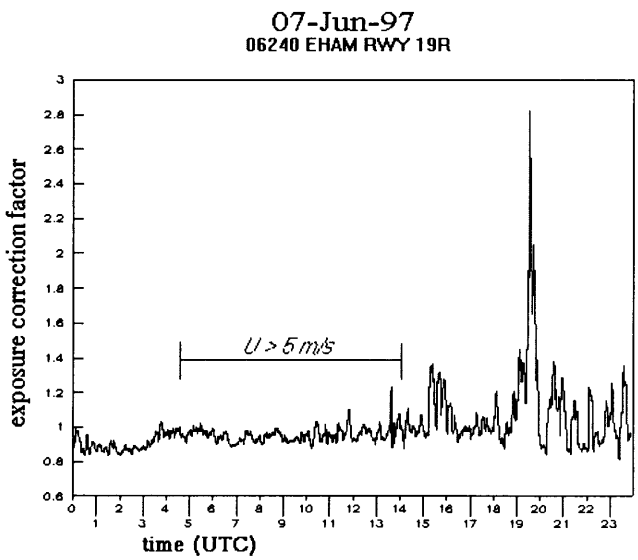

Fig. 3, F as a function of time

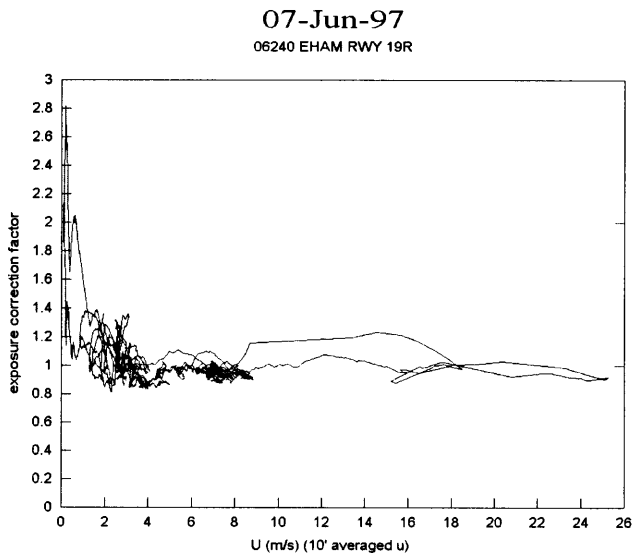

Fig. 4, F plotted versus U

In fig. 3, F is presented as a function of time and for the same period as in figs. 1 and 2. Note the rather bizarre behaviour of F after approx. 15:00 UTC. This behaviour can easily be explained since the constraint with $U>5$m/s is not fulfilled at that time. In this figure the interval for which U>5m/s, is 05:00 to 14:30 UTC, when F is stable. By plotting F versus U this statement can easily be understood since F is rather constant with wind speeds above 5 m/s (see fig. 4). Using the data set of F for $U>5$m/s, statistical analysis will provide an average value of F and its uncertainty, shown as a bar graph in fig. 5. From this set it follows that F = 0.96±0.05 (data measured on 07-June-1997 at WMO 02240 - Amsterdam Airport Schiphol, EHAM-RWY19R).

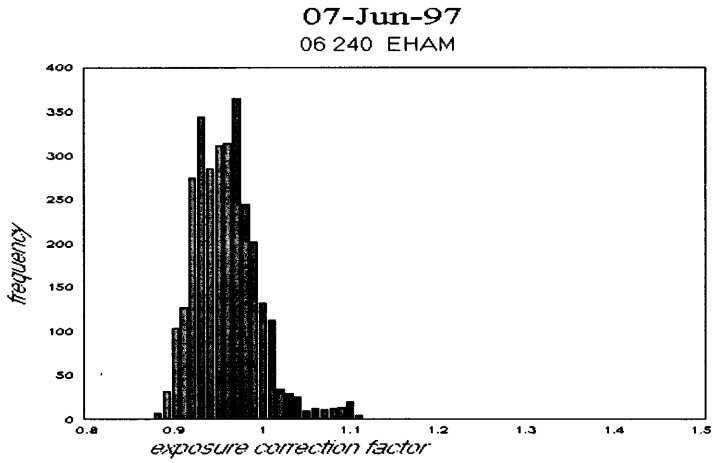

Fig. 5 Frequency distribution of F. From this distribution it follows that F = 0.96±0.05

Representativity and the exposure correction factor

Wieringa [6, 7] has stated that potential wind data are excellent material for interpolation with distant wind stations or for large-scale mapping of wind. This statement can be illustrated by comparing two nearby wind stations, but with a rather different siting: 1) WMO 06248 (Wijdenes), 52°38'N, 05°10'E, and 2) WMO 06249 (Berkhout), 52°39'N, 04°59'E. Both stations have a mutual distance of 13km. The first station is situated on a shoreline besides a dike with flat open water in the SE and a rather rough terrain in the NW. For this purpose a wind data set of May 2000 is used consisting of 10' average values and the associated standard deviations. Wind speed values with $U>5$m/s are selected for data analysis. Data of U and σ_U where used for the determination of F_1=F[06248] and F_2=F[06249]. Since F will be dependent of the wind direction (see Benschop [5]), F_1 and F_2 are derived for the various wind sectors. In fig. 6, F_1 and F_2 are presented as a polar diagram giving a bright impression of both F

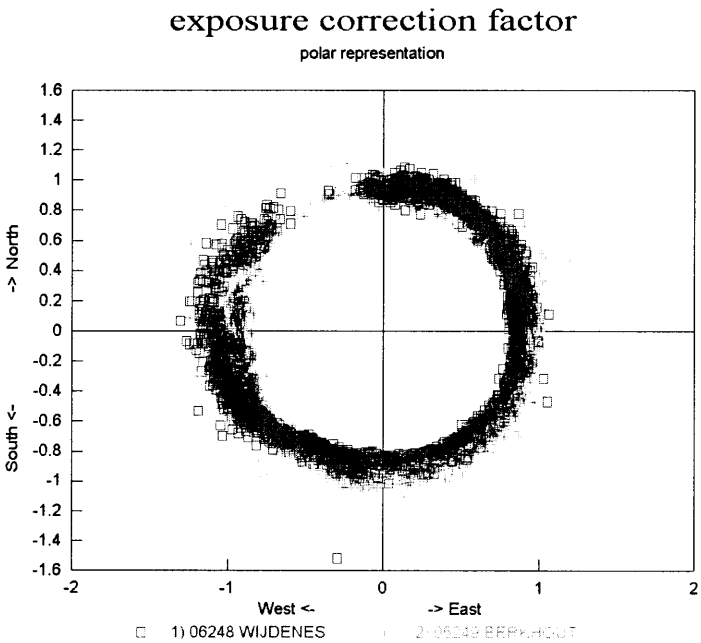

Fig. 6, a polar diagram of the values F_1 and F_2 calculated directly from eq. (6) using the 10' average values U and σ_U. from May 2000. Only values, with U > 5m/s are used. Note that during this period wind from the NNW was scarce. Note also the typical differences for both stations, which can easily be explained by the terrain circumstances of 06248 (Wijdenes): Open water in the SE, rough terrain in the W.

for the various wind directions. In fig.7, F_1 and F_2 are presented as a function of the wind direction, but *averaged* over intervals of 20°. By taking into account these factors the values of U for both stations can be converted into their potential wind speeds U_p for further comparison. A measure for representativety of a station for a specific area can be determined after calculating the correlation coefficient R of a wind speed data set of two nearby stations. To determine this coefficient, data of U from both stations are used, *i.e.* $R = R(U_1, U_2)$. It is found that:

R(measured 10' averaged wind speed) = $R(U_1, U_2) =$ 0.795
R(potential 10' wind speed) = $R(U_{p,1}, U_{p,2}) =$ 0.917

The result, $R(U_{p,1}, U_{p,2}) >> R(U_1, U_2)$ demonstrates the usefulness of exposure correction.

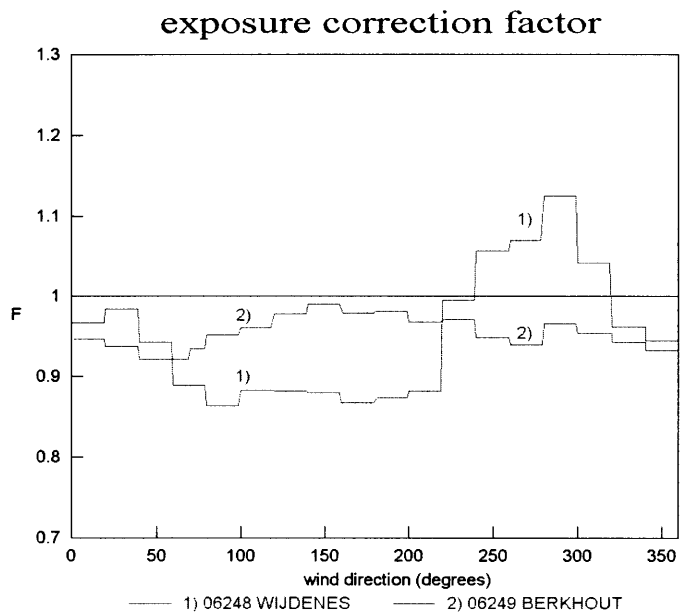

Fig. 7, F_1 and F_2 calculated after averaging and for wind direction sectors of 20° wide (see also fig. 6)

Conclusion

Turbulence measurements as part of operational meteorological observations for synoptical purposes provide direct information of terrain roughness. The method using standard deviations is a simple tool for the calculation of the potential wind speed providing a higher degree of representativity.

References:

[1] Van der Meulen, J.P.(1998), "Wake Vortex Induced Wind Measurements at Airfields" (presented at TECO-98), in Instruments and Observing Methods report No. 70 (WMO/TD - No. 877, WMO, Geneva, 1998), pp 139.

[2] Guide to Meteorological Instruments and Methods of Observation (WMO-No. 8, sixth ed., WMO, Geneva, 1996)

[3] Wieringa, J. (1973): "Gust factors over open water and built-up country," Boundary-layer Meteorology 3(1973)424

[4] Beljaars, A. (1988): "The Measurement of Gustiness at Routine Wind Stations" (presented at TECO-1988), in Instruments and Observing Methods report No 33 (WMO-TD No. 222, WMO Geneva, 1988), pp. 311

[5] Benschop, H. (2000), "Representativity of wind measurements in The Netherlands", this conference report.

[6] Wieringa, J.(1996), "Representativity of Extreme Wind Data", in "Hydrology of Disasters" (ed. V.P. Singh, Publ. Kluwer, Netherlands, 1996), pp. 19.

[7] Wieringa, J.(1997), "Representativity problems of wind stations", E.U.-COST Seminar on Data Spatial Distribution in Meteorology and Climatology, Voltera, Italy, 1997.

COMPARAISON ENTRE UNE STATION METEO TRADITIONNELLE ET UNE STATION METEO AUTOMATIQUE

Beltrano Maria Carmen, Perini Luigi
Ufficio Centrale di Ecologia Agraria (UCEA), Via del Caravita 7/A 00186 Rome – Italy
Tel. 0039 06 6793376 -06 6793804 - fax 0039 06 69941564
E-mail: cbeltrano@politicheagricole.it; l.perini@politicheagricole.it

Prémisse

Depuis sa création en 1879 le siège de l'Ufficio Centrale di Ecologia Agraria (UCEA), organe scientifique et technique du Ministère des Politiques Agricoles et Forestières (MIPAF) qui opère dans le domaine de l'agrométéorologie, se trouve en plein centre de Rome dans les locaux du Collège Romain. Dans ces mêmes locaux se trouve le plus ancien observatoire de Rome connu sous le nom de *"Roma - Collegio Romano"*. Sa création, dûe aux Jésuites qui à l'époque occupaient les locaux du Collège, remonte à la moitié du 16e siècle. L'observatoire était déjà à l'époque réputé en Europe pour sa valeur scientifique. A partir de 1782, des observations météorologiques régulières commencèrent à être faites et en 1787, la Tour Calandrelli (haute de 66,4 m s.l.m) qui domine la place du Collège Romain au cœur de Rome, fut construite à des fins de pur Observatoire.

Jusqu'à présent les observations ont toujours été faites au même endroit, et ce en utilisant des instruments de plus en plus modernes mais dont les mesures se sont toujours avérées être comparables aux précédentes, permettant ainsi d'établir en 200 ans d'observations une série de données homogènes. L'importance scientifique de l'Observatoire de Rome – Collège Romain repose sur cette longue série de données congruentes qui constitue une base efficace pour l'étude du climat de Rome et de ses variations climatiques liées aux effets de l'urbanisation.

Introduction

Depuis Août 1998, une station automatique Campbell CR10, appartenant au Réseau Agrométéorologique National du Ministère des Politiques Agricoles et Forestières, a été placée aux côtés de la station traditionnelle. Pendant un an et demi les deux stations météo ont fonctionné en même temps l'une à côté de l'autre. Les mesures provenant de l'instrumentation traditionnelle et de cellê automatique ont été comparées et analysées de façon à évaluer si l'on pouvait encore considérer les données météorologiques du Collège comme étant homogènes. Dans le tableau 1, les caractéristiques techniques et fonctionnelles des instruments employés par les deux stations sont reportées.

Tabeau 1 - **ROMA COLLEGIO ROMANO CARACTERISTIQUES TECHNIQUES DES DEUX STATIONS DE MESURE**

STATION TRADITIONNELLE

INSTRUMENTS	CARACTÉRISTIQUES	UNITÉ DE MESURE	ETENDUE DE L'ÉCHELLE	PRECISION	SENSIBILITÉ
Abri météorologique	Bois de larix				
Thermo - hygrographe	À lame bimétallique À cheveux	°C %	- 15 + 45 °C 0 - 100 %	±1 % ± 3 %	0,5 °c 5 %
Thermomètre à minimum	À alcool	°C	- 30 + 50 °C	± 0.2 °C	0.2 °C
Thermomètre à maximum	À mercure	°C	- 30 + 50 °C	± 0.2 °C	0.2 °C
Psychromètre d'August	À ventilation artificielle 6 m/s	%	- 30 + 50 °C	± 0.2 °C	0.2 °C
Pluviographe	Collecteur 10 dm^2	mm	10 mm	± 2 %	0,2 mm
Baromètre Fortin	À mercure	mmHg		± 0,5 %	0,1 mmHg
Barographe	Anéroïde	mmHg	80 mmHg	± 0,5 %	0,5 mmHg
Héliographe	Campbell - Stokes	heures et decimaux			
Anémomètre enregistreur	Girouette Moulinet à coupes	degrés ° km/h	0 - 360° 0 - 100 km/h	± 5° 0,5 - 1,5 m/s	0,5 m/s

STATION AUTOMATIQUE mod. CR10 Campbell

CAPTEUR	CARACTÉRISTIQUES	UNITÉ DE MESURE	ETENDUE DE L'ÉCHELLE	PRECISION	SENSIBILITÉ
Température	Résistance PT100 à ventilation	°C	- 40 + 60 °C	± 0,3 K	0.2 °C
Humidité	Résistance à ventilation	%	0 - 100 %	± 1 %(5 - 95%) ± 2%	0,5 %
Précipitation	Relais	mm		± 0,2 mm	0,2 mm
Pression atmosphérique	Potentiomètre	hPa	0 - 690 bar	± 0,3 %	
Durée d'insolation	Cellule photoélectrique	minutes	0,4 - 1,1 µm	± 3 %	10uV/W/m^2
Direction du vent	Potentiomètre	degrés	0 – 360°	±2%	0,6 m/s
Vitesse du vent	Magnétomètre	m/s		±1% 10-5 m/s) ±2% (>55m/s)	0,2 m/s

Les senseurs de température et d'humidité de la station automatique ont tout d'abord été installés à l'intérieur de l'abri météo sur la façade Nord de la Tour à côté des instruments de type traditionnel. Ainsi, pour s'assurer que les deux types d'instruments répondent toujours aux standards de construction, des contrôles sur la fonctionalité et le

calibrage des deux systèmes de mesure ont été effectués pendant quelques temps. Les données relevées par les deux stations ont été analysées et confrontées quotidiennement, et après une période de tests, le 21 mai 1999, les senseurs de température et d''humidité ont été déplacés à l''extérieur de l'abri météo. Sur la terrasse de la Tour, se trouvent, l'un à côté de l'autre, à peu près à la même hauteur, le collecteur du pluviographe traditionnel et le senseur d'insolation, qui se trouve à environ 8 mètres au dessus de l'héliographe Campbell-Stokes placé, quant à lui, sur le parapet de la terrasse au sud de l'observatoire.

Au cours de la période d'essai, pendant la saison estivale de 1998, il s'est avéré que souvent, en principe durant les premières heures du matin, le senseur des précipitations indiquait quelques millimètres de pluie tandis que le pluviographe traditionnel n'en indiquait pas et en effet il faisait beau temps. Situations inexplicables d'autant plus qu'en présence de précipitations, les deux systèmes de mesure relevaient des données de valeurs très légèrement différentes. Par ailleurs il arrivait parfois d'obtenir des valeurs de rayonnement global horaire qui ne correspondaient pas à celles attendues pour des valeurs correspondantes d'insolation et trop variables au cours de journées belles et chaudes. De même le phénomène ne s'expliquait pas pour les valeurs de rayonnement etant donné que les différences pouvaient se vérifier indifféremment à des moments divers de la journée et donc ne pouvaient être attribuées au calibrage du senseur. Après un certain temps, grace à des contrôles continus le mystère a été dévoilé: il s'agissait d'une mouette qui parfois se posait sur le collecteur du pluviographe provoquant au moment de son décollage des oscillations du mécanisme d'enregistrement du pluviomètre ou parfois se perchait sur le pyranomètre couvrant le senseur et provoquant ainsi des altérations dans les mesures. Ainsi le problème a été résolu en plaçant une protection autour du collecteur du pluviographe et autour du pyranomètre.

Instruments et Méthodes

Entre les mois d'août 1998 et décembre 1999, les deux stations ont fonctionné sans discontinuité et les valeurs relévées ont été analysées et comparées selon plusieurs critères, et ce pour évaluer l'homogénéité des deux séries. Les données examinées dans ce document sont: température minimum, température maximum, humidité entre 8heures et 14heures, insolation, précipitations.

Sur la feuille électronique Excel, les données relevées par chacune des stations ont été ordonnées: les séries ont été établies tenant compte uniquement des données auxquelles était associé le code flag zéro, équivalent à "donnée valable". Les donnés ont été comparées seulement quand les couples étaient complets et valables. La comparaison entre les deux séries de données s'est faite à deux niveaux: tout d'abord des graphiques ont été élaboré avec les couples de séries de données, ensuite des contrôles d'homogénéité ont été faits utilisant le logiciel de statistique SPSS.

Contrôle graphique

Ce test montre le cours des deux séries et leur eventuelle superposition. Une ligne d'interposition a été rajoutée afin de mettre en évidence les différences non accidentelles mais stables en utilisant, selon le paramètre, les régressions polynômiales (comme dans le cas de la température), ou celles linéaires (comme dans le cas de l'humidité).

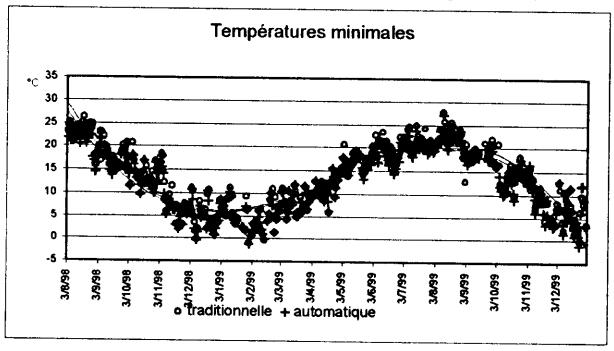

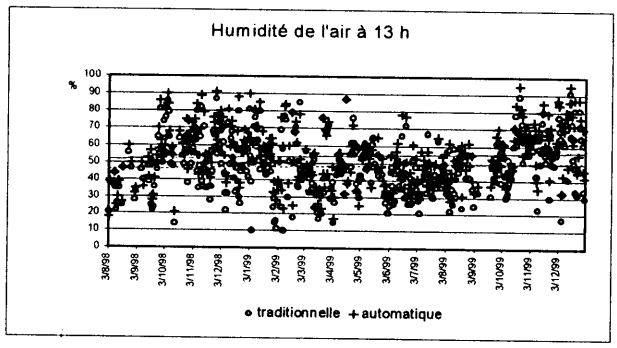

Pour les températures, le graphique relatif aux températures minimales montre une légère sous-estimation des valeurs relevées par la station automatique; cette caractéristique est plus evidente pendant la période estivale. Le grafique relatif aux températures maximales montre une meilleure superposition des deux séries de données.

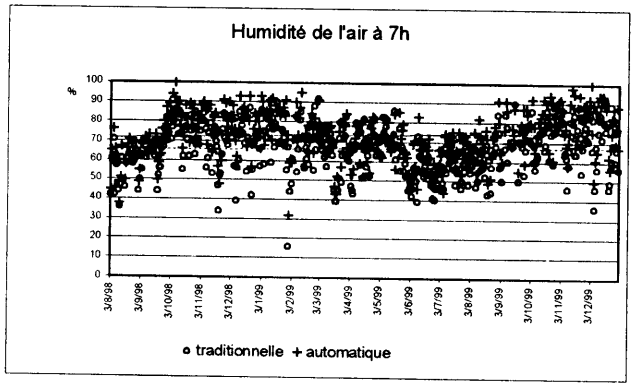

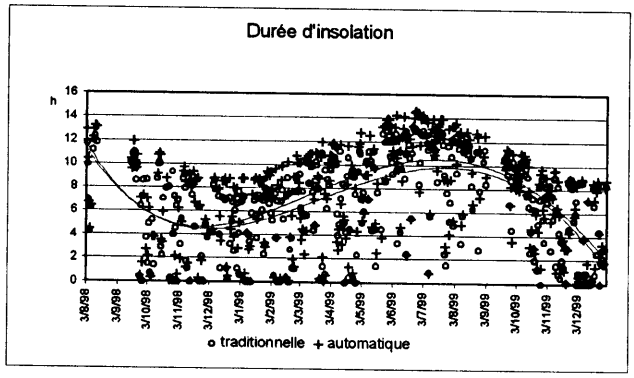

Pour l'humidité de l'air, les grafiques relatifs aux observations de 7:00 h et de 13:00 h, (T.M.E.C.) mettent en évidence une constante sur-estimation de la station automatique pendant toute la periode de l'année. Pour l'insolation, le graphique montre une légère superposition entre les deux séries. Toutefois, les lignes de regression mettent en évidence une sur-estimation de la station automatique pendant la période printemps - été.

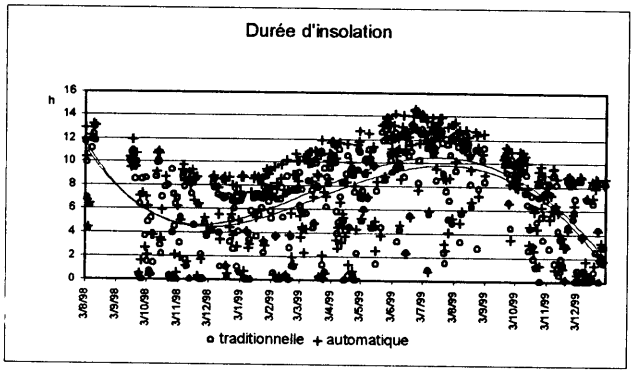

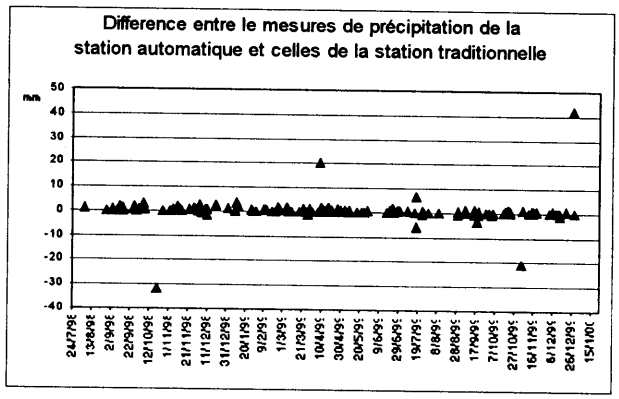

Pour les précipitations, on a pris en considération seulement les cas de pluie remarqués par au moins une des stations; après on a calculé les differences entre les mesures de la station automatique et celles de la station traditionnelle. Ansi, il a été possible de mettre en évidence que, souvent, la station automatique sur-estime les précipitations et surtout de reperer les differences importantes. L'analyse et le contrôle de ces données et des annotations rapportées dans les bulletins d'observation de la station traditionnelle ont permis d'expliquer les cas de grande sur-estimation: la cause a été recherchée, dans tous les cas, dans de fortes chutes de grêle qui ont provoqué l'ébranlement du pluviographe, en causant un certain nombre de basculements qui ne corrispondaient pas à des réelles précipitations.

Tests statistiques

Pour les deux séries de données on a calculé des statistiques descriptives. En particulier, on notera une très forte correlation entre les couples de données de température et insolation, comme le montre le tableau 2.

Pour évaluer les éventuelles differences entre les données, un test sur l'homogénéité des deux séries a été appliqué. Il a été réalisé en employant le test de statistique de Kolmogorov – Smirnov. Ce test a permis d'évaluer objectivement la congruence entre les données relevées par les deux stations. Un test à deux cueux a été effectué, avec significativité du 0,99. Les résultats ont été insérés dans le tableau 3 et confirment une dishomogénéité des mesures d'humidité et de précipitations relévées par la station automatique.

Tableau 2 - Correlation

Paramètres	Station traditionnelle		Station automatique		Correlation
	moyenne	d.s.	moyenne	d.s.	
Température minimum	13,6	6,8	12,9	6,5	0,99
Température maximum	21,0	7,6	21,2	7,5	1,00
Insolation	6,9	3,8	7,4	4,2	0,95
Humidité à 7:00 h	66	12,4	73	12,1	0,93
Humidité à 13:00 h	49	16,2	54	15,8	0,96
Précipitation	3,2*	-	3,2*	-	0,92

* médiane

Tableau 3 - Test de Kolmogorov-Smirnov

Paramètres	n° cas station traditionnelle	n° cas station automatique	difference absolu	Z max de Kolmogorov-Smirnov
Température minimum	464	464	0.075	0.107015
Température maximum	465	465	0.026	0.106900
Humidité à 7.00 h	487	487	0.207	0.104457
Humidité à 13.00 h	425	425	0.155	0.111817
Insolation	418	418	0.100	0.112749
Précipitation	169	169	0.195	0.177321

Conclusion

La sostitution d'une station traditionnelle par une station automatique pose une série de problèmes liés à la continuité de la série historique des données relévées au même lieu. L'expérience conduite à l'Observatoire de Rome Collège Romain témoigne que si pour certaines mesures et certains paramètres il est possible de mettre en évidence un rapport satisfaisant entre les séries de données provenant de la station traditionnelle et celles de la station automatique,

comme dans le cas de la température et de l'insolation. Pour d'autres paramètres, comme l'humidité et les précipitations, les differences peuvent être si importantes qu'il est impossible de considérer les deux séries comme homogènes et continues. Sans doute, on doit rechercher la cause de ces differences soit dans la position differente des senseurs, soit dans les caracteristiques techniques des instruments.

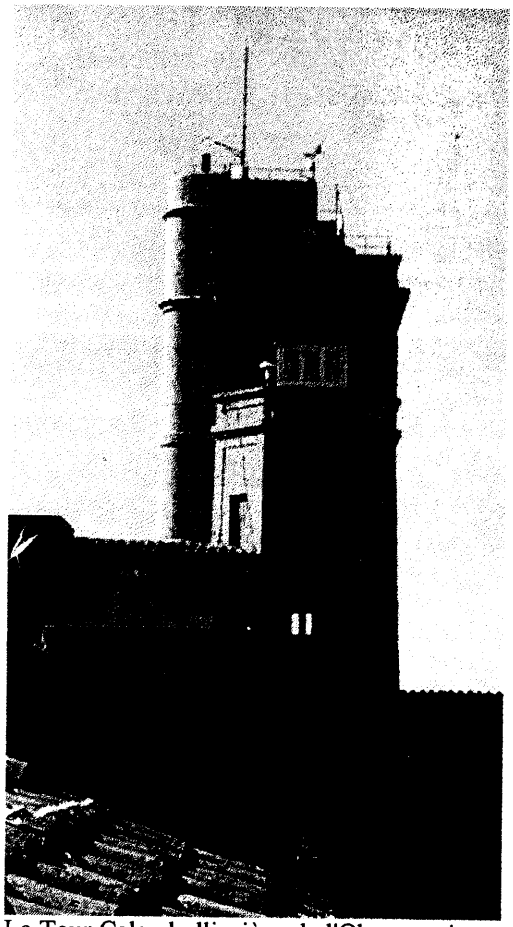

La Tour Calandrelli, siège de l'Observatoire

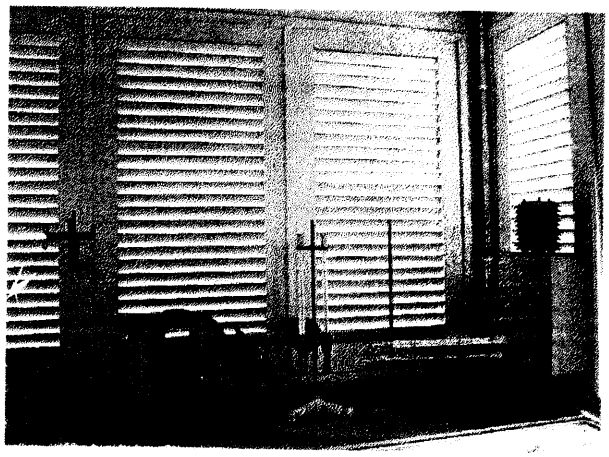

L'abri metéorologique où sont situés les thermometrès, le Thermo - hygrographe, le psycromètre, le senseur de pression.

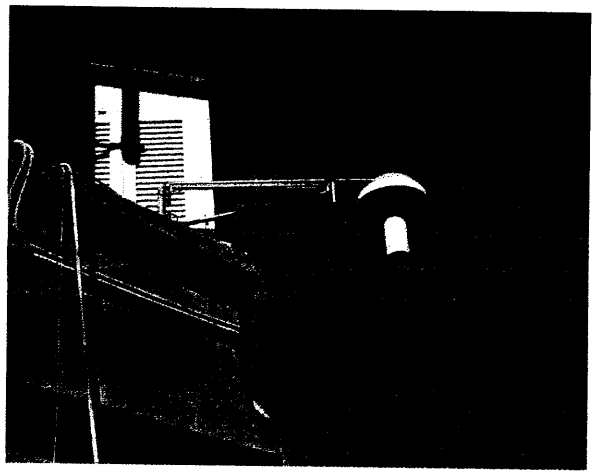

Les senseurs de température et humidité, dehors de l'abri.

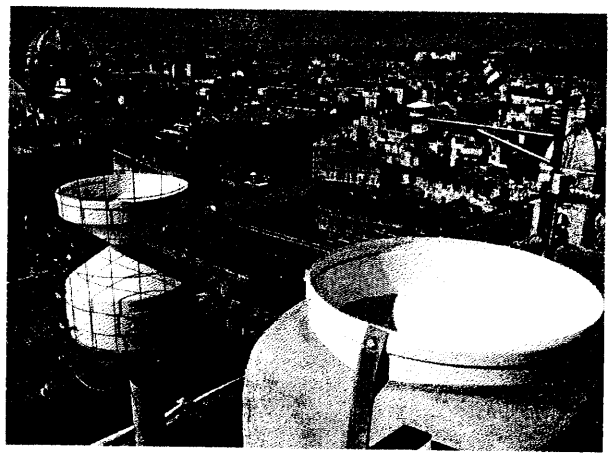

Les pluviographes et en second plan le radiomètre et le senseur d'insolation

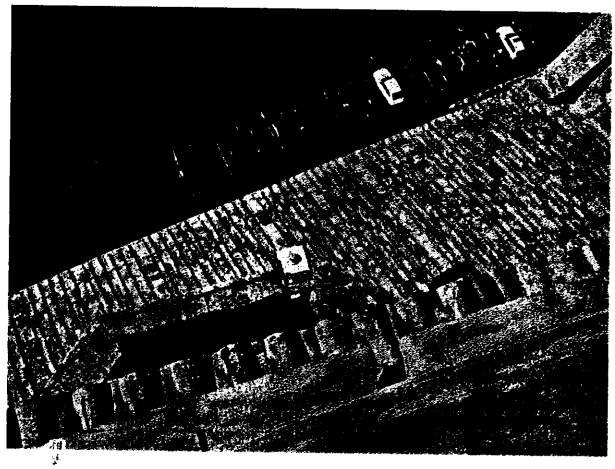

Le radiomètre et l'héliographe au dessous de la terrasse de couverture de la Tour

1 MEASUREMENT TECHNOLOGY, PERFORMANCE, AND QUALITY ASSURANCE

1.1 Surface Observation Systems

1.1.3 Instrument Design

Meteorological sensors for fully automated surface observation systems

Jochen Dibbern, Deutscher Wetterdienst, Postfach 10 04 65, 63004 Offenbach, Germany
Karl-Heinz Klapheck, Deutscher Wetterdienst, Postfach 65 01 50, 22361Hamburg, Germany
Imre Szabó, Deutscher Wetterdienst, Postfach 65 01 50, 22361 Hamburg, Germany

Introduction

The German Meteorological Service (DWD) is currently modernising its ground based observing network (Messnetz 2000). Economical constraints make him to replace parts of the visual observations of the human observer by automatic devices and software algorithms. In addition the data acquisition systems will be improved and changed by more compact or cheaper ones.
New sensors have been tested in co-operation with research institutes and industry. Among others systems for the determination of the precipitation type have been tested and a contract for feasibility studies on the improvement of forward scatter instruments had been placed.

Comparison of Present Weather Sensors (PWS)

The automatic acquisition of many weather elements as for example air temperature, pressure etc. has already taken place because a physical quantity could be simply converted to an electrical quantity suitable for processing , but it is not easy to take a machine and imitate the view of the human eye and its interpretation in the brain, when complex weather phenomena like the present weather are observed. If you have a good camera with remote coupling you can partially replace the human eye and acquire cloudiness, perhaps precipitation. But at the remote station again an observer has to look on a screen. Fortunately devices have been developed that automatically convert the present weather – that means precipitation y/n, type and intensity of precipitation – into an appropriate code number. Will the observer and the devices get the same results? This question made DWD to compare four different Present Weather Sensors with each other and with the corresponding observers messages.
Three of the Present Weather Sensors use optical scattering: type VPF-730 from HSS company, type FUMOSENS from Impulsphysik company and FD12P from Vaisala company, the forth one, type POSS from Andrew company, uses microwave radiation. The optical sensors were installed at Braunlage in the German low mountain range where you have a high frequency of events of liquid precipitation and of solid precipitation in the winter season. The station was permanently occupied by observers during the testing period from July 1995 to May 1997. The POSS was available only at later times and it was installed at Hamburg and the messages from Hamburg airport were taken for comparison in this case [1].
In a first step the discrimination of precipitation y/n and the type were evaluated. The observer always records the present weather observation with the highest ww-code number acc. to WMO Table no. 4677 in the time interval from 20 to 7 minutes before the hour, the sensors send telegrams in one minute or 15 seconds time intervals. The sensor data set was evaluated in the following way to get a representative sensor code number output for the 13 minutes interval: a class number was adjoined to the different code numbers found in the 13 minutes interval, the lowest ww-code is class 1, the next higher code is class 2, etc. The product of class number and the frequency of each ww-code was computed. If there was precipitation, the ww-code with the highest product number was representative provided it was messaged at least two times. If there was no precipitation seen by the observer and the PWS has sent at least two times ww 00-03 (no significant weather) the representative PWS code was set to 00. In the other cases the highest PWS code was taken as representative in the 13 minutes interval, mostly fog or haze event numbers. In this way the percentual correspondences between the human observer and the PWS were calculated and are given in the upper part of Figure 1 for precipitation y/n, drizzle, rain, snow, liquid and solid precipitation. Though the liquid precipitation events are the sum of drizzle and rain events, the percent number is larger than the averaged drizzle and rain percentages, because in the case drizzle the PWS could have found either drizzle or rain or something else. The events of solid precipitation include graupel and hail. The best result for finding a right type of precipitation is 69 % with an optical sensor and 81 % with the POSS sensor. Because the POSS output code was not ww-code conform a matching table had to be built before.

In a second step an investigation was done to see whether PWS code numbers did exactly match the observer's one. This means a comparison with reference to the intensity of the precipitation events. Besides the exact matching a tolerable correspondence was defined: the number differs by one step within the precipitation group, light rain is like strong drizzle and vice versa, the PWS messages the main term (40, 41, 42, 50, 60, 70, 80), the observer messages an interrupted event but the PWS messages an uninterrupted event. As seen in the lower part of Figure 1, the percentage numbers get distinctly lower compared with the numbers of the upper part of Figure 1.
Though the POSS generally shows the best results it is not reliable in discriminating rain and snow in the -1° to 5°C range, a frequent situation in German winter season. Up till now the results did not encourage DWD to put any of the sensors into network operation.

Improvement of visibility measurement with the scattering method

A transmissometer was compared with a scatterometer for possibly replacing the double spaced type by a single spaced compact type at airports. At moderate and heavy rainfall distinct differences between the two types were noticed ranging from 2000 m to about 500 m in the worst case. This fact was the reason for placing a contract for a feasibility study to find improvements for the scattering method. The Impulsphysik company was instructed to do and to formulate conclusions from the physical analysis and computations done by the Meteorological Institute of the University of Kiel and the DLR Institute of Oberpfaffenhofen .
While the transmissometer will fake a slightly high visibility in the case of rain caused by increased forward scatter the scatterometer will overestimate the extinction due to a small scattering volume and incorrect signal processing.
In the scope of the study the scattering characteristics of different fog-, haze – and precipitation models were analysed and possible changes in the instrumental arrangement were shown. The wavelength of the light source had no significant influence on the scattering phase functions. With haze- and fog models the phase functions had the smallest deviations from each other at 32° scattering angle but the estimated measurement uncertainty is still >>10%. At 143° the deviation of the model groups is rather wide and the quotient of 32° and 143° could determine the model group, estimating an uncertainty of <10%.
Different rain drop models will also have small deviations at 32°, but that doesn't hold for solid precipitation models. The latter differ distinctly from the liquid models in the range from 70° to 120°. The quotient of measurements at 32° and 90° should be about 135 for rain drops, 0.84 to 9.9 for snow and 0.28 to 0.84 for graupel.
In a small scattering volume often only one precipitation particle is in the volume at a time. It makes a strong signal so that precipitation could be realised and therefore be processed separately or be eliminated (single particle processing). In the case of rain 32° scattering and separate determination of the 'big' particles extinction part would be a solution. With solid precipitation particles should have a second receiver at 90° to realise them. The extinction component of these particles is to be measured in a separate sensor for instance at 0° in the same device as a transmission. The low particle number in the scattering volume might request an average over several minutes.
Alternatively an external device may be used to yield the extinction component of the hydrometeors. A disdrometer is a suitable device [2]. It measures falling speed and size of the particles and determines the particle size distribution and extinction. Limiting characteristics of disdrometers are a threshold radius for detection and the uncertainty at the falling speed of solid particles with different forms and orientation. Generally with two devices you have two separate measuring volumes and the delicate task to couple the devices.
So there are six possible modifications of the scatterometer as seen in Figure 2 (solid lines: basic equipment) and listed in Table 1.

Disdrometer test

A disdrometer type 'PARSIVEL' from PMTech company is under test at DWD as a candidate for providing present weather information resp. additional data for visibility determination. Short period operational test locations were Hamburg and a the mountain station 'Zugspitze' (2960 m). Preliminary results are:

- liquid and solid precipitation is recognised with different intensity steps.
- drizzle is hardly discriminated from rain, because the threshold diameter is 0.3 mm.

- graupel isn't discriminated from snow because the velocity is often in the same range.
- the amount of precipitation is generally given too low at small rates (drizzle !) whereas it is given too high at high precipitation rates. As reference a raingauge was used.
- on sunny days it tends to message 'drizzle': scintillation seems to produce increased signal noise.
- vertical winds apparently influence the velocity measurements at mountain locations.

Further tests are intended to get more present weather data esp. at hail and to find reliable size distributions to deduct the extinction value of precipitation.

References

[1] Szabó, I. et al., 2000: Present weather Sensoren. Final report, DWD Hamburg, Germany.

[2] Löffler-Mang, M. et al., 2000: An Optical Disdrometer for Measuring Size and Velocity of Hydrometeors. J. Atmos. Oceanic Technol. 17, 130-139

modification		uncertainly in %			
		fog	haze	liquid precip.	solid precip.
A	32° scattering single particle processing -	<10 %	60 %	<10 %	300 %
B	32° scattering single particle processing external disdrometer	<10 %	60 %	dependent on disdrometer	dependent on disdrometer
C	32°, 143° scattering single particle processing external disdrometer	<10 %	<10 %	dependent on disdrometer	dependent on disdrometer
D	32°, 90°, 143° scattering single particle processing -	<10 %	<10 %	<10 %	300 %
E	32°, 90°, 143° scattering single particle processing external disdrometer	<10 %	<10 %	<10 %	dependent on disdrometer
F	0°, 32°, 90°, 143° scattering single particle processing -	<10 %	<10 %	<10 %	dependent on transmission

Table 1: Possible scatterometer modifications

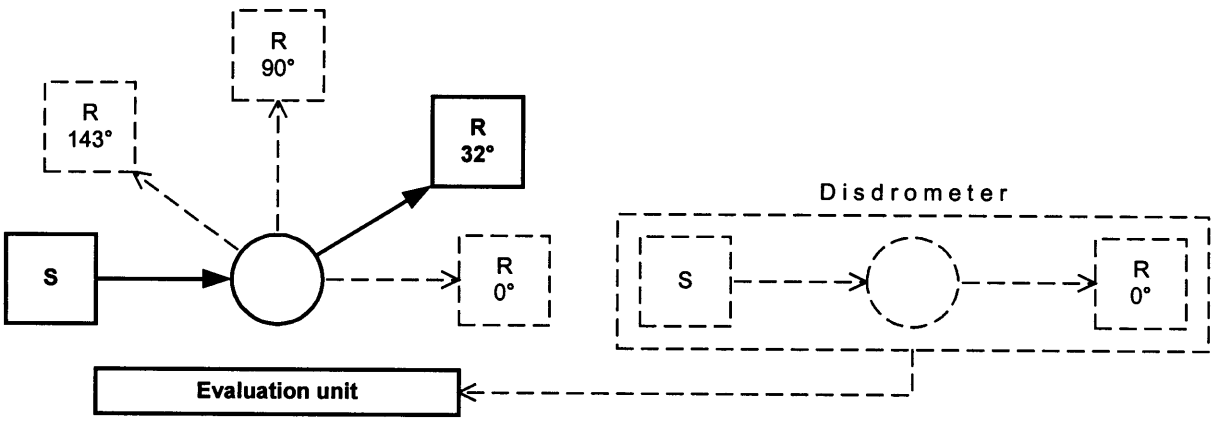

Figure 2: Basic configuration (solid lines) and modifications (dashed lines); S: lightsource, R: Receiver

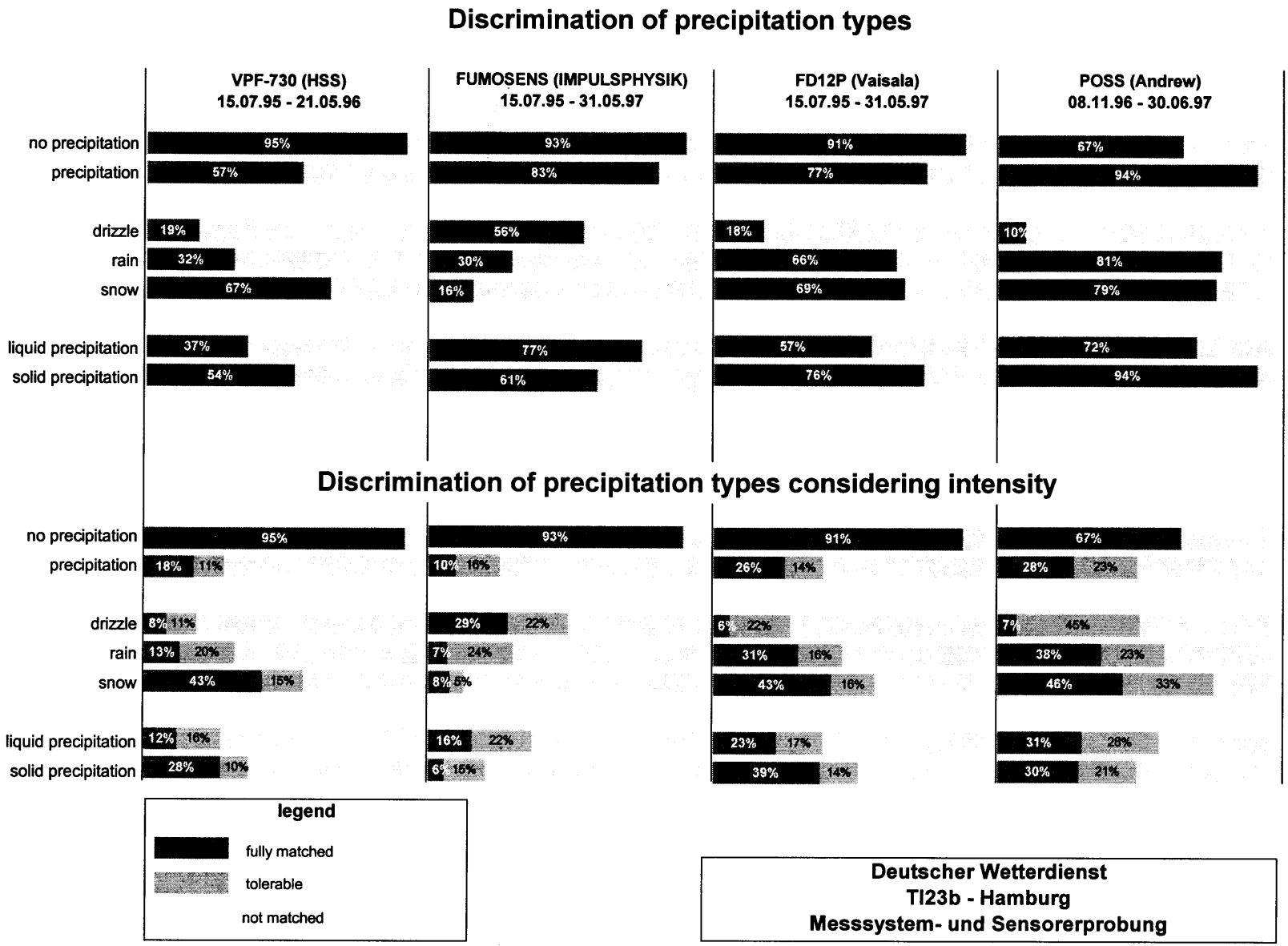

Figure 1: Comparison of PWS output with synop messages

Infra Red Thermal Imaging Cameras as an Observing Tool.

S.J. Keogh, S. Dewey, D. Hatton, D.W. Jones

The Met. Office, Beaufort Park, Easthampstead, Wokingham, RG40 3DN. United Kingdom.

Tel. +44 (0)1344 855828, Fax. +44 (0)1344 855897, Email. skeogh@meto.gov.uk

1. Introduction.

As the need for further automation grows it is becoming more important to evaluate new ways of making measurements that are usually performed subjectively by humans. Observations of cloud type and cloud cover are usually performed by humans. This paper describes the work done by The Met. Office in exploring the potential of infra red (IR) camera systems that may in future provide 24 hour observations. These measurements are performed using visible (Hatton et al, 1998, Rowbottom et al, 1988) and IR images, which are now distributed over The Met. Office intranet system.

Several types of imaging systems can be employed to record information about clouds. Visible cameras and image intensifiers can be used but these require the scene to be illuminated either by the sun or by a light source. A near IR image intensifier can have an IR lamp to illuminate the scene at night but will not produce images of cloud as this would require an enormous amount of energy from the lamp to illuminate the cloud base. Image intensifiers also exhibit 'flare' when a bright object is in the image frame and can be permanently damaged if the light is bright enough to saturate the sensor.

Thermal cameras however work on the principle of the thermal IR radiation emitted from the source. IR thermography is a passive sensing technique that requires no illumination of the scene. Thermal IR cameras therefore work just as well at night as they do in daylight.

The thermal IR technology utilised in our studies exploits the 8-14 micron region of the electromagnetic spectrum. Some thermal IR cameras exploit the 3-5 micron region of the spectrum but these tend to be used for high temperature applications because the peak in the thermal emission spectrum shifts to shorter wavelengths at higher temperatures. In the past thermal camera systems used cryogenic or Stirling cycle coolers to reduce the sensor noise but now many thermal cameras use thermoelectric coolers to stabilise the sensor at a low temperature. Some manufacturers refer to these systems as 'uncooled' but this simply implies that no external means of cooling is required. This is mainly for economic reasons as external methods such as cryogenics and Stirling cycle coolers are very expensive to run operationally.

2. The camera systems.

2.1 Initial trials.

Several IR cameras have been evaluated at The Met. Office experimental site at Beaufort Park over the past 18 months. Two cameras were initially tested which were manufactured by Inframetrics (now taken over by FLIR systems) and Raytheon (Dewey, 1999).

2.1.1 Inframetrics thermacam PM 295.

This camera has three fixed calibrated temperature ranges and we used the -40 to +90 ^{o}C range. However, the camera was modified by the manufacturers to give lower 'uncalibrated' readings down to –60 ^{o}C. This can be important for discriminating between cirrus and clear sky. The signal in the camera is digitised over 32768 radiance levels. The camera has two forms of image output - PAL and tgram (tgram requires a special PC card). The images are also analysed in the Thermogram software provided by the manufacturers. The camera has 320x240 pixels.

2.1.2 Raytheon Palm IR 250.

This portable IR camera produces B/W images in NTSC format only. It allows for contrast adjustment in the scene but is not capable of radiometry. The camera has 320x240 pixels.

2.1.3 Initial camera intercomparison.

The two IR cameras were mounted on a pan and tilt unit along with a visible colour camera, which would enable the observer to verify the cloud type estimates in the IR with a visible camera estimate. The IR camera housings were fitted with germanium windows.

2.1.4 Results – Palm IR.

The Raytheon Palm IR 250 was not capable of reporting the temperature of the objects in view because it is not designed for radiometry. However, it was quite adequate for the purposes of imaging cloud and determining cloud cover, although clouds at different temperatures in different parts of the image would appear to be at the same temperature due to the way that the images were scaled. This meant that inferring cloud height information from the images was not possible. There was also some 'fringing' where there were strong temperature gradients in the images because of the way the images were processed by the camera. This is a problem with many camera systems. An example image from the Raytheon Palm IR is image 5 in Annex 1.

2.1.5 Results – Inframetrics PM295.
The Inframetrics PM295 camera produced some interesting images of cloud structures. Some of these are shown in images 1-4 in Annex 1. The camera was also able to produce some quantitative measurements of scene temperature, although because of radiance errors arising from the germanium window and atmospheric attenuation the absolute temperature estimates from the camera are not reliable.

2.2 The current camera arrangement.
The camera currently being evaluated is a Thermovision Alert MT (a later version of the PM295), distributed by FLIR systems. This camera has a sensor array of 320x240 pixels. It produces an interpolated PAL output image as well as digital data via an S-video link. The gain and temperature measurement range can be adjusted via camera control software.

The IR camera is mounted next to a visible camera. This arrangement is shown in figure 1, both the visible and IR cameras being mounted on a pan and tilt unit. A PC controls the pan and tilt unit whilst simultaneously capturing PAL video images from the cameras using a PC based framegrabber. The PC produces a suite of IR and visible images that make up a complete panoramic mosaic of the sky.

Figure 1. Visible and IR camera set-up (arrow).

2.3 Image distribution.
The resulting panorama gives the observer a full hemispherical view of the sky. The camera images are then available to observers on The Met. Office intranet. The images can be transmitted from the remote site by conventional telephone line, ISDN or using direct TCP/IP communications.
The camera views can then be accessed easily and used either as a diagnostic tool to aid forecasters or for the quality control of observations being remotely and automatically reported e.g. from an automatic weather station.

3. Cloud identification.

Fractional cloud type identification can be difficult for the observer, especially when there are several cloud layers. This is because the amount of visible radiation being scattered within the clouds makes it difficult to detect cloud edges with the human eye. However, thermal IR cameras view thermal IR radiance. Clouds at different heights will radiate according to their temperature. This makes it easier to determine the location of cloud edges on the thermal IR images than on visible images. IR cameras are also capable of seeing cloud structure through haze when an observer may not be able to see clouds at all.

Several examples of cloud types as viewed in the thermal IR are shown in images 1-5 (Annex 1) and described in table 1.

Table 1. Image descriptions.

Example cloud type(s).	Image number(s)
Cumulus.	2
Altocumulus	3,4
Stratocumulus/Cirrus	5
Cumulonimbus	1

Cloud cover estimates are an important element of aviation reports as well as being used by forecasters. They may also be used to verify the performance of forecast models. Visual estimates of cloud cover are error prone because although the observer can report a cloud cover of 8 octas it can be the case that the IR camera sees holes in the stratus layer(s). In this situation the IR camera would provide a more accurate estimate of fractional cloud cover for different cloud types and layers. However, it is debatable as to whether an accuracy of better than 1 octa is useful.

4. Other potential uses for thermal IR cameras.

4.1 Ground temperatures.
Conventional ground temperature measurements are made using a glass sheathed platinum resistance thermometer (HMSO – Observers Handbook). These thermometers are unreliable for measuring ground minimum temperatures because they are in poor thermal contact with the ground – particularly in the case of a grass surface. Thermal cameras offer a non-contact means of determining the surface temperature. However, the emissivity of the surface must be known before the surface temperature can be determined. Several laboratory studies of ground surface emissivity exist (e.g. Wilber et al, 1999), which are mainly for satellite remote sensing applications but are transferable to surface observations (Keogh et al, 2000).
Absolute temperature determination from IR cameras is difficult because the cameras' protective window

and the intervening atmosphere modify the radiance received by the sensing element. Compensating for these effects is not a trivial process and therefore ground temperature estimates to an accuracy of better than 1°C are not practical operationally at this time. Image 6 shows a scene taken when the ground was thawing after a frost. Various buildings and instruments are visible in addition to some cumulus cloud on the horizon (the grey scale imposed used here may mean that these features are not meaningful in this black and white paper).

4.2 Present weather determination.
Rain has the effect of reducing the contrast in IR images such that the image appears to have a reduced level of surface detail. An experienced observer should be able to notice the lack of surface detail in the images and attribute it to rain or fog. This could be particularly effective when the IR camera is used to add confidence to readings from present weather sensors and visibility meters.

5. Discussion.

5.1 Limitations of IR camera systems.
IR camera systems cost a large amount of money because the technology is not supplied in large quantities. As the potential of IR cameras is realised the price will inevitably come down due to the increase in demand for these systems. However the market is changing very rapidly such that any current model of IR camera may be superseded in less than one year. This will make it difficult to produce consistent systems for the observational network as the specification of the cameras change.

Observers will also require some training to interpret IR imagery and to pick out the subtle image details that will enable them to determine present weather and to recognise different cloud scenarios, especially at night when there is no visible data to help in the cloud recognition process.

5.2 Advantages of IR systems.
IR systems can offer full 24-hour observing capability with no discernible difference between day and night operation. The human eye cannot determine cloud cover and type under poor light conditions and in haze whereas IR technology requires no background illumination of the sky whatsoever. Unlike visible cameras IR cameras do not flare when the sun is in the image. When the cost of IR cameras becomes 'affordable' then it would be expected that the installation of such cameras in remote locations could give cloud observations in areas where there are no observers.

Cloud identification has been demonstrated by The Met. Office to be possible using thermal IR systems. Thermal IR sky images could potentially prove to be as useful to the meteorological forecaster as the X-ray has proven to be for the medical profession. As the technology is explored further meteorologists may find other applications for thermal IR cameras that are not mentioned here.

5.3 Operational considerations.
Currently 'off the shelf' thermal IR cameras are too expensive to be an observing tool for widespread use. However, informed opinion is that it would be possible to develop an IR camera to a specification that meets the meteorological requirements for about 1/3 of the current market cost.

The arrangement of the cameras needs to be considered very carefully. The cameras must be placed in a waterproof housing to protect them. In addition the housing must have an IR window with very high transmission in the 8-14 micron wavelength range e.g. anti-reflection coated germanium has ~96% transmission. These housings were not commercially available from manufacturers during the evaluation period and so they had to be specially constructed by The Met. Office for the purposes of these trials.

6. Future work.

The discussion above relates to the use of cameras as an aid to the manual observing process whether used locally or remotely. The next stage in the process of observation automation is to develop techniques for automatic analysis of such images, both to identify cloud types and amount, and as a qualifier to other observation data.

7. References.

Dewey, S., 'Infra Red Trial Report', The Met. Office, OLA Technical Report No. 16, August 1999.

Hatton, D., Jones, D.W., Rowbottom, C.M., 'Technical Experiences of Using a Video Camera to Make Remote Weather Observations', WMO Instruments and Observing Methods, TECO-98, May 1998.

Keogh, S.J., 'An Investigation of the Potential of Infra Red Cameras for the Determination of State of the Ground', The Met. Office, OLA Technical Report, July 2000.

HMSO, 'Meteorological Observer's Handbook', 3rd Edn, Her Majesty's Stationary Office, 1975.

Rowbottom, C.M., Hatton, D.B., Jones, D.W., 'Operational Experiences in the Use of Video Camera Images to Augment Present Weather Observations', WMO Instruments and Observing Methods, TECO-98, May 1998.

Wilber, A.C., Kratz, D.P. and Gupta, S.K., 'Surface Emissivity Maps for Use in Satellite Retrievals of Longwave Radiation', NASA / TP-1999-209362, August 1999.

ANNEX 1. Selected images.

Note. These are colour images and may not reproduce well in black and white. More information is available from the authors.

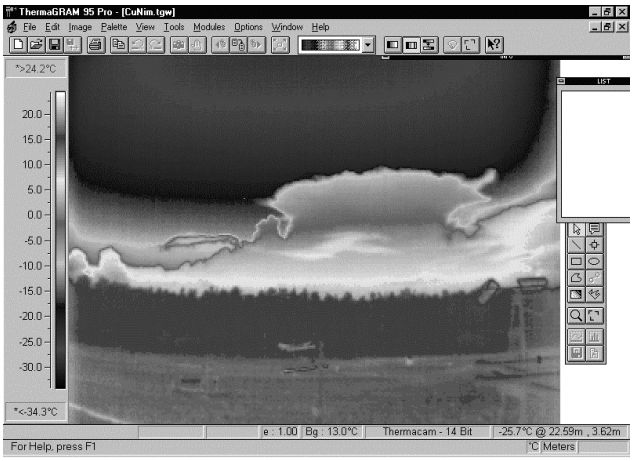

Image 1 Cumulonimbus anvil.
Inframetrics thermacam PM 295.

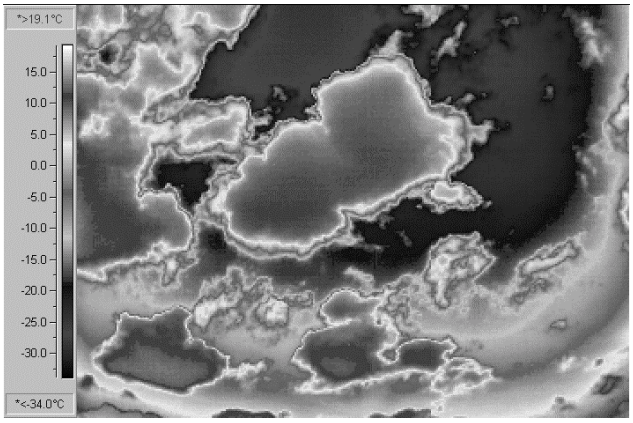

Image 2 Cumulus cloud.
Inframetrics thermacam PM 295.

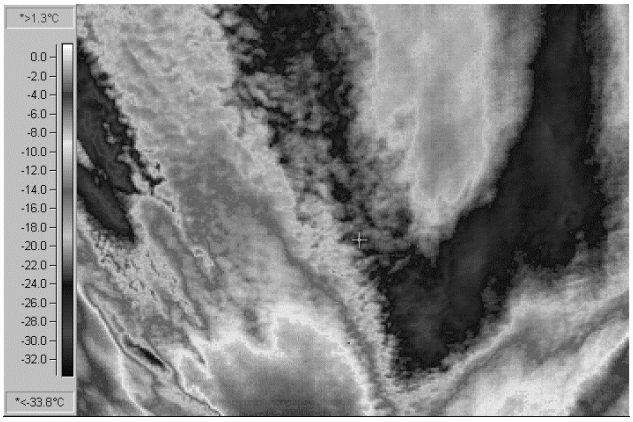

Image 3 High altocumulus.
Inframetrics thermacam PM 295.

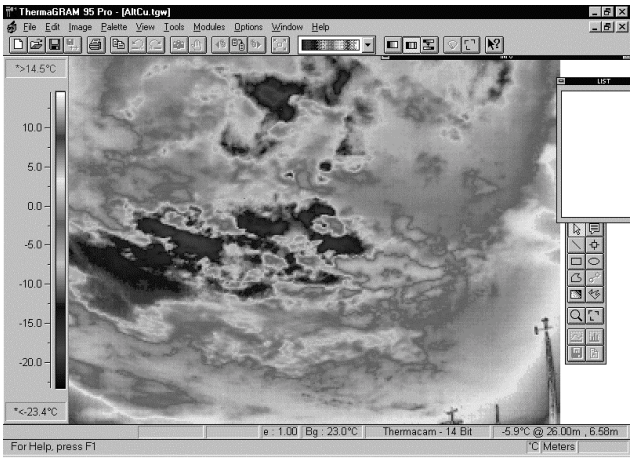

Image 4 Altocumulus.
Inframetrics thermacam PM 295.

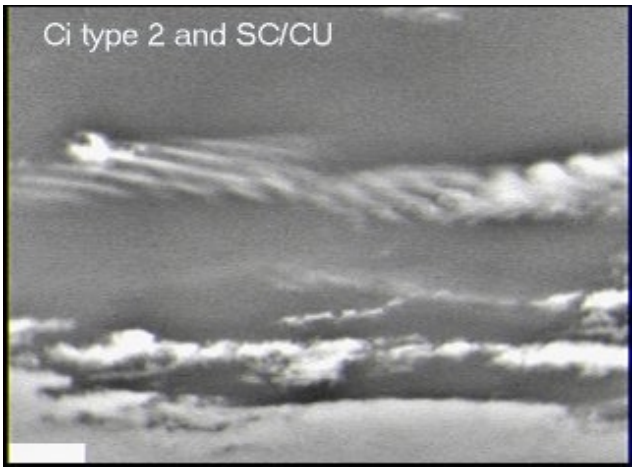

Image 5 Cirrus, cumulus and stratocumulus.
Raytheon Palm IR 250.

Image 6 Defrosting ground, cumulus.
Thermovision Alert MT.

DETERMINATION AUTOMATIQUE DE L'EPAISSEUR DE NEIGE SUR LES AEROPORTS AU MOYEN D'UN SYSTEME EMBARQUE SUR VEHICULE.

J. L.GAUMET, M. ZEPHORIS, F. ZANGHI,
Météo-France, Direction des Systèmes d'Observation
7 Rue Teisserenc de Bort
78195 TRAPPES France

1. INTRODUCTION.

La formation brutale d'une couche de neige, même relativement peu importante, est un phénomène météorologique redouté par les gestionnaires des grandes plate-formes aéroportuaires. Ils doivent rapidement en communiquer l'épaisseur aux pilotes après avoir effectué des relevés représentatifs en différents points de la piste, et ensuite, prendre des décisions de fermeture provisoire si la couche est trop épaisse ou le plus souvent envisager le déblaiement. Pour arriver à de telles situations, il suffit de quelques centimètres de neige, épaisseur à partir duquel les principaux avions ne sont plus certifiés pour atterrir.

Actuellement, après une précipitation neigeuse et quelle qu'en soit l'importance, des relevés manuels sont effectués en certains points seulement de la piste pour éviter une trop longue fermeture des pistes concernées, opération toujours très coûteuse pour les compagnies et l'aéroport. De plus, ces relevés manuels n'ont pas toujours la représentativité nécessaire, pour bien connaître l'ampleur du phénomène.

Pour remédier à ces inconvénients, Aéroport De Paris (ADP) a décidé de faire appel aux conseils de Météo-France pour définir un système de mesure de l'épaisseur de neige au moyen d'un dispositif métrologique embarqué sur un véhicule de piste, donnant en temps réel le profil de contaminant tout au long du parcours avec une précision minimale de l'ordre de 0,3 cm et ceci pour des épaisseurs allant de quelques millimètres à quelques dizaines de centimètres.

2. DEFINITION DES BESOINS.

L'équipement de mesures automatiques installé sur un véhicule de piste devra répondre aux besoins opérationnels définis par A.D.P, au départ du projet, suivants :

- Précisions des mesures conformes aux recommandations de l'annexe 14 de l'Organisation de l'Aviation Civile Internationale OACI :
  - 2 cm pour la neige sèche.
  - 1 cm pour la neige humide.
  - 0,3 cm pour la neige fondante.
- Mesures effectuées en déplacement à des vitesses de l'ordre de 50km/h.
- Prise en compte des problèmes liés au véhicule : insensibilité aux projections de neige, aux oscillations du véhicule et à la surélévation du mobile due à la présence de neige écrasée sous les pneumatiques.
- Fonctionnement du système par conditions météorologiques difficiles (température négative, brouillard) et de nuit comme de jour.
- Transmission et utilisation en temps réel des mesures de hauteur de neige dans le centre de décision de l'aéroport.
- Système simple à mettre en œuvre sans qualification spécifique et avec sécurité maximale des personnels.

3. METHODE DE MESURE.

3.1. *PRINCIPE.*

Pour atteindre la précision de mesure demandée, une mesure optique sans contact a été retenue afin de déterminer la distance du capteur à la surface de la neige. Un faisceau laser cylindrique de faible diamètre est dirigé verticalement vers le sol. L'énergie lumineuse diffusée est alors utilisée pour observer le spot lumineux sur le sol. Sur un montage solidaire du laser, une caméra CCD est placée pour recevoir le spot lumineux et former une image de celui-ci. C'est la position du pic correspondant qui donne la mesure de

distance par l'intermédiaire d'une loi de transformation. Ce principe est connu sous le nom de triangulation laser (Figure 1).

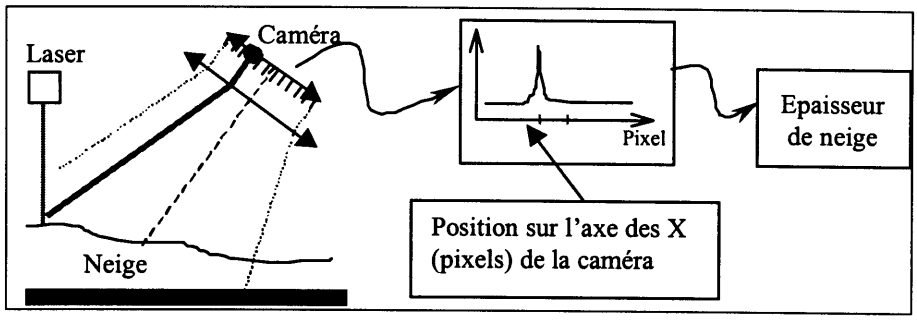

Figure 1 : Schéma de principe du dispositif

3.2 *DESCRIPTION DE LA METHODE.*

Pour l'obtention d'une mesure réaliste et fiable de la hauteur de contaminant, il est nécessaire de se donner deux références :

- Une référence de déplacement horizontal.

Elle est réalisée par l'intermédiaire d'une roue de référence, solidaire de l'ensemble caméra/laser. Elle doit être absolument maintenue en contact permanent avec la piste.

- Une référence de mesure verticale.

Elle est réalisée au départ de l'expérience en effectuant une interpolation entre plusieurs mesures de référence (référence 0 pour un sol non recouvert, références 50mm et 100mm réalisées avec des cales). Il est alors facile de déduire l'épaisseur de neige par différence entre d'une part la hauteur mesurée et d'autre part la hauteur fixe séparant le montage optique et le sol non recouvert de neige.

4. DESCRIPTION DU PROTOTYPE.

Le système est constitué d'un laser à sécurité oculaire absolue (classe 1) et d'une caméra CCD.Le réglage de l'axe optique du laser dans le plan de vision de la caméra est une nécessité absolue. Pour éviter tout déréglage à bord du véhicule, l'ensemble est protégé des vibrations par des « silent-blocs ».
Le signal vidéo extrait de la caméra, est traité à l'aide d'une électronique très rapide qui le convertit en valeur numérique transmise via liaison RS 232 à un PC portable. Un logiciel traduit cette valeur en hauteur connaissant la loi d'étalonnage.
Avec le type de roue choisi, le système est capable de traduire une valeur de hauteur de neige tous les 55 cm puis de faire la moyenne de ces valeurs tous les 100 m de piste.
L'ensemble du système de mesure est intégré sur une remorque à 2 roues. Des roues de vélo fines ont été choisies afin d'avoir une bonne pénétration de celles-ci dans la neige assurant ainsi la même référence de hauteur du système par rapport au sol qu'il y ait ou non de la neige (Brevet Météo-France).

5. RESULTATS D'ESSAIS DU PROTOTYPE.

Pour valider le système, des essais ont été faits d'une part sur les pistes de l'aéroport d'Orly en l'absence de neige et d'autre part en montagne , dans les Alpes, en présence de neige.

5.1. *ESSAIS SUR PISTE EN L'ABSENCE DE NEIGE.*

Ces essais avaient pour but de démontrer que le système fonctionnait bien tout en mettant en évidence qu'il suivait au millimètre près les moindres irrégularités de la piste en meilleur état d'Orly. Cet objectif a été atteint ; la figure 2 montrant une faible dispersion des mesures avec un écart-type inférieur au millimètre.

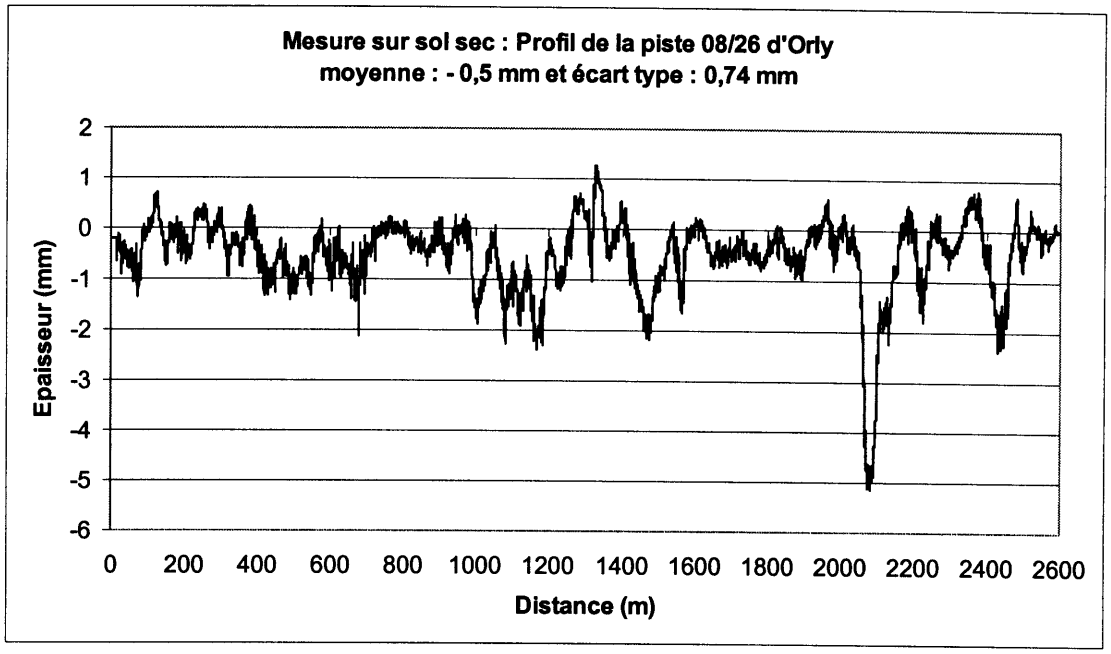

Figure 2 : Profil de la piste d'Orly 08/26 sans neige

5.2. *ESSAIS EN MONTAGNE EN PRESENCE DE NEIGE.*

Les tests en montagne ont été effectués en mars 2000 pendant trois épisodes significatifs de chute de neige sur une boucle de circuit routier de 1200 mètres peu fréquentée (soit 2200 mesures environ). La courbe de profil (figure 3) fait apparaître une grande similitude entre les différents passages sur le circuit. Le nombre de points de mesure reste équivalent d'un passage à l'autre, ce qui prouve que l'appareil reste bien constant. On remarque que les zones plus ou moins enneigées sont dues à la présence d'arbres. La moyenne des écarts entre le premier et le second passage est de –0,7mm avec un écart-type de 4,9mm. La figure 4 décrit une chute de neige importante avec une montée de l'épaisseur de celle-ci d'un passage à l'autre (34,8mm entre le deuxième et le troisième passage, soit une chute de neige de 200mm/heure). Les relevés manuels effectués simultanément avec un réglet montrent un bon accord entre les 2 types d'observation.

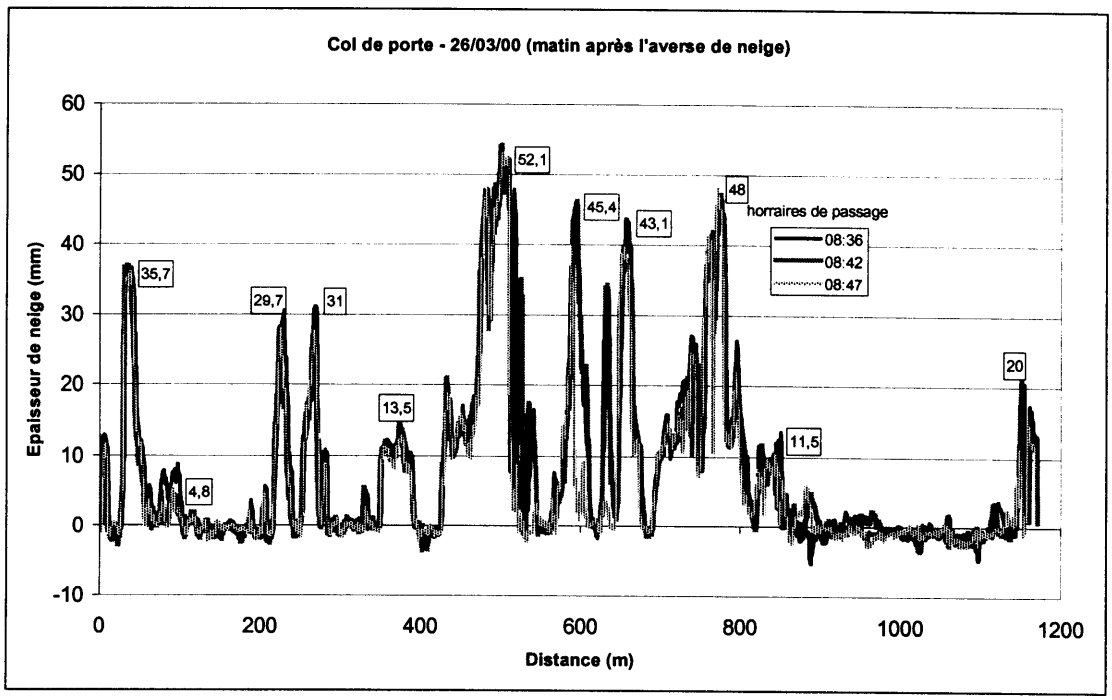

Figure 3 : Hauteur de neige en fonction de la distance parcourue : superposition de 3 passages successifs

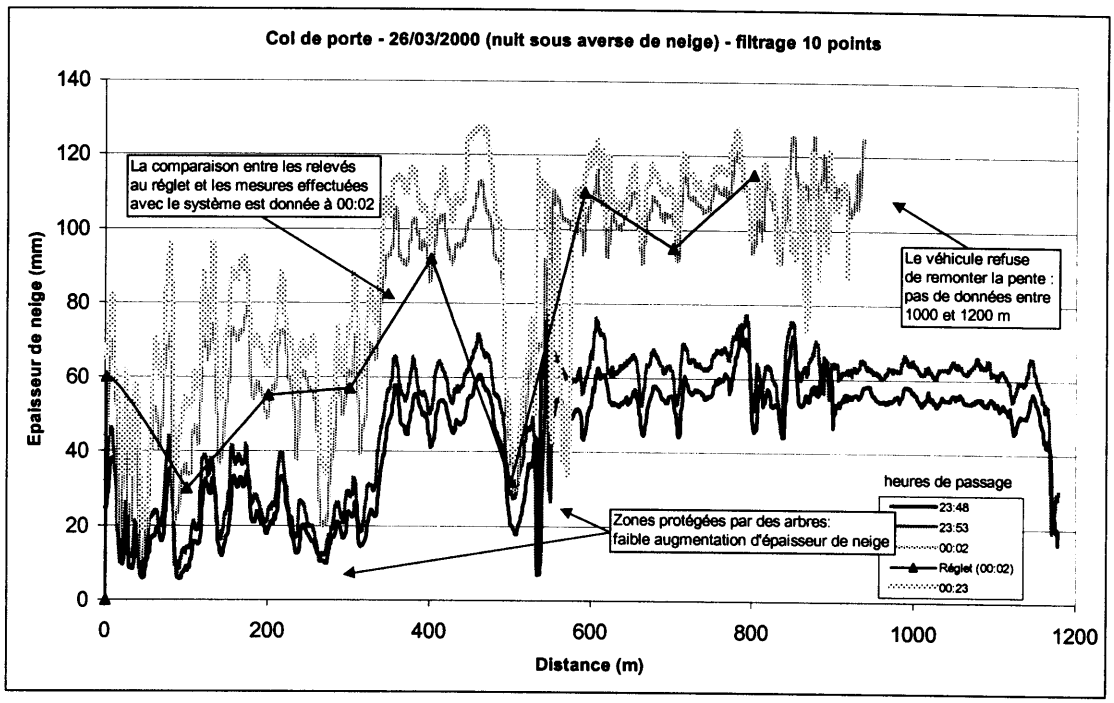

Figure 4 : Evolution temporelle de la hauteur de neige en fonction de la distance parcourue (4 passages successifs sur un même parcours)

5. CONCLUSION.

Le système présenté ici a subi de nombreux essais qui ont démontré qu'il répondait très bien aux spécifications techniques et opérationnelles initiales. En particulier, pour toutes les neiges fraîches et blanches, la précision de la mesure est de l'ordre de 2mm. La neige fondante translucide d'épaisseur de quelques millimètres, de même couleur que le bitume, est plus difficilement mesurée (2 à 5mm). Le positionnement du système de mesure à l'arrière du véhicule ne modifie pas la qualité des mesures. Le problème des oscillations du véhicule est résolu par un filtrage efficace des données sans perte d'information utile. Enfin, la visualisation de la couche de neige peut être effectuée en temps réel. Aéroport De Paris, satisfait de ces essais, va aborder la prochaine saison hivernale en mode opérationnel à Orly avec ce nouveau capteur d'épaisseur de neige.

6. REFERENCES.

E. Telmar, J.L Gaumet, M. Zéphoris, F Sarter. Détermination automatique de faibles épaisseurs de neige sur les pistes d'aéroport, par triangulation laser. Direction des Systèmes d'Observation, rapport interne, juin 1999.

J-L. Gaumet, M. Zéphoris, F. Zanghi, C. Pelte et P. Roulet. Détermination automatique des faibles épaisseurs de neige sur les pistes d'aéroports. Plaquette destinée à la deuxième réunion Internationale sur la performance en freinage des avions utilisant les pistes chargées de contaminants. MONTREAL-QUEBEC, 02 et 04 novembre 1999.

M. Zéphoris, J-L. Gaumet. Dispositif de mesure de l'épaisseur d'une couche de neige. Brevet d'Invention en France n° 9913703, le 03 Novembre 1999.

C. Rougier, F. Zanghi. Traitement des données du système de mesure d'épaisseur de neige et Notice d'utilisation du système de mesure d'épaisseur de neige. Direction des Systèmes d'Observation, TRAPPES, Janvier 2000.

F. Zanghi, C. Rougier, J-L. Gaumet et M. Zéphoris (Météo-France) et P. Roulet (ICARE) et C. Pelte (SEREPS). Essais du système mobile de mesure d'épaisseur de neige sur piste d'aéroport. Rapport d'essai, Direction des Systèmes d'Observation, TRAPPES, Mai 2000.

Calibration and Control Methods for Tipping-Bucket raingauges

Michel Leroy
Météo-France, Direction des Systèmes d'Observation, BP 202 78195 Trappes, France

Michel.leroy@meteo.fr

Tipping bucket raingauges are not recent and high technology instruments but are widely used over the world. The quantity of precipitation is a basic climatologic measurement and probably the most important to human activities. The largest instrumental networks are set for this measurement. Both for economic and technical reasons, the measurements are increasingly automated and raingauges with a transducer are used. This allows the knowledge of precipitation quantities at low time steps along with daily values. Several types of transducer may be used. Tipping bucket raingauges are an old technique. Newer technology is now available, especially weighing one. The purpose of this paper is not to compare the different techniques or instruments but to focus on tipping bucket problems as they are still widely used.

1. Advantages and problems related to tipping bucket raingauges

The main advantages of tipping buckets are
- The simplicity of the system, easy to understand and therefore to maintain.
- A nearly non electronic sensor.
- A low cost system, due to the 2 upper points.

The main disadvantages are
- The difficulty of adjustment of the tipping buckets
- The need for a cone necessary to guide water into the bucket. This cone is therefore sensible to clogging.
- The loss of water (underestimation) at high rainfall intensity.
- The need to heat at a negative temperature.

The simplicity and low cost of a tipping-bucket raingauge often surpass the disadvantages and explain the very wide use of this type of sensor. The low cost is the main reason why tipping-buckets are used by Météo-France.

These past years, Météo-France has conducted several tests and studies on raingauges, in particular to optimise their heating (see M. Zephoris & al., TECO-98). Characteristics of tipping buckets problematic have been deeply analysed.
Many designs of tipping-bucket raingauges exist on the market with various collecting surfaces and tipping masses. The examples in this paper are based on a 400 cm2 sensor using tipping buckets adjusted for 8 g. This leads to a 0.2 mm resolution. The techniques described are also applicable to different designs.

2. Underestimation at high intensity

The bucket tip is not instantaneous. Water falling during the tip may be lost. For example, for a rainfall rate of 120 mm/h, we have a tip every 6 s (with a 0.2 mm resolution). If the tip has a duration of 300 ms, the loss will be 5% (0.3/6). The duration of the tip is depending on the inertia of the system (the inertia momentum related to the swing axe) and the momentum generated by water inside the bucket. All this is design dependent. The smaller is the inertia; the faster is the tip. The measurement resolution is also a factor. A bucket adjusted for 0.1 mm will tip 2 times more than for 0.2 mm and the loss of water may be doubled. The loss increases with intensity as the period between 2 tips decreases. The loss should be proportional to the intensity; but at high intensity, the dynamic of water falling into the bucket helps the tip. Therefore, the loss is reduced.
Underestimation with intensity is seldom documented by manufacturers. As some adjustment procedures are made at high intensity (50 to 100 mm/h for example), the associated underestimation has to be taken into account in the procedure. This is also seldom done. For a high intensity of 200 mm/h, typical underestimation

errors are -10%. But we have tested a raingauge design (widely sold) exhibiting underestimation errors as large as -40% ! This design was sold to us with an error curve with intensity, which is uncommon, but this curve was completely wrong, being established for another bucket capacity than the model that we bought.
Underestimation with intensity may be no longer a disadvantage of tipping-bucket technique. Corrections may be applied by the acquisition systems, taking in account the time between two successive tips and a correction curve.
All this leads to a need to clearly document the error curve with intensity. To establish this error curve, several systems may be used. We will describe the system used by Météo-France.

3. Calibration bench

We use a bench composed of an electronic weighing machine, a peristaltic pump, both connected to a standard PC with dedicated software. The electronic weighing machine has a 0 .01 g resolution, a 5 kg range and outputs the measurements on an RS232 line to the PC, 10 times per second. A water container is weighed. A tube injects water into the buckets through a peristaltic pump. This pump is also controlled by the PC, both for its speed and start and stop. With (8 g, 0.2mm) buckets, this bench allows the generation of 3 mm/h to 250 mm/h intensity range. The range may be adjusted by the selection of different tubes. The tip detector (such as a contact closure) is connected to a junction signal of an RS232 line of the PC. The dedicated software controls the pump, sets a given intensity, counts a selected number of tips, gets the mass variation of the water container. It outputs the measured precipitation quantity (n*8g), compared to the decrease in mass on the balance, and calculates the difference expressed in %. A succession of tests at various intensities may be programmed, leading to an automatic establishment of an error curve with intensity. A typical duration for a test series is 90 minutes. An example of an error curve is given.

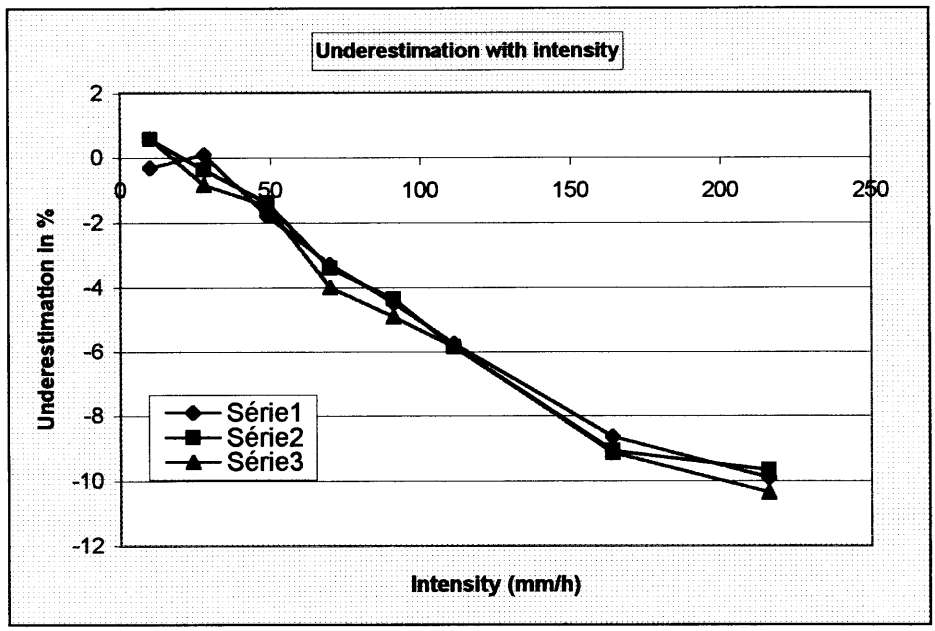

The uncertainty associated with the calibration bench is about 1%.
The repeatability of test series is depending on the tipping-bucket design, especially on the water retention of buckets. The repeatability is typically better than 2%, both from successive tests with the same sensor than with sensors of the same design (after setting).

4. Checking a raingauge adjustment in the field

A calibration bench is a laboratory tool. In the field, besides a visual inspection and manual cleaning, it is advisable to check the tipping-bucket settings. The easiest way to do it, is to pour a known quantity of water inside the cone. This method is recommended by several manufacturers, some of them selling specific accessories for that. Two accessories are needed :

- A water container to set a given water quantity. This container must allow knowing the water quantity with a high level of confidence, say with an uncertainty lower than 1%. A drum (such as some sold by some manufacturers ...) is not well fitted as the uncertainty on the water level leads to a non negligible uncertainty on the volume. It is better to use a flask with a narrow neck, the water level being adjusted in the narrow neck. Such flasks are common on laboratory equipment catalogues. Météo-France is using a 1 litre flask. 3 mm in the neck corresponds to 1 ml of water. Taking in account the flask tolerance, the flask

and water dilatation with temperature, an uncertainty lower than 0.5% may be easily reached on the water volume with this flask. The cost of a flask is less than 50 Euros.

- A system to limit the flow to the buckets. This system may be a calibrated cap with a hole, the water container being inverted in the cone. Météo-France is using a shutter with a trench, set in the cone's bottom.

To take in account the normal loss of water with intensity, the intensity generated by the method must be known. The mean intensity is known by dividing the quantity by time. The intensity varies during the test as the water pressure decreases with the water level in the cone. Météo-France has developed a piece of software to record the tips during the test. The measurement of time during two successive tips allows the evaluation of the bucket imbalance.

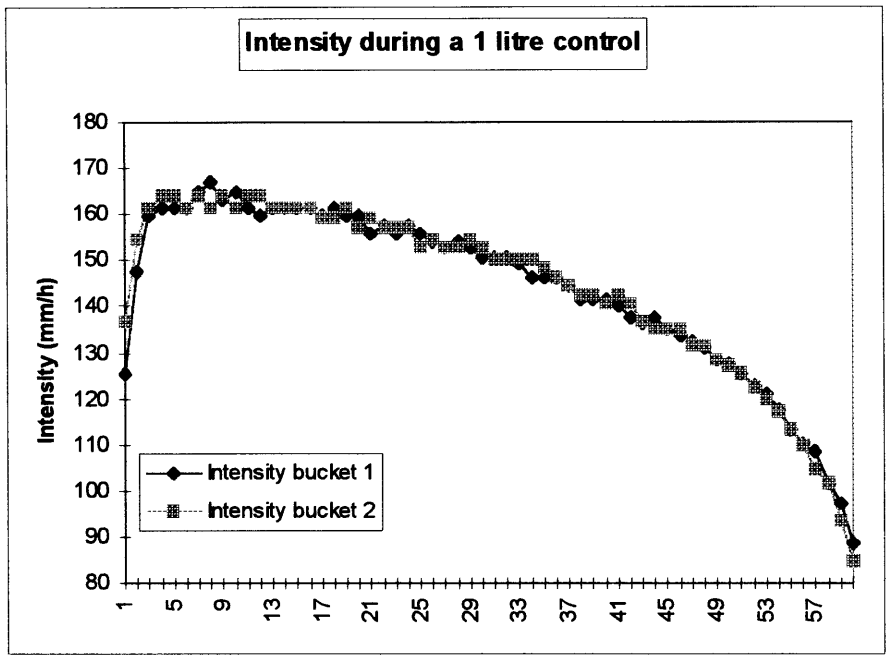

This curve shows the intensity variation during a control. Considering that the time variation of intensity is roughly linear such as the error curve with intensity on the intensity range covered, the normal deficit due to the loss with intensity may be directly inferred from the error curve and the mean intensity during the control. The mean intensity during this control was 144 mm/h.

With the curves shown in this paper, the normal loss is 8 % for 150 mm/h. 115tips should be recorded with a well-adjusted gauge. 112 and 118 limits are used during a field check. If the control duration is within given limits (to check the applied intensity) and the number of tips is within the limits, the control is successful. Otherwise, an adjustment is necessary.

To limit the uncertainty of the applied correction about intensity losses, it could be better to use a system designed to limit the flow to low values (say 50 mm/h). A 1 litre control will last 30 minutes. With a 150 mm/h intensity, the control duration is reduced to 10 minutes. Though the uncertainty of the intensity corrections is slightly increased, it is preferable to reduce the control time to increase the probability that the control will be regularly done in the field. The longer is the control, the higher is the risk that the control will not be properly done (human factors exist when a working day in the field is getting long).

5. Bucket imbalance

A bucket imbalance is not dramatic as an under adjustment of one will compensate an over adjustment of the other. For low quantities and odd numbers of tips, the compensation will not completely occur, but will be hidden by the resolution associated with the gauge. There will always stay an uncertainty of about 0.2 mm (the bucket resolution) because a bucket could be nearly full before or after a precipitation event. A large imbalance will slightly change the error curve with intensity. Experience shows that an imbalance of up to 10% between the buckets may be accepted. The accepted imbalance tolerance must be set to avoid a long process of the individual adjustment of each bucket. Some sensor designs avoid this problem with a system allowing the setting of the two buckets with only just one screw.

6. Tipping bucket adjustment

The adjustment may depend on the intensity. It is much better to adjust the buckets for a low intensity (say 8 g for intensities below 10 mm/h). Underestimation at high intensity may then be corrected during field measurements, by using the known intensity error curve. Several techniques may be used to make the setting. A knowledge of the raingauge model used allows knowing the correspondence between a one turn of the setting screw and the mass setting off the tip.

6.1 Using a pipette

It can be a manual or electronic pipette. Many designs are available. The uncertainty of the water quantity injected into a bucket with a pipette may be lower than 0,1 cm^3 (1.25% with 8 g buckets). It is very difficult to adjust the setting to an exact quantity of 8 cm^3 which would be at the exact (unstable) equilibrium. Making the setting with lower and upper limits, for example 7.8 g and 8.2 g, is much better and repetitive. The buckets must not tip over for 7.8g. They must for 8.2g. This method is objective (Yes or no). The limits used depends on the accepted tolerance (and on the repeatability of the tips, which may be related on the water retention of the buckets which may vary with time, and on the way to pour the water into the bucket). This method allows the setting of each bucket. It can be long (up to 60 minutes).

6.2 Using a calibration bench

A calibration bench as described above may be used for the buckets setting. Two methods may be used.

- By setting a low intensity (< 10 mm/h) and turning the setting screws after the tips, noting the water mass injected. Several tips are necessary to compensate the measurement variability. The advantage of using a low intensity is a direct setting for 8 g. The disadvantage is the time needed. Waiting at least 72 seconds (if intensity is < 10 mm/h) between two tips is long.
- By setting a higher intensity, taking in account in the setting the loss due to intensity. If the intensity used is 60 mm/h, there is a tip all the 12 seconds. Using the error curve presented above, the loss is 3%. The setting must be done for 7.75 g 12 seconds are enough to adjust the setting screws. The setting of the 2 buckets may be done in less than 5 minutes.

6.3 Using a checking with 1 litre

The loss with intensity and the intensity during the control must be known and taken in account. As mentioned above, the imbalance between the buckets may be also evaluated by recording and using the time between successive tips. The control results after pouring 1 litre allow knowing the mean adjustment of each bucket. The setting screws can then be turned to adjust the buckets, if knowing the correspondence between one turn of the screw and the mass setting off the tip. After adjustment, a second control is needed for a (final) check.

6.3 Dry setting

Another solution is to adjust the setting by replacing water with a dry mass (fitted to the bucket shape) into the bucket. Such as the pipette method, it is not practicable to adjust the tipping to an exact mass. It is better to make the setting with 2 limits, one giving a tip, the other not. This can be done by adding a light washer. The advantage of this method is that it is very fast and is not disturbed by water retention in the buckets. A disadvantage is that it is not done in realistic conditions, with no water retention en the buckets. A good solution is to check the setting with 1 litre or a calibration bench. The advantage of using a calibration bench is to supply a calibration curve (as a proof) with the sensor.

7. Conclusion

Though based on old principles, the tipping-bucket raingauges adjustment and quality control may still be improved. Besides the definition and selection of a new tipping-bucket raingauge model, Météo-France is setting and formalising the procedures for calibration and control.
The instrument's aspects must not be neglected but it must not be forgotten that the major causes of errors for precipitation measurements are the wind effects and the influence of siting and exposure.

A PROCEDURE TO IMPROVE MEASUREMENTS OF DEW POINT BY AUTOMATIC WEATHER STATIONS

W.R. Sparks, D.W. Jones and D.B.Hatton
The Met. Office, Beaufort Park, Easthampstead, Wokingham, Berkshire, RG40 3DN, United Kingdom
Tel: 44 (0)1344 855603 Fax: 44 (0)1344 855897

ABSTRACT

The psychrometer is the traditional instrument for measuring ambient humidity for meteorological observations. This may be a wet and dry bulb thermometer exposed in a naturally or artificially ventilated Stevenson style screen, or a more precise instrument such as an Assmann psychrometer. However, for reliable results these instruments require regular maintenance, including the exchange of the wet bulb wicks and refilling of the water reservoir; they are also difficult to operate when the wet bulb temperatures are below freezing. These problems are aggravated when the psychrometer is used on an automatic weather station and consequently many AWS designs use an electronic hygrometer for measuring ambient relative humidity. Many of these, however, are less accurate than a well maintained psychrometer, particularly at high values of RH and they may also exhibit changes in calibration with time and with temperature.

This paper describes an algorithm developed for operational use on AWSs equipped with both an electronic RH probe and a psychrometer. The electronic probe provides the operational measurement of RH and hence the reported dew point, but when conditions are suitable for accurate measurements from the psychrometer the latter is used to update the calibration correction to the electronic humidity probe and to check that the probe remains responsive to rapid changes in relative humidity. The procedure allows improved accuracy in the reported dew points, and the period between laboratory calibrations of the probe to be extended.

INTRODUCTION

Most automatic weather stations operated by the United Kingdom Meteorological Office are equipped with both an electronic relative humidity probe (referred to below as the probe) and two platinum resistance thermometers configured as dry-bulb and wet-bulb (referred to collectively as the psychrometer). These three sensors are exposed in a naturally ventilated thermometer (Stevenson) screen.

At present the probe and the psychrometer are treated as independent instruments. The reported dew point is taken from the psychrometer unless the wet-bulb temperature is 0°C or less. This practice can produce large errors when the wet-bulb dries or the relative humidity is low and the wind is very light. Also, unacceptable jumps in reported dew point can occur when the probe is brought into use, especially if the probe has been in the field for some time and its calibration has changed.

The proposed procedure uses the strengths of one type of sensor to compensate for the weaknesses of the other.

The strengths of the psychrometer are:

(a) good long-term stability of the platinum resistance thermometers,
(b) sensors can be checked in the field,
(a) accuracy can be restored by replacing the wick,
(b) it is most accurate at high relative humidity.

Weaknesses of the naturally ventilated psychrometer are:

(a) the wet-bulb may become dry,
(b) it is not accurate at low humidity,
(c) it is not accurate at low wind speeds,
(d) it is not accurate when the wet-bulb temperature is below 0°C.

Strengths of the probe are:

(a) it can be calibrated to give required accuracy over a wide range of relative humidities and ambient temperatures,
(b) the accuracy is largely unaffected by wind speed.

Weaknesses of the probe are:

(a) errors of several percent relative humidity may develop between calibrations which are normally at intervals of six months,
(b) sensors may become less responsive to rapid changes in relative humidity after a few months in the field

PROCEDURE CARRIED OUT BY THE AUTOMATIC WEATHER STATION

The following procedure is carried out automatically each minute

---

Read dry-bulb temperature
Read wet-bulb temperature
Read probe relative humidity
Read wind speed (1-minute mean at 10 metres)
Apply correction to obtain corrected probe relative humidity (RH) [Note 1]
Apply lag to dry-bulb temperature to estimate probe temperature [Note 2]
Calculate probe dew point using corrected probe RH and estimated probe temperature

<u>If wind speed < 5 knots OR wet-bulb temperature ≤ 0.5°C then END</u> else [Note 3]

Calculate psychrometer relative humidity
Calculate psychrometer dew point

<u>If wet-bulb is dry then END</u> else [Note 4]

Update correction to probe [Note 5]
Update variance of probe dew point [Note 6]
Update variance of psychrometer dew point [Note 6]

Notes

1 A different correction is allowed for each 5% range of relative humidity.

2 The temperature of the probe lags the dry-bulb temperature by about 90 seconds and the probe's internal temperature sensor is not stable enough to ensure long-term accuracy of dew-point measurements. The additional lag of the probe temperature is not a major problem when the sensors are exposed in a conventional thermometer screen but can cause large errors when a rapid response temperature sensor is used (Richardson et al 1).

3 The naturally ventilated psychrometer does not provide accurate measurements of relative humidity and dew point when the wet-bulb temperature is below 0.5°C or the wind speed is too low.

4 The difference [psychrometer dew point - probe dew point] is smoothed by an exponentially filter with a time constant 5 minutes.

If this smoothed value is > 0.5 + (dry-bulb temperature - probe dew point) * 0.15 then the wick is assumed to be dry.

5 The probe correction, for the appropriate relative humidity pentad, is updated using the relationship

new correction = old correction*(1-k) + (psychrometer RH - probe RH)*k

where k = 0.0006942.

This is equivalent to a time constant of 24 hours if the same correction is updated each minute but in practice the time constant will usually be longer.

6 The variance of minute-to-minute changes in the probe dew-point and the psychrometer dew point are updated using a relationships of the type

new variance = old variance *(1-k) + k*(this value - last value)^2

where k = 0.0006942 which gives a lag of about 24 hours.

PERFORMANCE OF THE AUTOMATIC WEATHER STATION PROCEDURE IN THE FIELD

Figure 1 Identification of a drying wet-bulb

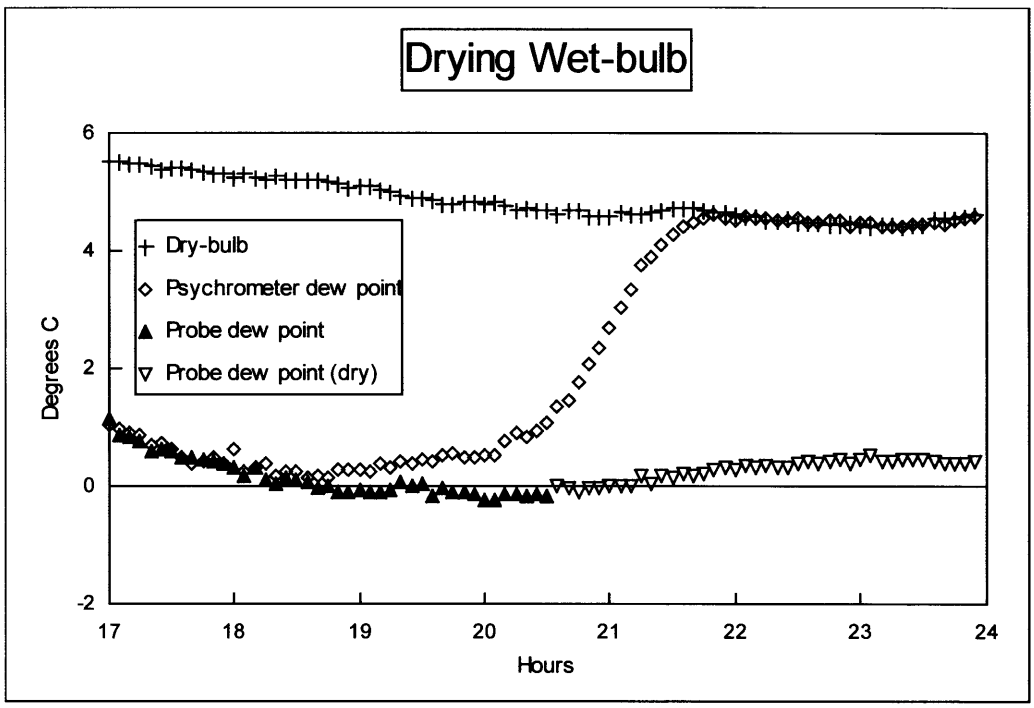

A key element in the above procedure is detection of a dry wick and Figure1 shows how it performed in the field. The figure shows values of dry-bulb temperature, psychrometer dew point and probe dew point over a period of seven hours during which the wet-bulb was allowed to dry. Until about 1810 the psychrometer and probe are in good agreement but after that the psychrometer dew point increases while the probe dew point falls slightly. At about 2035 the procedure recognised that the wet-bulb was dry. This is shown by the by the probe dew point plot changing from solid triangles to open triangles.

Another feature of the above procedure is comparison of the sensitivity of the probe and the psychrometer. Although there is a considerable diurnal variation in the magnitude of minute to minute changes in dew point it was found that the ratio of the probe response to the psychrometer response remained relatively constant throughout the day. This makes it easy to monitor the sensitivity of the probe and withdraw it from service if it becomes sluggish.

When conditions allow the psychrometer to provide accurate measurements the procedure adjusts the corrections to the probe to keep it in agreement with the psychrometer. Figure 2 shows how corrections determined by reference to the psychrometer compare with those found in the laboratory at the end of the field trial.

The points labelled 5degC, 10degC & 25degC show the corrections determined in the laboratory at those temperatures. The points labelled Psychrometer show the corrections produced in the field by reference to the psychrometer at an average temperature of 14°C. When the probe was installed in the field all corrections were set to zero and were allowed to develop over a period of a month. The corrections produced by reference to the psychrometer at high relative humidity are about 1%RH lower than those found in the laboratory and this difference increases to about 1.5%RH at 55% RH. No corrections with reference to the psychrometer are plotted for relative humidity less than 40% because there were too few periods with relative humidity below 40% during the field trial for the corrections to be changed form the initial value of zero.

Figure 2

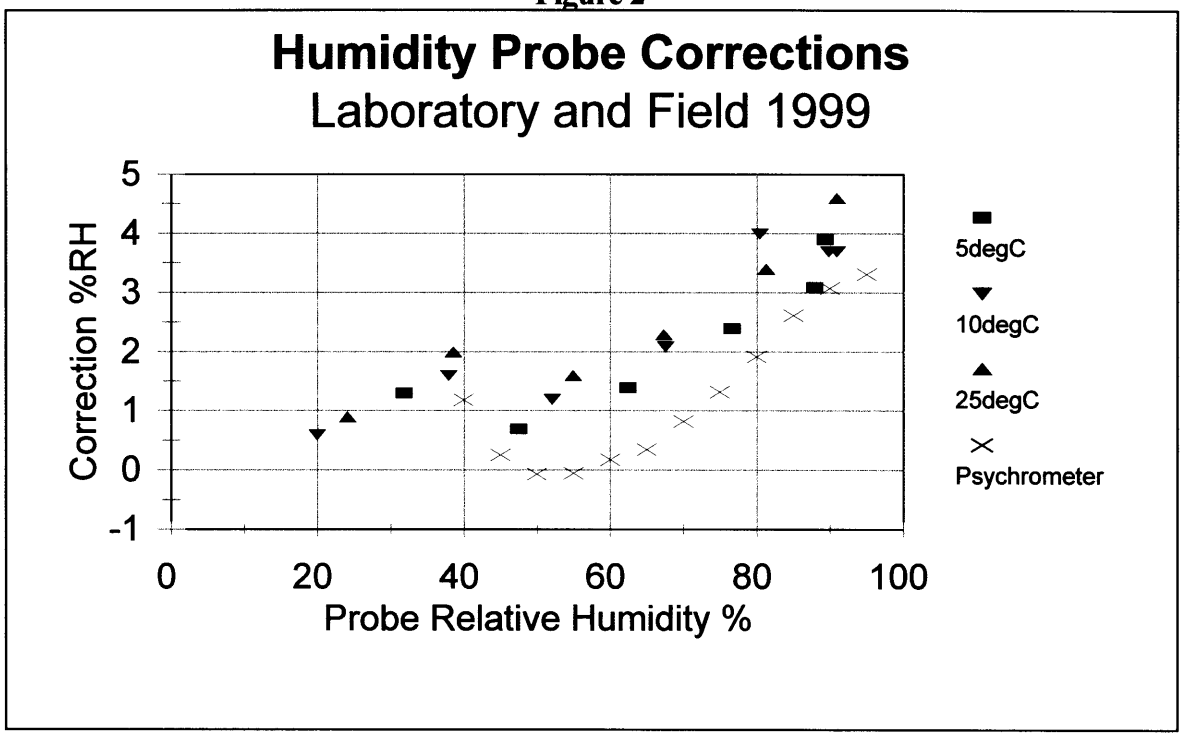

DISCUSSION

The procedures outlined above offers the possibility of maintaining accurate measurements of relative humidity and dew point from an automatic weather station in a temperate climate. It reduces errors due to the slow calibration drift of an electronic humidity probe and eliminates the gross errors that can occur when a wet-bulb dries. It allows humidity probes to be kept in the field longer between laboratory calibrations, which could have considerable economic benefit.

These advantages do not come without effort. Good caretaker maintenance of the wet-bulb is essential to ensure that the wick is clean and is supplied with pure water. The automatic weather station manager must monitor the sensitivity of the probe and the corrections that are developing. Loss of sensitivity, excessive sensitivity or rapid change of corrections indicate the need to change the probe.

REFERENCE

1. Richardson, S.J., Fredrickson, S.E., Brock, F.V. and Brotzge, J.A., Combination Temperature and Relative Humidity Probes: Avoiding Large Air Temperature Errors and Associated Relative Humidity Errors, 10th Symposium on Met. Observations & Instrumentation, American Meterological Society. pp 278 - 283.

New Automatic Observation Method of Evaporation
- Class "A" Evaporation Pan -

Lee, Bu-Yong, Park, Byoung-Yoon, Woo, Hyung-Taek

Department of Environmental Science, Catholic University of Taegu
Kyongbuk 712-702, Republic of Korea
bylee@cuth.cataegu.ac.kr

1. Introduction

The measurement of evaporation from the surface of land and water has been one of important meteorological elements in the study of atmospheric science. The currently used methods of measuring evaporation volume are experimental method, numerical interpretation method, and the use of Class "A" Evaporation Pan. Of these methods, the use of Class "A" Evaporation Pan estimates evaporation by measuring changes in water depth in the pan that are obtained from hook gauge and vernier scale by observer. This method measures water level by 0.1mm. Up to present, several instruments for automatic water level recording have been produced. However, they have not been used in weather station since their measurement accuracy has not reached to the level of 0.1mm recommended by WMO. This study was, thus, conducted to develop water level measurement sensor for the use of Class "A" Evaporation pan and examine its validity by observing water level in Pan.

2. Comparison of Methods of Automatic Evaporation Measurement

2.1 Current Method of Automatic Evaporation Measurement

The current method measures the distance to water surface from the fixed position. This measurement method records water level changes by electric signal resulting from rotation angle changes of rotating equipment that is turning round in accordance with water level changes and is connected to buoyant equipment with a wire. This method has, however, the problem of measurement accuracy having more than ±0.5mm error due to the effect of frictional force.

2.2 New Method of Automatic Evaporation Measurement

Our new method converts changed volumes of water level to those of buoyant force and then transforms buoyant changes into electric signal by using straingauge loadcell. This method has the advantage of increasing measurement accuracy by eliminating moving part causing error.

3. Results

3.1 Experimental Verification of Newly Developed Instrument

Tabel 1 shows both values of true depth obtained from calculation and values of depth measured by water level measurement sensor devised by us according to every 1mm change of water level in experimental water tank.

Table 1. The values measured by new instrument

No	True Depth(mm)	Measured Depth(mm)
1	0.00	0.00 (0.00)
2	1.00	1.02 (+0.02)
3	2.00	2.00 (0.00)
4	3.00	3.03 (+0.03)
5	4.00	4.00 (0.00)
6	5.00	4.99 (-0.01)
7	6.00	5.97 (-0.03)
8	7.00	6.97 (-0.03)
9	8.00	7.97 (-0.03)
10	9.00	8.97 (-0.03)

As shown in table 1, the new instrument measured changes in water level up to 0.01mm level and the errors of measured values against true depth were within the range of ±0.03mm at 9mm full scale.

3.2 Comparison of Observed Data and Measured Values in Field Station

The validity of new instrument was examined by comparing its measured values with values recorded by observer obtained from August 21 to September 3, 1997. The data measured and observed during 9 days from August 21 to 29 were shown in table 2.

The recorder used in observation was 21X datalogger made by Campbell Scientific, Incorporated. In table 2, Observer is observed values, measured by observer, in Class "A" Evaporation Pan installed at Suwon Meteorological Station located in Gyeonggi Province. New method is values measured by new instrument. Precip. is the amount of rainfall during the observation period, and W/S is wind speed. The values in parenthesis are the differences between observer and new method.

Table 2. Comparison data of new method during 21 to 29 August 1997 at Suwon

Date	Observer	New Method(mm)	Precip.	W/S(m/s) 9AM
8. 21	2.4	2.8 (+0.4)		3.3
8. 22	4.7	4.9 (+0.2)		0.5
8. 23	3.7	3.1 (-0.6)		1.5
8. 24	3.2	3.7 (+0.5)		1.0
8. 25	4.4	3.5 (-0.9)	7.1	4.0
8. 26	2.4	2.4 (0.0)	0.7	3.0
8. 27	3.9	4.5 (+0.6)		1.7
8. 28	3.6	3.8 (+0.2)		0.5
8. 29	3.0	2.1 (-0.9)	1.4	2.0
Total	31.3	30.8 (-0.5)	9.2	

As shown in table 2, the maximum difference between observed and measured values was 0.9mm for 2 days and other recorded data were revealed below than that value. There were rainfalls during August 25, 26 and 29. In a case of August 26, observed value was equal to that measured by new instrument. While the total evaporation measured by observer during the observed period was 31.3mm, new method showed 30.8mm. The difference in the total amount of evaporation between two methods was 0.5mm.

We also attempted to show the possibility of hourly measurement of evaporation by new instrument. Fig. 1 shows the evaporation rate per hour during April 24 to 26, 2000. Maximum evaporation rate was 0.6mm around 3PM and markedly decreased during the night on 24 April.

The new instrument developed by this research can record water level changes less than 0.1mm. The very small error was found in the total evaporation values between observed method and new one. These results clearly prove that new instrument follows up and records water level changes accurately.

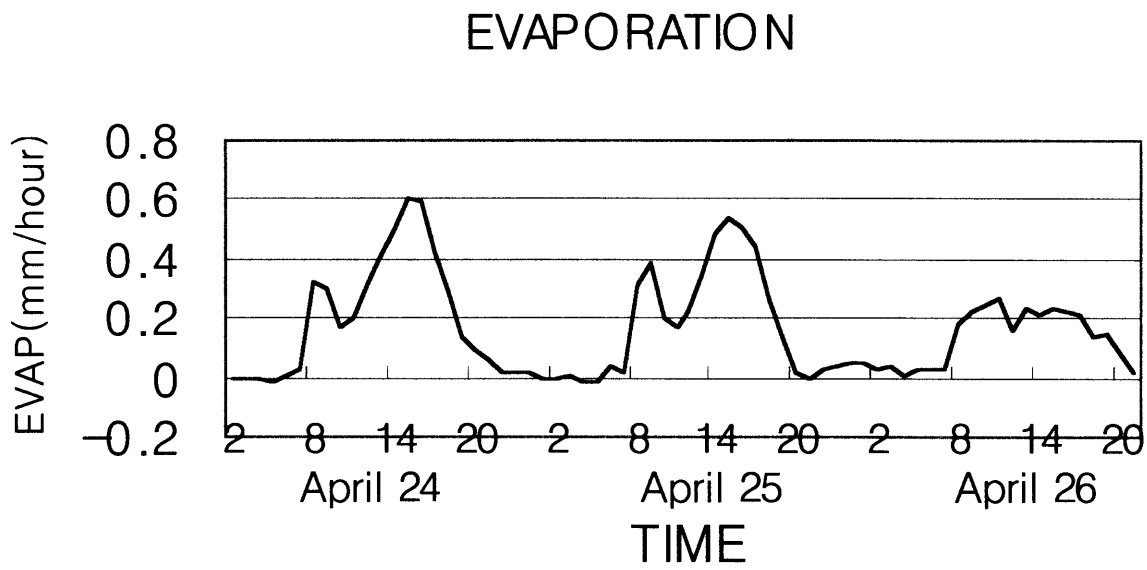

Fig. 1. Example of evaporation measurement by new instrument during 24 to 26 April, 2000 at NIAST study field at Suwon.

4. Conclusion

The following results were obtained from the experiment and field test of evaporation recorder

1) New method accurately measures water level less than 0.1mm
2) Automatic measurement of evaporation per hour is possible
3) Automatic evaporation recorder with the level of 0.1mm can be made for the use of evaporation observation.

Reference

Assouline, S. and Y. Mahrer, 1996 : Spatial and temporal variability in microclimate and evaporation over lake Kinneret : Experimental evaluation., American Meter. Soc. 35, 1976 ~ 1084.

Bolsenga, S.J., 1975 : Estimating energy budget components to determine lake Hron evaporation. Water Resour. Res. 11, 661~666.

The Application of the RARR in the Surveillance of Urban Rainfall Distribution

Fang Guoliang

(Shanghai Meteorological Research Institute. Shanghai 200030)

Shao Lingling

(Shanghai Central Meterological Observatary.Shanghai 200030)

Abstract

Remote automatic rainfall recorder is an intelligent measuring apparatus. It can offer us real time rainfall data of different periods according to various requirements and provide forecast the urban rainfall distribution in order to modify short range forecast in time. Its intelligent synthetically statistical function can also offer the overall and correct rainfall measurement for the plan of urban draining works and display rainfall in real time the apparatus can be a rainfall observation of the network. The observation of weather radar can be modified by comparing with the observation of the network so that the rainfall development process can be revealed correctly and the first hand data for scientific research of the short-range rainfall can be provided.

Keywords: Remote automatic rainfall recorder, weather radar

Preface

As storm rainfall is a kind of the catastrophic weather in the cities of our country, basing upon the status of Shanghai area and the demands of production of the industry and the agriculture, we developed an intelligent measuring apparatus -- Remote Automatic Rainfall Recorder(RARR), which can collect, store and display data automatically, offer real-time and different periods information of cumulate rainfall to help forecasters know the case about the urban rainfall distribution and amend short range forecast in time. The intelligent and synthetically statistical function of RARR can also provide the overall and accurate rainfall measurement for the programming of urban drainage system and the design of agricultural irrigation project. In addition to its characteristics mentioned above, RARRs can be set up to form a rainfall observation network, which contrasts with the weather radar so as to revise its observation result of rainfall, reveal the developmental and evolutive process of rainfall system timelier and more precisely and provide the first-hand information for the research of short-term precipitation forecast.

Performance and Technique Indexes of RARR

RARR is specially used in the automatic collection, disposal and storage of rainfall data, which is composed of the mainframe, the precipitation rainfall sensor and so on. Equipped with sixteen soft buttons, DC/DC board with highly bright LEDs, the mainframe consists of CPU, RAM, CU(Counting Unit), etc. The sensor, flexible and accurate, is like a tipping bucket, showing original design and high reliability, and still has a set of real-time control software. There are two standard RS-232C interfaces in RARR(fig.1), one connected to the remote modem and another to the computer. When it rains, the sensor convert the rainfall information into the pulse signals, and simultaneously, CU takes count automatically and CPU reads data once per minute, which will be stored in RAM and displayed on the LED board. The rainfall data of different periods can be shown by touching

the soft buttons mentioned earlier to help the observers grasp the rainfall status in the observation area at any moment. Furthermore, for the convenience of forecasters, RARR is equipped with calendar and timer.

The technique indexes of RARR are as follows.

The range of rainfall measured		1~200mm/h
	Resolution	0.1mm
	Precision	<10mm, (±)0.4mm
		>10mm, (±)4mm

Near 40 RARRs can be distributed throughout the different parts of Shanghai area such as organs, villages and towns, streets, parks and so on to form a network of remote observation spots (seen in fig.2). At each spot, the precipitation can be displayed by the RARR as it reaches 0.1mm, and the rainfall info can be transmitted to the control center in time in the case of online to the local network.

The Observation of Rainfall

The content of observation

To get the intensity and distribution of rainfall of the city in time, RARR may work from 8 p.m.(Beijing time, same as follows) of the previous day to 8 p.m. of the current day with a sampling time of one minute, and save data automatically. If time passes 8 p.m., the new rainfall data will be stored as another day. RARR can preserve the data of the latest two days. Besides the instantaneous rainfall, precipitation within one hour, as well as two and three, can be shown on the LED board by pushing the relevant buttons at any moment to represent clearly the evolution of rainfall system. If the rainfall runs over the given value, which can be set manually, RARR will give an alarm. Connected to the computer with a printer, RARR can also print the maximal intensity values of rainfall within ten minutes and one hour and the time when they emerge in table.

The actual records of rainfall data

There generally appeared a rainstorm, even heavy, in Shanghai area at 4 p.m. on Jun 24, 1996 affected by the southward movement of the intense JiangHuai rain band. Up to 4 p.m. on 25th, there were 12 of near 40 remote observation spots in the urban area whose measuring precipitation reached about 100mm/24h(shown in table 1). The statistics of the rainfall shows that its distribution in the city was spatio-temporally nonuniform and there are three time pieces with the concentrated rainfall like 4 p.m. to 5 p.m. on Jun 24 and 7 a.m. to 9 a.m. on Jun 25. In Nanshi District, the precipitation rainfall that is 111.4 mm in the Xiao Dongmen Street spot is about one time as mush as that which is 56.7 mm in the government spot. The same thing happens in another two spots, Nanxiang and Loutang in Jiading District. However, the maximal rainfall intensity in one hour appears in Loutang, which is 35.6 mm, and that in ten minutes in the government of Nanshi District, which is 24.7 mm. The concentrated rainfall in this spot would cause seeper most readily, though its precipitation is not too much. In the course of this rainstorm, due to the real-time rainfall information provided by RARRs continually, each related department of the city made a good preparation so that there were no streets with seeper except some district without drainage systems. Compared with the rainstorms in the last several years, which led to the seeper in hundreds of streets and thousands of dwelling houses, such situation improves more nowadays.

The Comparison between the Data of the Weather Radar and those of the RARR

The weather radar can display the planar distribution of the rainfall area, detect its echo intensity and quickly figure out the rainfall intensity and precipitation in a diameter of 2 to 200 kilometers area. However, this is only an indirect way to get the results, and it's a rather complex process to work out the rainfall intensity through the echo signal value of the weather radar. Now in our country, the density of the distribution of rainfall station is so sparse that it's difficult to acquire the exact rainfall intensity and precipitation in a certain area. In contrast to the weather radar, the RARR can make a good complement. The high density distribution of the RARR makes it possible to

provide many kinds of accurate and timely rainfall data of different periods of time in urban area. The weather radar can estimate the rainfall intensity, rainfall distribution and the total precipitation on each spot in its scanning area and get the rainfall information in large area. Therefore, RARR and the weather radar can be used cooperatively to improve the rainfall surveillance and prediction by the meteorological departments.

There are several methods, such as Z-I relation, (标准目标法)standard targets, (电磁波衰减法)electromagnetic wave attenuation, (正交偏振法)orthogonality polarization and so on, for the quantitative rainfall measurement of the weather radar. At present in the daily work, Z-I relation is in the most common use. With the measured echo power, the radar reflectivity factor Z can be numerated by the radar meteorological formula and then get the rainfall intensity I via Z-I relation. Usually, the precipitation is obtained by the rainfall intensity multiplying its duration, so the precipitation in a certain area can be achieved by the time integral on it. To make a comparison, Table 2 shows these two kinds of data obtained in a torrential rain process from 16 p.m. to 18 p.m. on Jun 24, 1996. It can be seen that these two kinds of data show the same tendency of variation of rainfall, and also that there in the real cases exists a certain deviation deriving from Z-I relation of the weather radar. In Z-I relation formula, the parameter A and b are not constant for firstly, the variability of actual rainfall may cause their deviations, secondly, the variation of the falling speed of rain drops by that of the vertical velocity of air may do the same job and thirdly, the measure error of echo signals and the change of the refraction coefficients of radio wave along with its attenuation functions the same way in its travel process. Therefore, in the course of the quantitative rainfall measurement of the weather radar, the measured drop-size distribution data and the statistic of A and b in Z-I relation formula should be used to increase its veracity in terms of the temporal and local situation.

The error revision of the rainfall estimation of the weather radar with the measured records of the RARR

The research suggests that for the middle latitude areas and the radar the wavelength of which be from 5 cm to 10 cm, Z=200I is the typical formula to estimate the rainfall. But, in fact, Z-I relation is not unique in the rainfall estimation. It changes with different places, seasons and rainfall types, and its A and b also change even in the same rainfall course mainly due to the spectrum variety of drop-size distribution. Consequently, the error of the rainfall estimation of the weather radar results primarily from the change of Z-I relation. It's impossible, however, to measure raindrop size distribution every time in the practical work to calculate A and b, so the data of the RARR may be employed to calibrate the rainfall estimation of the weather radar.

To begin with, the data from N RARRs acquired in time are compared with the data from the weather radar at the corresponding observation points to ascertain the divergence between the actual value by the RARR and that by Z-I relation. Next, the latter at each point is multiplied by a revision factor to get the regional rainfall distribution. The concretely adopted formula is as follows:

$$\overline{(G/I)} = (I/N) \sum_{i=1}^{N} (G_i/I_i)$$

In which ($\overline{(G/I)}$)is the revision factor,(G_i)the hourly precipitation by the RARR and (I_i) the rainfall by the weather radar.

The data by the RARR are used to adjust those by the weather radar, which can not only have the advantages of high-resolution and large-scale rainfall distribution, but also improve the accuracy of rainfall measurement.

Conclusion

1.The application of the RARR makes better the disadvantageous situations that there are only several rainfall observation spots, and provides the related branches a better understanding of the real-time rainfall conditions;

2. As an intelligent measuring device, the RARR can gather data automatically, display the actual rainfall of different periods of time and offer integral and accurate rainfall data;

3. Due to different kinds of factors that give birth to divergence, there exists a definite error in measuring the rainfall intensity at an observation point by the weather radar and also a deviation between the rainfall data of the RARR and those of the weather radar.

4. By employing both the data of the RARR and those of the weather radar, the deviation in the rainfall measurement through the weather radar can be reduced by a simple revision.

References

[1] JunYi Xu etc., The theory and application of one chip microcomputer,The Sci-Tech publishing house of Shanghai,1988.

[2] Edward A.Brandes,Proceeding of NEXRAD Doppler Radar Symposium/Workshop,1982.

[3] A.M.Borovikov etc., Radar Measurement of Precipitation Rate,A.Moscona,Copyright Israel Program for Scientific Translations,1970.

[4] B.SIJIEPANIANKE,Radar's application in meteorology, The Sci-Tech publishing house,1979.

[5] DaZhang Tang,HongYuan Guo etc.,The preliminary discussion of Z-I relation, Journal NANJING Institute of Meteorology,1,91-101,1978.

1 MEASUREMENT TECHNOLOGY, PERFORMANCE, AND QUALITY ASSURANCE

1.1 Surface Observation Systems

1.1.4 Solar Radiation Observations

ABSOLUTE CALIBRATION OF PYRGEOMETERS: A PROPOSAL FOR A WORLD RADIOMETRIC REFERENCE FOR LONGWAVE IRRADIANCE MEASUREMENTS

Rolf Philipona
Physikalisch-Meteorologisches Observatorium Davos, World Radiation Center, (PMOD/WRC)
Dorfstrasse 33, CH-7260 Davos Dorf, Switzerland
Tel: +41 81 417 5131, Fax: +41 81 417 5100, E-mail: rphilipona@pmodwrc.ch

Atsumu Ohmura
Institute for Climate Research, ETHZ
CH-8057 Zürich

ABSTRACT

The World Standard Group (WSG), a group of seven absolute pyrheliometers located at the World Radiation Center in Davos, manifests the World Radiometric Reference (WRR) for shortwave irradiance measurements and is in WMO regulations since 1981. For upward and downward longwave irradiance measurements however, no such standard nor reference is available at present. Due to the importance of longwave radiation in relation to radiation budget, cloud forcing, greenhouse effect and climate change research this shortcoming needs to be addressed and a WRR for longwave irradiance measurements need to be established. This in particular, since instrument calibration and measurement techniques were drastically improved in recent years, making accurate and reliable long-term measurements a perfect tool for climate change observation.

1. INTRODUCTION

Atmospheric longwave irradiance is usually measured with hemispherical (2π) receivers on flat horizontal surfaces. Pyrgeometers are the most prominent instruments to measure longwave irradiance in climatological networks. The most widely used Eppley Precision Infrared Pyrgeometer (PIR) was improved over the last 25 years. New instruments like the CG4 pyrgeometer from Kipp&Zonen show very promising advantages with respect to dome heating and spectral transmission. Investigations on calibration methods, instrument characterization and measurement techniques at PMOD/WRC (Philipona et al., 1995) let to a deeper understanding and drastic improvements of pyrgeometer calibration and measurements. The Baseline Surface Radiation Network (BSRN) round-robin calibration experiment (Philipona et al. 1998), demonstrated that PIRs are stable and that calibration results of individual black-body calibration sources used worldwide are within 1 to 2 percent to each other. Field measurements at the BSRN initiated first International Pyrgeometer and Absolute Scanning Radiometer Comparison (IPASRC-I) demonstrated the limits of pyrgeometer measurement precision if one is using individual black-body calibration factors. Improvements of precision, or intercomparability between instruments, were demonstrated on the basis of a final field calibration, comparing pyrgeometers with an absolute reference standard instrument. As reference standard a sky-scanning absolute instrument was used, which was build at PMOD/WRC based on a commercial pyroelectric detector and a reference black-body source. Sky radiance at a narrow viewing angle is compared to radiance measurements in the well characterized reference black-body source. The absolute value of hemispherical downward longwave irradiance is determined by Gaussian quadrature integration over 32 sky radiance measurements at predetermined directions.

Improvements on pyrgeometers, calibration apparatuses and measurement techniques up to the level adequate for a world radiometric reference for longwave irradiance measurements will be presented. Results of the BSRN round-robin and IPASRC-I experiments will be presented, showing drastic improvements of pyrgeometer measurements achieved with field calibrations.

2. PYRGEOMETERS

Pyrgeometers and pyrradiometers are instruments used to measure atmospheric and terrestrial longwave irradiance. In meteorological and climatological networks, pyrgeometers are preferred over pyrradiometers primarily because of their long-term stability due to their very stable silicon domes compared to polyethylene domes of pyrradiometers. Pyrgeometer silicon domes, and their interference filter deposited on the inside wall, blocking shortwave radiation below 4 microns, provide the additional advantage to directly measure the longwave component, whereas pyrradiometers measure shortwave and longwave irradiance from which the shortwave component, separately measured with pyranometers, has to be subtracted.

In climate research as well as for meteorological longwave radiation measurements, the Eppley PIR pyrgeometer is the most used instrument (Drummond et al. 1970). Mayor improvements over the last 25 years,

like the change from a KRS-5 to a silicon dome, the dome temperature measurement and its appropriate evaluation formula (Albrecht et al., 1974), as well as the improved dome temperature measurement and extended pyrgeometer formula (Philipona et al., 1995), made the PIR, if correctly deployed, a stable and reliable instrument. Thermal dome effects, which were the largest source of errors, have well been taken care of with the new three thermistors dome temperature measurement.

The CG4 pyrgeometer from Kipp&Zonen has been brought on the market very recently and is a new version of their CG1 pyrgeometer. The CG1 with its flat window had a full view angle of only 160 degrees, whereas the new CG4 has a meniscus shaped dome providing 2π hemispherical view. To achieve optimal thermal conductivity between dome and body the meniscus shaped dome is clamped with an aluminum ring onto the pyrgeometer body. This sandwich construction and high thermal conductivity of silicon, makes the dome an almost integral part of the aluminum body and temperature differences between dome and body, and hence thermal dome effects, are almost non existent in the CG4.

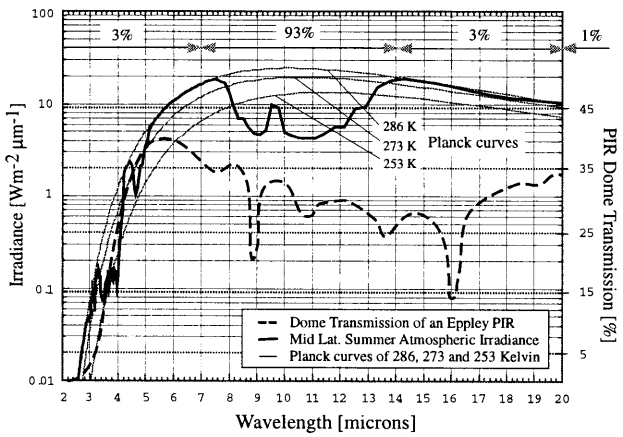

Fig. 1: Planck calibration curves compared to a MODTRAN calculated spectra of mid latitude summer longwave irradiance at Davos (1580m a.s.l.), and dome transmission of a PIR pyrgeometer.

Hence, errors due to thermal effects of silicon domes have been minimized on state of the art pyrgeometers, but spectral transmission effects of the silicon domes, and their shortwave blocking interference filters, is another concern making spectral sensitivity of pyrgeometers very wavelength dependent. Uncertainties with respect to absolute measurements arise in particular with pyrgeometer calibration made in black-body radiation sources. As shown in figure 1, Planck spectral curves from black-body sources are very different from spectral curves of atmospheric longwave radiation. If the spectral sensitivity of a detector measuring atmospheric radiation would be flat over the entire spectrum, say from about 2 to 100 microns, there would be no harm to calibrate the detector with Planck curves, since all wavelength would be treated equally. But PIR dome transmission is low, transmission curves are not at all flat as shown in figure 1 and transmission goes up only between 3 and 5 microns, which means that PIRs do not treat all wavelength with equal sensitivity. These curves can actually be quite different, and although the CG4 dome transmission is higher and improved, it is still not spectrally flat and hence subject to the same problem. Depending on calibration temperature and atmospheric longwave spectrum, which can strongly vary for different temperatures and water vapor amount, certain wavelength may be over- or underestimated during measurements and hence create considerable uncertainties. Further uncertainties are due to possible inhomogenity of the interference filter deposited on the inside wall of the spherical PIR dome. Deposition of the interference filter is easier on the flat meniscus shaped dome of the CG4 and therefore more uniform. Additional errors are due to the cosine effect even though longwave radiation from large zenith angles is small.

2. BLACK-BODY CALIBRATION

Pyrgeometers have always been calibrated with black-body radiation sources. Thermal radiation at intensity levels close to atmospheric radiation is easily generated in black-body cavity radiation sources, working in the range from ambient temperature to about 30 Kelvin below, and emitting Planck spectral radiation at emissivities of almost unity. In contrast to atmospheric longwave radiation, which has a maximum at the zenith and is zero at the horizon, black-body radiation sources show a different radiation pattern emitting uniform longwave radiance over all zenith angles.

With the aim of improving the consistency of longwave radiation measurements within their network, the BSRN community started in 1994 a pyrgeometer calibration round-robin experiment, to test individual black-body calibrations made worldwide. A set of five PIRs was sent around and was individually calibrated by eleven laboratories in seven different countries. Participants were supposed to use their own methods and calibration devices whereas the five standard pyrgeometers and a data acquisition system with a non-intrudable computer program was provided. The round-robin experiment was conducted in a "blind" sense in that the participants would have no knowledge of the results of others until the experiment was completed.

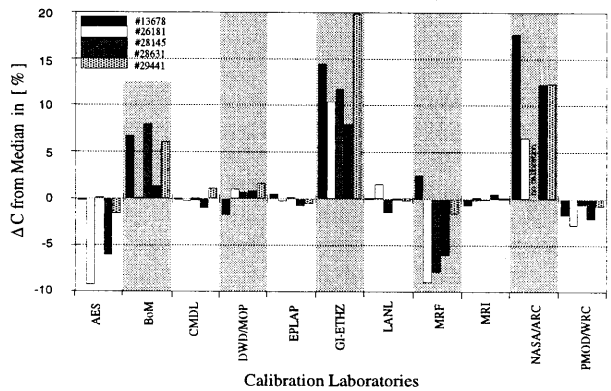

Fig. 2: BSRN Pyrgeometer calibration round-robin comparison results.

The responsivities C [$\mu V/Wm^{-2}$] determined by six of the eleven institutes were within about 2% of the median for all the five PIR pyrgeometers (see Fig. 2). Among the six laboratories, the absolute deviation around the median for each instrument is less than one percent. This small scatter suggests that PIR pyrgeometer were stable during the two years of the experiment and that six different calibration devices reproduce the responsivity C of PIRs consistently.

3. REFERENCE SKY RADIOMETER

With thermal effects of pyrgeometer domes being minimized and black-body radiation sources reproducing calibration factors, or responsivity values C, consistently, uncertainties due to spectral and directional response, connected to dubious pyrgeometer dome transmission and cosine effects, have still to be addressed in particular with respect to correctly measuring absolute values of atmospheric longwave irradiance. Since these uncertainties are all directly related to black-body pyrgeometer calibration, a new approach comparing pyrgeometer measurements to an absolute reference longwave instrument was taken.

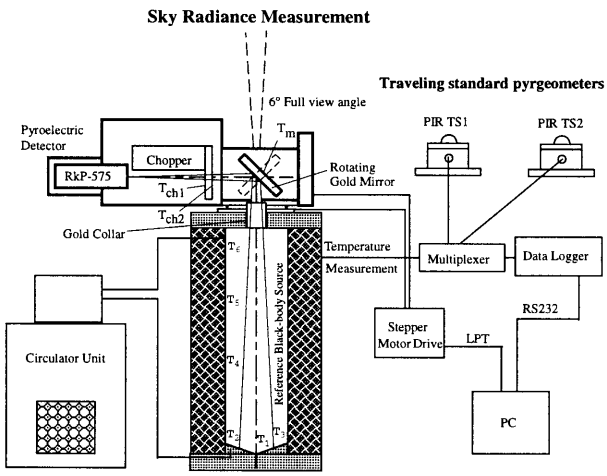

Fig. 3: PCSR absolute reference to field calibrate pyrgeometers.

The Planck Calibrated Sky Radiometer (PCSR) shown in figure 3 serves as absolute reference instrument and is based on a completely different design and measurement principle. In order to prevent errors related to spectral sensitivity, a cavity-design pyroelectric detector has been chosen and no window or optical component except of an high reflecting gold mirror positioned at 45 degrees is in the beam path from the detector to the sky. Thus, the relative spectral response of the PCSR is almost flat decreasing by only 4 percent from 2 to 15 microns, which is the most important spectral part for atmospheric longwave radiation measurements. It further decreases by another 6 percent out to 30 microns. Also, the PCSR does not measure hemispherical as pyrgeometers do, but scans the sky with a narrow full view angle of 6 degrees. Two rotation stages, one for rotating the gold mirror around its horizontal axis and one for rotating the entire detector head azimuthally, allow to point the probe beam to any direction into the sky and also vertically down into the reference black-body source for calibration. With 32 sky radiance measurements, taken during a scan, a Gaussian quadrature integration is used to calculate the hemispherical longwave irradiance. Since no window nor any filter is installed in the beam path, sky scans can only be made during night time to prevent shortwave radiation disturb longwave radiance measurements. Also, for high quality measurements, scans should be made during rather homogeneous clear sky situations.

The Planck calibrated sky radiometer (Philipona, 2000) is designed as an absolute reference standard instrument. In contrast to solar shortwave irradiance which in absolute cavity radiometers is substituted with electrical power and hence traced to an absolute standard of electrical power, the PCSR longwave sky radiance measurement is compared to radiance, measured in a reference black-body source. The emittance of this black-body source is accurately known and its temperature is traced to the absolute temperature standard of the Swiss federal office of metrology. Calibration procedure and sky radiance measurements are interleaved and are referred to the chopper temperature which is also traced to the temperature standard and hence allows to determine the absolute value of longwave irradiance.

4. FIELD INTERCOMPARISON

In fall 1999 the BSRN community, in collaboration with scientists of the Atmospheric Radiation Measurements (ARM) program, conducted the first international pyrgeometer and absolute sky-scanning radiometer comparison (IPASRC-I). 15 pyrgeometers of which 8 standard Eppley PIR, 6 PMOD/WRC modified PIRs and 1 Kipp&Zonen CG4 pyrgeometer were compared to the PCSR sky-scanning radiometer and to transfer model calculations at the U.S. Southern Great Plains (SGP) Cloud and Radiation Testbed (CART) site. The aim of IPASRC-I was to evaluate present precision levels of pyrgeometer field measurements relative to each other and with respect to absolute measurements of downward longwave radiation.

The 15 participating pyrgeometers were chosen from a broad international community. To their USER or PMOD black-body calibration factors a common black-body calibration was performed at NOAA/CMDL preceding the intercomparison. All pyrgeometers were equipped with ventilation systems and tracking shade discs, and 1 minute integrated readings were recorded. During 8 consecutive days of measurements, pyrgeometers were compared to each other and to nighttime PCSR absolute measurements. Using balloon sounding and ancillary measurements, 4 clear sky morning time slots could be compared to transfer model calculations.

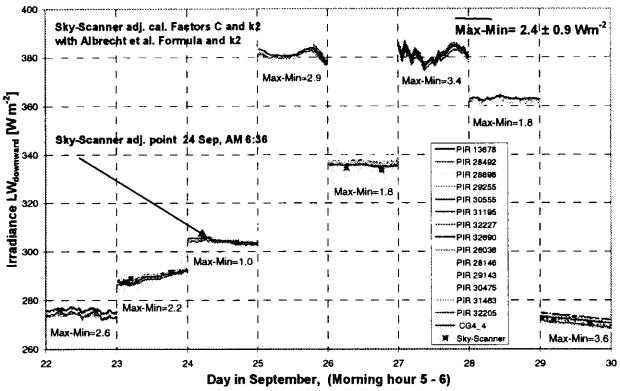

Fig. 4: IPASRC-I nighttime (AM 5-6) intercomparison of all 15 pyrgeometers using FIELD calibration factors.

The 15 pyrgeometers were intercompared with USER and CMDL black-body calibration factors using the standard Albrecht et al. pyrgeometer formula, and for the 7 modified pyrgeometers (6 mod. PIRs and 1 CG4) PMOD calibration factors and the new Philipona et al. formula was used. Additionally all pyrgeometers were field calibrated using the sky-scan result on 24 Sep. at UT 11:36 as target value to which all pyrgeometer measurements were adjusted by changing their calibration factors C and k_2. With the new FIELD calibration factors longwave downward irradiance was then recalculated for all the 8 days and compared.

Calibration Factors	Pyrgeometer formula and Cal. Factors used	Number of Pyrgeometers involved	Nighttime Max-Min ± Stdev [W m^{-2}]
USER	Albrecht et al. with *C, K*	All [15]	11.9 ± 3.0
CMDL	Albrecht et al. with *C, K*	All [15]	8.4 ± 1.3
PMOD	Philipona et al. *C, k1, k2, k3*	Modified [7]	3.4 ± 0.5
FIELD	Albrecht et al. with *C, k2, K*	All [15]	2.4 ± 0.9
FIELD	Philipona et al. *C, k1, k2, k3*	Modified [7]	1.2 ± 0.4

Table 1: Average Max-Min values over 8 days with different Cal. Factors.

As shown in figure 4 and table 1 the average difference between Maximum and Minimum pyrgeometer reading over 8 days (night hour AM 5-6) is getting smaller from USER to CMDL and to PMOD calibration factors used. However, if we use the FIELD calibration factors the difference is further reduced by a factor of three. For all 15 pyrgeometers the Max-Min is down at 2.4 Wm^{-2} with the FIELD calibration factors, and for the modified pyrgeometers Max-Min goes from 3.4 to 1.2 Wm^{-2} from PMOD to FIELD calibration factors. Hence, comparative field calibration drastically improves precision of pyrgeometer measurements. With respect to absolute values intercomparisons have shown pyrgeometer measurements and transfer model calculations to be within 1 to 2 Wm^{-2} to the PCSR absolute measurements. A more detailed description of these results, including daytime measurements, is in preparation.

5. DISCUSSION

Dome effects due to inhomogeneous and inadequate spectral and directional transmission produce errors and hence uncertainties on pyrgeometer field measurements. Errors are mainly related to calibration factors determined with radiation sources different from atmospheric longwave radiation, such as black-body sources. A sophisticated analysis of individual domes which would allow adequate spectral and directional corrections is very expensive and still not satisfying. IPASRC-I demonstrates, that modified and new pyrgeometers in combination with the extended pyrgeometer formula showed much better results over original PIRs. However, a final field calibration, comparing pyrgeometer measurements to a reference standard improves intercomparability of pyrgeometers again by a factor of three. Hence, pyrgeometer black-body calibration is a first step to determine the dome correction factor and approximate values of the calibration factors. The final calibration factors C and k_2 are much more accurately determined by field comparison to an absolute reference standard.

6. WRR FOR LONGWAVE IRRADIANCE

The World Radiometric Reference for shortwave radiation is inadequate for longwave radiation due to the large difference of intensity. Reference standard instruments traced to absolute temperature standards, like the PCSR, will have to be used as absolute reference for longwave irradiance measurements, and in particular for final field calibration of pyrgeometers. The low level of uncertainty now reached with pyrgeometer measurements make longwave irradiance one of the most promising element for greenhouse related climate change research.

REFERENCES

Philipona, R., C. Fröhlich, Ch. Betz, 1995: Characterization of pyranometers and the accuracy of atmospheric longwave radiation measurements. Appl. Opt., **34**, pp 1598-1605.

Philipona, R., et al., 1996: The baseline surface radiation network pyrgeometer round-robin calibration experiment. J. of Atmospheric and Oceanic Technology, **15**, pp 687-696.

Drummond, A.J., W.J. Scholes, and J.H. Brown, 1970: A new approach to the measurement of terrestrial long-wave radiation. WMO Tech. Note 104, pp 383-387.

Albrecht, B., M. Peollet, and S.K. Cox, 1974: Pyrgeometer measurement from aircraft. Rev. Sci. Instrum., **45**, pp 33-38.

Philipona, R., 2000: The Planck calibrated sky radiometer: an absolute instrument to measure atmospheric longwave radiation. Appl. Opt., submitted for publication.

Investigations of night-time zero offsets at short-wave broadband radiometers

Klaus Behrens and Dr. Klaus Dehne
Deutscher Wetterdienst
GB Forschung und Entwicklung
Meteorologisches Observatorium Potsdam
Postfach 60 05 52
D-14405 Potsdam, Germany
Tel.: +49 331 88893 20 Fax: +49 331 88893 36
E-Mail: klaus.behrens@dwd.de

Abstract

The improvement of the radiation measurements concerning the zero offsets is one of the main goals of pyranometrical research. In a first part the results are discussed of special investigations of the zero offsets in dependence on different ventilation of the domes of CM21 pyranometers as well as of comparisons of CM21, CM22 and a STAR-pyranometer. It is shown, that the night-time zero offsets are mainly influenced by the combination of atmospheric long-wave radiation and fan ventilation power. Furthermore, the results are presented of a long-term investigation (about five years) of night-time zero offsets from routine measurements of pyranometers at the BSRN station at Lindenberg (Germany).

Introduction

The zero offset is defined as the output of the short-wave radiometer device if no short-wave radiation is received.
Principally, both the radiometer and the connected data acquisition device contribute to the zero offset, but the latter - measured simply by a short circuit - should be at modern systems of lower orders of magnitude.
All effects which influence the temperature difference T_0 between the receiver surface and the body of the heat sink belong to the physical sources of zero offsets at thermal receivers - as used in broadband radiometers like pyranometers and pyrheliometers. In the case of a thermopile receiver having n junctions with an EMF of k µV/K and of a radiometer responsivity of R µV/Wm^{-2} the offset irradiance E_0 corresponding to an offset effect of T_0 is given by $E_0 = n\,k\,T_0 / R$. If n=100 and k = 30 µV/K and R = 10 µV/Wm^{-2} ("low temperature thermopile") a T_0 of ± 0,01 K generates already an offset error E_0 of ± 3 Wm^{-2}. Such T_0 values could be produced first of all by:

a) Long-wave radiation, received through the domes
b) Different heat transfer to the receiver surface and the heat sink body caused by
   - front passage or gusts etc.
   - daily course of air temperature.

To reduce the zero offset in the case of pyranometers different measures have been applied:

a) Exposure of the active receiver body and the heat sink body in an equivalent position below the dome, realized in the STAR-pyranometer (receiver surface with black & white segments) for instance.
b) Use of two glass domes (realized in nearby all pyranometers having black receiver surfaces).

Recent improvement: Use of two 4 mm thick quartz domes (more mass and heat conductivity) as realized in the CM22.

c) Ventilation of the outer dome, or more consequently: ventilation of the pyranometer casing (containing the heat sink) and the outer dome successively with the same air stream. The number of such ventilated pyranometers has been increased in the last decade.

The aim of this paper is to demonstrate the reduction of zero offsets by the above mentioned measures for the relatively simply detectable zero offset at night-time. The results of examples measured in the field may be supplemented at the end by long-term values of the German BSRN-Station in Lindenberg.

Performance of night-time offset measurements

The measurements of night time offsets of pyranometers were performed mainly during March 2000 and June 2000 at the National and Regional Radiation Centre in Potsdam (φ = 52,37°, λ = 13,08°, h = 89 m).
The measurement in March should show first of all the reduction of night-time offset **by ventilation** of typical black surface pyranometers. Three Kipp & Zonen pyranometers of type CM21 ventilated by a 5 W-fan of Eigenbrodt (Königsmoor / Germany) were used. The pyranometers are encapsulated in a cylindrical table-casing at which the fan is flanged to blow the air around the pyranometer body.
The air leaves the casing between the radiation shield of the pyranometer and the foot of the outer dome and streams against the dome from all sides. For the standard operation the fan needs only (5 W, 24 V); the air is not pre-heated, the speed of the air is about 1,5 m/s.
To demonstrate the ventilation effect the three simultaneously operated pyranometers are ventilated with the standard power, with the half power and without any power, respectively.

The measurement in June 2000 were performed after the procurement of one of the new "thick quartz dome"-pyranometers of the Kipp & Zonen type CM22, announced as "low offset device". It has been compared with the classical **low offset pyranometer** type "STAR" (Ph. Schenk, Wien) and the "thin dome" pyranometer CM21. Both CM-pyranometers are ventilated (5 W power) while the STAR-pyranometer was unventilated. Later on the CM22 was also operated without any ventilation as the STAR-pyranometer.

The pyranometer output was recorded by data loggers "COMBILOG" of Friedrichs (Hamburg, Germany). During the experiment a short circuit together with the highest resolution of the logger was used to test the influence of the acquisition device. The registered voltage of the short circuit fluctuated within 0 and -0.7 µV. At a typical responsivity of 10 µV/Wm^{-2} the contribution of the logger is about -0,07 Wm^{-2}.

Results

The investigations of the night-time zero offset were done by analyzing the pyranometer output if the sun was more than 5° below the horizon and no short-wave radiation disturbed the measurements.

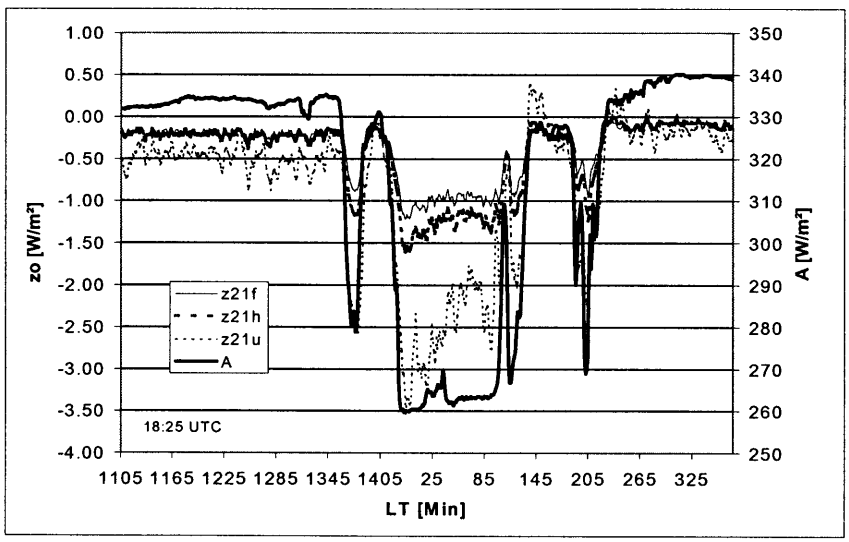

Fig. 1: Night-time zero offset of three different ventilated CM21 (z21f: full power; z21h : half power; z21u: unventilated) and the corresponding long-wave downward radiation A Potsdam, 00-03-06/07

Figure 1 shows a typical picture of the course of the long-wave downward radiation A at changing cloudiness together with the courses of the night-time zero offset of the three (by different power ventilated) CM21 pyranometers. The three offset curves follow more or less the changes of the long-wave downward radiation. The curves of the full power (z21f) and of the half power (z21h) ventilated devices are relatively close together with offsets up to about -1,5 W/m². The unventilated pyranometer (z21u) shows a larger offset than the ventilated instruments. Especially during rapid changes of A the offset of the unventilated devices reaches values of about -3,5 W/m².

Figure 2 presents the corresponding scatter diagram displaying the correlation between the long-wave downward radiation and the night-time offsets. At first this picture gives an impression about the strength of the correlation between the zero offset at different ventilation power and at second it

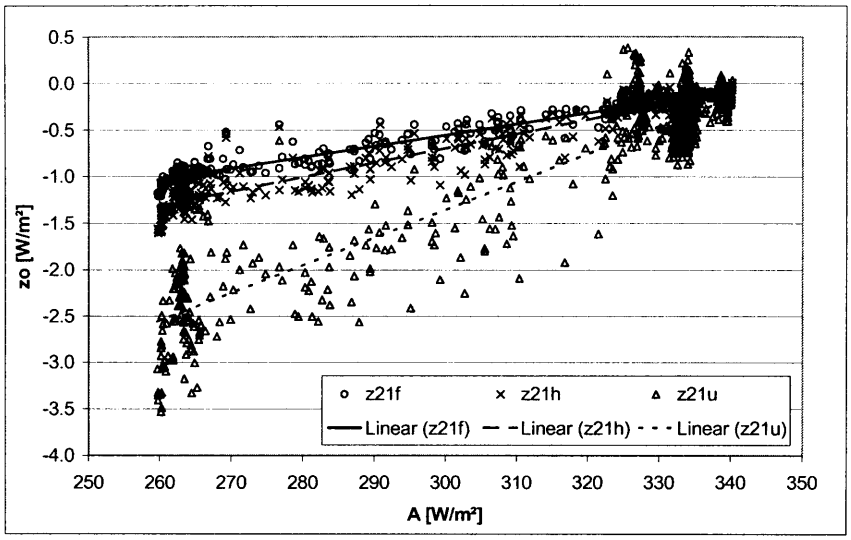

Fig. 2: Scatter plot of the night-time zero offset of different ventilated CM21 (z21f: full power; z21h: half power; z21u: unventilated) and the corresponding linear regression lines in dependence on long-wave downward radiation A
Potsdam, 00-03-06/07

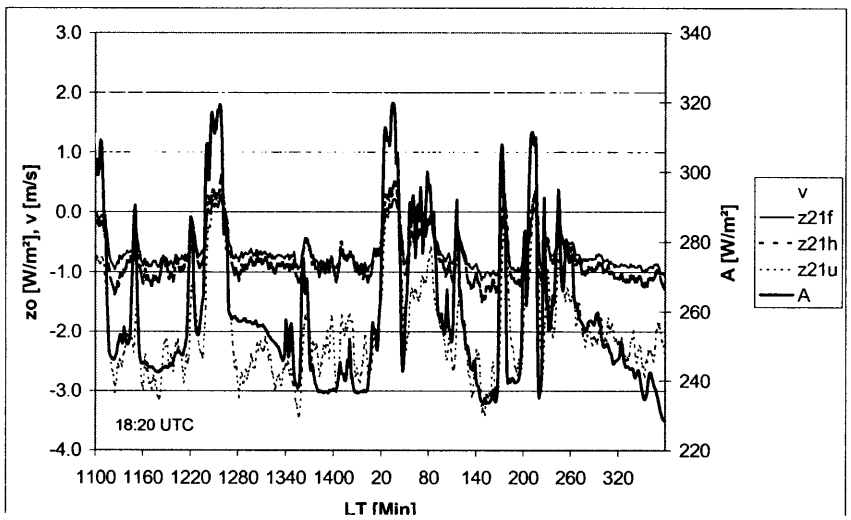

Fig. 3: Night-time zero offset of three different ventilated CM21 (z21f: full power; z21h: half power; z21u: unventilated) and long-wave downward radiation A together with natural wind speed v
Potsdam, 00-03-03/04

Table 1

Date	a	b	c
00-03-06	z21f	1,2	0,982
	z21h	1,5	0,974
	z21u	3,0	0,927
00-06-24	z21f	1,2	0,937
	z22f	0,6	0,943
	zSTu	0,2	0,591
00-07-09	z21f	1,2	0,856
	z22u	1,5	0,860
	zSTu	0,5	0,760

Legend:
z21f: CM21 full power ventilation
z21h: CM21 half power ventilation
z21u: CM21 unventilated
z22f: CM22 full power ventilation
z22u: CM22 unventilated
zSTu: STAR-pyr. unventilated

shows the bigger scattering as well as the bigger dependence of the unventilated pyranometer on long-wave downward radiation A.

Furthermore it is visible that there is a small difference but remarkable between the full and half power ventilated pyranometers.

Additionally to the zero offset of the CM21 and the long-wave downward radiation Figure 3 implies the natural wind speed measured by a ultrasonic anemometer at the level of the pyranometer domes. There is nearly no influence of the wind speed on the offset. A correlation coefficient of r = 0,18 between the wind speed and zero offset of the unventilated CM21 confirms this statement.

Typical courses of a CM21 (z21f), a CM22 (z22f) - both ventilated by full power - and an unventilated STAR-pyranometer (zSTu) together with the corresponding long-wave downward radiation A are shown in Figure 4. In comparison with Figure 1 it is evident that the zero offset of the STAR-pyranometer and of the CM22 are smaller than those of the CM21. Furthermore, the influence of rain on the zero offset is demonstrated. The rain droplets effect - at least by evaporation - a cooling of the domes with the consequence of a more or less rapid decline of the offset at all (!) pyranometers. After some minutes the offset follows again the changes of the long-wave downward radiation because of the adaptation of the system receiver/dome.

Table 1 gives an overview about the dependence of the night-time zero offset at the used pyranometers with the respective ventilation power (Column a) on the long-wave downward radiation at selected days which was investigated by a regression analysis. Column b shows the

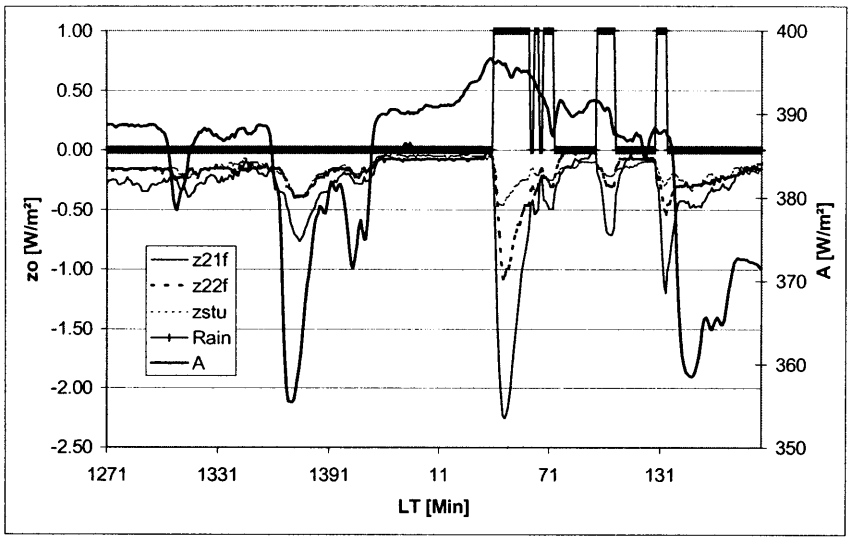

Fig. 4: Night-time zero offset of a CM21 (z21f: full power ventilation), CM22 (z22f: full power ventilation), a STAR-pyranometer (zSTu: unventilated) and long-wave downward radiation A together with signed rain (Rain=1)
Potsdam, 00-06-14/15

change of the offset caused by a change of 100 W/m² in long-wave radiation. The correlation coefficients are presented in Column c. All ventilated pyranometers are only very little (≤1,5 W/m²/100 W/m²) influenced by changes in long-wave radiation. The ventilated CM22 and the unventilated STAR-pyranometer reach similar results at an offset level of < 0,3 Wm^{-2}. The zero offset of a CM22 without any ventilation is nearly in the same level as a full power ventilated CM21.

The correlation coefficients of the unventilated CM21 and the STAR-pyranometer are remarkable lower than in the case of the unventilated CM22. This may be interpreted that the improvements at the CM22 reduce "thermal noise". The experiment showed that a stable and strong air stream in the case of the investigated pyranometers with a black receiver surface (CM21, CM22) enables much lower zero offsets than specified in the "CIMO Guide" [1].

The investigated data of a time series of about five years routine measurement concerning the zero offset of the with 5 W steadily ventilated CM21 installed at the German BSRN station Lindberg are in good agreement with the results found in this experiment; the nightly means are within ±1,5 Wm^{-2}.

Conclusive remarks

a) It is recommendable that other radiation centres (main stations) at which other types of pyranometers and / or fans are in use should repeat the investigations of night-time zero offset because of its relatively low need of additional man-power.

b) To estimate the undesired zero offset component of the measured signal of solar irradiance the determined results of night-time zero offset can be evaluated qualitatively. At night-time the long-wave cooling effect dominates generally and causes the negative sign of the offset. During the sunny day the received solar fluxes should reduce or (over) compensate this long-wave effect by heating the domes first of all (absorption of IR-solar energy). The dome ventilation of the outer dome by fan or wind should reduce the resulting effect to an amount which is not higher than during clear-nights.

c) In the last issue of the "CIMO Guide" Table 7.5, p. I.7-9 [1] the pyranometers are classified according to acceptable limiting values of errors in a list of characteristics. In the case of zero offsets the effect of 200 W m^{-2} net long-wave radiation or of a linear temperature change of 5 Kh^{-1} has to be equivalent to less than 7 Wm^{-2} and 2 Wm^{-2}, respectively, for pranometers of "high quality". At least the first value seems with regard to the presented results too high. This will be controlled by laboratory experiments at the Met. Obs. Potsdam soon.

d) Concerning the used pyranometers: At pyranometers with "low-temperature thermopile" 1000 Wm^{-2} generates only a temperature difference of about 3 K. That means low tilt and linearity errors but higher zero offsets. At the Star-pyranometer the disadvantages arise with the ageing of the white paint and the relatively large receiver surface combined with the shallow dome.

Reference:

[1] WMO: Guide to Meteorological Instruments and Methods of Observation, Sixth Edition, WMO-No. 8, Geneva 1996

****

Automatic indirect observations of sunshine duration

Luis F. Nunes, Fernanda Carvalho

luis.nunes@meteo.pt, fernanda.carvalho@meteo.pt

Department of Observation & Networks, Meteorological Institut - Portugal

Rua C Aeroporto de Lisboa, 1749-077 Lisboa

1. Introduction

During recent years, Portuguese Meteorological Institute (IM) has been upgrading the national meteorological network, by installing new Automatic Weather Stations (AWS) at sites where manually operated stations are to be replaced (fully or partially) by AWS, because the growing need of having all data available in real (or near real) time and in digital format. However, these AWS observations can not replace all the classical observations, like sunshine duration, which have been recorded using the well-known Campbell-Stokes sunshine recorder for many years, instead, automatic and near real-time global radiation data in true solar time, is available every 10 minutes, measured with CM-11 pyranometers.

There are several reasons for continuing the sunshine duration observations, the main one is related to long climatic data series and another one is to satisfy the needs of many users (hydrologists, agronomists, engineers, etc) who are still depending on sunshine duration data for several applications. Since the AWS are measuring radiation instead of sunshine duration, some approach should be made to automatically simulate the sunshine duration observations, using the radiation data.

The automatic estimation of daily sunshine duration (DSD), based on CIMO recommendations, was tried for the stations where global and diffuse radiation data was available, for those the AWS processing systems were programmed to calculate and transmit the DSD in the 06 UTC SYNOP reports. But this method is not possible to apply directly for most part of AWS because only few stations are equipped with shaded pyranometers. So, an algorithm was prepared to estimate the direct irradiance (I_D) as a function of observed global irradiance (I_G) and using global (I_G*) and diffuse (I_S*) irradiances for clear sky conditions, estimated by a Simplified Radiation Transfer (SRT) Model, previously developed for Portugal mainland, that considers geographical (lat., long., alt.) and atmospheric (ozone, aerosols and precipitable water) effects.

2. The Method

From the definition of direct irradiance, follows: $\mathbf{I_D = (I_G - I_S)/\cos z}$

Where z is the zenith angle, I_S is the diffuse irradiance and I_G is the global irradiance.
To overcome the lack of diffuse irradiance observations at most of AWS, this variable (I_S) can be estimated by the following expression, if we calculate (using the SRT model) the global (I_G*) and diffuse (I_S*) irradiance values for clear sky conditions:

$$\mathbf{I_S / I_S^* = I_G^* / I_G}$$

This relation says that, in cloudy sky conditions (or any other conditions) diffuse irradiance increases by the same amount that global irradiance decreases with respect to clear sky conditions. Then, the following algorithm is used to calculate the hourly sunshine duration:

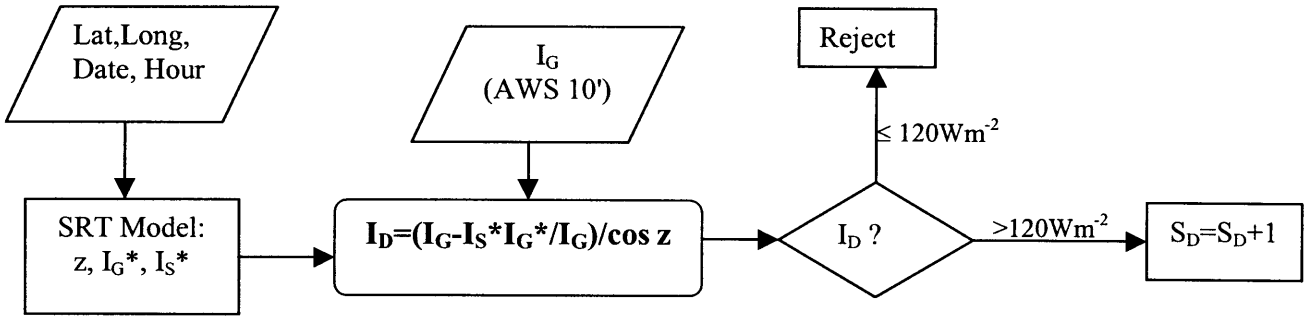

All the variables are calculated for 10 minutes period, to allow the estimation of 10 minute values for I_D, which are compared with the WMO threshold of 120Wm^{-2}; if the values are above the limit, the hourly sunshine duration (HSD) is increased by 10 minutes. The estimation of DSD is made by the sum of all HSD values for the same day.

3. Stations, sensors and data analysis

The sensors used at AWS for measuring global irradiance I_G are connected to electronic data-loggers for automatic integration every 10 minute, and these records are sent every hour to the IM Central Offices and also to the local PC at main synoptic stations. These pyranometers are installed at 2m height, close to the AWS processing system, and, in many cases, is not close to the Campbell-Stokes recorder. Global radiation data (I_G) from several months from three stations of the mainland network were used to calculate HSD by the proposed algorithm, and the results compared to Campbell-Stokes hourly readings. The series of differences between estimated and measured sunshine duration (HSD' - HSD) are shown in the next Figures. The data series used were the followed:

January/2000 to May/2000 from Bragança - 5 months
January/1999 to Dec/1999 from Coimbra - 12 months
January/1999 to May/2000 from Lisboa - 17 months

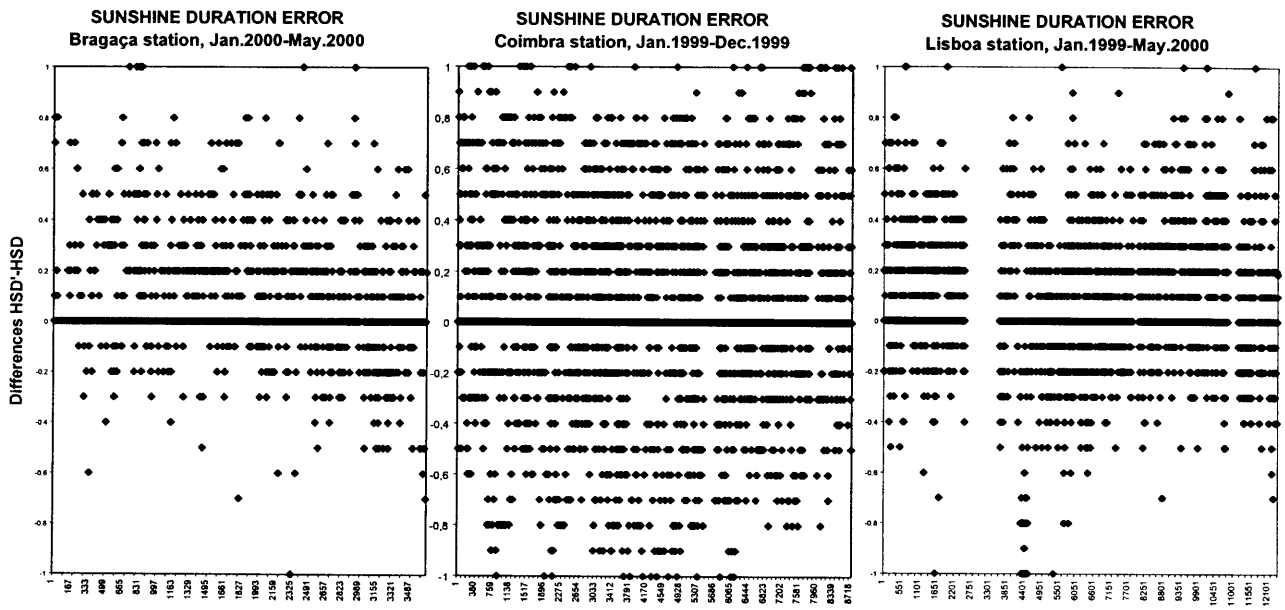

The stations used for this work, located at Bragança (41.80°N, 6.73°W, 690 m), Coimbra (40.15°N, 8.47°W, 171 m) and Lisboa (38.71°N, 9.15°W, 104 m) were selected to represent different climatic regions of Portugal/Mainland, respectively, the North (small city on inland mountains), the Centre (medium city near the coast, on the edge of mountain/flat landscape) and the South (large city, next to the coast, with complex topography).

The frequency distribution of differences HSD' - HSD' are shown in next histograms.

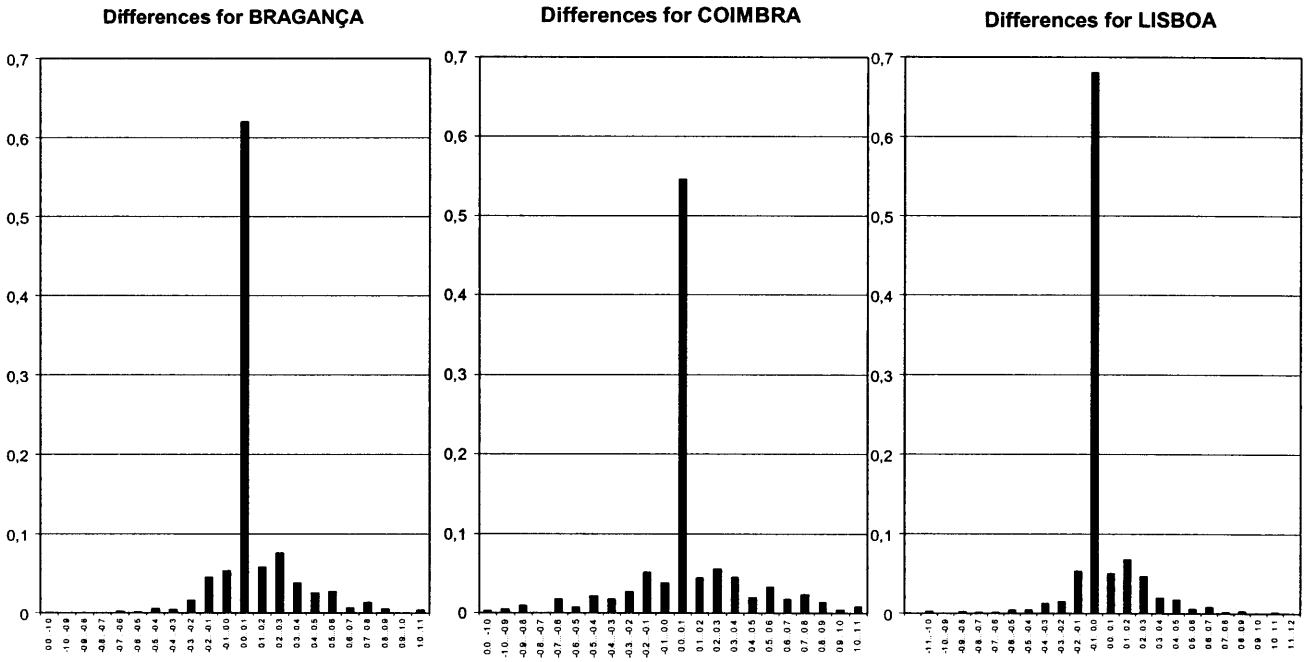

Because at these stations the global radiation sensor and the heliograph are installed at different places and at different heights, we expected to have larger systematic errors, instead, the small values found for the bias (0.03 – 0.05) and for the average deviation (0.09 – 0.17), reveals that there are no significant installation and exposure differences.

Regarding the dispersion of error values given by the standard deviation (0.2 – 0.3) and the RMS error (0.2 – 0.3) some investigation can be made about the causes of random errors, which can be related to operational procedures. The main identified aspect that may affect pyranometers performance is the frequency and efficiency of glass dome cleaning, that can be affected by the changes in meteorological conditions (rain, dew, dust, etc), which makes more difficult to keep it clean. Other aspects to investigate are the influences of the constancy of leveling, and of desiccator status and the eventual need for replacement of silica gel.

One of the major concerns, regarding global radiation measurements should be the calibration issue for sensors in use, but, fortunately, with the results of these 3 stations, it seams that there is no significant influence of the calibration factor degradation, during the several months period of the analyzed data, in spite the lack of calibration procedures during that period, which should be carried out at least once a year according to WMO recommendations.

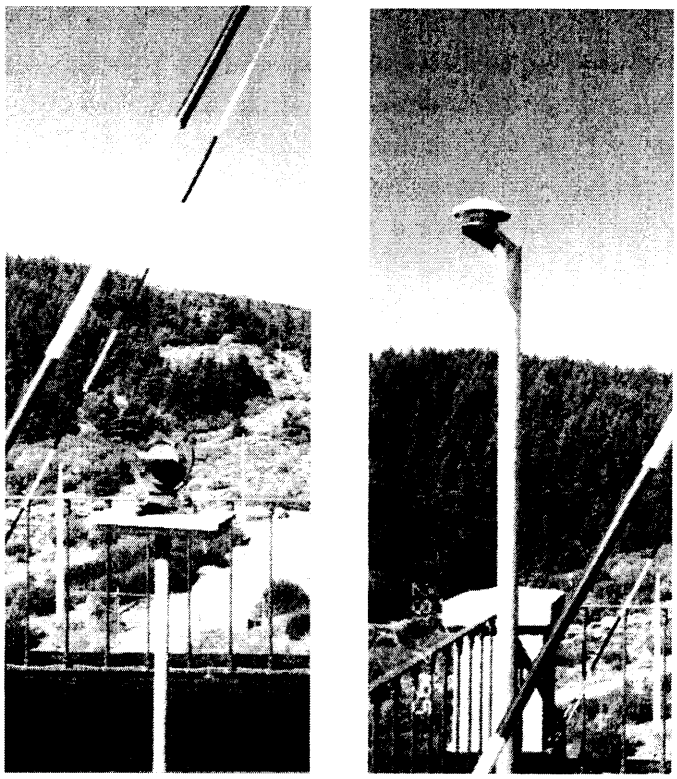

Examples of installations of Campbell-Stokes sunshine recorder and Kipp & Zonen pyranometer at synoptic station

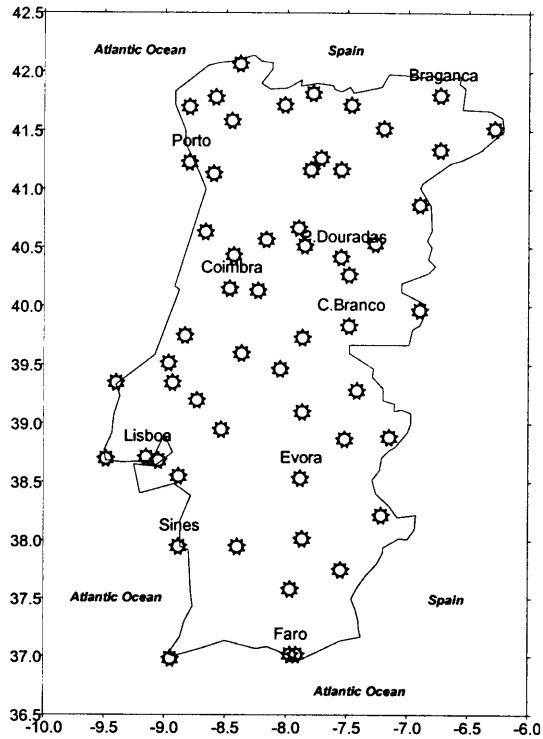

Portuguese solar radiation network
Stations currently operating

4. Current and Future Work

In order to verify the operational capabilities of the method described above, the algorithm was implemented to run automatically in a standard PC (Pentium based) to calculate the sunshine duration every hour, using the 10 minute global radiation data measured at Lisboa station. This program is intended to be working continuously for several months, to evaluate its performance and data availability. After this testing period, the algorithm is going to be installed at all synoptic stations where there are professional observers and modern PCs available. This system will allow to have automatic hourly values of sunshine duration available locally and will allow to calculate also the daily sunshine duration. For the non-synoptic AWS the HSD and DSD will be calculated at IM's Central Offices.

In spite of the results presented, it is premature to abandon the Campbell-Stokes sunshine recorder. On the other hand, to investigate the aspects indicated in the previous paragraph, we need to have longer data series for further analysis and comparisons, to evaluate how significant is the influence of those aspects. Besides, for climatological purposes the use of estimated HSD and DSD values needs longer comparisons in a time series context. So, for the next 2 or 3 years all the existing Campbell-Stokes sunshine recorders will continue in operation at stations where that would be possible. The records of these observations, from a set of few stations (≅10 sites), will be read and digitised to be compared with the results of the described algorithm, to allow making some adjustments, if necessary. After that period and since the operation and maintenance costs of the Campbell-Stokes recorders aren't very high, the intention is to keep them in operation for many years at all possible stations (where personnel is available), for purposes of backup instrument and also to serve as a source of possible corrections, mainly at 9 principal radiation stations.

A SENSOR FOR THE HORIZONTAL COMPONENT OF SOLAR RADIATION

J. C. H. van der Hage

Institute for Marine and Atmospheric Research

Utrecht University
Princetonplein 5
3584 CC, Utrecht
The Netherlands

tel: 0031-2532908 fax: 0031-2543163 e-mail: j.c.h.vanderhage@phys.uu.nl

INTRODUCTION

Erect bodies, like many plants, humans and high buildings, collect radiation on vertical surfaces rather than on horizontal surfaces. Climatological radiation sensors are designed to measure the radiation collected by horizontal surfaces like fields or oceans. For radiation studies on erect bodies another sensor is required: the "Horizontal radiation sensor" or H-sensor.

Optimal spacing of individual plants in a crop is a matter of great economic importance. There may be cases where H is a more relevant parameter in determining the optimal spacing than global radiation G. This will have to be verified.

THE H-SENSOR

Global radiation G is defined as the downward shortwave irradiance on a horizontal surface according to:

$$G \equiv \int_0^{2\pi} L \cos\theta \, d\omega \qquad (1)$$

L is the radiance in any direction, θ is the zenith angle of L and $d\omega$ is an infinitesimal solid angle in the direction of L. This definition implies that G is the vertical component of solar radiation and that a complementary horizontal component H can be defined as:

$$H \equiv \int_0^{4\pi} L \sin\theta \, d\omega \qquad (2)$$

Basically G is measured by collecting the light falling on a plane horizontal circular surface. And basically we measure H by collecting the light falling on the cylindrical surface of a vertical cylinder (see fig.1). But to improve the sine response of a real H-sensor we allow the top-surface to collect some false light as a

compensation for reflection loss at the cylindrical surface. Therefore the top surface of a real H-sensor is not completely blind (see fig.1).

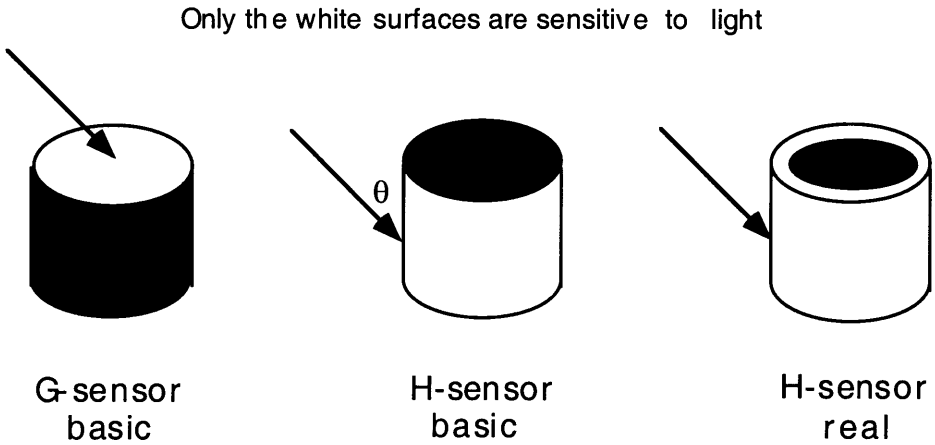

Fig.1: Concepts of G- and H-sensors

The directional response of a real H-sensor is presented in fig.2. This graph shows $R(\theta)/\{R(90^o)*\sin\theta\}$ as function of θ where $R(\theta)$ is the response to collimated light incident on the sensor at an angle θ with the cylinder axis of the sensor. $R(90^o)$ is the response in the reference direction perpendicular to the cylinder axis.

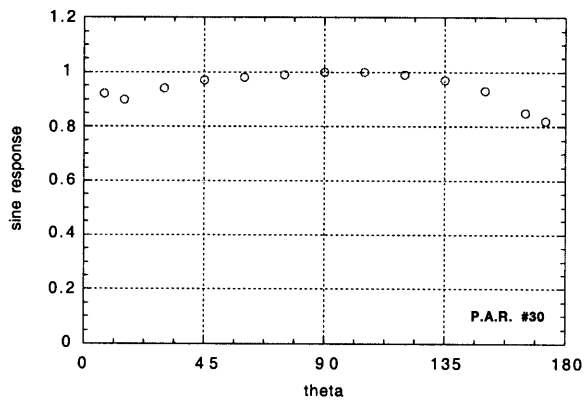

Fig.2: Directional response of an H-sensor

The spectral response of the H-sensor is determined by the diode mounted inside the instrument. For P.A.R. measurements we apply a silicon-diode VTB8440B by EG&G Vactec. This diode has an infrared rejection filter and a spectral range between 330 and 720 nm with a maximum response at 580 nm.

For N.I.R. measurements we apply a silicon diode BPW34FA by Siemens. This diode has a visual light rejection filter and a spectral range between 700 and 1100 nm with a maximum response at 880 nm.

An H-sensor is calibrated against a G-sensor with the same spectral properties, in a collimated light beam in a dark room. The calibration is based on eqs.(1 and 2). The H-sensor is positioned in the beam under $\theta_H = 90^o$ and a reading is taken. Then the H-sensor is replaced by the G-sensor, positioned under $\theta_G = 0^o$ for another reading. Now $\sin\theta_H = \cos\theta_G = 1$ and consequently G = H according to eqs.(1

and 2). For an absolute calibration the G-sensor had previously been compared with a Kipp solarimeter under a clear sky.

G- AND H-CLIMATOLOGY

In an idealized radiation field under a cloudless sky and over an open field both G and H can be expressed as a function of solar time (see appendix). Fig.3 is the result of this calculation for Beijing at 40° latitude in midwinter (left) and midsummer (right). Note that in midwinter there is much more horizontal radiation than global radiation. In this situation it is definitely more advantageous for a plant to collect H- than to collect G-radiation.

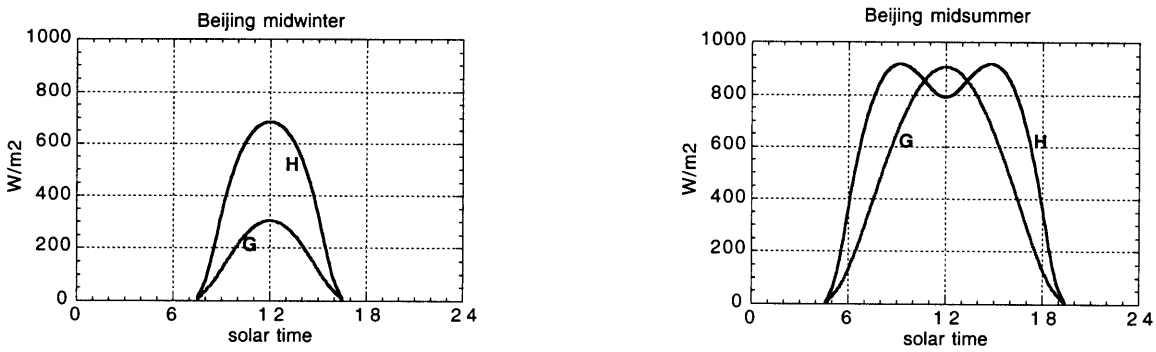

Fig.3: G and H calculated in an idealized radiation field for Beijing (lat.40°) in midwinter (left) and midsummer (right).

In midsummer H is moderated around noon because then the contribution of direct radiation to H decreases with increasing elevation of the sun. The dip in the H-curve is relatively shallow because the diffuse contributions to H, both downwards and reflected from the ground, remain significant at noon.

Tsunoda (1959) reported that highly productive rice varieties have leaves more vertical than those of the cultivars of lower productivity. This observation may be explained by fig.3: An erect morphology protects plants from extreme vertical radiation loads around noon in the tropics and it also enables them to profit from relatively high intensities of the horizontal radiation in the morning and the evening, thus increasing the number of productive hours per day.

In Beijing the maximum value of G varies from 900 Wm^{-2} in summer to 300 in winter while H_{max} varies only from 900 to 700 Wm^{-2} in the same period. Not only in Beijing but all over the world the H climate of the open field is less extreme than the global radiation climate. The diurnal variation of H resembles a square function better than G does and, compared to G, H is low in the tropics and high in polar regions.

MEASURING THE RADIATION DOSE

Closed stands of plants can be considered as horizontal surfaces receiving radiation G like a solarimeter does. Isolated individuals can sometimes be considered as cylinders. The H-sensor, in combination with a G-sensor, allows an absolute experimental determination of the radiative flux P intercepted by a cylinder in any irregular radiation field (e.g. on a forest floor). Van der Hage (1995) has shown that the flux P intercepted by a vertical cylinder with radius r and height h is:

$$P = \pi r^2 G + 2rh H \qquad (3)$$

This exact determination of P was not possible before the introduction of the H-sensor. Conventionally only G, the vertical component of the radiation field is measured and P is then approximated on the basis of an assumed angular distribution of the radiation field. The assumed angular distribution can be supported by a measured value of the ground albedo α.

At first sight eq.(3) does not feature α. That may seem incorrect because the reflective properties of the ground must affect P; but closer inspection reveals that the reflected contributions to P are incorporated in the measured value of H.

APPENDIX

The diurnal variations of G = G(t) and H = H(t) in fig.2 for an idealized radiation field were calculated from the following expressions:

Global radiation: $$G = G_o + G_\downarrow \qquad (4)$$

Horizontal component: $$H = \left(\frac{\pi\alpha}{2} + tg\theta\right) G_o + \frac{\pi}{2}(\alpha+1) G_\downarrow \qquad (5)$$

Direct radiation: $$G_o = S\,\tau^{1/\cos\theta} \cos\theta \qquad (6)$$

Diffuse radiation: $$G_\downarrow = S\,(0.271 - 0.294\,\tau^{1/\cos\theta})\cos\theta \qquad (7)$$

Solar zenith angle: $$\cos\theta = \sin\psi \sin\delta + \cos\psi \cos\delta \cosh \qquad (8)$$

with:
- S is the solar constant (1380 Wm^{-2})
- τ is the transmission factor of the unclouded atmosphere (0.6)
- α is the ground albedo (0.25)
- ψ is the geographical latitude (40°)
- δ is the solar declination (midsummer: 23.5^o, midwinter: -23.5^o)
- h is the hour angle $(t-12)*2\pi/24$ with **t = solar time**

The expressions (4), (6), (7) and (8) are by Gates (1980), expression (5) is by Van der Hage (1993).

REFERENCES

Gates,D.M., "Biophysical ecology", Springer Verlag, New York,115-118, 1980.

Van der Hage, J.C.H.: The horizontal component of solar radiation, Agric.Forest Met. **67**, 79-93, 1993.

Van der Hage, J.C.H.: Intercepted flux and the horizontal component of solar radiation, Theor. Appl.Clim., **52**, 143-149, 1995.

Tsunoda,S. , A development analysis of yielding ability in varieties of field crops, Jap.J.Breed. **9**, 161, 1959.

PERFORMANCE EVALUATION FOR PYRANOMETERS

Lu Wenhua and Mo Yueqin
Chinese Academy of Meteorological Sciences
46 Baishiqiao Road, Beijing 100081, China
Tel./ Fax. 86-10-68406866, E-mail Lwh@cams.cma.gov.cn

1 INTRODUCTION

The performance of two models pyranometer (model DFY4 and model TBQ-2) made in China has been tested. We have mainly studied the long-term stability of sensitivity, nonlinearity, temperature dependence, directional response (cosine and azimuth), tilt effect, response time and et al. Sensitivity and response time are tested in outdoor exposure and others are tested on the laboratory test facility for solar radiation instruments. In our measurements we used a personal computer in conjunction with data logger and output of instruments can be measured and processed automatically. Model PSP pyranometer made in EPPLEY laboratory of USA is used as a reference instrument and its dissemination of the value of the quantity can be trace back to WRR. Main error for pyranometers is concluded according to a great of test data and analysis. It is very useful for observation and study of solar radiation.

2 PERFORMANCE OF TEST

Five instruments for each model are tested, which serial numbers are 0060, 002, 0053, 0058, 011 for model DFY4 and 9303, 9312, 9311, 9317, 9313 for model TBQ-2.

2.1 Sensitivity and Long-term Stability Test

Table 1 The Results of Sensitivity Test ($\mu V \cdot W^{-1} \cdot m^2$)

Date	0060	002	0053	0058	9303	9312	9311	9317	9313
93. 11. 25	8. 589	8. 146	8. 008	8. 191	8. 564	8. 441	9. 002	8. 853	8. 264
94. 03. 01	8. 454	8. 474	7. 458	8. 658	8. 321	8. 367	8. 643	8. 475	8. 528
94. 03. 02	8. 460	8. 524	7. 570	8. 606	8. 285	8. 286	8. 623	8. 495	8. 436
94. 03. 03	8. 373	8. 480	7. 753	8. 622	8. 310	8. 320	8. 646	8. 507	8. 450
94. 03. 04	8. 402	8. 499	7. 960	8. 610	8. 287	8. 241	8. 581	8. 461	8. 446
94. 03. 05	8. 283	8. 410	7. 939	8. 562	8. 279	8. 304	8. 686	8. 541	8. 341
94. 03. 07	8. 178	8. 298	7. 476	8. 612	8. 259	8. 237	8. 433	8. 174	8. 066
94. 03. 09	8. 335	8. 480	7. 416	8. 583	8. 227	8. 383	8. 595	8. 536	8. 396
94. 03. 14	8. 367	8. 512	7. 475	8. 638	8. 322	8. 413	8. 620	8. 622	8. 359
94. 03. 15	8. 322	8. 486	7. 478	8. 581	8. 296	8. 452	8. 625	8. 612	8. 292
94. 04. 13	7. 973	8. 273	7. 214	8. 285	8. 250	8. 405	8. 755	8. 588	8. 340
94. 09. 22	8. 176	8. 490	7. 647	8. 522	8. 298	8. 521	8. 793	8. 827	8. 512
94. 09. 23	8. 225	8. 525	7. 680	8. 535	8. 343	8. 608	8. 880	8. 829	8. 470
95. 05. 22	8. 090	8. 410	7. 120	8. 563	8. 271	8. 423	8. 703	8. 718	8. 615
95. 05. 25	8. 157	8. 428	7. 155	8. 548	8. 285	8. 456	8. 753	8. 727	8. 569
Average	8. 292	8. 429	7. 557	8. 541	8. 306	8. 390	8. 677	8. 598	8. 406
MRE	-3. 85	-3. 36	5. 97	-4. 10	3. 11	2. 60	3. 75	-4. 93	-4. 04

Note: MRE is a maximum relative error.

Pyranometer No.20461 (model PSP) is used as a reference instrument and No.20463 (model PSP) is regarded as a monitoring instrument. Data are collected every two minutes. Sensitivity is tested in different seasons and

weather condition (clear day, nebulous, cloudy and less than 5 m/s wind speed).

The experiment is covered 18 mouths and the results are listed in table 1. It shows that the sensitivity of pyranometers is dispersed which occurs at the condition of lower solar elevation angle (less than 30°) and lower temperature (less than 0℃). The maximum relative error is about 6%. This is a combined error caused by nonlinearity, temperature dependence, directional response, zero drift of the instrument and et al.

2.2 Nonlinearity Test

The test facility consists of mechanism and a solar simulator that the spectrum components do not change with irradiance. Test point is respectively at irradiance of 250, 500, 750 and 1000 W/m². Nonlinearity is given by $\delta_L=(V/V_{500}-1)\times 100\%$. In the formula V is the output of pyranometer and V_{500} is output of pyranometer when the irradiance is 500 W/m². The results are given in Fig.1 and Fig.2. The results show that the nonlinearity error are all within ±2.0% and the maximum error is in the lower irradiance.

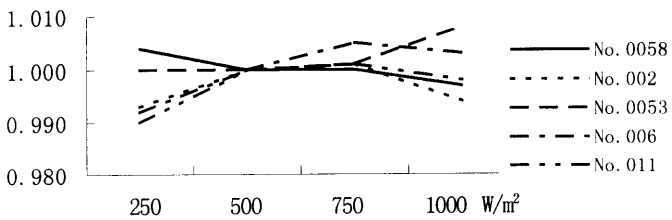

Fig. 1 Nonlinearity of DFY4

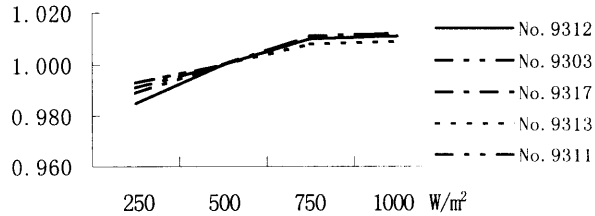

Fig. 2 Nonlinearity of TBQ-2

2.3 Temperature Dependence Test

Temperature dependence is tested on the laboratory test facility with temperature test chamber. We change the temperature in the chamber while the irradiance is unchangble and then the outputs of instruments are measured. The temperature point is respectively at -30.0℃, -20.0℃, 0.0℃, 20.0℃, 40.0℃ at irradiance 1000 W/m².

Temperature coefficient is given by $c=(V_{T2}/V_{T1}-1)/(T_2-T_1)$, V_{T1}, V_{T2} is respectively output of instrument in the formula when the temperature is T_1, T_2. The results are given in the table 2. Temperature coefficient is not constant, but the average is within ±0.1%/℃ except No.0053.

Table 2 Temperature Coefficient (%/℃)

No.	-30.0~-20.0℃	-20.0~0.0℃	0.0~20.0℃	20.0~40.0℃
0053	-0.08	-0.06	-0.16	-0.22
0058	0.03	0.03	0.01	0.05
0060	0.04	0.02	0.00	-0.03
002	0.09	0.08	0.05	0.04
011	-0.02	-0.05	-0.05	-0.04
9303	0.08	0.06	0.06	0.04
9313	0.07	0.04	0.04	0.05
9311	0.12	0.05	0.03	0.05

2.4 Directional Response

Directional response can be divided into cosine response and azimuth response.

2.4.1 Cosine Response Test

Cosine response test is made use of studying the directional character of incident beam. The irradiance is adjusted to 1000 W/m² on the laboratory test facility. First the output of instrument (V_0) is tested in $\theta=0°$ (θ is zenith angle), namely solar elevation angle h= 90° , then the solar elevation angle h is adjusted to 80° to measure the

output of instrument. Each angle of measurement is at 90° , 80° , 70° , 60° , 50° , 40° , 30° , 20° , 10° . The output of instrument for solar elevation angle 90° (θ =0°) is tested again.

Cosine response error is calculated by formula $\delta_\theta = (V_\theta / V - 1) \times 100\%$. In the formula the relation between θ and h is $h = 90° - \theta$, V_θ is the output of instrument at θ, and $V = V_0 \cdot \cos\theta$ is an ideal value at θ and V_0 is the average of two outputs of instruments at θ =0° . The results are listed in the table 3.

Table 3 The Relative Error for Cosine Response (%)

No.	80°	70°	60°	50°	40°	30°	20°	10°
0058	0. 15	0. 35	0. 51	0. 68	0. 70	0. 63	1. 34	-3. 80
0060	-0. 97	-2. 40	-2. 29	-1. 32	1. 59	2. 73	-4. 81	-16. 31
002	1. 56	0. 99	1. 73	2. 58	3. 68	5. 57	8. 65	13. 51
0053	-0. 11	-0. 19	-0. 27	-0. 21	-0. 04	-0. 06	-0. 21	-0. 45
011	-0. 05	0. 26	0. 68	1. 44	2. 63	3. 73	5. 49	10. 66
9311	-0. 26	-0. 35	-0. 32	-0. 19	0. 70	1. 74	1. 36	-0. 91
9312	-0. 27	-0. 29	-0. 28	0. 01	0. 90	1. 74	2. 13	1. 30
9313	-0. 42	-0. 93	-1. 63	-2. 39	-3. 10	-3. 95	-6. 24	-13. 55
9317	-0. 30	-0. 41	-0. 72	-0. 54	0. 18	0. 97	0. 19	-1. 92
9303	-4. 75	-0. 13	-0. 19	-0. 11	-0. 16	-0. 16	-0. 59	-2. 35

2.4.2 Azimuth Response Test

The method of azimuth response test is similar to the cosine response test. The output is measured at solar elevation angle 10° . The test point is at intervals of 30° within directional 0~360° and it's at 0° , 30° , 60° , 90° , 120° , 150° , 180° , 210° , 240° , 270° , 300° and 330° which is 12 points together.

Table 4 The Relative Error for Azimuth Response (%)

No.	0°	30°	60°	90°	120°	150°	180°	210°	240°	270°	300°	330°
0058	0. 18	0. 32	0. 25	-2. 13	0. 73	3. 99	3. 72	1. 47	-2. 74	-1. 65	-2. 95	-1. 18
0060	-3. 35	-3. 77	1. 08	4. 09	5. 26	1. 08	-2. 85	-0. 76	0. 24	-1. 34	0. 75	-0. 43
002	0. 12	-0. 83	-0. 31	2. 45	3. 96	3. 31	2. 66	0. 33	-0. 35	-3. 74	-3. 09	-1. 28
0053	-4. 57	-3. 64	-2. 25	-0. 70	1. 77	2. 16	0. 84	4. 02	5. 26	3. 86	-1. 24	-5. 50
011	-3. 76	-4. 55	-7. 06	-8. 61	-4. 72	0. 00	2. 63	8. 25	7. 00	4. 84	4. 49	1. 50
9311	2. 98	4. 21	3. 89	2. 27	0. 00	-2. 14	-4. 34	-3. 95	-2. 59	-2. 33	-0. 26	2. 27
9312	0. 33	0. 33	0. 66	0. 53	-0. 28	-0. 01	0. 73	0. 26	0. 12	-0. 96	-0. 96	-0. 75
9313	-6. 67	-4. 95	-4. 29	0. 29	4. 39	6. 52	7. 25	6. 36	2. 59	-0. 28	-4. 54	-6. 67
9317	-6. 21	-6. 70	-4. 98	-4. 41	0. 26	4. 35	6. 48	7. 22	6. 32	2. 55	-0. 31	4. 57
9303	0. 51	-0. 01	-0. 15	-0. 74	-0. 15	-0. 45	-0. 08	-0. 66	0. 95	0. 51	0. 21	0. 07

Azimuth response error is given by the formula $\delta_A = (V_Z / V_{Z0} - 1) \times 100\%$. V_Z is the output of each azimuth and V_{Z0} is an average of outputs at solar elevation angle 10° .

The results are given in the table 4. It shows that the error of azimuth response is in -8. 61%~8. 25%. According to the observation condition in use we should test 6 points, namely 60° , 90° , 120° , 240° , 270° , 300° and its error should be less than 5 %. Pay attention to that the direction of pyranometer must be the same whether in the test or in the observation, i.e. the cable of pyranometer points to north.

2.5 Tilt Effect Test

Output is measured when the instrument is in level (tilt angle 0 ° first. Then they are tested at 45° , 90° , 135° and 180° respectively. The point in level is tested again. The average of two values in level is regarded as reference value (U_0) to calculate the tilt response error. The results is calculated by $\delta_T=(U/U_0-1)\times 100\%$. U is the output of instrument each angle.

The results are listed in table 5. The errors of DFY4 are within ±1.0%. But TBQ-2 are within ±3.0%.

Table 5 The Relative Error for Tilt Response (%)

Tilt Angle	0058	0060	002	0053	011	9311	9312	9313	9317	9303	20463	20461
45°	0.27	-0.19	0.66	0.00	0.22	0.97	0.66	0.73	0.96	1.12	-0.32	-0.34
90°	-0.39	-0.29	0.29	0.03	-0.37	1.48	1.02	1.22	1.52	1.84	-0.32	-0.36
135°	0.07	-0.05	0.32	-0.21	-0.09	2.12	1.78	1.95	2.25	2.67	-0.40	-0.38
180°	0.43	0.25	0.32	-0.09	-0.05	2.60	2.79	2.78	2.95	3.09	-0.51	-0.48

2.6 Response Time Test

The response time are tested in both indoor and outdoor. The results are less than 30 second (99 % response).

3 CONCLUSION

By the test of performance for pyranometer model DFY4 and TBQ-2, their sensitivities are within 7 ~ 9 $\mu V \cdot W^{-1} \cdot m^2$, nonlinearity is less than 1.2%, average temperature coefficient is less than 0.1% / ℃, maximum cosine error is less than 16.5%, maximum azimuth error is less than 9%, response time (99% response) is less than 30 second and maximum tilt error is less than 3%. It is of great importance to improve the quality of pyranometers and evaluate solar radiation measurement.

REFERENCES

WMO. Guide to Meteorological Instruments and Methods of Observation. Sixth Edition. WMO No.8,1996.

China State Bureau of Quality and Technical Supervision. Verification Regulation of Pyranometer JJG458-96. Chinese Metrology Press, 1996.

Lu Wenhua, et al. A Laboratory Test Facility for Solar Radiation Instruments and its Applications. 1998. WMO/TD: No.877, 361-364.

International Organization for Standardization, 1990 b: Solar Energy Field Pyranometers Recommended Practice for Use, ISO/TR 9901.

UV and Visible Solar Radiative Fluxes above Arctic Sea Ice

Alexander Los[1], Stefan R. de Roode[2], and Peter G. Duynkerke[3]

[1] Kipp & Zonen B.V., Roentgenweg 1, 2624 BD Delft, The Netherlands, email: alexander.los@kippzonen.com
[2] Univ. of Washington, Dept. of Atmosph. Sciences, Box 351640, Seattle, WA 98195-1640, USA, email: roode@atmos.washington.edu
[3] Univ. of Utrecht, Princetonplein5, 3584 CC Utrecht, The Netherlands, email: p.g.duynkerke@phys.uu.nl

Abstract

As part of the FIRE III (First ISCCP Regional Experiment) Arctic Cloud Experiment, actinic flux measurements were made above the Arctic Sea ice during May 1998. FIRE III was designed to address questions concerning clouds, radiation and atmospheric chemistry in the Arctic sea ice region. The actinic flux is the relevant radiative parameter needed to determine the photochemical reaction rates. Moreover, it is discussed that the actinic flux may be used to determine vertical absorption profiles and the net irradiance, provided that the single scattering albedo is known.

Introduction

Photodissociation of atmospheric key molecules, such as O_3, NO_2, CH_2O (formaldhyde), and H_2O_2 (hydrogen peroxyde) by solar ultraviolet radiation plays an important role in atmospheric chemistry [1]. The radiative parameter that determines the photodissociation rate of chemical species is the actinic flux, which is defined as the incident radiance integrated over all solid angles [2]. The actinic flux therefore describes the radiative energy intercepted by molecules, whereas the irradiance describes the flow of radiant energy through the atmosphere [3]. Thus, radiance incident from all directions contributes to the actinic flux. For this reason it is also referred to as the mean intensity, or as 4π-radiative flux.

An unambiguous description for actinic flux calculations is presented in [2], which was followed by several investigations of actinic fluxes, e.g. [3], [4], [5], [6], and [7]. However, there is no simple linear relationship between the monochromatic actinic flux and the irradiance, as was shown from actinic flux observations reported by [5]. The effect of a high surface albedo on the actinic flux was discussed on the basis of observations made by, e.g. [8], [9], and [10]. In [11] actinic flux measurements collected by means of a tethered balloon in Atlantic stratocumulus were presented.

This study presents actinic flux measurement performed above the arctic sea ice at the SHEBA (Surface Heat Balance of the Arctic Ocean) ice camp (76°N, 166°W) during May, 1998. This measurement campaign was part of the FIRE III ([1]) Arctic Cloud Experiment, which was designed to address questions concerning clouds and radiation in the arctic sea ice region [12]. The arctic region is characterized by a high surface albedo, large solar zenith angles and the frequent occurrence of low stratus clouds. UV-A and visible actinic fluxes, at a wavelength of λ=365 nm and λ=550 nm, respectively, were measured continuously by two 4π-radiometers installed at 1.5 m above the surface, whereas vertical profiles of the visible actinic flux at λ=550 nm, were obtained at least once a day from tethered-balloon observations.

Theory

The monochromatic actinic flux, F(λ), can be computed by integrating the local radiance, $I_\lambda(\Phi,\theta)$, over the solid angle $d\omega=d\mu d\Phi$:

$$(1) \qquad F(\lambda)=\frac{1}{4\pi}\int_{\Omega} I_\lambda(\mu,\phi)\,d\omega$$

where μ is the cosine of the zenith angle, θ, Φ is the azimuth angle, and Ω=4π (solid angle). The monochromatic net irradiance, E(λ), is defined as:

$$(2) \qquad E(\lambda)=\int_{\Omega} \mu I_\lambda(\mu,\phi)\,d\omega$$

An equation that describes the relation between the irradiance E and the actinic flux F in horizontal homogeneous optical media can be derived from the radiative transfer equation which reads [15]:

$$(3) \qquad \mu\frac{dI(\mu,\phi)}{d\tau}=I(\mu,\phi)-\frac{\varpi}{4\pi}\int\wp(\mu,\phi;\mu',\phi')\,I(\mu',\phi')\,d\omega' \;-\; \frac{\varpi}{4\pi}\wp(\mu,\phi;\mu_0,\phi_0)\,S_o\,e^{-\tau/\mu_0}$$

where τ is the optical depth of the homogeneous layer obtained by integrating the extinction coefficient β_e over the layer height, $\wp$ is the scattering phase function, μ_o is the cosine of the solar zenith angle, and ϖ is the single scattering albedo. The irradiance $E_0(\tau)$ represents the direct component of solar radiation in the

[1] First ISCCP (International Satellite Cloud Climatology Project) Regional Experiment

atmosphere, defined as $E_0 = \mu_0 S_o e^{-\tau/\mu_0}$, S_0 being the extraterrestrial solar constant. According to [2] the actinic flux, F_0, obtained from the direct solar radiance, and E_0 are related as $F_0=E_0/\mu_o$.
The integration of Eqn (3) over $d\omega$ and using $F_0=E_0/\mu_o$ yields the relation between E and F, reading

$$\frac{dE}{d\tau} = (1-\varpi)F \tag{4}$$

If absorption can be excluded, i.e. when ϖ =1, the net irradiance E will be constant throughout the optical medium, which means that radiative energy is conserved. However, for ϖ < 1, which may be encountered in clouds the net irradiance E will decrease towards cloud base, indicating that radiation is absorbed within the cloud layer. Moreover, if the single scattering albedo is known very accurately, the change in E can be found by measuring the actinic flux. A possible advantage of this approach is that it requires only one 4π-radiometer, rather than two separate radiometers for the downward and upward components of the irradiance. Because radiance is not weighted with μ in the actinic flux, the orientation of 4π-radiometers is not of importance, whereas radiometers measuring irradiance need to be installed perfectly horizontal.

Results

The visible 4π-radiometer used for this study was newly developed for the FIRE III experiment. It has a maximum spectral response in the visible light part of the spectrum at 550 nm, and is described in [13]. Two identical visible 4π-radiometers were used, one which was attached to a balloon and one which was attached to a mast at 1.5 m above the surface. The actinic flux measurements are estimated to be accurate within 10%. The input parameters that need to be specified in the TUV model [14] are the cloud optical depth, the albedo of the snow-covered sea ice, the surface pressure, and the vertical atmospheric profile of temperature. The mean cloud optical depth was derived from surface-based and, if available, aircraft observations. The measured broadband shortwave surface albedo at the site was approximately 0.8, which is a value typically representative for a pristine snow surface. A summary of the tethered-balloon soundings made between 7 and 9 May 1998 is presented in Table 1.

Table 1: Cloud characteristics for the five selected tethered-balloon soundings made above the Arctic Sea ice. Start time is given in decimal Julian day, JD. The cloud cover for the Arctic stratus cases was approximately unity.

Case	Start (JD)	μ_o Start	μ_o End	$\bar{\tau}$	Cloud type
2	127.73	0.30	0.36	5±2	Stratus
5	128.77	0.36	0.42	17±4	Stratus
7	129.17	0.33	0.27	12±4	Stratus
8	129.31	0.15	0.10	10±4	stratus (thinning)
9	129.80	0.40	0.45	8±4	Fog

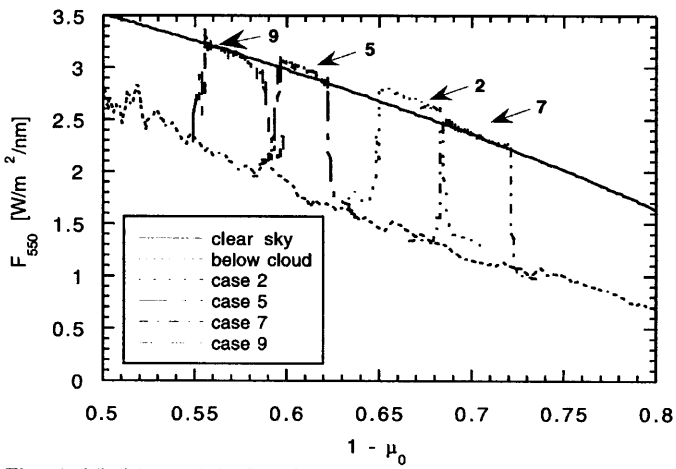

Fig. 1: Visible actinic flux from measurements made at 1.5 m above Arctic sea ice surface (labelled 'clear sky' and 'below cloud') and from tethered-balloon soundings in Arctic stratus for different cases. The balloon soundings are summarized in Table 1).

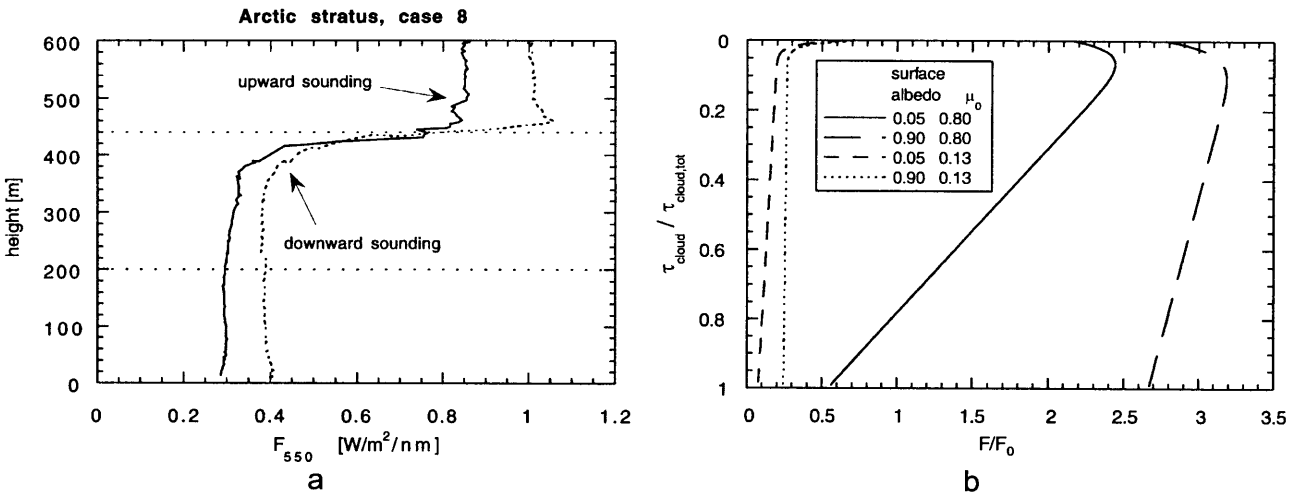

Fig. 2: (a) Measured vertical actinic flux profiles for visible radiation in Arctic stratus above sea ice (case 8, see summary of balloon soundings in Table 1). Horizontal dotted lines depict cloud base height and cloud top height. (b) Modelled in-cloud actinic flux profiles for different solar zenith angles, μ_0, and different surface albedo values. The modelled profiles, shown for the relative cloud optical depth $\tau_{cloud}/\tau_{cloud,tot}$, are normalized with F_0.

In Fig. 1 the observed actinic flux above stratus clouds, and surface observations during both clear and cloudy skies are presented. The surface observations during cloudy skies (labelled 'below cloud') and one of the balloon soundings (case 5) were made simultaneously. The actinic flux above the cloud is nearly the same as the observations performed at 1.5 m above surface during clear sky. This can be explained by the fact that the effective albedo of the arctic sea ice and the cloud is only slightly larger than the ground albedo alone. Below the cloud, however, the actinic flux is lower than during clear sky conditions. The observations and model results reveal that actinic fluxes below clouds are – in first approximation – varying with the cloud optical depth due to changes of the radiation intensity by cloud reflection. The varying actinic flux as function of cloud height can be seen in the vertical profiles, shown in Fig. 2a. The visible actinic flux profiles in Fig. 2a are obtained from observations in arctic clouds of case 8. The nearly constant vertical profile of the actinic flux in the lower part of the arctic cloud layer is due to the rather low value of the net irradiance associated with low values of solar zenith angles. Modelled actinic flux profiles for comparable conditions, i.e. high surface albedo and low solar elevation, depicted in Fig. 2b, are in good qualitative agreement with observations. The maximum of the profile is largest in the upper 50 m near cloud top. The modelled actinic flux profiles in Fig. 2b reveal that the height of the maximum depends on the solar zenith angle and that the magnitude of the maximum is changing with the surface albedo. The peak in the actinic flux profiles is visible for large μ_0 values only, i.e. for small solar zenith angles; because direct solar radiation penetrates deep into the cloud field, the diffuse radiation field inside the cloud is increased by the direct solar radiance.

Conclusions

The diurnal cycle of UV-A (λ=365 nm) and visible (λ=550 nm) actinic fluxes during clear and cloudy conditions was measured by two 4π-radiometers, installed just above the ice surface. In addition, vertical profiles of the visible (λ=550 nm) actinic flux through low arctic stratus clouds were observed by means of tethered-balloon soundings. The cloud optical depth was obtained from surface based microwave radiometer observations and, if available, in-situ observations made by the NCAR C-130 aircraft. Above the cloud layer the actinic flux was found to be almost the same as during clear sky conditions. This can be attributed to the fact that the effective albedo of the arctic sea ice and the cloud is only slightly higher than the ground albedo alone. The observed vertical actinic flux profiles in arctic stratus were nearly constant with height, except in a shallow layer near the cloud top where the actinic flux significantly increased with height. By integrating Eqn (3) over $\mu d\omega$ an expression is obtained, which describes the observed vertical actinic flux profiles. More details on the interpretation of the observed profiles is given in the poster P1.1.4(4)M. In [16] the results of the present analysis are given in greater detail.

Acknowledgements

The aircraft data collected by means of the C-130 of NCAR were kindly supplied by Ron Ruth and Krista Laursen. The authors thank NCAR and its sponsor, the National Science Foundation, for allowing them to use the observational data. The microwave radiometer data were kindly provided by Dr. J. Liljegren (Iowa State University). The authors wish to thank the many people of the FIRE/SHEBA community for giving logistical support by bringing the equipment to the SHEBA ice camp and for assisting on the site.

References

[1] Crutzen, P. J., and P. H. Zimmermann, The changing photochemistry of the atmosphere, Tellus, 43AB, 136-151, 1991.

[2] Madronich, S., UV radiation in the natural and perturbed atmosphere, in Environmental effects of UV (Ultraviolet) Radiation, pp. 17-69, CRC Press, Boca Raton, 1993.

[3] Zeng, J., S. Madronich, and K. Stamnes, A note on the use of the two-stream delta-scaling approximation for calculating atmospheric photolysis rate coefficients, J. Geophys. Res. , 101, 14,525-14,530, 1996.

[4] Van Weele, M., P. G. Duynkerke, Effect of clouds on the photodissociation of NO2: observations and modelling, J. Atmos. Chem., 16, 231-255, 1993.

[5] Van Weele, M, J. Vilà-Guerau de Arellano, and F. Kuik, Combined measurements of UV-A actinic flux, UV-A irradiance and global radiation in relation to photodissociation rates, Tellus, 47B, 353-364, 1995.

[6] Los, A., M. van Weele, and P. G. Duynkerke, Actinic fluxes in broken cloud fields, J. Geophys. Res., 102, 4257-4266, 1997.

[7] Landgraf, J., and P. J. Crutzen, An efficient method for online calculations of photolysis and heating rates, J. Atmos. Sci., 55, 863-878, 1998.

[8] Junkermann, W., Measurements of the J(O1D) actinic flux within and above stratiform clouds and above snow surfaces, Geophys. Res. Lett., 21, 793-796, 1994.

[9] Shetter, R. E., C. A. Cantrell, K. O. Lantz, S. J. Flocke, J. J. Orlando, G. S. Tyndall, T. M. Gilpin, C. A. Fischer, S. Madronich, and J. G. Calvert, Actinometric and radiometric measurement and modeling of the photolysis rate coefficient of ozone to O(1D) during Mauna Loa observatory photochemistry experiment 2, J. Geophys. Res., 101, 14,631-14,641, 1996.

[10] McKenzie, R. L., K. J. Paulin, and S. Madronich, Effects of snow cover on UV irradiance and surface albedo: A case study, J. Geophys. Res., 103, 28,785-28,792, 1998.

[11] Vilà-Guerau de Arellano, J., P. G. Duynkerke and M. van Weele, Tethered-balloon measurements of actinic flux in a cloud-capped marine boundary layer, J. Geophys. Res. , 99, 3699-3705, 1994.

[12] Curry, J. A., and 26 Coauthors, FIRE arctic clouds experiment, Bull. Amer. Meteor. Soc., 81, 5-30, 2000.

[13] Van der Hage, J. C. H., and S. R. de Roode, An isotropic light sensor for measurements of visible actinic flux in clouds, J. Atmos. Oceanic. Technol., 16, 1698-1701, 1999.

[14] Madronich, S., UV radiation in the natural and perturbed atmosphere, in Environmental effects of UV (Ultraviolet) Radiation, pp. 17-69, CRC Press, Boca Raton, 1993.

[15] Goody, R. M., and Y. L. Yung, Atmospheric radiation. Theoretical basis, 2nd Ed., 519 pp., Oxford University Press, 1989.

[16] Stephan R. de Roode, Peter G. Duynkerke, Wim Boot, and Jeroen C.H. Van der Hage, Surface and Tethered-Balloon Observations of Actinic Flux: Effects of Arctic Stratus, Surface Albedo, and Solar Zenith Angle, submitted to J. Geophys. Res., 2000.

****

1 MEASUREMENT TECHNOLOGY, PERFORMANCE, AND QUALITY ASSURANCE

1.1 Surface Observation Systems

1.1.5 Quality Observations

Representativity of wind measurements in The Netherlands: a discussion on methods of transforming observed values to the area involved

Henk Benschop
Royal Netherlands Meteorological Institute KNMI
Department of Observations and Models
P.O. Box 201
3730 AE De Bilt
The Netherlands
Telephone: +31302206383
Telefax: +31302210407
e-mail: benschop@knmi.nl

Abstract of the paper

The data of the measurements of windspeed and winddirection should be representative for areas as specified by the users, especially in the framework of synoptic meteorology, climatology and aeronautical meteorology. However the roughness of the field around the observation sites, e.g. buildings, trees, forest, hills, walls etceteras, can have a high impact on the values of the winddata. In he case of an inhomogeneous landscape this influence is also dependent of the winddirection. These circumstances make it insure what grade of representativity the measurements will have. At Royal Netherlands Meteorological Institute a method is developed to transform the data, especially on windspeed, to the area involved. This method will be presented and discussed.

Representativity of measured windspeed on synoptic scale

The goal of the observations of windspeed and -direction at a height of 10 meter above the landsurface is to get an idea of the present behaviour of the horizontal surface wind in the region. Of main interest is to get an accurate idea of the windsituation on a synoptic scale. The distribution of the meteorological observation network in the Netherlands, and the distance between the observation points, especially for measuring windspeed and winddirection, has been based on statistical research by J.Wieringa. The conclusion was that with a separation of 30 km between 2 observation points in a homogeneous landscape, for 90% of the time the difference in windspeed is less than 5%. With a density of the network like this, the archived winddata can also be used for an analysis of incidents (e.g. stormcalamities), and for climatological studies.
(See fig.1).

On the base of the results of the research with respect to the scale of density, the selection of weatherstations in The Netherlands has been done. However, although The Netherlands is mainly a flat country, at most of the stations the goal of the measured windspeed - to get an accurate idea of the horizontal windsituation in the region - will be influenced by the roughness of the terrain near the observation site. The scale of roughness depends on the number and type of obstacles, the vegetation, the topography and other terrainobjects. It means that any roughness of the terrain causes a difference between the measured windspeed and the windspeed which is representative for the region.

To correct for this terrain influence on the average windspeed a shelterfactor has been developed by Wieringa (ref.1, 2). This factor is a relation between the measured average windspeed, mostly at a height of 10 meter, and the virtual windspeed that would be measured if the terrain close to the site (radius < 1 km) would be completely flat.

The calculation of this factor has been based on the hypothesis that the windspeed at a height of 60 meter above the landsurface is rather constant in a large region of a homogeneous landscape and objects not higher than ca. 20 to 30 meters. The procedure for the calculation is to transform the measured value of average windspeed u_{obs} to a present value of the average windspeed at 60 meters height and after that to transform back to a virtual 10 meter value of the average windspeed u_{virt} in a completely flat terrainsituation. The function on transformation the windspeed is in fact the logarithmic vertical windprofile formula at neutral atmospheric conditions (ref. 2, 3).

$$u = (u^* / \kappa) / \ln (z/z_0)$$

κ (Kappa) is the Von Karmanconstant ($\approx$0.4)
u^* is the friction velocity of the air
u is the average windspeed
z is the measuring height
z_0 is the scale of roughness of the terrain: roughnesslength

The result of the transformation is the following shelterfactor F:

$F = u_{virt} / u_{obs} = \{ \ln (10/z_{0p}) / \ln (60/z_{0p}) \} * \{ \ln (60/z_{0s}) / \ln (z/z_{0s}) \}$

z_{0p} = roughnesslength in the case of flat terrain ($z_{0p} \approx 0{,}03$ m)

z_{0s} is the roughnesslength around the site of the windobservation (mostly dependent of the winddirectionsector)

z is the measuring height of the sensor (normally 10-m)

Using the above mentioned values for z and z_{0p} (resp. 10 m and 0,03 m) one can calculate the shelterfactor in this specific situation:

$$F = 0{,}764 * \{ \ln (60/z_{0s}) / \ln (10/z_{0s}) \}$$

There are several methods for estimating z_{0s}. The operational method at the KNMI is based on the relation between the standarddeviation of the windspeed and the roughnesslength, as well as the relation between the gustfactor G and the roughnesslength. Herewith the gustfactor is the maximum gust in an observing period (u_x) divided by the average windspeed in the same period (u): u_x / u. This method follows the principle the rougher the terrain the more variability there will be in the horizontal windspeed. This derivation is focussed on the median value of a datasample of gustfactors: <G>. As result of the, partly statistical, analysis the following relation between the median gustfactor <G> and the roughnesslength z_0 is found:

$$G = f_T * \left(1 + \frac{1.42 + 0.3 * \ln\left(\frac{10^3}{U_t} - 4\right)}{\ln \frac{z}{z_0}}\right)$$

z is the observation height z, normally 10-meter

U_t is the gustlength: u * t (u: average windspeed, t: duration of the gust)

f_T : 1 in the case of an avering period of 10 minutes

1,1 in the case of an averaging period of 60 minutes,

Using 1-hour values (f_T = 1,1), a mean gustlength $U_t \approx 50$ meter and the above mentioned roughnesslength $z_0 = z_{0s}$, one can find:

$$\langle G \rangle = 1{,}1 * \{1 + [1.42 + 0.3 \ln 16] / [\ln (10/z_{os})] \}$$

The effect of the terrain roughness on the measured windspeed is minimised by using the theory on the shelterfactor. For all the weatherstations in The Netherlands, where windspeed is measured, the shelterfactors per windsector of 20° have been calculated. Every two years an update calculation of those factors is made because of possible modifications in the roughness.

Representativity of measured windspeed at airports, especially Airport De Kooy

To get (real time) information about the windfield at an airport, especially to the windfield at take off and touch down zones of the runway, one should think of a representativity of the measured horizontal windspeed (and winddirection) for a region of about 5 x 5 km^2. The conditions with respect to the representativity are dictated by the rules of the ICAO (ref.4.)

An important weatherstation at the northwest side of The Netherlands is the observation station WMO 06235 situated at Airport De Kooy. In the framework of this station a windmast of 10-meter height has been located. The observations of windspeed and winddirection at this site have several goals. The main objectives are:

a) to give a representative view on the local horizontal windfield at the field of the airport, especially at touchdown and take off positions, including helispots;
b) to give a representatively synoptic and climatological view on the windfield in this countryside of The Netherlands: rather flat agriculture country with some small towns, canals and low dunes beside the seacoast;
c) to give a representatively synoptic and climatological view on the windfield at the near seasurface: Noordzee, Waddenzee, and IJsselmeer.

The windmast has been situated at the north side of the airportfield at a distance of about 300 meters from touchdown zone 22 of the runway. A smaller distance to the runway is difficult because of the influence of landing or departing aeroplanes or helicopters (turbulence, vortices, and so on) on the windmeasurements. In the present situation the measurements are reasonably representative for the airportfield in general and the touchdown zone 22 especially. However the roughness of the country at the north direction of the windmast is large, because of the buildings of the city

Den Helder, trees of 10 meter high along the roads, and other objects within a distance of about 200 meters from the site. Therefore, the representativity of the windmeasurements on a larger scale is doubtful. The effect of the terrain roughness near the observation site on the measured windspeed can be minimised using the shelterfactor.

The results of the calculation of the present shelterfactors per winddirectionsector of 20 degrees at the windobservation site of weatherstation De Kooy are presented in table 1.

Sector (degrees)	Gustfactor <G>	Roughnesslength z_0 (m)	Shelterfactor F (z=10m,z_{0p}=0,03 m)
000-020	1,883	0,424	1,197
020-040	1,707	0,169	1,100
040-060	1,531	0,032	1,002
060-080	1,455	0,009	0,961
080-100	1,472	0,013	0,970
100-120	1,531	0,032	1,002
120-140	1,531	0,032	1,002
140-160	1,531	0,032	1,002
160-180	1,531	0,032	1,002
180-200	1,478	0,014	0,973
200-220	1,490	0,018	0,980
220-240	1,483	0,016	0,976
240-260	1,483	0,016	0,976
260-280	1,579	0,057	1,029
280-300	1,707	0,169	1,100
300-320	1,795	0,284	1,148
320-340	1,883	0,424	1,197
340-360	1,895	0,445	1,204

Table 1. Shelterfactors of the windsite of weatherstation De Kooy

Using the values of the shelterfactors one can calculate per winddirection the virtual average windspeed out of the measured values of average windspeed and to get in this way a representative view on the windsituation at this part of The Netherlands.

As mentioned above, the shelterfactor has been based on a transformation of the windspeed to a virtual windspeed at flat terrain (z_0 = 0,03 m). To realise the option "to give a representatively synoptic and climatological view on the windfield at the near seasurface ", one can also transform the measured windspeed to a virtual wind above seasurface by using the roughnesslenght of seasurface ($z_0 \approx$0,002 m). This gives a method in hand to estimate the average windspeed above near seasurface and to get an accurate idea of the windfield in this area of the North Sea, Waddenzee, IJsselmeer.

Conclusions

The shelterfactors make it possible to calculate per winddirection the virtual average windspeed out of the measured values of average windspeed and in this way to get a representative view on the windfield on synoptic scale in the concerned region.

References

1. Gust factors over open water and built-up country, J.Wieringa, Boundary-Layer Meteorology 3 (1973) 424-441;
2. An objective exposure correction method for average wind speeds measured at a sheltered location, J.Wieringa, Quart.J.R.Met.Soc (1976) 102, pp 241-253;
3. Windstructure in strong winds below 150 m, H.A.Panofsky, Wind Engineering 1(1977), pp 91 -103;
4. International Civil Aviation Organisation ICAO, 'Meteorological Service for International Air Navigation, International Standards and Recommended Practices', annex III to the convention on International Civil Aviation, 13th edition, 1998.

****

Fig. 1. Distribution of synoptic windstations in The Netherlands, situation may 2000

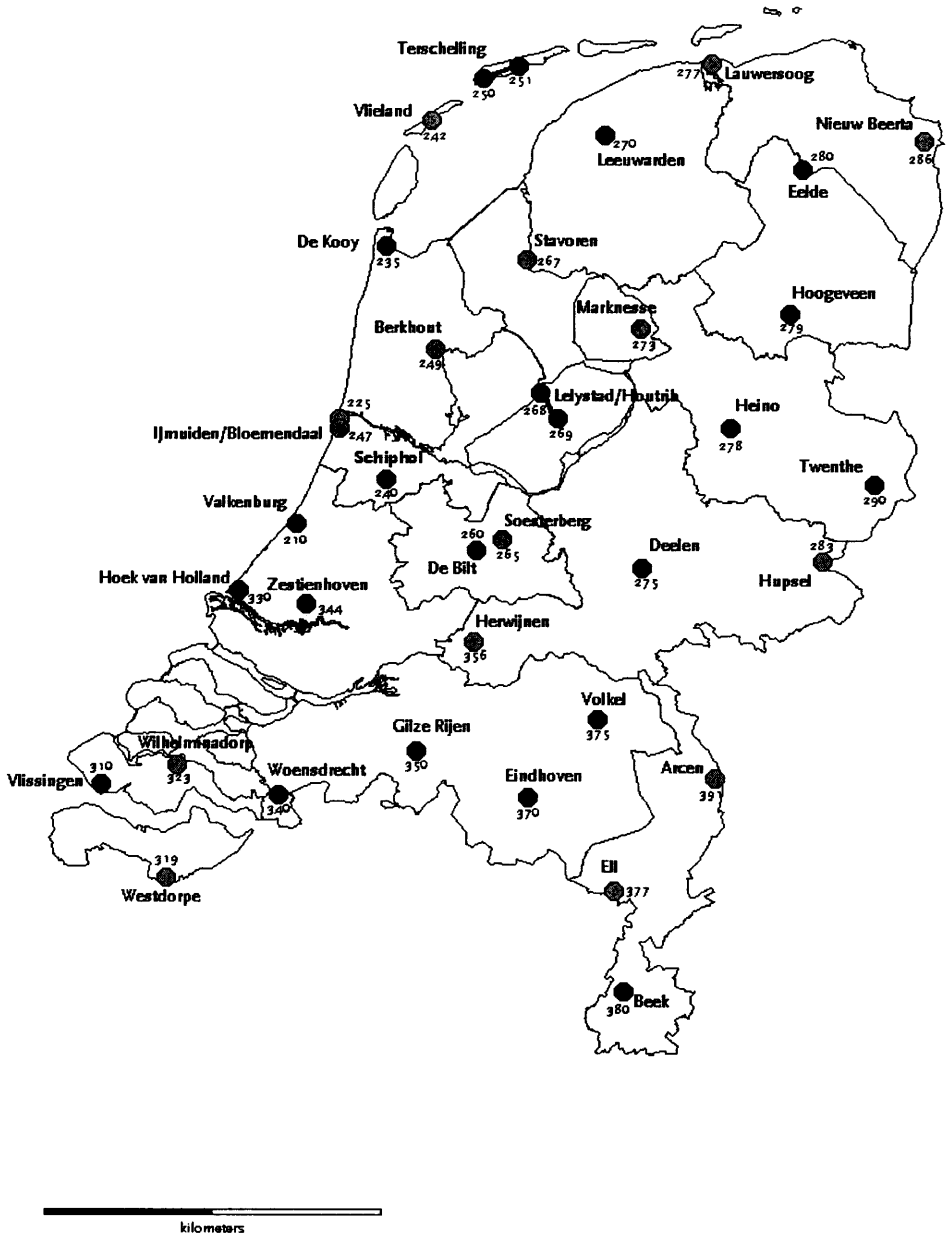

ПОЛНАЯ МОДЕЛЬ КОРРЕКТИРОВКИ ОСАДКОМЕРНЫХ ДАННЫХ, МЕТОДИКА И АЛГОРИТМ ОЦЕНКИ СИСТЕМАТИЧЕСКИХ СОСТАВЛЯЮЩИХ ПОГРЕШНОСТИ

Голубев В.С., Коновалов Д.А. Государственный гидрологический институт,

Богданова Э.Г., Ильин Б.М. Главная Геофизическая обсерватория

23, 2- я линия, 199053, Санкт – Петербург, Россия Тел. (812) 323 3517, 323 1167

Факс (812) 323 1028, ISHIKLOM@ZB3267.SPB.EDU

ABSTRACT

A full model of correction of the results of precipitation measurements are presented which takes into account systematic errors conditioned by aerodynamic characteristics of the precipitation gauge as well as evaporation-condensation processes and wetting of the precipitation collector. Amount of false precipitation catched by the precipitation collector during snowstorms is assessed.

Введение

Полная модель корректировки осадкомерных данных позволяет оценить действительное количество осадков, поступивших из облаков на поверхность земли в пункте наблюдений, путем учета систематических погрешностей, вызванных аэродинамическими свойствами осадкомерной установки, процессами испарения-конденсации и смачивания в осадкосборнике, а также ложных осадков, попадающих в осадкосборник за время общей и низовой метелей. Научное обоснование методики корректировки осадков приведено в работах авторов [1-3].

Оценка систематических погрешностей производится по результатам срочных наблюдений на метеорологических станциях. Для получения действительных значений осадков используются сведения о типах приборов, характеристиках места их размещения, а также метеорологических элементах, явлениях и процессах в срок и между сроками наблюдений.

Разработанные совместными усилиями сотрудников Государственного гидрологического института и Главной геофизической обсерватории им. А.И. Воейкова методика и алгоритм корректировки осадков реализованы в виде компьютерной программы для расчета действительных значений осадков, измеренных осадкомером Третьякова в срок наблюдений.

С учетом результатов взаимосравнения ВМО измерений твердых осадков (1986-1998гг.) разработанная программа корректировки может быть адаптирована к данным, полученным по другим типам осадкомеров.

Полная модель корректировки

Вычисление действительных значений осадков выполняется по формуле

$$P=K(P^{*} + \Delta P - P^{*}_{f1} - P^{*}_{f2}), \text{ мм}, \qquad (1)$$

где K - коэффициент, учитывающий систематическую погрешность связанную с воздействием аэродинамических факторов на результат измерений осадков;

$P^{»}$ - результат измерения осадков по измерительному стакану;

ΔP - поправка, компенсирующая систематические погрешности измерения осадков, возникающие вследствие смачивания внутренней поверхности осадкосборника, испарения осадков из него и конденсации влаги на поверхности внутренних стенок;

$P^{»}_{f1}$ - поправка, учитывающая количество ложных осадков, попавших в осадкосборник за время общей метели;

$P^{»}_{f2}$ - поправка, учитывающая количество ложных осадков, попавших в осадкосборник за время низовой метели.

Коэффициент K рассчитывается путем осреднения данных за отдельные сроки наблюдений (τ) по формуле :

$$K = 1 + A_0 \frac{\sum_{1}^{n} (\mu(\tau) \cdot U_h(\tau))^2}{n}, \qquad (2)$$

где A_0 - эмпирический параметр;

$\mu(\tau)$ - коэффициент перехода от значений плотности воздуха при стандартных параметрах атмосферы к плотности при реальных условиях;

$U_h(\tau)$ - скорость ветра на высоте приемного отверстия осадкосборника;

n - число сроков метеорологических наблюдений между сроками измерения осадков.

Величина поправки, учитывающей погрешности измерения осадков за счет смачивания, испарения и конденсации (ΔP,мм) рассчитывается в зависимости от вида осадков и относительной влажности воздуха:

- в случае измерения жидких осадков, при $r \le 95\%$ по формуле:

$$\Delta P = 0.069 \ln(100 - r) + 0.009, мм, \qquad (3)$$

при r>95% $\Delta P = 0.1, мм;$

- в случае измерения твердых осадков, при $r \le 95\%$ по формуле:

$$\Delta P = 0.097 \ln(100 - r) - 0.15, мм, \qquad (4)$$

при r>95% : $\Delta P = -0.2, мм;$

- в случае измерения смешанных осадков, при $r \le 95\%$ по формуле:

$$\Delta P = 0.158 \ln(100 - r) - 0.449, мм; \qquad (5)$$

при r>95%: $\Delta P = -0.2, мм.$

В формулах (3) - (5) r – относительная влажность воздуха, осредненная из всех срочных ее значений ($r_a(\tau)$) от срока установки осадкосборного сосуда до срока измерения осадков (смены сосуда) включительно, %.

При расчете действительных значений осадков по формуле (1) принимается:
при $P^{»} + \Delta P < 0,\ P = 0$

Количество ложных осадков, попавших в осадкомер за время общей метели $(P^{"}_{f1}, мм)$, вычисляется по формуле

$$P^{"}_{f1} = \sum_{1}^{n1} J^{i}_{f1} \cdot \tau^{i}_{f1}, \qquad (6)$$

где J^{i}_{f1} - средняя интенсивность ложных осадков за период, в котором наблюдалась общая метель, между двумя сроками наблюдений за метеоэлементами, мм/час;

τ^{i}_{f1} - продолжительность общей метели за этот же период ($\tau^{i}_{f1} \le 3$ час.), час;

$n1$ - число промежутков наблюдений, в которые наблюдалась общая метель ($n1 \le n - 1$).

Интенсивность ложных осадков J_{f1} за счет общей метели в срок наблюдений вычисляется по формуле

$$\text{при} \quad U_h(\tau) > 4{,}2 \text{ м/с} \qquad J_{f1} = 0.033\left(U_h^{2.2} - 4.2^{2.2}\right)\frac{1}{\mathrm{K}_{f1} U_h} \cdot \mathrm{B}_h L_{f1}, \quad (7)$$

Коэффициент захвата дефляционных частиц при общей метели K_{f1} вычисляется по формуле:

$$\mathrm{K}_{f1} = 1 + 0.0215 \cdot \mu^2 \cdot U_h^2, \quad (8)$$

Коэффициент, учитывающий концентрацию дефляционных частиц на высоте приемного отверстия осадкосборника B_h, вычисляется по формуле:

$$\mathrm{B}_h = \frac{2}{h - h_S} \cdot \ln\frac{2}{z_0} \cdot \left(\ln\frac{h - h_S}{z_0}\right)^{-1}, \quad (9)$$

где h - высота приемного отверстия осадкосборника над поверхностью земли, *м*;

h_S - высота снежного покрова на метеорологической площадке, определяемая по данным ежедневных измерений по постоянным снегомерным рейкам, *м*;

Коэффициент, учитывающий насыщенность метели (L_f), вычисляется по формуле:

$$L_f = th \cdot \frac{3\text{Ч}(\text{А})}{1000} \quad (10)$$

Ч - длина разгона метели по данному направлению ветра, *м*.

Количество ложных осадков, попавших в осадкосборник за время низовой метели (P^{*}_{f2}, *мм*), вычисляется по формуле

$$\mathrm{P}^{*}_{f2} = \sum_{1}^{n2} J^{i}_{f2} \cdot \tau^{i}_{f2}, \quad (11)$$

где J^{i}_{f2} - средняя интенсивность ложных осадков за счет низовой метели за период , в котором наблюдалась низовая метель, между двумя сроками наблюдений метеоэлементов, мм/час;

τ^{i}_{f2} - продолжительность низовой метели за этот же период ($\tau^{i}_{f2} \le 3$час.), час;

$n2$ - число промежутков наблюдений, в которые наблюдалась низовая метель ($n2 \le n - 1$).

Интенсивность ложных осадков при низовой метели в срок наблюдений вычисляется в зависимости от состояния снежного покрова перед началом низовой метели. Выбор формулы производится сообразуясь с последовательностью фиксации наблюдателем времени снегопада, общей метели и низовой метели.

Предварительные результаты испытания модели

В настоящее время авторами проводятся испытания разработанной программы корректировки срочных значений осадков на материале трех станций северо-западного региона РФ (С.-Петербург, Воейково, Винницы) и четырех станций Арктики и Камчатки (Диксон, Тикси, Каменское, мыс Лопатка).

Из рассмотрения результатов корректировки по станциям северо-западного региона вполне очевидно, что в данных климатических условиях, где в исследуемый период метелей практически не было, разработанная методика и программа корректировки надежно применима. Все рассчитанные значения поправок вполне адекватно отражают влияние соответствующих метеорологических параметров и условий защищенности установки осадкомера.

При попытке применить предложенную модель корректировки в условиях Арктического побережья возникли трудности, связанные с неопределенностью или отсутствием исходных параметров, необходимых для расчета ложных осадков. К их числу относятся такие характеристики, как вид метели и состояние поверхности снежного покрова. При сильных ветрах и интенсивной дефляции различие между низовой и общей метелью часто становится весьма приблизительным, и кроме того, во время сильной метели практически невозможно определить, выпадает ли снег из облаков, или поднят с поверхности снегового покрова в процессе дефляции, либо присутствуют оба процесса одновременно.

Характеристика состояния снежного покрова, от которого сильно зависит интенсивность дефляции и структура дефляционных частиц, также практически не отражается в материалах стандартных метеорологических наблюдений.

Все это приводит к большим случайным ошибкам в определении количества ложных осадков в условиях сильных продолжительных метелей, и делает неопределенными результаты корректировки за отдельные сроки или сутки.

Дальнейшее усовершенствование модели корректировки в части учета ложных осадков, на наш взгляд, требует дополнительных исследований в направлении изучения региональных климатических особенностей метелевого режима и увязки с особенностями структуры снежного покрова, которая, в свою очередь, формируется под влиянием температурно-ветрового режима региона.

Литература.

1. Golubev,V.S., Bogdanova,E.G., 1996: Point measurements of solid precipitation. In,Proc. of the workshop on the ACSYS solid precipitation climatology project Reston, VA, USA,12-15 september 1995.WMO/TD No.739,1996. 8-29.

2. Golubev, V.S., Bogdanova,E.G., Simonenko, A.Yu.,1997:

The effect of blizzards on the precipitation gauge readings and proposals on the experimental check of the correction method of precipitation data in Arctic region. In. Proc. of the workshop on the inplementation of the Arctic precipitation data archive at the Global Precipitation Climatology Centre. Offenbach, Germany, 10-12 July, 1996. WMO/ TD No. 804, 1997.74-79.

3. Голубев В.С., Коновалов Д.А., Симоненко А.Ю., Товмач Ю.В. –Корректировка измерений осадков и качество откорректированных данных.- Метеорология и гидрология, 1999г., №1, с.103-113.

A Method of Field Calibration of Automatic Weather Stations

By Hu Yufeng, Zhou Weixin
Chinese Academy of Meteorological Sciences, Beijing, China
Tel.: (+8610) 68406976, Fax: (+8610) 68406976
Email: weixin@mail.sparkice.com.cn

1. Problems with periodic calibration of AWSs

It is practically impossible to bring the whole Automatic Weather Stations (AWSs) already in use back to lab and do periodic calibration. A normally used method is to use travelling standards to compare with the AWS in field. If a problem is found, the questioned sensor is sent back to lab for calibration. However, there are several points need to be considered with this method:

On one hand, the quality of calibration in field is often compromised with the complexity of the equipment and procedures. For example: (1) It needs to be proved that the travelling standard can reconstruct the true value in field. (2) During comparing, homogeneity and stability of the measurand are required. (3) If the present weather is used as experimental condition, calibration is carried out at only one point (or within a very narrow range) in the allowed range. Under such circumstance, the result from a single point calibration can not substitute that from a full-span calibration. (4) The other equipment and the environmental condition related to the comparison should be ensured. (5) The downtime of normal operating due to calibration has to be taken into consideration.

On the other hand, the important difference between the calibration of the sensor used in AWS and the calibration of the sensor in ordinary application is ignored. Especially, when a present sensor in AWS needs to be replaced with a calibrated one, the well known "substitution error" may happen.

2. Relationship between periodic calibration and instrument accuracy

Accuracy of an instrument is the sum of all-random errors and undetermined system errors during measurement. Accuracy of an instrument has to be decided with strict model-test. As normally accepted, instrument accuracy could be represented by the following equation.

$$\Delta = \sqrt{\left(\delta_1^2 + \delta_2^2 + \delta_3^2 + \delta_4^2 + \delta_5^2 + \delta_6^2\right)} \qquad (1)$$

where, Δ : accuracy of an instrument;

δ_1 : the sum of errors of the standard and experimental error during calibration;

δ_2 : residual indication error of the calibrated instrument after adjusting;

δ_3 : the basic error of an instrument (normally calculated as square root of the sum of squares of repeatability error, hysteresis error and non-linearity error);

δ_4 : the influence error by variety of influence quantities;

δ_5 : indication drift between two calibrations;

δ_6 : tracking error caused by the limit of the response to fast change of measurand.

In principle, the purpose of the periodic calibration is to ensure accuracy of AWS, and it targets the indication drift (δ_5) of the instrument. Indication error of the instrument against standards during calibration is a determined system error, which has to be corrected. Thus, the periodic calibration of AWS should include comparison with a standard to find the indication error and correction (or adjustment) accordingly. The view that it is unnecessary to adjust as long as indication error is within accuracy is not correct.

Based on the analysis of the relationship of periodic calibration and instrumental accuracy, and taken into consideration of problems of the normally used method as stated above, we propose a two-step calibration method of AWS.

3. Principles of two-step calibration of AWS

Accuracy-related AWS measuring chain includes a sensor, an amplifier, a multi-switch, and an A/D converter and computation part of the computer program. We can divide it into two parts, a sensor and a condition circuit, and calibrate them separately (see fig.1). From practice, we find that in the whole measuring chain, the sensor has the most influence in AWS accuracy. Thus, the emphasis of two-step calibration is on the sensor. The sensor is calibrated in full span in lab, which is the same as traditional whole instrument calibration in respect of the controlled measurand, standards, environmental condition and comparison procedure, with the differences mainly in analysis of the comparison data. In field, we use a well-calibrated sensor to replace the one that needs to be calibrated, and calibrate the condition circuit with a high precise signal generator. Obviously, the equipment and procedure for this method is much simpler than whole instrument calibration in field.

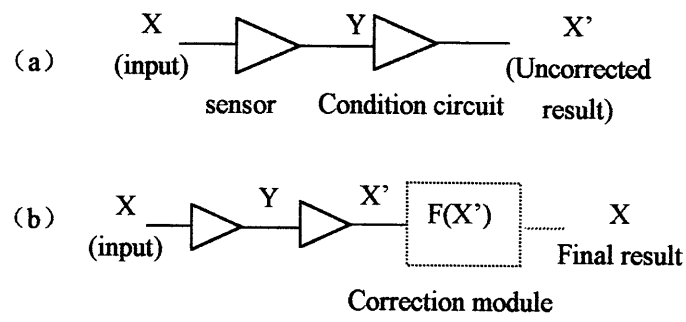

Fig.1 the diagram of measuring chain of AWS

The key to two-step calibration is how to determine respectively calibration parameters of both the sensor and the condition circuit, which can be used by computers within the AWS. Taken a Pt resistance sensor as an example (reference to table 1), Let X represents the excitation applied to the sensor (i.e. temperature), R represents the output of the sensor (i.e. resistance). And let Y represents the temperature equivalent to the output of the sensor, which can be calculated from resistance by means of the normal characteristic curve of the sensor. The relationship curve between R and X is called the characteristic curve of the sensor, and the relationship curve between Y and X is called the calibration curve of the sensor (see

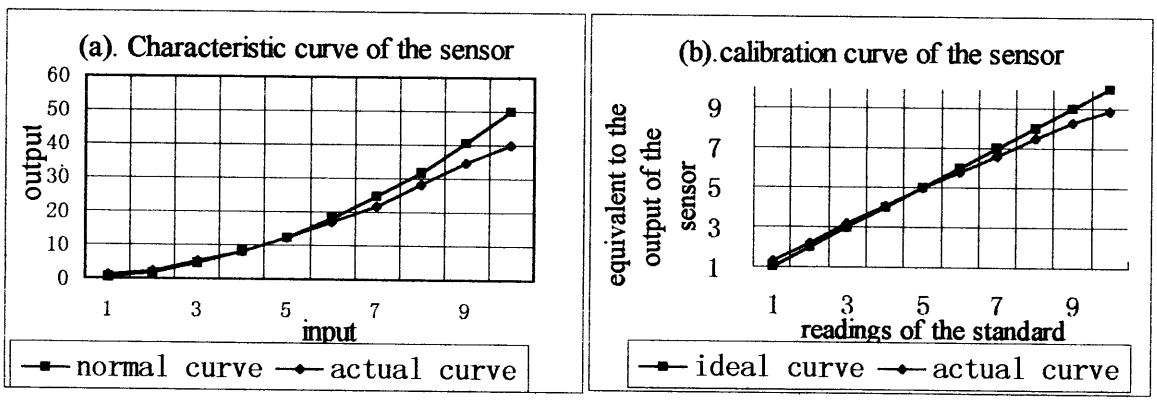

Fig.2 comparison between the characteristic curve of a virtual sensor and its calibration curve

fig.2). Usually, $Y \neq X$. So, the actual characteristic curve of a sensor is not the same as the normal characteristic curve of this kind of sensor. Although the characteristic curve of the sensor may be very complex, the calibration curve can, however, be fit as a straight line as the following. The error of the liner regression equation is small enough (see table 1)

$$X = A_1 + B_1 * Y \qquad (2)$$

Where, A_1 is the intercept of the liner equation, which is liner regression of the calibration curve, and B_1 is the slope. They are regarded as the calibration parameters of sensor.

Similarly, the liner regression equation for the calibration curve of the condition circuit can be written as:

$$Y = A_2 + B_2 * X' \quad (3)$$

Where Y is the equivalent of the input of the condition circuit (or the output of the sensor), X' is the output of the condition circuit. A_2 is the intercept of the liner equation, and B_2 is the slope. A_2 and B_2 are regarded as the calibration parameters of condition circuit.

Table 1. An example of calibration of a actual Pt resistance sensor

T[1] (℃)	Rn[2] (Ω)	Ra[3] (Ω)	Te[4] (℃)	err. 1[5] (℃)	err. 2[6] (℃)	err. 3[7] (℃)
-40.00	84.027	84.014	-40.03	-0.03	-0.12	0.02
-30.00	88.037	88.030	-30.02	-0.02	-0.11	0.00
-20.00	92.037	92.040	-19.99	0.01	-0.08	0.00
-10.00	96.024	96.038	-9.96	0.04	-0.06	-0.01
0.00	100.000	100.027	0.07	0.07	-0.02	0.00
10.00	103.964	104.002	10.10	0.10	0.01	-0.01
20.00	107.917	107.968	20.13	0.13	0.04	0.00
30.00	111.857	111.922	30.17	0.17	0.08	0.00
40.00	115.787	115.869	40.22	0.22	0.12	0.02

[1]: actual temperature

[2]: normal resistance, $Rn = f(T) = 100\times(1+aT+bT^2+cT^3)$

where, a=3.97E-3, b=-5.84E-7, c=-4.22E-12

[3]: actual resistance

[4]: temperature equivalent to Ra, $Te = f^{-1}(Ra)$

[5]: uncorrected error

[6]: residual error only correcting the zero

[7]: residual error after correcting by means of liner regression equation

Once we get the calibration parameters of both the sensor and the condition circuit, the indication errors of these two parts against the standards can be corrected easily.

The error due to comparison experience of the sensor and/or fitting calibration line is one of components of δ_2, defined as δ_{21}; accordingly, the error due to the calibration of condition circuit and/or e fitting calibration line is defined as δ_{22}. The sum of them corresponds to the residual error δ_2 of whole instrument calibration in lab, more or less.

4. Correction equation for two-step calibration

Combine equation (2) and (3), we get:

$$\begin{aligned} X &= A_1 + B_1 * Y \\ &= (A_1 + B_1 * A_2) + B_1 * B_2 * X' \end{aligned} \quad (4)$$

In fig.1(b), let

$$F(X') = A_3 + B_3 * X',$$

Then

$$A_3 = (A_1 + B_1 * A_2), \quad B_3 = B_1 * B_2 \quad (5)$$

Thus, F(X') is the required correction equation, which should be added into the computation module of AWS. The coefficients of this equation are derived form calibration parameters (A_1, A_2, B_1, and B2). In above equation X' is the well-known uncorrected result. However, after calling the function F(X'), the final output of AWS should be equal to the true value, at least theoretically.

5. Other important issues involved in two-step calibration

Of course, the normal characteristic curve (or the equation) used in calculating calibration parameters must be the same used in AWS.

To get accurate experience data during calibrating sensor, it is important to use electric measuring instrument satisfying accuracy requirement. Usually, the AWS itself is disabled to do it as a standard electric measuring instrument. This accuracy requirement depends on analysis of total errors of sensor calibration should be ensured in practice.

Similarly, the signal generator used in calibration of the condition circuit should have enough accuracy. Especially in field, the accuracy can be achieved. Best of all, the signal generator is a special smart function generator.

To transfer calibration parameters accurately, A_1 、 A_2 and A_3 should have more decimal point position than that one included in the final result. B_1 、 B_2 and B_2 should have more efficient digits than that one included in the factor to multiply by it.

6. Conclusion

In order to keep accuracy of AWS used in field, it is necessary to calibrate them periodically and correct the constant error found. To achieve this goal, we divide AWS measuring chain into two parts, the sensors and the condition circuit, and calibrate them in two steps. The calibration of sensors, which have more influence on measuring accuracy of AWS, is carried out in lab, while replacing sensors and calibrating the condition circuit with a signal generator are done in field. In this way, the complexity related to whole instrument calibration and both errors and operation cost resulted from it are limited. Although characteristic curves of sensors are non-linear, for most measuring instruments, it is accurate enough to use liner regression instead of the actual calibration curve. Using the coefficients from the liner equation makes it possible and easy to transfer the result of calibration. The equation (5) derived above can exactly correct constant errors found theoretically without the substitution error.

It is much simpler with much better result to use this two-step calibration than to use traveling standards to calibrate AWS as a whole instrument in field. This method can be used not only for AWSs, but also used in hydrology, environmental monitoring, and those with complicated systems, such as on some industrial sites.

(End)

CORRECTIONS OF THE WIND-INDUCED ERROR OF TIPPING-BUCKET PRECIPITATION GAUGES IN SWITZERLAND USING NUMERICAL SIMULATION

B. Sevruk, Y.-A. Roulet and V. Nespor
Climate Research ETH Zurich, Switzerland: sevruk@geo.umnw.ethz.ch

Common precipitation measurements using elevated can-type gauges are subject to systematic error mostly due to wind field deformation above the precipitation gauge orifice, wetting and evaporation losses, splash-out and splash-in, blowing snow, etc. (Sevruk, 1982; 1993). An elevated precipitation gauge systematically distorts the wind field above the gauge orifice and forces the wind speed to increase over the gauge orifice (blocking effect). Due to the adverse wind action, some of the lighter precipitation particles are borne away before reaching the gauge and are lost for the measurement. The wind-induced loss depends on wind speed, the weight of precipitation particles and the gauge construction parameters, the most important is the use of wind shield. The dependency is non-linear (Sevruk, 1989; Goodison et al., 1998; Nespor and Sevruk, 1999). The loss amounts on average to 2 - 10 % of measured values of rain and up to 60 % of snow for unshielded gauges and wind speeds greater than 4 ms^{-1} (Goodison et al., 1998). Since the wind-induced error during snowfalls can be ten times larger than for rain, the fraction of snow in total precipitation is a very important variable.

Correction procedures are different for rain and snow. They have been developed for different types of precipitation gauges and various time intervals according to the availability of necessary input data, such as the precipitation intensity and weather situation (different drop-size distribution exists for different types of rains but the same intensity), wind speed, temperature, rain/snow amounts etc. They are based either on empirical field methods using the WMO reference standard (Sevruk and Hamon, 1984; Goodison et al., 1998) or numerical simulation as described by Nespor and Sevruk (1999). In addition, the water equivalent of fresh snow and snow cover and the snow dept have also been used to assess the "true" snowfall and to derive correction procedures (Sevruk, 1983: 1986a; 1987; Sevruk et al, 1998). In the case of simulation the wind-induced error is estimated by computing the wind field around the gauge using computational fluid dynamics software and by numerical simulation of precipitation particle trajectories in the computed flow field. Figure 1 shows the results of simulation for two unshielded precipitation gauges as used in Switzerland: the common daily gauge by Hellmann and the automatic station gauge ASTA.

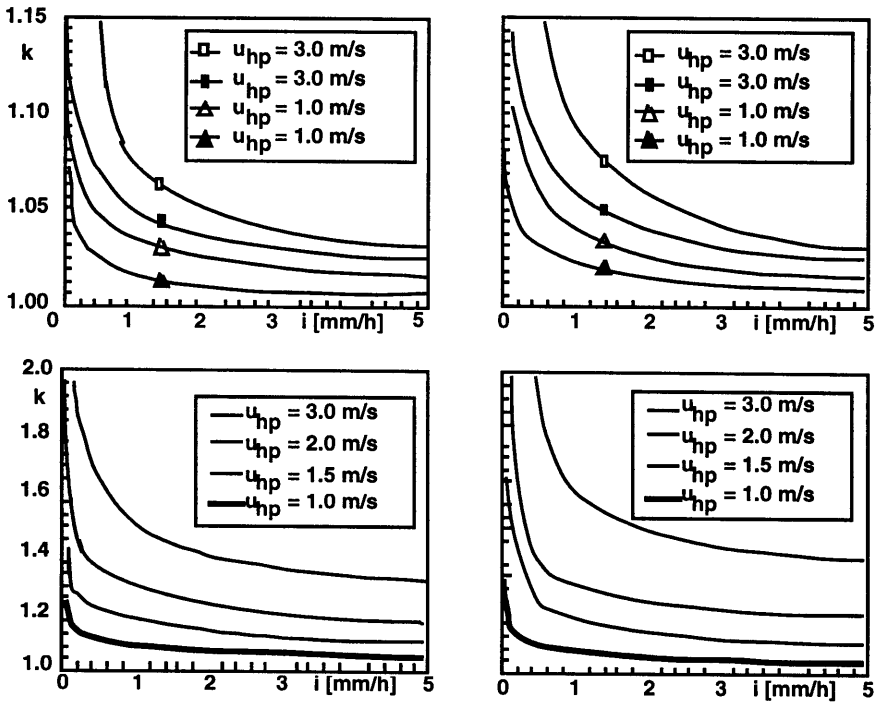

Figure 1: Conversion factor k defined as the ratio of "correct" and measured precipitation for rain (top) and snow (bottom) for the Hellman gauge (left) and the ASTA gauge (right) in dependency of wind speed u_{hp}, intensity i and type of weather situation according to Nespor and Sevruk (1999). Void symbols in the top diagrams refer to orographic rain and black ones to showers. Note different scales for rain and snow. For shielded gauges k can be reduced to 50 and 70 % for snow and mixed precipitation, respectively (Goodison et al., 1998).

The simulation has many advantages as compared with the rather costly empirical methods. Once the methodology is developed, correction procedures for any type of precipitation gauge can be made on computer very fast, within weeks. For field tests more years are necessary. Moreover, during field tests with heated gauges the losses of precipitation catch due to heating should be separately accounted for. This presents a rather difficult problem. The agreement between the results of empirical and theoretical procedures is fairly well as showed by Sevruk and Nespor (1998). Having developed a correction procedure for a given type of a gauge, the problem consists primarily, in the resolution and availability of input data. This poses no problems for the automatic meteorological stations where hourly values of many variables are available but it is a serious disadvantage of common gauge sites with only one precipitation observation per day. Here, interpolations are needed practically of all variables (Sevruk, 1986b). In Switzerland, there are up to 72 automatic stations (ASTA) as compared with 400 common (Hellmann-type) gauge sites. They are more or less regularly distributed over the whole territory including high altitude regions up to 4000 m a.s.l. and providing hourly values of almost all meteorological variables on line. The rain/snow separation can be assessed at the automatic stations according to the weather situation from the Weather Bulletin and the hourly temperature t [°C] as follows. For rain: t min = 2; for snow: t max = -2; for mixed precipitation (50 % rain, 50 % snow): t interval = -2 and 2 °C. The level of wind measuring instruments above the ground is commonly higher up to ten times (20 m) above the precipitation gauge orifice (1.5 - 2.5 m). This can be accounted for using the reduction procedure based on the logarithmic vertical wind profile and degree of gauge site protection as shown by Sevruk and Zahlavova (1994). The latter can be directly measured at site using a theodolite or assessed from the metadata. In some cases, the fish eye pictures of gauge sites are also available. One-third out of all ASTA gauge sites in Switzerland is exposed, more than one-third is mostly exposed, eight gauge sites are mostly protected and only two are completely protected. The ASTA gauge is heated during the winter season. The registration follows tipping-bucket principle. Generally, this type of recording gauge seems to be less reliable than manual gauges as for instance, the Hellmann gauge (Sevruk, 1996).

For different reasons only 64 (out of 72) gauge sites have been considered in the study. The season considered, from December 1996 to February 1997, was characterised by small wind speeds at the level of the gauge orifice on days with precipitation. On average it amounted to only 0.9 ms^{-1} at 51 gauge sites (13 hill sites excluded). One fourth of all hours with precipitation showed snow and one third mixed precipitation. The rest was rain. The average hourly correction, the losses due to heating, evaporation and wetting excluded, amounted to 18 % of the measured precipitation. Since the mean hourly corrections could be small, the maximum values are generally large. At each gauge site the maximum hourly correction amounts at least to 100 %.

Table 1
Mean hourly corrections in per cent of measured values and input variables at the gauge sites with large corrections, December-February 1996/97.

Legend:
P - total of measured precipitation, [mm]
u - daily wind speed, [ms^{-1}]
$\underline{u}$ - daily wind speed average over the period of precipitation, [ms^{-1}]
t - daily temperature, [°C]
$\underline{t}$ - daily temperature average over the period of precipitation, [°C]

Gauge site	Altitude	P	Correction	u	$\underline{u}$	t	$\underline{t}$
Weissfluhjoch	2690	123	70	2.6	4.5	-5.7	-7.8
Säntis	2490	439	56	4.2	5.2	-4.5	-6.3
Gütsch	2287	251	62	4.4	4.9	-4.1	-6.1
Moleson	1972	168	71	3.3	5.4	-1.3	-2.4
La Dôle	1670	382	68	5.8	7.8	-0.5	-0.9

Table 1 shows corrections and input variables for gauge sites with the largest corrections. Such gauge sites are mostly situated in the mountains in altitudes above 1500 m a.s.l. On the 14th February 1997 during the snowfall with a strong wind of 8 ms^{-1} only one third of the "true precipitation" was measured on the top of the Saentis (2490 m a.s.l.) and only 10 % during one hour. The average of 10 hours with maximal corrections amounts to 320 % at Weissfluhjoch (2690 m a.s.l.) and more than 100 % for 21 gauge sites. The reason for such large values is the combination of snow with strong winds. Small corrections occur in the lower parts of Ticino, in the

Central Switzerland (Lucern, Altdorf), inner-alpine valleys (Disentis) and in gauge sites in Midland with small wind speed and fraction of snow (Wynau, Zurich, Bale and Berne).

The regional corrections vary considerably as seen from Table 2. For this aim, the Swiss territory has been subdivided into six regions. They represent different climate conditions in Switzerland such as the dry inner-alpine (Grison, reg. I; Valais, reg. III, particularly the Rhone valley) or the humid south-alpine climate (Ticino, reg. II) and the high alpine climate (Prealps/Alps, reg. IV) as well as the windy (Jura, reg. VI) and less windy (Midland, reg. V) climate.

Table 2
Regional corrections, frequency and intensity of precipitation types, December - February 1996/97.

Region		Altitude [m asl]	P* [mm]	Correction [%]	Number of hours rain	snow	mixed	Intensity*+ rain	snow	mixed
I Grison	(9)	1542	90	21	22	85	66	0.5	0.5	0.6
II Ticino	(11)	1080	174	5	83	90	113	0.5	0.7	0.6
III Valais	(10)	1301	199	17	64	90	78	0.7	1.1	0.7
IV Prealps	(11)	1037	209	28	92	71	86	0.7	1.1	0.8
V Midland	(15)	565	177	8	167	21	66	0.7	0.4	0.7
VI Jura	(8)	937	213	27	147	39	126	0.7	0.4	0.8
All territory	(64)	1045	178	18	101	63	87	0.7	0.8	0.7

Brackets indicate the number of gauges * refers to measured values + [mmh^{-1}]

The largest corrections of all regions result for the Prealps/Alps and Jura and the smallest ones of only 5 and 8 % for the Ticino and Midland, respectively. The variability of corrections arises from combinations of all relevant variables including the number of hill gauge sites with larger wind speed and amount of precipitation. This can be demonstrated by two regions I and VI, Grisons and Jura, respectively. They show quite different wind speed and temperature but almost the same correction magnitude of 21 vs. 27 % (Tab. 2). The mean altitude of all eight-gauge sites in Jura is less than 1000 m vs. above 1500 m in Grison. The mean wind speed and temperature during precipitation periods in Jura amounts to 3 ms^{-1} and 2 °C, respectively and the number of hours with precipitation is 312 (102 snow and 210 rain). In Grison, wind speed amounts only to one-half of that in Jura (1.6 ms^{-1}), but due to high altitude the temperature amounts to -3 °C (5 °C smaller than in Jura!) and the total number of precipitation hours only to 173 (118 snow and 55 rain). The number of snow hours is more or less the same (102 Jura vs. 118 Grison) but the number of rain hours in Grison is no more than one-fourth of these in Jura. Due to this and to low temperatures and despite the small wind speed the corrections in the region of Grison still amount to a respectable 21 %.

Regional differences in precipitation amount, duration and intensities of rain, snow and mixed precipitation exist but there are no differences at all in the average intensities of different forms of precipitation over the entire territory of Switzerland. As seen from Table 2 they amount to 07; 0.8 and 0.7 mmh^{-1} for rain, snow and mixed precipitation, respectively. The large intensities of snow in Ticino, Valais and Prealps/Alps are caused by heavy snowfalls of a few extreme events as seen from Table 3 and possibly also by the heating of precipitation gauges. The heating can cause the reduction of melting of snow accumulated in the gauge to a few last hours of the snowfall period. Generally, the duration of the low-intensity snowfall is not recorded properly using heated gauges because the accumulated snow tends to evaporate. Thus only larger amounts of snow can be recorded. This, of cause, increases the recorded intensity of snow. In the Grison no heavy snowfalls occur frequently and the intensity of snow is small. In the regions V and VI of Midland and Jura with the smallest altitude and the total seasonal snow amount of only 8 - 15 mm and generally, high temperatures during precipitation periods no frequent heating is necessary and as again snowfall intensity is small.

In order to see the effect of averaging over smaller and larger time intervals using the non-linear dependency of the wind-induced error (Fig. 1) daily corrections have been compared with the daily sum of hourly corrections. The variables needed for the correction of daily precipitation totals are based on the average over all hourly values with precipitation during a particular day. The day was defined from 0700 am of the present day to 0700 am of the following day. The average hourly correction amounted to 18 % vs. daily correction of 19.5 % of the measured precipitation. The overestimation of only 1.5 % (equal to 6 % of correction amount) seems negligible. But as can be seen from Table 3 the combinations of actual intensities and wind speeds during a day can vary widely, particularly during longer precipitation periods at the high altitude with large correction

values (e. g. snow). This can cause large differences between the total of hourly and the daily correction.

Table 3
Extreme values of hourly precipitation intensity, wind speed and the ratio of daily and total of hourly corrections

Gauge site	Altitude [m asl]	Date	Duration [hours]	Correction day/Σ hours ratio	Intensity min	max. [mmh^{-1}]	Wind speed min.	max [ms^{-1}]
La Dôle	1670	2.12.96	20	1.4	0.1	2.1	4.8	12.8
La Dôle	1670	19.12.96	21	1.8	0.1	4.8	4.2	11.5
Chasseral	1599	13.02.97	15	2.0	0.1	4.4	4.3	9.9
La Chaux F.	1018	13.02.97	18	0.3	0.1	4.5	3.6	6.8
Säntis	2490	1.12.96	15	2.0	0.1	2.9	0.7	10.4
Säntis	2490	18.02.97	15	1.5	0.1	6.6	1.5	13.0
Moleson	1972	5.02.97	12	1.3	0.5	2.6	1.7	10.8
Pilatus	2106	18.02.97	15	1.9	1.2	4.2	1.2	4.2

In this connection it should be noted that for precipitation periods with frequent breaks and the registration interval of one hour the actual corrections are generally biased. The reason is that the "true" precipitation duration can be often smaller than the registered number of hours with precipitation. This means the smaller observed intensity as compared with the real one. Yet the smaller intensity means the larger correction. This effect and the above-mentioned differences in hourly and daily corrections indicate that the smaller the time period considered the more accurate the correction of the wind-induced error. In order to estimate the optimum correction interval, the corrections of one minute, 10 minutes and one hour intervals should be analysed.

Summary: The wind-induced error of hourly precipitation measurements of 64 gauge sites of the Swiss Automatic Network (ANETZ) from December to February 1996/97 amounted to 18 % of measured precipitation. The corrections vary considerably between gauge sites and regions. The smaller ones occur in the lower parts of Ticino and the larger ones in the Alps.

References

Goodison, B. E., P.Y.T. Louie and D. Yang.: WMO solid precipitation measurement intercomparison, World Meteorol. Org., Geneva, Switzerland, WMO/TD-No. 872, 212 pp, 1998.

Nespor, V. and B.: Sevruk: Estimation of wind-induced error of rainfall gauge measurements using a numerical simulation. J. Atmos. Ocean. Techn, 16(4), 450-464, 1999.

Sevruk, B.: Methods of correction for systematic error in point precipitation measurement for operational use. World Meteorol. Org., Geneva, Operational Hydrol. Rep., 21, WMO-No. 589, 91 pp., 1982.

Sevruk, B.: Correction of measured precipitation in the Alps using the water equivalent of new snow. Nordic Hydrology, 14(2), 49-58, 1983.

Sevruk, B.: Conversion of snowfall depths to water equivalents in the Swiss Alps. In: B. Sevruk (Ed.) Proc. Workshop on the Correction of Precipitation Measurements. Zürcher Geographische Schriften, ETH Zürich, No. 23, 81-88, 1986a.

Sevruk, B.: Correction of precipitation measurements: Swiss experience. In: B. Sevruk (ed.). Proc. Workshop on the Correction of Precipitation Measurements. Zürcher Geographische Schriften, ETH Zürich, No. 23, 187-196, 1986b.

Sevruk, B.: On difficulties of checking storage gauges in winter. In: Proc. 13th Conference of Carpathian Meteorology. Institut of Meteorology and Hydrology, Bucharest, 169-174, 1987.

Sevruk, B.: Wind-induced measurement error for high-intensity rains. WMO Instruments and Observing Methods Rep., No. 48, WMO/TD- No. 328, 199-204, 1989., Geneva.

Sevruk, B.: Checking precipitation gauge performance. In: S. Couling (ed.). Measurement of airborne pollutants, 89-107, Butterworth Heinemann, Oxford, 1993.

Sevruk, B.: Adjustment of tipping-bucket precipitation gauge measurements. Atmos. Research., 42(1-4), 237-246, 1996.

Sevruk, B. and W.R. Hamon: International comparison of national precipitation gauges with a reference pit gauge. Instruments and Observing Methods Rep., World Meteorol. Org., Geneva, No. 17, 135, 1984.

Sevruk, B. and V. Nespor: Empirical and theoretical assessment of the wind-induced error of rain measurement. Water Science and Technology, 37(11), 171-178, 1998.

Sevruk, B., M. Paulais and Y.-A. Roulet: Correction of precipitation measurement using fresh snow as reference. Proc. WMO Technical Conference on Meteorological and Environmental Instruments and Methods of Observation, World Meteorol. Org., TECO-98. WMO/TD-No. 877, 349-352, 1998.

Sevruk, B and L. Zahlavova: Classification system of precipitation gauge site exposure: Evaluation and application. Internat. J. Climatol., 14(6), 681-689, 1994.

ACCREDITED CALIBRATION LABORATORY OF THE HYDROMETEOROLOGICAL INSTITUTE OF SLOVENIA

Silvo Žlebir
Hydrometeorological Institute of Slovenia
Vojkova 1/b, 1000 Ljubljana, Slovenia
Tel.: +386 1 478 4306, E-mail: silvo.zlebir@rzs-hm.si

Introduction

Regular and accurate calibrations are important factors of quality assurance in classical and automated surface observing and measuring networks. For this reason, we have set up in Slovenian Hydrometeorological Institute our own calibration laboratory. Laboratory is primarily intended for calibration of instrumetation, used in the measuring network of our institute. At the moment we have facilities to calibrate instruments for temperature, humidity, barometric pressure and ozon (O_3), but we are setting up also calibration facilities for other air-quality instrumentation (SO_2, NO_x and CO), solar radiation and for hydrological (water level) instrumentation. For all these quantities, we attempt to assure the highest quality of calibration work with known and well defined uncertainties and traceability to national and/or international level.
Slovenia is setting up a so-called distributed system of primary national standards, which means that different laboratories will be carriers for different primary national standards. As standards for all physical quantities in Slovenia are not set up yet, we are also competing to be a carrier of primary standard for some of them. According to the foreseen future development of the Hydrometeorological Institute of Slovenia into commercialization, we also itend to offer some of the laboratory's capacities for the market. These are the reasons why we already started a procedure of accreditation of our laboratory. Besides, also national legislation urges us to be accredited. Nowadays, our laboratory is accredited according to the EN45001 standard and ISO25 Guide for termometry, we plan to be accredited also for calibration of humidity, barometric pressure and ozon measuring instruments in near future.

Capabilities and equipment of the laboratory

TEMPERATURE:
Laboratory is equipped for calibration of classical mercury thermometers, electronic thermometers with displays, platinum resistance thermometers, thermistors and thermographs. As a media, we use computer controlled bath with a water/glycol mixture in the temperature range of -20°C to +50°C and an air chamber in a temperature range of –20°C to +40°C. Working standards are Pt100's, which are regularly calibrated against primary standard Pt25 SPRT with the aid of DC resistance bridge. Pt25 is also regularly calibrated in laboratory fixed points, which are the triple point of water and the Galium melting point.. Other equipment used in calibration process are precision multimeters and standard resistors. External traceability is linked to DKD (Deutsche Kalibrierdienst) accredited laboratory in Germany for Pt25 SPRT and fixed points and to RvA-NKO accredited laboratory at Slovenian Institute for Quality and Metrology for multimeters and standard resistors. Best measurement capabilities(BMC), as evaluated from uncertainty budget and stated in COFRAC accreditation contract no.2.1404, is 45 mK for calibration of thermistors and platinum resistance thermometers and 90 mK for mercury thermometers. Calibration performances in water triple point and galium melting point have been improved recently and BMC'a are now 1.0 mK and 1.5 mK, respectively. Laboratory is now making effort to improve the performances and BMC of calibration in air chamber. To this goal, useful volume of the chamber will be decreased.

Calibration of automatic weather stations' sensors is fully automatic procedure, where measurement PC controls the bath, working reference and measurand. It also calculates uncertainties and measurement differences in preset calibration points.

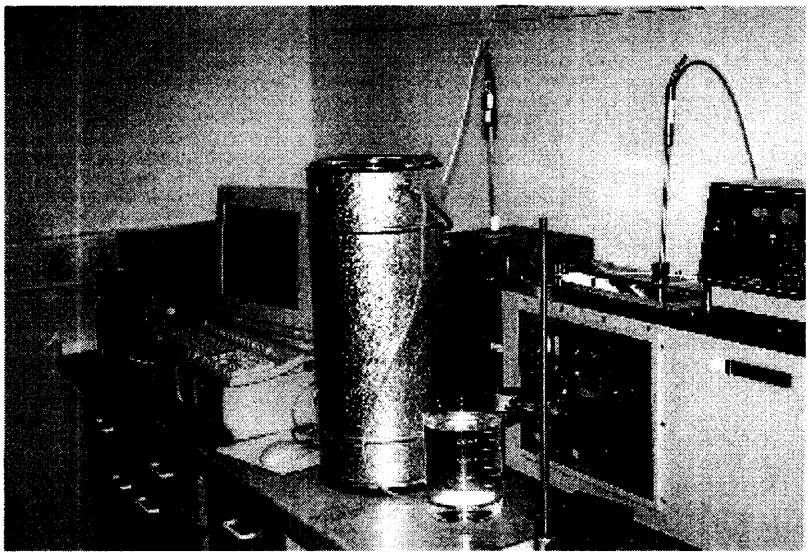

Picture 1

Part of the thermometry laboratory equipment, including Galium melting point and calibration bath

BAROMETRIC PRESSURE:
Laboratory equipment enables calibration of mercury barometers, barographs, mechanical barometers and electronic barometers in the range of 100 hPa to 1100 hPa. Occasionaly, also altimeters and radiosondes are calibrated. To obtain stable pressure in this high range, Th. Friedrichs barometric pressure chamber is used. Primary laboratory reference is a Desgranges & Huot precision digital force dynamometer, combined with a piston cylinder assembly, which lineary transforms pressure into force. Precisely defined masses, which are used to check and recalibrate the dynamometer, are also a part of the instrument. This reference instrument is externaly traceable to French BNM-LNE, its ucertainty being in the range of 6 Pa. Pressure in the whole measuring circuit is controlled by the automatic pressure controller.
Working references of the laboratory are Setra and Vaisala precision barometers. Procedure for calibration of electronic barometers and barometric sensors is also automated.
Estimation of the BMC's for barometry is in the phase of evaluation. It is expected to be somewhere about 10 Pa.
Accreditation procedure for barometry is now going on.

HUMIDITY:
For calibration of humidity instruments and sensors, chamber with a high degree of stability in temperature and humidity is used as media. At the moment, electronic psychrometer, calibrated and traceable to German PTB is used a primary laboratory reference instrument. Two sigma uncertainty for calibration is 3-4 % of relative humidity. We are now setting up a new laboratory system, where dew point instrument, traceable to French CETIAT laboaratory will serve as a reference. For calibration of capacitive humidity sensors, we are also using saturated salt solutions as reference materials for certain humidity points.
Calibration of humidity is possible in following ranges:
from -20 °C to -10 °C - RH range 10% to 80%
From -10 °C to +10 °C - RH range 10% to 90%
over 10 °C - RH range 10% to 98%

OZON:
Calibration of UV photometric O_3 analyzers is made by comparison to a reference standard instrument (calibrator) of a higher rangee. Calibration is traceable to Czech national standard, located at the Hydrometeorological Institute of Czech Republic. Calibration in our laboratory can be done in the range of 0 – 500 ppb, with uncertainty depending on the calibration point, lowest being about 10 ppb.
Also calibration of ozon analyzers is in preparation for accreditation.

Other capabilities of our laboratory include calibration of solar radiation sensors, visibility instrumentation, water level sensors/instruments and analyzers for air composition of SO_2, CO, NO, NO_2 and dust particles. For these quantities, full analysis of uncertainties is not done yet. Fully documented traceability to higher level is also a subject of future work.

Accreditation process

Accreditation is an official confirmation for the laboratory that it is qualified for doing calibration for certain field. In Slovenia, process of accreditation for calibration and testing laboratories has begun few years ago. Until now, there are ten calibration laboratories accredited and among them, laboratory of the Hydrometeorological Institute was the sixth one. As Slovenian national accreditation body is actualy setting-up, foreign European accreditation bodies are included in accreditation procedures. Our laboratory is accredited for temperature calibrations by COFRAC, Comite Francais d'Accreditation, the French national accreditation body. Relevant standards were EN 45001 and ISO Guide 25, additional documents were requirements from COFRAC. Accreditation certificates by both, the Slovenian accreditation body and COFRAC, were imparted to our laboratory in May 1999.

To fulfil all the accreditation requirements, laboratory set up effective, well documented quality system. Quality manager of the laboratory, who takes care for the implementation and development of the quality system, was named among the laboratory staff. Assessments of both, the quality system and the technical competence of the laboratory, were done by assessors, named by COFRAC and Slovenian accreditation body. When assessing technical competence of the laboratory, staff of the laboratory, working premises, equipment of the laboratory and its internal and external traceability, calibration procedures, uncertainty evaluation and documentation were all audited.

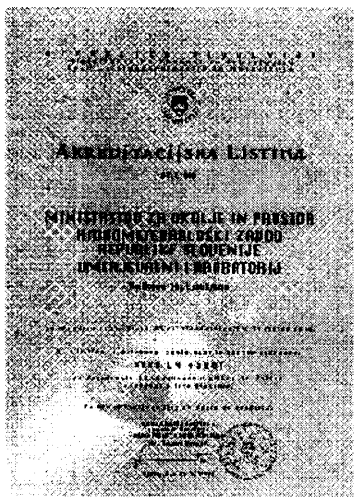

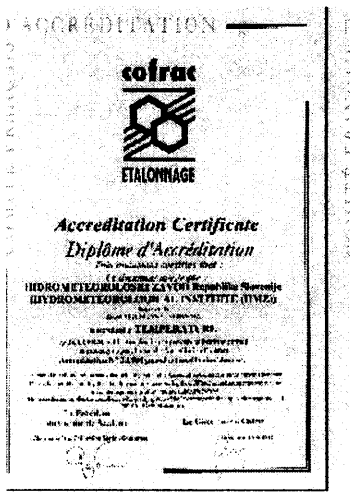

Picture 2

Accreditation certificates of the calibration laboratory of the Hydrometeorological Institute of Slovenia

Conclusion

According to the strategy of the Hydrometeorological Insitute of Slovenia toward the quality of our services, we set up a calibration laboratory to support the quality of data on our meteorological and environmental measuring network. At the moment, laboratory covers almost all the needs of the measuring network regarding calibrations. It has facilities for calibration of sensors/instruments for temperature, humidity, barometric pressure, solar radiation, visibility, water level and air-composition. Laboratory is accredited now for thermometry, but the process of accreditation is resuming for hygrometry, barometry and ozon measurements. Accreditation is one of the key factors that ensure high level of quality of our data and its traceability to the international level.

References

(1) WMO Guide to Meteorological Instruments and Methods of Observation; World Meteorological Organization - No.8, Sixth Edition, Geneva 1996

(2) ISO/IEC Guide 25: General requirements for the competence of calibration and testing laboratories, 3rd edition 1990. International Organization for Standardization, Geneve, Switzerland

(3) Exigences A Satisfaire Par Les Laboratoires D'Etalonnage Accredites Ou Candidats A Une Accreditation, Modalites D'Application, Document COFRAC N° 2002, 3ème Édition - Novembre 1994

(4) Reglement D'Accreditation, Document COFRAC N° 2005, Révision 05 - Décembre 1999

A SIMPLE TOOL FOR RECORDING METEOROLOGICAL INSTRUMENT SITE EXPOSURE

D.B. Hatton and M. Parker
The Met. Office, Beaufort Park, Easthampstead, Wokingham, Berkshire, RG40 3DN, United Kingdom
Tel: 44 (0)1344 855831`Fax: 44 (0)1344 855897 Email: dbhatton@meto.gov.uk

Introduction

The quality of many meteorological observations, particularly when part of a climatological network, is highly dependant on the exposure of the sensor used to take the measurements. This is particularly true of rainfall, radiation and wind, but can also be significant for other variables. Most sensors have 'ideal' exposure conditions, but frequently compromises have to be reached because of site limitations and the proximity of potentially disturbing objects.

In the urban environment, where sites may be less than ideal for synoptic meteorological measurements, but which nevertheless have significant anthropological relevance, it may be considered that representative measurements will include the effects of nearby objects. In this situation any obstructions to sensor exposure on the site may be accepted as part of the normal exposure, but need to be quantified.

For whatever reason, it is important that the exposure of sensors is characterised regularly so that account can be taken of changes that occur, for example when trees grow or new buildings are constructed.

In the past The Met. Office carried out site surveys to assess the exposure of rain gauges, using an inclinometer and compass to determine the amount of shelter. This required measurements to be taken and manually logged at 10° intervals around the compass. It was a time consuming task that could be difficult in windy conditions. These instruments are not easy to use, and mathematical errors can also be introduced when transferring the readings from eye level to gauge top.

The solution

The use of a camera with fish eye lens was considered as one solution to the problem, but there were several drawbacks. Readily available camera systems were expensive, and it was not possible to mount the camera with the lens in the position at the top of the rain gauge, without actually removing the rain gauge. Even if a modern digital camera was used, the images could not be easily viewed in real time. The positions and elevations of objects could only be measured after applying an overlay with corrections for lens characteristics and distortion.

The idea of using a hemispherical dome as a reflector was conceived and a prototype was made from an old discarded glass lighting globe, which was painted black on the inside and inscribed with lines indicating azimuth. This device was of a suitable size to fit on the top of a rain gauge and, after aligning the azimuth markings to north, the reflected 360° panorama could be viewed from vertically above. Only a very simple calculation was necessary to determine the correct positions for a further set of inscribed circles that would indicate the angular elevation of all surrounding objects. From this it was a simple matter to observe and note down the relevant details.

The step from prototype to production of the relatively small numbers required was surprisingly difficult without incurring excessive development or manufacturing costs. The glass domes with an optically acceptable finish were no longer available, and in any case, they were rather fragile for operational use in the field.

Moulded products were ruled out because of the high initial tooling costs, with no guarantee of a satisfactory result. There were no other off the shelf products available with an acceptable optical finish and of the right size.

As modern computer controlled machining techniques became available, a manufacturer was eventually identified with the capability of manufacturing hemispherical domes from austenitic stainless steel. These could be polished to provide an optically acceptable finish, at quite a low unit cost. It was then a simple machining task to inscribe scale lines of azimuth and elevation. A small magnetic compass was inset on top of the dome to provide an easy facility for alignment.

Figures 1 and 2 show the reflector in an early version mounted on a plywood base with a carrying slot, and which provides an adapter for easy location on a 5 inch rain gauge. It is an easy matter to change the base to suit any other application. Figure 3 shows the dome mounted on a plastic base with a pair of small spirit levels attached, to assist with alignment.

In use, the complete surrounding panorama can be viewed by eye and a photograph taken with a camera, either hand held (see figure 1), or mounted on a small tripod. The image is already marked with an elevation and azimuth scale and it is easy to see at a glance where objects exceed the acceptable minimum elevation angle and could affect the instrument exposure. The intrusion of the observer into the image is minimal, and a tripod mount will reduce this further. By using a digital camera, the image can be immediately downloaded to a laptop PC, checked, and stored in a site record file.

These devices have been tested by inspectors from The Met. Office and have proved to be very useful for checking rain gauge exposure, and also for ensuring that radiation sensors are exposed in positions that are clear of obstructions.

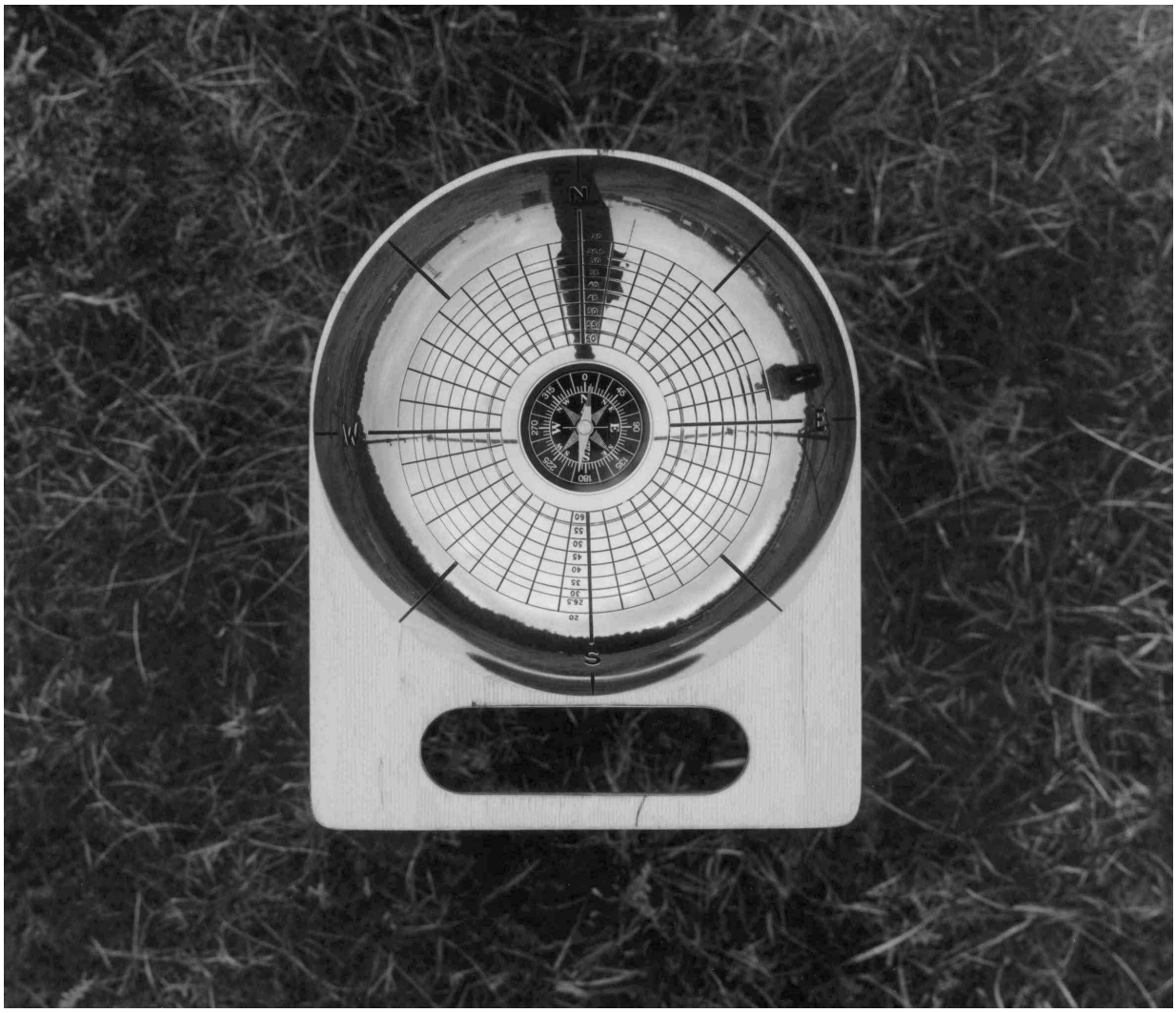

Figure 1 Plan view
The circular rings are marked to show the elevation of objects in the range 20° to 60°

Figure 2 Side view of dome mounted on a 5 inch rain gauge

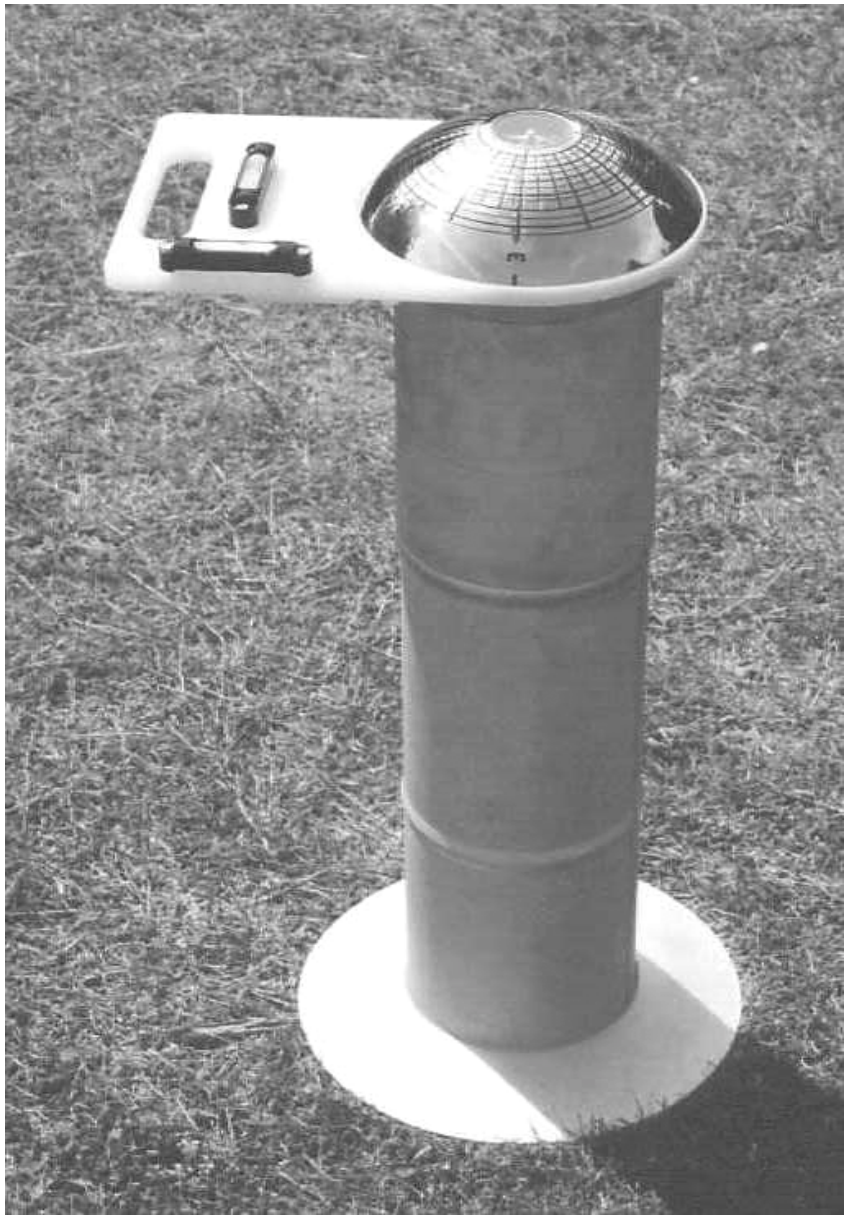

Figure 3 Dome with alternative base and spirit levels

ACCELERATION AND DECELERATION OF A CUP ANEMOMETER IN A WIND TUNNEL AND IN NATURAL TURBULENCE

W.R. Sparks, D.W. Jones and D.B. Hatton
The Met. Office, Beaufort Park, Easthampstead, Wokingham, Berkshire, RG40 3DN, United Kingdom
Tel: 44 (0)1344 855603 Fax: 44 (0)1344 855897

ABSTRACT

Accurate wind observations require instruments whose calibration and dynamic characteristics are known. For cup anemometers in particular, the 'basic' calibration is easily achieved for different steady state wind speeds in an accredited wind tunnel, however this will not characterise the performance in field conditions of turbulent winds.

This paper describes a method of determining the dynamic response of a cup anemometer based on additional wind tunnel measurements to determine the acceleration and deceleration characteristics necessary to calculate the constants in the anemometer's equation of motion.

By comparing two similar anemometers with different distance constants it will be shown that the equations determined in the wind tunnel accurately predict the performance in natural turbulence.

1. INTRODUCTION

The characteristics of the cup anemometer have been extensively studied and reported in the literature. There is general agreement that the response of the instrument can be well approximated by an equation of the form

$$\mathbf{L*du/dt + u = v} \quad \cdots\cdot \quad (1)$$

where $\mathbf{L = D/[a*u + (1-a)*v]}$

$\mathbf{u}$ = the wind speed indicated by the anemometer

$\mathbf{v}$ = the horizontal wind speed to which the instrument is exposed

$\mathbf{t}$ = time

$\mathbf{D}$ = the anemometers distance constant

$\mathbf{a}$ = dimensionless constant

Equation (1) is a generalisation of one given by Taiichi Hayashi[1] who based his derivation on the work of Schrenk[2].

Although there is general agreement on the form of equation (1) there is no such agreement on the value of '**a**'. Those who have studied both acceleration and deceleration of the cup anemometer [e.g. Taiichi Hayashi[1] and Hyson[3] usually follow Schrenk[2] in assuming that **a** = 0.5 while those who concentrate on acceleration of the instrument [e.g. Lockhart[4] and the Handbook of Meteorological Instruments[5]] adopt the value **a** = 0. For these two values of '**a**' there are classical analytical solutions to equation (1). The Handbook of Meteorological Instruments[5] gives the solution for **a** = 0 and Taiichi Hayashi[1] gives the solution for **a** = 0.5. However, equation (1) can be solved for any value of '**a**' by numerical methods.

This paper will show that the value of '**a**' can be determined by simple tests of the anemometer in the wind tunnel and that equation (1) then provides a good guide to the performance of the instrument in the field.

Amongst the errors of the cup anemometer identified by MacCready[6] are the '**u**' errors that result from the inability of the instrument to follow rapid variations in the horizontal wind speed and the errors that arise if the anemometer does not have a cosine response to winds that depart from the horizontal. Since equation (1) allows only the '**u**' error to be calculated the non-cosine response errors must be eliminated when anemometers are compared in the field. Errors due to non-cosine response can be estimated from wind tunnel studies, but in this study were eliminated through the use of externally identical anemometers with different distance constants.

2. THE ANEMOMETERS

The instruments studied were a Vector Instruments A100L anemometer and an internally modified version of this instrument, referred to in this paper as the A100M.

The A100L has three conical plastic cups 50mm diameter on a rotor with overall diameter 150mm. The body of the instrument has a diameter of 55mm and a height of 60 mm. The body contains an infrared light source and detector, and an electronics module that provides both a pulse output and a voltage output proportional to wind speed. Only the pulse output was used for high frequency measurements in this investigation to avoid contamination of the results by time constants in the electronics module.

The A100M was produced from an A100L by removing the electronics module to make space for a heavy flywheel attached to the bottom of the rotor shaft. This increased the moment of inertia of the rotating parts of the instrument by a factor of about 2.5 without changing the instrument externally.

Steady-state calibrations in the wind tunnel showed that linear calibration curves could be used with both instruments to give measurements with a standard error of estimate of 0.05 m/s or less, over the speed range from 2.5 m/s to more than 20 m/s.

3. ACCELERATION OF THE ANEMOMETERS IN THE WIND TUNNEL

The wind tunnel was set to a constant speed and the anemometer was released from a lower speed and allowed to take up the air speed in the tunnel. The speed of the anemometer in the wind tunnel was controlled at start speeds different from the wind flow by a simple electrically driven shaft that could be instantaneously disengaged from the anemometer rotor. The rate of rotation of the anemometer was measured by counting pulses over periods of 0.125 seconds.

The expected speed of the anemometer was calculated using equation (1) and compared with the measured speed. The parameters '**D**' and '**a**' were adjusted to minimise the root-mean-square difference between expected and observed speeds.

A number of different starting speeds and values of '**a**' were tried, but it was found that the simple procedure of releasing the anemometer from rest and assuming that **a** = 0, gave a value of '**D**' that provided as good a fit for all start speeds as any more complex procedure or assumption. Following Lockhart[4], observed speeds less than 30% of the final

wind speed were discounted to ensure that the response motion had recovered sufficiently from the initial forced stall condition.
Sixteen runs of the A100L with final speeds from 2.7 m/s to 15.1 m/s gave 1.95 metres for the mean value of '**D**' with a standard deviation 0.161 metres. The value **D** = 2 metres was adopted for all subsequent work.
Twelve runs of the A100M with final speeds from 5.0 m/s to 10.5 m/s gave 4.95 metres for the mean value of '**D**' with a standard deviation 0.38 metres. The value **D** = 5 metres was adopted for all subsequent work.

4. DECELERATION OF THE ANEMOMETERS IN THE WIND TUNNEL

The anemometer was driven at an indicated speed of about 40 m/s and released to take up the speed of the wind tunnel. The speed indicated by the anemometer was measured by counting pulses over periods of 0.125 seconds. Anemometer time was synchronised to logger time by starting calculations at the mid point of the 2nd period during which the indicated speed was less than 40 m/s.

4.1 Deceleration in still air

Equation (1) shows that when **v** = 0 the value of **L** depends on **D/a** so that only one of these parameters can be selected independently. The simplest assumption is that '**D**' has the same value for deceleration as for acceleration and to adjust '**a**' to give the best possible fit to the observations.

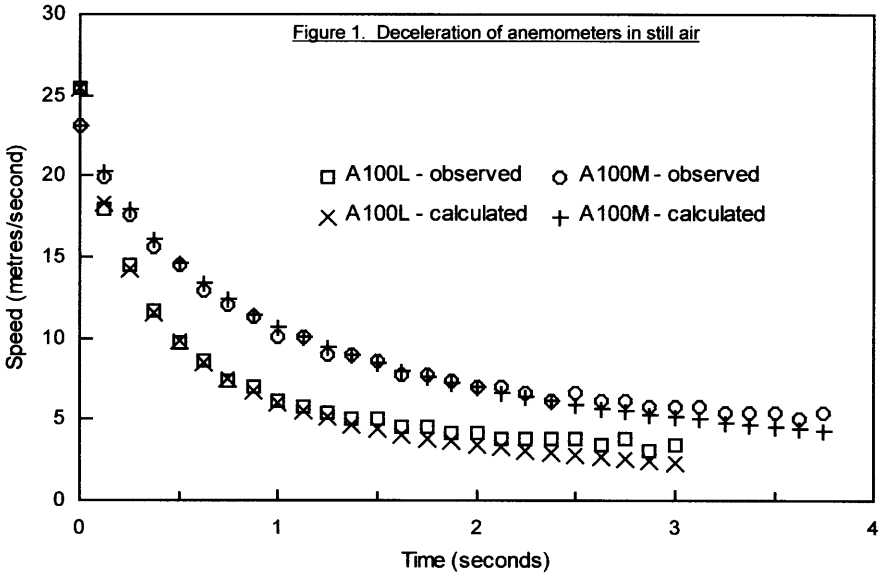

Figure 1 shows the results for one run of each anemometer. Agreement between observed and calculated values is good at high speeds but significant differences appear as the instruments slow. A possible cause of the error at low speeds is that the anemometer created a local swirl of air and was not actually decelerating in still air towards the end of its motion. A value of '**a**' was chosen to minimise the errors while the anemometer was decelerating rapidly.

Four runs of the A100L (with D = 2 m) produced 0.25, 0.24, 0.25 & 0.26 as values of **a.**
Four runs of the A100M (with D = 5 m) produced 0.25, 0.25, 0.26 & 0.26 as values of **a.**
The value **a** = 0.25 was used for both anemometers in all subsequent calculations.

4.2 Deceleration in moving air

'**D**' has been determined by acceleration tests and '**a**' has been determined by deceleration in still air. There are no other adjustable parameters in equation (1) but it is of interest to study how well the equation predicts deceleration in moving air. Figure 2 shows the agreement between calculation and observation for three runs of the A100L. Agreement is not exact but it is satisfactory. Similar results were obtained for the A100M.

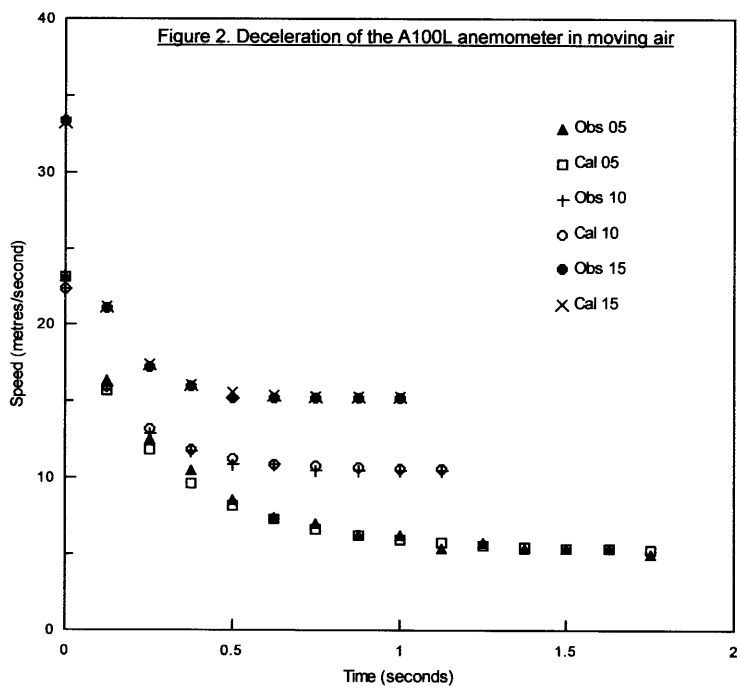

5. SUMMARY OF ANEMOMETER EQUATIONS

Results in the wind tunnel suggest that a good approximation to the dynamic response of the anemometers is provided by equation (1) with

$\mathbf{L} = \mathbf{D}/\mathbf{v}$ for acceleration and $\mathbf{L} = \mathbf{D}/(0.25\mathbf{u} + 0.75\mathbf{v})$ for deceleration
$\mathbf{D} = 2$ metres for the A100L and $\mathbf{D} = 5$ metres for the A100M.

Writing $\mathbf{du/dt} = \mathbf{S}$, equation (1) may be rearranged to give

$$\mathbf{v} = \{\mathbf{u} + (\mathbf{u}^2 + 4\mathbf{DS})^{1/2}\}/2 \quad \text{for acceleration} \qquad \cdots\cdot (2)$$
$$\mathbf{v} = \{2\mathbf{u} + [4\mathbf{u}^2 + 12(\mathbf{u}^2 + 4\mathbf{DS})]^{1/2}\}/6 \text{ for deceleration} \qquad \cdots\cdot (3)$$

Given a series of high-frequency observations from which '**S**' may be approximated, equations (2) and (3) can be used to estimate the true value of '**v**', independent of anemometer lag.

6. PERFORMANCE OF THE ANEMOMETERS IN THE FIELD

6.1 Exposure and data recording

The anemometers were exposed at The Met. Office site at Beaufort Park in Southern England. Beaufort Park contains many trees and buildings and is more turbulent than most anemometer sites. It is, therefore, a good place to investigate the effect of an anemometer's distance constant on its performance.

The anemometers were mounted 10 metres above the ground on a horizontal cross arm 45mm diameter. Vertical rods supporting the anemometers above the cross arm were 16mm diameter. The distance between the centres of the anemometers was 600mm and the centres of the cups of the anemometers were 445mm above the top of the cross arm.

The wind speeds indicated by the A100L and A100M were recorded by counting output pulses over periods of 0.25 seconds. For each run data were recorded for 10 minutes. On 17 days between 14 November 1997 and 4 January 1998 61 runs were recorded. Average speeds for the runs ranged from 2.97 m/s to 9.99 m/s and the maximum 3-second gusts varied between 4.99 m/s and 23.85 m/s.

6.2 High frequency response of the anemometers

The high frequency response of the anemometers was investigated in two ways:

a) by comparing of the highest ¼ second value from each anemometer in each data set,

b) by comparing of the lowest ¼ second value from each anemometer in each data set,

Equations 2 and 3 were applied to the series of values of **u** measured by the A100L anemometer to estimate a series of values of **v** corrected for the lag of the instrument. When calculating $\mathbf{v}_n$, **S** was approximated by $(\mathbf{u}_n+1 + \mathbf{u}_{n-1})/(2\delta)$ where δ is the time step between values in the series. This series of values calculated from the A100L measurements is denoted by **LC**.

Measurements made directly by the A100L are denoted by **L** and those made by the A100M are denoted by **M**.

Equation (1) with **D** = 5 metres and **a** = 0.25 was applied to the **LC** series to calculate expected values for an anemometer with the characteristics of the A100M. These values are denoted by **MLC**.

If both the **L** and **M** anemometers are subjected to the same turbulent air flow and equation (1) accurately describes their response, we should expect **M** values to be the same as **MLC** values since it should make no difference whether the smoothing effect of the anemometer is applied mechanically through the inertia of the instrument or numerically through equation (1).

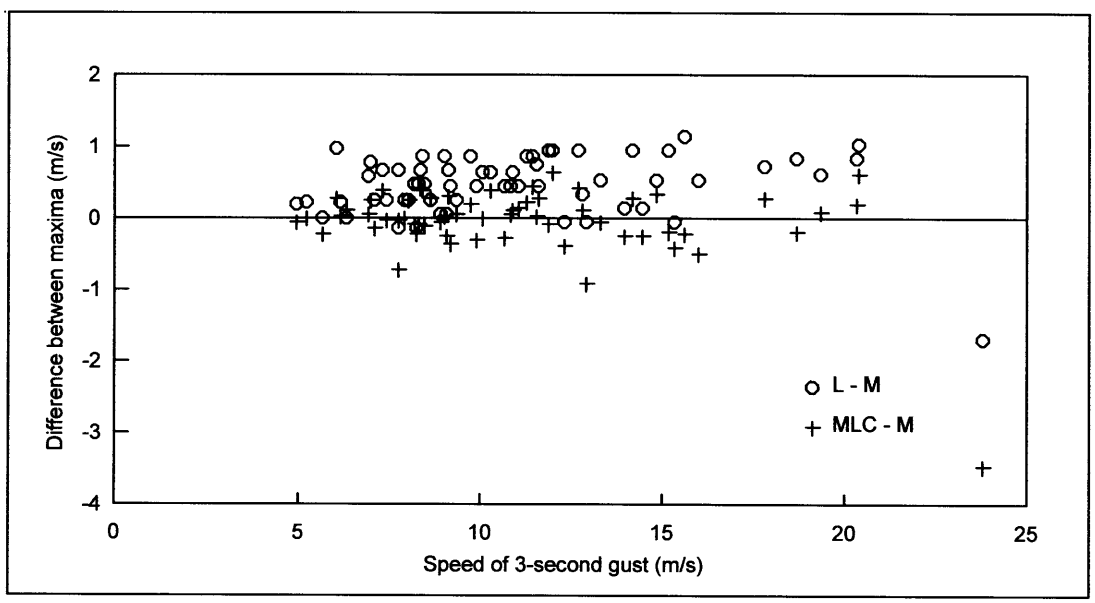

Figure 3. Differences between maxima v 3-second gust speed

Figure 3 shows differences between the maximum ¼ second gusts in each run. There is considerable scatter in the individual differences and the values at the highest gust speed are clearly anomalous. Nevertheless, the statistics are convincing. The average value of **L-M** is 0.403 m/s with standard deviation 0.432 m/s and the average of **MLC-M** is -0.045 m/s with standard deviation 0.531 m/s. As expected, the A100L with a distance constant of 2 metres indicated slightly higher gusts than the A100M which has a distance constant of 5 metres. The **MLC** values, calculated from the **L** values by applications of equations 2, 3 and 1 show very good agreement with the directly measured **M** values.

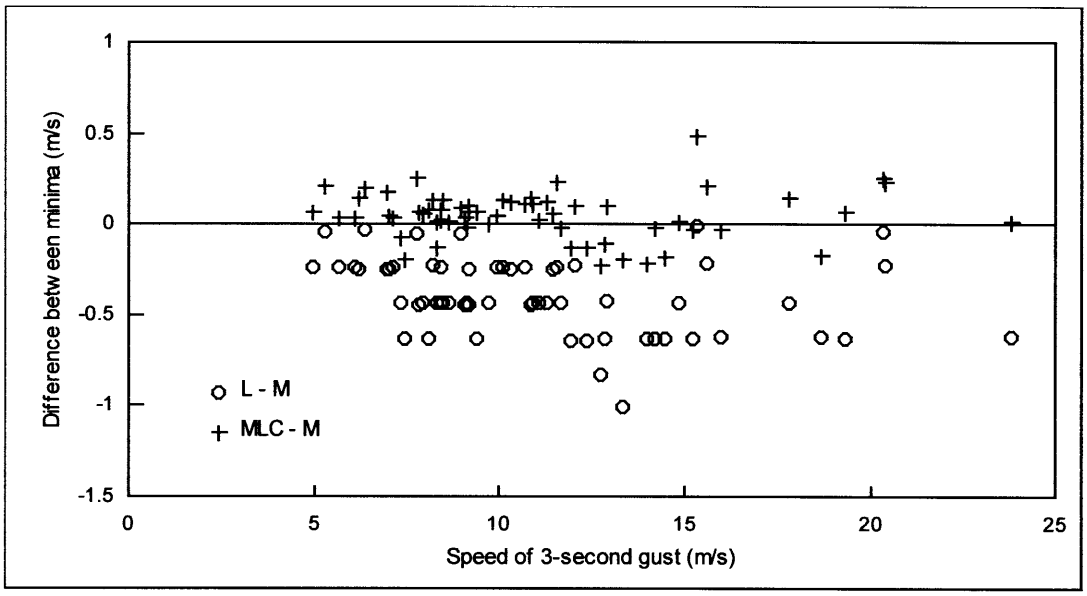

Figure 4. Differences between minima v 3-second gust speed

Figure 4 shows differences between the minimum ¼ second values measured by each anemometer in each data set plotted against gust speed. As expected, the anemometer with distance constant 5 metres does not decelerate as quickly as the one with distance constant 2 metres and **L-M** is generally negative. The average value of **L-M** is -0.397m/s with standard deviation 0.206 m/s. **MLC** is in good, but not perfect agreement with **M**. The average value of **MLC-M** is +0.052 m/s with standard deviation 0.132 m/s. A 't' test shows that the probability that **MLC-M** is 0 is only 0.004. Nevertheless, agreement between theory and observation is good enough for practical purposes and is within the uncertainty of the calibration of the anemometers.

7. DISCUSSION

By comparing two externally identical anemometers with different distance constants it has been shown that a simple differential equation accurately describes the dynamic response of a cup anemometer in a turbulent atmosphere.

The distance constant '**D**' of the anemometer is easily measured in a wind tunnel and once the distance constant is known the only other constant in the equation '**a**' can be determined by observing the deceleration of the instrument in still air.

Shortage of space prevents a full discussion of some important aspects of this work such as the numerical solution of the anemometer equation. These details and a fuller analysis of the performance of the instruments in the field can be found in Sparks (1998)[7].

References

1 Dynamic response of a cup anemometer. Journal of Atmospheric and Oceanic Technology, 4, 281-287, 1987, Taiichi Hayashi.

2 Ober die Trägheitsfehler des Schalenkreuz-Anemometers bei schwankender Windstarke. Z Tech Phys, 10, 57-66. 1929, Schrenk, O.

3 Cup anemometer response to fluctuating wind speeds. Journal of Applied Meteorology, 11, 843-848, Hyson, P.

4 Anemometer performance determined by ASTM methods. Journal of Atmospheric and Oceanic Technology, 4, 160-169, 1987, Lockhart, T.J.

5 Handbook of Meteorological Instruments (second edition), Part 4, Measurements of surface wind, HMSO. London, 1981, Meteorological Office.

6 Mean wind speed measurements in turbulence. Journal of Applied Meteorology, 5, 219-255, 1966, MacCready, P.B.

7 The performance of a cup anemometer in laboratory and field. Met O (OLA) Technical Report No. 15, The Met. Office, Bracknell, England, 1998, Sparks, W.R.

1 MEASUREMENT TECHNOLOGY, PERFORMANCE, AND QUALITY ASSURANCE

1.2 Upper-air Observation Systems

Keynote Paper

The Composite Upper Air Observing System, a challenge for the future work of CIMO

John Nash

The Met. Office, Beaufort Park, Easthampstead, Wokingham, Berks RG40 3DN,UK

Tel: -44-1344-855649;Fax:-44-1344-855897: e-mail:jnash@meto.gov.uk

1. Introduction

In this paper, I shall look at some of the challenges the Upper Air Working Group of CIMO faced in the last decade. Some of these remain to be resolved. Originally, this Working Group consisted of a relatively small number of national experts who in practice had worked together for many years. However, in the last three years it has developed into a much larger joint meeting between a new generation of upper air experts, (including those working on ground based remote sensing) and a significant number of commercial manufacturers. In this time, a variety of urgent problems have affected the upper air portion of the WMO Instruments and Methods of Observation programme (IMOP), Canterford (2000). These have been resolved partly in meetings of the Upper Air Working Group and partly by specialized meetings organized by WMO relying on contributions from core members of the Upper Air Working Group.

I will consider the issues relating to radiosonde operations and to the operational introduction of ground based remote sensing systems, including wind profiler radars. Potential problems resulting from the use of a more integrated approach to operational upper air networks including aircraft and satellite-based observations will also be discussed.

2. Composite Upper Air Observing System

In 1990, radiosonde measurements could still be considered the core of the Global Observing System. Satellite based systems were able to produce cloud pictures that were extremely useful to forecasters, but the sounding products from passive satellite radiometers were not providing the full benefits claimed for the global coverage of that observing system.

Ten years later, the techniques for using the satellite radiometer measurements have improved, and consistent positive benefits have been found in numerical forecasts for longer than 24 hours. Furthermore, in the last two years, measurements from a new generation of microwave radiometers (AMSU-A and -B) on NOAA satellites have improved numerical forecast capability, as soon as made available. Similarly, there has been progress in the provision of upper winds derived from tracking cloud and water vapor structure using geostationary satellites.

The advances in the satellite sector have been supported by large amounts of temperature and wind reports made available from commercial aircraft operations. The availability of the aircraft data has followed from improved real time communications to the aircraft in flight. Widespread acquisition of measurements is now being attempted in many regions under a variety of international agreements. Commercial aircraft can provide information of similar accuracy and vertical resolution to radiosondes for temperature and wind over the height range of aircraft operations, but the timing and availability of observations may be variable. Aircraft relative humidity observations are not yet widely available, apart from prototype experiments.

On the ground, wind profiler radars are providing a reliable operational service in several countries, and infrared or microwave radiometers are under development to provide measurements of temperature and water vapour at similar temporal resolution to the wind profilers. Wind profilers plus ground based remote sensing can provide wind and temperature measurements continuously at high temporal resolution, but are more expensive to operate than collecting the aircraft information and can only be fully exploited in numerical forecasting as operational data assimilation techniques improve.

Considerable scientific effort is focussed on the use of ground based reception of Global Positioning System (GPS) satellite signals to derive measurements of total water vapour amount. This could be cost effective in countries that deploy widespread GPS sensor networks for monitoring seismological events.

Finally, many ideas are circulating on methods of deploying dropsondes or targeting unmanned aircraft over the oceans to provide insitu measurements with better vertical resolution than satellite sounding systems.

Thus, the radiosonde system, whilst still a very important part of the upper air component of the GOS can no longer be considered the core of the system alone. In many eyes, it has already been superceded by some of the other systems mentioned above. Given the drive to reduce the cost of the operational upper air networks the choice of the mix of observing systems for the integrated observing network for GOS and GCOS is a major part of the current work of CBS.

- **In this context, the manufacturers of upper air systems require clear guidance as to the probable resultant mix of systems, in order to plan development and the necessary manufacturing capacity.**

This requires an integrated approach between the network planners and those with practical experience in the implementation of new systems, expertise that is mostly found in CIMO. If incorrect advice is generated it could lead to economic problems for the manufacturers, and escalate the costs of conventional upper air observing systems.

- **Advice should also be generated for members (+CBS) on the newest types of observing systems; e.g. GPS total water vapour or techniques for targeted insitu observations.**

3 Progress with radiosondes

Radiosonde observations were not replaced by satellite observations in the 1980s or 1990s, as initially predicted by some meteorologists. In practice, most radiosonde measurements also made significant progress in reliability, accuracy and vertical resolution. Fig.1 shows results from a radiosonde comparison measurement performed at Ascension Island in 1999. In Fig. 1(a), the temperature measurements of at least one system were obtained with a vertical resolution of better than 20 m, from the surface to balloon burst. Accuracy of the more reliable sensors is probably better than 0.5 °C. Differences between the different radiosondes were not as large as 1°C at any point during the ascent. Relative humidity measurements were of sufficient speed to resolve the main humidity changes with height in at temperatures down to -70°C or even lower in some cases. However, probable accuracy was between 5 and 10 per cent, at best, and there are significant differences even in low level cloud. The R.H. sensor providing the most rapid response at -80°C was the Meteolabor Snow White Chilled mirror hygrometer, with the Vaisala RS90 measurements also agreeing closely at pressures down to 130 hPa. In Fig.1 (b) wind measurements were obtained with a vertical resolution of 300m from the surface to balloon burst with accuracy probably better than 1 ms^{-1} using a Vaisala GPS windfinding system. Most of the variation in the vertical in the wind structure was not transient and could be seen in measurements made 3 hours earlier. Currently, the advice used in coding such wind measurements into a TEMP message is inadequate, allowing errors of 5 ms^{-1} in interpolating between reported significant levels. In many cases the coding of the message introduces much larger errors than the observing system limitations. This coding practice persists because the coding authorities did not accept the advice of the Upper Air WG. However, at least two more changes have been subsequently introduced to the TEMP code by CBS without consultation to the Upper Air WG on the costs that this would incur on existing upper air systems. Selection of significant levels for TEMP messages is not easily standardized, and should not be necessary if BUFR code is implemented.

- **The methods of dealing with upper air code changes require significant improvement in future. A move away from TEMP to an agreed BUFR code needs to be managed as soon as possible.**

Unfortunately, wind measurements of the quality shown in Fig.1 are not always obtained with the GPS radiosondes currently in use.

- **Improvement of the reliability of the GPS wind measuring system is clearly another major challenge for the immediate future**

All the systems used at Ascension were installed in a matter of hours after shipment from the UK for the experiment. This reflects a significant advance in radiosonde systems supplied by the better international manufacturers since the start of the WMO Radiosonde Comparisons in 1984. Temperature and wind can be measured as accurately as most users require. Ground stations have been reduced in size so that they are readily transported installed, and are easy to operate. The progress has been the result of collaboration between the manufacturers, certain national research institutes and members of the CIMO Working Group +CIMO Members exploiting advances in modern technology.

4. Meeting user requirements

Mesoscale and local forecasting requires temperature and humidity measurements with high vertical resolution in the lower troposphere, preferably about 100m or less. Radiosondes provide the necessary measurements of both variables on a widespread basis. The accuracy of the radiosonde temperature measurement in the lower troposphere is well suited for the users. Unfortunately variation in systematic bias from batch to batch in relative humidity measurements undermines the potential usefulness of the better radiosonde relative humidity measurements, even in the lower troposphere. If a radiosonde measurement with a low bias of 3 or 4 per cent in cloud is assimilated in a numerical analysis with any strong weighting, the measurement tends to destroy the representation of the cloud.

- **The reduction of instability /contamination during manufacture, storage and flight and the elimination of significant systematic bias from the radiosonde relative humidity measurements constitutes one of the major challenges for both manufacturers and operators during the next decade**

The magnitude of error causing the problem is within existing WMO user requirements for the accuracy of upper air relative humidity measurements, quoted as rms error of 5 per cent R.H.. This generalized user requirements really needs more detail than is currently considered necessary. The stated requirements are not in line with the policy of adjusting radiosonde relative humidity measurements (always increasing the values) used in numerical forecasting.

- **Instrumentation experts dealing directly with customers and manufacturers should be included in discussions of user requirements and not sidelined from these processes.**

5. Integrating radiosonde with aircraft and wind profiler measurements

Recent observing system experiments have indicated that radiosonde observations may not be contributing as much as expected to the accuracy of current numerical forecasts. The radiosonde measurement samples mesoscale atmospheric structure in detail. The local forecaster uses this detail, but it is often not fully assimilated in the numerical model because differences from the background forecast fields are not supported by many other observations.

If radiosonde observations were less expensive and were deployed regularly at spacing in the horizontal that would define the mesoscale fields directly, a more accurate assimilation of the mesoscale structures would result. This happens to a limited extent in many research campaigns, especially those based on dropsonde observations. The typical scale of persistent mesoscale structures near the British Isles is illustrated in Fig.2. This shows an estimate of the horizontal wind structure observed at 70 km spacing in a severe storm that passed over the British Isles on 24 December 1999. At 18 UTC the surface low pressure associated with the storm was deepening very rapidly and was centered at about 55°N 6°W. At 12 UTC the early stages of the storm had been over the sea to the southwest of the UK and had not been observed by the radiosonde network. The storm caused significant structural damage and flooding in southern England. Two plan views are shown through the storm with wind speed contoured using isotachs. The first section in Fig.2 (a) is at a height of 1 km and the second in Fig.2 (b) at 3 km. The dashed contour line indicates the extent of rain near the surface derived from weather radar measurements, with four areas of strong precipitation indicated by the shaded areas inside thick contours. The arrows indicate the wind direction. At 1 km there were three main areas of strong winds. The strongest winds were at about 51°N 4°W at 18UTC, with winds higher than 40 ms^{-1} in advance of the surface cold front. This area was associated with gusts of 25 to 30 ms^{-1} at the surface. The second area was over the eastern side of England 51°N 1°E with maximum winds of about 35 ms^{-1} and surface gusts between 15 and 25 ms^{-1}. A third more limited area with winds as high as 35 ms^{-1} was at 53°N 6°W in colder air near the center of the depression, where surface gusts as high as 35 ms^{-1} were observed in the most unstable air. The winds in this third area strengthened rapidly with time to about 45 ms^{-1} at 1 km when passing over a radiosonde station in northern England 6 hours later. At 3 km the strongest winds were over 50 ms^{-1} and were observed at 50°N 6°W. The detailed mesoscale picture of the storm was made possible by the wind profiler network in western England (four sites spaced apart by about 150 km). Observations from Doppler weather radar at Dublin, Ireland, aircraft observations in southeast England and a limited number of radiosonde measurements at 18 UTC from UK stations complemented the profiler measurements. Most of these measurements were not used in real time by the numerical forecast, since the observing systems were still under evaluation before acceptance as operational systems. Estimating winds at this horizontal spacing over the UK only became possible in 1999.

The UK mesoscale model 6 hour forecast showed major differences (greater than 10 ms^{-1}) from the observed structure shown here, consistently underestimating the winds in advance of the cold front. Thus, the radiosonde network on its own could not provide sufficient upper air information to correct the forecast, and the model-forecast field was unable to interpolate adequately between the available observations.

- **However, addition of the aircraft and wind profiler measurements will facilitate exploitation of the detail in the radiosonde measurements. A support infrastructure is needed to ensure the long-term compatibility of the three types of measurements. The quality of aircraft and wind profiler measurements may degrade slowly with time. If these changes are to be detectable and rectified, there must be a core of upper air measurements that are reliable. A reliable radiosonde network would best provide this core.**

The possible contribution of high temporal resolution measurements from a wind profiler is illustrated in Fig.3. Measurements from the 915 MHz wind profiler sited at 50°N 5°W are shown from 13.00 until about 19.00 UTC on 24 December 1999. Observations were derived at 5-minute intervals with minimal quality control. The upper time- height section shows signal to noise for the observing mode operating at 200m vertical resolution. In dry air conditions, the profiler does not normally see strong signals above 3 km, so the strong signals up to about

9-km indicate the presence of ice crystals in upper cloud. The second time height section shows wind speed, approximately equivalent to a section from about 54°N 3°E to 49.5°N 7°W in Fig.2. The heavy rain at 50.5°N 3.2°W in Fig.2, passed over the wind profiler at about 17.10 UTC. At this time the winds at 4 km in Fig.3 dropped from 42 to 32 ms^{-1} . The winds at 4 km increased again to near 55 ms^{-1} just after 18.00 UTC, when the signal power dropped rapidly. The very strong winds at this level were associated with dry air intruding into the frontal region. Thus, temporal resolution of much greater than an hour is important both for operational modeling of the system and for research. The third time height section is equivalent to the second, but observed at 60 m vertical resolution to improve the vertical resolution of the observations close to the surface. The strongest mean surface winds were observed between 16.00 and 16.30 UTC, where the 35 ms^{-1} contour in Fig.3 was consistently closest to the surface. The fourth time height section shows the vertical velocity observed at high resolution. The vertical velocity measured here is usually that of the precipitation. The transition from pale to dark shading at around 2 km near 14.00 UTC indicates the level where ice crystals are melting to rain. Later, near the passage of the cold front at about 17.00 UTC the melting is taking place at a lower level.

The wind profiler radar not only provides wind measurements, but its signal power, spectral width and vertical velocity also provide information about precipitation [and significant changes in relative humidity in the vertical when dry]. The use of such a system should not only be considered in terms of wind measurements, but also the other information it can provide. For instance, wind profilers of this type ought to provide useful information on rainfall or the depth of the convective boundary layer in many tropical countries. In similar fashion, winds from Doppler weather radars need to be integrated with the other systems considered here.

- **The challenge to CIMO is to provide guidance on the practical aspects of operating wind profilers. Wind profilers have operational limitations and these must be spelled out to Members. Guidance should be given to the manufacturers and research centers in hardening designs to be effective in countries where maintenance effort may be limited. Similarly, guidance is required in optimizing data processing algorithms. Effective communication of the high temporal resolution data at the necessary speed to users is also an important issue.**

A consequence of the diversification in upper air instrumentation in a composite network may be that a single Member instead of running 10 manned radiosonde stations may opt for 2 manned radiosondes, 4 automated launchers and 4 profilers, plus aircraft measurements. Is it efficient to support such a network with specialized staff as an individual Member? Should support be contracted out to the manufacturer, or should it be centralized on a regional basis with several Members funding support to the different types of systems?

- **CIMO should consult with the manufacturers and the network managers in recommending cost-effective methods of supporting future upper air networks.**

There is potential to make significant progress in upper air networks in the next decade. This will probably be easier for winds than for temperature and relative humidity measurements. Changes in the operational networks must be introduced at a rate that sustains progress and does not undermine the stability of the GOS and GCOS. The resultant mix of observing systems will differ between regions, reflecting variations in manpower costs and the practicality of deployment of certain types of equipment.

6. Resolution of outstanding problems

6.1 Radiofrequency issues

During the World Radio Conference in 1992, part of the 400.15 to 406 MHz band was allocated to the Mobile Satellite Service in a manner preventing continued long term use by radiosonde operators. Subsequently, meteorological services have had to take actions to retain the necessary radiofrequency to maintain operations, both at frequencies near 403 MHz and also at frequencies near 1680 MHz. ITU-R, responsible for the allocations, had no documentation about the Meteorological Aids Service, (with radiosondes the most common type of system). This documentation has now been generated through the activities of a limited number of national experts and help from a manufacturer. CBS organized most of the special meetings to develop WMO policy for future radiofrequency use, but the chairman of the CIMO Working Group also chaired these meetings and is a member of the CBS Steering Group on Radiofrequency Co-ordination. Whilst the necessary progress was made, the workload was concentrated too heavily on the chairman of the working group. Attempts to standardize the performance of radiosondes are under way in some regions, and CIMO must be represented in these negotiations

- **It is essential for the future that an upper air (CIMO) support group must contain a nominated radiofrequency expert to be responsible for these issues.**

Radiofrequency issues remain a challenge. Historically, there was very limited radiofrequency use near the radiosonde bands allowing many countries to develop their own national spectrum

use. In some cases, radiosonde transmitters are used that are not capable of staying within the specified MetAids service spectrum. This cannot continue because global allocations proposed for satellite systems will prevent national arrangements in future.

- **Thus, it is essential that all national radiosonde services use radiosonde transmitters that are capable of staying well within the internationally allocated bands, using receivers that can cope with interfering signals towards the edge of the allocated bands. All relevant members have access to the necessary technology, and this must be introduced within a decade.**

6.2 Replacement of Omega Radiosondes

The closure of the Omega radionavigation service led to major investments in new radiosonde equipment. The generation of advice to Members relied heavily on core members of the Upper Air Working Group, but in many cases the advice appeared as products from CBS, because CBS assumes responsibility for network operations. The Upper Air WG correctly steered certain manufacturers away from relying on VLF signals as a global solution to the problem. The correct assessment of the status of GPS versus modern radiotheodolite was reported. However, for a variety of reasons most Members decided on implementation of GPS radiosondes with the associated higher cost of consumables, rather than radiotheodolites using cheaper radiosondes. Radiotheodolites were implemented in the Caribbean, with a manufacturer contracted to maintain the systems rather than the national services.

The GPS radiosonde systems were not very reliable in the first few years of operation. After five years, many of the problems have now been resolved. However, this has involved the issue of new processing software to many sites. Many Members do not have an infrastructure for managing such updates. It can be expected that many Members will be asked to change the radio receiver in their ground system before too long, as the manufacturer changes over to digital radiosonde transmissions. Similarly, members are being requested to upgrade to a new radiosonde with improved sensors. Whilst modern systems are generally reliable, it is not possible to run an upper air system for 20 years without any effort to provide serious technical support for the system. Thus, it is important that Members organize methods of training and support for those staff who are to keep track of the technical status, and implement necessary upgrades.

- **CIMO needs to address the issue of training in maintaining an upper air network, i.e. at the supervisor/ technical support level, rather than purely the operator.**

CIMO/CBS have to work together in monitoring progress, but the current structure of CBS struggles to supply the necessary expertise to CIMO.

- **In restructuring the work of WMO, consideration should be given to retaining a forum where the upper air system operators, technical experts and manufacturers meet to decide on operationally important issues. This ought to include members of the research community who are also interested in furthering the capability of the upper air observing system.**

The radiosonde system is vulnerable because there are currently no other international support groups apart from the CIMO group.

The problems encountered with GPS radiosondes have illustrated the importance of storing raw data for diagnostic purposes during a flight, when new systems are not functioning well. It is probable that radiosonde stations in future will be treated more like other remote sensing sites. As well as the observation, the radiosonde system should also transmit engineering status and housekeeping software output back to a central monitoring point (whether a regional center or the manufacturer).

- **CIMO needs to develop the use of housekeeping information, raw archives and system diagnostics from remote radiosonde sites, and the associated interfaces to the regional network center or manufacturer.**

6.3 Year 2000 problem

Co-Operation between manufacturers and the major users worked reasonably well in identifying and rectifying the problems, but again relied too heavily on a limited number of personnel to take the critical actions.

6.4 Poor Performance of national systems

One outstanding problem that has yet to be resolved is the poor measurement performance of several national radiosonde systems. Although large efforts have been made, the measurement quality offered to the user seems to have stuck for nearly 20 years.

- **CIMO has to address the problem of improving the general standard of radiosonde observations worldwide, perhaps through greater use of bilateral collaboration.**

Reference:

Canterford, R. (2000) - Major challenges facing WMO Member countries in operating and maintaining meteorological and environmental instrument networks and the role of CIMO. Proceedings of TECO-2000.

FIGURE 1(a)

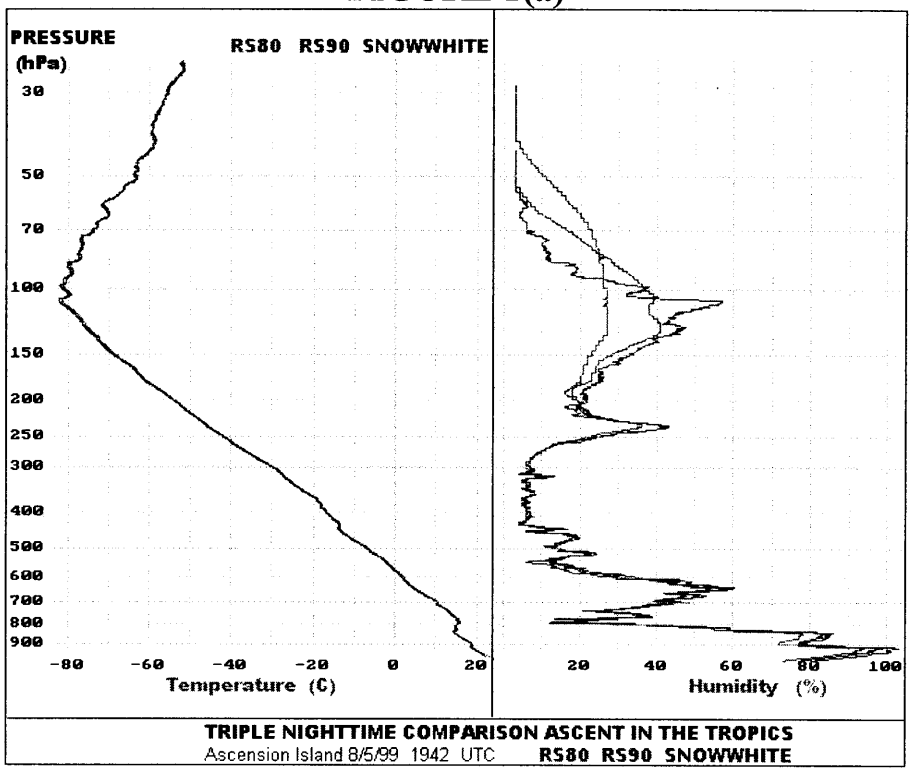

FIGURE 1(b)

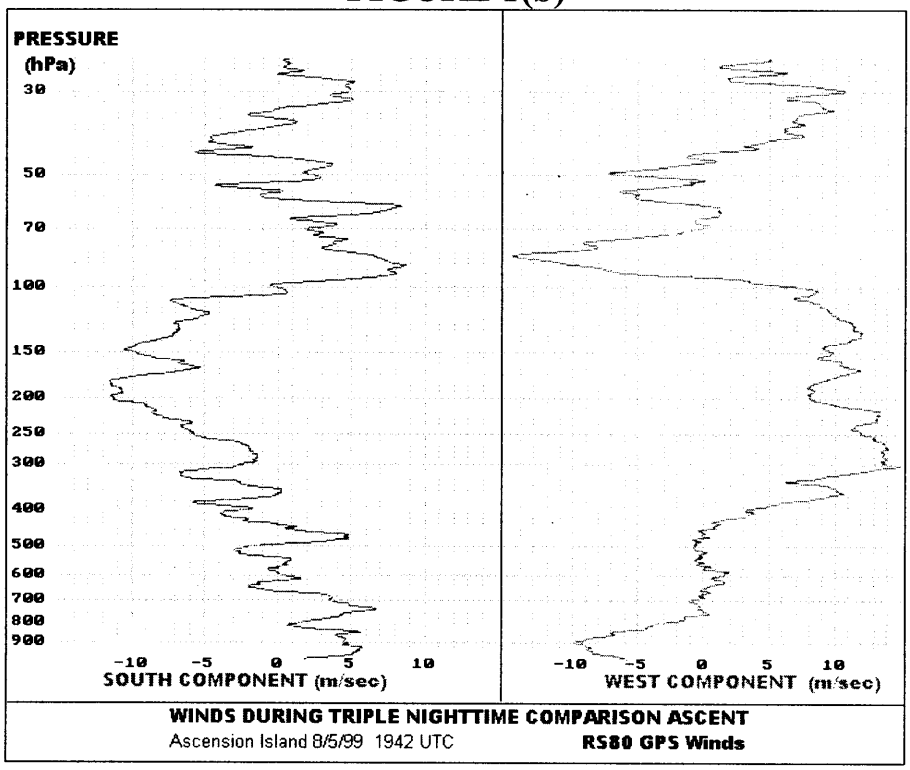

Fig.2(a) Wind speed [ms-1] for 1000 m at 18 UTC on 24.12.99

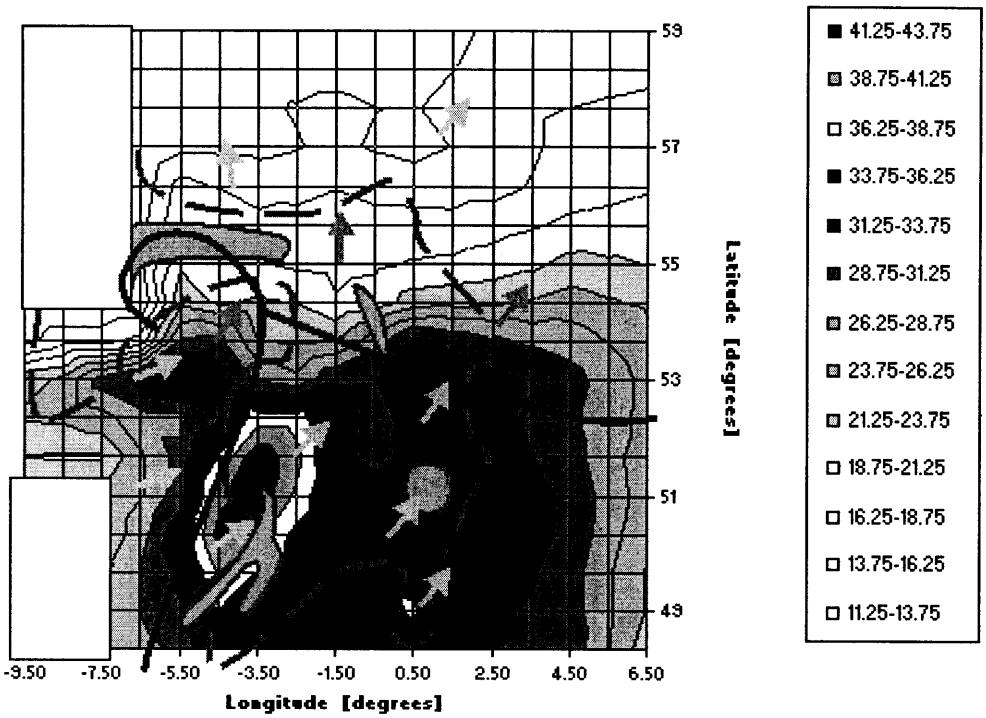

Fig. 2(b) Wind speed [ms-1] for 3000 m at 18 UTC on 24.12.99

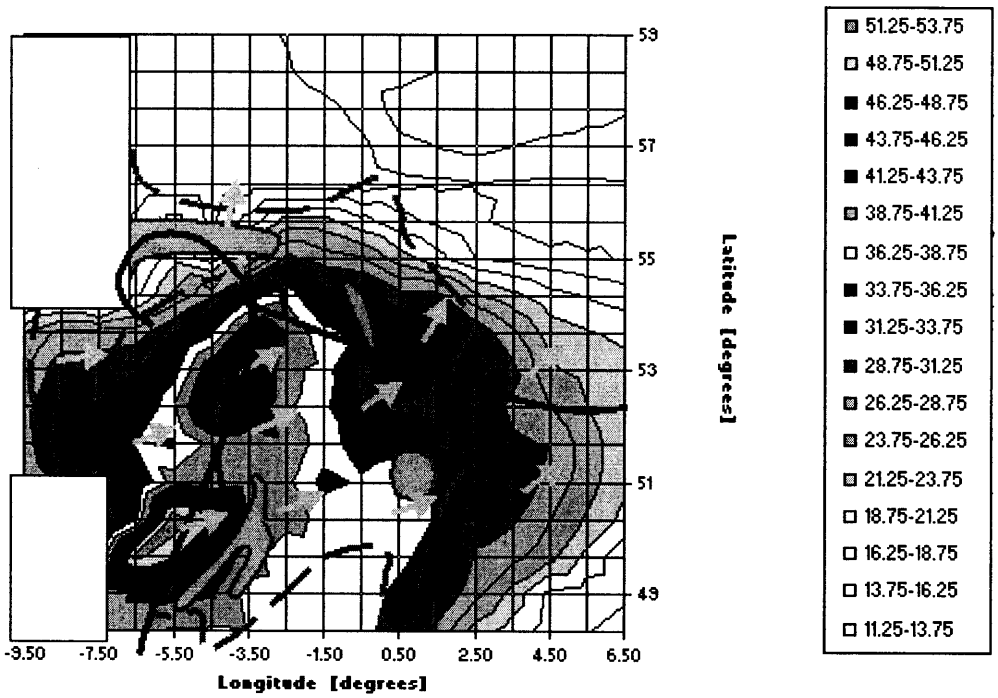

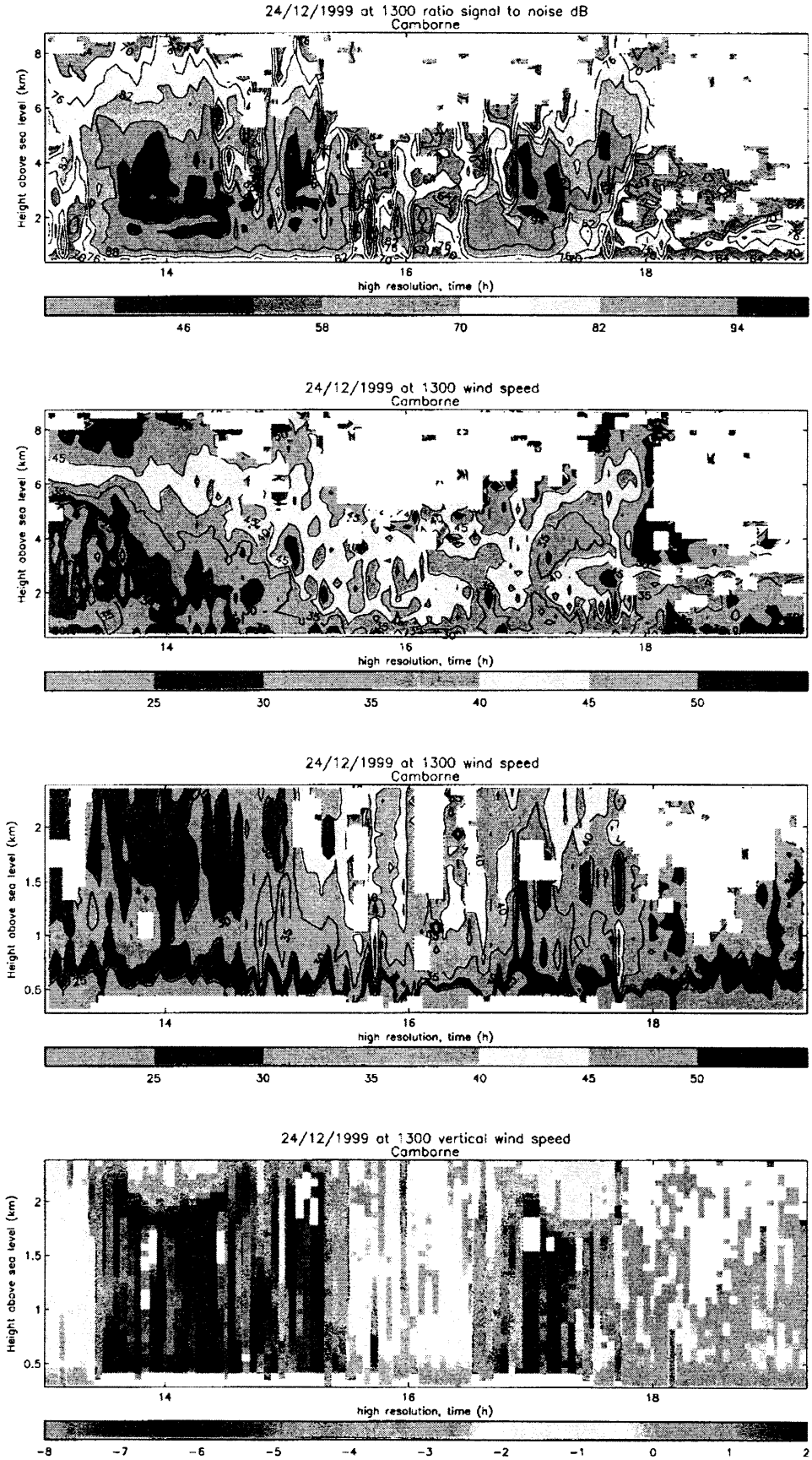

Figure 3. Detailed measurements from a wind profiler in a severe storm, 24/12/99 Camborne, Cornwall (50N 5W)

1 MEASUREMENT TECHNOLOGY, PERFORMANCE, AND QUALITY ASSURANCE

1.2 Upper-air Observation Systems

1.2.1 In-situ Upper-air Observation Systems

The Preliminary Experiment of Deriving

Integrated atmospheric Water Vapor from Ground-based GPS

He,ping, Xu,baoxiang, Zhou, xiuji
Chinese Academy of Meteorological Sciences
(46 Baishiqiao Road Beijing P.R. China, 100081)
Li, yanxing
National bureau of Earthquake
(7 NaiHuo Road Tianjing P.R. China, 300180)

ABSTRACT

The field experiment named "Huamex" was conducted in China from May to June 1998. In this experiment, a regional GPS-network that included three ground-based GPS receiving stations (Shantou, Yangjiang and Haikou) was established to estimate integrated atmospheric water vapor (IWV). In this paper, the comparison of IWV derived from GPS and radiosondes for a 51-day period at ShanTou station is given. Both had an average bias of 6.5mm, the root-mean-square difference was 4.3 mm. The GPS/IWV (IWV derived from GPS) varied periodically with time and it had an obvious period of 7.2 days on the average. Moreover, GPS/IWV were compared with per hour cumulated precipitation. Obviously there was a good coincidence between them. The variation period was similar to that of surface precipitation. Form the time-series of GPS/IWV, we note the accumulating and releasing process of water vapor was obvious. The surface precipitation happened while atmospheric IWV reduced.

Keywords GPS, dry delay, wet delay

1. Introduction

Water vapor plays a critical role in atmospheric physical process. It helps us to study the vertical stability of atmosphere, the constructions and evolution of storm systems and energy balance of earth-atmosphere system. Using GPS to estimate atmospheric IWV is a promising method and it was developed in 90s. In 1992, Bevis et al. put forward the principle of estimating atmospheric water vapor with ground-based GPS. In 1993, the GPS/STORM experiment was hold in the U.S. This experiment was analyzed by Rocken et al. (1995) with a relative method. (Using GPS to estimate the relative value of IWV among the GPS stations and using Water Vapor Radiometers to measure the absolute of IWV at a reference station, thereby determining the correction to transform relative IWV into absolute IWV at every station). Later in the data reanalyzing for GPS/STORM, Duan and Bevis put forward a new approach to estimate absolute value of atmospheric IWV without calibrating by Water Vapor Radiometers. In China, researches in this field have being done a lot in recent years [1]-[5]. Especially, we established Ground-based GPS receiving stations during Huamex experiment period (from May to June 1998), expecting to obtain some information about atmospheric IWV. The experiment was successful; the preliminary analysis shows that it is a promising remote sensing technique for deriving atmospheric IWV.

2. Field experiment and GPS data processing

Two temporary GPS stations were established at Shantou and Yangjiang during Huamex in 1998. The GPS receiver at Shantou was set at the meteorological platform, and at Yangjiang was located about 2 meters away from the meteorological platform. Two GPS receivers observed continuously from May 5th. to June 26th. Simultaneously, the GPS receiving station of Haikou observed continuously during the experiment too. Table1

shows the geographical data of each station.

Raw GPS data obtained at the stations of Shantou, Yangjiang and Haikou were processed with the GAMIT software. Data collected from some long distance stations like Shanghai, Tianjin(China), TSKB(Japan), IRKT(Russian) and Kitab(Uzbekstan) were also used in order to introduce some very long baselines. The computing yielded total zenith delays with a temporal resolution of 30 minutes.

3. Method estimate atmospheric IWV

The GAMIT software was used to estimate the zenith delay caused by the neutral atmosphere. The zenith neutral delay has two components; they are dry delay and wet delay. The surface pressure measurements are used to compute the dry delay. The dry delay is subtracted from the zenith neutral delay to obtain the wet delay, which is then transformed into IWV.

This paper adopts following formula (advised by Elgered at el.) to calculate dry delay:

$$Z_h = [(2.2779 \pm 0.0024)mm \times hpa^{-1}]\frac{P_0}{f(\lambda, H)}$$

where P_0 is surface barometric pressure at the station, λ is geographical longitude, H is sea level elevation of the station, and $f(\lambda, H) = [1 - 0.00266\cos(2\lambda) - 0.00028H]$

Atmospheric integrated water vapor (IWV) is the total quantity of water vapor overlying an unit area on the earth's surface expressed as the height of an equivalent column of liquid water. It somewhat relates to zenith wet delay. Businger et al.[7] provided the following empirical formula:

$$PW = \prod \times ZWD$$

$$\prod = \frac{10^6}{\rho_w R_v [k_3 / T_m + k_2]}$$

where ρ_w is water vapor density, R_v is gas constant of water vapor, and T_m is weighted mean temperature (Davis et al. 1985),

$$T_m = \frac{\int (P_v / T) dz}{\int (P_v / T^2) dz}$$

$$k'_2 = k_2 - mk_1$$

$m = M_w / M_d$ is mole ratio of water vapor to dry air, k_2, k_2, k_3 are coefficients in the empirical formula of atmospheric refractive index N (Smith and Weintaub 1953),

$$N = k_1 \frac{P_d}{T} + k_2 \frac{P_v}{T} + k_3 \frac{P_v}{T^2}$$

where P_d is barometric pressure of dry air, and P_v is water vapor pressure. $\prod$ is a coefficient relative to meteorological parameter, it can be given an approximate constant value of 0.156. For simplicity, this paper adopts $\prod$ as $\prod$=0.156 in computing.

4. Preliminary Conclusion and Discussions

We analyzed the data from GPS, radiosonde and precipitation of the three stations. The GPS/IWV were yielded at 30-min intervals. The comparison of GPS, radiosonde estimates of atmospheric IWV at SHANTOU station for 51-day period of the experiment, is shown in Fig.1. Also the precipitation data is drawn on the Figure. The abscissa is observation time (hour), the ordinate is IWV (mm), and the second ordinate is precipitation (mm/h). In the figure, continuous curve is GPS estimates of IWV, small dots are radiosonde estimates of IWV, and vertical volumes are precipitation.

Due to the advantage of continuous observation, the method of estimating IWV from GPS can quite well illustrate the variation of atmospheric IWV in high temporal resolution. It is continent for us to determine the accumulating and releasing processing of water vapor. It is sometime accumulated sometime released in accordance with the weather process. But it can not be expressed in radiosonde data of twice a day.

Although, there were differences between GPS estimates and radiosonde estimates at same observation time, both had an average bias of 6.5mm and the root-mean-square difference was 4.3 mm, the tendencies of IWV estimated from GPS and radiosonde were same.

In the fig.1, it can be seen from the time series of IWV estimated from GPS that the evolution of IWV is periodic. Amplitude varies violent and the period of wave with average amplitude of 33mm is 7.2 days.

It can also be seen that the general developing tendency of IWV with time is increasing, and there may be something to do with seasonal variation of atmospheric humidity, which is lower in May and higher in June. Table 2 shows the statistics of IWV in May and June, the mean value of IWV increases 6.9mm from May to June.

Furthermore, the data of precipitation are drawn on the same figure (Figure 1) in order to observe how the atmospheric IWV varies with ground surface precipitation. GPS/IWV varies periodically by the rule of increasing rapidly, relative stability and then decreasing violently. Its variation period is similar to that of surface precipitation. The phenomenon is very often and clear that heavy rain companies the decreasing of IWV in time. especially before strong precipitation happens the atmospheric IWV reduces sharp. Maybe there is a close coincidence between them.

In this paper, GPS data from Huamex are processed routinely, compared and analyzed preliminarily. And later further analysis and research will be done. Preliminary analyzed results indicate that there are many prominent advantages to use GPS technique in observing atmospheric IWV and it is a promising technique.

Tanle1: geographical data of each station

Station Name	longitude	latitude	elevation(m)
SHANTOU	$116^0 41'$	$23^0 24'$	7.3
YANGJIANG	$111^0 58'$	$21^0 52'$	23.8
HAIKOU	$110^0 21'$	$21^0 02'$	13.9

Table2: the statistics of IWV from May to June 98,SHANTOU station

Month	Average(mm)	Max(mm)	Min(mm)
May	46.9	62.3	31.7
June	53.9	68.4	40.0
differences between June and May	6.9	6.1	8.3

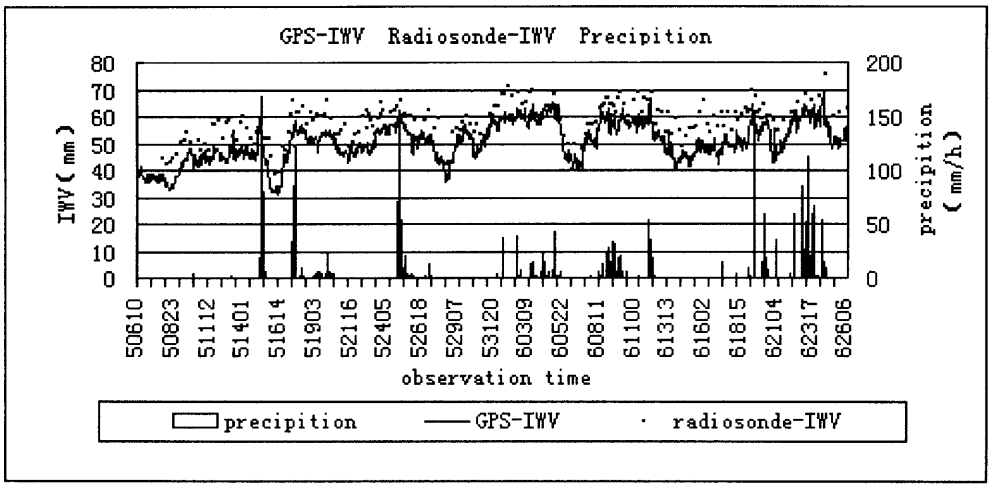

Fig.1: The comparison of IWV estimates derived from GPS and radiosonde for 51-day period at SHANTOU station, and the data of precipitation

Acknowledgements

This research was supported by 95-ZHUAN-03 and G1998040909.And we would like to thank Professor Ge, runsheng, Zhang, peiyuan (Chinese Academy of Meteorological Sciences) and Hu, xinkang (National bureau of Earthquake), for their kindly support.

5. References

[1]Mao, jietai, The application of GPS in the field of meteorology, 1993,4:45-49

[2]Li, chengcai, Mao, jietai et al., Sensing water vapor by GPS, Chinese Science Bulletin, 1999.2, Vol.44, No.3.

[3]Peng, hong, Ge, runsheng, Zhou, xiuji 1997, The application of GPS in the field of atmospheric sounding, collected works of atmospheric remote sensing, Meteorology Publisher

[4]Mao, jietai, Li, jianguo, 1997, Sensing the distribution of water vapor in eastern area of China by using GPS, Center of Meteorological satellite, collected works of the study of meteorology, 12-20.

[5]Yang, hongmei, Ge, runsheng, Xu, baoxiang, analysis neutral atmospheric water vapor from single sounding station, meteorology, 1998.9, Vol.24 No.9 P8-11

[6]Elgered G, Divis J L, Herring TA, et al. Geodesy by radio interferometry: water vapor radiometry for estimation of the Wet Delay. J G R, 1991, 96: 6 541-6 555

[7]Bevis M, Busiger S, Chiswell T, et al. GPS meteorology: mapping zenith wet delays onto precipitable water. J Appl Meteor, 1994: 33,379~386

[8]Businger, s, et al., The Promise of GPS in Atmospheric Monitoring, Bulletin of the American Meteorological Society, 77(1), 5-18(1996)

[9]Rocken, C, et al, GPS/STORM- PS Sensing of Atmospheric Water vapor for Meteorology, Journal of Atmospheric and Oceanic Technology 12(3),468-478(1995)

[10]Wave, R, et al, GPS Sounding of the Atmosphere from Low Earth Orbit: Preliminary Results, Bulletin of the American Meteorological Society,77(1),19-40(1996)

[11]Duan J, Bevis M. GPS meteorology: direct estimation of the absolute value of precipitable water. J Appl Meteor, 1996, 35: 830-838

OVERVIEW OF NWS RADIOSONDE SYSTEM REPLACEMENT

Richard D. Thomas, Jr. and Carl A. Bower, Jr.
National Weather Service
National Oceanic and Atmospheric Administration
1325 East-West Highway
Silver Spring, Maryland 20910
United States of America
Facsimile: (301) 713-0959
Email: richard.thomas@NOAA.gov

1.0 INTRODUCTION

The radiosonde is one of the most critical observational tools for obtaining atmospheric measurements required for numerical prediction, research models, climatology, and regional forecasts. It is an instrument, carried aloft by a balloon, which measures the ambient pressure, temperature, and moisture during its flight. A radio signal containing the information is sent down to a ground station where it is processed into various reports or observations. The radiosonde's position or movement can be tracked by various methods to determine a sounding of wind speed and direction.

Rawinsonde observations (a radiosonde tracked to also determine winds) form the backbone of weather forecasts and upper air analyses as part of the World Meteorological Organization's World Weather Watch. They are critical input to numerical weather prediction models, severe weather prediction, air pollution transport prediction, aviation operations, and the study and prediction of global climate change. They also serve as the benchmark from which estimates of satellite and ground-based thermodynamic profiler temperature and moisture retrievals are derived.

Given the critical importance of this observing program in supporting the National Weather Service (NWS) mission and the various adversities facing the program, the NWS has begun an effort to totally replace its current network of 40+ year old systems with a modern system that will operate within a much reduced frequency spectrum, avoid increasing maintenance difficulties, and be more effectively integrated with other systems at modernized NWS offices.

2.0 CURRENT NWS OPERATIONAL NETWORK

Of the more than 800 upper air stations around the world, the United States supports a network of over 100 upper air observing stations that reaches from the Caribbean to Pacific islands, and from Alaska to south of the equator. These include those located at NWS-staffed stations, contractor-staffed stations, stations staffed by other agencies, and stations staffed by other countries. Approximately 75,000 radiosondes are flown annually at NWS supported sites. Observations from NWS stations are taken twice daily.

The current radiosonde system in use at most NWS location operates in the 1670-1690 MHz frequency range. It consists of a large ground-based radio-direction finding antenna and radio receiver which tracks the location of the radiosonde and receives signals transmitted. Data are then passed to an IBM PC/XT for processing into meteorological messages that are disseminated across the world.

3.0 ASSESSMENT OF NEED

There are a number of issues which threaten the continued operation of this critical component of the NWS infrastructure. The main two issue areas relate to maintenance of the current system and its requirement for a large radio-frequency band in which to operate.

The mechanical portions of the system are 1950's vintage and are becoming more difficult to maintain. Over 90% of the system parts are commercially obsolete. Numerous integrated circuit chips used throughout the system are particularly difficult to replace. Due to the age of the equipment, failures are increasing such that the number of parts repaired has more than doubled in the past 6 years. The NWS has now completed an effort to procure stockpiles of these old components from the original manufacturers or integrators. Given current failure rates, the system should be repairable through 2004. After that, catastrophic outages are anticipated. The supply of parts necessary to maintain the outdated IBM PC/XT computer is only sufficient to last 1 to 2 years. The software used in this computer must be rewritten before it can be used on a newer computer. Maintenance work is further complicated by a lack of modern diagnostics support (software or test equipment), and requires extensive training and experience to diagnose problems manually.

At some stations, additional ground equipment (transponders) provide special tracking of the radiosondes when they are carried over the horizon in high wind situations. This transponder equipment uses vacuum tubes which are no longer supportable. In 1990, 33 stations had transponder units. Currently, there are only two stations remaining which have the equipment still functioning, resulting in the loss of high altitude wind data which may be degrading numerical weather prediction models.

The current generation of radiosondes are very inefficient in their use of radio-frequencies, due mainly to the lack of frequency stability in the transmitters and the lack of tuning accuracy. As a result of the Omnibus Budget Reconciliation Act of 1993, the U.S. Government reallocated 5 MHz (1670-1675 MHz) to the private sector on January 1, 1999. The current ground systems will be very susceptible to interference from new transmitters operating in this frequency band, which could result in lost data during portions of the radiosonde flights, or inability to operate the system at all. Furthermore, steps must be taken to tune the radiosonde transmitters to a higher frequency to avoid causing interference to new receivers operating in that same frequency band. This will increase the interference already being experienced between radiosondes and data transmissions from meteorological satellites.

4.0 REPLACEMENT PROGRAM OBJECTIVES

The NWS has several primary objectives in replacing its current network of radiosonde systems, as outlined in Figure 1.

- Maintain system availability
- Reduce use of radio-frequency spectrum
- Distribute higher resolution datasets
- Distribute both processed and unprocessed data

Figure 1: Replacement System Objectives

System availability will be maintained by utilizing more reliable components in the replacement system. The other major objective is related to the reduction in the use of radio-frequency spectrum. The new system must coexist with other users in the same or nearby spectrum band through the use of stable transmitters and robust ground receiving equipment.

In addition, there are several other objectives associated with the implementation of new data processing software. The distribution of higher resolution data sets will allow numerical prediction models and researchers to use the full set of observed data, where the current system does not disseminate or archive all of the data sent by the radiosonde. These products, as summarized in Figure 2, will be distributed in near real-time. The data sets will include both processed and unprocessed data, which provides the best data quality (corrected for solar radiation effects on sensors) to users, and yet supports the needs of climate researchers who require data continuity by allowing them to reprocess the original data from old observations using new algorithms.

- WMO Coded Messages
  - Transmitted in two parts (Surface to 100 hPa, above 100 hPa)
  - Mandatory and significant levels
- RADAT Message
  - Coded message
  - Flight levels crossing the freezing point
- Distributed Data Sets
  - Transmitted in two parts (Surface to 100 hPa, above 100 hPa)
  - Administrative data
    - Station, flight, radiosonde, and balloon information
    - Surface weather conditions
  - Time stamped data
    - Height and Pressure
    - Temperature (with and without radiation correction) and Humidity
    - U/V wind components
    - Lat/Long position
    - Quality indicators
    - Time resolution matching radiosonde
- Archive Data Set
  - All data in above sets
  - Additional processed data

Figure 2: Summary of data sets to be distributed by the replacement system.

5.0 SYSTEM OVERVIEW

The replacement radiosonde system will consist of several components (Figure 3) which will be acquired in separate acquisitions. The telemetry subsystem (antenna and receiver) is to be a generic design which will allow the ground system to work with different brands of radiosondes. This is critical to maintaining competition in the acquisition of the radiosondes in order to keep costs under control throughout the lifetime of the system. The radiosondes will be purchased in combination with a signal processing subsystem that will decode the proprietary signals from the radiosonde into a standardized meteorological data stream which is passed to the NWS upper air workstation. The workstation will be a Pentium computer running Windows NT, which will in turn be connected to the Advanced Weather Interactive Processing System (AWIPS) local area network. Automated surface observing equipment now used throughout the NWS network are often located too far from the radiosonde release point to be representative of the environmental conditions. Therefore, surface weather observing equipment (temperature, pressure, humidity, and wind) are required at the point of the balloon release to baseline the remainder of the radiosonde sounding. Finally, at a small number of locations (about 10), a balloon inflation and launch shelter will be used to inflate and release the balloons where a more controlled release is required due to obstacles in the surrounding area. In many of these cases, the shelters will be located on the rooftop of the office building. Manual inflation and release of the balloon is not practical in those circumstances.

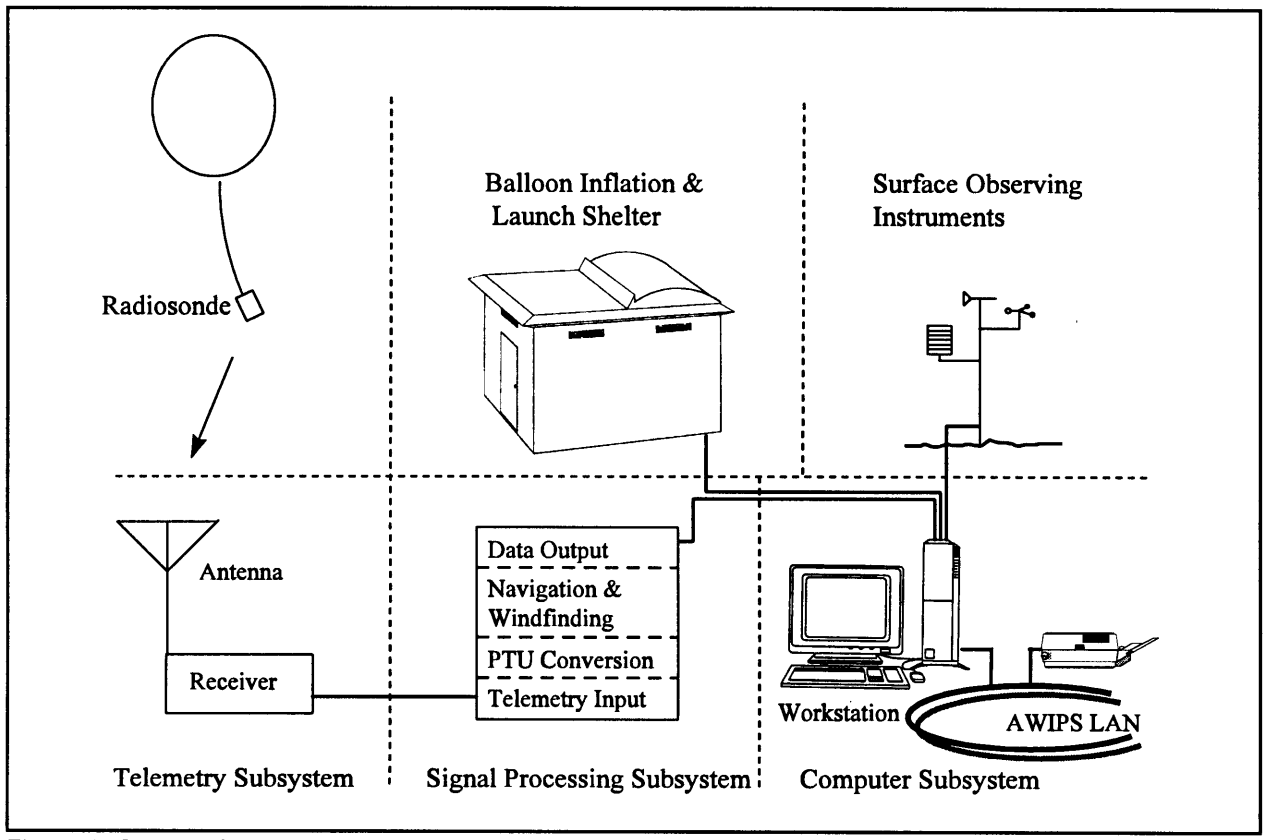

Figure 3: System Overview

In August, 1999, a contract was awarded to International Met Systems (formerly ATIR U.S., Inc.) for the telemetry subsystem, shown in Figure 4. The antenna tracks the radiosonde, providing the 1660 - 1700 MHZ radio data to the receiver located on the back of the dish assembly, which down converts the signal to 107 MHZ for the Signal Processing System. The Data Communications Equipment provides a fiber optic link back to the office (within 2000m) where the main workstation is located, as well as provides voice communications between the office, antenna location, and launch area. The radio receiver is state-of-the-art and uses standard cell-phone components. The characteristics of the antenna are listed in Figure 5. The servoed parabolic dish was chosen due to it's superb performance, low cost, and high reliability. The usually lower reliability of moving mechanical parts have evolved over the past 10 years to become very reliable mechanisms. The dish can be split for easier transport. The low inertia pancake motor drives are maintenance-free, lubricated for life. The system will include a comprehensive suite of built-in-test features for both continuous monitoring of the hardware and software states, as well as special off-line diagnostic tests.

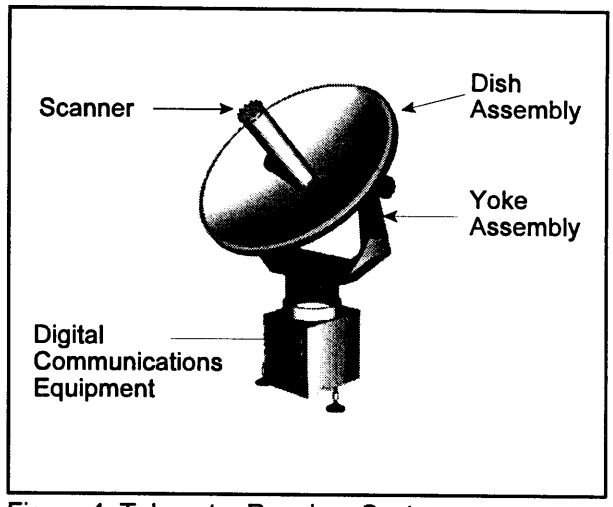

Figure 4: Telemetry Receiver System

- 2.0 meter diameter fiberglass parabolic dish
- Lightweight construction
- Rugged, corrosion resistant materials
- Easy access to subassemblies
- Pedestal provides environmentally controlled 19" rack for DCE and SPS
- Use of current NWS radomes will be required
- Uses proven, low risk technology

Figure 5: Antenna Characteristics

The replacement system will use Global Positioning System (GPS) wind-finding techniques in order to meet NWS accuracy and availability requirements. In January, 2000, contracts were awarded to two radiosonde manufacturers (Sippican, Inc. and InterMet Systems) for the development and submission of GPS radiosondes for evaluation by the NWS. Those products determined to meet the NWS radiosonde specification will be placed on a Qualified Products List, from which future acquisitions will be made. No significant change in radiosonde sensor performance is anticipated with the new system at this time (compared to the current NWS operational radiosondes).

6.0 IMPLEMENTATION SCHEDULE

The acquisition of the various system components shown in Figure 3 began in 1999. Necessary modification and integration of commercially available components is occurring during 2000, with implementation of systems at the field sites beginning in late calendar year 2001 and continuing into 2005. The implementation schedule will be phased across three or more years in order to keep the necessary annual funding at lower levels.

7.0 SUMMARY

The NWS must take immediate steps to avoid further degradation of its radiosonde system network. Plans are underway to replace the current system with a GPS-based system within the next 4 to 5 years. The new system will have to meet more stringent requirements associated with the use of radio-frequency spectrum, and will eliminate many of the maintenance issues associated with the current system.

Additional requirements and specification documents (as well as procurement information) can be found on the NWS Observing System Branch's web site at http://www.rrs.nws.noaa.gov.

THE NEW PHASE ARRAY AEROLOGICAL RADAR – MARL

Alexei Ivanov, Alexander Azarov, Alexander Kochin
Central Aerological Observatory, Dolgoprudny, Russian Federation
Tel: (095) 408-76-85; Fax: (095) 576-33-27
Victor Chistuhin
Moscow Institute of Electronic Engineering, Russian Federation
Tel: (095) 530-10-29; Fax: (095) 530-22-33

1. INTRODUCTION

It is known that there are three systems of windfinding that consists in determining radiosonde coordinates during the flight and finding the height: radiotheodoliting, radar-tracking and navigational. Each method has its advantages and disadvantages. Conventionally in Russia a radar-tracking method is used, which provides high accuracy in determining wind and altitude, confirmed in some intercomparisons of radiosondes [1], autonomy, i.e. independence from navigational signals, low cost of radiosondes. Now the aerological network of Russia uses mostly the radar-tracking system AVK-1 with a high-power transmitter and parabolic antenna 1,8 m in diameter. On the net now there are 102 AVK radars. They also are used in some other countries. Its high power consumption and increasing costs of operation and maintenance made it necessary to develop a new radar.

2. THE NEW AEROLOGICAL RADAR

The aerological radar of a new generation MARL-A (Fig. 1) is created on the basis of active phase array antenna with 64-th independent transceiver modules. The electronic control of a beam is carried out by a computer in both coordinates - in an elevation in limits +70...-40 grad, in an azimuth in limits + - 25 grad. The antenna plane has an incline of 30 grad to provide the scanning range of elevation from - 10 grad to +100 grad. In azimuth, near the limits of the electronic scanning range, the antenna is additionally turned mechanically. The step of electronic scanning of 0,05 grad, is provided by 4-digit phase shifters.

The power of the transmitted impulse necessary for receiving the return signal from the super-regenerative receiver of radiosonde is only 100 w. This is two orders of magnitude lower than in AVK-1, which is the result of using special methods of signal filtration and correlation processing. The pulse length is about 0,8 μs. The tracking range is 200 km.

The procedure of distance measurements and sonde tracking, processing of telemetry signal, compiling upper-air telegrams, and collecting data archives is performed in the PC of operator. This PC is connected via data links to the MARL receiver and on-board (industrial) computer. Fig. 2 shows the structural diagram of MARL-A, while Figs. 3 and 4 show a PC screen in two modes.

Structurally, MARL consists of an antenna post, with all blocks in microelectronic implementation, and PC of an operator. The antenna post is covered by a radiotransparent windshied.

PARAMETERS OF MARL-A

1	Dimensions the phased array antenna (64 devices)	1,8 x 1,4 M
2	Precision of angular tracking (root-mean-square deviation from datas AVK-1) - In an azimuth - In an elevation angle	 0,15 grad 0,1 grad
3	Transmitted power - In pulse - Medial	 100 Watt 0,1 Watt
4	Tracking distance - Precision - Maximum range	 + - 30 m 200 km
5	Operating frequency	1680 + - 5 MHz
6	Consumed power	less than 500 Watt
7	Weight (without windshield of a shelter)	250 kg

3. RESULTS OF TESTS

In testing, special attention was paid to the directional diagram of the antenna array, to the precision of sonde tracking over two angular coordinates and tracking reliability,

especially at large distances, including a possibility of fast recapture a sonde after tracking loss.

Figure 5 shows experimentally checked up phase-array antenna's pattern in the horizontal and vertical planes. The width of the main lobe is not changed by an up to 10 deg. deviation from the normal. At a decline of up to 20 deg., the diagram broadens by 10 %. At a maximum decline of +/- 60 deg. in elevation, the main lobe broadens by 30 %.

The precision of the angular radiosonde tracking with MARL was determined in comparison with the data on the angular coordinates of AVK-1 radiosonde launched on one suspension, and also the performance of the Sun tracking using a radiotheodolite mode of MARL-A.

In Fig. 6, an example of a simultaneous launching MARL and AVK radiosondes is presented. The results show a good agreement with RMS errors: 0,1 ... 0,15 deg.

It is quite useful to examine elevation tracking of a radiosonde at descent [2]. The elevation angle is likely to vary uniformly at descent, the beginning of the nonuniformity implying the influence of an underlying surface on an antenna directional characteristic. In experiments with MARL-A, the critical angle of a place was + 4-6 deg.

To estimate tracking quality in range, an experiment to recapture a radiosonde released at the neighboring upper-air server was conducted. The radiosonde was recaptured at 168 km distance.

4. CONCLUSION

The new aerological radar MARL-A with low power emission now is in production for some stations of the Russian network. The main parameters of MARL-A are better than that of AVK-1. Radiosondes which are used with a new radar are the same as used with AVK, that is MRZ-3A, but on the frequency 1680 MHz. The price of MARL-A and operational expenses are more less than for traditional big radars.

REFERENCES

1. A. Ivanov, A. Kats, S. Kurnosenko, J. Nash and N. Zaitseva. WMO International Radiosonde Comparison – Phase III (Dzhambul, USSR, 1989). WMO Report on Instruments and Observing Methods, № 40,1991.
2. D. Call. Comparing the Windfinding Performance of a New Phase Array Radiotheodolite with GPS Radiosondes. Reports of TECO – 98 (Casablanca, Marocco, 1998). WMO Report on Instruments and Observing Methods, № 70, pp. 165-168.

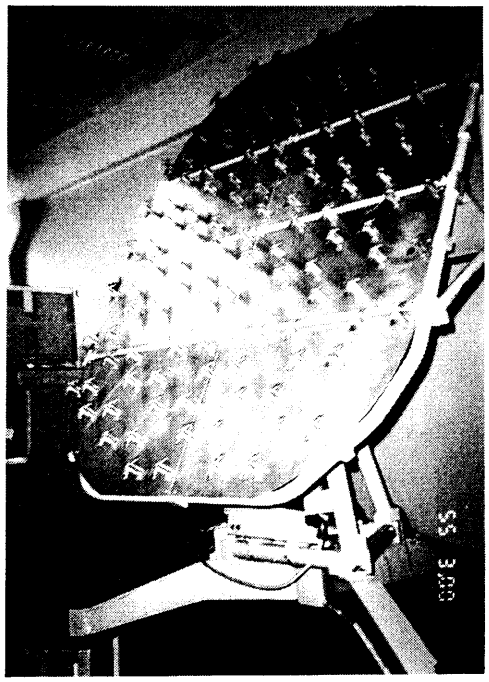

Fig 1. MARL-A

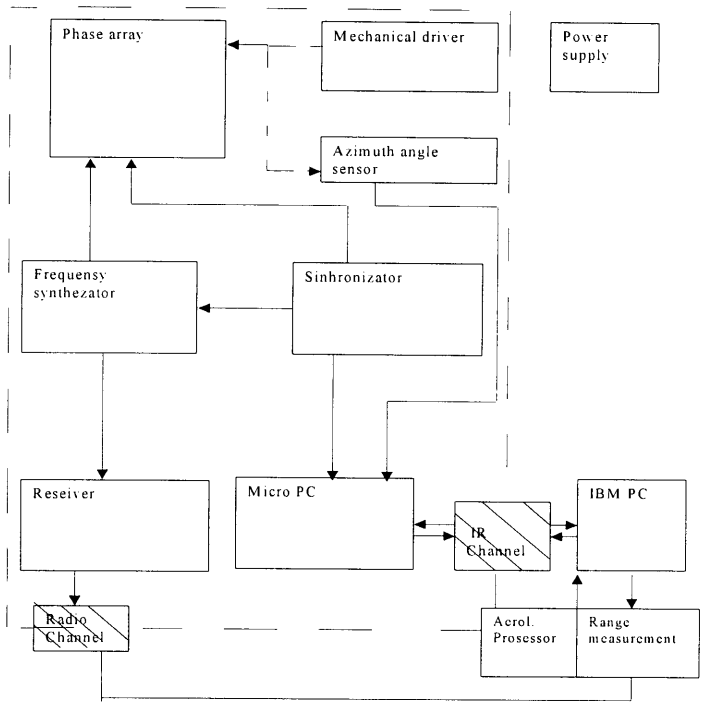

Fig 2. Structure of MARL - A

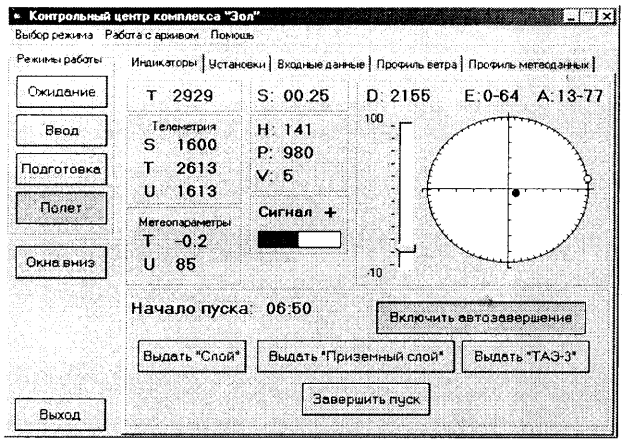

Fig 3. View of screen in a base mode

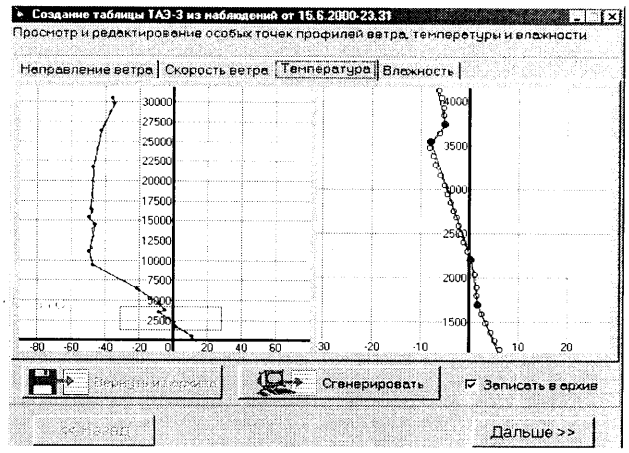

Fig 4. View of temperature profile

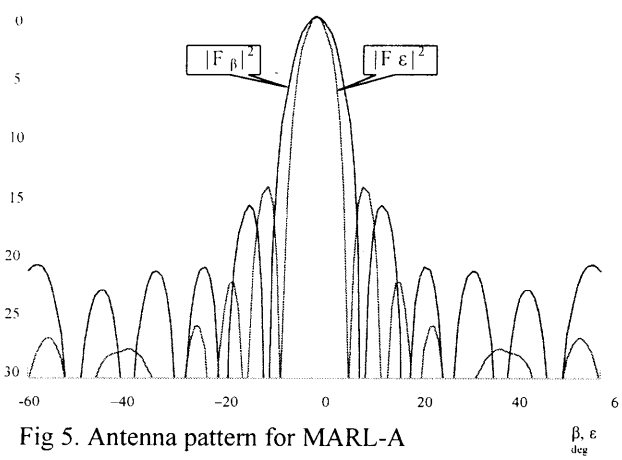

Fig 5. Antenna pattern for MARL-A

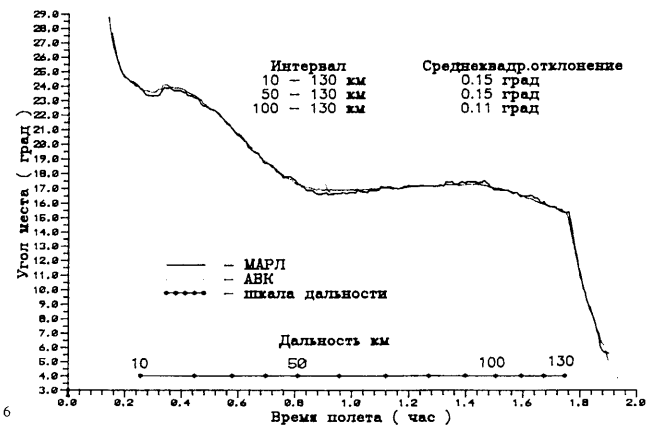

Fig 6. Comparision of elevation angle between AVK and MARL

New Technology in Upper Air Observations

R. E. Smout, J. B. Elms, D. R. Lyth and J. Nash
The Met. Office, South Road, Easthampstead, Wokingham, Berkshire, RG40 3DN UK
Fax: +44 1344 855897 email resmout@meto.gov.uk

Introduction

The Met. Office (UK) has made the decision to move from an observation network dominated by manual observations to a highly automated observation network by 2002. As a consequence, almost all the operational systems in the UK upper air network will be changed and some radiosonde stations will close or be moved. The current Vaisala PC-CORA ground systems will no longer be used for main operations.

Upper Air data for the GOS are expected to be provided by four Vaisala Autosondes, with two manned radiosonde stations retained at the current GCOS site, Lerwick, Shetland and Camborne in Cornwall. In addition three boundary layer and two tropospheric wind profilers will be used to provide continuous measurements of upper wind.

This report is concerned with the test and development activities for radiosonde systems in the last year. Three topics will be considered.

1. Testing and development of operational interfaces for the new Vaisala DigicoraIII ground station.
2. Testing of GPS windfinding systems. UK Autosonde operations need the option of GPS windfinding if there are problems with the Loran-C navigation chain in Europe. Defence test ranges require accurate low level GPS winds, as the wind finding radars used for the last 40 years are at the end of their working life. Graw and Sippican GPS radiosondes are being used to obtain height measurements to provide an independent check on radiosonde pressure sensors.
3. Flight testing of the Vaisala RS90 radiosonde, before introduction into operational service.

DigicoraIII - Characteristics

DigicoraIII is a PC based system whose software runs under Windows NT4. It was chosen by competitive tender to replace the PC-CORA ground system, which could not support GPS wind measurements. DigicoraIII is flexible enough to meet both civilian and defence Met. Office user requirements, and will also be incorporated into the Vaisala Autosondes. This will allow The Met. Office to standardise on one sounding system. DigiCoraIII software allows remote access via a telephone line; this will simplify software support, software upgrades and detailed diagnostics of system failure. Vaisala Oy will provide software support under a service level agreement. DigicoraIII will also allow several ascents to be processed and displayed simultaneously so that the manned sites can take over flight processing control from subsidiary sites, if required.

DigicoraIII has extensive archives of raw and edited data. At the end of each flight all raw data pressure, temperature, humidity and wind information whether it be Loran or GPS are stored. If there are problems with an ascent, Vaisala Oy have diagnostic software that can determine whether the problem was interference, a bad radiosonde or some other factor beyond the operator's control.

An early version of DigicoraIII with a partial operator interface was deployed at Ascension Island in April/May 1999. This was for an AMSU-B satellite water vapour radiometer verification test, MOTH [Measurement Of Tropospheric Humidity], in collaboration with the UK Met Research Flight. A fuller operational DigicoraIII evaluation was conducted at Camborne in March 2000. A number of operational system problems were found that would have prevented contractual acceptance as an operational system. However there were no discernible differences in the computed pressure, temperature and humidity values when compared to the current PC-CORA system. Differences were found between the Loran winds from PC-CORA and DigicoraIII. The Loran test was conducted with DigicoraIII having the same line fitting length and smoothing settings as used with PC-CORA. Towards the end of some flights, DigicoraIII winds were less reliable than from PC-CORA. Vaisala have resimluated the flight measurements with more active smoothing, and DigicoraIII winds then appear of similar quality to those from PC-CORA. An updated version of DigicoraIII software is undergoing operational testing at Lerwick and the earlier system faults have now been mainly eliminated.

GPS Radiosonde

GPS wind measurements with winds computed using a sample period of 1-minute (approximately 300m vertical resolution) were tested at Camborne in April 2000. GPS winds were compared with simultaneous Cossor radar winds and at low levels with winds from a Metek Sodar.

The Graw radiosonde was the simplest to prepare for operation, whilst the Sippican radiosonde was the most difficult. The Graw radiosonde does not have an unwinder, the Sippican radiosonde has a 30 metre unwinder and the Vaisala radiosonde has 60 metres making it the most difficult to launch in strong winds. Vaisala RS80 GPS winds had most interpolation and missing data, (about 2 per cent of the total winds

reported), similar to the current operational data loss at UK overseas stations. The winds from Graw and Sippican GPS radiosondes agreed most closely with the Cossor Radar. DigicoraIII winds oscillated with an amplitude of about 1 to 1.5 ms^{-1} and period of about 30 seconds relative to the radar winds, see Fig. 1. This happened when flown alone or on flights with other radiosondes. It was not seen in Vaisala GPS tests at Camborne using an early version of MW15 software (Elms, et al.1997). Fig. 2 shows the RMS differences of simultaneous measurements by the Vaisala, Graw and Sippican radiosondes with respect to the radar for the southerly wind component. The results for the westerly wind component were similar. The standard error of the radar measurements was expected to be about 0.2 ms^{-1} shortly after launch, increasing to about 0.3 ms^{-1} by the end of the flight. The results in Fig.2 indicate measurement errors in the Sippican were similar to those of the radar, and those found for the Vaisala system in 1997. The Graw measurements have larger errors, mostly because the processing smoothed variations in winds more than expected for 1-minute samples.

At low levels the Sippican measurements were the most reliable. However, it would be preferable to enter the surface wind observation after launch, rather than before, so the surface wind could be timed to match with launch in both Sippican and Graw systems.

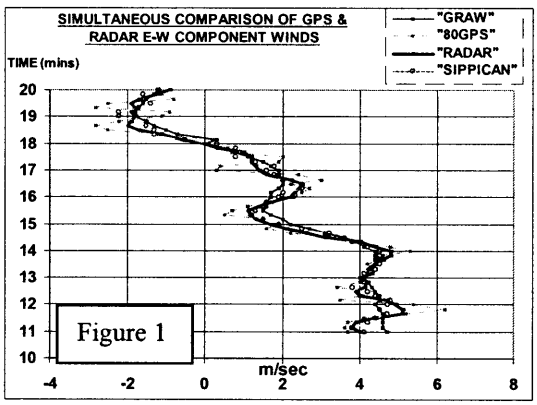

Figure 1

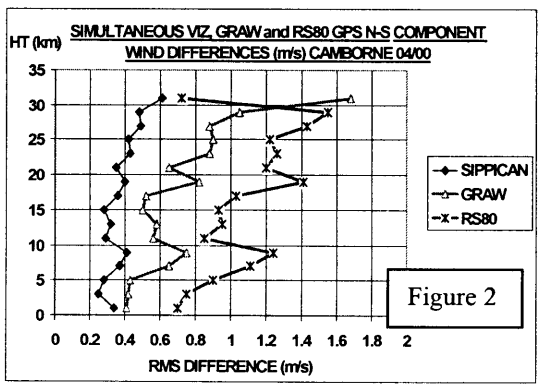

Figure 2

RS90 Radiosonde

The RS90 radiosonde is described in Paukkunen and Jauhiainen (1998).

Vaisala RS90 Tests

The RS90 was first tested internationally in 1995 at Wallops Island, Schmidlin, (1998). The UK Met. Office tested a revised version in August 1998 at Camborne, but this was in very dry and sunny conditions and it was judged necessary to perform another acceptance test in wetter, windier conditions before operational introduction. This test was performed in March 2000, with the RS90 radiosondes flown in parallel with the Meteolabor Snow White chilled mirror hygrometers. Comparison flights with the Snow White were also part of the MOTH test on Ascension Island in early 1999 and a second MOTH test at Visby, Sweden in December 1999.

Relative humidity results

In the UK test in 1998 the RS90 humidity sensor was not regenerated before launch (heated for several minutes to drive off contaminants), but in 1999 and 2000 the sensors were regenerated before performing ground control checks.
Three systematic problems have become clear as the result of the UK deployments of the RS90 humidity sensors.

1. Contamination of the humidity sensor when emerging from low cloud.
2. Day/night differences in relative humidity measurements.
3. Batch Differences in Calibrations.

Contamination in Low Cloud

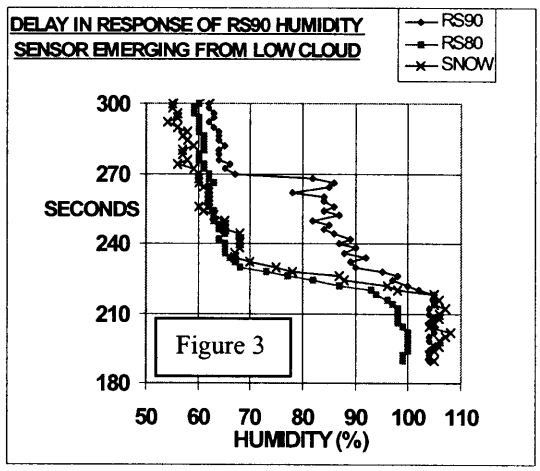

Figure 3

The two RS90 humidity sensors are not covered, and rely on alternate heating of the sensors to drive off contamination during an ascent. However, in the recent Camborne acceptance trial, the pulse heating was not strong enough to drive the water off the sensor when emerging from relatively thin low cloud, in situations where the cap on the RS80 relative humidity sensor prevented contamination. This occurred on several occasions. An example is shown in Fig. 3. In this example there was a 30-second delay before the RS90 humidity dropped to the correct value of around 60 percent.

Day Night Differences

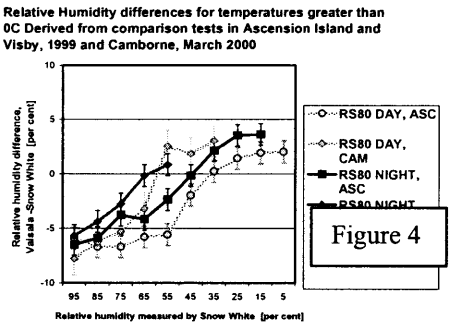

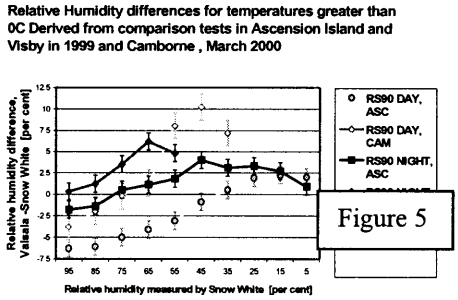

Figures 4 and 5 show comparison results from large numbers of triple radiosonde comparisons between Vaisala RS80 H-Humicap, Vaisala RS90 and Snow white chilled mirror hygrometer. The Snow White is not assumed to be an absolute reference but is used to be independent of the two Vaisala radiosondes. However, comparison of Snow White measurements in upper cloud between day and night indicate that any day-night difference in the measurements is not large. In Figure 4 the average day night difference between the RS80 and Snow White is about 2 per cent R.H. In Figure 5 the day-night difference is about 4%. During the day the RS90 sensors are heated by the sun's solar radiation. The relative humidity reported is for a temperature higher than ambient, and is thus lower than the true value for the correct air temperature. This day-night difference in the RS90 increases significantly by at least 10% in the upper troposphere.

Observed Batch Differences in Calibrations

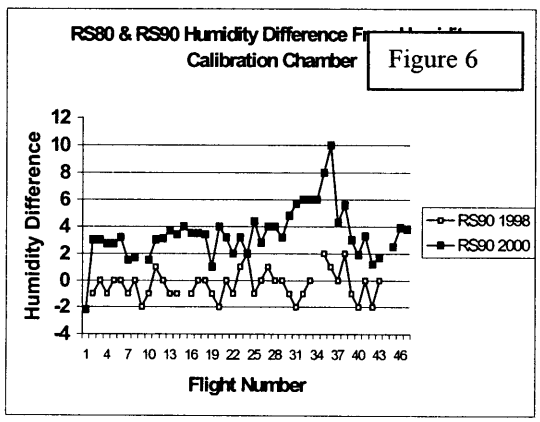

During the two tests at Camborne, an additional humidity check was made prior to launch by placing each radiosonde in a humidity chamber. Figure 6 shows the results. In August 1998 the RS90 was not regenerated before launch and in March 2000 there was a regeneration procedure in use. In March 2000 the RS90 humidity check data were consistently higher than in the 1998 test. This explains the offset between the Camborne and Ascension Island results at high relative humidity in Fig. 5. The check results for the RS80 did not change between tests, and these radiosondes were more consistent relative to the Snow White than the RS90 measurements. Vaisala Oy have now stated that regeneration should only be used with radiosondes that have been regenerated before calibration in the factory. Thus, the acceptance test must be repeated once this type of radiosonde becomes available.

Hence the introduction of the RS90 radiosonde is to be postponed until the problems are resolved.

RS90 Temperature Performance

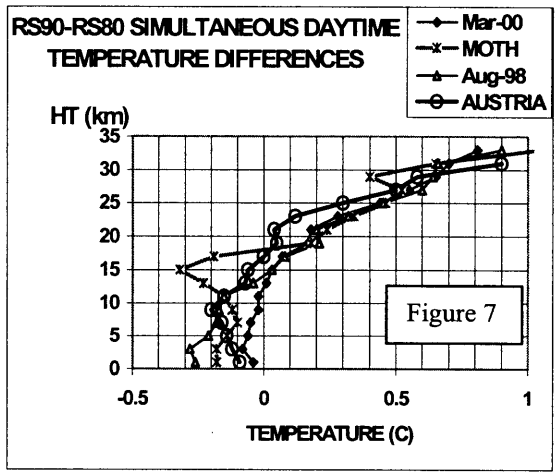

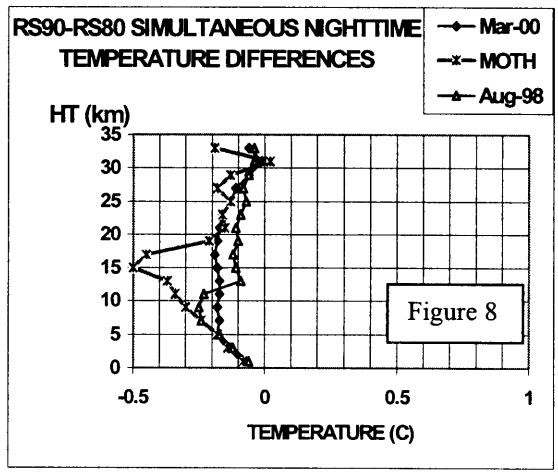

Figures 7 and 8 show the mean differences between the temperature measurements made during daytime and night-time in the three main UK tests. At night the most significant differences occur near the tropical

tropopause. At temperatures near –50°C, the RS90 appears to have a "calibration difference", of between –0.1°C and –0.2°C relative to the RS80, see the comparisons between 20 and 25 km. The difference in time constant of response probably causes the RS90 to report lower temperatures, on average by between 0.1°C and 0.2°C at 10 km. In the tropics it appears that both calibration and time constant differences have increased in amplitude to give an overall difference of –0.5°C between the two radiosonde types. In the daytime, Fig. 7 also includes a fourth data set designated "Austria" from Paukkunen and Jauhiainen (1998). All four tests show similar RS90-RS80 differences, as a function of height apart from in the upper tropical troposphere, where the increased difference seen at night is also present in the day. The differences in the stratosphere between the two-radiosonde types is not trivial for climate change studies and needs adequate explanation. The differences must lie in the radiation correction schemes, which are of very different amplitude for the two radiosonde types, see Figure 9.

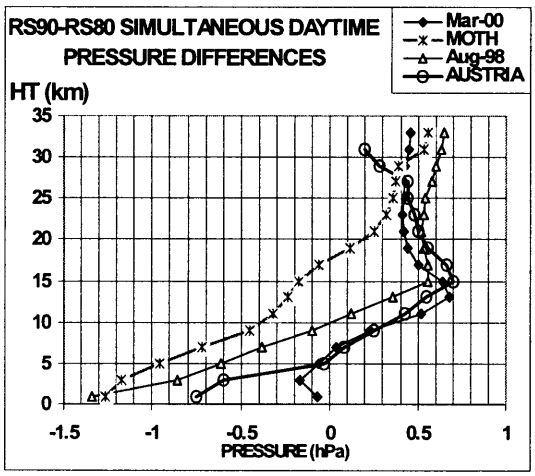

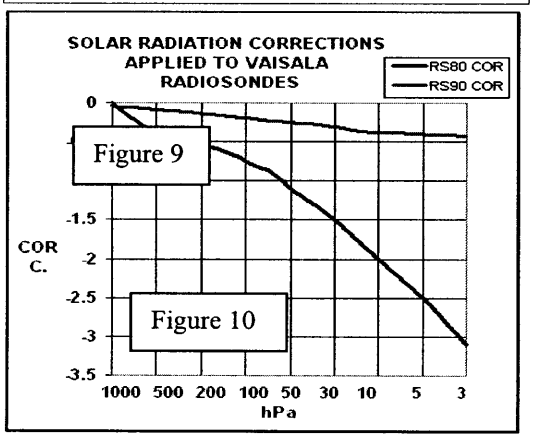

RS90 Pressure Sensor Performance

The differences between simultaneous measurements by the RS90 and RS80 pressure sensors are presented as a function of height in Fig. 10. Near the ground the RS90 usually indicates pressures lower than the RS80. The RS80 sensor has a positive pressure bias when its internal temperature is transitioning from a higher temperature to a colder temperature. In the stratosphere, the RS90 pressure sensor indicates pressures lower than the RS80 by about 0.4 hPa on average. In Fig.11, comparisons of simultaneous height measurements between the tracking radar and the two radiosonde types, indicates that in the 1998 test the pressure indicated by the RS90 was much closer to the truth at heights above 20 km than that of

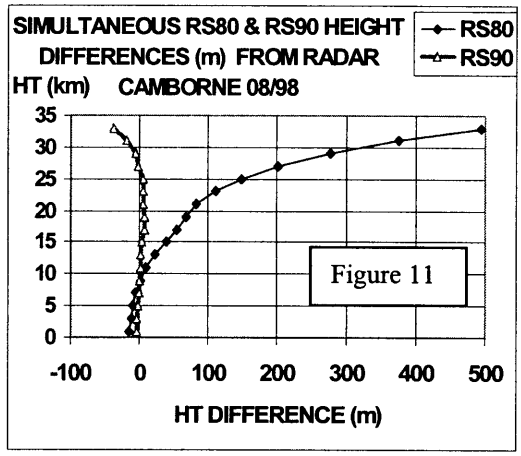

the RS80. Around 15 km, near the tropical tropopause, the relationship between the two pressure sensors differs significantly from mid-latitudes. This merits further investigation.

The pressure and temperature differences between the two-radiosonde types noted in the stratosphere, would be expected to produce the following step change in climate records at a round 10 hPa (31 km). In the daytime temperature would rise by 0.4 K on average and at night drop by 0.4K on average.

References:

A. Paukkunen, H. Jauhiainen (1998) RS90 Radiosonde into Operational Use TECO-98 WMO/TD No. 877 pages 237 - 240.

Schmidlin, F. J., (1998) Summary Of The WMO International Radiosonde Relative Humidity Sensor Comparison – Sept. 1995. TECO-98 WMO/TD No. 877, pages 185 - 187.

Elms, J.B., Nash, J and Stancombe, J.L. (1977) Second Evaluation of Vaisala GPS radiosonde system, Camborne. Remote Sensing Branch, Tech. Memo No.2 available from The Met. Office, Bracknell

THE DEVELOPMENT OF A RECOVERABLE RADIOSONDE: THE GLIDERSONDE PROJECT

Ken Howard[1], Michael Douglas[1], Nilton Renno[2], Davis Egle[3], and Frank Gallapher[4]

1 - National Severe Storms Laboratory, NOAA ERL, Norman OK
1313 Halley Circle
Norman, Oklahoma USA 73069
(405) 366-0500
Email: khoward@nssl.noaa.gov

2 - University of Arizona, Tucson, AZ
3- Egle Engineering Norman, OK
4 - University of Oklahoma, Norman, OK

1. INTRODUCTION

Radiosonde observations are widely considered to be the single most important component of the current atmospheric observing system, and have been the mainstay of the global observing network for more than 45 years. However, the global distribution of such observations remains very uneven, with the highest density in the middle latitudes of the Northern Hemisphere, while large tropical land areas in South America and in Africa are sparsely sampled. Although labor costs are a substantial fraction of the total cost of making such observations in developed countries, the so-called "expendable" radiosonde package dominates the sounding budget of most developing countries, and this cost generally determines both the number of stations that can be operated and the frequency of soundings. The cost of maintaining this worldwide network has been in recent years subject to scrutiny, and it is not clear is the network can been maintained at its present level, let alone expanded into the remaining continental data voids. Even developed countries are re-evaluating the frequency of soundings, in efforts to reduce budgets, and some networks are under serious financial stress.

2. CONCEPT

A proposed partial solution to these recurring cost problems is the development of a recoverable, reusable radiosonde system. The use of such a device would possibly allow for both an increased distribution of sounding sites and an increase in the frequency of sampling by the device with a corresponding significant reduction in the recurring cost. The ideal solution would consist of a reusable instrumentation vehicle, which could be launched in a manner consistent with present operation, but could be automatically returned to the launch point, or another designated recovery point, to allow for the recovery and reuse of the equipment. To provide an expanded distribution, the ideal device would also need to be designed to the lowest acquisition cost possible. The concept for a recoverable/reusable sonde was first proposed by Dean Lauritsen of the National Center for Atmospheric Research (NCAR). In United States Patent Number: 5,186,418 granted on February 16, 1993, Dr. Lauriten proposed developing a recoverable rawinsonde that would fly back to its launch point or suitable location with the vehicle guidance during descent utilizing a GPS based navigation control system.

The ideal solution is a reusable vehicle called the Glidersonde. The Glidersonde is a small-unpowered autonomous sailplane that carries meteorological sensors for the collection of atmospheric data in a comparable method to a radiosonde. The Glidersonde has a wingspan of less than one meter and a total flying weight of approximately 2.0 kilograms. The Glidersonde contains a Global Positioning System (GPS) receiver and a small microcomputer used in determining relative position and navigation decisions. The Glidersonde is carried aloft by a conventional gas-filled balloon measuring pressure, temperature, and humidity and position data as it ascends. At a preset altitude, the Glidersonde releases itself from the balloon. The aircraft naturally flies to a level attitude and the autonomous navigation system steers it to the home or alternate location. After reaching the home location, the glider circles while descending. At a preset altitude above ground, a parachute deploys and the Glidersonde is recovered. The vehicle can then be quickly refurbished and reused. A schematic diagram of a complete Glidersonde mission is depicted in Figure 1.

THE DEVELOPMENT OF A RECOVERABLE RADIOSONDE: THE GLIDERSONDE PROJECT

Ken Howard[1], Michael Douglas[1], Nilton Renno[2], Davis Egle[3], and Frank Gallapher[4]

1 - National Severe Storms Laboratory, NOAA ERL, Norman OK
1313 Halley Circle
Norman, Oklahoma USA 73069
(405) 366-0500
Email: khoward@nssl.noaa.gov

2 - University of Arizona, Tucson, AZ
3- Egle Engineering Norman, OK
4 - University of Oklahoma, Norman, OK

1. INTRODUCTION

Radiosonde observations are widely considered to be the single most important component of the current atmospheric observing system, and have been the mainstay of the global observing network for more than 45 years. However, the global distribution of such observations remains very uneven, with the highest density in the middle latitudes of the Northern Hemisphere, while large tropical land areas in South America and in Africa are sparsely sampled. Although labor costs are a substantial fraction of the total cost of making such observations in developed countries, the so-called "expendable" radiosonde package dominates the sounding budget of most developing countries, and this cost generally determines both the number of stations that can be operated and the frequency of soundings. The cost of maintaining this worldwide network has been in recent years subject to scrutiny, and it is not clear is the network can been maintained at its present level, let alone expanded into the remaining continental data voids. Even developed countries are re-evaluating the frequency of soundings, in efforts to reduce budgets, and some networks are under serious financial stress.

2. CONCEPT

A proposed partial solution to these recurring cost problems is the development of a recoverable, reusable radiosonde system. The use of such a device would possibly allow for both an increased distribution of sounding sites and an increase in the frequency of sampling by the device with a corresponding significant reduction in the recurring cost. The ideal solution would consist of a reusable instrumentation vehicle, which could be launched in a manner consistent with present operation, but could be automatically returned to the launch point, or another designated recovery point, to allow for the recovery and reuse of the equipment. To provide an expanded distribution, the ideal device would also need to be designed to the lowest acquisition cost possible. The concept for a recoverable/reusable sonde was first proposed by Dean Lauritsen of the National Center for Atmospheric Research (NCAR). In United States Patent Number: 5,186,418 granted on February 16, 1993, Dr. Lauriten proposed developing a recoverable rawinsonde that would fly back to its launch point or suitable location with the vehicle guidance during descent utilizing a GPS based navigation control system.

The ideal solution is a reusable vehicle called the Glidersonde. The Glidersonde is a small-unpowered autonomous sailplane that carries meteorological sensors for the collection of atmospheric data in a comparable method to a radiosonde. The Glidersonde has a wingspan of less than one meter and a total flying weight of approximately 2.0 kilograms. The Glidersonde contains a Global Positioning System (GPS) receiver and a small microcomputer used in determining relative position and navigation decisions. The Glidersonde is carried aloft by a conventional gas-filled balloon measuring pressure, temperature, and humidity and position data as it ascends. At a preset altitude, the Glidersonde releases itself from the balloon. The aircraft naturally flies to a level attitude and the autonomous navigation system steers it to the home or alternate location. After reaching the home location, the glider circles while descending. At a preset altitude above ground, a parachute deploys and the Glidersonde is recovered. The vehicle can then be quickly refurbished and reused. A schematic diagram of a complete Glidersonde mission is depicted in Figure 1.

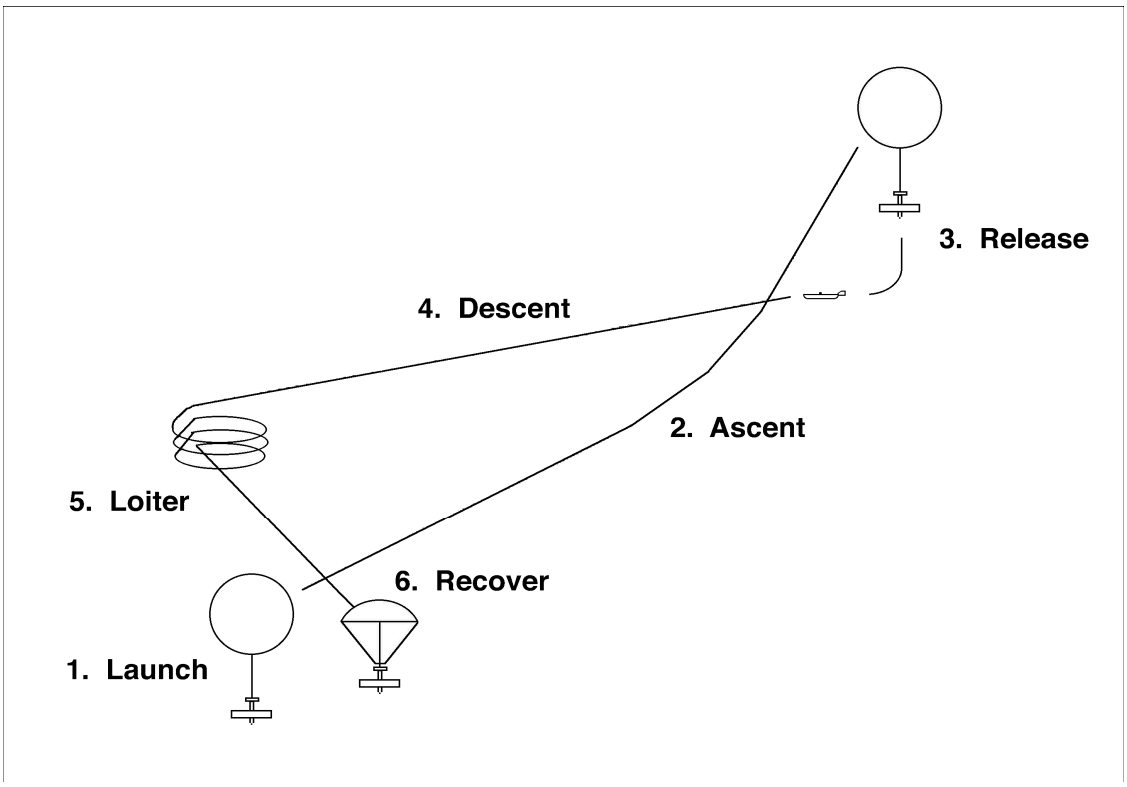

Figure 1. Glidersonde mission and stages (not to scale).

Data recovery can take one of two forms. The data can be stored internally in re-writable memory and downloaded after the vehicle is recovered or the data can be telemetered to a ground station as it is acquired. The data collection is equivalent in both accuracy and continuity to a standard radiosonde sounding. However, employing the Glidersonde vehicle, the meteorological sensor package is safely returned to be utilized over and again.

3. ENGINEERING ASPECTS

The basic engineering approach was to evaluate the mission requirements and design and develop a demonstration vehicle, at a minimum cost in a minimum time, to meet those project goals. To accomplish this task, a series of exploratory discussions was held to establish the mission requirements. These included specific payload definition, launch sites and their associated historical wind conditions, and automated return and recovery of the vehicle. Based on these discussions, it was established that the device would need to possess the following attributes: first the capability to be launched using the existing balloon launch systems and operate and acquire data consistent with existing procedures; second, the primary payload would consist of a standard radiosonde instrumentation package with limited flexibility to accept alternate devices (to enhance this flexibility and minimize interface constraints with proprietary radiosonde instrumentation, the device and its operation must be completely independent of the payload); third, possess an independent system to automatically navigate and return to the launch point; and fourth, possess an automated recovery system activated upon return to the launch point. To minimize development time and system cost of the Glidersonde, the maximum use of commercially available, “off-the-shelf”, components, utilizing present technologies, was employed.

The demonstration vehicle was constructed using Remote Controlled (R/C) model aircraft technologies to minimize development time. It is expected that advanced manufacturing procedures would be used for a commercialized version of the vehicle. The navigation & control system is the combination of a programmable micro-controller, a commercially available GPS sensor, and standard R/C model aircraft servos. The GPS provides the navigational position and tracking data to the micro-controller which in turn provides the necessary control input signals to the servos to have the vehicle track and return to the launch point.

The use of a commercial GPS system allows for a return accuracy within approximately 20 meters of the launch point. Once the vehicle is within this window, the system has the vehicle orbit within the window until recovery is initiated. The independent, automated recovery system consists of a sensitive altimeter (pressure device), a parachute release and deployment device, a recovery parachute, and a parachute-reefing device. The altimeter possess the capability to be preset with a defined offset with respect to the initial launch value at which a deployment device can be triggered. In the descent, once this specified relative altitude is reached, the deployment of the parachute is initiated. The deployment height is anticipated to be approximately 45 meters to allow the vehicle to avoid normal ground obstacles, such as water towers, etc., in the glide mode, but eliminate the drift /range problems with winds at the recovery sight. To eliminate the vehicle being drug over the ground and damaged due to surface winds, a ground contact parachute reefing system collapses the parachute. At this point the system can be refurbished and reused.

The navigation computer is the brain of the Glidersonde system. The microcontoller, which is a microprocessor with built-in memory and communications interfaces, performs all the computations and serves as the master controller for the vehicle components. In order to accomplish these tasks, several computer interfaces were developed: (1) the GPS interface, (2) the human interface, and (3) the control interfaces. The human operator determines at what altitude the vehicle will terminate its ascent.

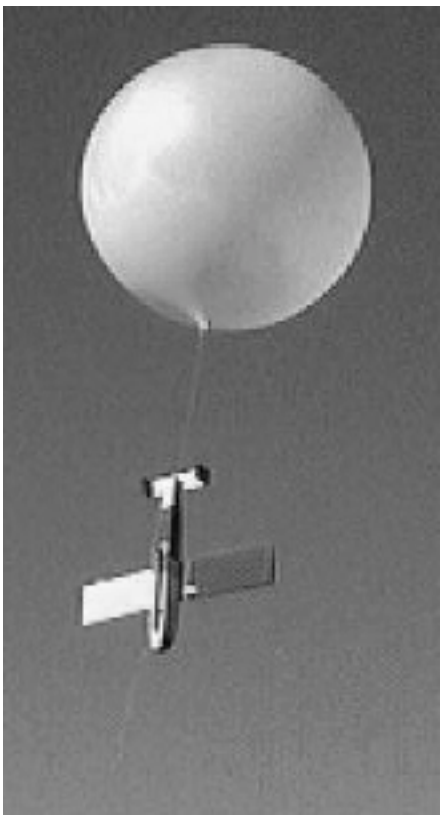

Figure2. Glidersonde in the ascent phase

The GPS interface feeds the navigation computer the data needed to perform the required manipulations. The control interfaces actually maneuver the vehicle, and terminates the ascent and descent phases. The computer reads input data from the GPS receiver and automatically separates the aircraft from the balloon, computes the course to the recovery area, and navigates the aircraft back to the recovery area completely without human intervention (autonomously).

4. TEST FLIGHTS

A long series of flight tests were conducted to develop the major components of the Glidersonde and to demonstrate the viability of the basic concept. During various phases of the development powered aircraft that were about the same size and flying characteristics as the Glidersonde were used. A complete data set from all test flights are shown in the Glidersonde URL. In every one of the tests conducted with the Glidersonde, the navigation system has performed as intended. A typical, but very short flight, is illustrated in Figure 3. This figure shows a screen capture of the display of the GSDataCapture program which plots the XY coordinates of the flight path as telemetered down to the ground station. During the flight, this display shows the current location of the glider. The text in the upper left hand corner of the display shows latest data telemetered to the ground along with the maximum altitude recorded for this flight and the home coordinates.

The current position of the glider is shown in the display as the small X drawn on the screen. The inset in the lower left-hand corner of Figure 3 identifies the features shown at the current location. The small drawn from the X visually shows the aircraft heading at this position, in this case, 334 deg. The line drawn toward the bottom of the inset is the path. Annotations have been added to the plot in Figure 3 to show the major events in the flight. These events are somewhat difficult to see in the static display but are very evident when the real-time display or a replay of the flight is seen. After the balloon was launched, it drifts SSE for as few seconds and then moves directly North and then NNW. The balloon was separated from the balloon about 400 m North and 150 m West of the home location. The release altitude for this flight was set for 1000 feet. The navigation computer then executed a left turn and pointed the vehicle toward home. The craft flew a portion of a circular path around home until, at the point indicated, the pilot assumed control and landed the glider.

A ROBOT PLANE METEOROLOGICAL SOUND SYSTEM

Ma Shuqing[1], Wang Gai[2], Pan Yi[2], Liu Zulun[2]

1 Atmospheric Observing Experimental Base CMA,44,zhizhuyuan road,bejing,china,(+8610)68415080,(+8610)67884851,msqing@163bj.com

2 Institute of Meteorological Sciences of Jiangxi Province

1. Foreword

The model UAV has been used to measure atmospheric environment before RPMSS appeared. The flight of model UAV can only be flying within visual range. Sounding scope is only about 1km. Besides, the model UAV has no location system. It can not position and measure wind. If we equip ground tracking system, it is too huge and loses flexibility. The appearance of GSP makes it possible to develop a new UAV aerosounde system. New UAV was planned in the United States for the tropic cyclone study under the supporting of WMO/CAS and ICSU [1]. In China, the development of UAV aerosounde system is included in Chinese Meteorology Administration "8th Five Year" plan. Now A robot plane meteorological sound system (RPMSS) has been developed.

2. General

A robot plane meteorological sound system consists of a mini robot plane , an air-borne digital radiosonde, and a ground-based subsystem. The flight of robot plane is controlled by the onboard auto-control system to proceed along a pre-designed flight line under the guidance of Global Position System (GPS). The flight track and meteorological data will be sent back to the computer of ground-based subsystem. Ground-based subsystem processes and displays the flight track and meteorological data real timely, and send control order to the plane. The aerosonde measures temperature, pressure, and humidity. Wind speed and direction are calculated from GPS data.

2.1 Mini PLANE

Fig.1 shows the photograph of the mini plane. The pneumatic layout combines the conventional and duck type layout [2]. The engine is on the tail of plane. The take off weight is about 12 kg. In order to verify the function of the plane, four test flights were conducted during the maximum ground wind speed up to 10 – 12 m/s. The plane's stability and serviceability are good. Another test flight has been organized by the Department of Science, Technology and Education of the CMA on December 18,1997. The flight is functioning normally with upper air wind speed of 18 --20 m/s. In this test, the plane flew away as far as 40 km.

Specification of plane:

Wingspan:	3.0m
Wing area:	0.62m^2
Airscrew diameter:	0.46m
Take off weight:	12kg
Maximum speed:	30m/s
Maximum lift ratio:	3m/s
Ceiling:	5km
Endurance:	4-8hr

2.2 schematic diagram of the system

The schematic diagram of the system is shown in Fig. 2.

The onboard equipment consist of:

1 Onboard computer
2 the converted circuit
3 GPS receiver, which can run after eight satellites in the same time. Its location error is 100 meter, speed error is 0.1m/s. It can give longitude、latitude、altitude、velocity and so on.
4 The transceiver, which adopts common VHF、UHF or other communication equipment. It sends information from modem to the ground.
5 Modem, with half duplex. The highest baud rate is 1200 bit.

6 Gyroscope, utilized to increase stability of the plane.
7 Telemetric receiver, to receive instruction from the ground based subsystem.

Ground equipment consists of:

1 Transceiver, matched with onboard equipment.
2 Modem, matched with onboard equipment.
3 Micro-computer, used to: receive, process, and display the data from the plane; write flight route and initialization data to the onboard computer before the plane takes off; dispatch instruction to the onboard computer.

2.3 structure of the control system

The onboard computer is the center of the control system, and the GPS receiver is the predominant information source. The reliability is most important for the onboard computer. The 80C198 single chip CPU is chosen for the onboard computer, which has abundant I/O function. The peripheral circuit adopts general programmable chip. The onboard computer has special advantages such as high integrating degree, small size, and low power consumption. The control system includes on board and grounded equipment.

Onboard computer software function module

1 Parameter install and diagnose module;
2 GPS information take over module;
3 Information handling module;
4 Mathematics operational module;
5 Route management module;
6 Servo management module;
7 Sensor information gather module;
8 Communication module.

In the onboard computer, each software module runs not in proper order and is dispatched through interrupt, and runs interactively. The onboard computer software system is a multitask system. Though, the complex level of software system is increased but integrated degree and reliability of hardware is raised, and the cost is reduced. Figure 3 is the automatic control flow chart.

3. Wind Velocity measurement

Measuring wind velocity by aircraft is usually conducted by measuring the difference of the air velocity and ground velocity of the aircraft[3] . The measuring of wind velocity by RPMSS is based on the horizontal air velocity return zero method during a plane circle flight or on the analytical method [4].

3.1 Horizontal velocity return zero method

Because the mini plane has very small turning radius, the horizontal velocity return zero method has been deduced to measure the wind velocity. When the plane flies a whole circle to the same point related to the air, the sum of the horizontal air velocity vector is zero, and the mean horizontal wind velocity equals to the mean the plane ground velocity. The mark returning to same point is the heading sensor output equal to the beginning value.

The relationship of the air velocity V_a, ground velocity V_g of the plane and wind velocity V is as follows:

$$V=V_g-V_a \qquad (3—1)$$

Assume the plane fly at constant speed along a horizontal circle, the longitude and latitude components can be expressed as:

$$V_{ax}=A\cos(\omega t)$$
$$V_{ay}=A\sin(\omega t) \qquad (3—2)$$

Where ω is the angular speed , A is the modulus of V_a. Integrating both sides of (3—2) obtains

$$\int_0^T V_{ax}dt=\int_0^T A\cos(\omega t)dt=0$$

$$\int_0^T V_{ay}dt=\int_0^T A\sin(\omega t)dt=0$$

where T is the time period of one circle flight. Therefore, the integrating of both sides of formula (3—1) divided by T give

$$\frac{1}{T}\int_0^T Vdt=\frac{1}{T}\int_0^T V_g dt=V \qquad (3—3)$$

It is that the mean horizontal wind velocity V is related only with V_g in the time period of T. V_g is given by GPS once per second, so

$$V=\frac{1}{T}\sum_{i=1}^{T} V_{gi} \qquad (i=1,\ 2\ldots\ T) \quad (3—4)$$

Vgi is the horizontal ground velocity of the ith second got from GPS receiver. If assume the longitude and latitude coordinates given by GPS at the ith second are Xi and Yi, then the components of Vg at X and Y direction are

$$V_{gxi}=(X_i-X_{i-1})$$

$$(i=1,\ 2\ldots\ T) \qquad (3—5)$$

$$V_{gyi}=(Y_i-Y_{i-1})$$

So, the components of horizontal wind velocity V at X and Y direction are

$$V_x=\frac{1}{T}\sum_{i=1}^{T} V_{gxi}=(X_T-X_0)/T \qquad (i=1,\ 2\ldots T)$$

$$(3—6)$$

$$V_y=\frac{1}{T}\sum_{i=1}^{T} V_{gyi}=(Y_T-Y_0)/T \qquad (i=1,\ 2\ldots T)$$

It can be seen that the measured horizontal wind velocity in this way is as the same as obtained by conventional wind measuring method in physical meaning. The mini plane flight track of 10 October 1995 on ground coordinate is shown in figure 4. It can be seen that the flight track is a helical line. If it were drawn in the coordinate system related to the air, the flight track would be a circle. The test flight study[4] shows the aerosonding results obtained by this system has good accuracy.

3.2 Analytical method of wind measuring

When the aircraft flies in the air along a circle with constant speed, in the ground coordinate the flight track of the airplane can be writen as:

$$X=V_{fx}t+r\cos(\omega t+\alpha)+C_x$$

$$Y=V_{fy}t+r\sin(\omega t+\alpha)+C_y \qquad (3\text{-}7)$$

Where X and Y are the ground coordinate of aircraft. Vfx and Vfy are the components of horizontal wind velocity at X and Y directions, r and ω is the radius and angular speed of the plane circular fight, α is the initial phase, Cx and Cy is the original coordinate of the circle center. Derivative X and Y versus time t, we can get

$$V_x=\frac{dX}{dt}=V_{fx}-r\omega\sin(\omega t+\alpha)$$

$$(3\text{-}8)$$

$$V_y = \frac{dY}{dt} = V_{fy} + r\omega\cos(\omega t + \alpha)$$

Formula (3-8) is unlinear function. In order to calculate, unfold formula (3-8) by Taylor series and omit the terms of two or higher order, obtain

$$V_x = (V_x) + \frac{\partial V_x}{\partial V_{fx}}\Delta V_{fx} + \frac{\partial V_x}{\partial r}\Delta r + \frac{\partial V_x}{\partial \omega}\Delta\omega + \frac{\partial V_x}{\partial \alpha}\Delta\alpha$$

$$V_y = (V_y) + \frac{\partial V_y}{\partial V_{fy}}\Delta V_{fy} + \frac{\partial V_y}{\partial r}\Delta r + \frac{\partial V_y}{\partial \omega}\Delta\omega + \frac{\partial V_y}{\partial \alpha}\Delta\alpha \qquad (3\text{-}9)$$

(V_x)、(V_y) are the values obtained from formula (3-8) using the original values V_{fx0}、V_{fy0}、r_0、ω_0、α_0. $\Delta V_{fx} = V_{fx} - V_{fx0}$, $\Delta V_{fy} = V_{fy} - V_{fy0}$, $\Delta r = r - r_0$, $\Delta\omega = \omega - \omega_0$, $\Delta\alpha = \alpha - \alpha_0$. In formula (3-9) there are 5 unknowns: ΔV_{fx}、ΔV_{fy}、Δr、$\Delta\omega$、$\Delta\alpha$. When N continuous groups of $(V_{xi}$、$V_{yi})$ values are obtained from GPS, there will be 2N five element one order functions. In order to eliminate the stochastic error, set 2N>5, solving ΔV_{fx}、ΔV_{fy}、Δr、$\Delta\omega$、$\Delta\alpha$ with least square method, and add them to V_{fx0}、V_{fy0}、r_0、ω_0、α_0. Put them to function (3-9), a series functions are setup again, solving them itinerately until ΔV_{fx}、ΔV_{fy}、Δr、$\Delta\omega$、$\Delta\alpha$ become smaller than preset criteria, then the wind velocity V_{fx} and V_{fy} with necessary accuracy are obtained.

When N=14,19, and 24, the standard error of longitude $\sigma_{\Delta Vxf}$ and latitude component of wind velocity $\sigma_{\Delta Vyf}$ equal to 0.27, 0.11, 0.05 and 0.24, 0.10, 0.04 (m/s) respectively;

4. Digital Electronic Radiosonde

It consists of electronic sensors, measuring circuits and digital processing unit. Fig. 5 shows the frame chart of this digital electronic radiosonde.

The temperature sensor is thermal resistance, humidity sensor is humidity sensing capacity, and pressure sensor is silicon pressure sensor. Measurement and processing is conducted by the processing unit consisted of measuring circuit and single chip computer. Gathered and processed digital data is compiled into airborne control unit data flow in intercept mode and transmitted to ground receiving system. In the radiosonde advanced sensors are used, the gathered data are processed, and the digital data is compiled into control data flow in intercept mode. It makes the radiosonde higher accuracy and higher stabilize capability of anti-interference.

Specification

item	range	accuracy
Temperature	-90 to 50°C	0.3°C
Humidity	0 to 100 % RH	5% RH
Pressure	5 to 1050 hpa	0.5 hpa

5. Test sonding

The wind profile measured by the RPMSS on 29 October 1997 02:05 (UTC) is shown in figure 6. The square points are obtained by conventional radiosonde nearby at 28 October 1997 23:45 (UTC). It can be seen the RPMSS can give more detailed data. Figure 7 shows the profiles of temperature, humidity, and pressure obtained at the same flight. The square points are comparing data as in above figure. RPMSS data shows the same trends as conventional radiosonding but higher sensibility and give more detailed data again.

6. Summary

RPMSS has the advantages as: small size, light weight, easy to move to remote sites, flexible, high accuracy, and would be widely used in atmospheric research, especially at remote areas.

New Radiosonde for Chinese Ground Equipments

Li Jiming and Feng Dali
Shanghai No.23 Radio Factory, Shanghai, China

1. Introduction

The conventional upper air sounding system in China, the GZZ2 Radiosonde-701Secondary Radar System, has been used since 1960's. It was once on the upper-middle level among the world sounding systems. However, with the rapid development of science and technology, especially with the large-scale operation of electronic radiosondes, this system lags behind a lot and must be upgraded.

As a radiosonde with mechanical deformed sensors and mechanical coding, GZZ2 works visibly with its backwardness such as low sensitivity, large radiation error and big lag coefficient, especially in high level. In addition, with the growing application of radio and telecommunication systems, the frequency interference of 400MHz makes the operation of GZZ2-701 system more and more difficult, especially in developed regions of eastern China.

To meet the operational needs of the future upper-air sounding in China, CMA has set definite demands on manufacturers for development of new sounding systems and/or reforming of the present system. GPS radiosonde system is set as the target of future upper-air sounding system in China, while considering the price factor, a transition scheme of 1680MHz secondary radar with new radiosonde is made firstly. During the 3 years period of gradual replacement with the new system for radiosonde stations all over the country, the 701secondary radar system is still used at part of station network and requires new radiosonde to improve its performance. Of course, GPS technique must be considered in the new radiosonde to meet the requirements WMO makes for GCOS stations.

So the new radiosonde for Chinese ground equipments should be as follows:

It should be better to fit three different systems: present 400MHz 701 secondary radar, near future 1680MHz secondary radar, and the future GPS windfinding system.

It should fulfill WMO's accuracy requirements for upper-air measurements, with a high S/N rate and an output power enough to get the range of 200km. It must be light, easy to use, stable to store, and low-priced.

It should adopt advanced technologies, high-grade devices, and up-to-date designs. To match different sensors and transmitters, modularization and seriation are adopted.

2. Description of the New Radiosonde

Shanghai No.23 Radio Factory has developed a new radionsonde (hereafter as Newsonde) to meet all needs mentioned above, which has won the bid from CMA.

The Newsonde is a microprocessor-based digital type. It contains the blocks of Sensors, Intelligent Conversion, Transmitter and Battery.

The temperature sensor nowadays is a new design of fast response rod thermistor, with the measuring range of +50℃~-90℃, and resistance of 10~700kΩ. Its length is 10mm, and diameter including the high reflection coating is only 1mm. In future, a metal wire may also be used. The humidity sensor is a small chip of hygristor, with performance of broad measuring range, high reliability, good changeability and fast response, and the dimension of 35×6×1mm. Capasitive humidity sensor may also be used later. As for the pressure sensor, two types can be chosen: a capacitive aneroid capsule with 25mm diameter and 3~8pf

capacitance variation in 1050~10hPa range, and a solid state silicon pressure sensor, both are sensitive and with very small lag.

The Intelligent Conversion has very good compatibility to all kinds of sensors as it can input all variable parameters such as resistance, capacitance, voltage, and current. It can also fit different transmitters compatible to radiotheodolite and secondary radar, and as well as GPS receiver. Through R/V, C/V converters or amplifier signals from temperature, pressure and humidity sensors are input to the multiplexer. The A/D converter is a software-based double integration type, with conversion resolution of more than 14 bits. A microprocessor is used to control the multiplexer and the A/D converter, and process the digitalized PTU signals. At most 7 parameters can be processed in the Conversion, with sampling period of 1 second, 0.2 S of which is used for radiosonde data, total 21 bytes including sonde ID, and 0.8 S is idle time used for transmitting ranging signal or re-transmitting GPS signals (see following Figure).

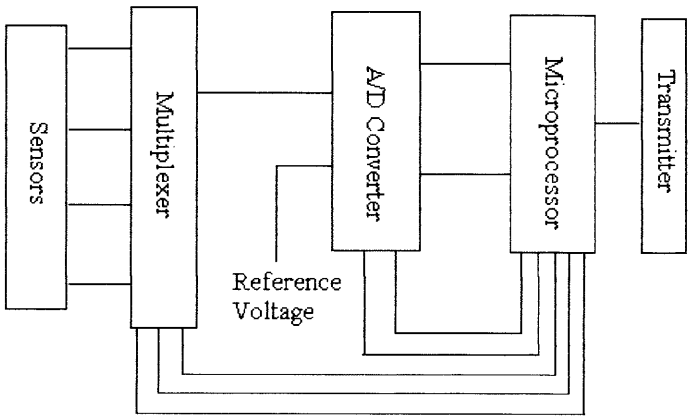

The power source is 20V water-activated magnesium-cuprous chloride battery. Calibration data is stored in a floppy disk that is supplied with radiosonde, and meanwhile the calibration curve can also be provided. The instrument weighs about 300 g including battery.

3. Key Technologies

The Newsonde adopts some new hi-tech means to enhance its performance; let's see three of them.

i. Solid state silicon pressure sensor

It is a very sensitive semiconductor device, with high accuracy, small dimension, and very small lag. However, if no measure is taken, its temperature coefficient will be quite big, with 5% above 0℃ and over 7% bellow 0℃; and in addition, it is non-linear. The problem we have solved by software compensation, and it is tested well.

ii. Intelligent Conversion

There are many types of A/D converters for us to use. Considering that the sampling rate of radiosonde is not high, while its accuracy requirement is strict, and considering that the cost of radiosonde must be quite low, especially that our Newsonde has a price much lower than that of the similar ones in world , we adopt software-based double integration A/D conversion, with conversion accuracy of 0.2‰. Together with the single chip microprocessor, external integrator, comparator, and others, the Intelligent Conversion has a very stable conversion performance in low temperature as well as in normal temperature.

iii. Subcarrier Technique

When the Newsonde is for 701 secondary radar, it must be considered that the frequency interference should be reduced, and that 701 radar cannot be changed any. In 1970's, when we received the signals from an old type of electronic radiosonde with 701 radar we found that the radar transmitting signal changed the

radiosonde measuring frequency. A control device must be added to turn down the radar transmitter during receiving of radiosonde PTU signals and re-turn on radar transmitter during the idle time of PTU signals.

The problems we have solved by adding to the Newsonde a crystal oscillated subcarrier modulation, and also adding a special demodutator to the ground equipment, so as to reduce frequency interference, while no need to change radar transmitter switching.

30 in situ flights have been successfully made with this technique in the Newsonde to match 701 radar. Also the technique has been used in some GZZ2-701 stations, and will be in more and more other stations. The results are quite good; the flying height increases a lot. The annual average burst rate of balloon at Shanghai Upper-air Station has even enhanced from 49% to 95.6%.

4. Test Results (extract from the Test Report of CMA's Atmospheric Observing Experimental Base)

i. Static Test: From Dec.1998 to Jan.1999 the CMA's Atmospheric Observing Experimental Base held two static tests for the Newsonde from Shanghai No.23 Radio Factory. Each test works on 6 Newsondes extracted from 60 sets and 200 sets respectively. The results are in following table:

Temperature		Humidity		Air Pressure	
Requirement	Test Results	Requirement	Test Results	Requirement	Test Results
±0.3℃	1.±0.1℃ 2.±0.08℃	±5%RH (above-25℃) ±10%RH (bellow-25℃)	1.±3.6%RH 2.±1.8%RH	±1hPa (above 500hPa) ±2hPa (bellow 500hPa)	1.±0.66hPa 0.42hPa 2.±0.38hPa 0.24hPa

ii. Dynamic Tests: From Dec.1998 to Oct-Dec.1999 the CMA's Atmospheric Observing Experimental Base held two dynamic tests for the Newsonde from Shanghai No.23 Radio Factory.

a. First Test:

Five comparison flights were made with Vaisala's GPS system. The results show that average difference of pressure is within +1hPa and −1hPa, that of temperature is within 0℃ and −0.4℃, and humidity meets each other in low level.

b. Second Test:

From 20 Oct. 1999 to 6 Dec.1999 a total of 80 flights were made. The results of minute to minute synchronic comparison with Vaisala GPS sonde are as follows:

Air pressure: The difference to Vaisala GPS sonde is only 0.5hPa. Systematic error of one-year-stored Newsonde compared to GPS is smaller than that of newly-applied ones.

Temperature: The temperature records of Newsonde bias low at night but do not exceed −0.4℃. It biases high in daytime but does not exceed 0.4℃ bellow 100hPa and not exceed 0.8℃ in high level. The cause may be that the coating of thermistor is not thick enough, then the solar radiation error is too big.

Humidity: It biases not more than 3% lower in low level and biases high in high level of 300hPa above. The following table shows the results of international comparison of VIZ, AIR, GZZ2 to RS80 in 1989(*) compared with this test comparison.

Pressure	VIZ	AIR	GZZ2	Newsonde
900	1	4	-4	-2
700	1	1	-6	-3
500	6	6	2	0
300	10	9	7	6

It can be seen that Newsonde is better than GZZ2 and not too much different to VIZ and RS80 in low level, and the measurements of all four are bigger than RS80 in high level. But the difference of Newsonde is the smallest.

c. Standard deviations of Newsonde

Twin flight was held of two Newsondes with different transmitters each tracked by L-band radar and 701 radar. The standard deviations are as follows:

Air pressure: <1hPa;

Temperature: <0.1℃ at night and <0.2℃ by day;

Humidity: not more than 5% RH in whole troposphere.

5. Conclusions

After preliminary tests by users and examinations of in situ comparison flights, the Newsonde proves to be of high sampling rate, high measuring accuracy, excellent anti-interference, high reliability and low price, and fit to several types of Chinese ground equipment. If further improved, it will certainly enhance the quality of upper-air measurement and reliability of data acquisition in China.

Acknowledgements

The authors wish to thank CMA's Atmospheric Observing Experimental Base for strict tests and in situ comparison flights of the Newsonde; thank Prof. Huang Bingxun for submitting important suggestions for improvement on Newsonde tests and our paper.

References

*: Ivanov,A., Kats, A. , Kurnosenko,S. , Nash,J. , and Zaitseva,N. , 1991: WMO International Radiosonde Comparison, Phade III, Final Report. WMO, Instruments and Observing Methods. REPORT NO.40

New Stabilised Balloons for GPS Radiosondes

Jean Barat
Professor at the Pierre & Marie Curie University
Place Jussieu, Paris V, France
Tel: 01 64 47 42 90 E-Mail: jean.barat@aerov.jussieu.fr

Introduction

The in-situ wind measurements performed by the stations of the meteorological nets are usually obtained by tracking a balloon which is assumed follow the atmospheric flow with an appropriate system like i.e.: Omega or Loran C, Radiotheodolites, Meteorological radars.....). In these conditions the representativity of the wind measurement depends both on the balloon as a wind sensor and on the tracking system accuracy. Because the weak resolution of the tracking systems used until now, the meteorological balloons' performances as wind tracers have been more than enough. Problem began when more accurate tracking systems (like millimetric FPS16 radar used by the US ranges) have been used to obtain better wind measurements. In this case the meteorological balloons have immediately showed their limits and special balloons have been developed, like the famous Jimsphere which is still used since its introduction in 1965.

The recent arrival of GPS sondes in meteorological nets is completely changing the problem because the GPS locating accuracy is at least as good as the better tracking radars. In these conditions, classical meteorological balloons are no more adapted to GPS sondes; the accuracy of wind measurements being now too weak due to the bad behaviour of these balloons as wind sensors. As the cost of radiosoundings is very important for the nets, it is not possible to work with Jimsphere balloons which are very expensive (radar cost not included). We show in this paper how the use of a very simple and low cost aerodynamical appendix modifies totally the balloon's behaviour, without changing its structure and particularly its performance. A such stabilised balloon allow to produce winds that approach radar-Jimsphere quality.

Principle

The Reynolds number charactizing the flow around classical meteorological balloons (with ground diameter typically between 1.4 and 2 m) are supercritical up to altitudes of 10-12,000m, i.e. practically in the whole troposphere. This has two extremely important consequences

1) The balloon aerodynamic drag coefficient Cx is very weak (around 0.12). As this coefficient characterizes the ability of the balloon to follow the atmospheric flow it is not a good wind sensor and it will not restitute the fine structure of the wind profiles.
2) At supercritical Reynolds numbers the self-induced motions are erratic and occur over a broader band of frequencies so that the velocity of the GPS sonde is no longer representative of the atmospheric velocity.

Both phenomena are closely linked and it is difficult to study them separately. Practically, mostly of the second can be observed easily because of the very large radiosonde velocity amplitudes which are obviously not related to the atmospheric flow. To approach the real atmospheric velocity the radiosonde' manufacturers use generally an internal data processing which smoothes the radiosonde velocity on long time intervals so that erratic motions are reduced. In practice it brings to reduce the vertical resolution under 400-500m. This value is really insufficient in the low atmospheric layers especially if one takes into account the possibilities of the GPS tracking. In 1965 Scoggins designed the Jimsphere which is a surpressurized 2m diameter sphere with 398 roughness elements (cones). This configuration allows obtaining a narrowband of the self-induced motions with a vertical wavelength of about 25m and oscillations of about 3m/s. The vertical resolution of

the Jimsphere as a wind sensor is of 100m, i.e. a gain of factor 5 compared to meteorological balloons.

In order to obtain the same result with smooth meteorological balloons we have used to modify the supercritical flow around balloon an high Cx (>2) aerodynamic appendix (sail) fixed rigidly on its upper hemisphere. The longitudinal dimensions of the appendix are between 30 and 70 cm. Because the Jimsphere is turning on itself during the ascent the roughness elements must cover all its surface. On the contrary the sail is unique, its angular position remaining constant because the torque of the GPS sonde mass hanged below the balloon.

While the Jimsphere can only carry a light mass and is limited to 18 km the stabilised balloons are basically meteorological balloons with a bursting altitude depending only on their dimensions. Practically the system may be used with balloons up to 2000g and even more.

Results

Qualitative results

In the Figure 1 we compare the E/W GPS sonde velocity profiles obtained in the same conditions (string of 25m and 350g balloons) with a stabilised and a non stabilised balloon. The standard balloon was carrying a Modem type GL98 GPS sonde and the stabilised balloon a Vaisala RS80 GPS sonde. In order to present a better visual comparison we show in the Figure I a vertical expansion of the profiles. With the classical meteorological balloon large erratic velocity fluctuations (±6 m /s) are clearly evident: they cannot be caused by the atmospheric flow and they are artefacts related to the self induced motions at supercritical Reynolds number. Because the erratic behaviour of these motions the 120m vertical smoothing does not suppress them and the corresponding profile exhibits large amplitude noise (error). It is the reason for which the data processing used classically smoothes data over large intervals. On the other hand one observe on the 1 Hz stabilised balloon velocity profile regular oscillations of 2m/s amplitude quite comparable to that of the Jimsphere : the 120m vertical smoothed profile is now regular and the GPS sonde velocity is then quite representative of the atmospheric velocity.

Quantitative results :spectral analysis

To calculate the wind accuracy of a GPS sonde-balloon system and in particular to evaluate the error due to the balloon erratic motions (noise) it is useful to perform spectral analysis and then to calculate the vertical energy density of the GPS sonde velocity. If the erratic motions are negligible the vertical spectrum follows, function of the wave number, a 2.8 power law which correspond to the " universal spectrum theory ". If erratic motions become dominant it appears in the spectra a broader band of noise frequency so that the measured spectrum differ from the universal variation law spectrum. The comparison between the two spectra allow to define both the velocity error to a given vertical resolution (2) and the effective vertical resolution (3) which is defined as the wavenumber for which the noise dominated spectrum is twice its theoretical value. In the figure 2 we present the vertical spectra of the GPS sonde velocity calculated over all the troposphere both for the stabilised balloon and for the conventional balloon. The spectrum of the non stabilised balloon shows large deformation due to the self-induced motions and the vertical resolution which is calculated from the transition from signal domination to noise domination is 450m. At the inverse, on the stabilised balloon spectrum, the self-induced motion is apparent only at high wavenumbers so that the effective resolution is 120m . On other than the noise error is, for 100m resolution, equal to 0.8m/s for a classical balloon while for the stabilised balloons it is only 0.07m/s. Otherwise, following the NWS 99 definitions (4) the wind sampling period is thus 24 times superior to the one of the GPS sonde sampling (1Hz). In the case of an ordinary meteorological balloon the ratio grows to 90, that means a measurement availability rate falling to 1%. We assume an ascent velocity of 5m/s.

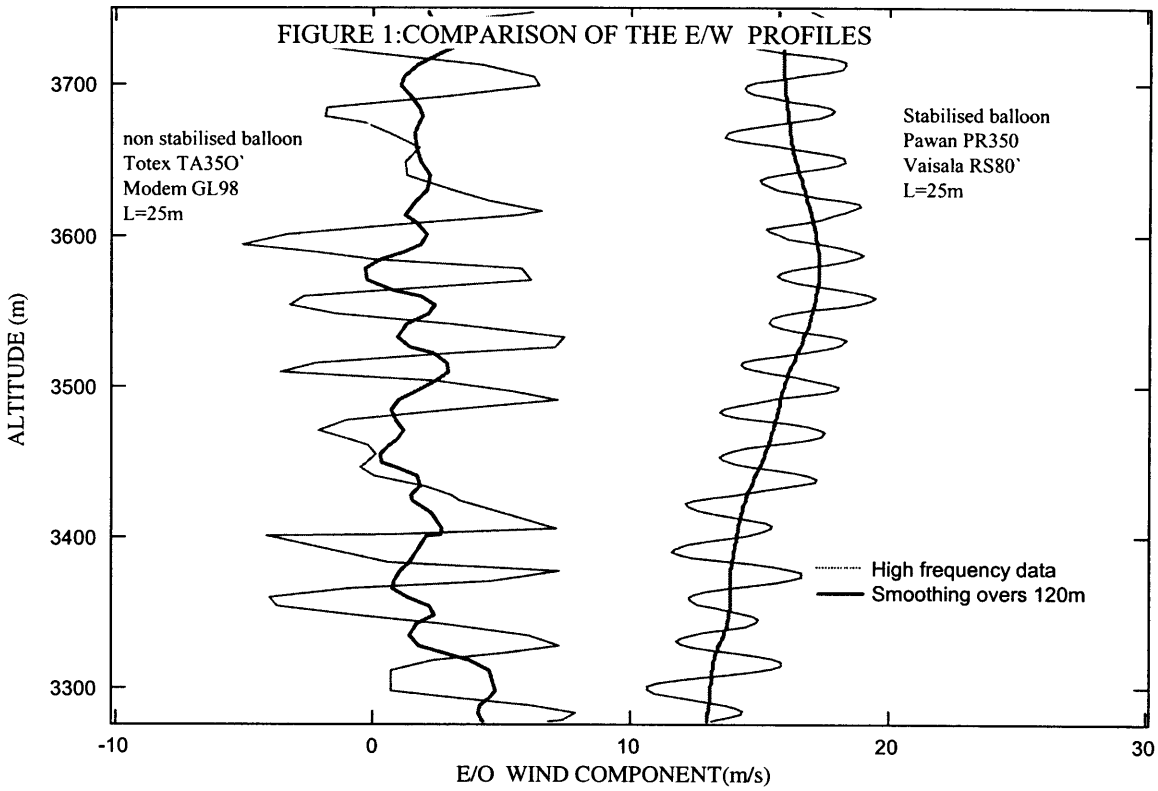
FIGURE 1:COMPARISON OF THE E/W PROFILES
non stabilised balloon
Totex TA35O'
Modem GL98
L=25m
Stabilised balloon
Pawan PR350
Vaisala RS80'
L=25m
High frequency data
Smoothing overs 120m
ALTITUDE (m)
3700
3600
3500
3400
3300
-10
0
10
20
30
E/O WIND COMPONENT(m/s)

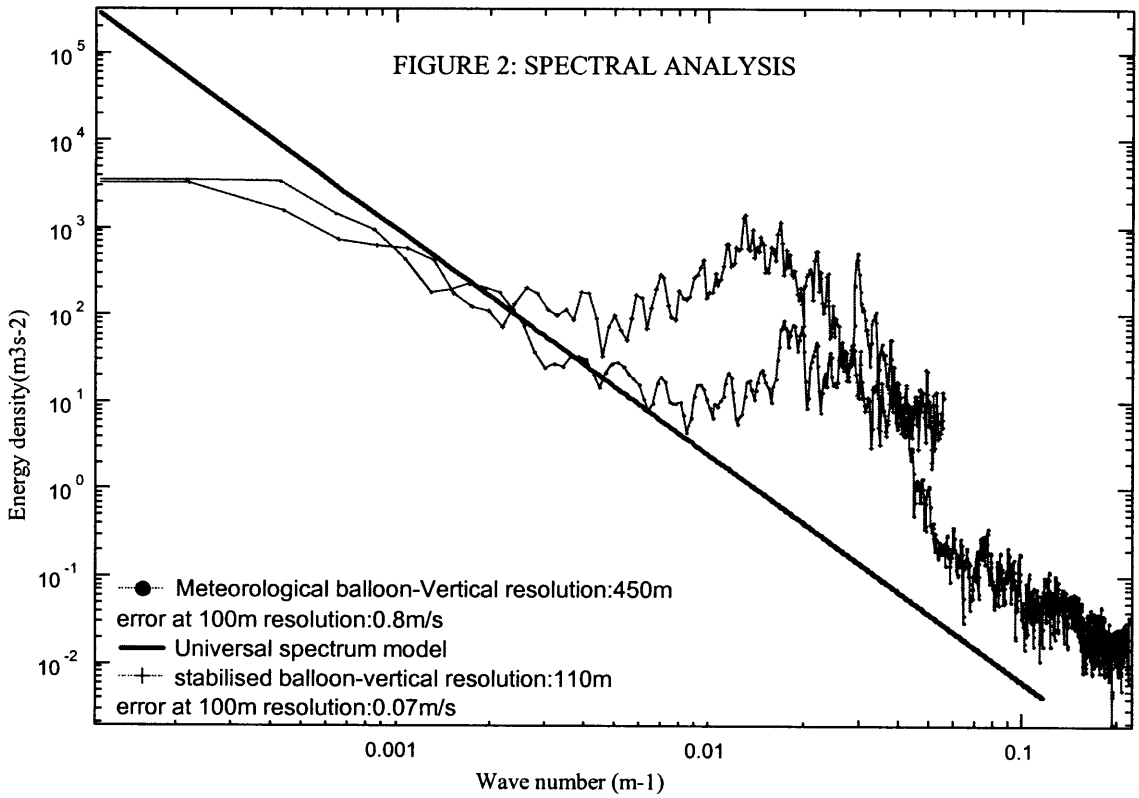
FIGURE 2: SPECTRAL ANALYSIS
Energy density(m3s-2)
10^5
10^4
10^3
10^2
10^1
10^0
10^-1
10^-2
Meteorological balloon-Vertical resolution:450m
error at 100m resolution:0.8m/s
Universal spectrum model
stabilised balloon-vertical resolution:110m
error at 100m resolution:0.07m/s
0.001
0.01
0.1
Wave number (m-1)

Conclusions

Paradoxically the recent arrival of the GPS sondes in meteorological nets has introduced a problem which was until then largely ignored. The high accuracy of the GPS tracking shows large erratic motions of the classical meteorological balloons which were occulted by the poor resolution of the old tracking systems. As described above these artefacts are related to the self induced motions of smooth balloons rising at a supercritical Reynolds number. In order to eliminate this effect 398 roughness elements (cones), 8 cm height, are used on the Jimsphere balloon so that the atmospheric flow is modified upstream. There are two conditions:

1 Use of a rigidically fixed appendix in order to fully transmit the aerodynamic forces to the balloon;
2 Act on the upstream airflow in order to modify its structure all around the balloon.

In the past several systems have been tentatively used to suppress or to reduce the effects of self induced motions. All were characterised by the fact that they acted behind the balloon and that they were not rigidly positioned on the balloon skin: we can mention solutions like to limit the radiosonde oscillations (damping by the neck of the balloon or by the string) or to use inverted parachute.

It is easy to note that these systems are not modifying the drag coefficient of the balloon itself and the wind measurement's accuracy cannot be improved therewith.

By using a single sail rigidly positioned on the upper hemisphere of a classical meteorological balloon we have presented in this paper a very simple and inexpensive system which totally modifies the balloon's behaviour as wind sensor. It allow to produce winds which approach the radar tracked Jimsphere quality. This has been showed during the tests conducted at Wandenberg, 2000 January, and which results have been recently presented(5).

References

(1) Scoggins J.R. 1967. Sphere behavior and the measurement of the wind profiles. NASA TN-3994,53p. Disponible au service d' information de la NASA, Washington DC 20546-0001J

(2) Barat Jean et Charles Cot,1995 : Accuracy analysis of Rubsonde-GPS Wind Sounding System. J. Appl.Meteor., 34, 1123-1132.

(3) Timothy.L.,Wilfong, Steve Smith and Christy Crosiar,1997 : Characteristics of High Resolution Wind Profiles Derived from Radar-Tracked Jimspheres and the Rose Processing, Program. J. Atmos.and Oceanic Technology, 14, 318-325

(4) Specification NWS-J070-RS-SP005 for Global Positionning System –Radiosonde and Signal Processing System, Nov 8, 1999.

(5) Timothy L. Wilfong,, Jean Barat, Christy L.Crosiar and Richard Walterscheid : Characteristics of Wind Profiles Derived from a Stabilized Balloon and Differential GPS Technology. Presented at the Meeting Range Missile, Orlando, September 2000

New instruments for Russian upper-air network

A. Balagurov, V. Grinchenko, A. Kats,
KOMET, 3/6, Pervomayskaya Str., 141700, Dolgoprudny, Moscow.Reg., Russia
Tel/fax: (+7-095) 4086104, e-mail: komet@mtu-net.ru

The WMO Comparison /3/ as well as the following upper-air data quality monitoring /4,5/ proved sufficient quality of Russian AVK ground stations wind-finding, but also revealed essential problems with temperature and especially humidity sensors of operational Russian MRZ-3 radiosonde. 2.2 mm white-painted rod thermistor has significant infrared radiation error /1/, rather slow time response and modest reproducibility /2/, while obsolete gold-beater skin humidity sensor at all concedes modern humidity sensors /2,6,7/.

Rapid implementation of market economy also forced Russian Federal Hydrometeorological Service (Roshydromet) to look for alternate vendor of radiosondes to avoid having sole radiosonde manufacturer. There was alternative choice on the market – proven in the same comparison Vaisala DIGICora-RS80 sounding system, but its direct introduction didn't provide secure investments. There were about 100 AVK ground stations deployed on the upper-air network quite recently.

In this situation it was found a rational direction to find a solution — combining in the same radiosonde world-wide known Vaisala sensors and proven Russian VHF transmitter-transponder unit, ensuring compatibility with existing ground station under its minimal rearrangement. Development of new radiosonde and interface equipment was ordered to Central Aerological Observatory of Roshydromet (CAO) under support of Vaisala, both financial and technical. New radiosonde received name RF95. It carries RSS80TU sensor unit of RS80 radiosonde without pressure capsule, adapter unit, including frequency divider to meet pass band of AVK receiver, and VHF transmitter-transponder, similar to one of MRZ-3. Foam plastic case of radiosonde was specially designed for optimal arrangement of sensor boom, all internal electronic devices and battery (the same as in MRZ-3).

The most complicated obstacle was the obsolete built-in ROM firmware of AVK dedicated computer. Its upgrade, demanding hand-made reprogramming, would request too many funds and time. Therefore, it was decided to utilize modern digital equipment, allowing arbitrary transformation of telemetry signal before input to AVK dedicated computer. It was designed special microprocessor-based interface unit RM95 to be installed into low-frequency telemetry channel of AVK. RM95 converts in real time telemetry frame of RF95 (~1.5 s) into one of MRZ-3 (~21 s), preserving the same relationships between dimensionless "y-parameters", used in calculations of temperature and humidity for both zondes. In this way RM95 doesn't require any information concerning calibration of specific radiosonde. The main difference to operator is choice of sun elevation to be put into AVK dedicated computer – special table was introduced from best fit of RSS80TU radiation corrections by ones of MRZ-3. RM95 is installed into free space of one of AVK unit and is powered by internal power sources of AVK. In shutdown state it doesn't influence usual operation of AVK with MRZ-3. Installation could be performed within several hours by one technician.

On 22 of April 1996 the first RF95 was launched in Dolgoprudny. Performed special laboratory and flight tests have validated chosen solutions. Also special tests with RS80-RF95 twin-flights were held in Dolgoprudny 13-14.05.96 (totally 5 flights). They showed reasonable agreement between RS80-DIGICora and AVK-RF95 observations (see **Fig.1**), taking into account AVK dedicated computer processing.

Roshydromet authorities approved results of RF95 development and approval tests. For manufacturing of RF95 Roshydromet established on the basis of CAO the Federal State Unitary Enterprise KOMET. In April 1997 experimental flights of brand-new RF95 were started in Dolgoprudny. At the same time it was started organization of production line. Essential support was received from RF95-NW – project, arranged according to the Agreement between Roshydromet and Finnish Meteorological Institute (FMI) on the support of aerological programmes during

01.08.1997 - 31.12.1999 on two Russian stations (St. Petersburg and Murmansk) using a new radiosonde RF95.

In September-October 1997 operational test of RF95 started on Voejkovo (nearby St.Petersburg) and Murmansk upper-air stations, which finished successfully in March 1998. Roshydromet authorities approved test results and RF95 was recommended for operational use on the Russian upper-air network. By the end of 1998 the development, production and purchase of special equipment, instruments and devices to be used for manufacturing of details and units, assembling, tuning and control of radiosondes RF95 was completed, relations with all subcontractors arranged. Radiosonde has passed all stages of tests, certification and licensing by Gosstandart of the Russian Federation and was brought into the State registry of instruments of the Russian Federation (registration №17225-98) with following technical specifications:

Temperature measuring range:	from –90 till +50 °C
Humidity measuring range:	from 0 till 100 %RH
Maximum allowed temperature error under operation conditions:	less than 1 °C
Maximum allowed humidity error under operation conditions:	less than 7 %RH
Sensors unit:	Vaisala RS80 radiosonde sensors unit
Power supply:	water-activated battery
Dimensions:	115x115x190 mm
Flying weight:	less than 300 g

New value has been added to RF95 usage by introduction to AVK ARM AEROLOG(ARM)– specialized workstation designed by KOMET. It includes PC with relevant software and microprocessor-based interface board US96, to be built into AVK unit, that performs LF telemetry signal measurements and identification(both of RF95 and MRZ-3), readings of digital radar-tracking data from AVK registers and transmitting information to PC via serial interface (all solution were made in coordination with developer of AVK). Workstation software implements all tasks relevant to upper-air data processing: input of sonde calibration data, conversion of engineering units into meteorological ones, base-line checking, pressure derivation and windfinding, preparation and transmitting of upper-air messages. It removes all restrictions, implied by application of RM95, that result in:

- full compensation of temperature influence on humidity measurements
- native Vaisala radiation correction scheme taking into account real vertical ascent rate and actual sun elevation changes during ascent
- complete use of RF95 high sampling rate and fast response sensors with higher vertical resolution.

At the same time application of PC brought up new attractive features:

- input radiosonde calibration data from disk files
- graphic presentation of profiles and graphical tools for selection of their prominent features (see **Fig. 2**)
- advanced raw and output data on-line and archive presentation especially for data quality analysis (see **Fig. 3**)
- data storage and archiving on PC instead of paper printout
- advanced communications capabilities with telephone modem or teletype adapter
- possibility of unreliable dedicated AVK computer elimination.

The first ARM was installed on Murmansk upper-air station by the end of October 1998. After week of training station's staff all alone started experimental operation with learning and in the mid of December 1998 ARM came to operational test. In 2000 Roshydromet authorities proved results of approval and operational tests and recommended ARM Aerolog to operational use on the Russian upper-air network.

Relevant changes were introduced into WMO Manual on Codes to reflect RF95 (with RM95) and ARM (with RF95 and MRZ-3) usage in 31313 group of TEMP message.

Since beginning of 2000 six Russian upper-air stations operate RF95 routinely, three of them use ARM Aerolog routinely and on two others it's installed on the trial basis. Already more than 5000 RF95 were launched on the Russian upper-air network. It's planned to increase amount of stations, using RF95 and ARM AEROLOG.

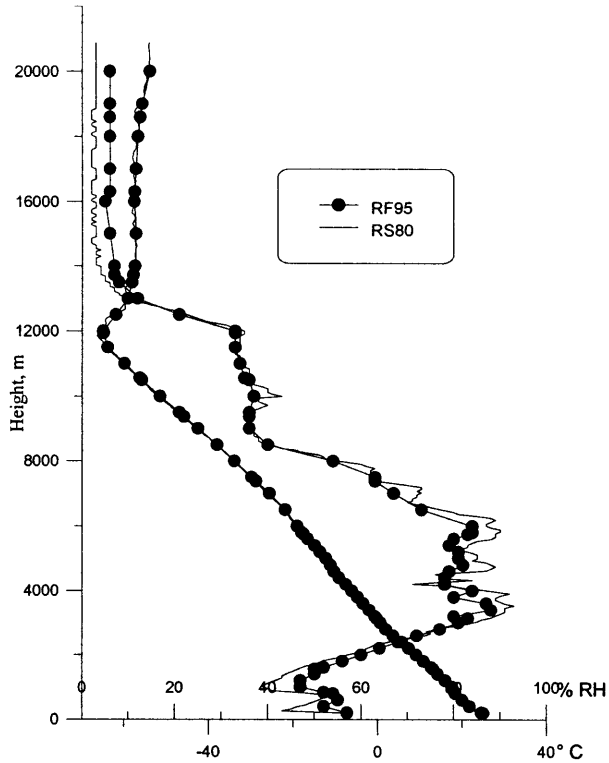

Fig.1 RF96-RS80 twin flight. 13/05/96-12UTC at station 27612.

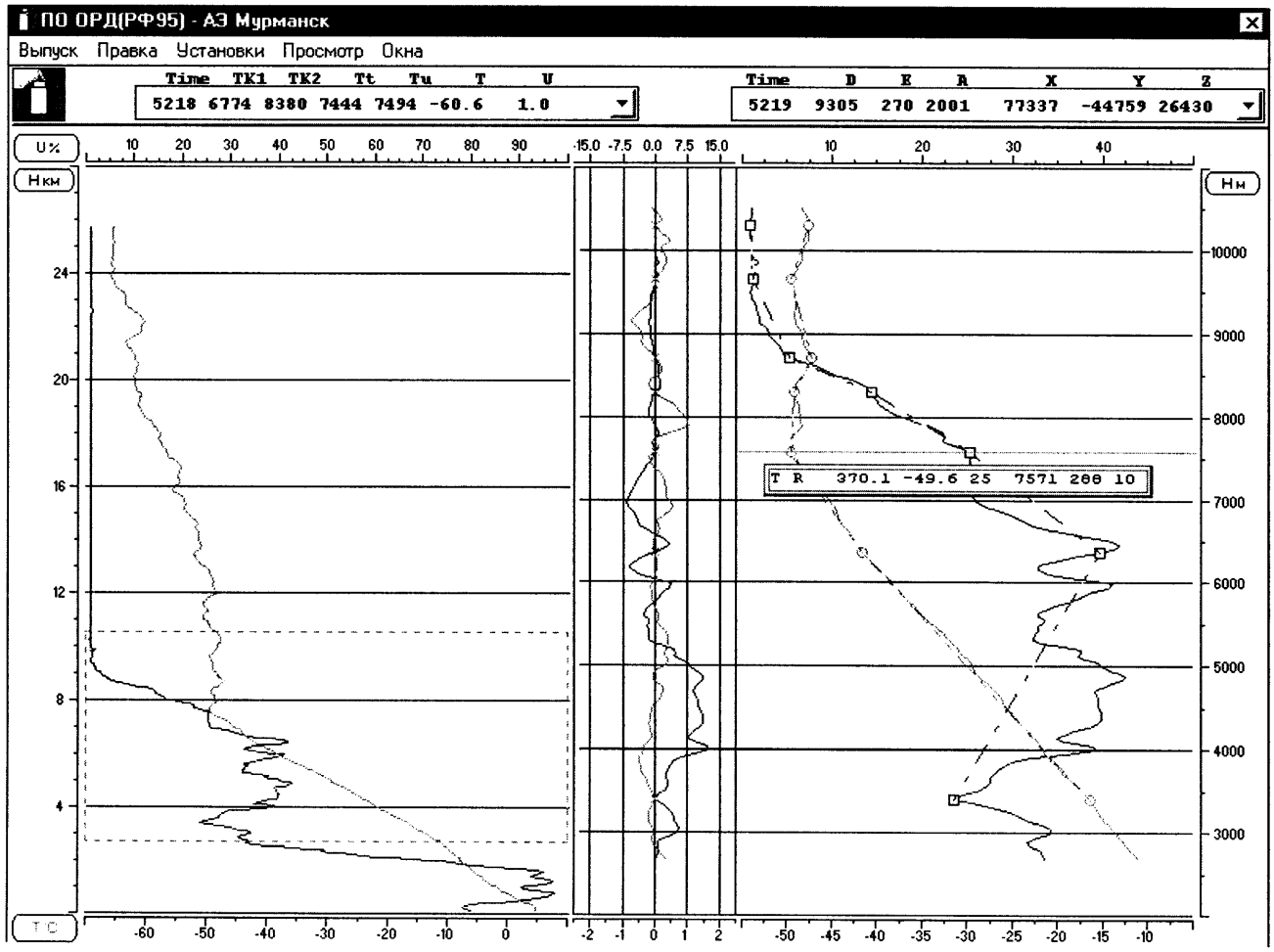

Fig. 2. ARM Aerolog significant point selection features(temperature and humidity). Ascent 9/10/1998-12UTC, station 22113.

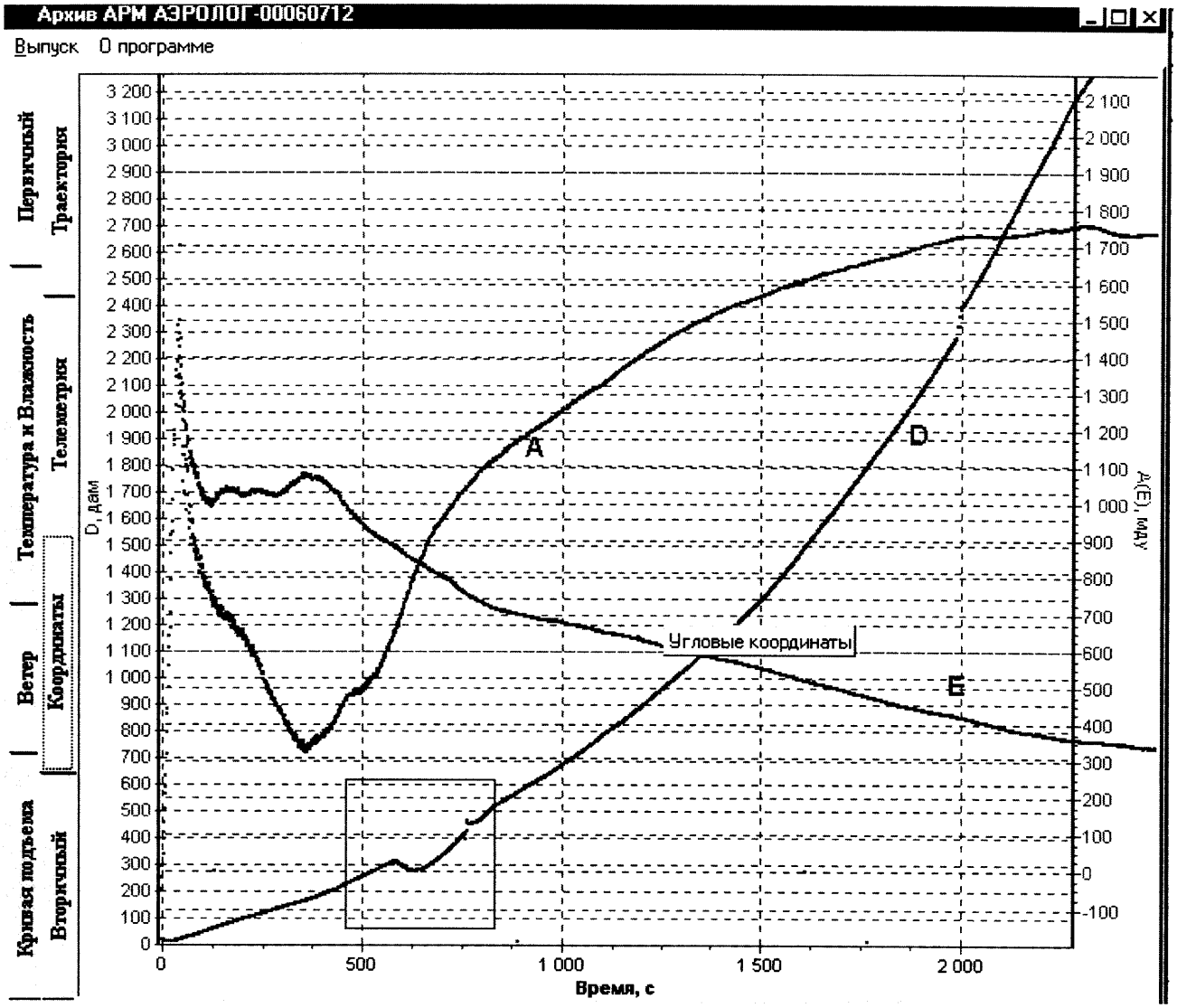

Fig. 3. Example of ARM Aerolog raw data presentation capability. Angular radar tracking data. Slant range(D) in dam, azimuth(A) and elevation(E) in °/0.06 versus time in s. Ascent 06/07/2000-12UTC, station 27612.

References:

1. M.B.Fridzon at all. 1988. Radiation Corrections in Radiosonde Measurement of Temperature. Meteorologia i Gydrologia [Soviet Meteorology and Hydrology], No. 6.
2. M.B.Fridzon. 1989. Estimation of Temperature and Humidity Radiosonde Measurements Errors on the USSR Upper-air Network. Meteorologia i Gydrologia [Soviet Meteorology and Hydrology], No. 5.
3. A. Ivanov at all. 1991. WMO International Radiosonde Comparison - Phase III : Dzhambul, USSR, 1989 / Final Report. WMO, Inst. And Obs. Methods, Rep. No. 40.
4. A. Ivanov, A.Kats. 1994. On the quality of measurements of geopotential heights of isobaric surfaces on the CIS upper-air network Meteorologia i Gydrologia, No. 3.
5. A.Kats, A.Ivanov , I. Potemkin. 1996. Automated system of upper-air network operation quality monitoring. Roshydromet scientific conference on results of in hydrometeorology and environment pollution monitoring.
6. A. Balagurov, A. Kats, N. Krestyanikova. 1998. Implementation and Results of the WMO radiosonde humidity sensors intercomparison (Phase I laboratory test). TECO-98. WMO, Inst. And Obs. Methods, Rep. No.70.
7. F. Schmidlin. 1998. Summary of the WMO International Radiosonde relative humidity sensor comparison - September 1995 - Phase II "Field test". TECO-98.WMO, Inst. And Obs. Methods, Rep. No. 70.

NEW RADIOSONDES FOR RUSSIAN SYSTEMS OF UPPER-AIR OBSERVATIONS

V.E.Ivanov[1], *S.P.Essyak*[1], *V.F.Lazarev*[1], *V.L.Volkov*[2], *G.S.Zakharova*[2], *V.T.Bogov*[3]

[1]Ural State Technical University, Ekaterinburg, Russia.

[2]Institute of Solid State Chemical of the Ural Centre Russian Academy of Sciences, Ekaterinburg, Russia.

[3]Joint-stock Company *METEO*, Ekaterinburg, Russia.

Phohe: (3432)427-646, Telefax: (3432)464-997, E-mail: meteo@emts.ru

ABSTRACT

In this paper quotes a description of the new radiosondes MRZ-10, intended for using with the radars AVK-1, "BREEZE" and with the radiotheodolite MARL-T.

In radiosondes are used new sensors, manufacted with the aid of microelectronic technologies: the humidity - based on the resistive thin-film structures of the polyvanadic acid and on the capacitive structures on the polimide films; the pressure - based on the silicon diaphragm with the integration piezoresistive pickoff. For high-precision measurement of the temperature is used a sensor, based on the thin platinum wire.

For the transmisson of the telemetric signals in radiosondes can be used superregenerative reciver-transmitter, which additionaly provides the possibility of measuring the slant range up to the radiosonde; and also can be used a transmitter with the high-stability of the carrier frequency 1680*MHz*.

For supplying the radiosondes are supposed to be used new battery packs with improved characteristics.

In the paper are discussing the peculiarities of the technical execution of new radiosondes; questions of the precision measuring of meteovalues under using the new sensors; and also there are quoted the results of the tests of theese radiosondes.

1. ВВЕДЕНИЕ

Аэрологические наблюдения, выполняемые с помощью радиозондов, являются в настоящее время основным источником информации о состоянии тропосферы и нижней стратосферы. На территории СНГ и ряда государств эти наблюдения проводятся российскими системами радиозондирования АВК-1/МРЗ-3 и "Метеорит"/МАРЗ-2, которые хорошо зарекомендовали себя в процессе их длительной эксплуатации. Однако на сегодняшний день они уже достаточно устарели, как в части используемой в них наземной аппаратуры, так и в части радиозондовых датчиков метеовеличин, которые в значительной степени определяют точность измерения параметров атмосферы. В настоящее время разработаны и внедряются на аэрологической сети новые радиозондовые системы, использующие современные малогабаритные радиолокационные станции "БРИЗ" и МАРЛ, производится также модернизация существующей на сети аппаратуры системы АВК-1.

Для использования в новых системах радиозондирования разработаны и готовятся к серийному производству на ОАО"МЕТЕО" радиозонды серии МРЗ-10 (в различных модификациях) с использованием высокоточных датчиков метеовеличин, выполненных на основе современных технологий.

В докладе обсуждаются особенности технической реализации новых радиозондов, рассматриваются вопросы точности измерения метеовеличин при использовании новых датчиков, а также приводятся основные характеристики этих радиозондов.

2. ДАТЧИКИ МЕТЕОВЕЛИЧИН

В новых радиозондах МРЗ-10 используются датчики трех основных метеовеличин, измеряемых при зондировании атмосферы - температуры, влажности и давления.

В качестве датчика температуры в радиозондах МРЗ-10, как и в радиозондах более ранних разработок (МРЗ-3, МАРЗ), используется полупроводниковй терморезистор, обеспечивающий среднеквадратичную погрешность измерения темпераурь не

более 0,5-0,7°С. В модификациях радиозонда МРЗ-10 с повышенной точностью измерения температуры используются металлические микрофольговые и тонкопроволочные терморезисторы, обеспечивающие повышение стабильности, улучшение динамических характеристик, а также уменьшение радиационной погрешности. Так в качестве образцового датчика температуры используется тонкопроволочный (платиновый) датчик [3], радиационная погрешность которого на высоте 30*км* не превышает 0,5°С, что позволяет использовать его в качестве метрологического средства для оценки точности измерения температуры сетевыми радиозондами в реальных условиях зондирования атмосферы.

В качестве датчика влажности в радиозондах МРЗ-10 используется интегральный пленочный датчик [2], чувствительный элемент которого выполнен на ситалловой подложке размером 8×4*мм* и представляет собой "сэндвич"-струкруру с верхним электродом из тонкого влагопроницаемого слоя золота. Его действие основано на зависимости диэлектрической проницаемости пленки полимерного сорбента от количества сорбируемой им влаги. Достоинствами этого элемента влажности является линейная характеристика преобразования, малый гистерезис, высокое быстродействие, широкий температурный диапазон измерений, высокая воспроизводимость характеристик. Выходным информативным параметром элемента является электрическая емкость в диапазоне 130-170*пФ*, при чувствительности $\approx 2{,}5\cdot 10^{-3}$ 1/%*RH*. Среднеквадратическая погрешность измерения относительной влажности воздуха таким датчиком не превышает 2%*RH*.

Для измерения атмосферного давления в радиозондах МРЗ-10 используется (при необходимости) интегральный кремниевый датчик мембранного типа, работающий на принципе поперечной тензоэдс. В настоящее время наибольших успехов в области создания таких датчиков добилась фирма *MOTOROLA*, разработавшая и изготавливающая большую номенклатуру датчиков давления для общепромышленного применения, которые при низкой стоимости имеют достаточно высокие метрологические характеристики. В радиозондах МРЗ-10 нами использован датчик типа MPX100A, содержащий только "чистый" тензоэлемент давления без каких-либо встроенных нормализующих и термокомпенсирующих схем. При этом требуемая точность преобразования давления (0,5-1,0*гПа*) достигается за счет индивидуальной градуировки каждого радиозонда при нескольких температурах окружающей среды и использования алгоритмического метода коррекции погрешностей.

В результате проводимых нами исследований золь-гель метода получения пленок сложных оксидных соединений элементов IV-VI групп периодической системы синтезированы материалы, обладающие комплексом свойств, которые могут быть использованы при разработке радиозондовых датчиков метеовеличин. Перспективными для практического применения являются пленки чувствительные к изменению влажности воздуха [1]. При нормальных условиях электическое сопротивление таких пленок (R) изменяется по логарифмической зависимости ($\ell gR=a+b\varphi$) в интервале относительной влажности вохдуха (φ) от 12 до 98%. Проведенные испытания показали, что датчик выполненный на основе таких пленок обеспечивает основную погрешность измерений влажности воздуха не более 2%*RH*. Получены также пленочные материалы с электропроводностью близкой к безактивационной в интервале относительной влажности φ=12-59%, при температурах до +70°С и с почти прямолинейной зависимостью от φ. Оценка комплексного влияния влажности и температуры воздуха на электропроводность пленок показала возможность достаточного точного учета температурной погрешности при измерении влажности. Кроме изучения воздействия указанных метеопараметров (температура и влажность воздуха), проводятся исследования поглощения ультрофиолетового излучения некоторыми составами пленок. Последнее может быть использовано при построении радиозондовых озонометрических датчиков.

3. СТРУКТУРЫ РАДИОЗОНДОВ, ОБЕСПЕЧИВАЮЩИЕ ПРЕОБРАЗОВАНИЕ ВЫХОДНЫХ ПАРАМЕТРОВ ДАТЧИКОВ В ТЕЛЕМЕТРИЧЕСКИЕ СИГНАЛЫ

Преобразование выходных параметров датчиков метеовеличин в темететрические сигналы осуществлятся в радиозондах МРЗ-10 с помощью вторичных частотных измерительных преобразователей, в которых для достижения инвариантности к воздействию различных дестабилизирующих факторов, имеющих место при полете радиозонда, применяются структурные методы повышения точности с использованием

дополнительных опорных и калибрационных сигналов.

Структура частотного преобразователя, являющаяся базовой для построения всех типов вторичных преобразователей выходных параметров датчиков, используемых в радиозондах МРЗ-10, приведена на рис.1. Использование в нем метода развертывания во времени с изменением направления развертывания в примыкающих циклах обеспечивает исключение аддитивных составляющих погрешности, связанных с напряжениями смещения активных элементов схемы преобразователя. Резистивные высокоомные датчики, например, полупроводниковый терморезистор ($R_т$), резистивный датчик влажности ($R_в$), включаются во времязадающую цепь интегратора последовательно с высокостабильным опорным резистором ($R_о$) по схеме, аналогичной используемой в радиозондах более ранних разработок (МРЗ-3, МАРЗ). При этом сохраняется и используемый в них метод исключения мультипликативных погрешностей пребразования сопротивления этих датчиков, основанный на вычислении относительного параметра $Y=T_о/T_{т,в}$.

Преобразование параметров тензодатчика давления осуществляется описанным выше частотным преобразователем при подключении к нему специальной измерительной цепи (рис.2а), осуществляющей промежуточное преобразование параметров тензодатчика в напряжение ($U_{иц}$), модулируемое сигналом ($U_м$). Как видно из временных диаграмм (рис.1б), величина периода опорного сигнала ($T_о$) аддитивно входит в величину периода рабочего сигнала метеопараметра ($T_м$) и при выполнении вычисления относительного параметра $Y_м=(T_м-T_о)/(T_{мк}-T_о)$ осуществляется компенсация как мультипликативных составляющих погрешности, так и аддиивных, возникающих из-за невысокого быстродейсвтия активных компонентов схемы базового преобразователя и измерительной цепи. На выходе измерительной цепи датчика

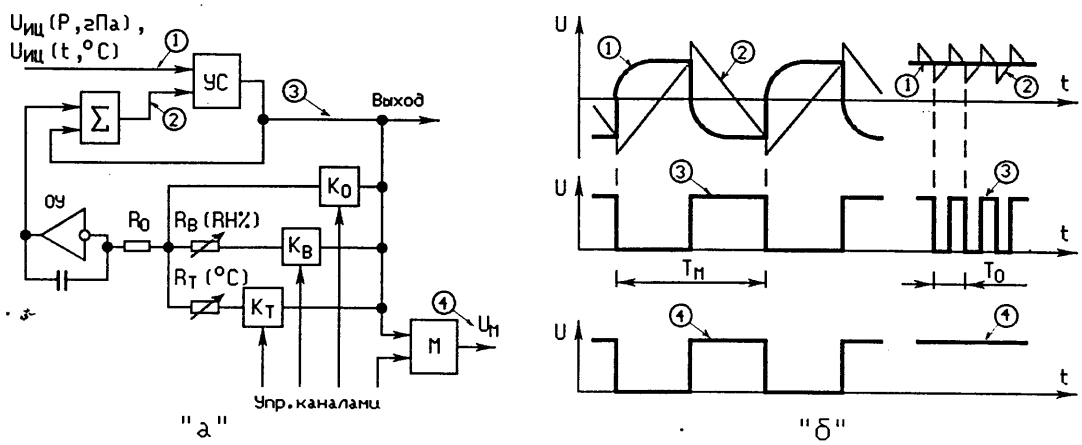

Рис.1. Структура частотного преобразователя выходных параметров датчиков метеовеличин (а); временные диаграммы напряжений, поясняющие принцип его работы (б).

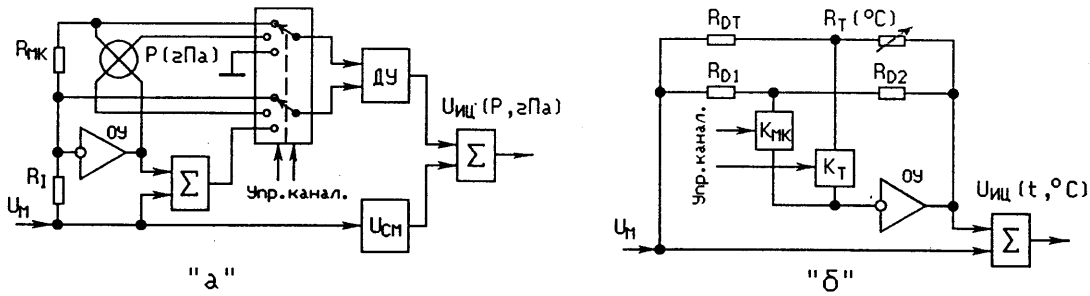

Рис.2. Структуры измерительных цепей для преобразованця выходных параметров тензорезисторного датчика давленця (а) и низкоомного проволочного датчика температуры (б).

давления последовательно формируются три напряжения: $U_р$ – рабочее (пропорцирнальное атмосферному давлению), $U_{мк}$ – мультипликативной коррекции, $U_{тк}$ – температурной корреции (пропорциональное внутренней температуре тензоэлемента датчика давления).

Преобразование сопротивления низкоомного микрофольгового или тонкопроволочного датчика температуры производится при подключении к базовому преобразователю (рис.1) измерительной цепи, структура которой приведена на рис.2*б*. На выходе этой измерительной цепи последовательно формируются два напряжкния $U_{Р}$ – рабочее (пропорциональное изменению сопротивления датчика), $U_{МК}$ – мультипликативной коррекции. Принцип преобразования здесь аналогичен описанному выше для цепи датчика давления.

4. РАДИОПЕРЕДАЮЩИЕ УЗЛЫ

В системах зондирования АВК-1 и "БРИЗ" в радиозондах применяются сверхрегенеративные приемо-передатчики (СПП), обеспечивающие передачу на одной несущей частоте 1780 (1680)*Мгц* телеметрической информации и формирующие ответный сигнал дальности, используемый для измерения наклонной дальности до радиозонда импульсным методом. При приеме запросного импульса мощностью до -90*Дб/Вт* СПП "отвечает" увеличением длительности одного из излучаемых радиоимпульсов (с частотой 800*кГц*) и уменьшением следующего, вплоть до его полного пропадания. Поэтому ответный сигнал по дальности воспринимается в РЛС сопровождения в виде "паузы" в излучении радиозонда, по которой легко определяется наклонная дальность. Для радиозонда используемого с радиотеодолитом МАРЛ-Т разработан радиопередатчик с несущей частотой 1680*Мгц*, стабильность которой не хуже 10^{-5}, а девиация телеметрическим сигналом составляет ±50*кГц*. Выходная мощность передатчика не менее 0,2*Вт*.

5. ИСТОЧНИКИ ЭЛЕКТРОПИТАНИЯ И КОНСТРУКЦИЯ РАДИОЗОНДОВ

Основные характеристики водоактивируемых электрохимических источников тока, используемых в качестве источника питания в радиозондах МРЗ-10, приведены в таблице 1. В нее включены как серийно выпукаемые батареи (28МХМ-0,2 и 36МХС-0,2), так и вновь разработанные (16МОВ-0,2 и 6МХС-0,4).

Таблица 1

Основные электрические и эксплуатационные характеристики радиозондовых батарей

Наименование параметра	Тип батареи			
	28МХМ-0,2	28МХС-0,2	16МХВ-0,2	6МХС-0,4
Электрохимическая система	Магний - хлорид меди(I)	Магний - хлорид свинца	Магний - оксиды ванадия	Магний - хлорид свинца
Разрядные напряжения:	27 $^{+18\%}_{-10\%}$	27 ±10%	18 ±10%	5,5 ±10%
	9,5 ±15%	9,5 ±10%	9,5 ±10%	
Разрядный ток, А	0,05	0,05	0,05	0,2
Время работы, час	2	2	2	2,5
Масса батареи, г (сух/акт)	120/150	135/185	120/150	100/130
Габаритные размеры, мм	80x80x40	70x70x30	60x75x30	50x50x22

Конструктивно радиозонды МРЗ-10 выполнены в унифицированном прямоугольном корпусе с размерами 110x110x170*мм*, который обеспечивает удобство размещения всех узлов радиозонда как во время хранения и транспортировки, так и в процессе работы. Полетная масса радиозонда не превышает 300*г*.

ЛИТЕРАТУРА

[1] V.Bondarenka, S.Grebinskij, S.Mickevičius, H.Tradauskas, Z.Martûnas, V.Volkov, G.Zakharova. Humidity sensors based on $H_2V_{11}TiO_{30.3}\cdot nH_2O$ xerogels. Sensors and Actuators, B55(1999), p.60-64.

[2] С.А.Крутоверцев, А.Е.Тарасова, С.И.Сорокин, А.В.Зорин. Микроэлектронные датчики для контроля влажности. Электронная промышленность, 1991, N5, с.31-32.

[3] В.А.Юрчук. Термометры для аэрологических измерений. Труды НИИГМП, 1975, вып.32, с.50-55.

RADIOSONDE SYSTEM OF CONDUCTING UPPER-AIR OBSERVATION

V.E. Ivanov, A.V. Gusev, O.V. Mironenko, R.A. Petrov
Ural State Technical University, Russia

1. ABSTRACT

Radiosonde system includs new compact radar "BREEZE" and radiosonde, which is raising by the gasfilled balloon. Design of this system was made at the Laboratory of upper-air equipments Ural State Technical University, and the manufacture of it, is realizing in "METEO" Joint Stock Company, Ekaterinburg, Russia.

System provides measuring the temperature, the humidity, the pressure, the speed and the direction of the wind in the atmosphere up to 40 km. Radar "BREEZE" operates on the carrier frequency 1680 (1780) MHz, it provides a precision measure of angular coordinates and slant range to the radiosonde (from 50m to 200km), by using a pulse reply of superregenerative receiver-transmitter on the radiosonde to the pulse interrogation of the radar. Besides, an average power of pulse interrogation, which is radiated by the radar, doesn't exceed 0.2W.

The possibility of employing the data of measuring the geometrical altitude (by using a radiolocation method) and the atmosphere pressure (by using a sensor, established on the radiosonde) for calculating the altitude of isobaric surfaces is a new qualitive characteristic of the system. On the one hand this will make it possible to raise the precision of measuring, which makes the system, under the high wind conditions and the considerable horizontal drift of the radiosonde, caused by them, and on the other hand this secures a possibility of non-statical phenomena's consideration in the atmosphere.

In this paper are discussing the results of the tests and the experimental exploitation of the radar "BREEZE"; is conducting the appreciation of the precision of measuring, which are made by the system, under different conditions of starting of the radiosonde. Nowadays are examined possible spheres of employment of the radar "BREEZE", which are connected with upper-air observations and the control of the environment.

2. ВВЕДЕНИЕ

В лаборатории аэрологического оборудования Уральского государственного технического университета по заказу ОАО "Метео" создана малогабаритная автоматизированная система радиозондирования «БРИЗ» для проведения аэрологических наблюдений [1].

Автоматизированная система «БРИЗ» относится к классу цифровых систем радиозондирования атмосферы с автоматической обработкой данных. При этом система «Бриз» обеспечивает возможность определения вертикальных профилей метеовеличин в следующих режимах:

- радиолокационном - определение координат зонда на основании измерения наклонной дальности до радиозонда с использованием активного ответа от суперрегенеративного передатчика зонда, а также измерений азимута и угла места.
- радиотеодолитном - определение координат зонда на основании измерения атмосферного давления, азимута и угла места.
- радиолокационно-теодолитный - определение координат зонда измерением как наклонной дальности до радиозонда, так и на основании измерения атмосферного давления, а также измерений азимута и угла места.

3. ОБЩЕЕ ОПИСАНИЕ СИСТЕМЫ «Бриз»

В состав системы «Бриз» входят:

– наземное оборудование РЛС «Бриз» - (радиолокатор или радиотеодолит), аппаратура предполетной проверки радиозонда, управления полетом и обработки метеоданных на базе ПЭВМ;

– комплект аэрологических зондов с датчиками различных типов. Информация по радиозондам, используемых системой «Бриз», приведена в статье «New radiosondes for Russian systems of upper-air observations» by Ivanov, Vjacheslav, et al. этого сборника.

В состав комплекса наземного оборудования РЛС «Бриз» входят:

- антенно-фидерная система (АФС). АФС обеспечивает быстрое электронное управление диаграммой направленности. В ближней зоне (дальность до 1км.) ширина диаграммы направленности по уровню 0.5 составляет 20°. Захват и удержание радиозонда в ближней зоне происходит в пределах ±40°. В дальней зоне ширина диаграммы направленности по уровню 0.5 - 6°, коэффициент усиления антенны не менее 26 дБ. Антенная система управляется высокоточным цифровым приводом. Волновая передача обеспечивает безлюфтовое вращение антенны при кругом обзоре по азимуту ± 360° и в пределах от -10° до + 130° по углу места. Такое построение АФС позволяет обеспечить высокую надежность и точность сопровождения радиозонда в экстремальных условиях. Общий вид АФС приведен на рисунке 1.

Рисунок 1. Общий вид АФС .

- Приемо-передающая система. Приемное устройство построено по схеме супергетеродина с тройным преобразованием частоты (коэффициент шума 1.5 дБ). В гетеродине используется синтезатор частоты с петлей ФАПЧ и цифровым управлением от микроконтроллера, что позволяет оценивать частоту радиозонда с точностью до 0.1 МГц. Передающее устройство полностью построено на полупроводниковых элементах. При средней мощности излучения 0.2 Вт. санитарная зона не превышает 4 м. Приемо-передающая система конструктивно размещена на шасси АФС, и допускает эксплуатацию в расширенном температурном диапазоне от -40° до +50°С.
- Система обработки и управления. Система обработки и управления обеспечивает:
  - управление антенной и приемопередающей системами в режиме ручного (по командам оператора ЦПУ) и автоматического сопровождения радиозонда;
  - измерение угловых координат радиозонда (угол места и азимут);
  - измерение наклонной дальности радиозонда;
  - сбор метеоинформации по каналу телеметрии, ее первичную обработку;
  - контроль функционирования и самопроверку системы с использованием эталонных тестовых сигналов при предстартовой подготовке и во время полета;
  - предстартовая проверка радиозонда;
  - прием команд и данных от центрального пульта управления (ЦПУ) и передача на ЦПУ измеренных значений параметров радиозонда и системы в целом для дальнейшей обработки и принятия решения по управлению системой и окончательной обработкой метеоинформации.

Все эти задачи решаются отдельными однотипными функциональными блоками, выполненными в виде печатной платы в стандарте МЭК 297-3 (размер 3U), соединенными через устройство коммутации и размещенными в одном корпусе. В настоящее время в системе используется 5 базовых модулей. Базовый модуль применен для решения различных задач по цифровой обработке сложных аналоговых радиосигналов и задач оптимального управления.

Наличие микропроцессора и микросхем программируемой логики позволяет оптимизировать структуру модуля в зависимости от требований поставленной задачи, оперативно перестраивать структуру модуля для решения новых задач по модернизации системы без ее аппаратной доработки. Структура модуля позволила осуществить эффективное распараллеливание процессов, ввести децентрализацию управления. Создание системы на основе базового модуля позволило существенно снизить затраты на изготовление и эксплуатацию системы [2].

- Центральный пульт управления. Центральный пульт управления предназначен для ручного и автоматического управления узлами и блоками РЛС «Бриз», окончательного сбора, обработки и отображения поступающей координатной и телеметрической информации, с последующей выдачей аэрологических данных в виде телеграмм и передачи их по каналам связи. Внешний вид ЦПУ приведен на рисунке 2.

В состав ЦПУ входит управляющая ПЭВМ, принтер и источник бесперебойного питания (обеспечивает автономную работу РЛС «Бриз» в течение 2-х часов). ПЭВМ, работающая под управлением специальной программы центрального пульта, выполняет следующие функции:

- автоматический контроль функционирования при включении изделия;
- предполетную проверку радиозонда;
- автоматическое и ручное наведение и сопровождение радиозонда, находящегося в свободном полете;
- определение и отображение относительных координат (азимута, угла места и наклонной дальности) и полетного времени радиозонда;
- обработку в реальном масштабе времени и отображение телеметрической информации от радиозонда о температуре, влажности и давлении в точке нахождения радиозонда;
- сохранение данных об относительных координатах радиозонда и параметрах телеметрической информации, привязанных к полетному времени, в виде файла- протокола на дисковых накопителях управляющей ПЭВМ;
- обработка аэрологических данных. Программа обработки аэрологических данных, их визуализация и формирование телеграмм для выдачи по каналам связи разработана специалистами Центральной Аэрологической Обсерватории, г. Долгопрудный и включена в программное обеспечение ЦПУ.

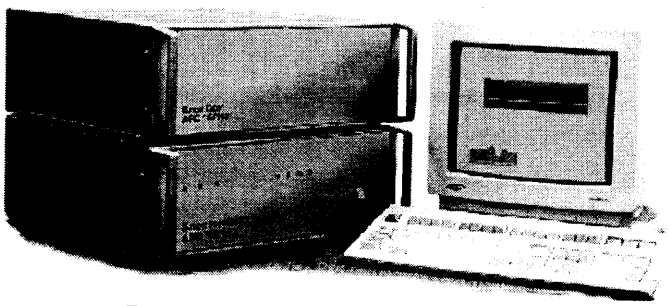

Рисунок 2. Внешний вид ЦПУ.

Интерфейс оператора и инженера обеспечивает отображение на экране ПЭВМ необходимой информации и ввод в систему команд управления от оператора и инженера. Интерфейс обеспечивает работу пользователя на одном из двух языков: русском или английском – выбор которого задается при начальной настройке станции. Особое оконное построение интерфейса обеспечивает наиболее удобное для пользователя размещение информации: группировку однородной информации в пределах одного окна, возможность перемещения этих окон на экране, возможность получения дополнительной информации в виде нового окна, возможность удаления с экрана окна, которое уже не нужно в данный момент. Важной особенностью окон является их перекрытие, т.е. одно окно может располагаться поверх другого.

4. ЭКСПЛУАТАЦИОННЫЕ ХАРАКТЕРИСТИКИ СИСТЕМЫ «БРИЗ».

Основные эксплуатационные характеристики системы приведены в таблице 1.

Основные эксплуатационные характеристики системы «Бриз». **Таблица 1.**

Минимальная дальность (до пункта выпуска радиозонда)	30 м
Максимальная дальность, не менее	200 000 м
Максимальная высота радиозондирования (максимально фиксируемая высота подъема радиозонда), не менее	40 000 м
Погрешности измерений:	
Среднеквадратическое значение погрешности измерения координат в режиме автосопровождения составляет, не более: по дальности, по азимуту и углу места	30 м 0,10°
Систематическая составляющая погрешности измерения координат в режиме автосопровождения составляет, не более: по дальности, по азимуту и углу места	20 м 0,1°
Среднеквадратические ошибки вычислений, не более: температуры воздуха скорости действительного и среднего ветра (от 0 до 75 м/с) направления действительного и среднего ветра (от 0 до 360°) атмосферного давления (от 1100мб до 2мб) относительной влажности (в пределах от 10 до 100 %)	0,1°С 1,0м/с 1,5° 2,0 мб 1,0 %

Для оценки эксплуатационных характеристик системы «Бриз» были проведены экспериментальные натурные испытания на аэрологических станциях Верхнее Дуброво г. Екатеринбург и г. Брест, республика Беларусь, по специально разработанным методикам. Испытания проводились во все времена года и подтвердили основные технические характеристики системы. Проверка технических характеристик системы проводилась методом спаренных выпусков радиозондов с синхронным измерением РЛС «Бриз» и комплексом АВК-МРЗ, эксплуатирующемся на аэрологической сети России. Оценки точности системы проводились с использованием образцовых средств измерений (оценка точности по угловым координатам и точности сопровождения радиозонда - оптическим методом, оценка точности по дальности - с использованием реперных точек, диаграммы направленности измерялись по разработанным методикам).

По результатам испытаний произведена доработка программного обеспечения ЦПУ РЛС: создан более удобный интерфейс оператора, с учетом рекомендаций пользователей, ускорен процесс выдачи телеграмм КН-04 (части А и В, С и D).

Время монтажа стационарной РЛС «Бриз» не превышает 8 часов. Общий вес системы не более 150 кг., конструкция системы позволяет вести монтаж РЛС без использования подъемных приспособлений.

5. ВЫВОДЫ

Результаты опытной эксплуатации показали, что система «Бриз» имеет реальные эксплуатационные характеристики, соответствующие современному уровню и требованиям ВМО к точности и качеству аэрологической информации. Система может быть использована для создания как стационарных РЛС, заменяющих устаревшие комплексы на сети стран СНГ, так и создание мобильных систем радиозондирования экологического мониторинга.

6. СПИСОК ИСПОЛЬЗУЕМОЙ ЛИТЕРАТУРЫ.

1. The new generation of upper-air observation equipment. By Ivanov Vjacheslav, et al. WMO technical conference on meteorological and environmental instruments and methods of observation. Report №70. Morocco 1998.
2. О некоторых принципах разработки цифровых радиотехнических систем. Б.Будаи, А.Гусев, В.Иванов, О. Мироненко. Инженерная микроэлектроника №2 1998г.

MESURES FINES DE VENT

A L'AIDE D'UN SYSTEME DE RADIOSONDAGE EQUIPE D'UN GPS 4D

MODEM	Tél. : 0 164 99 77 52 Fax : 0 164 99 77 53 E MAIL : mod@club-internet.fr
Z.A. de l'orme à bonnet - 91750 CHEVANNES-FRANCE	

Auteur : Patrick CHARPENTIER

La société MODEM a mis au point un nouveau procédé de Radio sondage en utilisant la technologie GPS.

1/Historique :

C'est à la suite d'une demande formulée par ESA (Agence spatiale européenne) en 1994 que la société Modem s'est intéressée au radio sondage. Il s'agissait à cette époque de trouver un moyen performant pour mesurer le vent.

A cet effet, il a été développé un nouveau ballon dénommé Méduse et une nouvelle sonde appelée GPS400PSK.

Les résultats extrêmement satisfaisant de ce système dont les objectifs et résultats seront décrit ci après ont motivé notre société pour développer un système complet de radiosondage vent + PTU adapté au marché météorologique.

2/Le système :

Le système se compose :

- D'une sonde GL98 qui associe les mesures de température et humidité aux mesures GPS complètes (y compris l'altitude) et les envoie au sol toutes les secondes.
- D'une station sol très compacte qui reçoit les données et effectue un traitement approprié pour éditer un message TEMP, PILOT ou autre.

Vent : Le système restitue la force et la direction du vent grâce aux mesures GPS. Ces mesures sont de deux ordres :

- mesures des positions dans les 3 dimensions par calcul de triangulation entre les signaux de trois ou quatre satellites minimums
- Mesure de la vélocité (vitesse) déterminée directement par le doppler provenant de la boucle de la porteuse et non pas par une différence entre deux positions.

- La vélocité est plus précise que la position sur des petites échelles de temps, alors qu'elle devient moins précise sur de grandes échelles.
- Notre système tient compte de ces deux méthodes de mesures afin de restituer les meilleures données possibles.
- Ces données sont comparées à celles qui sont au sol (GPS différentiel) afin de s'affranchir des perturbations liées aux erreurs satellitaires, aux problèmes de propagation, au brouillage volontaire éventuel.

PTU : Le système mesure la température grâce à une thermistance et tient compte de l'effet radiatif.

Le système mesure l'humidité grâce à un polymère capacitif et est corrigé en fonction de la température.

La pression n'est pas mesurée mais calculée à partir de l'altitude et des températures et humidités.

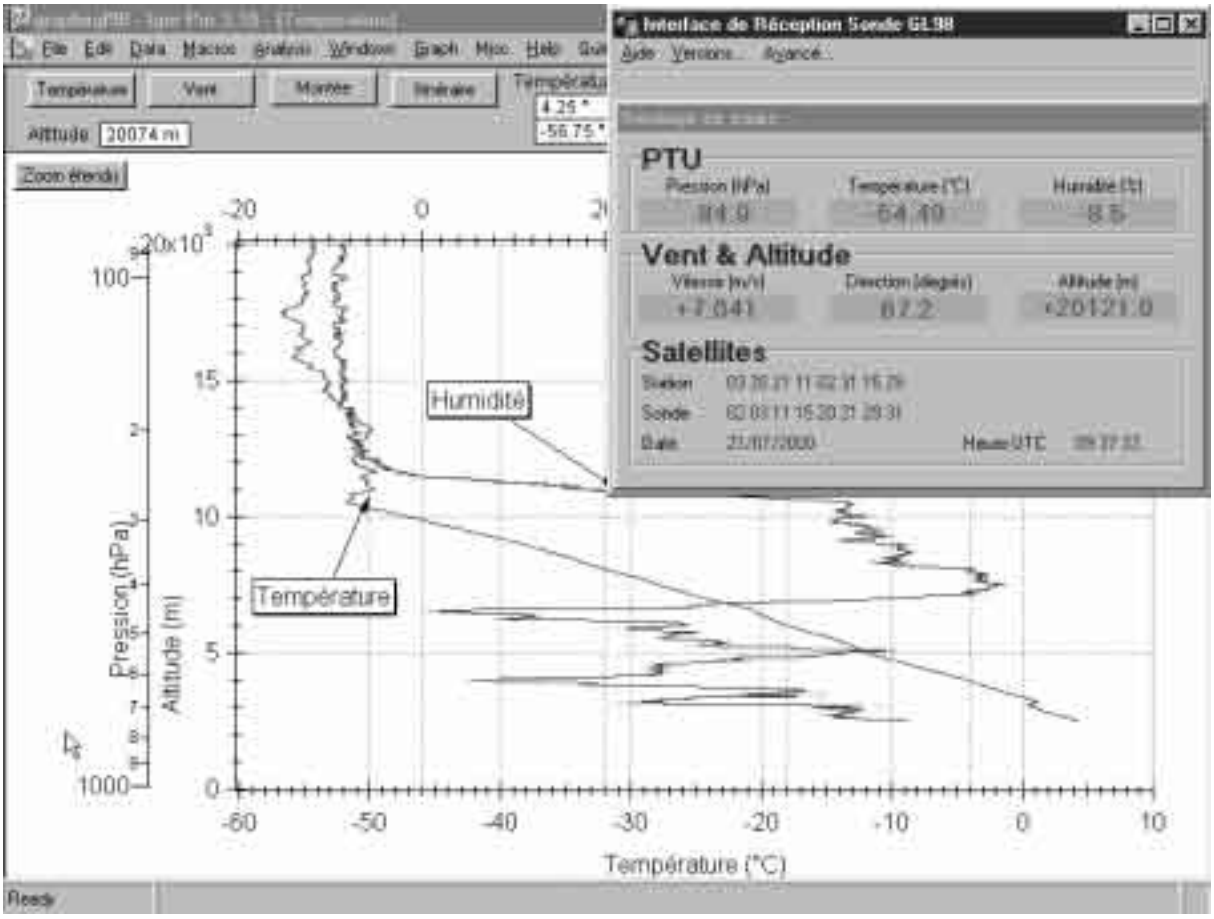

3/Mesure d'un profil vertical de vent

La précision d'un profil vertical de vent doit être mesurée sur l'ensemble du moyen utilisé, c'est à dire qu'il faut tenir compte de la précision de la sonde et du moyen de réception au sol mais aussi de la précision du ballon.

1/ Précision de la sonde :

localisation spatiale 10 m en x et y, 20m en z
composantes de la vitesse 0.2 m/s en u, v et w

2/ Précision du ballon recherchée :

erreur à 1 sigma <0.4 m/s pour une résolution de 100 m

Quel ballon choisir ?

Un ballon météo est un mauvais suiveur de vent, car il génère des mouvements parasites qui se traduisent par un vent apparent (bruit) qui n'a rien a voir avec l'atmosphère.
Ce bruit de mesure apparaît autour d'échelles de l'ordre de 700 à 800 m à cause de mouvements auto-induit liés à des variations aléatoires des points de décollement du sillage.
Ces mouvements auto-induits, contrôlés par le nombre adimensionnel de Reynolds de l'écoulement de l'air autour du ballon, couvrent pour les ballons météo classiques une large gamme de longueurs d'ondes (jusqu 'a 400m) avec des amplitudes de plusieurs mètres par seconde.

Les Jimspheres, Rubsondes, Capspheres, Méduses sont capable de résoudre des échelles de l'ordre de 200 m. Ce sont les ballons dit stabilisés.
Pour rendre un ballon plus stable, une solution consiste à augmenter la rugosité de la surface du ballon. On augmente ainsi la taille du sillage, ce qui a pour effet d'accroître la traînée et de diminuer les forces de portance.
Ces ballons sont donc conçus pour éviter les décollements aléatoires de la couche limite et absorber l'énergie turbulente du sillage.

Il faut y associer un vrai GPS car il donne une localisation tridimensionnelle et des mesures de vitesse Doppler plus précises que celles obtenues en dérivant la position.

4/ Les campagnes VERHT (mesure des profils de vent haute résolution et de température)

La première campagne VEHRT 1 a eu pour objet de valider le modèle décrivant le champ des fluctuations de vent en zone équatoriale et en cas de validation d'en ajuster au mieux les paramètres. Ce modèle était issu de nombreuses mesures effectuées sous nos latitudes, mais n'avait jamais été testé en zone équatoriale. Le champ des fluctuations de vent dépend de quatre dimensions, le temps et les trois dimensions spatiales, VEHRT 1 ne s'est préoccupé que de la dimension verticale et d'une certaine manière du temps.
Les moyens utilisés ont été le système de mesure ballon Méduse et sonde Modem
Les précisions de mesures ont été :

Température précision absolue 0.5 K
précision relative 0.03 K avec un temps de réponse < 4 s
Vent rapport signal/bruit =1 à 100 m de résolution.

Le résultat a été la détermination des paramètres d'un modèle du champ des fluctuations de vitesse et de température permettant une optimisation des charges structurales, environnement dynamique et pilotage des systèmes fusée-satellite Ariane.
La deuxième campagne VEHRT 2 par des lâchers simultanés en trois sites distants de 200 km, a permis d'accéder aux deux autres dimensions horizontales. Une première étude avait été

effectuée avec des données provenant de ROCHAMBEAU et de VEHRT 1 mesurées à des heures proches, mais les données de ROCHAMBEAU étaient de qualité médiocre (localisation du ballon, qualité du ballon), la simultanéité des sondages n'était qu'approximative et la distance entre les deux sites était trop faible.
Le résultat de cette deuxième campagne a permit de chiffrer l'influence des trajectoires obliques des lanceurs

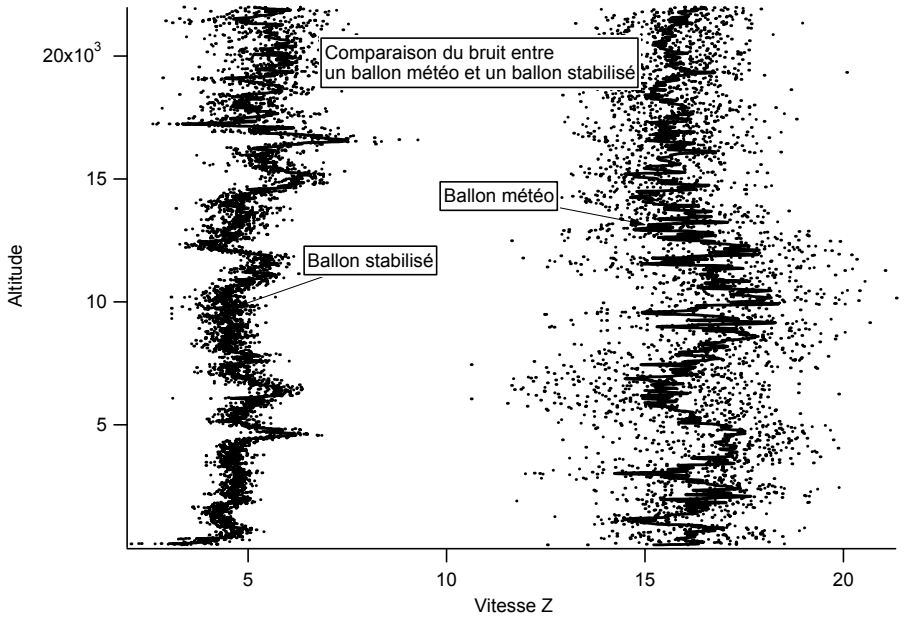

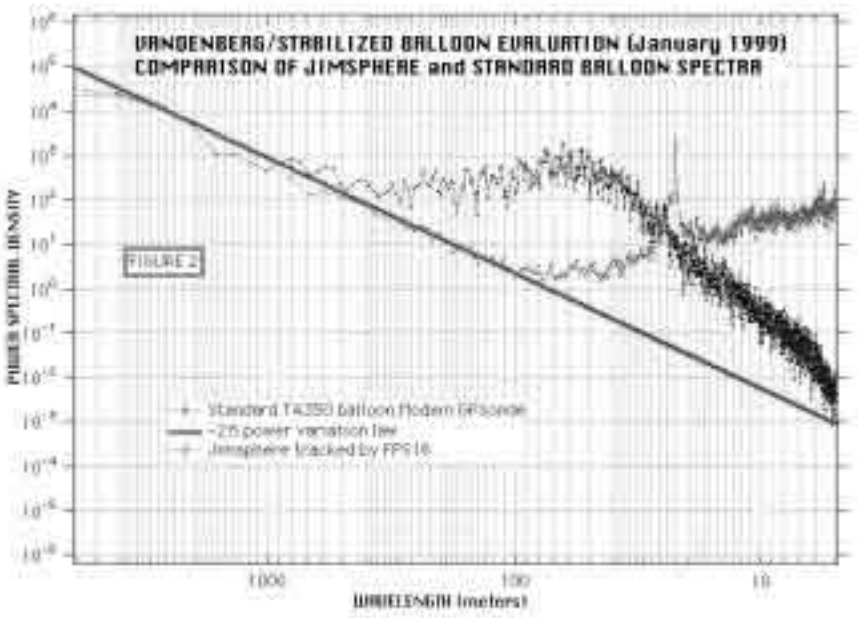

1 MEASUREMENT TECHNOLOGY, PERFORMANCE, AND QUALITY ASSURANCE

1.2 Upper-air Observation Systems

1.2.2 Remote Upper-air Observation System

OPERATIONAL EXPERIENCE OF A BOUNDARY LAYER WIND-PROFILER NETWORK

Nicola Latham, Tim Oakley, Myles Turp, John Nash

The Met. Office, Beaufort Park, Wokingham, Berkshire, RG40 3DN, UK
Tel: +44 (0)1344 855646, Fax: +44 (0)1344 855897, e-mail: nlatham@meto.gov.uk

Introduction

The Met. Office operates four Radian LAP3000 boundary layer wind profiler radars in the UK, located at Camborne and Dunkeswell in the South West of England and Pendine and Aberystwyth in Wales, see Table 1 and Figures 1 and 2. All systems are configured to use one beam to measure the vertical velocity and two beams to measure the velocity in two off-vertical directions. The three beam configuration was preferred to the five beam, as beam directions with high clutter do not have to be used and a more rapid observing cycle is achieved. The beams are cycled between a high mode, which supplies data up to 8km with 200m resolution (400m Dunkeswell) and a low mode which supplies data up to 2km with 60m resolution (100m Dunkeswell). The wind information is processed and may be presented as a wind barb plot as shown in Figure 4. The signal power, vertical velocity and spectra can also be presented for further analysis.

Location	Frequency	Antenna size	Installation Date
Camborne	915 MHz	2.61m x 2.61m	Nov 98 (upgrade from smaller system)
Dunkeswell	1290 MHz	2.61m x 2.61m	Feb 99
Pendine	1290 MHz	2.61m x 2.61m	Feb 99
Aberystwyth (development system)	915 MHz	1.74m x 1.74m	Nov 99

Table 1. The UK boundary layer wind profilers

Figure 1: The 915MHz wind profiler radar at Camborne.

The UK Wind Profiler Network

The UK wind profilers are intended to demonstrate the capabilities of a pilot network and contribute to the CWINDE programme (COST Wind Initiative for a Network Demonstration in Europe), as well as providing wind data to local and regional forecasts. The data are transmitted in real time via e-mail to Bracknell and archived in the operational database. Results are then monitored against the NWP model on a monthly basis to assess their performance and usefulness in the long term. Some weather radar data can also be processed to enhance the network over the British Isles during significant weather.

Figure 2. Wind profiler and weather radar sites in relation to Bracknell

Network Performance

Since installation during winter 98-99, there have been a number of hardware failures and numerous communications difficulties to resolve within the network. Both of the 1290MHz systems had problems with the final amplifiers on installation. These were not detected by the manufacturer's representatives. The malfunctions were difficult to detect as the expected performance in relation to that of the 915MHz system, was not well understood. Following total amplifier failure at each site and subsequent replacement, the network performance has improved and stabilised, while experience and statistics have been gathered to be used to identify problems.

Table 2 and Figure 3 illustrate the main causes of failure and the subsequent percentages of data available and data received in near time. The recent improvements shown by the availability statistics demonstrate the advantage of keeping spares accessible within the UK. Spare 915MHz and 1290MHz compatible components are in use in the Aberystwyth development system, while further 1290MHz components are kept at Bracknell. This spares policy shields, to some extent, the primary network of three profilers from the long lead times for repair or replacement.

Failure	**Total downtime (all sites)**
Receiver	37 days
Final Amplifier	101 days
Communications	50 days (real time only)

Table 2. Causes of profiler failure Nov 98 to May 00.

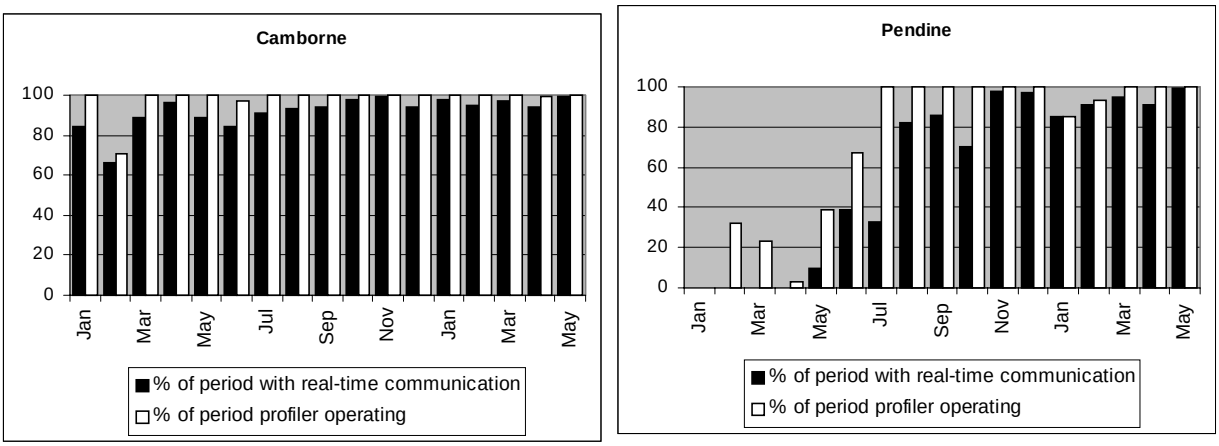

Figure 3: Percentage of data available in near time and off-line for two UK sites.

The improvements to the real time statistics reflect changes to the methods used for obtaining real time data via e-mail. In the earlier months the site systems pushed data to Bracknell. In this case the PC at the remote unmanned site tended to 'lock' in association with communication difficulties. This problem was resolved by switching the procedures so that data are pulled from the unmanned

sites to Bracknell. If the Bracknell computer locks it is easily reset. Although several data messages may still fail to be collected in any one period, the current set up has greater redundancy and allows quicker resolution of problems.

Data Products and Availability Against Height

Figure 4 gives two examples of data displays, latest 12hr versions of which can be found for an individual profiler at: www.met-office.gov.uk/sec5/CWINDED/cwinde99/cwinde99e.html. The example on the left shows wind speed and direction profiles for the 27th December over Camborne. This was at the time that a severe storm was causing much damage in southern France. The presence of a pronounced trough over the UK at heights of about 5 km at 14 UTC was poorly represented in the UK mesoscale model, although observed at all four profiler sites. The signal power plot on the right shows the development of the convective boundary layer between 08 and 18 GMT over Dunkeswell, detected in the profiler's low mode. This type of information from the boundary layer profilers will be used to generate information for forecasters on the temperature and humidity structure at the profiler sites in combination with radiometer observations.

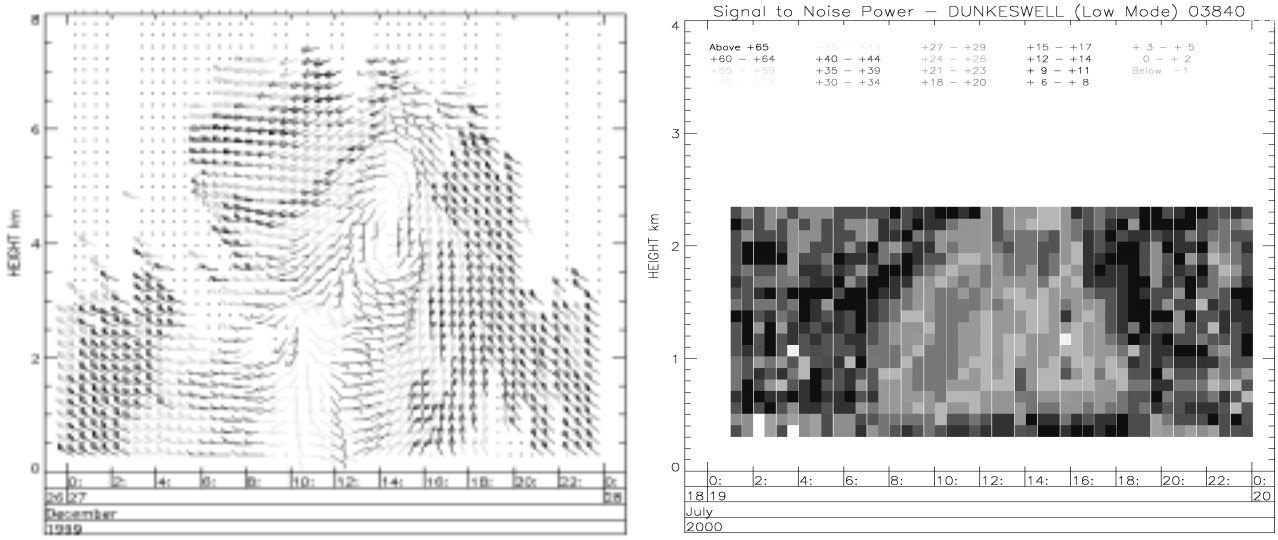

Figure 4: 24 hour wind barb plot (left) and 24 hour signal power plot (right).

The maximum height of data obtained by the profiler varies depending on conditions. Figure 5 shows the percentage of data messages received containing data at particular heights over a five month period at Pendine and Camborne. High mode data is regularly obtained up to 2.5km (75%), with a rapid decrease in availability in the 3 and 4km region.

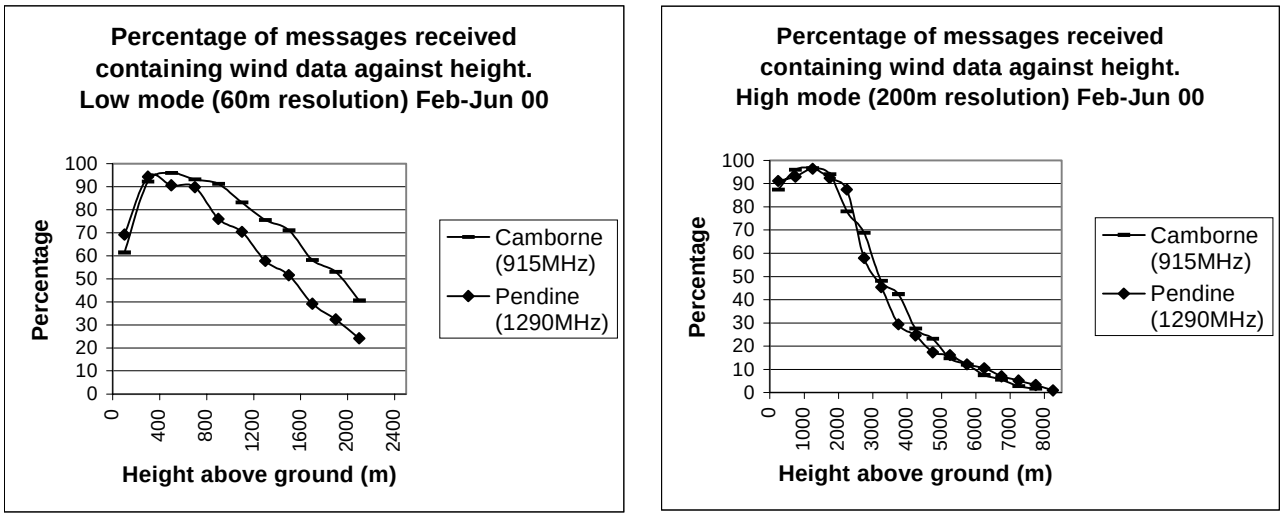

Figure 5: Percentage of data available against height for a 1290MHz profiler and a 915MHz profiler.

During the period shown, the vertical resolution of the 1290MHz system was reconfigured from 400m (high mode) and 100m (low mode) to match that of the 915MHz system. This enabled a comparison of performance to take place. It can be seen that in the low mode, at 60m resolution, the 1290MHz system records considerably less data in each height range above 800m than the 915Mhz system. The high mode, however with 200m resolution shows similar performance from the two systems. The 915MHz system is therefore better for obtaining high resolution clear air returns at lower levels, while the 1290MHz system benefits from higher returns in water/ ice clouds.

Use of Wind Profilers in Special Campaigns

In addition to the long term data archive that takes place for comparison against the UK Global model and analysis of network performance, UK boundary layer wind profiler data have been used for several short term special campaigns to support development of new systems.

The wind profiler at Camborne is located on an operational radiosonde site, which since early 1999 has supported campaigns to demonstrate a 78.2GHz cloud radar, a GPS water vapour receiver and a SODAR as well as multiple radiosonde comparisons. The boundary layer system at Aberystwyth has recently been installed adjacent to the MST profiler, LIDAR and another GPS water vapour receiver allowing further comparisons to be made. The comparison with the SODAR, for example, indicated a close match between the data at most heights, but confirmed the limitations of the profiler in the lowest two range gates, where the signal is not believed to be representative of the volume.

The example below illustrates a comparison of the wind profiler signal power plot displayed with a four minute temporal resolution and that of a cloud radar operating at 78.2GHz. The cloud radar information allows further interpretation of the wind profiler signal power product and as a complementary technique is a useful step towards automation of observations. Further details on this study are available from the author.

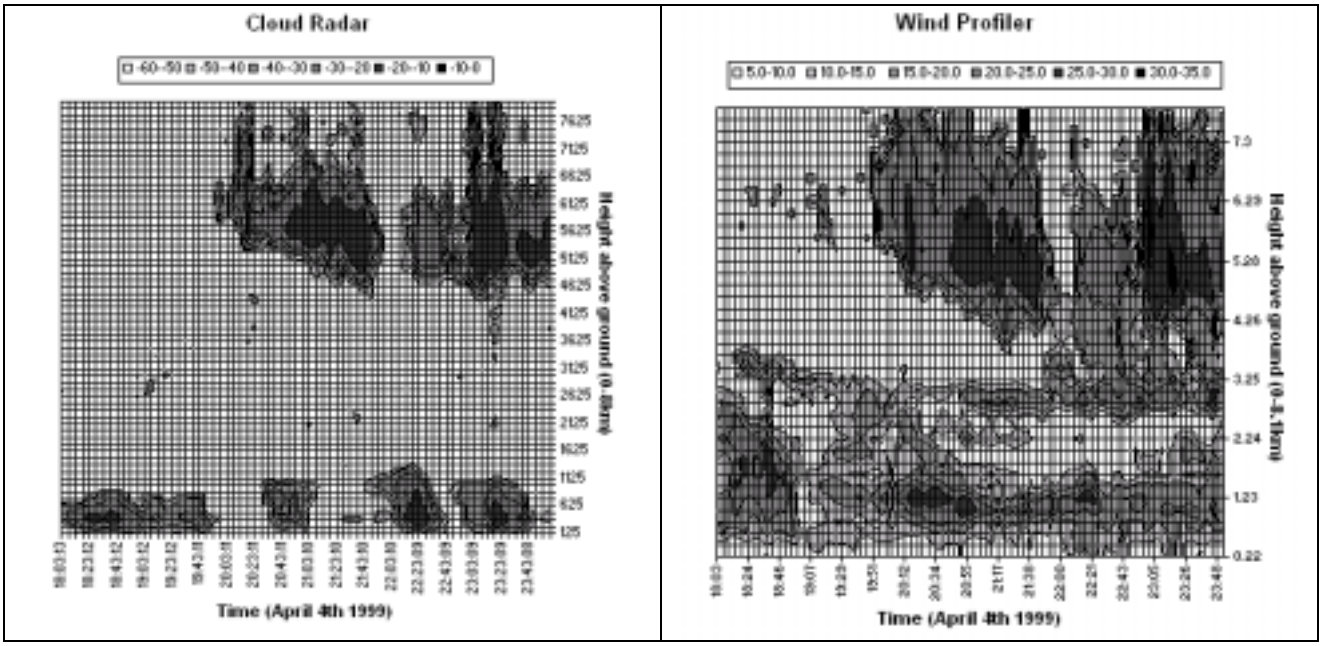

Figure 6: Signal plots for the 78.2GHz RAL Cloud Radar (left) and 0.915GHz Wind Profiler (right) for a six hour period over Camborne, April 1999.

Conclusion

The Met. Office has now decided that the wind profiler network will be handed over to be run as an operational service as part of a more fully automated upper air observing network.

Multiple Beam Statistical Analysis of Wind Profiler Data

P. Currier
T. Berthou
(Degréane S.A. 28 av. Font-Pré 83050 Toulon France)
(Tel.: (33)494 61 9292 Fax: (33) 494 61 0471)
(E-Mail: degreane@wanadoo.fr)

Abstract

Recent developments have enhanced the quality control of wind profiler radar data reducing the effects of interference, which can at times generate erroneous wind estimates.

Wind profiler data are usually processed at 4 levels:

digital signal processing of the time series (wavelets, FIR, pulse coding ...) ;
digital signal processing at the spectrum level (Merritt, multiple peaks ...) ;
consensus processing of the spectral moments ;
time / height continuity check at wind barb level (Weber Wuertz).

The quality control done at the wind barb level (i.e. Weber Wuertz) is used to differentiate between wind barbs generated by wind from those create by spurious echoes. Many of these spurious returns can be identified earlier in the processing chain.

The multiple beam statistical analysis of the different moments can be used at the consensus level to insure the basic premise of horizontal homogeneity of the atmosphere. This type of analysis is quite robust in rejecting spurious echoes that are accepted by the simple consensus algorithms. The analysis is presented along with its effect on the resulting wind barbs.

Introduction

Wind profiler radar are starting to be used operationally. The technique most commonly used by these radar is the Doppler Beam Swinging technique (DBS): the wind profiler makes at least three sequential measurements in different directions (Beam Swinging). The results are then combined to compute the three dimensional winds (U,V,W).

Operational use of wind profiler data requires extensive quality checks. The users usually prefer no data rather than erroneous wind measurements. Weber Wuertz type algorithms can flag many outliers. These algorithms reject neighboring wind estimates that present excessive wind gradients. There are, however, times when wind barbs are in error yet appear consistent. It is only when an experienced operator looks at the spectral data that these types of errors can be seen. Worse, certain errors can only be detected by examining a time / height history of the spectra and/or comparison with the other beams.

As a first step in increasing the wind barb quality check's robustness, various statistics of the consensus outputs are computed. These statistics are then compared with those of neighboring heights and other beams. This analysis easily detects cases where returns from different beams due to clear air, ground clutter, or rain would be combined.

Current Implementation

The following flow diagram illustrates the part of the processing chain.

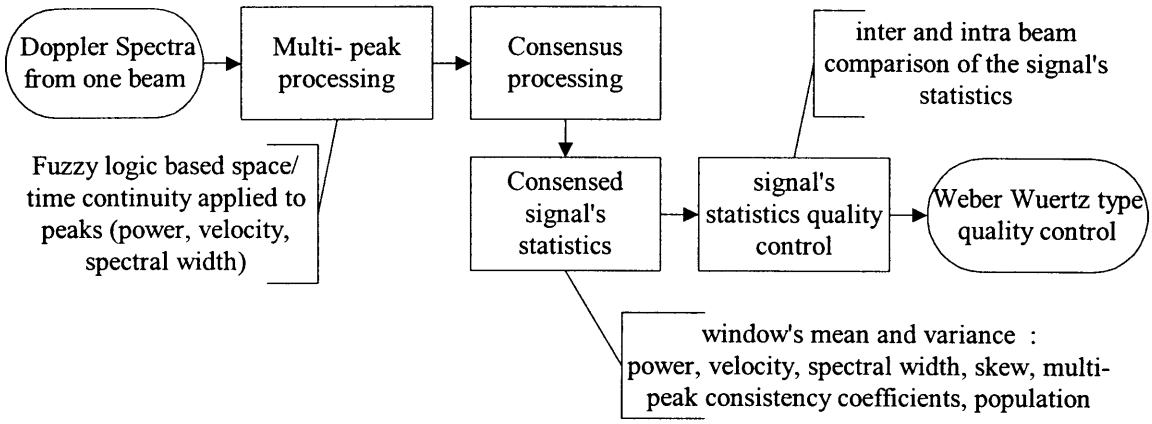

For clarity the feedback of the resulting profile output by the Weber Wuertz type quality control has been omitted (included in the other flow diagrams). The feedback loop is part of the automatic Doppler velocity scale adjustment mechanism.

The signal's statistics quality control is quite robust in eliminating data biased by ground clutter which has not been discriminated by the multiple peak processing and that is not detected by the Weber Wuertz type quality control. This method can even correctly processes data contaminated by ground clutter in all the beams over several identical heights.

One may be tempted to eliminate the Weber Wuertz type quality control. However, the two quality control algorithms do not process quite the same information and actually complement each other.

Extensions of the Method

Presently one of the greatest weaknesses in profiler processing is the lack of adaptability of the operating parameters to the changing weather. Essentially one or two operating modes are used to sound the atmosphere under all weather conditions.

The method can be used to feedback information to optimize the processing parameters:

- adjust the consensus duration and Doppler window width as a function of the wind's variability and /or return signal's Signal to Noise ratio. This allows for the automatic adjustment of the consensus parameters as a function of height.
- adjust the multiple peak processing to better discriminate between clear air returns and ground clutter (adaptive ground clutter rejection or removal).

The following flow diagram illustrates such a processing chain.

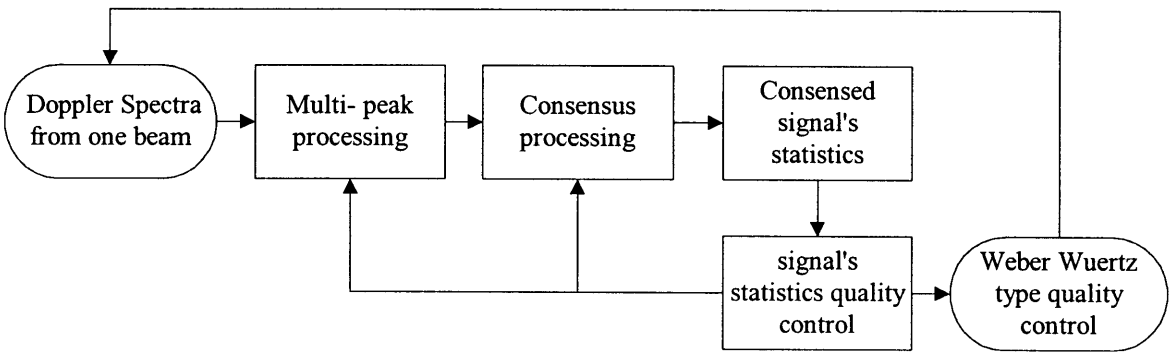

Certain applications require high time resolution wind profiles or even single cycle wind estimates. Using multiple processors it is quite simple to extend the architecture to build robust single cycle estimates directly from the output of the multiple peak processing, which is statistically constrained to the consensus output. In this case the system furnishes two outputs with independent update rates in parallel and in real time: one result based on a 15 minute or half hour consensus; the other based on a single cycle of measurements.

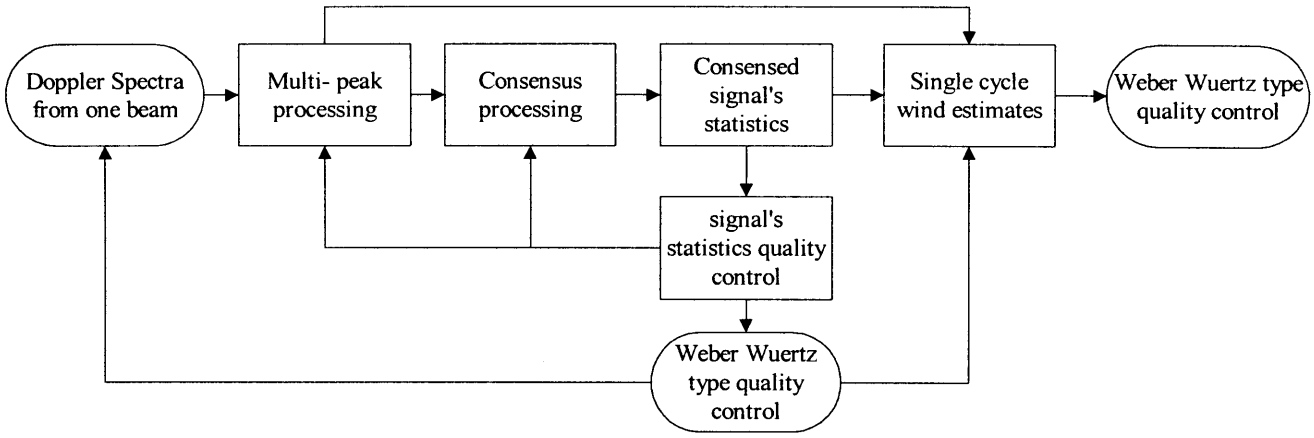

Conclusions

While simple and robust, this type of processing has not yet been implemented routinely. This tool can be used to adaptively set the wind profiler's operating parameters to optimize both the measurement capabilities and the quality of the wind estimates as a function of the changing weather conditions.

The first phase of implementation of this statistical analysis simply invalidates unacceptable measurements complementing a Weber Wuertz type quality control algorithm. The second phase is to feedback the information into the multiple peak analysis and consensus processing (adjusting the consensus time and velocity windows). The third phase is to develop robust single cycle wind estimates, which are statistically constrained to a consensus output calculated in parallel.

References

Clothiaux E. E., R. S. Penc, D. W. Thomson, T. P. Ackerman and S. R. Williams, 1994: A First-Guess Feature-Based Algorithm for Estimating Wind Speed in Clear-Air Doppler Radar Spectra. *J. Atmos. Oceanic Technol.*, **11**, 888-908.

Cornman L. B., R. K. Goodrich, C. S. Morse, and W. L. Ecklund, 1998: A Fuzzy-Logic Method for Improved Moment Estimation from Doppler Spectra. *J. Atmos. Oceanic Technol.*, submitted.

Griesser T., and H. Richner, 1997: Multiple Peak Processing Algorithm for Identification of Atmospheric Signals in Doppler Radar Wind Profiler Spectra, *COST 76 Profiler Workshop* May 12-16, Engleberg, Switzerland, 110-114.

Jaquier A., D. Ruffieux, and R. Stübi, 1997: Multi-Peak Analysis and Determination of Characteristic Heights with a Low-Tropospheric Wind Profiler, *COST 76 Profiler Workshop* May 12-16, Engleberg, Switzerland, 301-304.

Jordan J. R., R. J. Lataitis, and D. A. Carter, 1997: Removing Ground and Intermittent Clutter Contamination from Wind Profiler Signals Using Wavelet Transforms. *J. Atmos. Oceanic Technol.*, **14**, 1280-1297.

Merritt D. A., 1995: A Statistical Averaging Method for Wind Profiler Doppler Spectra. *J. Atmos. Oceanic Technol.*, **12**, 985-995.

Ralph F. M., P. J. Neiman, and D. Ruffieux, 1996: Precipitation Identification from Radar Wind Profiler Spectral Moment Data: Vertical Velocity Histograms, Velocity Variance and Signal Power - Vertical Velocity Correlations. *J. Atmos. Oceanic Technol.*, **13**, 545-559.

Schumann R., G.E. Taylor, F.J. Merceret and T.L. Wilfong, 1999: Performance Characteristics of the Kennedy Space Center 50 MHz Doppler Radar Wind Profiler Using the Median Filter/ First-Guess Data Reduction Algorithm, *J. Atmos. Oceanic Technol.*, **16**, 532-549.

Weber B. L., D. B. Wuertz, D. C. Welsh, and R. McPeek, 1993: Quality Controls for Profiler Measurements of Winds and RASS Temperatures. *J. Atmos. Oceanic Technol.*, **10**, 452- 464.

COMBINED TEMPERATURE AND WIND MICROWAVE PROFILER: RESULTS OF FIELD TESTING AND COMPARISON

Ivanov A.A., Kadygrov E.N., Viazankin A.S.
Central Aerological Observatory, Moscow, Russia
E-mail: attex@gin.global-one.ru, т./ф.+7(095) 408 7758

INTRODUCTION

Remote sensing of atmospheric boundary layer (ABL) temperature and wind profiles is important for a variety of studies, including air pollution, air-sea interaction, and short-term meteorological forecasting. During 1992÷1998 Meteorological temperature profiler (MTP-5) was successfully tested in many scientific field expedition. MTP-5 is a single-channel (5 mm) scanning microwave radiometer for measurement of temperature profiles in the altitude range 0÷600m with accuracy 0,5 K. In 1998÷1999 approximately the same radiometer was used for measurement of wind speed at altitude range 0÷250 m and for investigations of atmospheric turbulence. During August-September 1999 microwave remote sensing data (temperature profiles, wind profiles, parameters of atmospheric turbulence) were compared with the in situ data from 310-meters Obninsk Meteorological Tower.

TEMPERATURE MEASUREMENTS AND LAST COMPARISONS

Radiometric method of temperature measurements at atmosphere based on the measurement of thermal emission of the atmosphere in the millimetre wavelength band with the subsequent reconstruction of temperature profiles from the radiometric data [1, 2]. Previous comparisons with Tsukubo and Boulder meteo-towers have been described in [3,4]. At this report are presented a new data of MTP-5 comparisons with in situ sensors of Obninsk Meteorological Tower. The aim of those experiment was to test the other scheme of scanning which have been suggested for increasing of Tikhonov temperature reconstruction method stability [1, 5, 6]. Fig.1 represents the interval of standard deviation for various heights. The result was corrected with in situ sensors errors and systematic deviation.

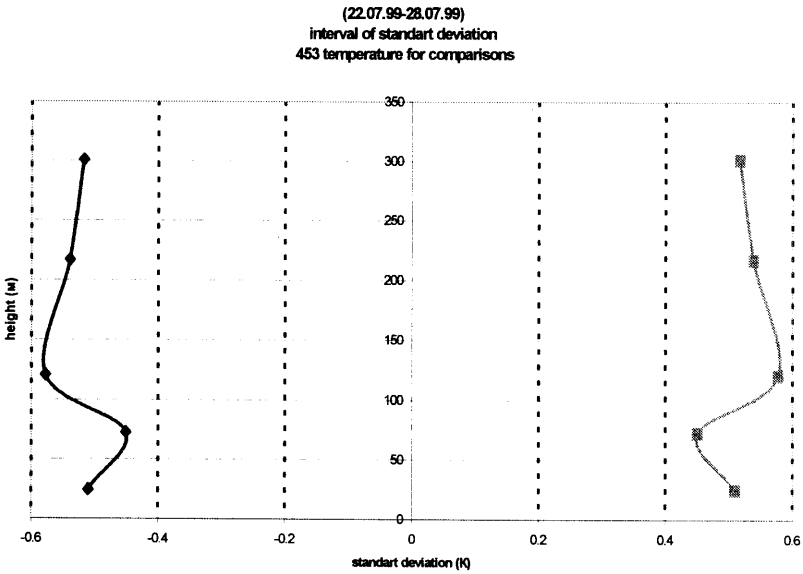

Fig.1

The fact is that the inversion situation at ABL have the time of birth and destruction about several hours. At that time sharp increase of aerosol concentration take place. Radiometric temperature observation in large industrial centres gives an opportunity to obtain dynamic picture of temperature distribution and to predict situation of ecological dangerous. The example of such situation which took place at Barrow station represented at Fig.2.

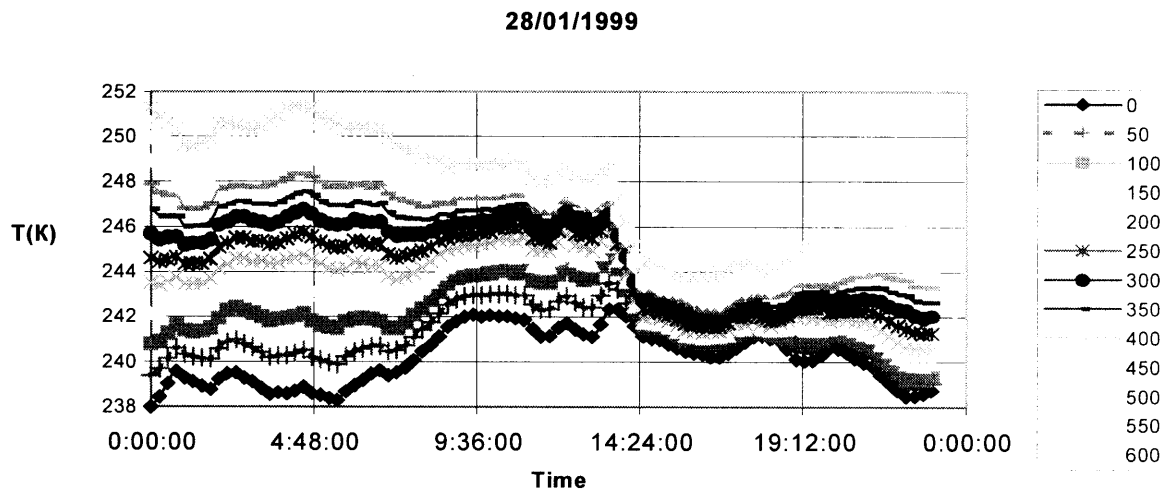

Fig.2.

INVESTIGATION OF TURBULENSE IN ABL

The possibility to use the thermal microwave emission of the atmosphere in the molecular oxygen absorption band centre at ν=60 GHz for detecting of temperature fluctuations have been shown in [5]. The fluctuation intensity of that emission is conditioned by turbulence pulsation of temperature and winds transfer in 300 m [6,7].

The opportunity of wind measurements by passive radiometers tuned at 60GHz are connected with two aspects. First is the space scale of detected atmospheric temperature inhomogeneities have the order of skin depth (300m). Due to Taylor hypothesis of the "freezing turbulence":

$$L \sim u_{wind} T \Rightarrow (if_u_{wind} \sim 10\frac{m}{sek}, T \sim 30\,\text{sec}) \Rightarrow L \sim 300m$$

The second is the result showed in [8] that the radiobrightness temperature fluctuation ΔTb from the turbulence pulsation ΔT(h) can be written:

$$\Delta T_b(\nu, \theta) = \frac{1}{\cos\theta}\int_0^H \Delta T(h)\gamma_\nu(h)\cdot\exp\left[-\frac{1}{\cos\theta}\int_0^h \gamma_\nu(h)dh'\right]dh$$

where: $\gamma_\nu(h)$ – molecular oxygen absorption coefficient; θ - sensing zenith angle, ν - frequency.

The instruments used in this work had following characteristics: Dicke-type 5-mm radiometers with the band width Δν = 3 GHz, sensitivity 0,03K at the 1 second integration time and antenna beam width 6°. Peculiarities of thermal emission at 60GHz made the measurements available in wide range of weather conditions (dry snow, fog, weak rain, presence of aerosol).

Three scanning radiometers have been used. One instrument have been occupied for atmospheric temperature stratification determination [9,10]. Two other worked in simultaneous mode. The zenith angles α and β changed from 0^0 up 90^0 (Scheme of experiment at Fig. 3.).Pulsation with the periods lying right to the meso-meteorological minimum on classical Kolesnikova-Monin spectrum have been of our interest.

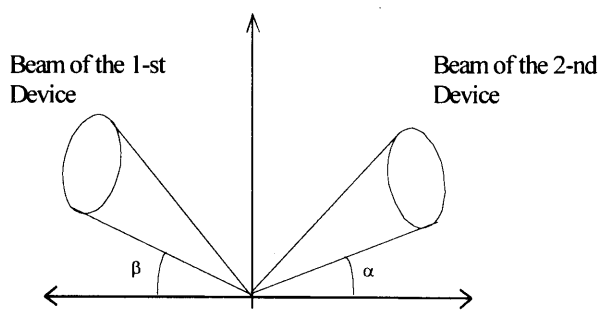

Fig. . 3

After the radiometer signal have been filtered in order to decrease instrumentation noise the data of in situ sensor and of one radiometer have been processed by Wavelet analysis. The results of the comparison presented at Fig.4 - Meteo Tower data and at Fig.5 - Radiometer data.

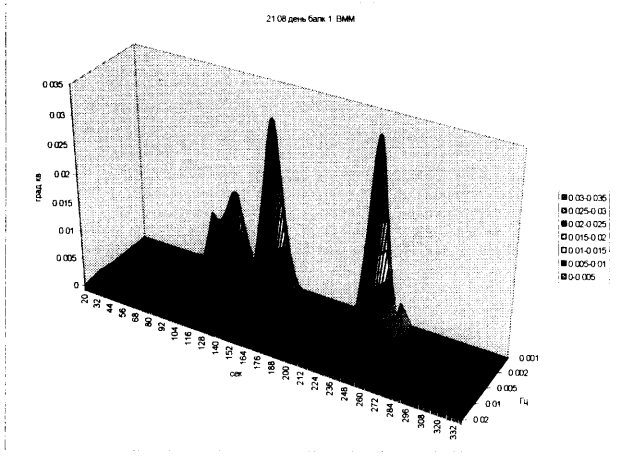

Fig.4

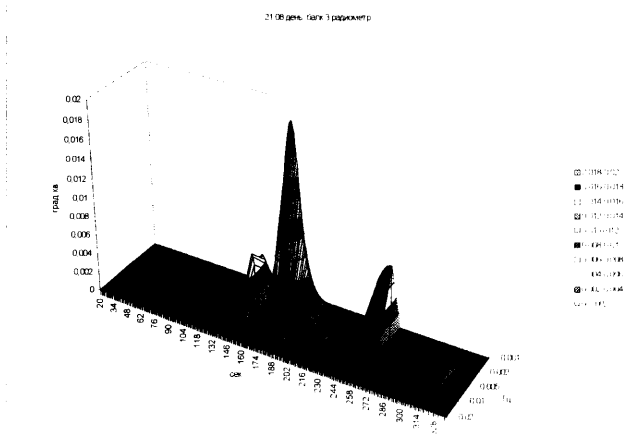

Fig.5

Comparisons of energy scale demonstrate good coincidence of in situ and remote data.

WIND SPEED DETERMINATION

Taking into account Taylor hypothesis of the «freezing» turbulence and making phase analysis one can determine wind speed and direction height profile in ABL. The preliminary estimations have showed that the accuracy of wind speed measurements is about ~1,5m/sek. Pulsations of the intertional interval have been chosen for apriori implementation of Taylor hypothesis while the transfer of temperature inhomogeneousis between spaces of radiometric sounding.

Radiometric results have been compared with meteo-tower data, some results of comparison are shown at Fig. 6.

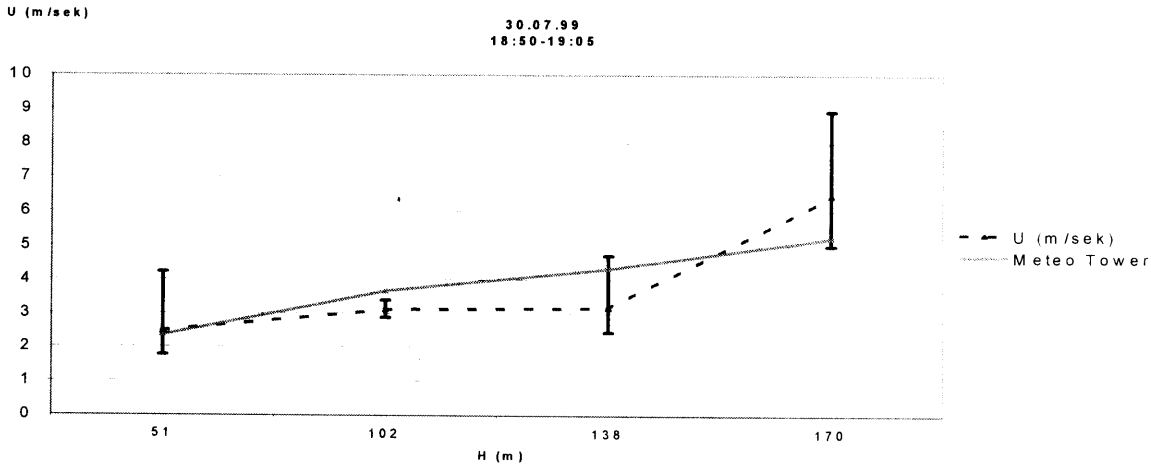

Fig.6

CONCLUSION

Scanning radiometers at 5-mm wavelengths gave excellent comparisons with in situ measurements with 310-meter Obninsk Meteorological Tower (August – September 1999). At the base of this investigations it will be possible to develop a new microwave remote sensing instrument for combined measurements of temperature and wind profiles at ABL.

REFERENCES

1. A. Ivanov, E. Kadygrov. WMO Report N 57, Instrument and Observing Methods, WMO/TD N 588, pp. 407-412, Geneva, 1994

2. A. Ivanov, E. Kadygrov, A. Lykov, E. Miller, D. Moiseev, A. Viazankin. WMO Report N 70, Instruments and Observing Methods, WMO/TD N 877, Casablanca, 1998, pp. 83-86

3.E.R. Westwater, Y. Han, V.G. Irisov, V. Lenskiy, E.N. Kadygrov and S.A. Viazankin. Remote sensing of boundary layer temperature profiles by a scanning 5-mm microwave radiometer and RASS: comparison experiments. Journ. of Atmosp. and Oceanic Tech., vol. 16, N 7, July 1999, pp. 805-818

4.Matsui I., Sugimoto N., Maksyutov Sh., Inoue G., Kadygrov E., Viazankin S. Comparisons of atmospheric Boundary layer Structure mesured with a Microwave temperature profiler and MIE scattering lidar, Jpn.J. Appl.Phys. v.35(1996), Pr.1, N 4A, April 1996, p.2168-2169

5. Kadygrov E.N., Troitsky A.V., Viazankin A.S. Investigation of Planetary boundary layer temperature by using microwave radiometers,Proc. of 4-th Int. Symp. On Tropospheric Profiling: Needs and technologies, 25 Sept., 1998, Snowmass, Colorado, USA, p.158-160.

6.V.D. Gromov, E.N. Kadygrov, A.S. Kosov, Remote sensing of atmospheric boundary layer at 5mm wave length, In: Proc.Symp. Wave propagation and remote sensing, Ravenskar, United Kingdom,8-12 June 1992, pp.3.4.1-3.4.5

7.A.V. Troitsky, E.N. Kadygrov, Atmospheric emission fluctuation of wave and turbulent origin in the absorption band O_2 ~5mm Proc. XXV-th General Assembly URSI, Lille,France, August 28-September 5, p.655 (1996)

8. Markina N.N., Naumov A.P., Sumin M.I. On global formulation of the reverse problem of remote atmospheric sounding in microwave range, Preprint N149, Gorky, NIRFI, 1981, p.47

9. Gajkovich K.P., Gromov V.D., Kadygrov E.N., Kosov A.S., Troitsky A.V. 1993, Thermal sounding of the atmospheric boundary layer in the Oxygen absorption band center at 60GHz, on IEEE Trans on Geosci.and Remote Sens.,vol.31, N1, pp.116-120.

10. Kadygrov E.N., Pick D.R. The potential for temperature retrieval from angular scanning single channel microwave radiometer and some comparisons with in situ observations. Meteorological Applications, UK, 1998, N5, pp.393-404

Automatic Cloud Coverage Determination by evaluation of thermal radiation differences[1]

Author: Mr. Klaus Heyn, Co-Authors: Mr. Ingo Schesonka, Mr. Stefan Engel
Institution: Jenoptik Impulsphysik GmbH,
Achter de Weiden 10, 22869 Schenefeld, Germany
Tel.: +49-40-83903-0, Fax: +49-40-83903-110,
E-mail: info@impulsphysik.com, Web: http://www.impulsphysik.com

---

Introduction:

In the framework of the world-wide activities for automation of weather observations the cloud coverage estimation has meanwhile pointed out to a critical term and seems not to be sufficiently fulfillable with the momentary available technologies.

All of the various technologies, which have been developed or are under development are up to now suffering from a number of certain disadvantages.

1. The classical human observer system
   - Works only at daytime
   - Has a limited low information update rate
   - Depends on subjective, individual factors
   - Is only able to estimate cloud coverage for more than one layer, if the clouds move sufficiently and the lower layer(s) is only partly covered
   - Is very cost intensive

2. The cloud coverage algorithms for ceilometer data
   - Have a natural limited information update rate, due to the statistical background of the method
   - Need a certain cloud movement for any cloud coverage estimation at all
   - Need a homogeneous cloud distribution for reliable results
   - Need all these facts to occur directly above the instrument(s)
   - Have a certain cloud height and detectivity limitation, depending on the cloud density

3. The various camera imaging analysis methods
   - Work only at day time
   - Need to shade direct sun radiation permanently (with sun synchronised movement), to prevent operational disturbances from the camera through the bright sun light
   - Are problematical to be adapted to an high reliable, all environment operationable and industrial manufacturable instrument

4. The infrared radiation analysis methods
   - Have not yet been in research and development status, where a reliable, all environment operationable and nearly maintenance free instrument could be manufactured for a reasonable price

The new developed Automatic Cloud Coverage Detector[2] ACCD™ from *IMPULSPHYSIK* overcomes with nearly all of the above mentioned disadvantages.

---

[1] © JENOPTIK *IMPULSPHYSIK* GmbH
[2] Patent pending

ACCD™ Measuring Concept[3]

In general one will find a different infrared radiation at a clouds covered sky in relation to the clear sky. This phenomena was intensively discussed in the frame of various research works in the past.

The ACCD™ uses this effect to decide whether a cloud is in the viewing field or not. During a defined and automatically running scan cycle, the infrared radiation is continuously applied to a infrared sensor element. A special narrow band filter selects the radiation within the atmospherical window between 8 and 14 microns.
Depending on measured radiation differences during a scan cycle the ACCD™ algorithm calculates the degree of cloud coverage.

The ACCD™ consists of a termination box and the sensor / electronics unit (see picture 1), which is mounted on a tilt / swivel head. This head is used to move the sensor unit in horizontal and vertical direction, so that the radiation of all segments from the sky can be scanned by using just one infrared detector. The applied viewing field of approx. ±5° for the detector enables a scan in six 360° cycles (each divided into thirty-six 10° segments) with elevation angles of 35°, 45°, 55°, 65°, 75° and 85° to cover the whole sky area of interest.

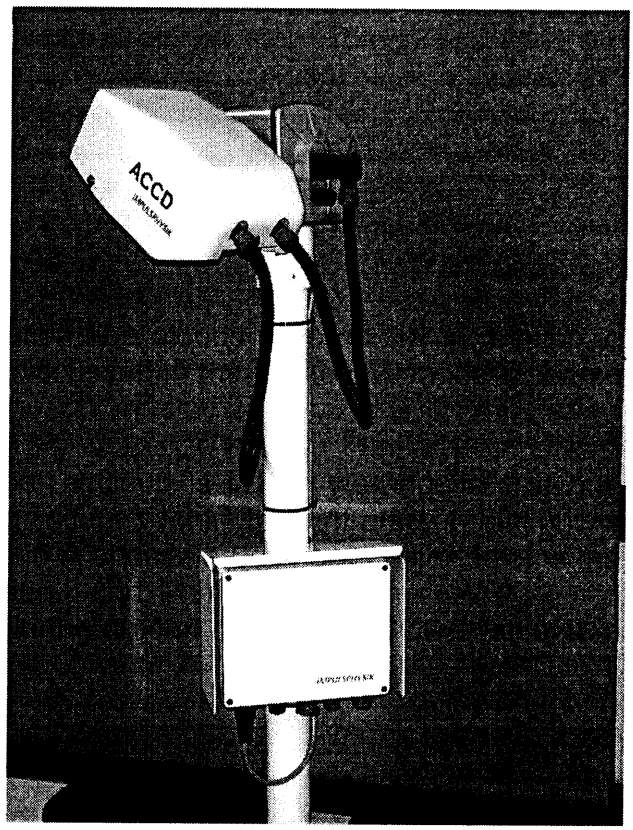

Picture 1

The neighboured measurement segments within each sampled 360° cycle and between the different sampling turns are evaluated for infrared radiation level. The cloud / no cloud decision for each scanned segment depends exclusively on the evaluation of detector signal differences. Beside this, the unique ACCD™ algorithm learns and adapts the sky clear radiation level to ensure a safe detectivity even for high cirrus clouds, which creates only small radiation differences.

The practical experiences show, that this method enables the ACCD™ even to evaluate cloud coverage situations, where ceilometers already fail.

[3] Patent pending

ACCD™ Measument Presentation

The cloud coverage information from the ACCD™ is typically presented in octas from 0/8 for sky clear up to 8/8 for overcast. A complete scan is finished in approx. every 90 seconds. In addition to the coverage information in octas the mnemonic code for cloud coverage is notified as well within the contents of the ASCII coded data telegram. The complete coverage information set is accessible through the serial standard RS-232 interface.

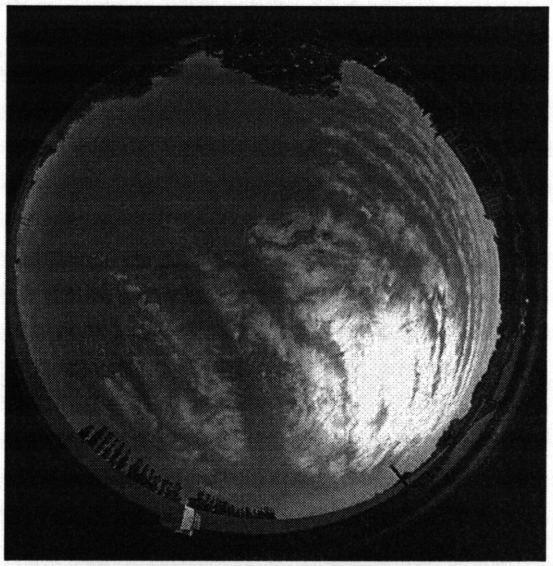

Picture 2

The detection example of picture 2 shows a situation with cirrus clouds above 35.000 ft in comparison with a "fish eye" image of the same cloud situation.

The used ACCD™ display software is especially developed for cloud coverage presentation showing a circular, observation-like format. This software analyses the contents of the ACCD™ data string and converts it into displayable screen segments at the workstation CRT. The display segments, which have been decided as covered by a cloud, are filled white against a blue background for the clear sky segments detected.

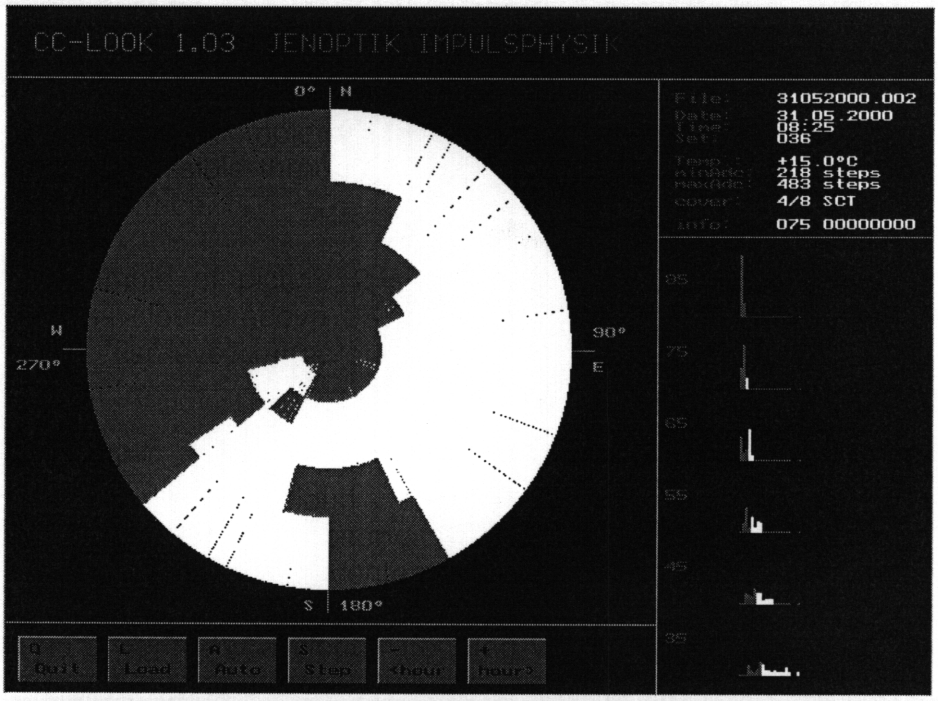

Picture 3

Beside this graphical presentation, the display informs about the calculated cloud coverage, the operational status of the instrument and the display gives an overview about the detected radiation levels within every 360° scanning cycle. For more information please contact the JENOPTIK *IMPULSPHYSIK* GmbH booth no. 14 at Meteorex-2000.

LONG RANGE SODAR

Improving the resistance of such a system to ambient acoustic noise

J. M. Fage
Remtech
P. O. Box 272406
Fort Collins, CO 80527 – U.S.A.

INTRODUCTION

Long-range Sodars (acoustic wind profilers) have been introduced about three years ago and have been installed world-wide.

While they initially were rather sensitive to ambient acoustic noise they now can operate with acceptable altitude range performance even when the environmental noise level reaches up to 55dBA.

This has been made possible by various signal processing techniques which are described hereafter.

New Noise Subtraction Technique

The frequency transfer function (in phase and amplitude) between the "active antenna" and the "reference antenna" allows a very efficient noise subtraction. The final acoustic frequency power spectrum can be cleaned by more than 15dB's decrease of the jamming source in the considered frequency zone.

This noise subtraction technique is also very efficient for removing spurious frequency peaks, which can be generated by electrical and/or magnetic influence.

Refined Adaptive Validation Criteria

The sodar software tries to achieve a given false validation probability. This one is very low: 4.0×10^{-5} chance per frequency band in each spectrum. As the acoustic environmental noise as well as spurious electronic peaks due to magnetic/electrical influences are statistically non-stationary the sodar stops emitting and "listens" only at regular time intervals. The real number of false validation during these periods for which no signal was emitted is used in two ways.

First the signal to noise (S/N) ratio per frequency band is adapted (increased or decreased) in order to keep the real false validation probability as close as possible to the false validation target.

Second at the end of the averaging period the number of validation threshold is also adapted based on the real false validations probability

Dual Mode Multi-Frequency Coding Technique

The Sodar operates with a wide frequency mode (3 frequencies standard, 5 with "NT" option) and a narrow frequency mode (9 standard, up to 15 with "NT" option).

The wide frequency mode uses emitted frequencies that are far enough from each other that their distance is larger than the largest expected Doppler shift and therefore provide a reference wind profile for the first part of the altitude range.

The narrow frequency mode uses more emitted frequencies with a shorter distance between them. Since this distance may be less than the maximum possible Doppler shift they can lead to a wind speed/altitude error.

These data are disregarded or properly corrected when compared to the wide frequency mode results.

The narrow mode covers the upper part of the Sodar range. It yields much more data and allows a much more efficient consensus technique based on many more independent measurements.

Five Beams Operation (Standard, up to nine beams with "NT" option)

The Sodar now operates on five beams by adding to the previous three (two tilted, one vertical) two new beams which are the mirror image of the 'direct' tilted beams.

The Sodar emits in sequence along each tilted beam and then immediately after along the corresponding symmetrical tilted beam.

The receiving sequence is activated simultaneously along each direct tilted beam and along its symmetrical beam.

The increased number of samples and the new possibilities offered for plausibility tests (as the symmetrical beam measurements must be equal in magnitude, and of opposite sign of those of the direct beam) result in a very significant range improvement.

The tables listed below are typical printouts from the Texas Natural Resources Control Commission Calaveras site.

Table 1: HEADER

BL#	MONTH	DAY	YEAR	HOUR	MIN	VAL1	VAL2	VAL3	VAL4
231	5	8	2000	12	30	699	554	529	0
SUP1	**SPU2**	**SPU3**	**SPU4**	**NOIS1**	**NOIS2**	**NOIS3**	**NOIS4**	**FEMAX**	**SOFTW**
0	1	1	0	765	411	391	0	0	711
FE11	**FE12**	**FE21**	**FE22**	**SNR1**	**SNR2**	**SNR3**	**SNR4**	**CHECK**	**JAM**
9	9	9	9	8	8	8	0	0	-9999

Table 2: DATA

ALT m	CT	SPEED cm/s	DIR deg.	S DIR	W	SW
3000	-9999	1089	141	-9999	-9999	-9999
2900	236	1081	139	17	-9999	-9999
2800	221	1075	136	17	-9999	-9999
2700	235	1091	132	17	-9999	-9999
2600	186	1122	129	17	-13	67
2500	181	1154	128	16	-34	71
2400	178	1188	133	14	-48	76
2300	168	1244	140	13	-42	78
2200	158	1336	148	13	-19	79
2100	148	1472	153	13	7	78
2000	138	1606	155	12	28	79
1900	127	1643	156	11	51	80
1800	117	1565	159	12	78	81
1700	110	1451	166	15	99	78
1600	130	1423	171	17	101	74
1500	132	1499	171	18	85	63
1400	124	1640	164	17	56	43
1300	117	1761	156	16	28	22
1200	109	1779	147	15	7	18
1100	102	1656	143	13	-16	36
1000	156	1430	145	14	-43	60
900	157	1168	157	21	-53	83
800	142	982	169	29	-39	87
700	136	886	169	32	-11	84
600	136	914	160	27	14	81
500	117	958	152	22	28	82
400	148	894	153	26	33	80
300	167	777	160	35	35	77
200	248	743	171	35	28	83
100	95	780	175	24	10	95

The Observation of Heavy Rainfall Event over China Using TRMM Data

M. Cheng, H. He, D. Mao, Y. Qi, Z. Cui, R. Shi and F. Zhou
Chinese Academy of Meteorological Sciences, Beijing 100081, P.R. China

1. Introduction

Heavy rainfall and/or floods brought by it have already caused the damage of property and the loss of human life (Cheng, 1994, Qi et al, 2000). On the other hand, heavy rainfall is the water resource especially for dry regions. In addition, rainfall is a key component of the Earth climate system, which may strongly affect the atmospheric circulation through the associated latent heat releases (Browning, 1990). Currently, besides the numerical meteorological model which is often used to study the heavy rainfall, there are three major techniques for the observation of heavy rainfall, i.e. direct measurement using rain-gauge, active remote sensing using radar (Collier, 1989, Cheng and Collier, 1993), and passive remote sensing using radiometer (Cheng et al, 1993, Cheng and Brown, 1995). Normally the radar is based on the Earth surface, and the radiometer is loaded onto satellite. The TRMM is the first meteorological satellite loading Precipitation Radar (PR). The PR together with on board Visible and InfraRed Scanner (VIRS) and TRMM Microwave Imager (TMI) form the most powerful capability to observe heavy rainfall from satellite. Therefore, some preliminary research has been carried out for the case study of heavy rainfall over the basin of Yangtze river using TRMM data at 2140 UTC on 20 July 1998 (or 05:40 BJT on 21 July 1998), which is described in this paper. TRMM derived precipitation products are also compared with rain gauge observation, ground radar data and mesoscale numerical model simulation results.

TRMM is a joint effort by National Aeronautic and Space Administration (NASA) and NAtional Space Development Agency of Japan (NASDA). One of the mission objectives is to test, evaluate and improve the performance of satellite rainfall measurements and estimate techniques. The satellite was launched on 27 November 1997 from Tanegashima, Japan. It has a circular orbit with altitude 350 km ranging between 35 degrees north and 35 degrees south of equator. Aboard the TRMM there are five instruments. Among them the PR, TMI and VIRS are the three primary instruments which constitute a rainfall measurement package. They work in a complementary manner.

The PR is the first space-borne meteorological instrument designed by NASDA to provide three-dimensional maps of precipitation structure. The measurements should yield invaluable information on the intensity and distribution of the precipitation, on the precipitation type, on the storm depth and on the height at which the snow melts into rain. The PR has a horizontal resolution at the ground of 4.3 kilometers and a swath width of 220 kilometers. It operates at 13.8 GHz with horizontal polarization. One of its most important feature is its ability to provide vertical profiles of precipitation from the earth surface up to a height of 20 km.

The TMI and VIRS were developed by Goddard Space Flight Center, NASA. TMI is similar to Special Sensor Microwave/Imager (SSM/I) on board the Defense Meteorological Satellite Program (DMSP). Instead of 4 frequencies, TMI has 5 frequencies (10.65 GHz, 19.35 GHz, 21.3 GHz, 37.0 GHz and 85.5 GHz) with dual polarization except 21.3 GHz. The additional 10.7 GHz is designed to provide a more-linear response for high rainfall rates common in tropical regions. The horizontal resolution of the TMI changes from 5 km at 85.5 GHz to 45 km at 10.65 GHz. A conical scan angle of 65 degrees provides a swath width of 760 km with the same resolution. The VIRS has 5 channels (0.63, 1.6, 3.75, 10.80 and 12.0 microns) with a swath width of 720 km and horizontal resolution of 2 km at nadir. The channels selected are similar to NOAA/AVHRR and GMS/VISSR. Thus the VIRS provides a link between

measurements made by TRMM rain package and those made simultaneously by the visible and infrared radiometers on operational polar and geostationary satellites. The primary sensors PR, TMI and VIRS in combination constitute TRMM as a 'flying rain gauge' to correct or calibrate the rain estimates made by other instruments such as GMS/VISSR, NOAA/AVHRR etc. The detailed description of TRMM sensor package is given by Kummerow et al.(1998).

3. The brief description of the case

On 20-22 July 1998, there occurred a continual heavy rainfall over the south of Hubei Province. On 20 July the heavy rain was mainly located over Sichuan province then moved to east and south. The rain continued eastward on 22 July and reached to coast area on 23 July. By analyzing reported rainfall data, it is found that the rainfall intensity on 21 July reached the peak. The rainfall amount reported by Wuhan weather station on 21 July is 285.7 mm within 24 hours. The peak period for this heavy rainfall was from 02:00 to 15:00 BJT on 21 July. The observed rainfall rate of 88.4mm/hr for the period of 06:00 to 07:00 BJT on 21 July was reported by Wuhan Weather Station. It is just after the TRMM overpassed Wuhan region. It has already been recognized that the heavy rainfall was produced from a mesoscale convective system.

4. Study of Heavy Rainfall Events

(a) 3-D Structure of Precipitation

The unique feature of PR is providing 3-D volume data of precipitation. From 3-D visualization, it is found that the precipitation system consists of many precipitation towers which form rain bands. These precipitation towers may be connected together in the lower layer but are separated in the higher layer. It is found that generally speaking, there is correlation between the rain rate at the layer of the height of 4 km and the height of precipitation tower, and the precipitation tower reaches up to 14 km with maximum rain intensity occurred at the centers of the tower for the horizontal direction and between the heights of 2-5 km for the vertical direction for this case.

(b) 3-D Structure Parameters of Cloud-Precipitation Systems

By viewing TRMM products for the case, following parameters of cloud-precipitation system can be obtained.

(1) The height of cloud top can be derived from TRMM infrared imagery
(2) Precipitation reachable height is derived from product of TRMM storm height.
(3) The height of zero isotherm can be derived from PR derived the height of bright band.
(4) The height of cloud base may be obtained from TMI derived 3-D cloud water content

5. Comparison Precipitation Product with Ground Truth and Simulation

Comparing Wuhan radar column maximum precipitation maps with PR derived one at 05:40 BJT on 21 July 1998. It is found that for the case, the patterns of precipitation are quite close, but the intensity may be much different. The precipitation intensity derived from the PR is generally smaller than one derived from the Wuhan radar. More comparison will be conducted in further study.

The rain guage hourly rainfall at 05:00-06:00 BJT on 21 July 1998 is analyzed: the rain gauge reported hourly rainfall distribution has a band shape with northwest to southeast direction. Within this band, there are three major centers with rain rates of 52, 31 and 26 mm/hr respectively. Comparing the rain gauge reported rain mao with the surface rain rate derived from

the combination of TMI and PR data, it is found that the general patterns of two rainfall maps are quite coherent. For example, the hourly rainfall distribution has nearly the same band shape as one given by PR and TMI combined product and the locations of three major centers are close. However, the rain guage network can not give the fine structure because of its coarse spatial resolution and the TRMM products can show more details of rain pattern. The difference of intensity on two maps is due to the TRMM product is instantaneous at 05:40 BJT and rain guage data are one hour average from 05:00 to 06:00 BJT, or due to TRMM gives less rain.

MM5 simulated results between 05:00-06:00 BJT on 21 July 1998, are used in this comparison. The simulated results give rain band but with different patterns and intensities. The simulation has bigger precipitation areas than ones derived from the observations and the simulated precipitation intensities are much smaller than those from observations. For example, the simulated top rainfall is only 13 mm/hr.near Wuhan, while rain gauge reported peak rainfall reaches 52 mm/hr.

6. Potential Research

Based upon the preliminary research, the TRMM data have displayed powerful capability to observe heavy rainfall and to estimate precipitation, although the current PR derived precipitation products seem underestimate the precipitation intensity. In order to fully benefit from the TRMM data, this research group have proposed following research subjects.

1) Studies of TRMM precipitation algorithms.

2) Validation of TRMM precipitation algorithms using more ground true data.

3) Retrieval of three dimensional structures of cloud-precipitation system using combination of the TRMM PR, VIRS and TMI data.

4) Estimation of precipitation using geostationary satellite data calibrated by the TRMM products for geostationary satellite have more temporal observing frequencies and spatial coverage. The principles are described by Lovejoy and Austin (1979), and Cheng and Brown (1995).

5) Calibration Chinese radar network using TRMM PR data. It is frequently observed that much different signals may be obtained for different radars while observing the same target. Because of the relative stable of the PR signal, a radar network should be benefited by the calibration using TRMM PR data.

6) Mesoscale model initialization and assimilation using the TRMM data to improve the accuracy..

Acknowledgements The TRMM products used in this study are provided by the Goddard Distributed Active Archive Center. Thanks also go to the meteorologists of Wuhan Central Meteorological Service who kindly provide the ground radar and rain gauge hourly precipitation data.

References

Browning, K.A., 1990: Rain, rainclouds and climate. *Quart. J. Roy. Met. Soc., 116, 1025-1056*

Cheng, M, R. Brown, and C.G. Collier, 1993: Delineation of rain areas using Meteosat IR-VIS data in the region of the United Kingdom. *J. Appl. Meteor.,32, 884-898*

Cheng, M. and C.G. Collier, 1993: An objective method for revcognizing and partially correcting bright band errors in radar images. *J. Appl. Meteor., 32, 6, 1142-1149*

Cheng, M. ,1994: *Estimate of precipitation using satellite, radar and rain gauge*, Ph.D Thesis, University of Bristol , 400pp

Cheng, M. and R. Brown, 1995: Delineation of precipitation areas by correlation of Meteosat visible and infrared data with radar data. *Mon. Wea. Rev. , 123, 2743-2757.*

Cheng M, H. He, D. Mao, F. Zhou, and B. Xiu, 2000: Retrieval of 3-D structures of cloud-precipitation system using TRMM data. *Submitted to Chinese Science Bulletin*

Collier, C.G., 1989: *Application of weather radar systems (A guide to uses of radar data in meteorology and hydrology)*, Ellis Horwood, Chichester, 290 PP

Grell, G.A., J. Dudhia, and D.R. Stauffer, 1994: *A description of the fifth-generation Penn State/NCAR Mesoscale Model (MM5).* NCAR Technical Note, 1994, NCAR/TN-398+STR ,138pp.

Kummerow C., Barnes W., Kozu T., Shiue J. and Simpson J. 1998 The Tropical Rainfall Measuring Mission (TRMM) Package. *J. Atmos. and Ocean Tech., 15, 809-817*

Lovejoy, S. And G.L. Austin, 1979: The delineation of rain areas from visible and IR satellite data for Gate and mid-latitudes, *Atmos. Ocean. 17, 1048-1054.*

Qi,Y., Q. Yi.. and M. Cheng, 2000: Numerical simulation for the "98.7" extraordinary heavy rainfall over the region of Hubei, *Submitted to Chinese Journal of Atmospheric Sciences (in Chinese).*

The Experiments on the Improvement and Application of GPS/PWV Technique in Shanghai area

Ding Jincai
(Shanghai Meteorological Center, Shanghai, 200030)
Wang Xiaoya Zhu Wenyao Yan haojian
(Shanghai Astronomical Observatory, Shanghai, 200030)

1. Introduction

Ground-based GPS meteorology is a new technique to measure precipitable water vapor (PWV) in air, it has been developing since the early 1990s. The physical basis for the measurement is the simultaneous observation of the signal delays from the GPS satellites to a given GPS receiver on earth ground. Since the zenith wet delay (ZWD) at a radio receiver is nearly proportional to the PWV, that is vertically integrated water vapor overlying the receiver. Thus

$$PWV = \pi \times ZWD \quad (1)$$

$$\pi = 10^6[\rho_1 R_w(k_3 / T_m + k_2')]^{-1} \quad (2)$$

where the ZWD is given in units of length and π is a dimensionless constant. ρ_1 is the density of liquid water , R_w is the specific gas constant for water vapor, The physical constants k_3 and k_2' are from the widely used formula for atmospheric refractivity, T_m is a weighted mean temperature of the atmosphere, defined as

$$T_m = \int_h^\infty (e / T)\, dz \;/\; \int_h^\infty (e / T^2)\, dz \quad (3)$$

T_m can be approximately estimated by surface temperature T_s as follows

$$T_m = 70.2 + 0.72T_s \quad (4)$$

This new technique can provide high accurate and continuous sequence of PWV data (hereafter called as GPS/PWV),which play important role in weather forecasts, numerical forecast and climate research, especially in mesoscale severe weather forecasts. Since 1997 Shanghai Meteorological center and Shanghai Astronomical Observatory conducted cooperatively a series of experiments to improve and apply the GPS/PWV technique. The goals of the experiments focus on testing the software system to calculate GPS/PWV and verifying the precision of PWV, evaluating the utilities in forecasting severe weather, such as heavy rains and so on, and improving the technique to satisfy the requirements of operational forecast in real time. The details are presented in the following three sections.

2. The first ground-based GPS/PWV experiment.

In this experiment six-day GPS data during July 26-31,1996 are collected from 23 national and IGS fiducial stations in East Asia, these stations form a regional GPS network. The software system to calculate GPS/PWV based on the precise orbits of GPS satellites is developed from GAMIT by Shanghai Astronomical Observation, named as SHAGAP. This software can obtain the zenith delays of the GPS satellites with the accuracy better than 1 cm. Employing SHAGAP the PWV/GPS data at 9 stations in China in interval of 2 hours are derived. For verifying the precision of PWV/GPS, the PWV data based on radiosondings (hereafter called as RADIO/PWV) at 00 UTC and 12 UTC on the same days at the same stations are derived, too. Fig 1 presents the results at ChangChun station and XiNing station. Both curves of the two types of PWV coincide well. The

mean deviation of GPS/PWV from RADIO/PWV are 3.74 mm. It is worth noticing that only the deviation on July 27 at XiNing station is very large, the magnitudes of RADIO/PWV are much less than that of PWV/GPS. In fact a moderate rainfall event occurred there on that day, it seems more reasonable that the PWV curve exhibits a peak with higher magnitude on that day. The comparing results prove that the software system is reliable and the precision of PWV/GPS data can fulfill the requirements of the weather forecasts.

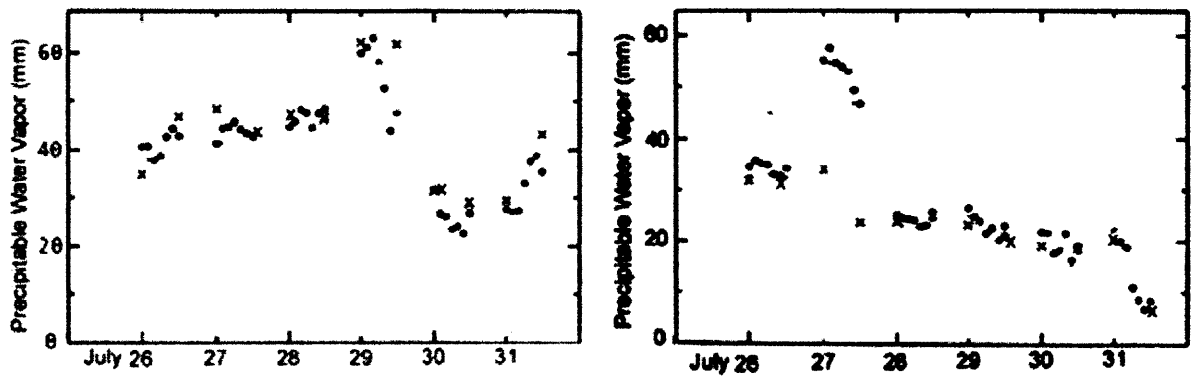

(a) ChangChun station (b) XiNing station

Fig 1. The comparison between GPS/PWV and RADIO/PWV data in July,1996 in China

(·) presents the PWV data based on GPS with interval of 30 minutes (GPS/PWV)

(x) presents the PWV data based on radiosondings with interval of 12 hours (RADIO/PWV)

3. The GPS/STORM experiment in Shanghai area.

As we known, water vapor in air is an important element for the generation and movement of various weather phenomena. A successful weather forecast depends closely on the precise and dense water vapor data. But now the standard observations of the water vapor in air at meteorological stations operate with radiosonde balloon only two times a day, at 00 UT and 12UT, respectively. And the distances between stations are over 300km mainly due to the expensive costs of the radiosondings. This is one of the main reasons why many mesoscale severe weather events fail to forecast. The precise and continuous GPS/PWV data can make up the above defect.

In order to evaluate the role of GPS/PWV data plying in indicating and predicting severe weather, a GPS/STORM experiment in Shanghai area was conducted in the periods of August 2-10 and 18-28, 1997 during which severe weather events occurred frequently. The GPS/PWV data were calculated in interval of 30 minutes at a IGS fiducial station in Shoushan, Shanghai. For comparing, the RADIO/PWV data at Baoshan meteorological station were calculated, too. The results and the relationship with severe weather events are illustrated in fig 2.

Firstly, there exist a period of frequent rainfall events during August 3-6. The GPS/PWV data exhibits frequent fluctuations, corresponding well with the frequent rainfalls. While, the six RADIO/PWV data from 00 UT, on the 3th to 00 UT on the 6th connect as an approximate straight line, without any obvious fluctuation. The reason is that most of the peaks and valleys of the GPS/PWV curve and the corresponding rainfalls in this period occurred between two times of radiosondings. Besides, a heavy rainfall occurred with 16.3mm at 23 UT and 12.3 mm at 24 UT on the 8th, respectively. Although both of GPS/PWV and RADIO/PWV data show a sharp peak at that time, the GPS/PWV data exhibit rapidly increasing after 12 UT on the 8th, it can indicate the occurrence of a heavy rainfall event earlier than RADIO/PWV data. If using RADIO/PWV data only, it has to wait until 00 UT on the 9th to know that the water vapor in air increased rapidly.

Besides it is worth notice that a severe weather event with thunderstorm, gale and heavy rain occurred at 07 UT on the 23th. The severe weather event lasted only one hour and the rainfall reached 68.8 mm an hour. But the RADIO/PWV data during 12 UT, 22th - 00 UT, 24th don't change obviously. Obviously, it is impossible for the radiosonding data to indicate a very short severe weather event happening in the middle time between two radiosondings. While the continuos GPS/PWV data show that the water vapor in air increased rapidly since 12 UT, 22th and reached a peak at 07 UT, 23th coinciding well with the time of the severe weather event. The above analysis results prove the advantages of continuous GPS/PWV data over RADIO/PWV data for indicating the severe weather events, especially the events lasting very short time.

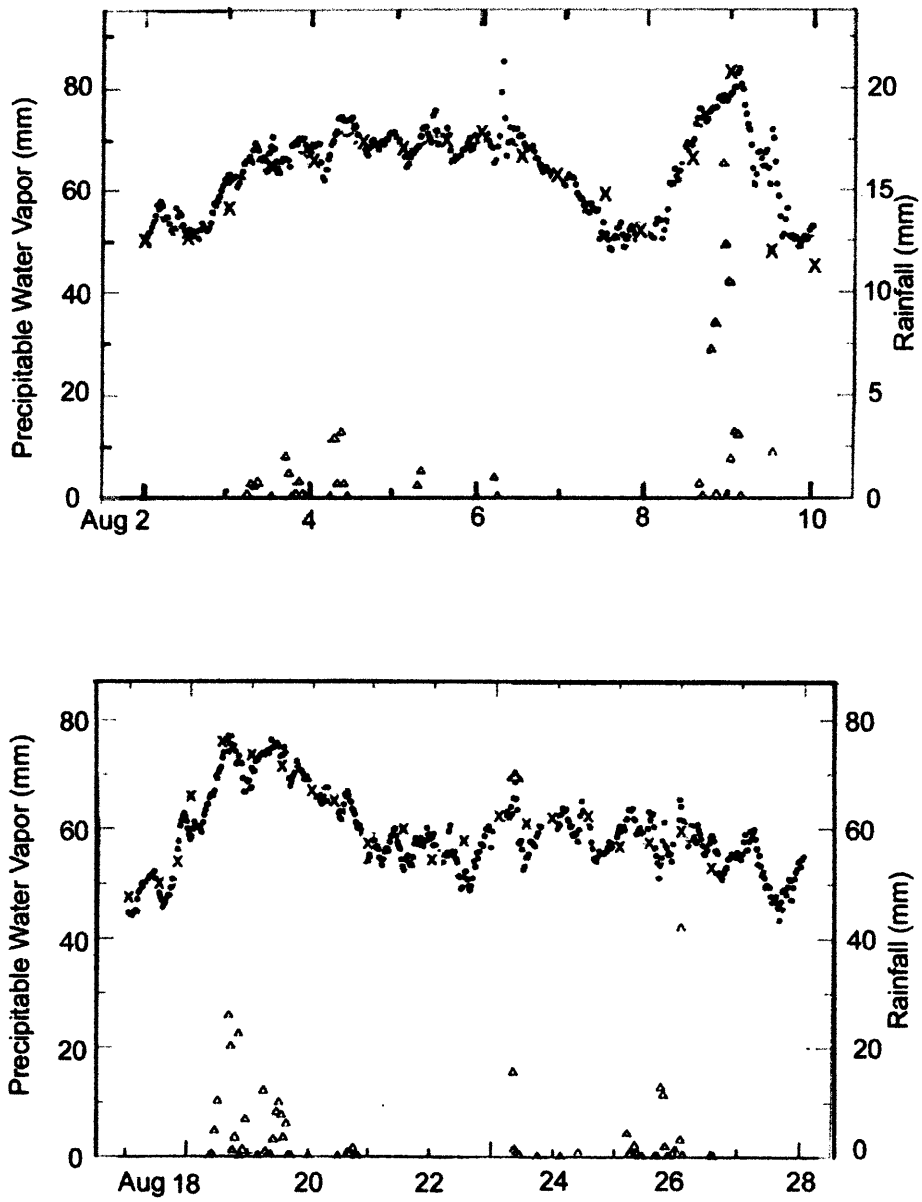

Fig 2. The comparison between GPS/PWV and RADIO/PWV data and the indicative role to severe weather events during GPS/STORM experiment in August, 1997 in Shanghai area. The abscissa marks the day and time (UT). (·) marks the GPS/PWV every 30 minutes and (x) marks the RADIO/PWV with interval of 12 hours, which are scaled by the left ordinate. (△) presents the rainfall per hour at Baoshan station scaled by the right ordinate.

4. The experiment to operationally calculate GPS/PWV in real time.

In order to realize the application of GPS/PWV data in the operational weather forecasts, The GPS/PWV data must be calculated and arrive at forecast room in very short time after the GPS signals are gathered. Generally, the delay of GPS signal is determined with the precise ephemerides or the fast speed orbits of the GPS satellite, but it should take at least 11 days for the precise ephemerides and 24 hours for the fast speed orbits of GPS satellites to be obtained. Fortunately, the IGS predicted orbits have been valid since March, 1997, the predicted orbits of GPS satellites in the next 24 hours and 48 hours can be obtained at 23:30 on every day. The accuracy of the predicted orbits is up to 50-80 cm. This makes it possible to calculate GPS/PWV with the predicted orbits in real time. Fig 3 illustrates the calculation results during the first period of GPS/STORM experiment. The thin dots mark the GPS/PWV data calculated with the precise ephemerides of GPS satellites and the dark dots mark the GPS/PWV data with predicted orbits of GPS satellites. Both of them coincide well. The mean square deviation between them is 0.2 mm, less than the accuracy of GPS/PWV by one order, almost without any influence on the accuracy of the GPS/PWV data. As mentioned above, the accuracy of GPS/PWV is 3.74 mm. This proves that the GPS/PWV data are reliable to be applied in operational weather forecasts in real time.

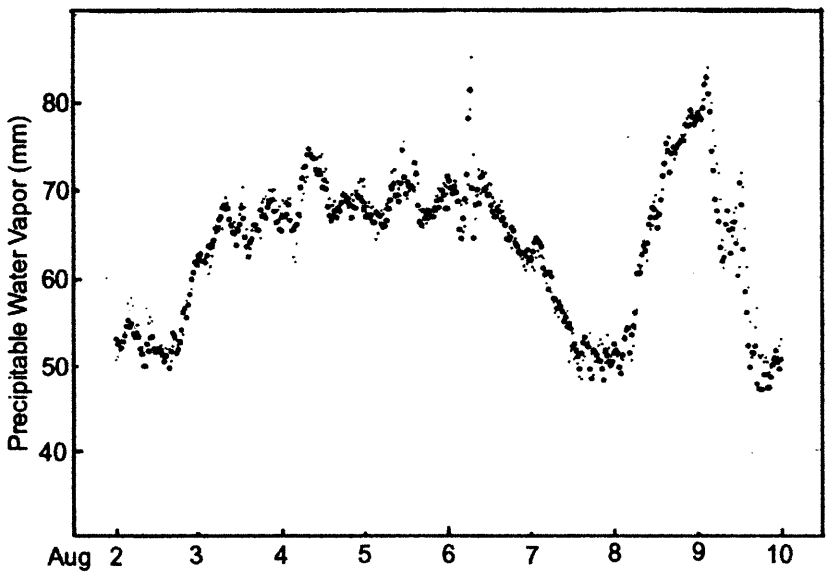

Fig 3. The comparison between the GPS/PWV data calculated with precise ephemerides and Predicted orbits of GPS satellites during the August 2-10,1997 in Shanghai, China.
The thin dot (.) marks the GPS/PWV data calculated with the precise ephemerides,
the dark dot (•)marks the GPS/PWV data with predicted orbits of GPS satellites.

QUALITY EVALUATION FOR THE COST 76 EUROPEAN WIND PROFILER NETWORK

N. Latham, J. Nash, T. Oakley, D. Lyth and M. Turp,
The Met. Office, Beaufort Park, Wokingham, Berkshire, RG40 3DN, UK
Tel: +44 (0)1344 855646, Fax: +44 (0)1344 855897, e-mail: nlatham@meto.gov.uk

Introduction – The European Wind Profiler Network

The United Kingdom was one of thirteen countries contributing to the European COST 76 (Co-Operation in the field of Scientific and Technical research) project, "Development of VHF/UHF Wind Profilers and Vertical Sounders in European Observing Systems". The project was established in 1994 with the aim of establishing a European wind profiler-observing network. The national meteorological services, research institutions and industry made contributions to the project.

In 1996, COST 76 agreed to initiate a campaign to network wind-profiler measurements in real time within Europe. Since then, significant progress has been achieved in networking wind profiler radars, and displaying upper wind information from Europe as part of the COST 76 CWINDE sub-project (CWINDE = **C**ost **W**ind **I**nitiative for a **N**etwork **D**emonstration in **E**urope). The profilers deployed in Europe are not of uniform type and thus networking such a variety of systems together requires flexibility in data reporting codes and in methods of data communication and also with quality evaluation software. The Remote Sensing Branch of the Met. Office, acting as the CWINDE project office, has developed the basic infrastructure for network operations, in collaboration with European partners within COST 76.

By CWINDE-99, 14 wind profiler systems supplied data in real time. During the MAP field phase in late 1999 up to twenty sites reported winds in real time. Currently 16 sites are reporting regularly.

Data availability

Data from these sites as supplied to The Met. Office are displayed in various formats on the web (www.met-office.gov.uk/sec5/CWINDED/cwinde99/cwinde99e.html), with plots updated every 30 minutes. A presentation of all current profiler wind data in the form of a thumbnail set is used by the project office to monitor data being received, so that any communications problems can be quickly resolved. Operators of the systems connected to CWINDE receive regular monitoring reports giving monthly details on the messages received, reported wind height coverage and summaries of the comparison of observations with short term weather forecast fields.

Identification of anomalous measurements

Wind profilers can produce large measurement anomalies, particularly if the operators have not adjusted operation to minimise the effects of ground clutter, sea clutter or intermittent sources of radio interference.

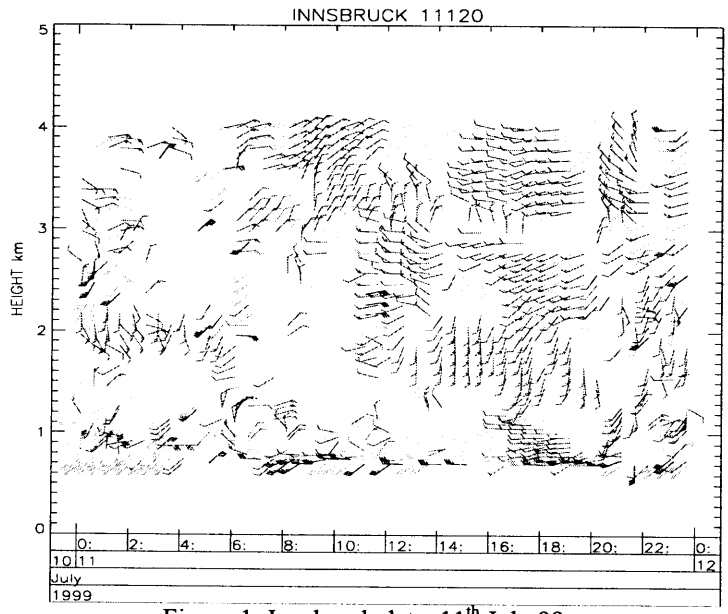

Figure 1: Innsbruck data, 11th July 99

Thus, the web display plots are also used to identify potential data anomalies. For instance, bird migration causes problems at some sites in the UK, but usually only for two or three hours after sunset on clear days. The validity of winds at this time of day can then be investigated by reference to signal power and vertical velocity plots. Figure 1 shows an example from a profiler at Innsbruck, Austria shortly after it was installed. Here, there were some spurious wind reports in the lowest range gates and also some spurious reports were escaping the system quality evaluation software at upper levels. The rate of occurrence of these types of errors can be quantified and operating procedures adjusted or referred back to the manufacturer to rectify the problem.

Quality Evaluation Techniques

(1) Against Numerical Forecast Fields

Wind direction and speeds provided by wind profilers have not always been as reliable as from radiosondes. Comparison against NWP model fields is a useful method for checking for systematic bias in wind direction or speed. Figure 2 shows part of a regularly used product from the CWINDE office, giving wind direction and wind speed bias compared to The Met. Office model's first guess (six hour) forecast field, averaged for a month. Comparisons with the measurements from the nearest radiosonde station are also presented to check whether the forecast fields are reliable or in error to some extent. In Vienna, the wind profiler is some distance from the radiosonde launch site, but using the forecast fields as a cross reference, the wind profiler measurements are shown to have a low direction bias and similar wind speed to the radiosonde measurements at heights of 2 km and above. However, nearer the surface the UK model forecast does not always represent detailed local flows (e.g. at 1 km) and a different method of cross-checking the wind measurements may be required, e.g. against aircraft measurements landing or taking off from the airport.

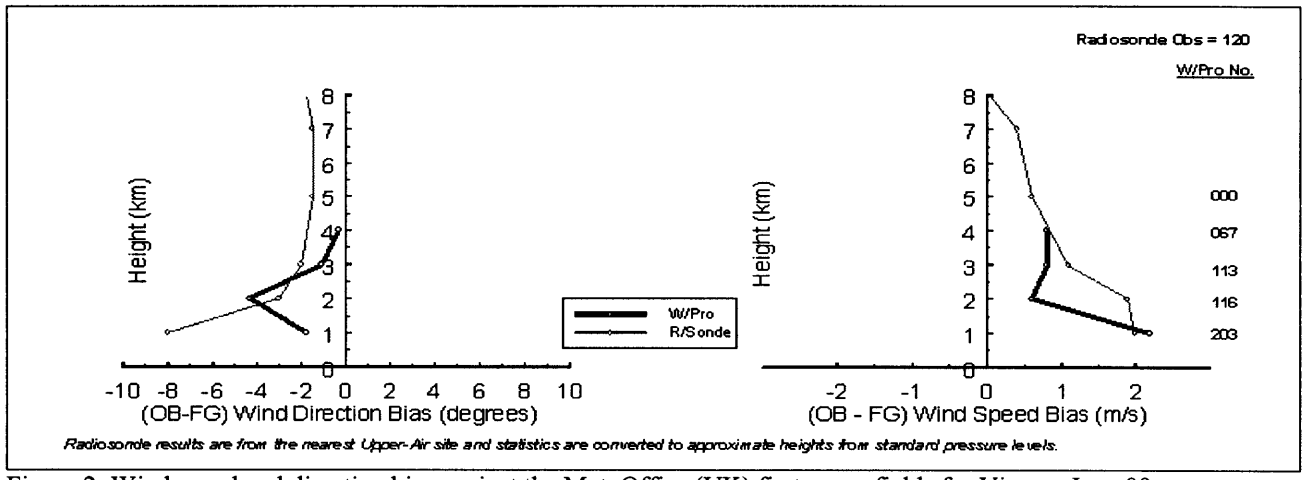

Figure 2: Wind speed and direction bias against the Met. Office (UK) first guess fields for Vienna, June 00.

(2) Specialised Tests Against Collocated Observations

The example given in Figure 3 shows the results of a comparison of wind direction between a wind profiler, RS80 radiosonde and a SODAR supplied by METEK. During a two month period, data from 194 RS80 radiosonde ascents were compared against nearest profiles from the wind profiler and SODAR. In general the profiler was performing well, however errors are occurring in the WP high mode at around 800m, resulting in a systematic bias of about 2° and a higher standard deviation relative to the radiosonde.

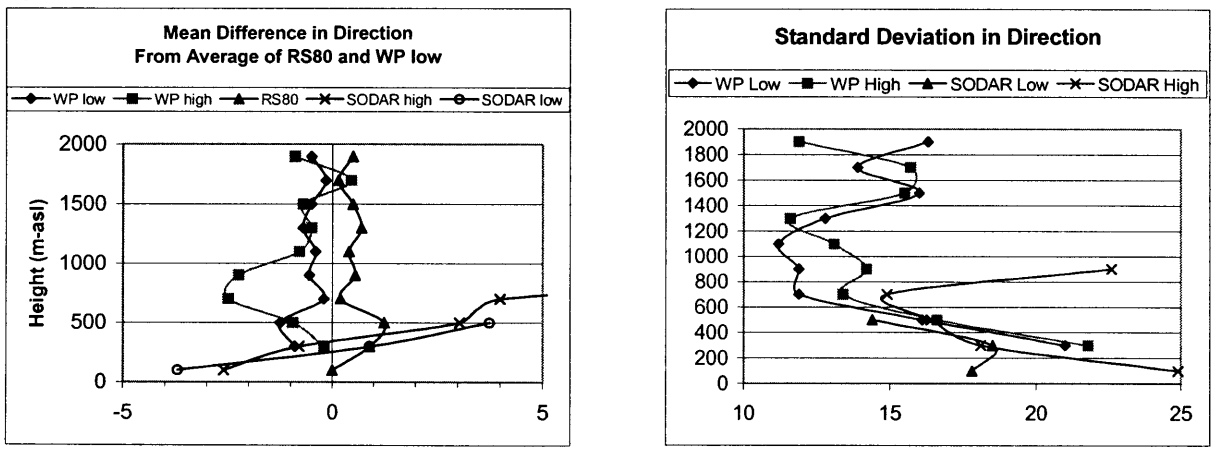

Figure 3: Comparison of collocated wind profiler, radiosonde and SODAR, Camborne, March-April 2000.

(3) Against Measurement Fields Generated By Integrated Observing Systems

As the wind profilers within Europe will have to function as part of an integrated wind observing system including measurements from radiosonde, aircraft and Doppler weather radar, CWINDE developed a plan view presentation for these types of wind measurements.

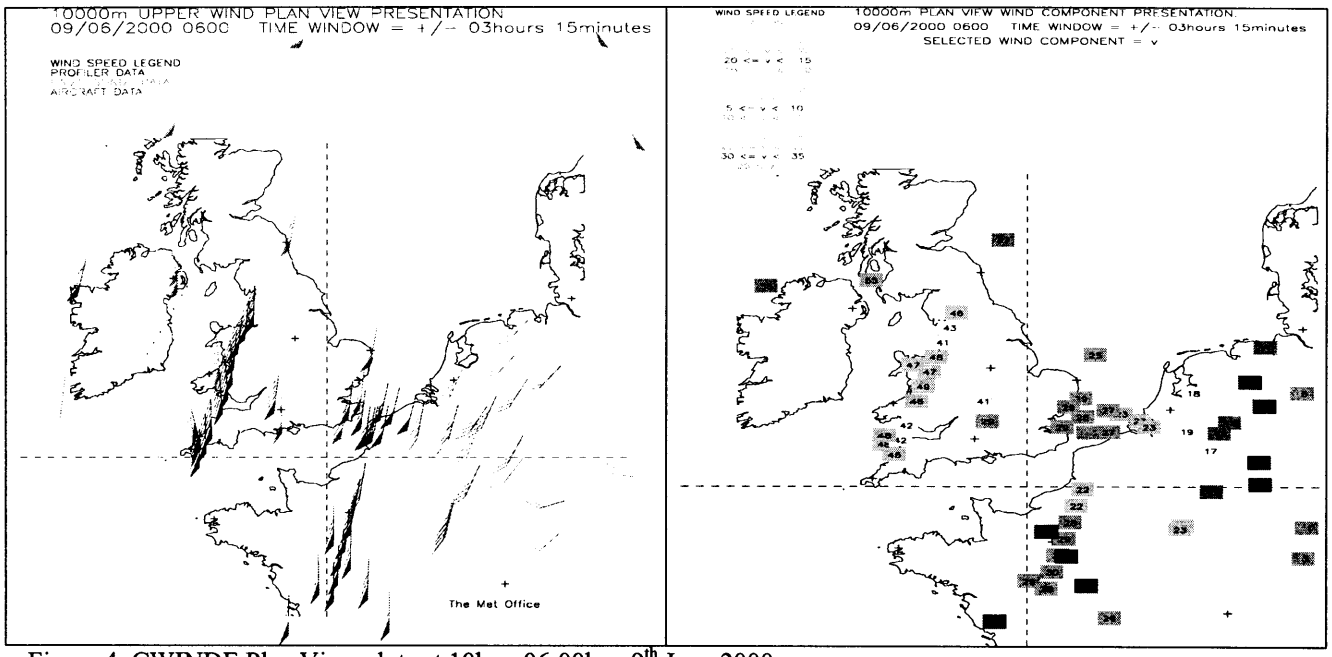

Figure 4. CWINDE Plan View plots at 10km, 06:00hrs, 9th June 2000.

Examples of these plots are also available on the CWINDE web site. The positions of aircraft and profiler wind measurements within ±3.25 hours are adjusted to the nominal time of the plot at 00:00 UTC [or 12:00 UTC], assuming that the weather systems are moving with a velocity close to that of the wind at 700 hPa. The radiosonde measurements are also time adjusted and take account of the drift of the balloon during ascent. An example of the plan view plot regularly available is shown on the left of Fig.4. The plot on the right is currently used for internal investigations within the CWINDE office and provides a numerical plot of the v component of velocity for this situation. At the height shown, there are observations from two profilers, Aberystwyth in western UK and La Ferte Vidame in northern France. The regular observations from the profilers are displaced from the observing site in a line with an orientation corresponding to a system velocity direction of about 200 degrees. The profiler observations are readily compared with the groups of aircraft observations over France and radiosonde and aircraft observations over the UK. In this case the observations from each observing type agree closely and there is no reason to query the operation of any of the systems. Evaluation of wind fields during CWINDE-97 and CWINDE-99 have identified serious anomalies in all three types of data, with large anomalies in some radiosonde measurements, spurious aircraft observations, and large scale malfunction in some profiler winds. This type of display facilitates quality evaluation of all three types of data and needs to be made available to upper air system operators on a regular basis, particularly as the manual checking of radiosonde observations is decreasing rapidly in western Europe.

Time Series

The atmospheric variability in wind, τ_u, has been shown, e.g. Kitchen (1989) to depend on the time separation, Δt_1, between samples as follows:- $\tau_u(\Delta t1) = b.(\Delta t1)^{\gamma}$ where b and γ are constants. γ is known as the structure function. For hourly or half hourly wind profiler measurements, experience with the better profilers in Europe leads to estimates of γ in the region 0.5 to 0.6 in the lower troposphere and lower stratosphere, and 0.6 to 0.8 in the upper troposphere near the height of the jetstreams.

If there is no correlation between the errors in each sample of a time series of wind profiler measurements, the rms deviation computed from the time series of measurements, $(\mathrm{rms}V_{obs}(\Delta t1)$ can be expressed as :-

$$(\mathrm{rms}V_{obs}(\Delta t1))^2 = (\tau_u(\Delta t1))^2 + 2.(\varepsilon_{obs})^2$$

where ε_{obs} is the standard vector error of the wind profiler measurement.

Figure 5 shows examples of $(\mathrm{rms}V_{obs}(\Delta t1))^2$ plotted as a function of height for two profilers in the UK, for the time separations shown. These are available on the CWINDE web page. If ε_{obs} were negligible compared to the real atmospheric variance, the left hand line in each case would be close to the value of $(\mathrm{rms}V_{obs}(\Delta t1))^2$ for a time separation of half an hour.

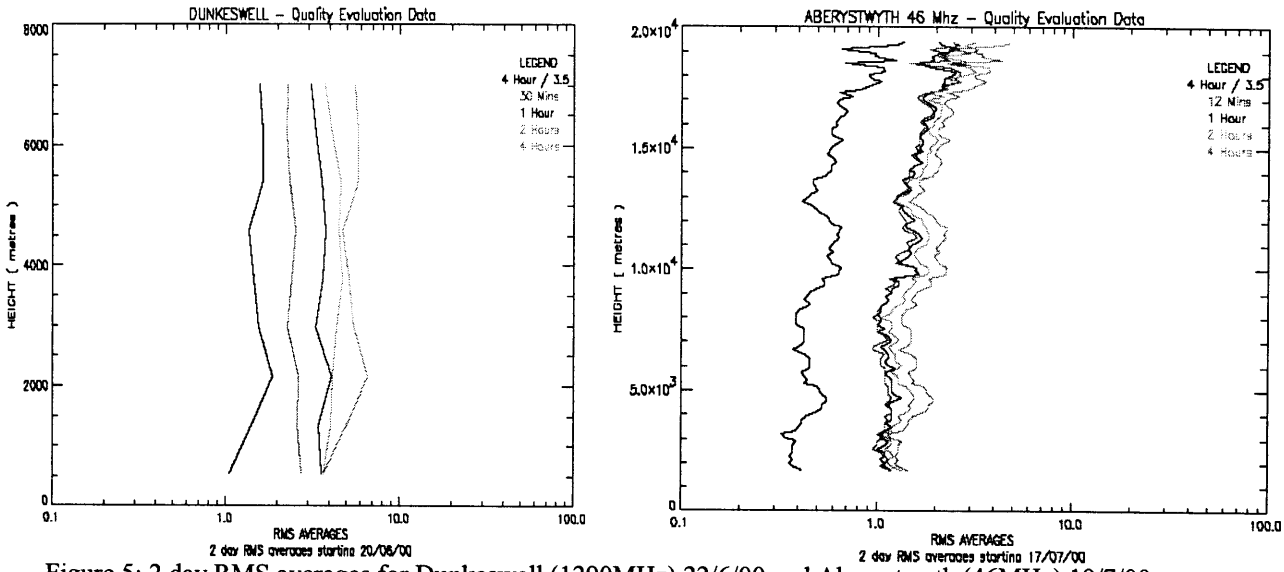

Figure 5: 2 day RMS averages for Dunkeswell (1290MHz) 22/6/00 and Aberystwyth (46MHz) 19/7/00.

These plots are not the easiest to interpret. It was intended to estimate the probable value of the structure function interactively and hence generate best estimates of profiler error. However, in practice this system did not work very consistently. Thus, it has been decided to produce estimates of the measurement error and atmospheric variance for a fixed set of possible structure functions, see Fig. 6. This will indicate whether the assumed structure function is critical in determining the estimated measurement error, or as in the sample in Fig.6, relatively insensitive.

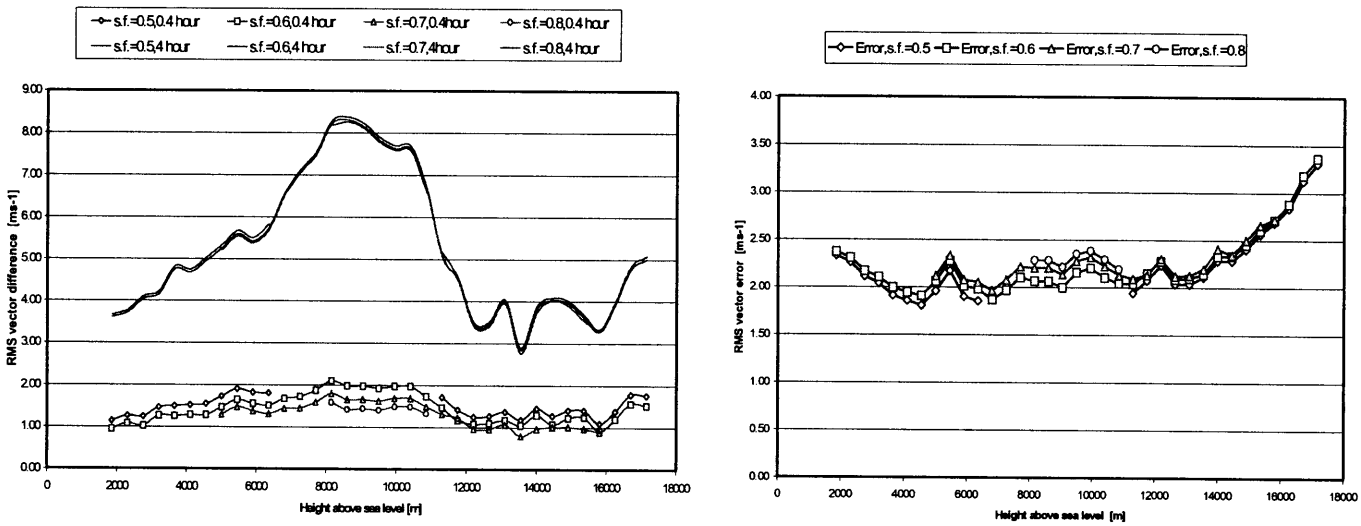

Figure 6: Atmospheric variance for 0.4h and 4 hour time separations (left) and estimate of random error (right), from the time series of measurements for a week in March 1999, Aberystwyth MST radar, for the structure functions indicated.

Conclusion

The development of a satisfactory set of quality evaluation products for the CWINDE network has taken longer than expected, because the work in developing the procedures was larger than originally estimated. A clearer picture of a satisfactory set of products is now emerging, but further development will be necessary in succeeding years, as less attention is paid in detail by the development staff responsible for the installation of the systems and more reliance is placed on the central quality evaluation procedures for flagging operational problems.

Reference

Kitchen, M. (1989) Representativeness errors for radiosonde observations. Q.J.R. Meteorol. Soc., **115**, pp 673-700

Distributed Transmitter / Receiver Design for Operational ST Wind Profilers

P. Currier
T. Berthou
(Degréane S.A. 28 av. Font-Pré 83050 Toulon France)
(Tel.: (33)494 61 9292 Fax: (33) 494 61 0471)
(E-Mail: degreane@wanadoo.fr)

Abstract

An operational VHF wind profiler using distributed solid-state transmitters and receivers has been operating since 1994. The simplicity of the design provides the phase coherence of the overall system. This architecture has many advantages over using a single transmitter / receiver design:

- significantly lower power output is required;
- excellent system noise figure;
- no « pseudo echo » when changing operating modes or switching beam directions;
- highly reliable;
- little maintenance required.

The overall cost of a distributed system is significantly lower than the equivalent centralized architecture having the same performance.

Pulse compression is required to take advantage of the high duty cycles (up to 20%) provided by the solid-state design. Multiple Inter Pulse Period pulse compression has many benefits over single IPP pulse compression:

- extremely low side lobes;
- large unambiguous distances;
- very robust to system non linearity;
- compatible with pulse shaping.

The high sensitivity of these radar makes them highly susceptible to various types of interference: vehicles, airplanes, precipitation, radio interference ... It is important to identify multiple targets in the measured Doppler spectra in addition to the clear air using multiple peak/feature spectral analysis.

Operational use of these radar requires reliable automated quality control based on signal statistics to identify valid clear air measurements.

Introduction

VHF wind profiler radar are used to measure winds in the troposphere and lower stratosphere. Typically they measure winds from 0.5/1.5 km up to 18/25 km with range resolutions between 150 meters and 1.5 km. The complexity of these instruments due to the combination of high power, large antenna surface and high sensitivity has kept these instruments mostly in field of atmospheric research.

Operational uses of wind profiler radar require relatively simple rugged systems able to operate unattended and which is incompatible with the traditional design of VHF wind profiler radar.

The use of distributed solid-state transmitters and receivers is the most cost effective design for operational systems. The main characteristics of the traditional (centralized) versus distributed design are presented in the following table:

	Centralized	Distributed
number of antennae	300	156
antenna surface	10000	3000
peak power	100000	20000
power x aperture	10^9	6×10^7

Overall, the distributed architecture is approximately "15 times smaller".

System Architecture

The main difficulty in distributed architectures is to maintain phase coherence of all the distributed elements. If phase coherence is not maintained, significant losses in the resulting antenna gain will greatly reduce the system's performance since it will affect both the receiver and transmitter chains. The phase coherence can be maintained either by use of phase lock loops or by a system which has intrinsic phase stability. The phase lock loop approach is complicated since the elements are distributed over several thousand square meters. The intrinsic phase stability approach is by far the cheapest and most reliable method. However great care must be used during the design to guarantee the resulting phase stability of the system. The elements influencing phase stability are mainly temperature variations, power supply variations, and the number of gain stages that are distributed. Consequently, the distributed elements must have a high thermal inertia, a single gain stage and the power must be furnished using a highly filtered direct current power supply. The resulting system architecture is given in the following figure.

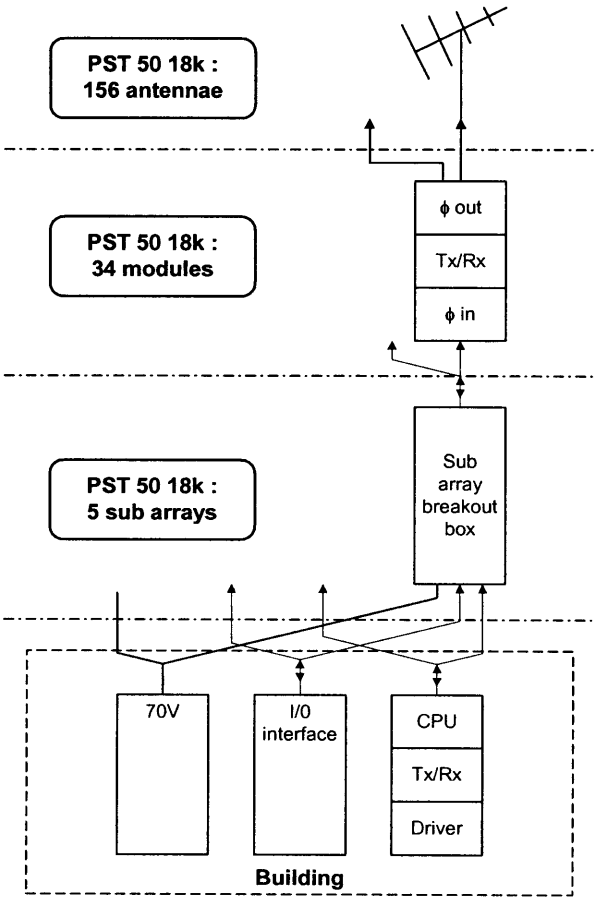

The 34 distributed solid-state transmitters and receivers contain a single stage receiver preamplifier (0.5 dB NF, 24 dB Gain) and one solid-state transmitter amplifier stage (17 dB Gain, 600 W peak). The beam forming is realized using one phase shifter on the input (ϕ_{in}) and one output phase shifter for each antenna (ϕ_{out}). This design minimizes system losses: both the system noise is optimized and the radiated power. Each module has extensive build in tests and furnishes a status message in real time. In case of a temperature or VSWR anomaly that may damage the module, the module automatically shuts down. Each module is completely independent from the others.

Because of the high thermal inertia of each module there are no significant thermal transient generated upon changing modes or beam directions: no "pseudo echo" generation that can mask the clear air signature.

The overall system is highly reliable. The failure of a module has not significant impact on the measurements: 10% to 20% of the system must fail before any noticeable effect on the instruments range coverage.

The system requires very little maintenance since there are no high voltages, no high power and very few moving parts.

Signal Processing

This system was designed from the ground up and benefits from the most recent signal processing algorithms. Some of the most innovative elements of the signal processing are

elaborate pulse compression;
second-generation intermittent interference rejection;
advanced multiple signal extraction;
statistical quality control.

Pulse Compression

Pulse compression is necessary in order to benefit from the high duty cycle available from solid-state transmitters: long pulses are phase coded in order to obtain a high spatial resolution. These new pulse compression techniques (Ghebrebrhan et al. 1992; Spano et al. 1996) have numerous advantages

very low sidelobes (reducing range ambiguities);
very robust against multiple trip echoes (large unambiguous range);
compatible with pulse shaping;
resistant to system non-linearities.

Intermittent Interference Rejection

The high sensitivity of these radar makes them highly susceptible to various types of interference: vehicles, airplanes, precipitation, radio interference. Often the interfering signals are present during a short time (an airplane or vehicle passing by) masking the clear air information. A second-generation intermittent interference rejection algorithm eliminates the contamination of such interference. This algorithm reduces significantly the spectral distortion introduced by the "Merritt algorithm" (Merritt 1995).

Advanced Multiple Signal Extraction

At times interfering signals present coherences that cannot be eliminated by the intermittent interference rejection algorithm (ground clutter for example). In such cases, the system must be able to process multiple signals and identify among these the clear air signature. The multiple signal extraction is statistically based and fuzzy logic is used to identify the clear air signal. These methods have been developed and refined continuously over the past eight years. Operational on several VHF and UHF wind profiler radars, this is the most robust processing available today.

Statistical Quality Control

The statistics of the resulting wind components are monitored in real time. This monitoring reliably detects and invalidates wind estimates that have residual interference contamination that would deteriorate quality of the wind measurements.

Conclusions

The architecture presented is a simplification of the remarkable MU radar used for atmospheric research. The distributed transmitter / receiver design for ST wind profiler radar is erroneously viewed as an expensive and complicated system. In view of the hardware's reliability and the robustness of the wind estimates furnished by this software/hardware architecture this new generation of VHF wind profiler radar is well adapted for operational deployment.

References

Fukao S., S. Kato, T. Aso, M. Sasada, and T. Makihira, 1980: Middle and Upper Atmosphere Radar (MUR) Under Design in Japan, *Radio Sci.*, **15**, 225-232.

Ghebrebrhan O. and M. Crochet, 1992: On Full Decoding of Truncated Ranges for MST/ST Radar Applications, *IEEE Trans. Geosci. and Remote Sensing*, **Vol. 30 No 1**, 38-45.

Merritt D. A., 1995: A Statistical Averaging Method for Wind Profiler Doppler Spectra. *J. Atmos. Oceanic Technol.*, **12**, 985-995.

Spano, E. and O. Ghebrebrhan, 1996: Pulse Coding Techniques for ST/MST Radar Systems: A General Approach Based on a Matrix Formulation, *IEEE Trans. Geosci. and Remote Sensing*, **Vol. 34 No 2**, 304-316.

1 MEASUREMENT TECHNOLOGY, PERFORMANCE, AND QUALITY ASSURANCE

1.3 Weather Radars and Lightning Detection System

A Lightning Detection and Location Network for New Zealand

Ralph A. Pannett[1], M.E., MIPENZ
Meteorological Service of New Zealand Limited

1. Introduction

A national lightning detection and location network requires large capital expenditure and significant ongoing operating costs. The business model under which Meteorological Service of New Zealand Limited (MetService) operates requires capital expenditure to show a return on investment above a certain threshold. In the past MetService was unable to establish a viable user market for lightning data at its real cost and therefore could not justify the establishment of its own network.

Transpower New Zealand Limited is the government 'State-Owned Enterprise' which owns and operates the network of high voltage transmission lines, substations, switchyards and control centres known collectively as the national grid. Transpower conducted a study in 1997 which indicated that a national lightning detection and location system would be clearly of economic benefit to its operations, e.g. optimisation of transmission line design, reduction in line patrol costs; and improved personnel safety.

Transpower invited MetService to make a proposal for the implementation of a lightning detection and location network (LDLN) to cover the New Zealand mainland and to provide data to Transpower with the performance specifications of 90% detection efficiency for lightning flashes greater than 5 kiloamperes, and a location accuracy of at least 0.5 km. Transpower would meet the capital cost of the system. Subsequently, in April 2000, Transpower awarded two contracts to MetService: installation of a lightning detection and location network; and operational delivery of lightning data to Transpower, with system maintenance and support for a period of 10 years.

MetService was responsible for project management, site acquisition, site works, securing telecommunications services, and assisting the supplier with system installation and commissioning. The MetService objective was to produce a high performance network for the lowest possible establishment and operating costs. These contracts retained ownership of the network equipment and lightning data by Transpower and MetService is in the role of a service provider. MetService has use of the data to effectively manage the network; to prove the utility of the data for public forecasting; and to develop information products for other clients with lightning-sensitive operations under commercial terms being negotiated with Transpower.

2. Selection of Lightning Detection and Location System

Holle and López [1] give a useful overview of the characteristics and application of the principal lightning detection methodologies. Global Atmospherics, Inc. (GAI) was chosen as the supplier of the LDLN. They proposed a system using IMPACT ESP sensors with data processing by their APA2000 software. The New Zealand network would benefit from the evolution of lightning detection systems and processing algorithms over many years (see introduction to [2]).

3. Sensor Operating Principles

Lightning discharges produce wideband electromagnetic radiation. The lightning cloud-ground (C-G) 'flash' may comprise several return 'strokes' to the initial leader charge from the cloud. The IMPACT ESP is a composite sensor which measures the electric and magnetic field signals above set thresholds in a bandwidth 0.4 kHz to 400 kHz, to determine by magnetic direction finding (MDF) the azimuth of the magnetic component; the time of arrival (TOA) of the electrical wavefront; and its signal strength and pulse shape.

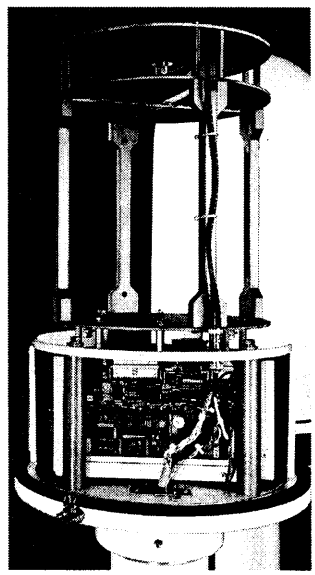

Figure 1 IMPACT lightning sensor

The sensor (Fig. 1) includes a flat plate electric field antenna; an orthogonal pair vertical loop antenna for MDF; and a GPS antenna for the sensor location

[1] The author acknowledges the permission of Transpower New Zealand Limited to publish this paper, and the assistance of Global Atmospherics, Inc.

and time reference. Comprehensive self-test and remote command functions are provided. The sensor output data format includes: station number, TOA in UTC to 50ns resolution, signal rise-time and peak-to-zero time, onset correction time, N-S and E-W magnetic field values, electric field value, time quality. The range-normalised peak field signal amplitude provides an estimate of the peak lightning current.

4. Sensor Site Selection and Optimisation

Good sensor siting is critical to the performance of the LDLN. GAI recommend baseline distances between sensors of the order of 300 km. The geometry of the New Zealand mainland (Fig. 2) is difficult to cover to good accuracy with a minimum number of sensors. MetService recommended likely sites mostly near to automatic weather stations on airfields (flat, open sites with power and communications services). From site latitude/longitude co-ordinates GAI ran computer models [2] which gave estimated iso-contours of detection efficiency and location accuracy for 17 site combinations until the desired quality of coverage was achieved with 10 sensors (Fig.2). The mean distance between pairs of adjacent sensors is 285 km with a standard deviation of 19 km. Over most of New Zealand a detection efficiency of better than 90% and a location accuracy of ±500m (median) should be achieved once systematic biases have been corrected.

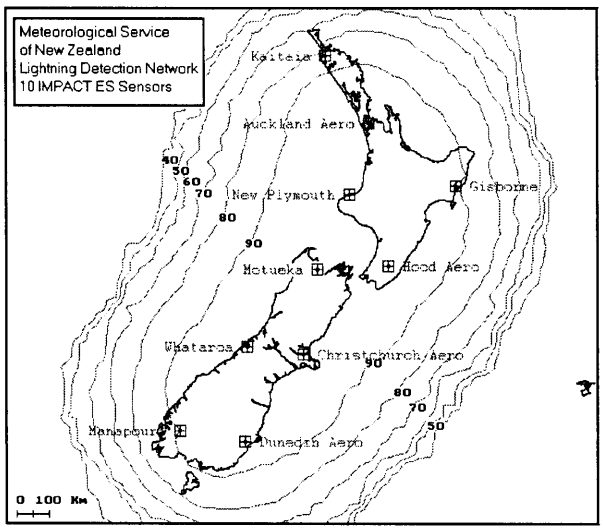

Figure 2a Estimated detection efficiency, %

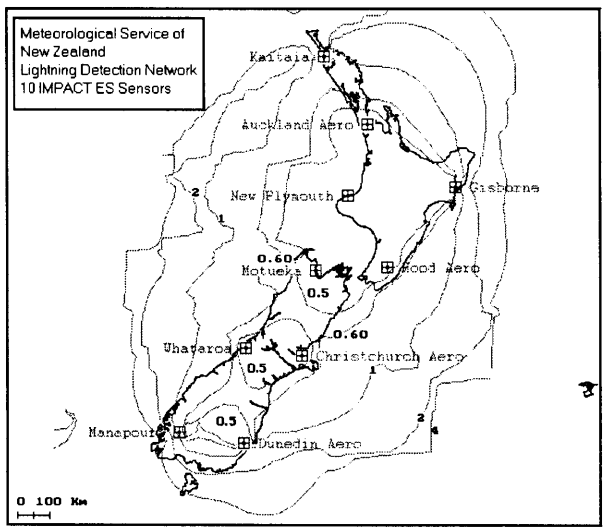

Figure 2b Estimated location accuracy, km

These site criteria were evaluated: physical environment, electromagnetic noise environment, ground conductivity (which affect sensor performance); road access, land acquisition and site works costs, access to power and telecommunications utilities (which affect installation cost); and transport access (which affects annual cost of maintenance). In order to reduce MDF errors, sites should present a nearly flat ground plane within 100 m radius with good conductivity and have no nearby grounded structures (trees, masts, buildings) which would distort the magnetic field; or underground or aerial power lines in which lightning can induce loop currents. For each of the initial selection of 17 sites, photographic and electromagnetic surveys were carried out. Following Fourier analysis of the data certain sites were rejected because interference exceeded the recommended limits, and 10 specific sites were identified.

At some sites noise pulses from electric fences were evident during the survey. In New Zealand the electric farm fence is commonly used as a temporary fence for controlled grazing of stock. These fences are energized by high voltage pulses with a repetition period of about one second and a rise-time similar to that of lightning C-G strokes. While a false signal which is detected only by a single sensor will be eliminated by the Location Processor, the regular pulses will create messages from the sensor, possibly masking a true lightning signal and increasing the message volume cost. GAI were asked to devise a solution that would reject the unwanted signals at the sensor so that they would not appear as messages. They designed new software commands for the control of the sensor message generation to reject signals with characteristics like electric fence pulses, by tuning five stroke parameters for the particular sensor site; and to reject pulses of low repetition frequency.

5. Network Communications

Fig.3 shows the lightning detection network configuration. Near real-time communications are required from each sensor to the central analysis computer. As each data message includes absolute time, communications

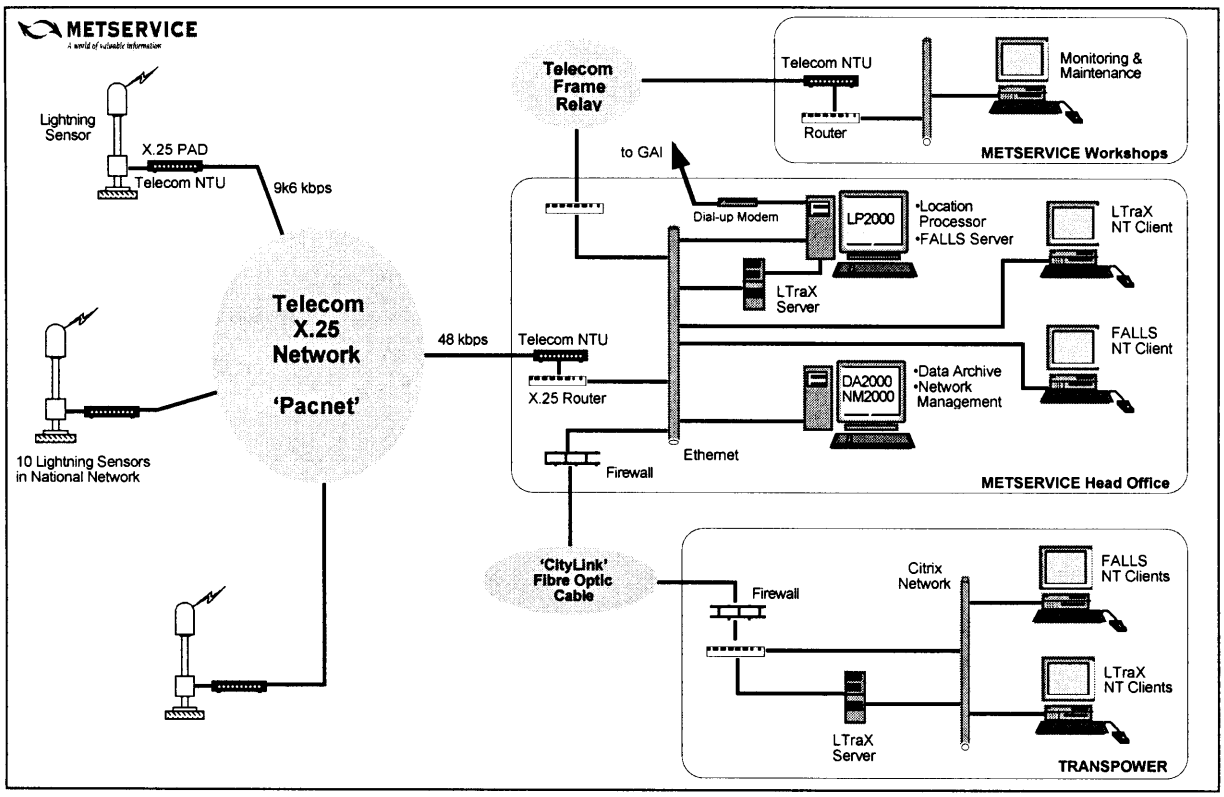

Figure 3 New Zealand National Lightning Detection and Location Network

latency of a few seconds is permissible until the central analyser receives data from all sensors that have detected a particular lightning stroke. The Telecom X.25 packet switch network (Pacnet) is employed because it is able to serve the rural locations of the most remote sensors and is cost efficient. Permanent virtual circuits were chosen to obviate circuit set-up delays. A circuit speed of 9.6 kbps from the sensors allows a sufficient maximum transfer of lightning data for multiple strokes, and a 48 kbps circuit to the central analyser has capacity to provide for the higher volume of concurrent messages from several sensors.

From the Central Processing System located in the MetService building, processed lightning data is made available to the Transpower computer network using TCP/IP protocol over a shared 'CityLink' high speed fibre optic cable with 'fire walls' at each end to maintain security.

6. Lightning Data Processing

Analysis of the sensor data is carried out on the GAI APA2000 system, comprising one Sun Microsystems Ultra 10 workstation with the LP2000 location processor software module, and a second workstation operating the DA2000 data archive module and the NM2000 network management module, all in a UNIX operating environment. The LP2000 collects the raw data from the sensors and provides the functions of control and configuration of sensors; archiving raw data; calculating lightning locations; and support of real-time lightning displays via their server software. It also enables remote support for the network by reading sensor parameters; running diagnostic routines; and downloading sensor software and parameters.

6.1 Detection Efficiency and Location Estimation

Lightning strokes with signal strengths below the sensor threshold, or with 'non-standard' waveshapes, or which cannot be correlated by several sensors, will not be reported. Detection efficiency is the percentage of actual strokes reported, and will vary from region to region with the geometry of the sensor locations. Network detection efficiency has been found empirically by comparing sensor outputs with records from a video camera array in the U.S. [3] and the GAI performance model is based on this data.

The estimated return-stroke position is located at the intersection of azimuth lines defined by sensors' MDF capability and the intersection of circular loci of TOA centred on the sensors. Errors in MDF (s. d. 0.9°) are due to non-verticality of the stroke near the ground, near-sensor distortions of the field and sensor measurement errors. Errors in TOA (s. d. 1.0 μs) arise from uncertainty in defining the peak field and differing propagation delays as the wavefronts travel over terrain and water of different conductivities. The

best estimate of stroke occurrence time is derived from the sensor TOAs. The more sensors participating, the greater redundancy and the better the accuracy of the estimate. On receipt of data from lightning sensors the Location Processor compares the times of the messages, decides whether they refer to the same event, and rejects noise messages. It then uses all available sensor measurements to optimise the location of the stroke by a least squares minimisation of a normalised chi-square statistic including the azimuth deviations from the expected value and the time deviations from the estimated return stroke time origin at the ground [2, 4].

The output of the Location Processor gives the stroke parameters: date and time, position (lat./long.), signal strength and polarity, peak current, number of sensors included in the determination, wave-shape timing, classification of cloud-to-ground or intra-cloud discharges; the dimensions of the axes of the position confidence ellipse and its orientation; and positional confidence (chi-square).

6.2 Data Archiving and Network Management

The DA2000 module is designed to handle many simultaneous requests for display of real-time or historical lightning data. This module collects real-time stroke data from the LP2000 and stores it in a Sybase™ relational database. Historical data may be filtered according to many parameters including date, latitude and longitude.

From replicated data streams on the TCP/IP LAN the NM2000 module can control all LP2000 processes. Thus the operation of the LP2000 may be monitored and it may be reconfigured, e.g. adding or removing sensors, changing measurement corrections. The NM2000 may log on to any sensor for diagnostic purposes. Network performance statistics may be logged and analysed for changes in performance.

6.3 Operational User Data Display

Display tools for operational use, planning and research are provided on computers at Transpower, MetService, and other client sites, via servers which are part of the Central Processing System. There are two principal tools available to users. LtraX™ (Real-Time Lightning Tracking Software) gives stroke polarity, intensity, location, and motion with respect to maps of significant features. Lightning events may be clustered and future development predicted to sound an alarm when specified targets are threatened. Historical data may be animated at selected rates. FALLS® (Fault Analysis and Lightning Location System) enables various analyses on past data for asset management. The FALLS server supports Sybase SQL.

7. Network Performance Evaluation and Optimisation

The LP2000 software calculates two quality statistics for the network stroke location accuracy. The *position confidence ellipse* from a two-dimensional location error distribution indicates the region within which the stroke originated with a probability of 50%. The length of the ellipse axes and its orientation will indicate the accuracy dependency on the geometry of available sensors. The *position chi-square* is a quality estimate from standard deviations of measurements from all participating sensors. A limit is set for the location processing so that if the chi-square value is exceeded, the stroke position value will be rejected.

The GAI model performance measures (see §4.) and data from the commissioning have established a baseline for the LDLN. After some months of lightning (and noise) data have been archived, MetService and GAI will examine the statistics to determine the effectiveness of the whole network (real detection efficiency and location accuracy), regional performance, and the performance of individual sensors. During the life of the LDLN it is expected that there will be changes in sensor environments. Tracking sensor statistics will show up systematic biases. These findings may suggest the need for the system optimisation service that GAI provides.

8. References

[1] Holle, RL & López, RE: Overview of real-time lightning detection systems for use by meteorological services, WMO/TD-No.570 *Instruments and Observing Methods, Report No. 51.*

[2] Cummins, KL, Murphy, MJ, Bardo, EA, Hiscox, WL, Pyle, RB, Pifer, AE: A combined TOA/MDF technology upgrade of the U.S. National Lightning Detection Network, *J. Geophys. Res.* 103, 9035-9044, 1998.

[3] Idone, VP, Davis, DA, Moore, PK, Yan Wang, Henderson RW, Ries, M, Jamason, P: Performance evaluation of the U.S. National Lightning Detection Network in eastern New York, 1. Detection efficiency; *J. Geophys. Res*, 103, 9045-9055, 1998.

[4] Cummins, KL, Burnett, Hiscox, WL, Pifer, AE: Line reliability and fault analysis using the National Lightning Detection Network: paper presented at the Precise Measurements in Power Conference, *National Science Foundation and Center for Power Engineering at Virginia Tech*, Oct.27-29, 1993.

The UK Met. Office's Upgraded Lightning Location System

Dr John Nash, Mr Eric Hibbett, Mr Greg Callaghan, Mr Paul Taylor,
Dr Noelle Daly, Mr Richard Burness and Mr Graeme West
The Met. Office
B3a Beaufort Park, Easthampstead, RG40 3DN, UK.
Email: jnash@meto.gov.uk
Fax: +44 1344 855897

Introduction

The Met. Office (UK NMS) has operated a VLF 'arrival time difference' (ATD) thunderstorm location system since 1986. This system is particularly suited to long range lightning detection, because of the choice of observing frequency (10 kHz), and the sophisticated processing involved. This long-range capability is vital for aviation forecasting over the North Atlantic and the Mediterranean. Though the location accuracy deteriorates with increasing distance from the current network in Europe, lightning flashes are regularly detected as far away as South America, Northern Africa and eastern Russia. There is a clear potential for expansion of this technology, to provide global coverage of thunderstorm activity.

Development

Since the 1940's, The Met. Office operated a magnetic direction finding system to locate lightning. This was called CRDF (Cathode Ray Direction Finding). This system worked quite well for many years, though it was extremely labour intensive requiring 32 staff. Bearing errors varied with time and led to undesirable location errors at long ranges.

A replacement system was introduced in 1986, which ran on VLF ATD (Arrival Time Difference) principles (Lee, 1986). This still required a full time operator, i.e. 4 staff. At a frequency of 10kHz, the ionosphere acts as a waveguide, and through multiple reflections, sferic waveforms from lightning flashes can travel thousands of kilometres. Most other lightning systems observe at higher frequencies, and so are not troubled by distant noise, because the sferics from long distances are attenuated. At higher frequencies, there is a sudden onset of the sferic that is relatively easy to time, whereas at VLF the leading edge of the received envelope is indistinct, and information about the whole waveform needs to be sent to the central processor. In practice, the extra communications requirement for a VLF system can be offset against the fact that few stations are required to cover a large area, compared with other commercial systems. By 1989, this version of ATD provided more accurate measurements at all ranges, and better thunderstorm detection efficiency than had been achieved in regular operations using CRDF.

The recent ATD hardware upgrade (Hamer, 1998) has removed the requirement for a full time operator and the system now runs with minimal checks on a daily basis. Imminent software enhancement efforts should result in an increase of the processing capability from 400 to 4000, and eventually to 12000 lightning strokes per hour. For lightning occurring over the UK, it will be possible to determine the flash type (cloud to ground or cloud to cloud), stroke polarity, stroke strength and the number of strokes per event.

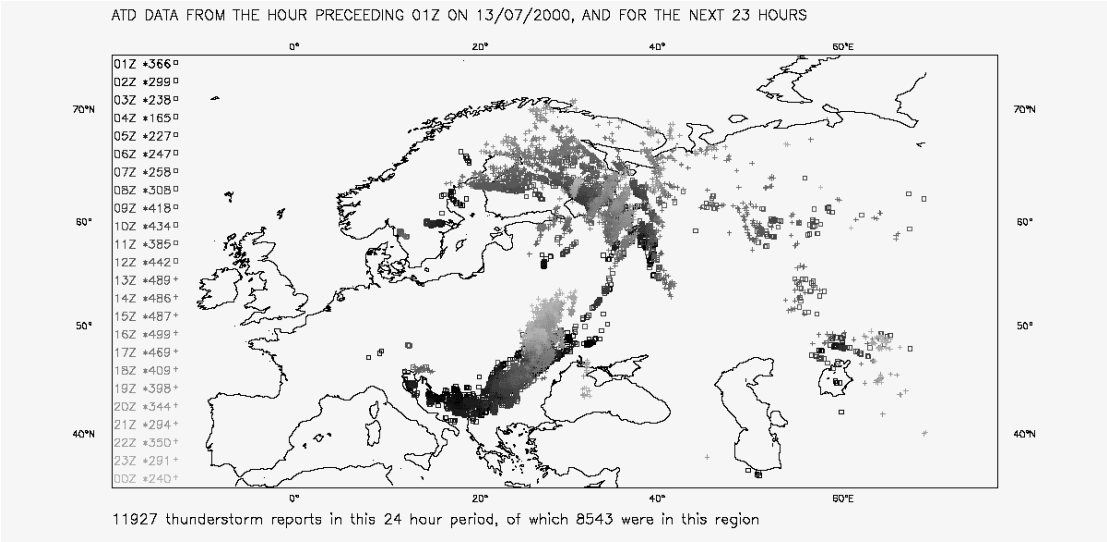

Figure 1 ATD fixes on 13/07/2000. Thunderstorms detected over Eastern Europe, Scandinavia and the Russian Confederation.

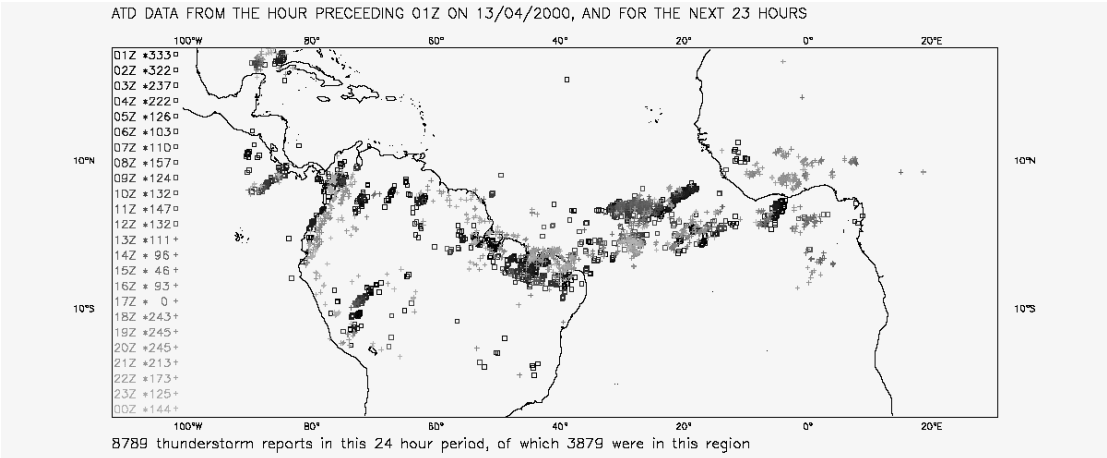

Figure 2 13/04/2000. A particularly active day along the ITCZ (Inter-Tropical Convergence Zone). The Andes are also triggering many lightning flashes.

The ATD Network

The ATD network consists of seven outstations, five of which are in the UK, and two in the Mediterranean (Cyprus and Gibraltar). The central control station is at the headquarters of The Met. Office in Bracknell, southern England. Accurate timing is fundamental for use of the ATD technique; therefore each outstation is equipped with two rubidium oscillators, which are regularly checked with GPS.

Lightning flashes detected at each of the outstations are sent to the control station, as well as the exact time of detection to an accuracy of 0.1 microseconds. Here, the waveforms are correlated, and the differences in arrival times are used to fix the flash location. Waveforms from at least four outstations are required to fix a flash. Having more than four waveforms results in better accuracy, as the location is calculated through an iterative process involving all waveforms and their associated ATD's. The location accuracy is also dependent on the geometry of the outstations taking part. If the fix is located within the bounds of the network in Europe (i.e. inside the quasi-triangle with Cyprus, Gibraltar and Scotland at each of the vertices) then the location accuracy is

usually around 5km, and less in the UK where it is about 1 to 2km. Outside of the immediate network, the accuracy reduces as all the outstations are 'looking' in much the same direction. For instance, in South America (~7000km from Britain), the expected error distributions are elliptical with the major axis of the ellipse corresponding to a location error of about 100km.

A significant factor in producing errors at long range is the varying height of the ionosphere. With correct modelling of the propagation path of the sferic through the Earth-ionosphere waveguide, errors should decrease. The incorporation of this algorithm is planned in the next two years.

The ATD central processor used to be a Perkin-Elmer machine, which was relatively slow. As it could only manage a peak processing rate of 400 flashes per hour, the outstations only sent the strongest flashes for processing; i.e. the weaker flashes that were detected at the outstation sensors were just thrown away. If there was a lot of local activity, then the distant flashes were too weak to be processed. Thus local saturation of the system resulted in negligible long-range coverage, as well as inadequate detection efficiency within the main European Service Area.

The recent upgrade has introduced a newer, much faster machine, a Hewlett Packard dual processor. This huge increase in speed and efficiency has increased the processing power to potentially 12000 flashes per hour. The process of writing and then debugging the software on the new machine, and bringing it to peak performance has been a lengthy one. The images shown in Figures 1 and 2 are of lightning detected with the new control station, which went operational in April 2000. They do not show the processor working at it's full capacity, but the rate is about 50% more than with the old machine.

Performance of the new processor

The new control station has been performing quite well, producing data about 95% of the time for the first three months. One of the best ways to evaluate the quality of the output is to compare it with data from another system.

EA Technology uses a magnetic direction finding technique to detect lightning over the UK. Most of their customers are from the electric utilities. They claim to have quite high detection efficiency, about 95% of all cloud-to-ground flashes should be detected by their system. This means that it is a good method of checking our ATD data. It should be noted that the EA network is based in Britain, so the quality of their location data degrades quite noticeably outside of the land masses of Britain and Ireland.

To make sure that we are comparing the same flash detected by both systems, the matching criteria is that they be separated by less than 0.05 seconds in time and by less than 200km. Figure 3 shows a contour map of the average distances between matched fixes. This distance is the least over the middle of the England. The data for this map is taken from March 2000, just before the new control station came into operational use. Figure 4 shows the same kind of map, but for data in May 2000, when the new control station was in charge. The maps are quite similar, which means that we can have confidence that the new control station is operating as well as the old one.

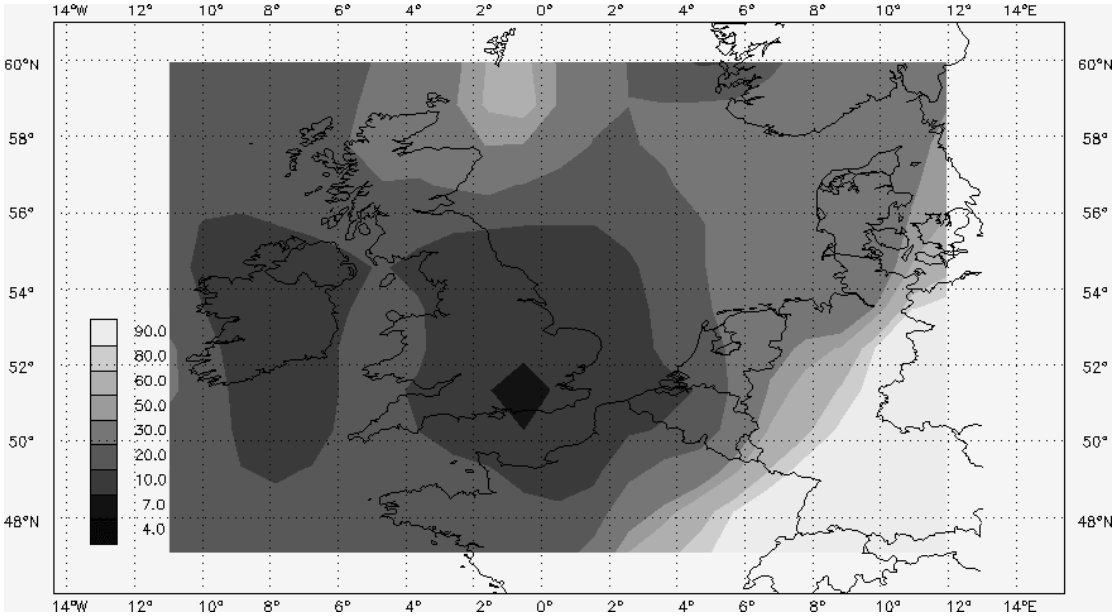

Figure 3 March 2000. The contours show the average distance (km) between matched pairs of EA Technology and ATD lightning fixes. Over the centre of England, the two systems agree to less than 7km, but father away, this agreement deteriorates, due mainly to the fact that EA Technology's system only covers the British Isles. This ATD data was taken when the old control station was in charge

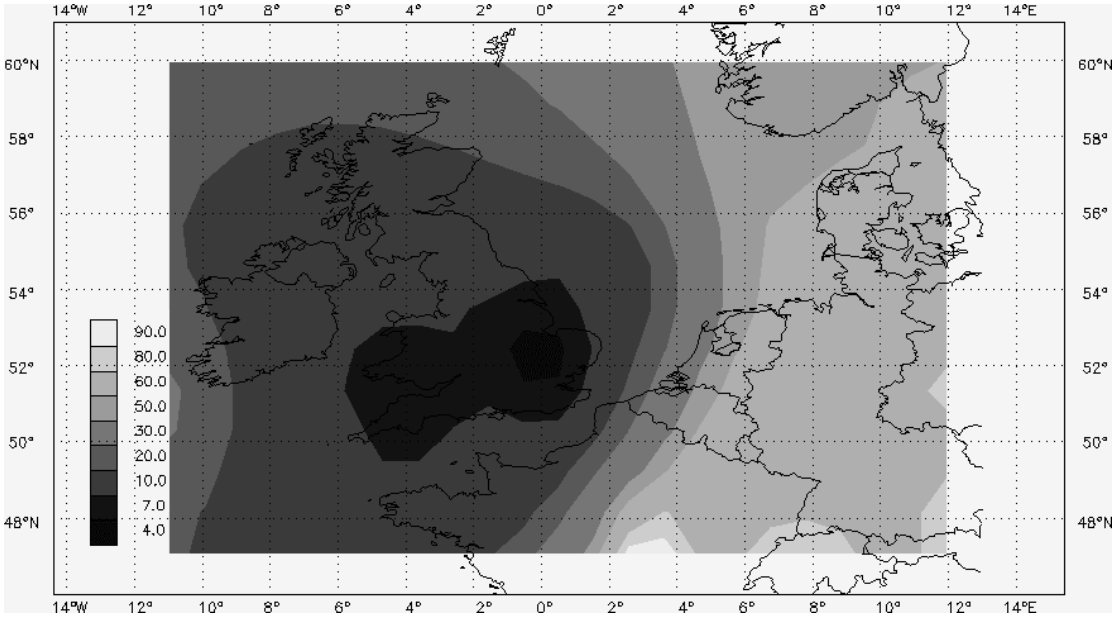

Figure 4 May 2000. With the new control station in charge, the contour plot looks much the same, verifying that the quality of ATD data remained the same after the new control station took over.

Conclusion

An upgraded version of the Met. Office ATD system was successfully introduced into operation in April 2000. The full processing rate of the new control station has yet to be exploited. With the higher rates of processing established later this year, it will be possible to provide a more consistent service to users at all ranges. More results shall be presented at the conference.

References

A.C.L. Lee, 'VLF ATD lightning location', Quart. J. R. Met. Soc. (1986), **112**, pp 203-229.

G.L. Hamer, 'The Met. Office's upgraded lightning location system', Phys. Chem. Earth, Vol. 23, No. 5-6, pp 619-622, 1998.

Gestion, efficacité et qualité des réseaux français de détection d'impacts de foudre.

Françoise Montariol
Météo-France, DSO/QMR/PMO, 42 avenue Coriolis, 31057 Toulouse cédex, FRANCE.
tél: (33) 5 61 07 98 81, fax: (33) 5 61 07 98 69, email: francoise.montariol@meteo.fr

Météo-France utilise en opérationnel, depuis des années déjà, plusieurs réseaux de détection d'impacts de foudre. Ces données sont devenues un atout important pour le prévisionniste, pour le suivi des orages et l'anticipation de situations dangereuses en prévision immédiate. Pour son propre usage en prévision, pour la climatologie et les études, Météo-France continue d'améliorer les réseaux foudre utilisés, la qualité de leurs données et l'étendue de leur couverture.

Le réseau français d'impacts de foudre au sol :

Le réseau français d'impacts de foudre au sol existe depuis 1987 et couvre désormais l'ensemble de la France métropolitaine et la Corse. Il comprend actuellement 28 capteurs dont 17 en France. Les 11 autres capteurs appartiennent à des réseaux de pays voisins : Suisse, Italie, Espagne et Autriche ; les données brutes des capteurs étrangers sont concentrées avec celles des capteurs français sur les concentrateurs de données foudre français, afin de participer aux calculs de localisation des impacts et d'améliorer les données du réseau, principalement dans les zones frontalières du pays.

Figure 1 : Le réseau français de détection d'impacts de foudre au sol.

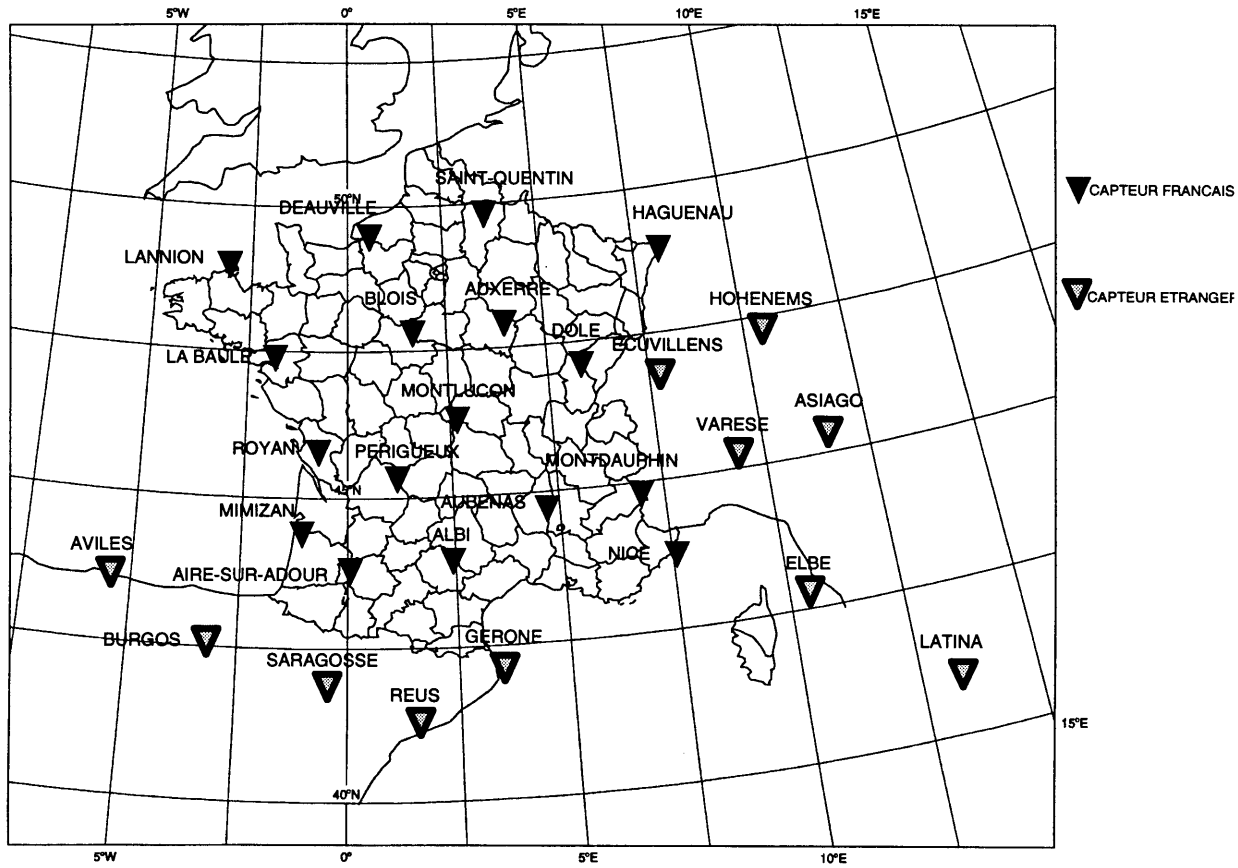

Le réseau initial a été mis à niveau en 1996 pour les capteurs, et en 1998 pour les concentrateurs. La technologie utilisée, "Impact" de la société Global Atmospherics Inc., est à base de triangulations et de différences du temps d'arrivée. La précision moyenne de localisation est désormais meilleure que 2 km sur la majeure partie du territoire métropolitain.

L'exploitation et la maintenance du réseau sont gérées par Météo-France et son partenaire Météorage. L'ensemble des moyens de télécommunications et de calcul sont maillés et doublés, et assurent ainsi une parfaite redondance et sécurité. Les données brutes des capteurs sont concentrées distinctement dans deux centres opérationnels, à Pau chez Météorage et à Toulouse chez Météo-France. Elles y sont traitées sur deux concentrateurs de données foudre qui se secourent mutuellement. Les données calculées sont alors stockées dans CATS, logiciel de base de données foudre développé par Météorage, sur des stations de travail également doublées. Les données d'impacts sont extraites de CATS pour la fabrication des produits foudre, spécifiques des besoins de chaque partenaire.
Météo-France alimente en données foudre toutes les 5 minutes, Météotel et Synergie, les terminaux de travail de ses prévisionnistes en région et département. Des fonctions élaborées de zooms, animations, cumuls, pointages, superpositions avec toutes les autres informations météorologiques observées, complètent les outils disponibles.

Les réseaux Safir régionaux :

Depuis 1991, un réseau de trois capteurs Safir détecte l'activité électrique intranuages et nuage-sol en région parisienne. La technologie, commercialisée par Vaïsala-Dimensions, est à base d'interférométrie. L'exploitation du réseau est réalisée à la Direction InterRégionale de Météo-France à Paris, sur deux concentrateurs qui se secourent mutuellement. Les données intranuages complètent les informations du réseau national, tout particulièrement pour la protection des plus gros aéroports français, situés autour de Paris. Les données sont disponibles pour les prévisionnistes régionaux en temps quasi réel sur console dédiée et au pas de 5 minutes sur leur poste de travail Synergie, équipé de fonctions de zoom, cumul, animations, noyaux, superpositions.

figure 2 : **Zone de détection SAFIR Ile-de-France**

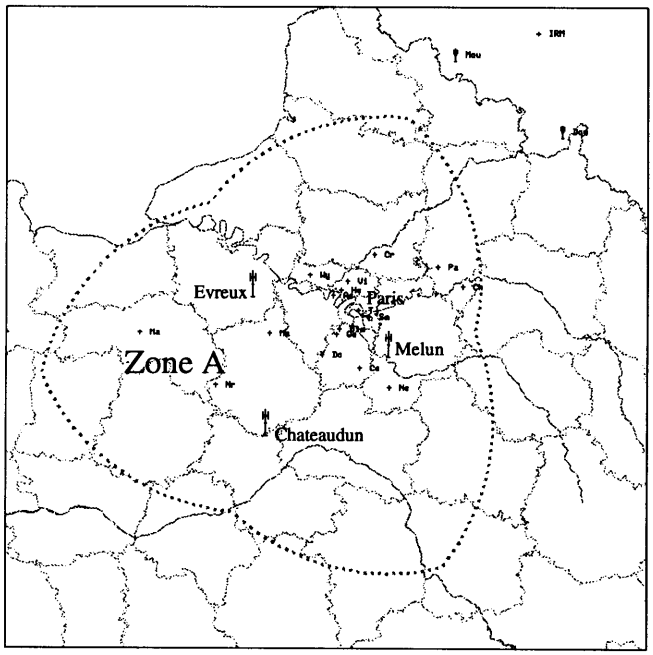

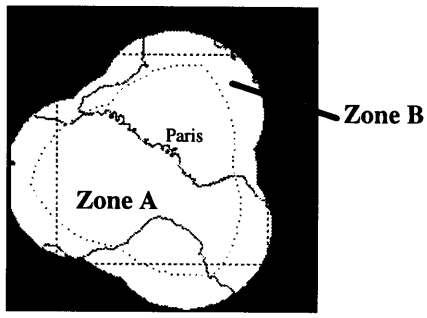

Enfin, l'été 1998 a vu l'installation d'un nouveau réseau régional Safir de détection totale dans le Sud-Est de la France. Il comprend aussi trois capteurs, il est géré par Vaïsala-Dimensions, utilisé par Météo-France et destiné à l'étude des phénomènes orageux intenses, dans une zone française très active orageusement.

Etudes et gestion de la qualité des réseaux :

La redondance des équipements et le pupitrage des chaînes d'exploitation foudre 24 heures sur 24 assurent un taux élevé de disponibilité des données. Pour le réseau de détection d'impacts au sol plus étendu, la panne d'un capteur n'affecte pas la qualité du réseau. En cas de problème réellement important, un message de service est envoyé aux prévisionnistes, soulignant la dégradation temporaire du réseau. Ce cas très rare a été expérimenté fin août 99, lors des problèmes des capteurs dus au roll over du GPS.

Un suivi régulier des données et de leur qualité complète ce dispositif. Pour le réseau d'impacts de foudre au sol qui couvre l'ensemble du territoire, un contrôle systématique de la qualité des données et du réseau est institué.

Les données d'état des capteurs sont analysées chaque mois et permettent d'établir un rapport de panne détaillé. En complément, l'efficacité relative de chaque capteur par rapport au réseau est vérifiée régulièrement, pour mettre en évidence l'apparition d'éventuels problèmes sur un capteur particulier.

La qualité des données produites est contrôlée périodiquement. Sur une grille de maille d'un demi-degré de latitude et de longitude couvrant le pays, des cartes d'isolignes sont produites pour trois indicateurs, paramètres qualitatifs issus des calculs du concentrateur de données foudre : la moyenne du demi-grand axe de l'ellipse de localisation à 50%, le nombre moyen de capteurs participant à la localisation d'un impact et le nombre de calculs n'aboutissant pas à une localisation. La cause d'éventuelles anomalies est systématiquement recherchée.

Les erreurs angulaires systématiques des capteurs sont corrigées par le calcul de paramètres de correction d'erreur angulaire, introduits dans les concentrateurs. Ce calcul est réactualisé annuellement.

L'ensemble des paramètres d'état et de qualité des capteurs est conservé depuis 1996 dans une base de métadonnées du réseau foudre, accessible pour les études climatologiques ou de recherche.

Les projets en cours :

Amélioration de la qualité du réseau de détection d'impacts au sol :

La rénovation du réseau en 1996, achevée en 1998, a amélioré la précision du réseau de détection d'impacts au sol d'un facteur supérieur à 4, par le changement de l'électronique du capteur pour un modèle neuf et plus sensible, par une sophistication des méthodes de localisation et par un accroissement de la puissance des concentrateurs de données foudre. Paradoxalement, cette rénovation a mis en évidence d'autres problèmes de limitation et de qualité du réseau, qui étaient masqués par les problèmes antérieurs plus importants. En particulier, certains capteurs présentent des problèmes résiduels d'autotest et d'erreurs angulaires aléatoires, donc non corrigibles.

Sur les conseils du constructeur, deux types de mesures ont été effectués sur les sites des capteurs :

- des relevés topographiques précis de l'environnement immédiat du capteur, indiquant la pente et la nature du sol, l'élévation et l'importance d'éventuels obstacles dans un rayon de 200 mètres autour du capteur
- des mesures d'interférences électromagnétiques, surtout dans la bande de 1 kHz à 350 kHz scrutée par le capteur, et utilisée pour de nombreuses émissions autorisées en France : radio grandes ondes, radiobalises et radiophares aéronautiques, système de radiopositionnement Loran C, signaux de synchronisation d'horloges, transmissions de signaux sur les lignes électriques EDF, défense nationale.

Les relevés topographiques ont permis de classifier les sites en 3 catégories : bon, correct ou à déménager de préférence. Toutefois, les capteurs à déménager ne correspondaient pas aux capteurs perturbés et semblaient convenablement corrigés par les paramètres de corrections d'erreur angulaires.

Par contre, les mesures d'interférences électromagnétiques ont mis en évidence de gros problèmes de perturbations sur certains sites, correspondant effectivement aux capteurs perturbés. Aucune perturbation d'origine locale n'a été mesurée ; mais, près de la moitié des sites subissent des perturbations significatives d'origine distante, dont 4 sites très bruités. Les émissions radio grandes ondes sont responsables de l'essentiel des interférences. En tête, l'émetteur de France Inter à 162 kHz, situé en plein centre de la France, d'une puissance de 2 MW, est pourtant distant de 100 km des plus proches capteurs, les plus bruités. Ce constat rend inutile tout déménagement.

Le constructeur G.A.I. a alors testé en laboratoire un filtre réjecteur de bande pour la fréquence de 162 kHz. Validé, ce filtre a été installé sur deux capteurs à l'essai fin septembre 99. Les autotests de ces deux capteurs sont devenus bons, et des paramètres de correction d'erreur angulaire efficaces ont pu être calculés. Il reste à contrôler que l'efficacité relative de ces capteurs n'est pas diminuée par le filtre. Ceci sera fait dès que suffisamment de données seront disponibles sur toute la zone de couverture des deux capteurs. Si ce filtre est efficace, il pourra être généralisé aux capteurs qui en ont besoin et testé pour d'autres fréquences perturbatrices.

Extension de la couverture du réseau :

Les échanges de données de capteurs avec les réseaux des pays voisins permettent de limiter les coûts et d'améliorer notablement la couverture des zones frontalières. Le problème des frontières maritimes reste posé.

En 1999, l'Instituto Nacional de Meteorologia en Espagne, la société CESI en Italie, Météorage et Météo-France en France ont décidé d'associer leurs réseaux pour un test de 4 mois, afin d'évaluer l'apport du réseau commun pour la détection des impacts de foudre sur la Méditerranée occidentale. Les données ont été concentrées chez Météorage en temps réel, via internet ou liaisons spécialisées déjà existant. Elles ont été traitées sur un concentrateur de données foudre dédié aux tests et utilisées en temps réel par le service de Prévision Marine de Météo-France. Elles ont également été analysées et recalculées en temps différé afin rechercher les meilleurs paramétrages possibles. Un exemple de situation, le 13 novembre 1999, est présenté en figure 3 ci-dessous.

Le test a été validé par les quatre partenaires au premier semestre 2000 pour la couverture de la Méditerranée occidentale, de l'Adriatique, du golfe de Gascogne et de la Manche. Le réseau maritime conjoint a redémarré le 22 juin 2000, pour un nouveau test plus pérenne.

figure 3 : Impacts de foudre détectés par le réseau méditerranéen le 13 novembre 1999.

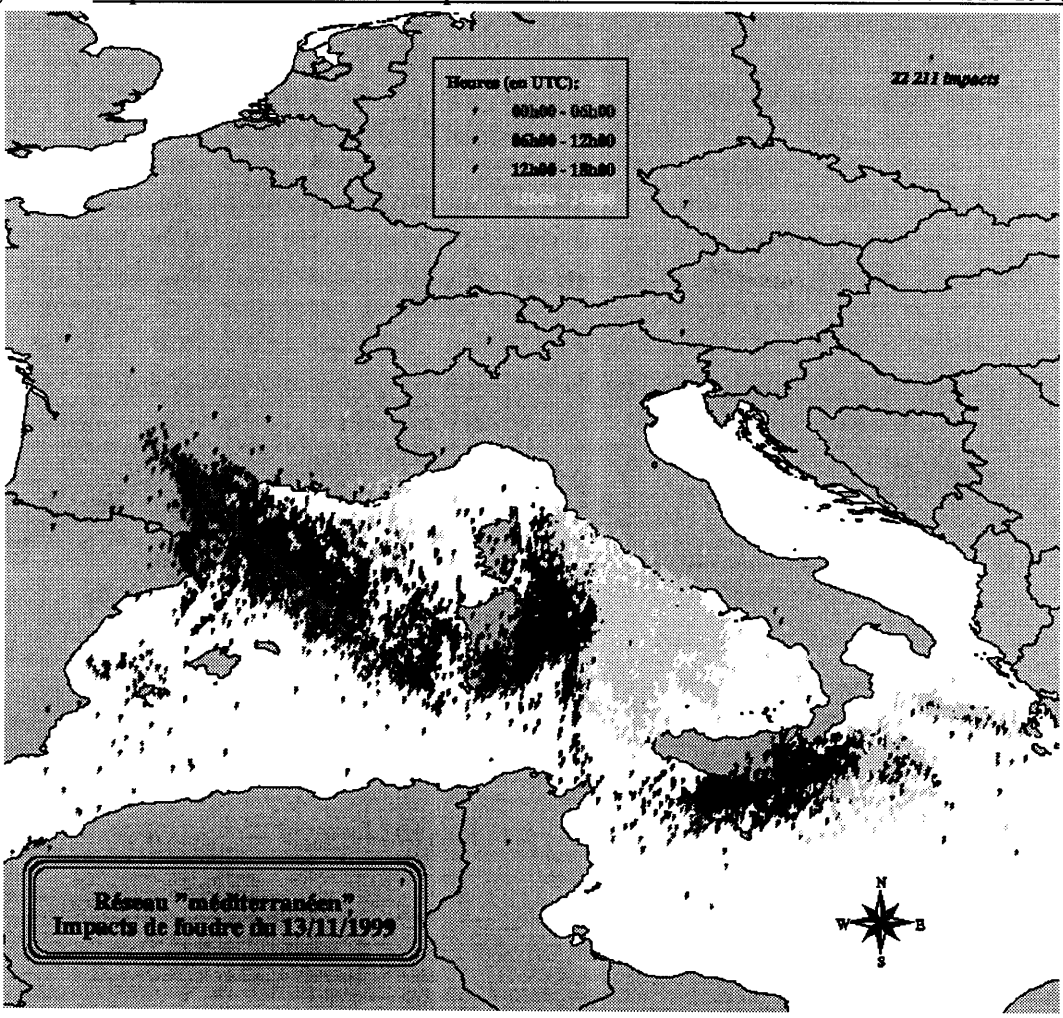

TOTAL LIGHTNING DETECTION TECHNOLOGY, APPLICATION IN WEATHER NOWCASTING

Philippe RICHARD
VAISALA DIMENSIONS - Europarc Ste Victoire - Bât 7 - 13590 MEYREUIL, FRANCE
Tel : (33) 4 42 12 64 64 - Fax : (33) 4 42 12 64 74 - email : philippe.richard@vaisala.com

I - INTRODUCTION

Lightnings and thunderstorms represent one of the major weather hazard to many fields of activity. Until recently it was only possible to record and locate the lightning strikes to the ground once they occurred but without any possibility of earlier identification and forecast of the thunderstorm. In order to provide a more useful information, research programs on lightning physics and thunderstorm phenomenology have been conducted at the French National Aerospace Research Agency (ONERA) during the 80's.

Based on the development of High Frequency electromagnetic techniques for the fine spatial and temporal analysis of atmospheric discharges, this research has conducted to the development of the first operational Total lightning localization system for lightning hazards early warning and thunderstorms forecast : SAFIR for : "*Surveillance et Alerte Foudre par Interférométrie Radioélectrique* ". This paper shall present the principles and applications of Total Lightning detection.

II - STORM DEVELOPMENT & TOTAL LIGHTNING ACTIVITY

Total lightning activity is made of Intra-Cloud (IC) and Cloud to Ground (CG) lightnings. It is closely related to the stage of development and intensity of thunderstorm cell, and can provide valuable information for storm early detection and monitoring.

The active phase of the storm starts when the lightning initiation conditions (strong electric field and high density of hydrometeors) are reached within the cloud. The activity during the storm development is made of Intra-Cloud Lightnings occurring between the main negative charge region (H ~ 6 km) and the upper positive charge region (H ~ 8-10 km).

The rate of internal discharges is well correlated with the development of the cell, and peaks during the thundercloud maximum vertical development. Concentrations of internal discharges are mainly associated with the convective areas.

Intra-cloud lightning is the main electrical manifestation of thunderstorms. It represents 70 to 90% of the total lightning activity of a thundercloud and can reach 99% in severe thunderstorms. Cloud to ground lightning activity develops during the maturity phase of the thunderstorm cell when the descent of the main core of hydrometeors enhances the electrification of the lower part of the cell, and consequently the probability of electrical discharge ignition closer to the ground.

Cloud to ground lightning activity peaks during the decay of the thundercloud and is preceded by a decrease of IC activity which can also precede strong downdrafts and intense precipitation at ground level (figure 1) (Ref. [1], [3], [5]).

BIRTH	STORM ONSET	DEVELOPMENT	MATURITY	DECAY / DOWNBURST
• Beginning of electrification mechanisms	• Beginning of internal electrical activity	• Intensification of intra-cloud lightning activity with storm development • Internal electrical activity reveals the severe storm areas	• Internal electrical activity culminates with the cell maximum vertical development • beginning of significant cloud to ground lightning activity	• Internal electrical activity decays, it precedes downburst phenomena • Cloud to Ground lightning phase culminates

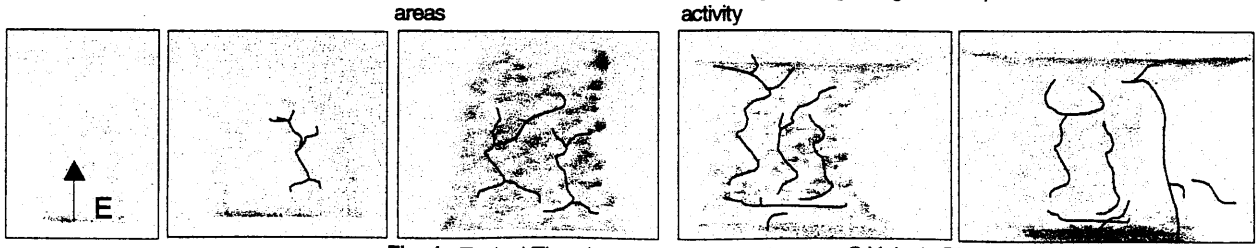

Fig. 1 : Typical Thunderstorm cell life cycle *© Vaisala Dimensions*

III - TOTAL LIGHTNING DETECTION AND LOCALISATION PRINCIPLES

Localisation of "Total Lightning" requires techniques capable to perform lightning detection over a wide range of characteristics, notably intensities of signals, and waveforms. For that purpose, the techniques developed for SAFIR system combine Very High Frequency (VHF) Interferometry for localization and Low Frequency (LF) detection for characterization. (Ref [6], [7])

Interferometric localisation provides on each detection station the time resolved angular direction of lightning phenomena.

It is based on the measurement of the phase differences of the lightning electromagnetic wave received on the different antennas of the detection station antenna array. These phase differences are directly related to the direction of arrival of the wave and are used to calculate the angular position of the source in azimuth (and elevation for 3D location).

2D or 3D spatial location is then obtained by triangulation on GPS time stamped angular directions given by at least two interferometric detection stations.

The interferometric technique is independent of the signal waveform since the measurement is made on the phase of the electromagnetic radiation. It can locate radiation sources produced by both cloud-to-ground and intra-cloud lightning phenomena, with a very wide dynamic range (100 dB). Such dynamic range enables to process signals from a large variety of lightning discharges phenomena (stepped leader, dart leader, recoil streamer, initial breakdown, return stroke,...) and simultaneously, without any gain adjustment, over a wide range of distances.

In addition, the fine time resolution of the measurement (typically 1 to 100 µs) combined with the fact that Interferometry can locate any radiation source independently of its waveform characteristics, allows to resolve the lightning discharge in a serie of successive located sources, and provides the full mapping of the lightning discharges. It represents a valuable source of information for the mapping of the total thunderstorm and lightning hazard areas.

Very High Frequency (VHF) is the range of frequency with the highest rate of lightning radiation. At the contrary of LF radiation which is dominantly produced by CG return strokes, and depends on the current intensity of the discharge, VHF is produced by a large variety of lightning phenomena including the low current intensity phenomena which cannot be detected at long distance in LF (Ref [2], [4]). VHF is thus an important choice for total lightning detection.

Low Frequency Detection (fast capacitive antenna) is used on each detection station in order to record the low to medium frequency CG return stroke electric field. LF radiation and propagation models are used to retrieve the main characteristics (polarity, peak current, rise time, decay time) of CG flashes.

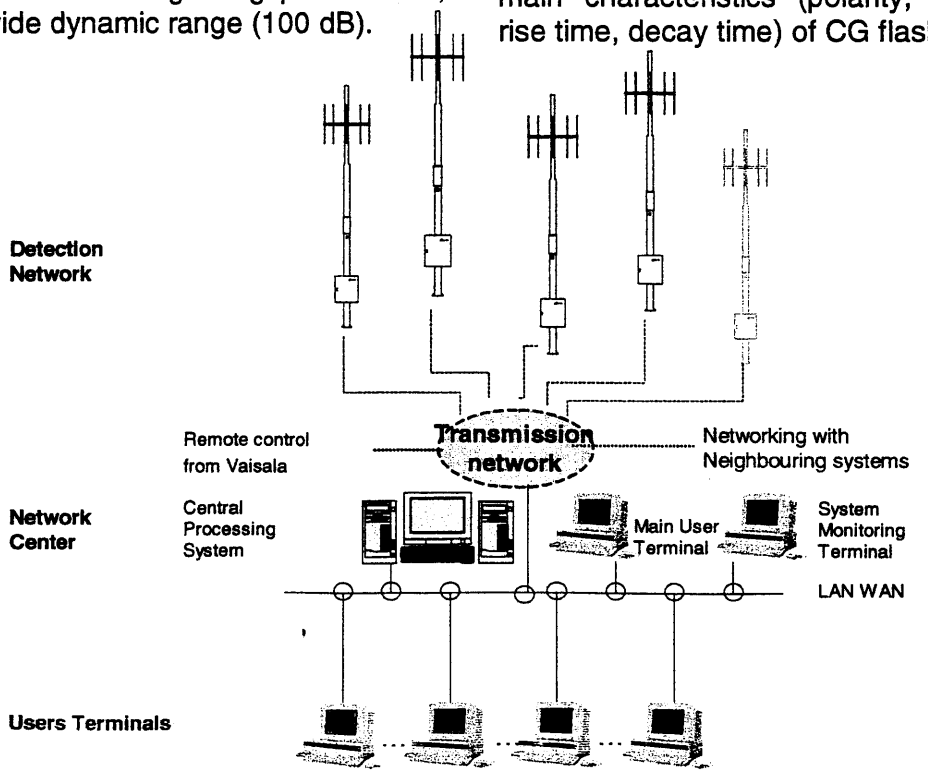

Fig. 2 : SAFIR SystemConfiguration

IV - OPERATIONAL INTERESTS OF TOTAL LIGHTNING DETECTION

The main interests of Total lightning detection reside in its practical contributions in the improvement of performances for thunderstorm early detection and nowcasting.

Improvement of thunderstorm monitoring and tracking efficiency

Intra-Cloud lightning activity represents a very high proportion of all lightnings produced by a thunderstorm.

In addition intra-cloud lightning extend over the whole active cell, and thus enable to delimit precisely the geographical limits of the lightning hazard areas.

Improvement of thunderstorms early detection

VHF radiation from Intra-Cloud lightning activity is the first sign of the thunderstorm electrical development detectable at long distance. It can precede CG activity by several tens of minutes and provides an early information for thunderstorm early detection as well as for early identification of developing

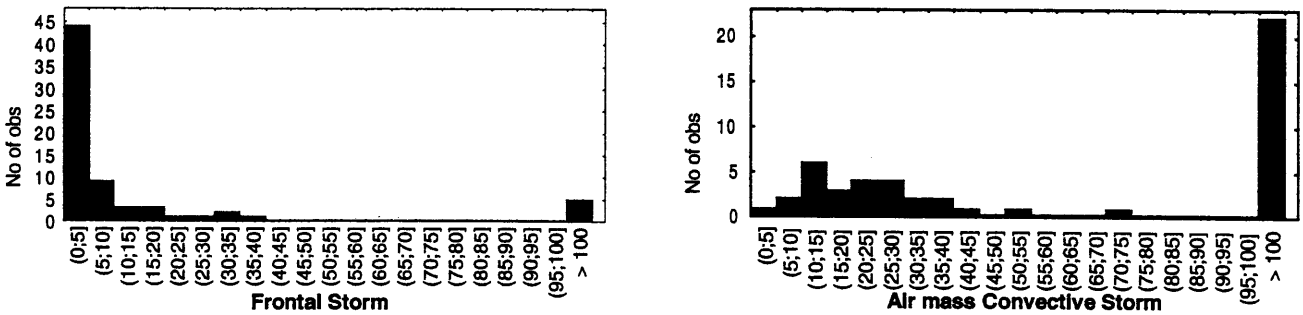

Fig. 3 : Distribution of Intra-Cloud versus Cloud-to-Ground Lightning ratios (4 min. time intervals) *from Kononov et al. [9]*

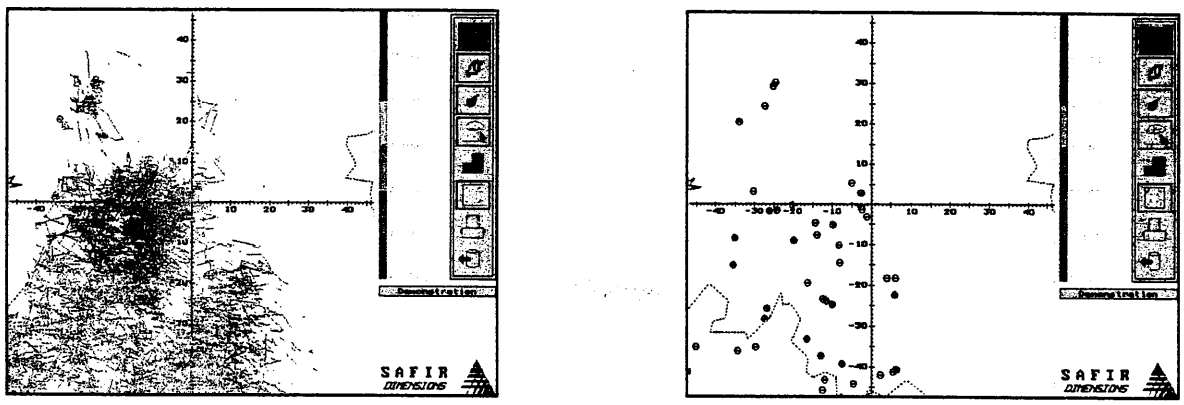

4A : Total lightning activity map

4B : Cloud to ground lightning activity map

Fig. 4 : Comparison of Total Lightning and CG lightning activity (Scale 100 * 100 km)

This is illustrated in *Figure 3*, where histograms of ratio between IC and CG flashes are presented for 2 different kinds of thunderstorm situations. In both cases, the activity is dominated by intra-cloud lightnings ; the practical consequence is illustrated in *Figure 4* where are presented both the Total Lightning map and the CG map for the same thunderstorm. Total lightning, with its predominant IC components provides at least one order of magnitude improvement in monitoring and tracking efficiency compared to cloud to ground lightning detection.

severe thunderstorm areas. Statistics of time delays between IC and CG detections are presented in *Table 1* for 3 cases of cumulated numbers of lightnings (1, 3 or 10 lightning(s) of each kind).

Depending on the criteria used for a new cell identification, the cases with 1 or 3 cumulated lightnings are representative of the early detection gain in time provided by Total lightning. Ten cumulated lightnings can be considered to be a minimum number to perform storm monitoring and tracking. The results of *Table 1* illustrate the very significant gain in time provided by Total lightning for storm monitoring compared to CG lightning detection.

	Δt<10 min	Δt : 10 - 60 min	Δt > 60 min
N = 1	53%	28%	19%
N = 3	29%	33%	38%
N = 10	10%	24%	66%

Table 1 : Distribution of time intervals between IC and CG activity for cumulated numbers of lightnings : 1, 3, and 10 (adapted from Kononov & al. [9])

Improvement of Identification and nowcasting of hazardous storm areas

A close correlation exists between the convective state and intensity of thunderstorm cell and the characteristics of its total lightning activity.

The monitoring of the rate and spatial density of total lightning activity enables to perform identification of strongly developing cells before severe phenomena at ground level during the thunderstorm decay such as high density of Cloud to Ground flashes, intense precipitations, and strong downbursts.

An exhaustive analysis of total lightning detection benefits for nowcasting is presented in reference [8].

Further nowcasting performances improvements are obtained through the data fusion between Total lightning activity and weather radar information. The two types of data constitute complementary informations on the cell characteristics which enable a better real-time description of stage of development and intensity of each thunderstorm cell (see Richard [10]).

Specific application real-time displays *(figure 5)* can thus be adapted for different fields of applications : from en-route or Terminal-area hazardous storm areas identification for aviation, to early identification of high precipitation potential cells for hydrology and flash flood nowcasting.

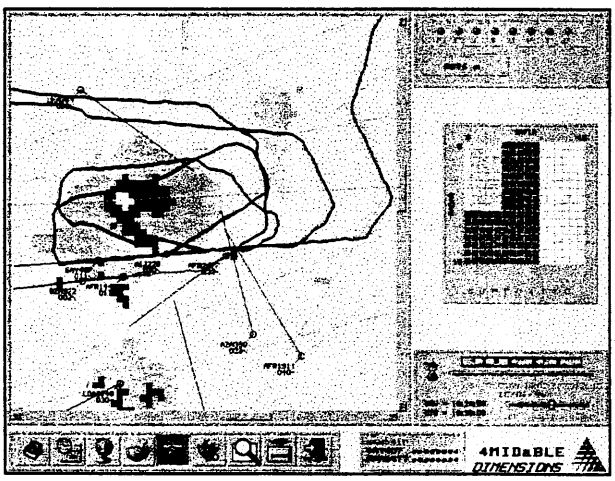

Application for Air-Traffic

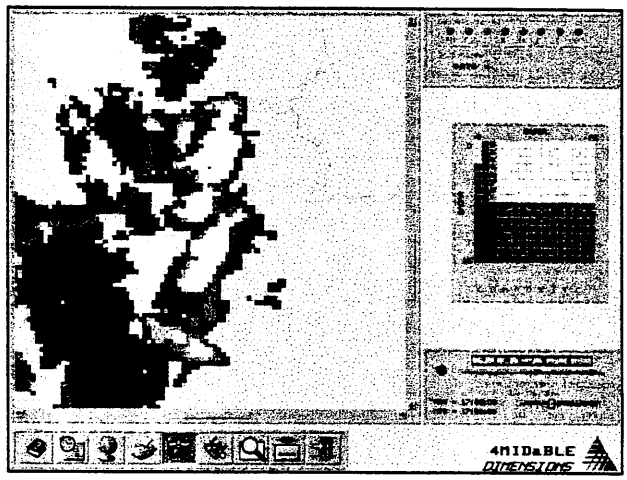

Application for Hydrology and flash flood forecast

Fig. 5 : Total lightning – Weather Radar Fusion examples

REFERENCES

[1] KREHBIEL (P.); "The electrical structure of thunderstorms ", Studies in Geophysics, The Earth Electrical Environment, National Academy Press, 1986.

[2] LABAUNE (G.), RICHARD (P.) and BONDIOU (A.); "Electromagnetic properties of lightning channels formation and propagation", Electromagnetics, Special issue on Lightning, 1988.

[3] LAROCHE (P.), MALHERBE (C.), BONDIOU (A.), WEBER (M.), ENGHOLM (C.), COEL (V.); "Lightning activity in microburst producing storm cells", 25th International Conference on radar meteorology, AMS, Paris June 1991.

[4] RICHARD (P.), DELANNOY (A.), LABAUNE (G.) and LAROCHE (P.); " Results of spatial and temporal characterization of the VHF-UHF radiation of lightning ", J. Geophys. Res., 91, D1, January 20, 1986.

[5] WILLIAMS (E.R.), WEBER (M.E.) and ORVILLE (R.E.); "The relationship between lightning type and convective state of thunderclouds",8th International Conference on Atmospheric Electricity, Uppsala, Sweeden, june 1988.

[6] RICHARD (P); " SAFIR, an operational system for thunderstorm early localization and lightning hazard warning ", International Conference on Lightning Protection – 1996

[7] RICHARD (P) ; " Propositions of methods of validation of Lightning localization systems performances " , International Conference on Lightning Protection – 1998

[8] WEBER (M.E.), WILLIAMS (E.R.), WOLFSON (M.M.), GOODMAN (S.J.) ; "An Assessment of the Operational Utility of a GOES Lightning Mapping Sensor", Project Report NOAA-18, Unclassified, MIT Lincoln Laboratory, Lexington, Massachusetts, February 13, 1998

[9] KONONOV et al; "Space-temporal variations of electromagnetic radiation of thunderstorms in the process of their evolution", 25th International Conference on Lightning Protection, ICLP Rhodos 2000 Sept. 2000

[10] RICHARD; "Storm nowcasting for aviation with total lightning weather radar data fusion,International Conference on Lightning and Static Electricity, Toulouse, France, June 1999

China New Generation Radar

Ge Runsheng Zhu Xiaoyao
Jiang Haiyan Wang Lixuan

(Chinese Academy of Meteorological Science, 46 Baishiqiao Road, Beijing 100081, China
Tel:+86-10-68407296, Fax:+86-10-68406493, Email:lianghh@ihw.com.cn)

1.Introduce

China is carrying out the plan of China New Generation Radar (CINRAD), using full-coherent Doppler weather radar to take the place of the old digital weather radar in the meteorological operational radar network. By using CINRAD, the ability of estimating precipitation will be improved and the wind field information in rainfall area can be obtained to remote detect more effectively those disastrous weather such as typhoon, rainstorm, mesoscale cyclone and tornado and so on. According to the broad area and different topography and geography conditions in china, CINRAD has two wave bands, S band (2800-3000Mhz) and C band (5300-5500Mhz). There are three types of radar, which correspond with the needs of CINRAD and have passed test and begin to set up radar stations to do trial run. They are CINRAD-S_A (WSR98D), CINRAD-S_C (714SDN) and CINRAD-C_C (3830).

2.Main parameters of CINRAD

CINRAD uses pulse Doppler system using klystron as the end transmitter to reach the full- coherent ability. CINRAD has high-gain, low-sidelobe and narrow-beam antenna that has good detecting capability. Receiver with wide dynamic range can estimate precipitation well. High-speed radar signal processor provides real-time echo intensity, radial velocity and spectrum-width. The high-capability data processing system provides real-time and processed graphic and image produces of

radar. See chart 1 of main parameters of CINRAD.

3.Technique features of CINRAD

(1) CINRAD has a strong detecting ability. The minimal echo intensity which S_A, S_C and C_C can detect at 200km from radar is better than –1.5dbz so that they can warn effectively disastrous weather around 400km.

(2) CINRAD concerns calibration of radar. There is a device that can test the dynamic quality of power, noise factor and receiver and then calibrate automatically radar and improve the ability of estimating precipitation.

(3) CINRAD has a stead coherent feature so as to be able to observe accurately average radial velocity and velocity width and has a software with dual PRF so as to extent the unfold velocity and distance range to provide large-range wind field information.

(4) CINRAD has a strong ability to process data and can provide a lot of radar products. S_A has deployed WSR-88D application software. S_C and C_C also has abundant processing products.

4.Further development

(1) CINRAD is developing the dual-linear polarization technique to improve the ability to estimate strong precipitation and precipitation phase. CINRAD will add a function of dual-linear polarization detection.

(2) CINRAD is developing a set of meteorological application software being able to be suitable for China according to Chinese actual precipitation condition and weather evolvement feather.

Chart 1 Main technical parameters of CINRAD

Types / Parameters	CINRAD-S_A (WSR 98D)	CINRAD-S_C (714SDN)	CINRAD-C_C (3830)
Frequency	2700-3000	2700-2900	5300-5500
Antenna diameter	8.54m	8.54m	4.3m
Beam width	0.99°	≤1.0°	≤1.0°
Antenna gain	≥45db	≥44db	≥44db
Side-lobe power level	≤-27db	≤-29db	≤-29db
Antenna scan model	PPI, VOL	PPI, RHI, VOL	PPI, RHI, VOL
Pulse power	≥650kw	750kw	300kw
Pulse width	1.57μs, 4.71 μs	1μs, 4μs	1μs, 2μs
PRF	318-1304Hz	300-1300Hz(1μs) 300-450Hz(4μs)	300-1300Hz(1μs) 300-450Hz(2μs)
Frequency stability	10^{-11}	10^{-11}	10^{-11}
Middle frequency	59.5491MHz	60MHz	60MHz
Receiver dynamic range	>94db	>90db	≥95db
Noise factor	4.0db	≤4.0db	≤3.0db
MDS		≤-107dbm(1μs) ≤-113dbm(4μs)	≤-107dbm(1μs) ≤-110dbm(2μs)
Signal processing method	PPP	PPP, FFT	PPP, FFT
Clutter cancel method	IIR	IIR	IIR
Clutter cancel ratio	30-50db	40-50db	30-50db
Unfolding processing	Software	Dual PRF	Dual PRF
Data processing software	WSR-88D software	Real time PPI, RHI, Basic data products, Physical value products	Real time PPI, RHI, Basic data products, Physical value products

Le réseau ARAMIS de radars-précipitations : démarche pour une utilisation quantitative

Jean-Luc CHEZE
Météo-France - DSO/CMR - 42, avenue Coriolis 31057 Toulouse cedex
Tel : (33) 5 61 07 98 62 – Fax : (33) 5 61 07 98 69 – Email : jean-luc.cheze@meteo.fr

Depuis 1984, Météo-France exploite le réseau ARAMIS qui comporte maintenant 15 radars-précipitations. Les premières utilisations du réseau ARAMIS étaient orientées vers la détection des zones précipitantes et potentiellement dangereuses. Depuis, Météo-France a cherché, en particulier par le projet HYDRAM, à utiliser les capacités de mesure des précipitations par radar pour affiner et quantifier la détection des zones dangereuses, ainsi que leur prévision.
Les objectifs visés sont :

- la mise à disposition d'images de lames d'eau radar 15 ou 30 minutes (ce terme désigne des images de quantités de précipitations cumulées sur une période donnée) de nos utilisateurs internes, en particulier des prévisionnistes de Météo-France,
- la mise au point d'outils de production et de diffusion en temps réel d'images de lames d'eau pour les utilisateurs hydrologiques,
- la prise en compte de l'information radar pour améliorer la climatologie des précipitations en complément des données pluviométriques.

L'utilisation quantitative des données radar, point commun aux 3 objectifs, nécessite de travailler en parallèle dans 2 directions. La première direction est la maîtrise de la qualité des données radar de base et la correction de biais systématiques pouvant affecter les mesures radar ; cette maîtrise constitue une tâche essentielle mais difficile lorsque l'on opère un réseau de 15 radars. La seconde direction est la mise en oeuvre de traitements permettant la correction des erreurs liées à la physique de la mesure (Atténuation par les fortes précipitations, erreurs liées au Profil Vertical de Réflectivité, ...). Par ailleurs, la diffusion de ces produits doit s'accompagner d'une formation et d'une information des utilisateurs encore plus complète.

Dans cette communication essentiellement consacrée à nos actions dans cette première direction, nous allons d'abord préciser notre approche basée principalement sur des comparaisons radar/pluviomètres sur de longues périodes. Comme une illustration de cette approche et de sa pertinence, nous présenterons quelques résultats de comparaisons de cumuls quotidiens de précipitations obtenus à partir de radars ou des pluviomètres sur plusieurs mois à forte pluviométrie.
Ensuite, nous décrirons dans quelles conditions nous avons démarré la diffusion d'images de lames d'eau en temps réel à destination des utilisateurs internes et externes.
Finalement, nous évoquerons les autres actions engagées par Météo-France pour améliorer les performances de nos systèmes radar.

1 – Analyse de la qualité des données radar et corrections des biais systématiques

Avant de mettre en œuvre des procédures de correction des données radar, il était d'abord nécessaire de se livrer à un diagnostique des performances de notre réseau radar. Pour cela, nous avons mis en oeuvre des comparaisons de champs de précipitations obtenus séparément à partir des données radar et de données de pluviomètres dans les conditions décrites ci-après.

Rappelons que le réseau est actuellement composé de 15 radars (10 en bande C et 5 en bande S) produisant des images de réflectivité toutes les 5 minutes. Ces images sont archivées systématiquement dans une base dédiée par la Division de Climatologie de Météo-France. Ces images comprennent 512 x 512 pixels de 1 kilomètre de côté avec les réflectivités codées sur 54 niveaux.
Les données pluviométriques sont extraites de la base de données climatologiques de Météo-France qui inclut plus de 3800 points de mesure des précipitations, englobant les stations synoptiques, les stations automatiques et les postes tenus par observateurs climatologiques. Le plus petit pas de temps de mesure commun à tous est le pas de temps quotidien.
Le champ de précipitations radar est calculé en convertissant simplement les réflectivités radar en intensités de précipitations par la relation de Marshall-Palmer. Les données ponctuelles des pluviomètres sont analysées à l'aide d'une méthode d'interpolation spatiale (krigeage) de manière à obtenir un champ de précipitations sur la même grille que les données radar. Il est alors possible de calculer, pour chaque pixel de l'image radar, le rapport entre les cumuls de précipitations déduits soit du radar, soit des pluviomètres.
Si l'on suppose que le champ de précipitations est assez « lissé » pour que les erreurs dues à l'interpolation soient minimisées (cela est généralement vérifié quand les cumuls sont réalisés sur une période suffisamment longue), la comparaison peut être utilisée pour évaluer les performances du radar et détecter certaines erreurs de la mesure radar.

Figure 1 : Rapports pluviomètre/radar sur les cumuls mensuels de précipitations de Septembre 1998 pour le radar de Toulouse

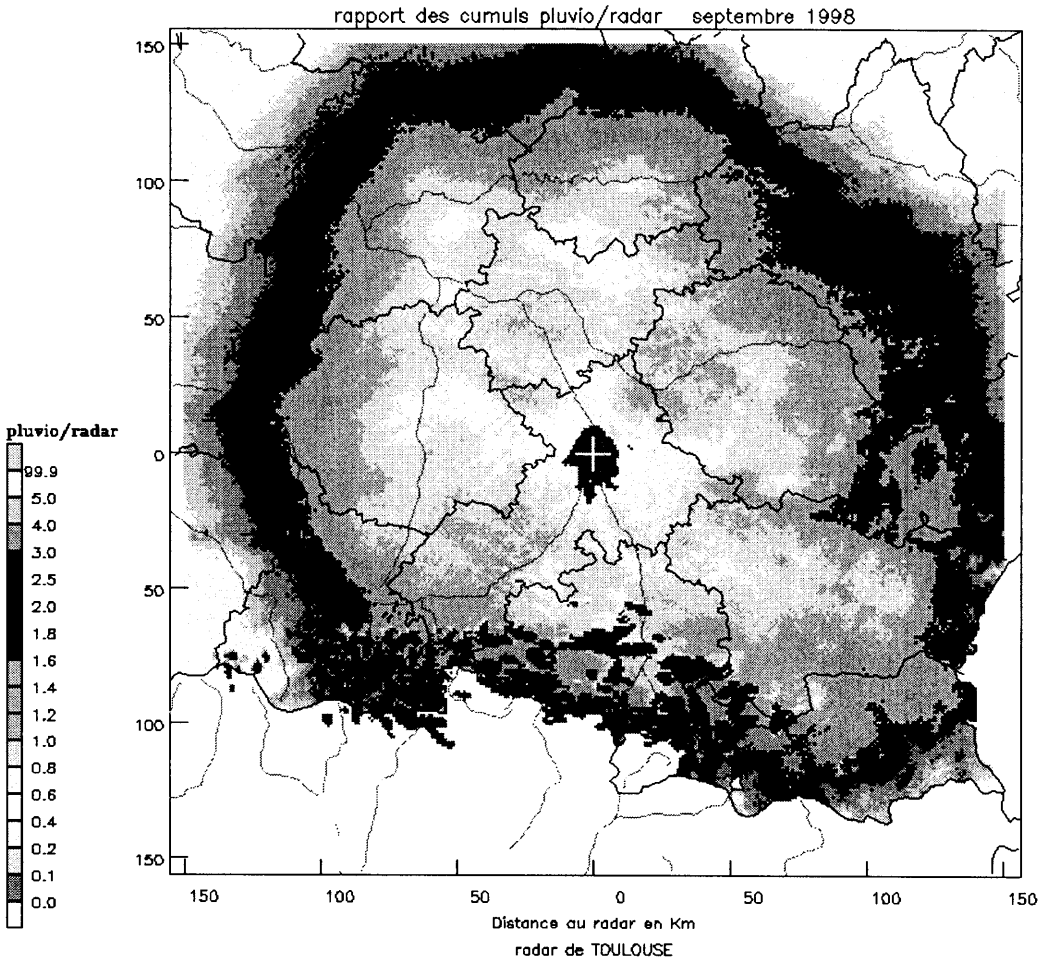

Figure 2 : Valeur moyenne (haut) et écart-type (bas) en fonction de la distance des rapports pluviomètre/radar sur les cumuls mensuels de précipitations de Septembre 1998 pour le radar de Toulouse

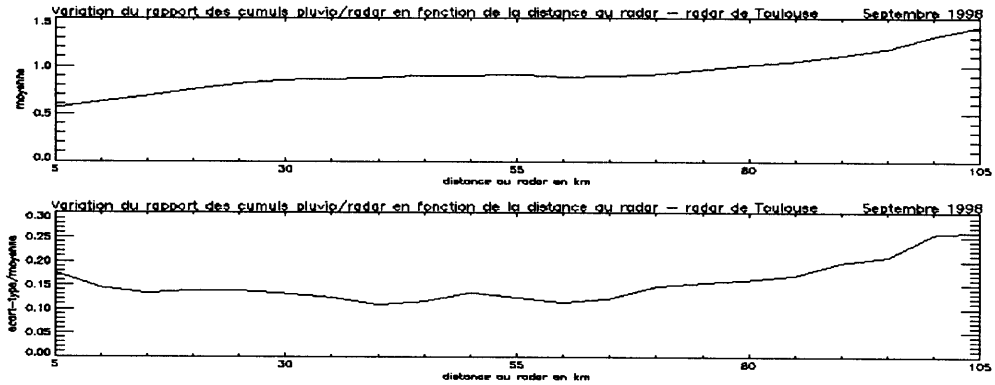

La figure 1 est un exemple d'une telle analyse réalisée pour le radar de Toulouse pour le mois de Septembre 1998. L'image est centrée sur le radar et chaque pixel représente le rapport entre les cumuls de précipitations obtenus soit à partir des pluviomètres , soit à partir du radar : une valeur plus grande (petite) que 1 représente une sous-estimation (sur-estimation) du radar. Quelques éléments significatifs peuvent être déduits de ce type de figure :

- le rapport croît fortement avec la distance au-delà de 80 à 90 kilomètres en raison des effets de la présence d'eau en phase et de remplissage partiel du faisceau qui produisent des sous-estimations du radar,
-le rapport croît plus rapidement dans certaines directions (par exemple dans la direction ESE) en raison d'effets de blocage partiel du faisceau,

- de fortes sur-estimations du radar existent sur les zones d'échos de sol, mais ces zones ont été masquées en gris sur cette image.
Une quantification de ces effets de la distance peut être aisément obtenue en calculant le rapport moyen sur des couronnes concentriques de 5 en 5 kilomètres. La figure 2 donne un exemple des courbes ainsi obtenues correspondant aux variations de la valeur moyenne (haut) et de l'écart-type (bas) en fonction de la distance. Les zones affectées par les échos de sol sont exclues de ces calculs.
Entre 20 et 90 kilomètres, le rapport moyen est à peu près constant autour d'une valeur de 0,8 pour le radar de Toulouse et l'écart-type reste de l'ordre de 0,15. Une première conclusion est qu'une réponse stable et fiable du radar peut être attendue dans un domaine, certes limité, mais bien défini, à condition que l'on ait bien caractérisé les zones concernées soit par des échos de sol soit par des blocages partiels importants du faisceau. La valeur moyenne du rapport donne une estimation du biais systématique qui est attaché aux mesures radar en comparaison avec les données sol et peut être utilisé comme un facteur de correction pour le calcul d'images de lames d'eau à partir des données de ce radar.

Cette méthode s'avére efficace pour évaluer les performances d'un radar et la qualité de ses données et présente une bonne alternative à la pratique plus répandue d'ajustement en temps réel à pas de temps fin par un réseau de pluviomètres. Cependant, elle ne peut pas prendre en compte les erreurs fluctuant rapidement dans l'espace et dans le temps comme les propagations anormales ou l'atténuation par les fortes précipitations.
Du fait d'une possible variation saisonnière de ce rapport, cette analyse doit être répétée périodiquement, par exemple sur une base mensuelle. Cela est réalisé opérationnellement tous les mois pour chacun des 15 radars du réseau ARAMIS.

2 – Comparaison de cumuls quotidiens radar et pluviomètres

Dans le but l'évaluer la pertinence d'une approche utilisant ces facteurs correctifs pour produire des images de lames d'eau radar, nous avons comparé les cumuls quotidiens dérivés des données radar avec des mesures de pluviomètres sur plusieurs mois, incluant des situations stratiformes et convectives et couvrant différentes saisons.
Pour faciliter ces comparaisons, nous avons comparé des cumuls quotidiens. Pour un tel travail de comparaison, le choix des critères est très important. Les critères suivants ont été utilisés en priorité :

- Le coefficient de corrélation entre les 2 séries de cumuls quotidiens du mois
- Un critère appelé C50 : ce critère est respecté si le rapport radar/pluviomètre est compris entre 0,5 et 1,5. Par exemple, si le pluviomètre mesure 10 mm, le cumul radar doit être compris entre 5 et 15 mm.

Seuls, les cumuls quotidiens supérieurs à 5 mm ont été pris en compte pour le critère C50.
Les tables 1, 2 et donnent les valeurs du facteur correctif et des 2 critères pour différents mois et pour 3 radars du réseau ARAMIS.

Tableau 1 : facteur correctif mensuel

	Nov. 96	Dec. 96	May 97	Aug. 97	Oct. 97
Abbeville	1.7	1.8	1.4	1.6	1.6
Trappes	1.3	1.3	0.7	0.6	0.6
Bourges	0.9	0.7	0.9	0.9	0.9

Tableau 2 : coefficient de corrélation mensuel pour les cumuls quotidiens

	Nov. 96	Dec. 96	May 97	Aug. 97	Oct. 97
Abbeville	0.84	0.89	0.9	0.89	0.92
Trappes	0.82	0.91	0.93	0.91	0.91
Bourges	0.83	0.94	0.92	0.9	0.89

Tableau 3 : valeur mensuelle du critère C50

	Nov. 96	Dec. 96	May 97	Aug. 97	Oct. 97
Abbeville		88	90	76	83
Trappes	75	70	81	71	77
Bourges		87	88	84	80

La variabilité d'un mois à l'autre du facteur correctif (voir tableau 1) est représentative de celle que l'on observe généralement pour des radars qui n'ont pas connu de dysfonctionnement particulier. Dans le cas du radar de Trappes, le changement de valeur du facteur correctif entre Décembre 96 et Mai 97 est dû à une modification de la procédure d'étalonnage électronique de la chaîne de réception.

Les résultats satisfaisants en terme de coefficient de corrélation (tableau 2) et de critère C50 (tableau 3) sont également représentatifs de ce qui peut être attendu pour un radar dans de bonnes conditions de mesure, c'est à dire en l'absence de panne du système radar et dans un contexte de zone à faible orographie.
Il est important de noter qu'une telle procédure d'analyse mensuelle des données radar est un bon moyen d'identifier des changements de comportement du radar et ainsi, de détecter ou d'anticiper certaines pannes ou dysfonctionnements.

3 – Diffusion opérationnelle d'images de lames d'eau radar

Pour favoriser une utilisation plus quantitative des données radar, nous avons démarré en Mai 1997 la production et la diffusion en temps réel d'images de lames d'eau radar pour chacun des radars du réseau ARAMIS. Ces images représentent, sur le même domaine que les images radar instantanées et avec la même résolution de 1km par 1 km, la quantité de précipitations sur les 15 ou 30 dernières minutes codée en dixièmes de millimètres. Dans cette première version, un nombre limité de traitements sont intégrés : le facteur correctif mensuel est pris en compte et un algorithme, appelé correction d'advection, compense les erreurs liés au sous-échantillonnage temporel. Les images sont concentrées dans un centre national à Toulouse et rediffusées par satellite. Ainsi, ils sont accessibles dans tous nos centres météorologiques au travers des terminaux utilisateurs METEOTEL et SYNERGIE. Ces images sont susceptibles d'être également mises à disposition d'utilisateurs externes, en particulier les services d'annonces des crues.
Un tel usage, plus quantitatif, dans un contexte opérationnel en temps réel demande encore plus de formation et d'information des utilisateurs finaux. Pour améliorer la circulation de l'information, nous avons mis en place une procédure pour concentrer puis rediffuser vers ces utilisateurs finaux des informations sur les pannes et les changements de comportement des systèmes radar au moyen de courts messages qui sont diffusés par satellite comme les images radar et visualisables sur les mêmes terminaux.

4 - Conclusion et perspectives

En réponse aux besoins des utilisateurs internes et externes d'une information plus détaillée en temps réel sur les champs de précipitations pour le suivi de situations météorologiques et autres applications hydrologiques, Météo-France a développé un dispositif opérationnel pour produire et diffuser des images de lames d'eau radar sur un pas de temps de 15 ou 30 minutes. Un tel usage quantitatif suppose des données radar de très bonne qualité. L'analyse des performances des systèmes radar, principalement basée sur des comparaisons avec des données sol sur de longues périodes, est une composante essentielle de notre approche, dans la mesure où elle peut produire des facteurs correctifs destinés à compenser les biais systématiques et contribuer à l'identification de problèmes affectant les systèmes radar et ainsi à l'amélioration générale de la qualité des données radar.

En complément, il est nécessaire de minimiser l'effet des autres sources d'erreurs telles que les effets de blocage partiel du faisceau, de l'atténuation par les fortes précipitations ou du Profil Vertical de Réflectivité. Météo-France poursuit des travaux sur la correction de ce type d'erreurs qui pourront être intégrées dans les futurs versions de produits radar.
Au delà de ces améliorations que l'on peut apporter aux données des radars conventionnels qui constituent actuellement notre réseau, il est nécessaire d'explorer les apports des techniques radar plus avancées. Dans ce domaine, Météo-France soutient un effort de recherche de laboratoires français, en particulier le CETP, pour le traitement des données à diversité de polarisation. Les possibilités déjà démontrées de correction de l'atténuation, de compensation des fluctuations des distributions de tailles des gouttes et de contribution à l'identification des types d'hydrométéores ouvrent des perspectives encore plus grande de développement de l'utilisation quantitative du radar pour les applications hydrologiques.

5 - Références

Andrieu, H. and Creutin, J.D. (1991) Effect of the vertical profile of reflectivity on the rain rate assessment at ground level. Preprints of the 25th conf. on Radar Meteor. Am. Met. Soc. Paris, 832-835.

Chèze J.L., F.Helloco, F.Sevault, F.Mesnard, H. Sauvageot, J.J Vidal and J.P. Dupouyet, 1998. Flood Forecasting from Radar Derived Rainfall Estimates in the Central Pyrénées Range. European Commission COST-75 Action Final Seminar on Advanced Weather Radar Systems, Locarno, 23-27 March 1998.

Joss, J. and Waldvogel, A. (1989) Precipitation estimates and vertical reflectivity profile correction. Preprints of the 24th conf. on Radar Meteor., Am. Met. Soc., Boston, 682-688.

Kitchen, M and Jackson P.M., (1993) Weather radar performance at long range. Simulated and observed. J. Appl. Meteor.,32,975-985.

Sauvageot, H. ,1992 Radar Meteorology. Ed. Artech House, 366 p.

Testud J., E. Le Bouar, E. Obligis and M. Ali-Mehenni. The rain profiling algorithm applied to polarimetric weather radar. J.Atmos.Oceanic Technol., Vol. 17, N°3, pp. 332-356 .

A NEW RETRIEVAL TECHNIQUE FOR SINGLE-DOPPLER RADAR

Jiang Haiyan
(Department of Meteorology, University of Utah, SLC, USA Email: j.h.y@263.net)
Ge Runsheng
(Chinese Academy of Meteorological Sciences, Beijing 100081, China)

Introduction

Among all kinds of present detective ways, only Doppler weather radar can better obtain the information of wind field distribution and structure inside cloud body. However, single Doppler radar only can detect the radial component of wind and can not obtain directly the two-dimensional structure of wind field. It is one of main research topics of developing and applying Doppler weather radar how to retrieve the actual wind from the radial wind. In 1960s, VAD method[1][2][3] was presented, which can retrieve the average wind direction and velocity, the average divergence, stretched deformation, shearing deformation and vertical profile of wind field from the radial velocity with the uniform wind supposition. In 1970s, by supposing the local uniform wind field, VARD and VVP methods[4][5] were presented, which can obtain the two-dimensional wind field. Song Chunmei[6] and Tao Zuyu[7] then gave VAP(Velocity Azimuth Display) method based on the UW(Uniform Wind) method. VAP method also can obtain the two-dimensional wind field using geometric method with the local uniform wind field supposition. VARD and VVP method can hardly apply actually because of their sophisticated calculations. VAP method only fit to retrieve some relatively uniform wind field because of its supposition. This paper presents a new technique retrieving the two-dimensional wind field from mesoscale vorticity equation under some suppositions. It is called Vorticity-Divergence method.

1. Principle of V-D method

In radar polar coordinate(radar is at origin, r represents distance to radar, θ represents azithum), vertical vorticity ζ and horizontal divergence D usually considered in meteorology can be represented by:

$$\zeta = \frac{Va}{r} + \frac{\partial Va}{\partial r} - \frac{\partial Vr}{r\partial\theta} \qquad (1)$$

$$D = \frac{Vr}{r} + \frac{\partial Vr}{\partial r} + \frac{\partial Va}{r\partial\theta} \qquad (2)$$

Where V_r is radial velocity and V_a is tangential velocity.

After being analyzed and simplified properly, the mesoscale vorticity equation[8]becomes

$$\left[\frac{\partial\zeta}{\partial t} + u\frac{\partial\zeta}{\partial x} + v\frac{\partial\zeta}{\partial y}\right] + (f+\zeta)D - \left(\frac{\partial w}{\partial y}\frac{\partial u}{\partial z} - \frac{\partial w}{\partial x}\frac{\partial v}{\partial z}\right) = 0 \qquad (3)$$

Where every mesoscale physical variation is in rectangular coordinate. u, v and w are the three components of velocity. f is the vertical component of geostrophic vorticity and can be regarded as a constant within the range of radar detection. Two suppositions about equation (3) are presents to simplify it.

(a) $\frac{\partial\zeta}{\partial t} = 0$. This is local variation of vorticity. During the moment of radar detection, it is very little and can be omitted.

(b) ($\frac{\partial w}{\partial y}\frac{\partial u}{\partial z} - \frac{\partial w}{\partial x}\frac{\partial v}{\partial z}$)=0. This is twisting term. We suppose that the vertical velocity w is uniform in a small region under the condition of two-dimensional. So the twisting term can be omitted.

Then equation (3) will become:

$$u\frac{\partial\zeta}{\partial x} + v\frac{\partial\zeta}{\partial y} = -(f+\zeta)D \qquad (4)$$

In radar polar coordinate, equation (4) becomes:

$$Vr\frac{\partial\zeta}{\partial r} + \frac{Va\partial\zeta}{r\partial\theta} = -(f+\zeta)D \qquad (5)$$

Combining equation (1)、(2) with (5), the final retrieving equations of V-D method will be:

$$\begin{cases} \zeta = \dfrac{Va}{r} + \dfrac{\partial Va}{\partial r} - \dfrac{\partial Vr}{r\partial\theta} \\ D = \dfrac{Vr}{r} + \dfrac{\partial Vr}{\partial r} + \dfrac{\partial Va}{r\partial\theta} \\ Vr\dfrac{\partial\zeta}{\partial r} + \dfrac{Va\partial\zeta}{r\partial\theta} = -(f+\zeta)D \end{cases} \qquad (6)$$

A progressively approaching method is used in solving equation (6). Firstly the divergence term $-(f+\zeta)D$ can be simplified to –fD by supposing $\zeta=0$. Then Va on each grid will be solved from the simplified equation (6). The distribution of ζ can be obtained from equation (1) and the values of Va. Then by replacing the obtained values of ζ in the divergence term, equation (6) can be solved again. Thus the relatively true distributions of Va、ζ、D will be obtained by approaching progressively.

2. Preprocessing data

The data used in this paper come from CAMS 10cm Doppler weather radar. The range of PPI scanning azithum is 0 °～360 °, the sample interval is 1 °, the radial maximum distance is 300km, the distance resolution is 300m and the elevation is1.7 °。Preprocessing includes five step: (1): removing noise, (2) supply missing spots, (3) unfolding, (4) filtering, (5) interpolating onto retrieving grids. Unfolding is a critical step of preprocessing. Before unfolding we must determine whether the velocity data are one-degree folding, two-degree folding or multi-degree folding. The two-dimensional unfolding method is used here. First correct folding degree is selected according to the slope of adjacent points along radial direction. At the same time the great gradient velocity is considered in order that the unfolding is reasonable. Then unfolding along tangential direction is made just as along radial direction. The result shows that the two-dimensional unfolding method is feasible. After preprocessing, the two-dimensional horizontal wind field will be obtained by combining the radial velocity detected by Doppler radar with the tangential velocity solved by equation (6). The retrieving grid is selected in polar coordinate. in which the grid length is 3km×3 °. While displaying the wind field image, the grid in polar coordinate is changed into rectangular coordinate with a bilinear interpolation[9].The grid length 7.5km×7.5km in rectangular coordinate.

3. Analyzing the retrieving results

Retrieving experiments with Doppler radar observational data on July 11-13, 1994 are made to test V-D method. A strong precipitation happened in Hebei and Beijing area in China on July 11-13, 1994. The results are analyzed by being compared with the actual synoptic situation.

A storm rainfall happened in Hebei and Beijing area in China on July 11-13, 1994. From the 500pha stream field figure at 08:00(Beijing local time, all times in this paper are represented by using Beijing Local Time) and 20:00 on June 12, the south airflow near radar turned to southwest and became stronger. From the surface stream field figure at 14:00 and 20:00 on June 12, a vortex near radar can be seen. Fig. 1a, 1b,1c and 1d are two-dimensional horizontal wind field retrieved by V-D method from the Doppler radar data at 14:55, 15:51, 18:52, 22:53 on June 12, 1994. We can see the features of wind field from the continuous development of the four figures. The direction of the flow southeast to radar was southerly, but that northwest to radar was northerly. A vortex near radar has been formed. There was a divergence area northeast to radar. With the lapse of time, the southerly air flow southeast to radar became stronger and stronger gradually and the direction of wind turned to southwesterly. By about 22:00, a stream of southeasterly clear airflow has been formed. At the same time the westerly air flow northwest to radar still kept. The

vortex near radar was more and more obvious and the divergence area northeast to radar became stronger and stronger.

From the actual weather condition, when Doppler radar observed the development of vortex near radar, a stream of strong downdraught happened near Beijing airport about 40km northeast to radar station. The development of vortex in retrieving result is corresponding to the actual condition of the downdraught. The position of downdraught is just at the strong divergence area(Fig 1d). So the retrieving result is consistent approximately with the actual weather condition.

In addition, the retrieving results of V-D method are compared with that of VAP method. It shows that the structures of the airflow retrieved by the two methods are similar approximately from the large range. But from the slight structure of the airflow, V-D method has obviously better performance than VAP method. V-D method can respond rather well the slight structure of wind field such as small convergence and divergence area, but VAP method can hardly do this. It is probable that VAP method can hardly respond the microscale disturbance of wind field.

4. Conclusion

(1) V-D method is a new try to retrieve wind field from single-Doppler radar data. It can rather well describe microscale and mesoscale weather systems because of fully thinking of the effect of vorticity and divergence. The tests at first have proved that it can be used in many weather conditions.

(2) V-D method in this paper can only retrieve the two-dimensional wind field and have omitted the vertical term during simplifying the retrieving equations. During the actual mesoscale and microscale weather process, the impact of vertical term can not be omitted. It is necessary to expand V-D method to a three-dimensional retrieving method by applying the atmospheric continuity equation in V-D method.

(3) In addition, while using the vorticity and divergence in this paper, it is possible that the vortex, convergence and divergence in rather weak weather systems could be magnified. This will be studied and tested in the future.

References

1 Lhermitte R M and Atlas D. Precipitation motion by pulse Doppler radar. *Preprints Ninth Weather Radar Conf. Amer.Meteor.Soc.*, 1961. 218～223.

2 Caton P G . The measurement of wind and convergence by Doppler radar. *Preprints Tenth Weather Radar Conf. Amer.Meteor.Soc.*, 1963. 290～296.

3 Browning K A and Wexler R. The determination of kinematic properties of a wind field using Doppler radar. *J.Appl.Meteor.*, 1968,7: 105～113.

4 Easterbrook C C. Estimating horizontal wind fields by two dimensional curve fitting of single-Doppler radar measurements . *Preprints 16th Radar Meteorology Conf. Houston: Amer.Meteor.Sci.*,1975. 214～219.

5 Waldteufel P and Corbin H. On the analysis of single-Doppler radar data. *J.Appl.Meteor.*, 1979, 18: 532～542.

6 Song Chunmei, Ge Runsheng, Zhang Peiyuan. Detection and research on two-dimensional horizontal wind field from single-Doppler radar. *Proceeding of mesoscale meteorology.*Beijing, *Meteorological Press:*1~7.

7 Tao Zuyu. VAP method retrieving wind vector field from single-Doppler velocity field. *Acta*, 1992, 50(1): 81～90.

8 Yang Guoxiang, He Qiqiang, Lu Hancheng. *Mesoscale meteorology*. Beijing: *Meteorological Press*, 1989.

9 Gu Songshan, Jiang Haiyan, Liu Xiaoyang,*Doppler Velocity Display with TVGA Graphics Adaptor, Journal of Nanjing Institute of Meteorology*, Dec.1993: 446～450.

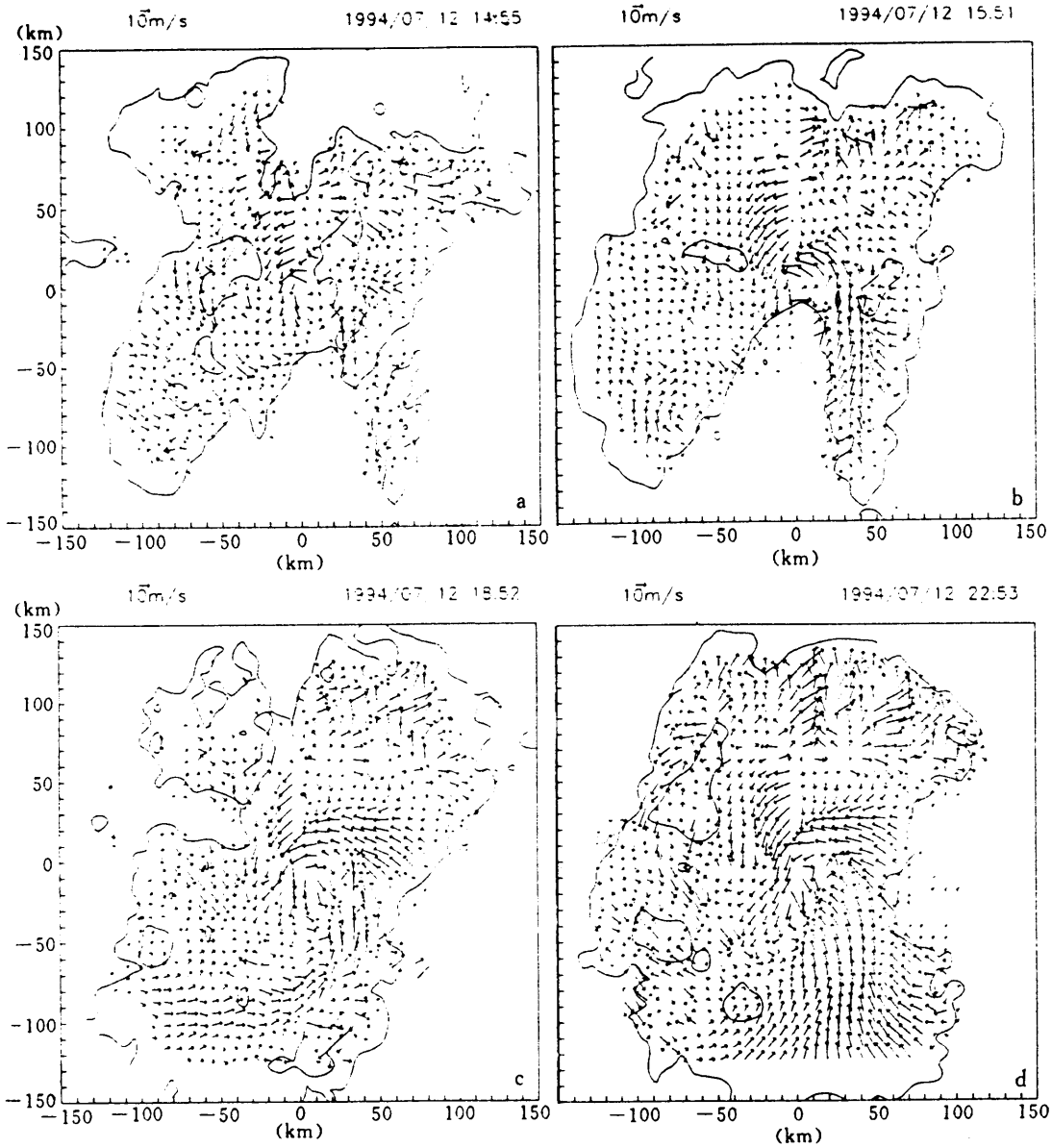

Fig.1 Two-dimension horizontal wind field retrieved by Vorticity-Divergence method on July 12, 1994 (the external profile is the isogram of echo intensity) (a) 14:55 (b) 15:51 (c) 18:52 (d) 22:53

Preliminary Study of Correction for Precipitation Attenuation of C Band Radar Data

M. Cheng① R. Shi① Z. Cui① Y. Qi① H. He ① Z. Cai① H. Xu ②

(①Chinese Academy of Meteorological Sciences, Beijing 100081; ②Huaihe River Commission for Water Resource, Anhui Bengpu 233001)

Address: Chinese Academy of Meteorological Sciences, 46 Baishiqiao Road Beijing 100081 China

Telephone: (010) 68406986 (o), Telefax: (010) 62175931 E-mail: minghu@public.east.cn.net

There are many applications for the radar measured precipitation [1,2, 3]. However, many factors still exist which limit the accuracy of radar measured precipitation. Therefore, it is a challenging task to improve the precipitation measurement accuracy [1]. For example, echoes in C and X band digital weather radars, which are widely used in China, may be strongly attenuated by hydrometeors in the path. This may strongly reduce the precipitation measurement accuracy. In 1954, based upon some hypothesis, Hitschfeld and Bordan[4] gave an analytical formula for the correction of hydrometeor attenuation. However, this technique failed to give reasonable results in practice. Since then, studies have shown that it is a difficult task to correct the attenuation. In HUBEX project which is under the frame of GEWEX (Global Energy and Water cycle EXperiment), the C band radar which is located in Fuyan, Anhui, P.R.C, was used in the field experiment in 1998. In this paper, based upon the C band radar observed data sampled from the observations with 10 minutes interval and rain gauge reported hourly rainfall data, an iterative method is used for the study of correction of hydrometeor attenuation.

1. Method and Data

Weather radar equation in unit of dBZ can be described as follow.

$$dBZ = dBZ_0 + dBC_e + 2\int_0^R K_{(dBZ)}\, dR \qquad (1)$$

where dBZ_0 and dBZ are the attenuated and corrected radar reflectivity factors respectively, dBC_e is the error caused by the calibration, R is the distance between the observation point and the radar., and K is the one way attenuation coefficient. In addition, there are following relations for K and Z.

$$Z = aI^b \qquad (2)$$

$$K = a' I^{b'} \qquad (3)$$

where I is precipitation intensity, a' and b' are parameters independent of precipitation intensity, but may vary with temperature of hydrometeors[5, 6]. a and b are parameters which may vary with radar location and type of cloud-precipitation system. In this study, a=200 and b=1.6 are chosen, which are widely used for stratiform precipitation, and Marshall and Palmer law[7] is used as the hydrometeor size distribution.

Based upon Equations 1 to 3, and Hildebrand[8] proposed iterative method, ignoring the term of calibration error, the iterative method used in this paper can be described as follow.

$$dBZ^{(n)} = dBZ_0 + 2\int_0^R K_{(dBZ^{(n-1)})}\, dR \qquad (4)$$

In this study, C band radar data are used. The radar is located at Fuyang city with the longitude of 115° 49' E, and latitude of 32° 55' N. Within the radar coverage, topography is quite flat. Plate I shows the radar reflectivity factors with the rain gauge positions (+). In this investigation, the radius of radar coverage is chosen as 250 km. The radar was operated in PPI mode with the elevation of 0.5° , 512 scanning lines for 360° rotation and the gate length of 1.0 km. The radar data were sampled every 10 minutes. In addition, 84 rain gauges reported hourly precipitation data are used in this paper.

2. Results and Discussion

Plate I-1 shows Fuyang radar observed reflectivity factor distribution at 10:01 BJT on 29 June 1998. From the plate, it can be seen that there are widely spread stratiform precipitation. The reflectivity factor may be higher than 50 dBZ and corresponding precipitation intensity may be bigger than 50 mm/hr. Therefore, the event can be classified as heavy rainfall. From the plate, it is found that the

reflectivity factor has its peak near the radar and gets weakening with the distance away from radar. The rain band had near west to east direction. Plate I-2 shows the corrected radar reflectivity factor distribution. The hydrometeor temperature of 20℃ is used in this correction procedure described above. From the plate, it can be seen that overall precipitation intensity is enhanced obviously, and the precipitation intensity of the whole rain band seems more uniform than uncorrected one. This is more closed to the property of stratiform precipitation. Therefore, the corrected precipitation field seems more reasonable.

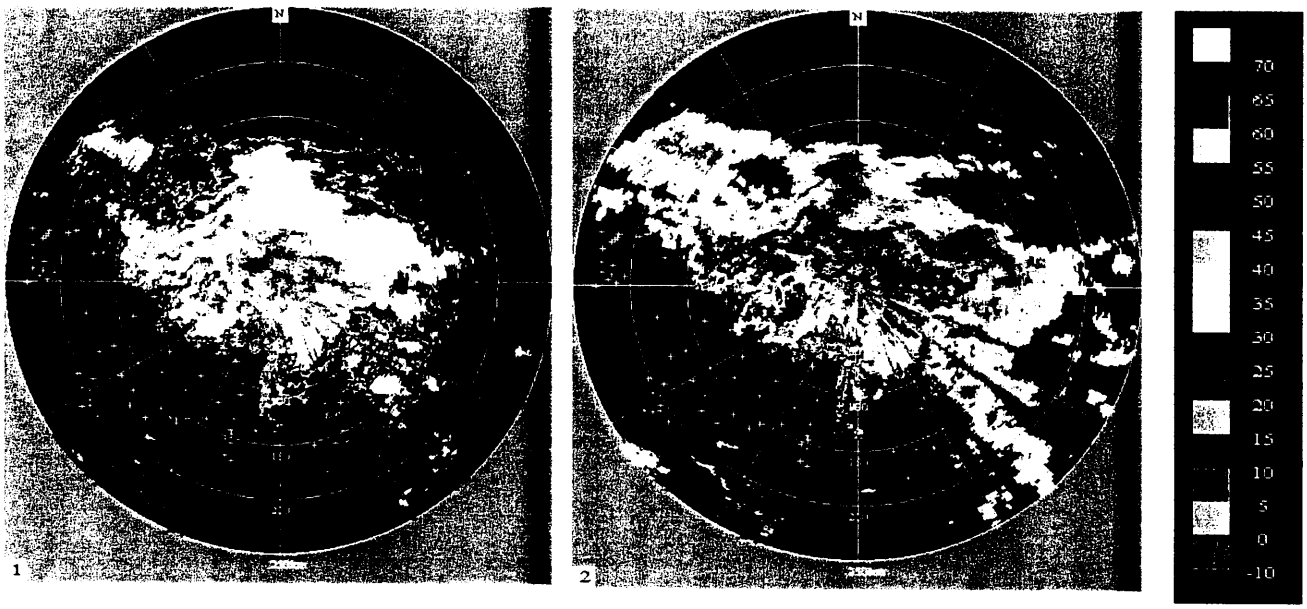

Plate I Distributions of Fuyang radar PPI reflectivity factor in the unit of dBZ at 10:01 BJT on 29 June 1998, derived from (1) direct observation, and (2) attenuation correction.

By comparing Plate I-1 with Plate I-2, it is found that two precipitation patterns are quite different. In Plate 1 representing the directly observed precipitation field, the relative weak echoes smaller than 30 dBZ are distributed in outer parts of the rain band. By analysis, this may arise from the attenuation of heavy precipitation for that case, which is confirmed by Plate 2. By further comparing two plates, it can be seen that most parts of green areas (smaller than 30 dBZ), located at outer parts of band and some isolated precipitation cells in Plate 1, turn to yellow or red color after correction in Plate 2. But there still are some green areas in Plate 1 keeping unchanged color after the correction (see Plate 2). These unchanged green areas mainly concentrate in the southwest direction relative to radar location. This is due to small portion of heavy rainfall in southwest direction, which makes the correction quite small. This fact also shows that the radar succeeded in detecting weaker precipitation in southwest direction. But the radar failed to do so in other directions for in which there was widely distributed heavy precipitation diminishing the signal from relative weak precipitation. This has been evidenced by rain gauge reported data. For the C band weather radar it has such property of direction dependence in detecting precipitation. Such directions vary with precipitation fields. It makes any attempts to reduce the precipitation attenuation effects through the range corrections quite difficult.

Figure 1 shows 84 rain gauges reported non-zero hourly rainfall with corresponding Fuyang radar derived directed observed and corrected hourly rainfall against the range between rain gauge and the radar at 10:00-11:00 BJT on 29 June 1998. Thick solid line with +, thin solid line with x and dotted line with * indicate rain gauge reported, radar observed rainfall before and after correction respectively. In the correction procedure, the hydrometeor temperature of 20^0C was chosen. The radar derived hourly rainfall is obtained by the trapeziform integration using 7 images sampled in the interval of 10 minutes. The relation of Z-I is chosen as $Z=200I^{1.6}$. By examining 84 rain gauges

reported hourly rainfall data from 10:00 to 11:00 BJT, the rainfall records from 23 rain gauges are used in this comparison. From Fig. 1, it can be seen that almost all rain gauges reported more rain than radar directed observation, and the ratio of rain gauge to radar directly observed hourly rainfall is getting bigger with the increment of the range between rain gauge and radar, while radar corrected hourly rainfall data are closer to rain gauge reported ones. By examining all 23 rain gauges reported hourly rainfall data, it is found that most of radar derived corrected hourly rainfall data are closer to rain gauge reported ones than those derived by direct observation. Therefore, by using the relatively simple correction procedure in this preliminary studies, the C band radar corrected precipitation is obviously improved, which can also be obtained at other observed times for the case.

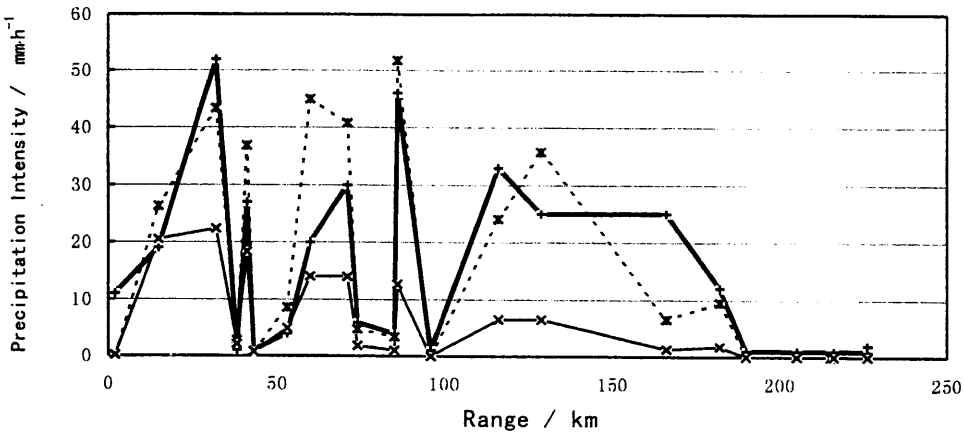

Fig. 1 Rain gauges (thick solid line with +) reported non-zero hourly rainfall with orresponding Fuyang radar derived directed observed (dotted line with *) and corrected (thin solid line with x) hourly rainfall against the range between rain gauge and the radar at 10:00-11:00 BJT on 29 June 1998.

From Fig. 1, it is also found that the correction scheme gives more rainfall for small ranges, which may be from imperfect Z-I relationship and unreal hydrometeor temperature, and/or ground cluster. And the correction scheme still underestimates rainfall in the range of 120-200 km, which may be due to partial filling of radar bean in such large range. These will be studied in future.

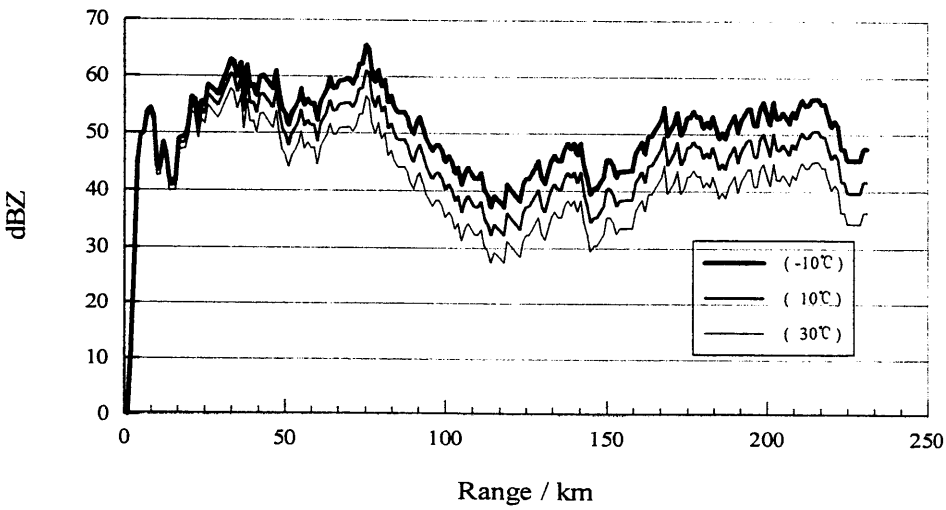

Fig. 2 The corrected Fuyang radar reflectivity factors for the scaling line at 308.0° at 10:01 BJT on 29 June 1998 for the hydrometeor temperatures of—10°C, 10° and 30°C respectively.

Figure 2 shows the corrected Fuyang radar reflectivity factors for the scaling line at 308.0^0 at 10:01 BJT on 29 June 1998 for the hydrometeor temperatures of -10^0C, 10^0 and 30^0C respectively. The selected three temperatures are possible temperatures for natural hydrometeors. From the figure, it can be seen that for this case, the hydrometeor temperature strongly effects the corrected radar reflectivity factor by reaching the difference of 10 dBZ in these three possible hydrometeor temperatures. Therefore, the temperature of hydrometeors has to be taken into account in an operational attenuation correction procedure.

Acknowledgement. The authors would like to thank Professor Zhou Xiuji for his support to this research, and two referees for their suggestions for the final version of this paper. The research is funded by Chinese Natural Science Foundation (Contract No 49705064), Chinese Ministry of Science and Technology (Contract No G1998040909), Chinese Meteorological Administration, and Chinese Ministry of Personnel (Outstanding Returned Oversea Scholar Program).

Reference

1 Cheng, M. Estimation of precipitation using satellite, radar and rain gauge data, Ph.D Thesis, University of Bristol, 1994, 400pp.

2 Collier, C G. Application of weather radar systems. A guide to user of radar in meteorology and hydrology. Ellis Horwood Ltd, 1989. 294pp.

3 Zhang Peichang, Dai Tiepi, Du Bingyu, et al. Radar Meteorology. Beijing: Meteorological Press, 1988. 329pp.

4 Hitschfeld W, Bordan J. Errors inherent in the radar measurement of rainfall at attenuating wavelengths. J. Met. 1954, 11: 58～67.

5 Qin Yu, Scattering and attenuation of electromagnetic wave at the length of 5 cm by rain, Corpus of Radar Meteorology .Beijing: Meteorological Press, 1981. 113～117

6 Herman, B. M., Battan, L. J. Calculation of Mie backscattering of microwaves from ice spheres. Q.J. Royal Meteorological Society, 1961, 87:223～230.

7 Marshall, J.S., Palmer, W.M. The distribution of raindrops with size. J. Meteor., 1948, 5:165～166.

8 Hildebrand P H. Iterative correction for attenuation of 5 cm radar in rain, J. Appl. Met., 1978, 17: 508～514

Introduction to CINRAD WSR-98D Signal Processor

He Jianxin Wang Ping

Beijing METSTAR Radar Company, Limited.

FuDao Building, 1/F East, No.11 Kaituo Road
Shangdi Information Industry Base, Haidian Distric
Beijing, 100085, P. R. CHINA
Tel: 86-10-62981245
Fax: 86-10-62981251
E-mail: bjradar@public.east.cn.net

1. Introduction

Building on its NEXRAD heritage, CINRAD incorporates many technological advances to further enhance performance, reliability and can be easily upgraded. These include an open system workstation platforms, VLSI DSP signal processor, network communications, real-time display, fibre-optical transfers, and new scan modes.

The CINRAD Signal Processor hardware contains two major subassemblies:

- Hardwired Signal Processor (HSP)
- Programmable Signal Processor (PSP)

The CINRAD Signal Processor block diagram is illustrated in figure 1 and its interfaces to other CINRAD subsystems is illustrated in figure 2. The following is a detailed description of the signal processor.

2. Hardwired Signal Processor

The Hardwired Signal Processor performs the following functions:

1) Prescaling of I, Q and Log data
2) Store interference detection tag and AGC position data
3) Synchronization and control of the transmitter and receiver
4) Control interface with the Programmable Signal Processor (PSP).
5) Pedestal Control

Compared with the NEXRAD HSP, the CINRAD HSP is programmable. It is redesigned based on VLSI PLDs (Altera Co. MAX9000S Series), which is in system programmable.
The in-system programmability (ISP) features facilitate prototyping during design development, streamline manufacturing, and increases design flexibility. ISP also enables quick and efficient upgrades in the field.

3. Programmable Signal Processor.

The data inputs to the PSP are either I and Q data or Log data from the HSP. Each data sequence consists of 32 bit floating point numbers in TI format. The PSP outputs are base data that the PSP sends to the RDASC Processor.

3.1 PSP Hardware

The PSP is programmable and re-programmable. It is one of a series of DSP PC Boards (PCI/C44S) Blue Wave Systems and is based on Texas Instruments' TMS320C4x family of Digital Signal Processors (DSPs). The main features of the board are:

- Four 60 MHz TMS320C44 processors, each with exclusive access to two banks of zero wait state Static RAM (SRAM) and a bank of Programmable Erasable ROM (PEROM).
- A full 32 bit PCI interface for rapid communication between the PSP and the PC.
- The four parallel communication ports on each C44 processor, which provides the primary method of interprocessor communication.

HSP-A and HSP-B are accessed from PSP via Blue Wave's DSPLINK2 interface. This interface provides fast parallel data transfer from/to HSP-A and HSP-B boards independent of the PCI bus.

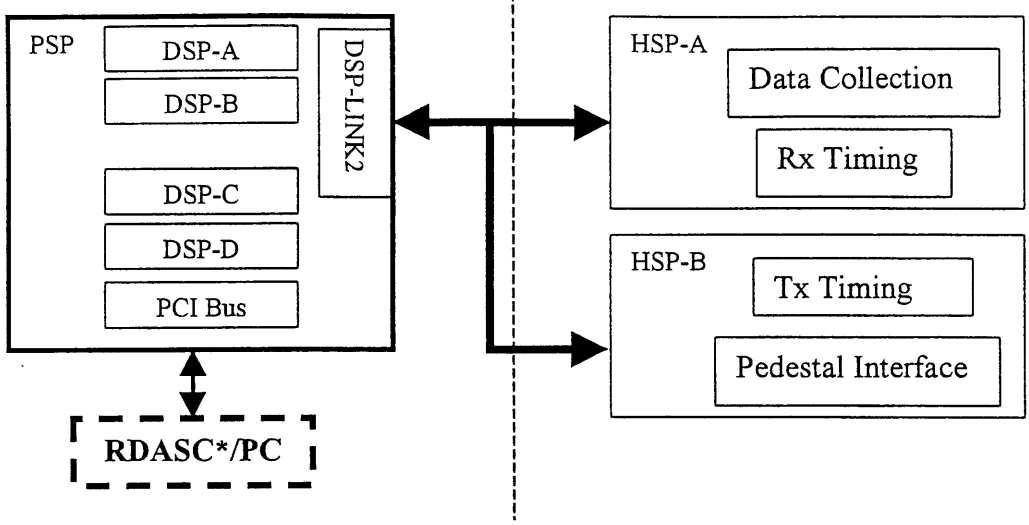

Note: *: RDASC- Radar Data Acquisition Status and Control. It is a radar monitoring and control program.

Figure 1 CINRAD Signal Processor Block Diagram

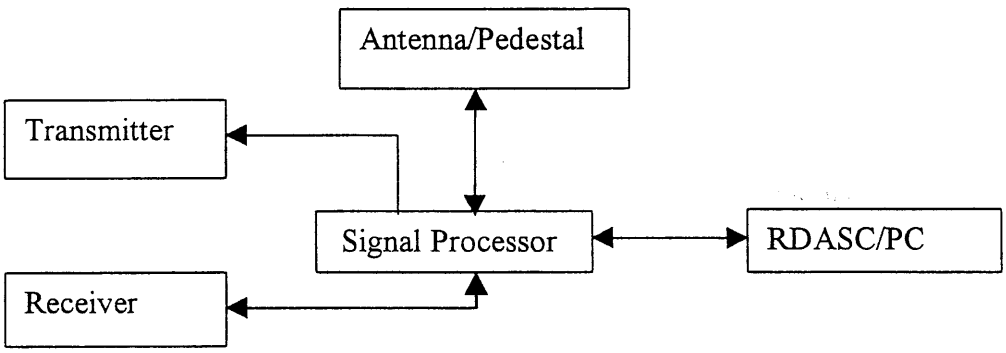

Figure 2 Signal Processor interface block diagram

3.2 PSP Hardware Functions

The hardware functions of the PSP are:

i. Accept I, Q, AGC Position, Log data and interference detection tags and distribute this data to the DSP units of the PSP.
ii. Accept fault localization data from the receiver and HSP
iii. Receive and Transmit data to the pedestal assembly
iv. Accept controls and supplementary data from the RDASC processor via the PCI bus and route it to the HSP.

4 Signal Processing Functions

4.1 The Z, V, and W estimates

Doppler radar receiver output data is processed to provide estimates of reflectivity, mean radial velocity, and spectrum width. The processor is capable of estimating reflectivity and velocity at signal-to-noise ratios down to and including -3 dB. The Z, V, and W estimates are discarded when the corresponding Signal-to-Noise ratio (SNR) is less than a set threshold value. Independent threshold values are used for the three estimates (Z, V, W) and a separate set of threshold values is used for each antenna scan strategy and each antenna scan rate used. All Threshold values are adaptable at the UCP(Unit Control Position), in increments of 0.5dB, over a range of SNR of at least -10dB to +10dB. There are many adaptation data values used to control data quality such as noise, TCN, TOVER etc. Outbound radial velocities are defined as positive velocities and inbound radial velocities are defined as negative velocities.

4.2 Ground Clutter suppression

Ground clutter contamination occurs when the returned signal from stationary or nearly stationary, non-meteorological targets is included in the base data. Ground clutter contamination has a significant effect on the accuracy of the base data. Since all products and algorithms are built from the base data, ground clutter contamination will affect both base data and derived products. A particularly sensitive product is the precipitation estimation.

The ground clutter suppression algorithm is designed to remove power from predictable ground sources returning high power and near zero velocity values. The notch width is an interval of velocity near zero where clutter suppression will be applied. Clutter suppression is applied in two fundamentally different ways. Automated clutter suppression can be performed by invoking the clutter maps (Include bypass maps and notch width maps) and adaptation data. Clutter filter bypass maps designate where not to apply suppression. A higher resolution bypass map minimizes loss of base data due to selection of clutter filtering. Clutter filter notch width maps that designate how much suppression to apply. The value of notch width required to achieve a specified amount of clutter suppression depends primarily on the clutter spectrum width. In turn, the clutter spectrum width depends primarily on antenna azimuth scan rate, wind velocity and terrain type. Operator defined clutter filtering is performed by defining a clutter suppression region. The degree of suppression selected for the region will be uniformly applied to all stationary targets in the region.

In CINRAD, fifth-order elliptic filter is implemented in order to achieve the required suppression level.

4.3 Interference Suppression

The Interference Detection Unit in the receiver sends an Interference Detection Tag (IDT) to the PSP (via the HSP) every time it senses in-band interference. PSP uses different processing method to minimize bias error for reflectivity and velocity estimates.

5 Signal Processing Flowchart

Signal Processing Flowcharts are illustrated in figure 3.

6. Acknowledgements

The authors wish to thank the members of the Signal Processing group of Metstar Radar Co., and American expert Fred Brenner.

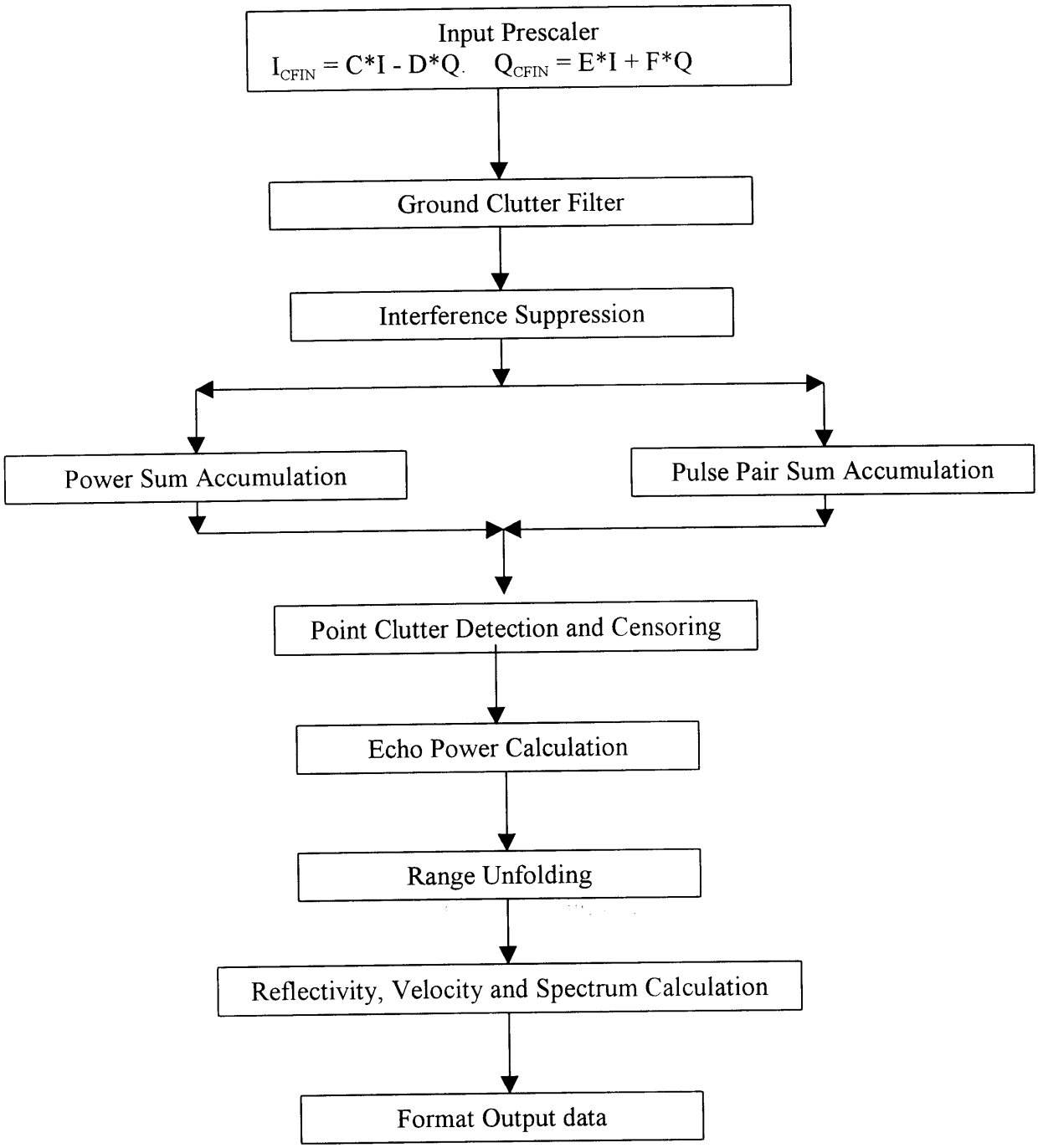

Note: C, D, E and F are coefficients for I & Q signal balance correction.

Figure 3 Signal Processing Flowcharts

Employment of an S-Band Vertically Pointing Radar

Jonathan J. Gourley[1], Kenneth W. Howard[2], Herb Winston[3]

[1] CIMMS/University of Oklahoma, Norman, OK, USA
National Severe Storms Laboratory
1313 Halley Circle
Norman, OK, USA 73069
ph: 405-366-0536
fax: 405-366-0472
email: gourley@ou.edu

[2]NOAA/National Severe Storms Laboratory, Norman, OK, USA

[3] URS/Radian Electronic Systems, Boulder, CO, USA

1. Introduction

Precipitation monitoring by radar during the cool season is complicated by poor low-level WSR-88D radar coverage in the U.S. Intermountain West (Westrick et al., 1999). Beam blockages from nearby terrain combined with the shallow nature of orographically enhanced precipitation limit the ranges at which reflectivity can be measured below the melting layer. The reliability of surface rainfall estimates from the operational precipitation algorithm diminishes as beam heights approach and exceed melting layer heights (Fulton et al., 1998). Within this zone of enhanced reflectivity, or radar bright band, precipitation overestimations can be as large as a factor of 10 (Smith, 1986). Above this layer, Kitchen and Jackson (1993) found that radars typically underestimate surface rainfall by a factor of 10 where beam overshooting is prevalent at far ranges (e.g., 200 km).

Wavelength	10.6 cm
Amplifier	solid state-low voltage, Class C
Peak Power	380 watts
Maximum Duty Cycle	10%
Antenna	3 meter shrouded parabolic dish
Beamwidth	3.2 degrees
Height Resolution	selectable: 60, 100, 250, 500 m
Maximum Height Sampled	21.4 km (typical)
Maximum Radial Velocity	20 meters per second (typical)
Spectral Points	128 (typical)
Dwell Time	35 seconds (typical)
Processor	DOS-based, personal computer
Sensitivity	-25 dBZe @ 10 km altitude
Power Requirements	110/220 VAC ± 10%, 5 amp
Recording	full Doppler spectra
Media	optical disk

Table 1. S-Band Precipitating-Cloud Radar System image and specifications.

During the winter of 2000, an S-Band Precipitating-Cloud Radar System was deployed in a "radar-hostile" region in Northern Arizona. Radar system specifications are given in Table 1. Spectral data were collected for several winter storms including one that produced over 75 mm of rainfall in the Phoenix metropolitan area. Reflectivity structures are analyzed for this storm that occurred from March 5-7.

2. Background

The S-Band vertically pointing radar was deployed in a prominent valley in Northern Arizona at Camp Verde. The site elevation is 949 m. The Flagstaff WSR-88D radar (KFSX) is 60 km away and resides at an elevation of 2286 m, while the Phoenix radar (KIWA) is 141 km

away and sits at 427 m. Figure 1 shows the radar horizons between the WSR-88D sites and Camp Verde. The white beams are those that are closest to the ground but clear it by more than 150 m (O'Bannon, 1997). Notice how the 0.5 degree beam from KIWA is partially blocked, yet utilized over Camp Verde. The S-Band deployment site is at the far right hand side of both plots.

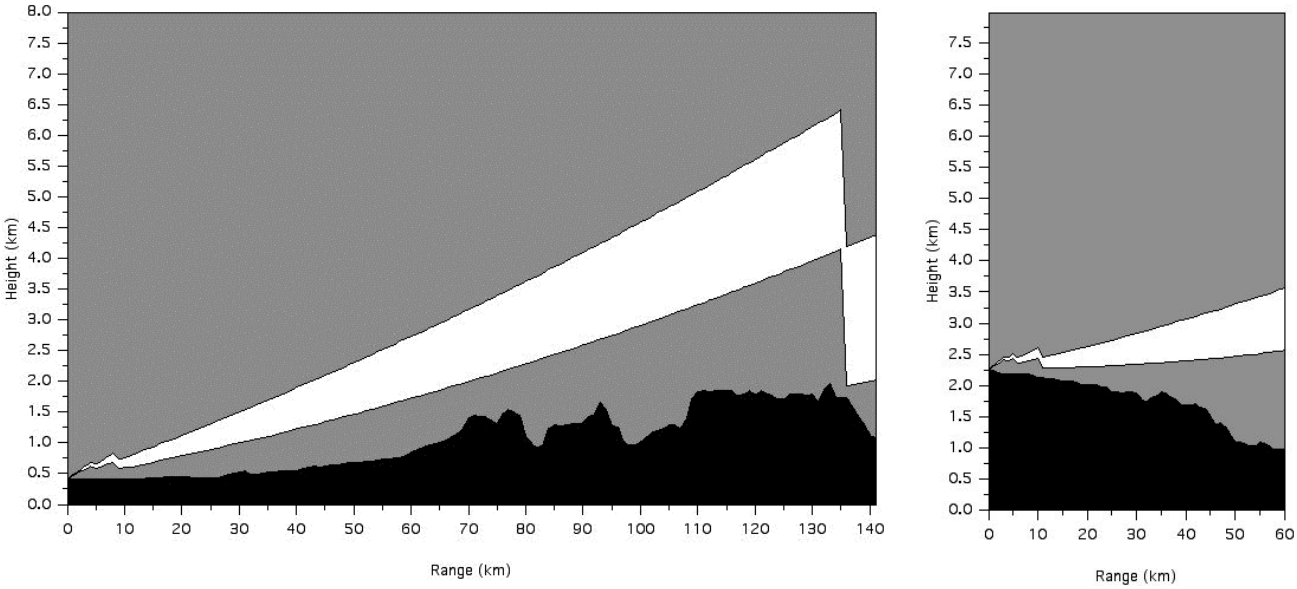

Figure 1. Cross-sections of KIWA hybrid scan (left) looking north and KFSX (right) looking west toward S-Band deployment site.

The lowest elevation angle from KFSX samples clouds over 1.5 km above Camp Verde. KIWA is able to capture data at a lower height above ground, but its sample volume is quite large. In addition, the beam is partially blocked by terrain and may result in degraded reflectivity values. Operationally, reflectivity data from partially blocked zones are adjusted based on the computed blockage. It is not well known whether these adjustment factors are accurate.

During winter storms in this area, the rain/snow line typically forms below the altitude of KFSX yet above KIWA and Camp Verde. With a melting layer near 1.5 km MSL, Fig. 1 shows that neither WSR-88D radar will sample rainfall below the melting layer. Instead, reflectivity and thus precipitation rates are derived from frozen hydrometeors measured aloft. Underestimations are likely in this scenario due to echo intensities decreasing with height above the melting layer, and the dielectric constant in the radar equation is assumed to apply to liquid hydrometeors. These radar sampling difficulties are not uncommon in the Intermountain West. As shown in the following section, detailed profiles of reflectivity provide useful information for QPE purposes, and may be used to augment future precipitation algorithms.

3. Results

Data are presented for 1000 to 1125 UTC on March 6, 2000. This winter storm produced stratiform rainfall at the S-Band site. Figure 2 shows time-height cross-sections of reflectivity data measured by WSR-88D radars over Camp Verde. The lower extent of the KIWA 0.5 degree beam is calculated to be 700 m above the ground at Camp Verde. However, beam depths are large, nearly 2.5 km in depth, leading to a smoothed depiction of actual vertical profiles. KFSX has smaller bin volumes, but they are over 1.5 km above the ground at the deployment site. Backscattered power is from frozen hydrometeors, and is thus not representative of surface rainfall rates.

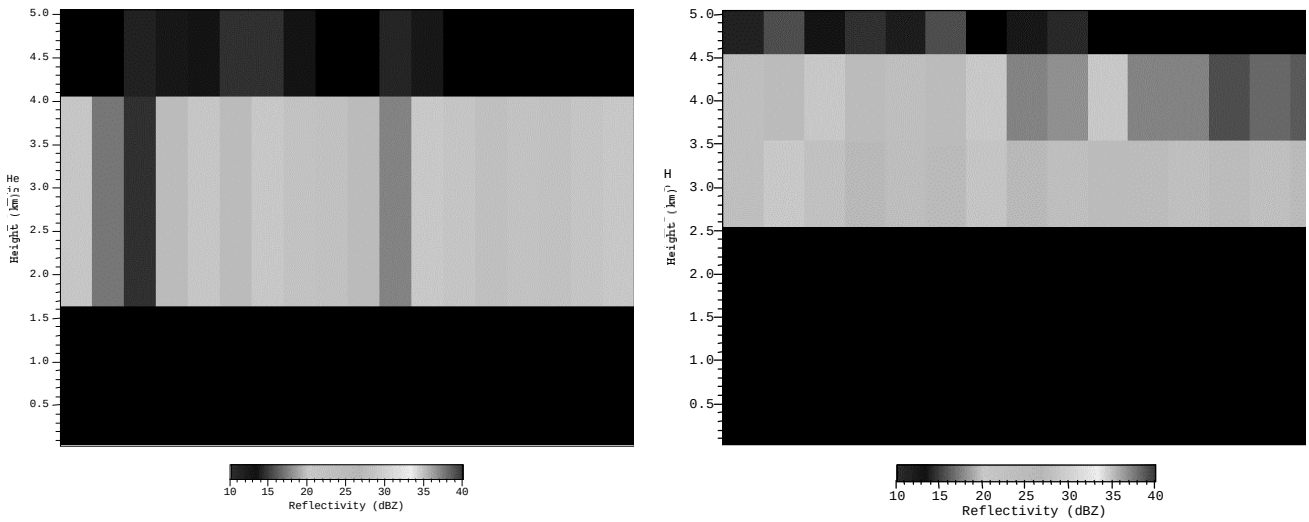

Figure 2. Time-height cross-sections of KIWA and KFSX reflectivity over S-Band deployment site. Time increases from 1000 UTC (left) to 1125 UTC (right).

Data collected from the S-Band vertically pointing radar show much more detailed vertical reflectivity structures. Figure 3 shows a time-height cross-section coinciding with the times presented in Fig. 2. The 45 m vertical height resolution captures a prominent layer of enhanced reflectivity from 1.5 to 1.8 km. This bright band reveals temporal variability as different densities of frozen hydrometeors slowly fall and melt. Since the melting layer is well identified, we can confirm that rainfall, and not snow, is reaching the surface. Moreover, S-Band reflectivity magnitudes measured just above the surface show little correlation with WSR-88D samples measured above the melting layer. This result suggests QPEs by operational WSR-88D radar systems are inaccurate for winter storms with low altitude melting layers.

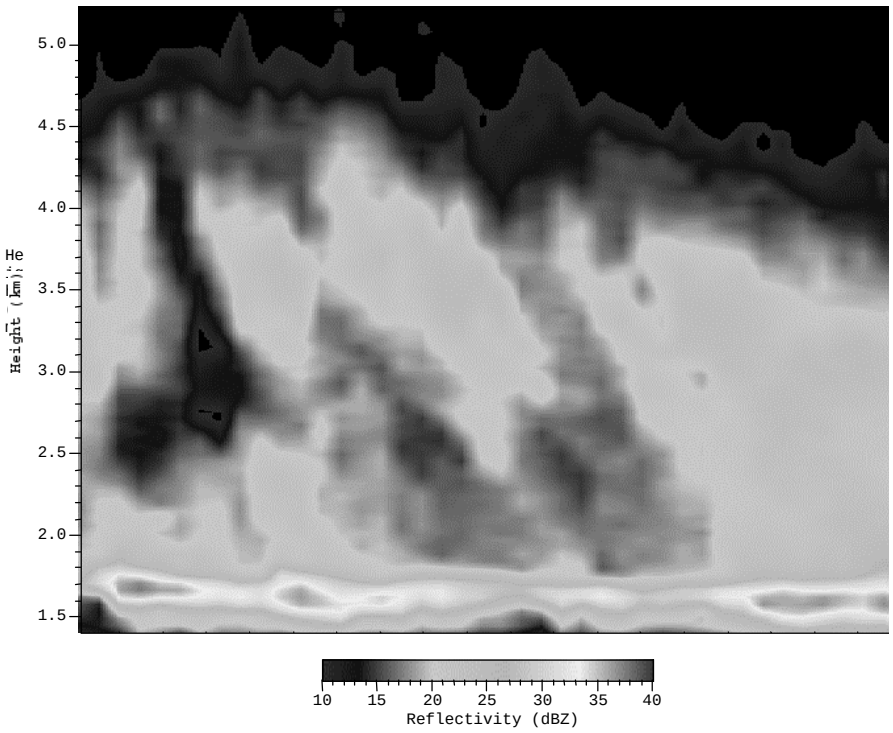

Figure 3. Same as for Fig. 2, except data are from S-Band Precipitating-Cloud Radar System.

4. Conclusions

The S-Band vertically pointing radar captures unprecedented detail in vertical reflectivity structures for winter storms over complex terrain in northern Arizona. It is capable of collecting high-resolution vertical profiles of reflectivity, velocity, and spectrum width. Future algorithms may be designed to utilize operational S-Band data to adjust and improve QPEs from WSR-88D radar or other remote sensors, such as satellites. Also, accurate detection of melting layer altitudes may be used to delineate frozen from liquid precipitation. Accurate QPE and precipitation typing will be useful for agricultural purposes, watershed management, flood control, avalanche forecasting, and handling of snow removal equipment for transportation during winter storms. It is hoped that this research-oriented radar will advance as a real-time observational platform.

5. Acknowledgments

We would like to acknowledge the Verde Natural Resource Conservation District for helping us operate the S-Band radar at Camp Verde. Also, Dave Carter from the NOAA Aeronomy Laboratory in Boulder, CO supplied us with code to read and convert our data. URS/Radian Electronic Systems provided the S-band radar used in this study. This project was made possible by funding from the Salt River Project in Phoenix, AZ.

6. References

Fulton, R. A., J. P. Breidenbach, D. J. Seo, D. A. Miller, and T. O'Bannon, 1998: The WSR-88D rainfall algorithm. *Wea. and Forecasting*, **13**, 377–395.

Kitchen, M., and P. M. Jackson, 1993: Weather radar performance at long range - Simulated and observed. *J. Appl. Meteor*., **32**, 975-985.

O'Bannon, T., 1997: Using a 'terrain-based' hybrid scan to improve WSR-88D precipitation estimates. Preprints: *28th Conf. on Radar Meteorology*, Austin, TX, Amer. Meteor. Soc., 2 pp.

Smith, C. J., 1986: The reduction of errors caused by bright bands in quantitative rainfall measurements made using radar. *J. Atmos. Oceanic Technol.*, **3**, 129-141.

Westrick, K. J., C. F. Mass, and B. A. Colle, 1999: The limitations of the WSR-88D radar network for quantitative precipitation measurement over the coastal western United States. *Bull. Amer. Meteor. Soc.,* **80**, 2289-2298.

Dual-Polarization and Processor Efficiency Enhancements of the DOE's Millimeter-Wavelength Cloud Radars (MMCR)

K.P. Moran, B.E. Martner, NOAA Environmental Technology Laboratory Boulder, Colorado, USA
H.A. Winston, URS/Radian International LLC, Boulder, Colorado, USA

1. Background

The use of millimeter-wave radars for cloud research has burgeoned in the last decade (Kropfli and Kelly, 1996). Much of this activity has been motivated by the need for more extensive and continuous monitoring of cloud conditions for climate research, aviation safety, and telecommunications. The high frequencies employed by these radars (typically 35 or 94 GHz) endow them with an inherent sensitivity advantage for detecting the very small hydrometeors of clouds compared to the lower frequencies used by storm surveillance radars. Thus, clouds themselves, and not just precipitating regions, can be observed and measured with high sensitivity and resolution using these "cloud" radar systems. Major disadvantages of the high-frequency radars include severe attenuation by rainfall (but not by snowfall) and limited range. The millimeter-wave radars are ideal for continuous ground-based observations of cloud conditions overhead, and episodic observations from research aircraft. A millimeter-wave radar is also the centerpiece for the international CloudSat satellite mission, to be launched in 2003.

The millimeter-wave cloud radar (MMCR) designed by NOAA's Environmental Technology Laboratory (NOAA/ETL) has been one of the primary systems in this technology growth (Moran et al., 1998). This 35-GHz radar is now built and marketed by URS/Radian International, LLC., through a Cooperative Research and Development Agreement (CRADA) with NOAA. The MMCR is part of the suite of instruments operated by the U.S. Department of Energy's Atmospheric Radiation Measurement (ARM) program (Stokes and Schwartz, 1994) at Cloud and Radiation Testbed (CART) sites in Oklahoma, Alaska, and on islands in the tropical western Pacific Ocean, where the radars are intended to operate for at least 10 years. An identical radar operated by NOAA/ETL has been used for shorter-term observations of clouds in the Arctic, Indian, and Pacific Oceans, and in Colorado and Massachusetts.

The MMCR is a vertically-pointing ground based, Doppler system, designed for long-term, unattended operations. In spite of very low transmitted power, it achieves excellent sensitivity, sufficient for detecting most visible clouds overhead, through its short wavelength and the use of a large antenna, long sampling duration (~1 sec), and signal processing and pulse compression techniques. Table 1 summarizes some of the radar's basic characteristics. Since its original design in the early 1990s, various minor improvements have been made to the radar system. NOAA and URS/Radian are now in the process of implementing two major upgrades: (1) replacing the radar's original data system with a more powerful processor, and (2) adding a dual-polarization measurement capability.

Table 1. Characteristics of the MMCR

Transmitter	TWTA, 100-W peak power
Duty Cycle	up to 25%
Antenna	6-ft or 10-ft diameter
Beam Width	0.3 and 0.2 deg.
Height Coverage	0.1 to 20 km
Height Resolution	45 m and 90 m, typically
Time Resolution	9 sec/mode, typical
Sensitivity	As good as -50 dBZ at 5 km
Operating Modes	programmable, typically cycles through 4 modes
Wavelength	8.6mm

2. The New Processor

The MMCR is a highly programmable system which allows the data collection to be optimized for the type of clouds that are under observation. The radar's sensitivity to a particular cloud observation is governed by variables such as transmitted pulse width, number of coherent pulse averages, pulse repetition frequency, number of incoherent spectral averages and the number of code bits used in pulse compression processing. These variables in turn influence the desired measurements such as maximum unambiguous velocity, range resolution, maximum range, range sidelobe artifacts and observation time. Numerous trade offs are possible and the radar routinely cycles through four independent modes designed to collect measurements for the particular clouds types encountered at individual radar sites (Moran, et al, 1998). Table 2 shows some of the operating characteristics of the four modes for the MMCR located at the Southern Great Plains CART site near Lamont, OK.

Table 2. Operating Characteristics for the MMCR's Four Scan Modes

Cloud Type	Stratus	Cirrus	General	Convective
Inter-pulse Period (μs)	68	126	106	106
Number of Coherent Avgs	10	6	6	1
Number of Spectral Averages	64	21	60	29
Number of code bits	8	32	not coded	not coded
Dwell Time (s)	2.8	1.0	2.4	0.4
Unambiguous velocity (ms^{-1})	±3.2	±2.8	±3.4	±20.3
Unambiguous Range (km)	10.2	18.9	15.9	15.9
Range Resolution (m)	45	90	90	90
Processor Efficiency (%)	31	12	29	4
Est. Sensitivity (dBZ at 5 km)	-47	-54	-42	-38

The operating characteristics of the radar were designed so that each mode has nearly the same observation time (time required to collect and process the measurements) of 9 seconds. Because the hardware and software overhead in the radar's signal processor varies with each mode, not all of the data that is available can be processed. The dwell time is that portion of the 9 seconds that is actually used in the cloud measurements and the processor efficiency represents that as a percentage. For the cirrus and convective modes the overall efficiency is low enough to have an impact on the performance of the radar.

The radar processor in the MMCR is based on the design of wind profiler radars, which exhibit many of the same operating characteristics as the cloud profiling radar. Observation times for wind profilers, however, are on the order of minutes and so processing overhead doesn't become a factor in the radar's performance. Cloud scientists, however, are often interested in observing the dynamics of cloud systems on as short a time scale as feasible. The narrow beamwidths of cloud radars means that short observation times of a few seconds present an opportunity to observe many independent samples of the cloud structure. Poor processor performance impedes the ability of the radar to shorten the observation time without affecting the sensitivity of the measurements.

A block diagram of the present and new MMCR radar processor is shown in Figure 1. The present architecture uses a specialized hardware pulse averager and a programmable digital signal processor (DSP) to implement the processing. As part of the radar upgrade a new radar processor architecture has been adopted that uses 5 programmable DSPs as shown. The advantages of the new design are the use of higher speed and multiple DSPs working in parallel to accelerate the cloud radar's processing power by a factor of eight. Not all of the available new processing power can be applied if other factors contribute to system overhead. Factors such as the time it takes to distribute the raw data and collect the processed results from the multiple DSP's contribute to system overhead. As an example, Figure 2 shows the level of expected improvements for different values of overhead for the cirrus mode. The new hardware will be operated under a new radar control software program, LAP®-XM that will replace the present (POP4) software. LAP®-XM was developed out of the need for a versatile radar control software environment that is easily programmed with new processing algorithms and operates under Windows NT.

The expected improvements in the processing speed will mean the temporal resolution for each mode will approach the dwell time without affecting the radar's sensitivity. Each mode may not reach the optimum dwell time, depending on the implementation. But there are numerous other tradeoffs that can be used to take advantage of faster processing. The sensitivity of a mode can be improved by increasing the number of spectral averages and leaving the observation time the same. An improvement in sensitivity also provides an opportunity to reduce the number of code bits used, which reduces the range sidelobe artifacts in modes that use pulse compression. The mode that is designed to observe convective clouds has the least radar ambiguities of all the modes. A faster processor would improve its sensitivity by nearly 7 dB which would put it in the same range as the stratus mode, perhaps eliminating the need for one of the modes, leaving room for a new mode in its place.

3. Dual-Polarization

As is the case with other high-sensitivity radars, the MMCR readily detects non-hydrometeor targets suspended in the air in addition to cloud droplets and ice crystals. Based on the currently available reflectivity and velocity measurements alone, it is usually not possible to distinguish between these two kinds of targets. This represents a major problem for ARM, where the goal is to determine the characteristics of clouds overhead in an automated fashion. The

problem is particularly bothersome in the afternoon at continental locations in spring, summer, and fall, when insects and bits of vegetation are commonly suspended aloft in the convective boundary layer.

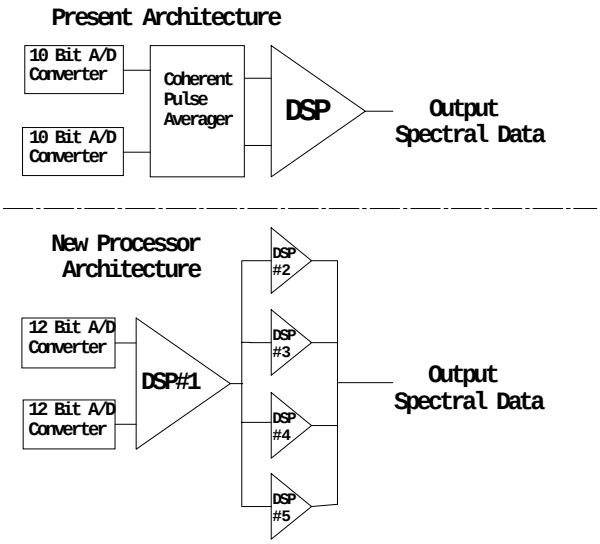

Figure 1. Diagram of the present and new processor architecture

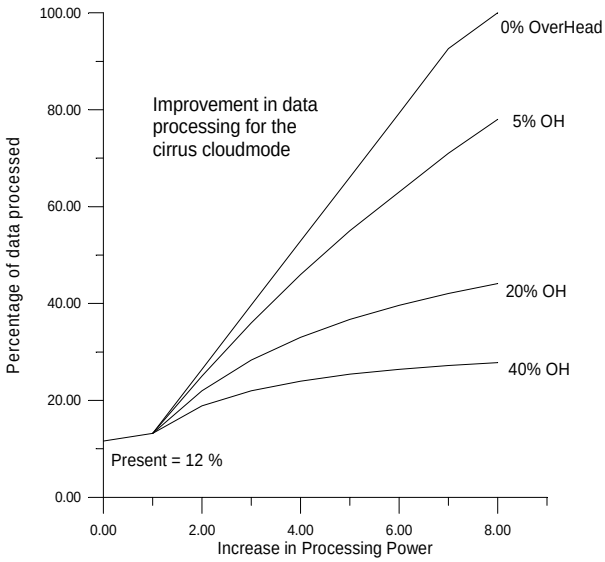

Figure 2. Expected Processing Improvements for different levels of system overhead (OH)

One approach to solving this problem is to add dual-polarization capability to the radar and use the resulting depolarization ratio measurements to provide information about the target shapes. This will allow the radar users to distinguish between the spherical droplets of stratus clouds and the comparatively non-spherical insects. Dual polarization may also be useful for distinguishing between various cloud hydrometeor types (such as droplets, column crystals and plate crystals), but the insect problem is the motivation for ARM to upgrade some of its radars to include dual-polarization measurements. Martner and Moran (2000) describe how ARM may implement this new capability into its automated cloud-mask algorithms to identify the stratus cloud regions and distinguish them from non-hydrometeor targets in the CART data stream.

The MMCR currently transmits linear polarization. Figure 3 is a block diagram showing the configuration for the dual-polar upgrade. In the upgrade the hardware is altered with the addition of an ortho-mode transducer (OMT) which separates the received signal into co-polarized and cross-polarized components. An additional electronic switch (#3 in the block diagram) is added to the receiver chain to allow the radar's single receiver to measure the co- and cross-polar signals on alternate pulses. Other switches protect the low-noise pre-amp while the transmitter is transmitting. A spare channel mode in the processor software is used for processing and recording the new cross-polar data. Dwell time is evenly divided between the two polarizations, thus sensitivity is reduced by 1.5 dB. The logarithmic ratio of the two nearly simultaneous signals is computed to determine the linear depolarization ratio (LDR), which is a function of the target particles' shapes and orientations. With some additional hardware changes the radar could transmit circular polarization and measure circular depolarization ratio (CDR) which would reduce or eliminate the sensitivity to particle orientations. Figure 4 shows an example of vertical profiles of co-polarized (a) and cross-polarized (b) returned power spectra for tests of the dual-polar MMCR in Colorado. The co-polar plot reveals three echo layers. The new cross-polar plot shows that the radar detected significant depolarization only in the lowest layer. This means that the lower layer definitely contained non-spherical particles, most likely insects. The significant amount of cross-polar signal could not have been caused by cloud droplets. This illustrates the basic idea for identifying the presence of insects in the MMCR data.

4. Summary

The MMCR is a high-sensitivity Doppler cloud radar which has already logged several years of detailed cloud observations at a number of locations. Upgrades to the system, now in progress, include replacing the processor with a multiple-DSP system, adaption of the LAP®-XM operating software and adding a dual-polarization measurement capability. These upgrades will provide improved observing/processing efficiency and flexibility and the ability to identify non-droplet particles, such as insects, which often contaminate the cloud data sets collected by the radars.

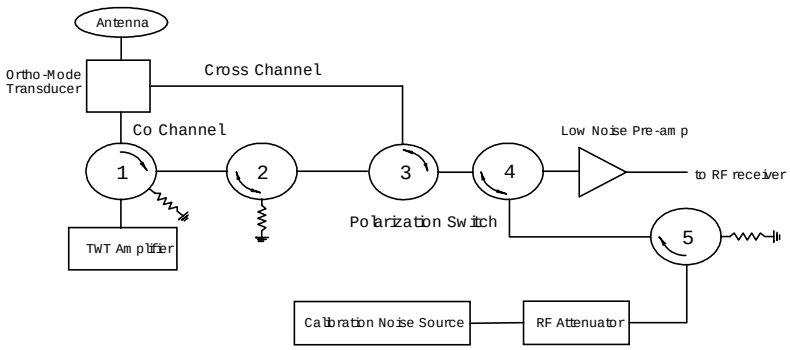

Figure 3. MMCR Dual Polarization Block Diagram

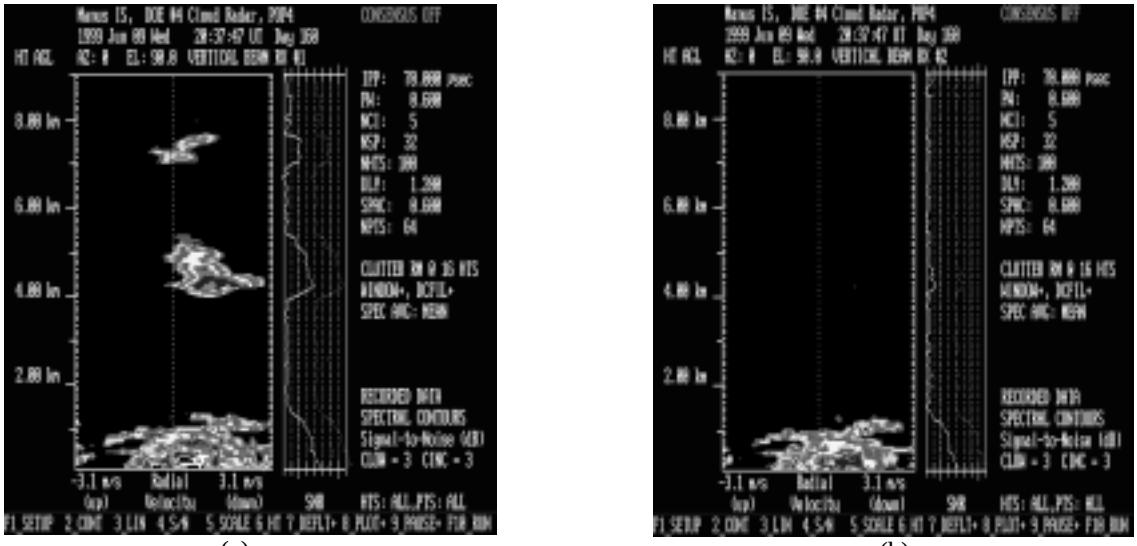

(a) (b)

Figure 4. Vertical profiles of (a) co-polarized and (b) cross-polarized echoes aloft observed during tests of the MMCR in Colorado.

Acknowledgments
Support for development of the MMCR and its upgrades has been provided by the U.S. Department of Energy' ARM program.

References

Kropfli, R.A., and R.D. Kelly, 1996: Meteorological research applications of mm-wave radar. *Meteor. Atmos. Phys.*, **59**, 105-121.

Moran, K.P., B.E.Martner, M.J. Post, R.A. Kropfli, D.C. Welsh, and K.B. Widener, 1998: An unattended cloud-profiling radar for use in climate research. *Bull. Amer. Meteor. Soc.*, ***79**, 443-455.*

Martner, B.E. and K.P. Moran, 2000: Using cloud radar polarization measurements to evaluate stratus cloud and insect echoes. *J. Geophys. Res.* (submitted).

Stokes, G.M., and S.E. Schwartz, 1994: The Atmospheric Radiation Measurement (ARM) program. *Bull. Amer. Meteor. Soc.*, **75**, 1201-1221.

Winston, H.A., K.P. Moran, B.E. Martner, M.J. Post, D.C. Welsh, D.A. Merrit, D.A. Hazen, 1998: Advances in profiling technology…. A new 8-mm Doppler cloud radar. Proceeding for the World Meteorological Organization technical conference on meteorological and environmental instruments and methods of observation, TECO-98, Casablanca, Morocco.

******

THE CAPABILITIES OF WEATHER RADARS TO DETECT DUST STORMS

Moustafa A. E. Amer

Egyptian Meteorological Authority
P. O. Box: 11784 Koubry El-Quoba, Cairo, Egypt
Tel.: 2849852, Fax: 2849857, E-mail: ma@idsc.gov.eg

1. WEATHER RADARS

1.1 Principles of Radar

Radar has been defined as " the art of detecting by means of radio echoes the presence of objects, determining their direction and range and recognizing their character. " In radar meteorology the term " object " is construed to mean anything in the atmosphere which returns to a receiver a detectable amount of power.

Radar is based on the principle that an electromagnetic wave is propagated through atmosphere at the speed of light and travels along straight lines. Thus, by means of antenna producing a narrow beam, in the manner of searchlight beam, one can scan with the antenna until a reflection is obtained and determine the direction to the reflecting object. Also, by measuring the time interval between the transmission of the radio energy and the reception of the reflected signal, the distance to the object can be easily calculated.

1.2 Radar Equation

The average returned power intercepted by the radar antenna, P_r can be given by

$$P_r = \frac{\pi^3 P_t G^2 \varnothing \varphi h}{1024 \lambda^2 \ln 2} \frac{|K|^2}{r^2} \Sigma D_i^6 \qquad (1.1)$$

where P_t is the radar transmission power, G is the antenna gain, $\varnothing$ and φ are the horizontal and vertical widths of the radar beam, h is the length of the outgoing radar pulse, λ is the radar wave length, K is a function of the complex index of refraction always less than one, r is the object range and D_i is the particle diameter.

Equation (1.1) can be written as:

$$P_r = \frac{C |K|^2}{r^2} \Sigma D_i^6 \qquad (1.2)$$

where C is a constant depending on the characteristics of the radar set.

2. DUST STORMS

2.1 Definition

Dust storm is dust raised from the ground by the wind and is carried upwards to height depending on the meteorological conditions and state of soil including the size of particles.

According to international convention a dust storm can be defined as a rapidly moving mass of air which contains large amount of dry opaque particles of diameters less than 100 microns and reducing the horizontal visibility to less than one kilometer.

In dust storms the wind and vertical currents may spread the dust over wide areas, lifting it to great heights, reducing surface, flight and slant visibilities to very low values.

2.2 Size and Concentration of Dust Particles

Measurements of size and concentration of dust particles of strong dust storms were made by Dr. El-Fandy (1951). He showed that the mean diameter of the dust particles is 4 microns while their concentration is 550 particles per cubic centimeter.

3. DETECTION OF DUST STORMS

3.1 Range of Detectable Dust Storms

For a dust storm to be detected by a radar set, its returned power intercepted by the radar antenna, should be greater than the radar minimum detectable signal.

Knowing the values of particles mean diameter and concentration of a typical dust storm (see 2.2), calculating the radar constant C and considering P_r as the minimum detectable signal of the radar; the maximum range of the dust storm can be calculated, such that the backscattered power from it is detectable, by using equation (1.2).

The author calculated the above mentioned range for different powerful radar sets. In each case the calculated range was several meters certainly less than the radar blind range.

3.2 Conclusion

It is concluded that weather radars cannot, to a large extent, detect dust storms.

References:

- Banoub, E. F. 1970, Sand Storms & Dust Storms in A. R. E. Met. Authority, Egypt.
- Battan, L. J. 1973, Radar Observation of Atmosphere. University of Chicago
- El-Fandy, M. G. 1951, Physics of Dusty Atmosphere.

****

Thailand Radar Network

Mr.Kasindej Dangintawat (Author),Mr.Chooseang Sinuthog (Co-author)

Thai Meteorological Department 4353 Sukumvit Road, Bangna, Bangkok 10260

Thailand

Tel. 662-3994582,662-39931681, Fax.662-3994582,662-3932628

E-mail : tmd@metnet.tmd.go.th

Thailand Radar Network is a weather monitoring and nowcasting tool. Composited precipitation data and storm tracking data etc. inputs are from 14 weather radar sites all over Thailand via satellite communication link. The system operation is an advanced computer system with high speed workstations and high resolution graphics. Each network radar sends products to the compositing centre in 15 minute intervals. When several radars are networked to a central data site, the advantages of greater forecasting range are immediately obvious. A forecaster can readily see precipitation across Thailand use the networked information to make decision for forecast and distribute to the public.

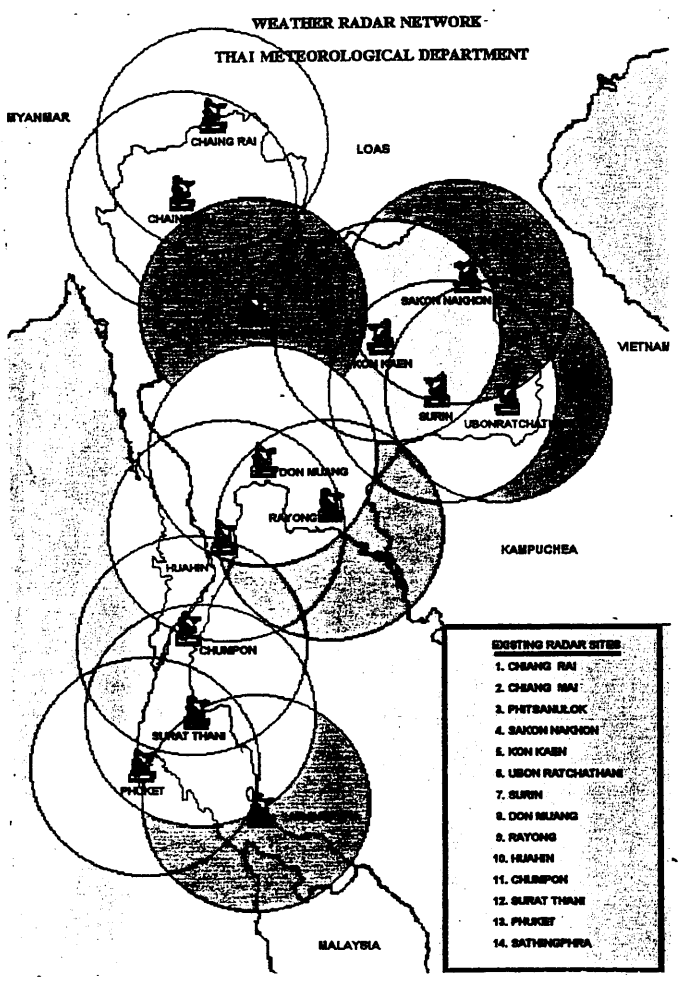

Figure 1 Thailand weather Radar Network

Thailand Radar Network (Figure 1.) was installed in 1997,now including 14 radar sites connected in the Network. General information on radar Network shown in Table 1. All of radar are from Enterprise Electronics Corporation USA. (EEC). These radar are equipped with Doppler facilities. The operating system is OSF/1 and the network is based on UNIX/RISC workstation with high resolution graphics .The composite Radar Networking Center (TMD Headquarter) is equipped with the DEC AXP3000-800 Workstation, Radar software at the Central site commanded to merging and distribution is called WARN which stand for Weather Radar Analysis Network. At each radar site control and display workstation is DEC 3000-600 and Compaq UA500 ,and software at each radar site is called EDGE stand for Enterprise Doppler Graphics Environment.

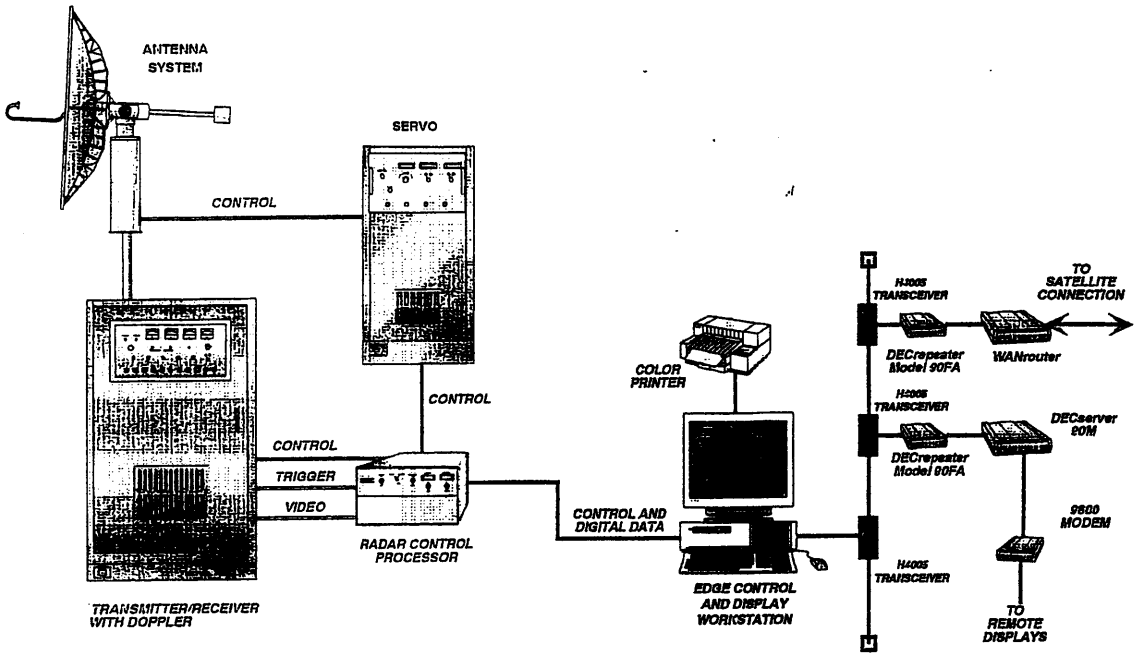

Figure 2 system at each Radar site

When radar site in networked is scan to collect the image data (Figure 3), it sends data to the central site automatic by schedule (every 27 minute of hour). Central site receives data for composite to Thailand pictures radar at 15 minute time intervals. All full resolution radar composites products displays will in turn be send from the central sites to all of radar site's workstation by satellite communication link in every hour. Observer workstation at each radar site can receive the composite images generated from the central site. (Radar composite is shown in figure 5)

The communication between central site and radar sites in the network is point-to-point multi channels and high speed single channel time shared TDM/TDMA network. The transmission speed at 19.2 Kbps. via Thaicom1 satellite .(Figure 4 show the diagram of satellite communication Link)

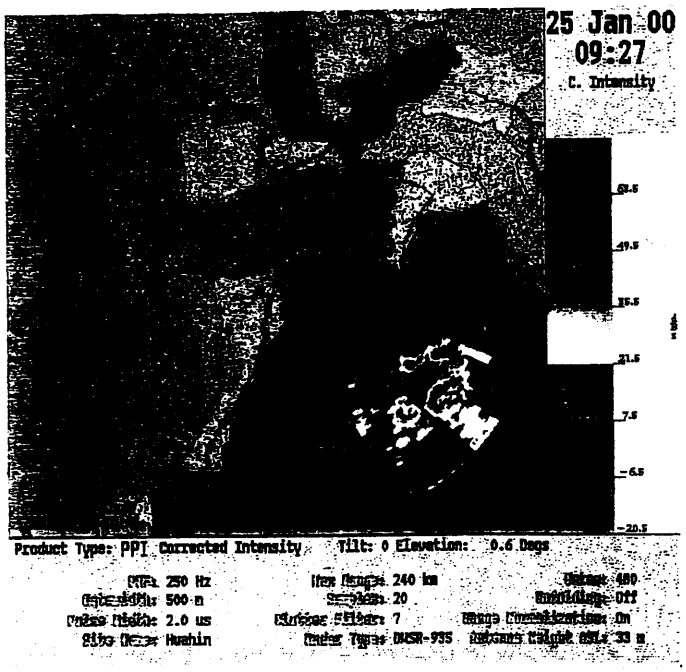

Figure 3 product of Hau Hin Radar site

PPI Corrected intensity range 240 km.

on Jan 25, 2000 09:27 GMT

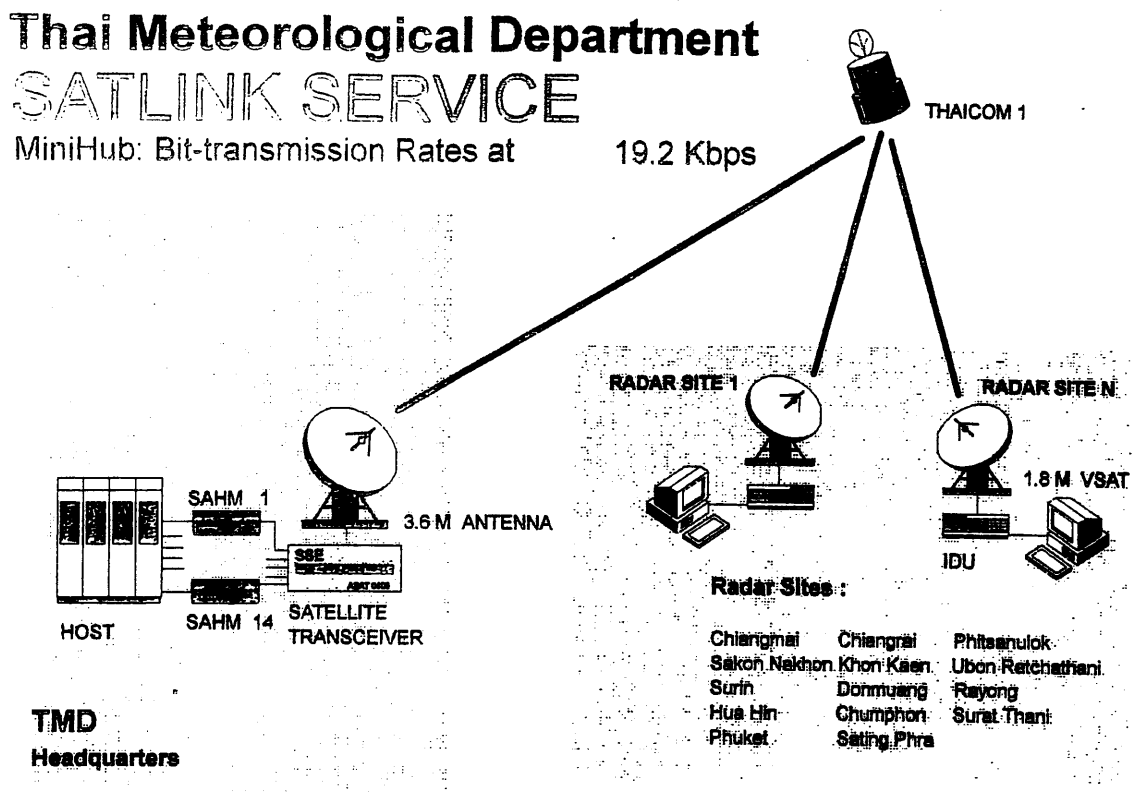

Figure 4 Satellite communication Link between central site and each Radar in Network

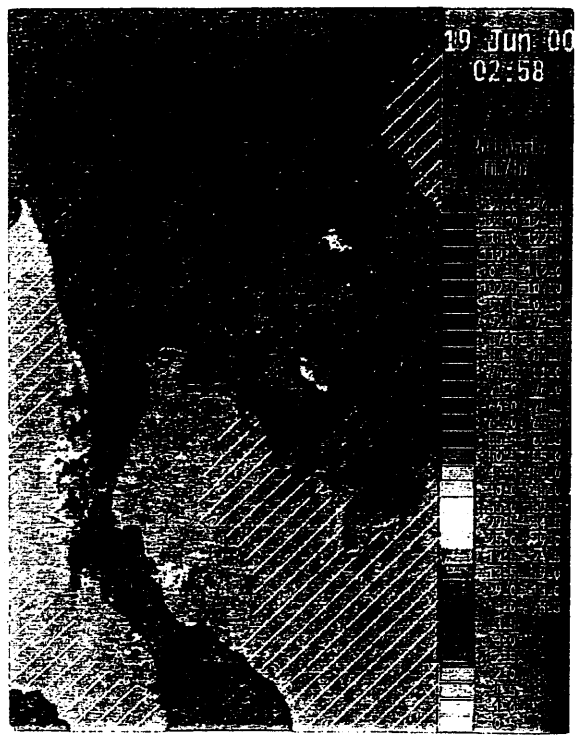

Figure 5 Thailand Radar picture composite on Jun 19, 2000 02:58 GMT.

Most of radar product frequently used are: PPI, RHI, CAPPI, Vertical cross section, Column maximum, Echo top, Precipitation accumulation, Vertically integrated liquid, Velocity azimuth display. Forecasters use Radar image information together with other meteorological data information, satellite data and numerical forecasts. In1997 before typhoon Linda hit Prachuab Kirikhan province(Southern part of Thailand), forecasters used radar image information data in making his decision to warning the public. At that time we can safeguarding of life and property. In conclusion, our Thailand radar network is working in good condition to produce detailed precipitation information in 24 hour for wide areas coverage all over Thailand .

Table 1 General information on Radar Network

No	Name	Manufacturer /Type	Band	Installation	Location
1	Chiang Rai	EEC/DWSR-93C	C	1993	Northern
2	Chiang Mai	EEC/DWSR-74C	C	1982	Northern
3	Phitsanulok	EEC/DWSR-74C	C	1982	Northern
4	Sakon Nakhon	EEC/DWSR-88C	C	1993	Northeast
5	Khon Khaen	EEC/DWSR-88C	C	1993	Northeast
6	Ubon Ratchathani	EEC/DWSR-93C	C	1993	Northeast
7	Surin	EEC/DWSR-74S	S	1976	Northeast
8	Don Muang	EEC/DWSR-88S	S	1992	Bangkok International Airport
9	Rayong	EEC/DWSR-74C	C	1981	Easthern
10	Hua Hin	EEC/DWSR-93S	S	1995	Southern east cost
11	Chumpon	EEC/DWSR-81C	C	1985	Southern east cost
12	Surat Thani	EEC/DWSR-88S	S	1993	Southern east cost
13	Sathingphra	EEC/DWSR-81C	C	1986	Southern east cost
14	Phuket	EEC/DWSR-88S	S	1990	Southern west cost
15	Central site Bangna (TMD Headquarter)	EEC		1997	Central

Abbreviations

C - Band = Frequency 5400-5700 Mhz.

S - Band = Frequency 2700-2900 Mhz.

DWSR = Doppler Weather Surveillance Radar

TMD = Thailand Meteorological Department

METNET = Meteorological Network Communication

EEC = Enterprise Electronics Corporation

Remarks

At present communication links in the Network between Central site and each radar site can be accomplished at only 6 radar sites . Before the end of this year (2000) communication link for the additional 3 radar sites will be improved for better radar compositing. In the near future MENET system will be further upgraded, resulting in being able to have data information all 14 radar sites to merge a composite data in the full system.

From NEXRAD WSR-88D to CINRAD WSR-98D

WANG CHONG WEN
Beijing METSTAR Radar Company, Limited
FuDao Building, 1/F East, No. 11 Kaituo Road
Shangdi Information Industry Base, Haidian District
Beijing, 100085, P.R.CHINA
Tel. (86-10) 62983703 ext. 15
Fax. (86-10) 62981251
E-mail: bjradar@public.east.cn.net

With its network of 165 systems, the US NEXRAD WSR-88D Doppler weather radar is widely regarded as the premier operational Doppler Weather Radar of our time. The CINRAD WSR-98D builds on the rich heritage of the WSR-88D by integrating proven NEXRAD technology with the latest advances in electronics, communications, and meteorological sciences. After three years of hard work, the first CINRAD WSR-98D system was delivered to the user by the end of 1999.

The features of the CINRAD WSR-98D including the operational mode, transmitter, receiver, signal processor, monitoring and control of radar system, radar product generation (RPG), principal user processing (PUP) and communication are described in the following paragraphs. See CINRAD System Block Diagram for system overview.

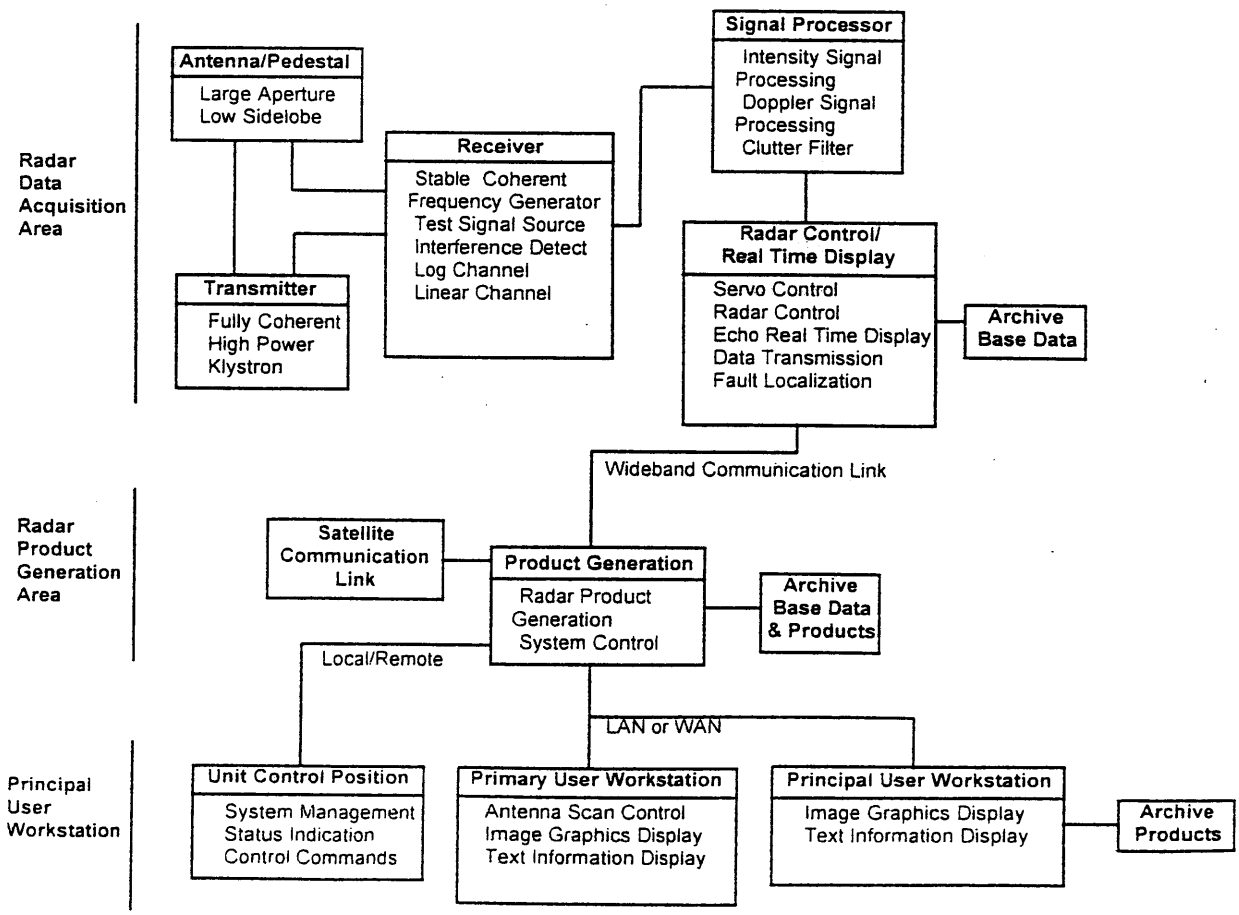

CINRAD System Block Diagram

There are two defined operational modes which are used to acquire the meteorological data necessary to detect the weather and translate the results into products. The modes are the Clear Air Mode and the Precipitation Mode. The Clear Air Mode can be selected manually only. The Precipitation Mode can be selected manually at any time and is also selected automatically whenever the system detects precipitation (based on pre-determined values and area coverage of reflectivity dBz).

To implement the operational modes, the CINRAD WSR-98D employs a set of pre-defined Volume Coverage Patterns (VCPs) to collect radar data. Each VCP is composed of specific antenna scan patterns, and specific transmitted waveforms with corresponding PRI patterns. There are four scan strategies 11, 21, 31, 32. The VCP 11, 21 are intended for precipitation mode, the VCP 31, 32 for clear air mode.

The radar transmitter unit consists of an amplifier/modulator and microwave system which generates and transmits RF power to the antenna pedestal. The equipment is modularized, remotely controllable, and self-monitoring with automatic fault location. A Transmitter Unit Fault Interlock system consisting of power supply monitoring, door interlocks, air pressure interlocks, air flow interlocks, over temperature sensor, oil level sensor, and oil temperature sensor is provided in the transmitter. The modulator includes overvoltage and overcurrent protective circuitry to prevent damage in the event of an open or short circuited load. Automatic recycling is provided to allow unattended operations. Continuous monitoring via built-in test equipment (BITE) provides a capability for fault isolation which can be accomplished at the RDA maintenance terminal.

The radar receiver is an EMI-shielded cabinet, housing the receiver components. Front and rear doors provide access to the receiver components. An inner swinging door provides the mounting surface for many of the modules. The remainder are affixed to the cabinet partitions, side walls, and slide-out shelves. The receiver channel comprises the analog signal processing circuits of the radar receiver with the exception of the front end (receiver protector and low-noise amplifier) which is located in the antenna/pedestal.

The radar receiver also includes the RF generator, RF test source select, and receiver interface. The receiver interface provides the signal interfaces between the receiver and the signal processor while maintaining electrical isolation via opto-isolators. It also provides holding registers for control data to the receiver from the signal processor.

The signal processor consists of a three-module set mounted in the expansion slots of the RDASC. It consists of two special-purpose modules together called the Hard-wired Signal Processor (HSP). The third module is a general-purpose programmable board called the PSP. The signal processor processes radar receiver outputs and sends processed data to the RDASC processor. The tasks performed by the hard-wired signal processor includes synchronization and control interface functions. The PSP performs clutter filtering and all other processing necessary to generate the base weather products of reflectivity, velocity, and spectrum width. The SP communicates with the RDASC processor over the computers high-speed PCI bus.

The clutter filters are 5-pole elliptical design having a controllable notch width. Each 250-meter range bin uses a separate clutter filter. Clutter filters are provided out to the full unambiguous range of the radar (510 km maximum). The design permits either filtered or unfiltered data to be

passed on to the signal processor. The filter notch widths are selected as a function of azimuth scan rate and the level of clutter suppression.

The RDASC Processor is a Pentium-based computer running Windows NT which provides the control of the RDA subsystem. The computer monitor displays the Maintenance Window which provides the operator-machine interface to the RDASC processor to allow monitoring, initiating test of the RDA, startup, initializing the processor, and loading the software into the processor as required. The RDASC also interfaces with the maintenance panel to control, monitor, and display various functions used during maintenance.

The CINRAD WSR-98D provides extensive performance monitoring and reporting. Items monitored in the tower and utilities area include outside and interior temperatures of the radome and shelters; presence of commercial and auxiliary prime power; diesel generator oil and coolant levels and temperature alarms; smoke and fire, and fire suppression system alarms; site and radome hatch entry; air filter alarms; and air conditioner alarms.

Pedestal monitoring includes reporting the status of stow pins, handwheel and protective interlocks, power supply performance, and angle encoder power. The pedestal electronics monitoring includes a loopback check of the digital interface, and a self test mode checks out and reports on operability of the analog loops of both axes. At a system level, pedestal performance monitoring includes attaining specified rate and/or position within a specified time period. Pedestal alignment can be checked against the position of the sun using an off-line test program.

Transmitter monitoring includes display and reporting of the status of the protective monitoring circuits discussed under the transmitter. In addition, transmitter status reporting includes position of the dummy load and pulse width switches, klystron heater warmup, redundant hardware failures and other maintenance required events, maintenance mode selected, and door interlocks. System level checks include monitoring of the response to high voltage on, dummy load and pulse width selection commands. Average RF power is monitored at the antenna and in the equipment shelter. Peak power is calculated from average power using the known duty cycle. The receiver Built-in Test Equipment (BITE) also has the capability to directly measure peak RF power.

Receiver and signal processor monitoring includes the capability to inject cw, pulse, delayed klystron output, and calibrated noise test signals into either the receiver front end ahead of any active circuits or into the input of the receiver cabinet in the equipment shelter. Test signal amplitudes can be varied from the receiver noise level to a saturation level. The test signals can be phase modulated pulse-to-pulse so that end-to-end checks of the signal processing for reflectivity, velocity and spectrum width base data can be made. Other performance checks and calibrations made during operational use of the equipment include calibration of the digital IF attenuator used in the Instantaneous Automatic Gain (IAGC) feature of the linear receiver channel, dc balancing and noise level check at the receiver output, and check of the amplitude and phase balance of the I/Q phase detector.

The RPG hardware consists of the RPG computer and associated peripherals. The RPG computer is a pentium-based machine operating under Windows NT. The computer monitor displays the Unit Control Position (UCP) Window which, along with the keyboard and mouse, provides the operator-machine interface to the RPG processor. A high-speed data printer is also included.

There are 75 products in the products set that is supplied currently. Most of the products are the

heritage of NEXRAD WSR-88D except the PPI, RHI and CAPPI products that have been added by METSTAR. The algorithms contained in the product generation software are same as used in the NEXRAD WSR-88D.

The advanced PUP Workstation is a newly designed weather data analysis station, which has been developed for many applications and incorporates the latest technology (Pentium PC) into the CINRAD WSR-98D design. The workstation provides the unique capability to display, manipulate, and analyze data quickly, and provides a seamless integration of data acquisition, display and manipulation for a great variety of weather products. Features include product compositing, overlays, looping, algorithm processing, and hard copy. The user can view one or multiple customized windows with single or composite weather images on the screen simultaneously.
The PUP Workstation receives data products from the WSR-98D Radar Product Generation (RPG) area and provides for the request, display, storage, annotation, and distribution of products by operational personnel. The PUP Workstation contains the dedicated hardware and software required for graphics processing, local control, status monitoring, local annotation, and product archiving.

The Wideband Communication（WBC）between the RDA and RPG is used to transmit base data and control information at data rates of 1.5M bps. The WBC is implemented with a 10/100M Local Area Network, the operating mode is Client-Server style. The server functions: Carrier Detection, connection requirement, connection acceptance, send-receive data, The client functions: connection acceptance, send-receive data. The communication protocol used is TCP/IP. Another option for WBC is a Spread Spectrum Communication System that is more smart and flexible than the MLOS system used in NEXRAD WSR-88D.
The Narrowband Communications（NBC）between RPG and PUP is for message exchange of basic products, derived products, alarms and other messages. The data rate is approximately 64kbps. According to the distance from RPG to PUP, the NBC may be implemented in Local Mode or Remote Mode. It is also Client-Server style, the Server is the RPG, the Client is the PUP. The protocol is X.25. By using a dedicated line or a leased line in the public data network with X.25 protocol, remote communication can be easily done.

The RDA, RPG and PUP computers used in the WSR-98D have hardware platforms and operating system are quite different from the WSR-88D. METSTAR has developed new and more friendly man-machine interfaces at the RPG and PUP workstations that has been well received by our user.

RADAR COMPLEX FOR ATMOSPHERE DYNAMIC CHARACTERISTICS MEASUREMENT

V.N. Efremov

Central Asian Research Hidrometeorological Institute,
SANIGMI, 72, K. Makhsumov str, 700052, Tashkent, Republic of Uzbekistan,
Phone Number: 7(3712) 35-81-56, Fax Number: 7(371) 133-20-25,
E-mail: UZHYMET@HMC.TASHKENT.SU

Nowadays pulse Doppler radar technique potentialities and advantages for measuring of the dynamic characteristics of atmosphere appear to be extensively known. However, it has been considered to be impossible to measure the wind field using single Doppler radar. It could be done using the system of 2 or 3 Doppler radars.

According to the existing method, proposed by Lhermitte and Atlas (1961) and worked out in details by Browning, Wexler (1968) and Caton (1963) the wind velocity can be determined using a single Doppler radar. The essence of this method is that the radial component is measured on along reserved circular outline with the fixed elevation angle and distance of signal strobbing. In this case the value and distance of the wind velocity are considered to be the characteristics averaged by area; restricted by the outline of scanning and considered to be applied to the point of radar installation.

It is known, that when antenna of Doppler radar is rotating by azimuth the law of radial component of the wind velocity change in the horizontal surface U_{pr} can be expressed by the equation as:

$$U_{pr} = U_o \cos(\alpha - \alpha_o) + C, \qquad (1)$$

where α_o and U_o is a direction and module of the wind velocity horizontal component, C is a constant, proportional to the wind field divergence. The majority of problems on interpretation Doppler radar observations come to the definition of these three parameters by the values of U_{pr}.

Let us assume that in the wind field measuring by method analogous to that one proposed by Lhermitte and Atlas the wind field is considered to be linear and homogeneous on the small segments of area and submitted to the law of change described by the equation (1). In this case it is enough to carry out 3 measurings of the radial component of the wind velocity on one of the segments of area with different azimuth angles in order to obtain the system of 3 equations:

$$\begin{aligned} U_{pr1} &= U_o \cos(\alpha_1 - \alpha_o) + C, \\ U_{pr2} &= U_o \cos(\alpha_2 - \alpha_o) + C, \\ U_{pr3} &= U_o \cos(\alpha_3 - \alpha_o) + C, \end{aligned} \qquad (2)$$

which can be easily calculated. Here α_1, α_2, α_3 and U_{pr1}, U_{pr2} and U_{pr3} respectively are azimuth angles of the chosen arc and values of the wind velocity radial component measured on these angles. The obtained values U_o, α_o and C appear to be the averaged characteristics of the wind field on the chosen arc section of the measurement outline and may be applied to a given point in space.

In practice more than 3 measurings are usually used. In this case we will obtain the equations with 3 unknown quantities, i.e. overdetermined system. To solve such systems the method of least squares for n couples of values of U_{pri} and α_i is to be used. This algorithm was applied to complex "Glissada". It allowed automatization of the processes of antenna conducting as well as surveying and storing information.

Complex "Glissada" includes the units of analogous and digital treatment of a signal and the system of antenna and personal computer control. As a personal computer IBM or compatible with them computers can be used.

The survey of information is conducted in the regime of antenna circular rotation. Operator introduces necessary quantity of elevation angles and azimuth step. All further operation is carried out by personal computer.

Information about radial component of the wind velocity in the process of surveying is reproducing on the screen of the monitor. At the right lower corner you can see date of measuring, time, elevation angle in degrees and azimuth step. Having passed this step, antenna is stopped, and radial component of wind velocity in 256 points up to the distance of 60 kilometres, which means every 240 metres, is measuring. Accuracy of measurement is 10 santimetres per second. Minimum azimuth step, which "Glissada" allows to do, is 0,6 degrees. Elevation angles are established with the same accuracy. In order to obtain such a picture we need only 1 minute. At the same time the field of reflectivity in DBZ may be also produced on the screen. All information about radial component of the velocity and reflectivity is remained in personal computer and may be reproduced as a table.

After all series of measurings are finished the computation of different wind characteristics is made. For example, we can compute the profile and vertical component over the radar (fig.1). On the first graph you can see module of the wind velocity in metres per second, on the second you can see the direction in degrees, on the third one vertical component of wind in metres per second is represented. Positive values of vertical component correspond to upward direction. Maximum height to which computation of different wind characteristics is made is determined by upper limit of cloudiness. The results of computation made by personal computer and arranged as a table may be reproduced into the screen of the monitor or printed.

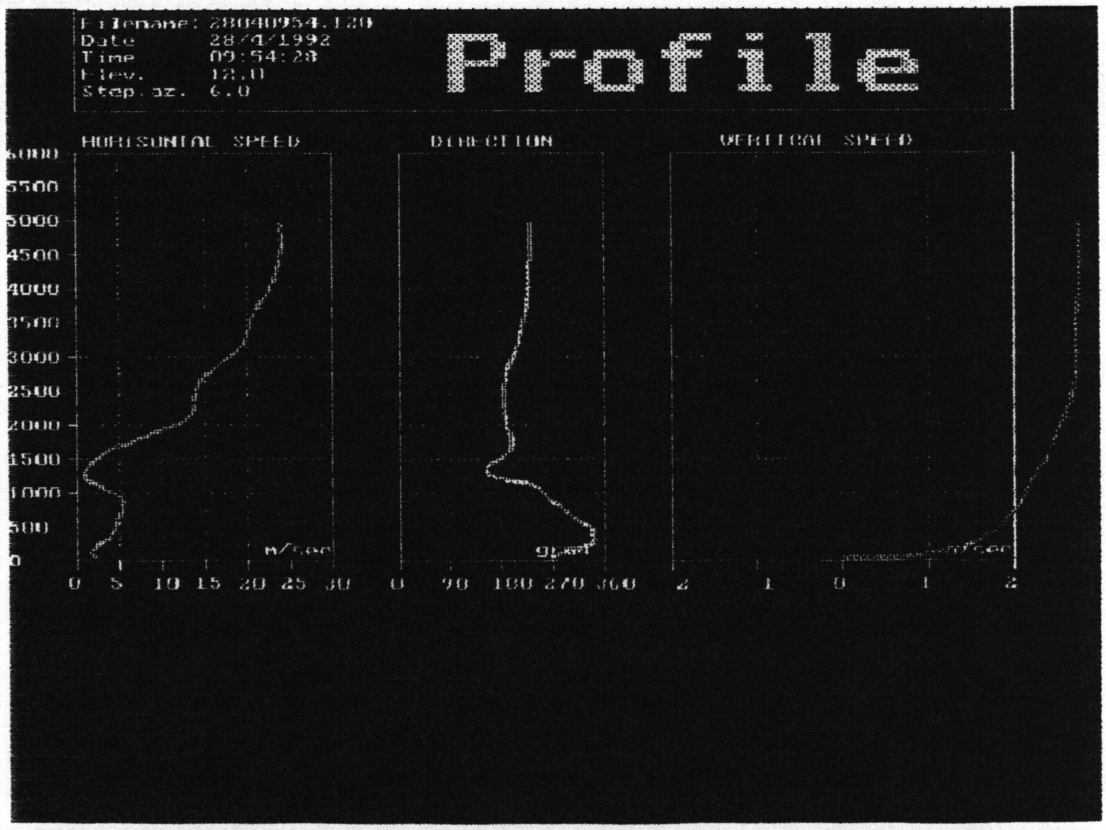

Fig.1. Profile of the wind velocity and vertical component

Besides profiles, complex "Glissada" enables us to compute the wind field in radius of 30 kilometres (fig.2). The accuracy of the module evaluation makes up 1 metre per second,

for direction it is 15 degrees. The network step may be chosen by operator equal to 2,5 or 5 kilometres. The scale of wind velocity is given at the right corner. Vectoral field shown in this figure does not belong to any definite level and resembles a cone with its peak in the place of radar location.

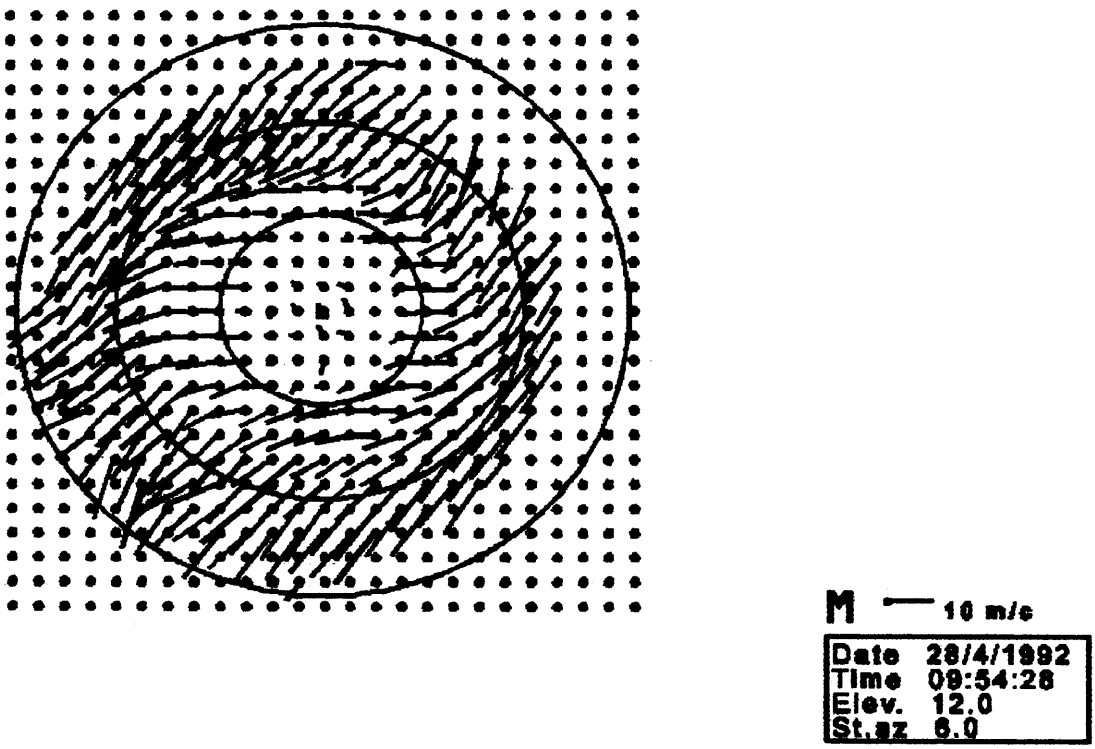

Fig.2. The wind field

Thus, algorithm of the solution of the inverse task of the wind field reconstruction by the values of radial component of the wind velocity enables to measure the wind velocity vector in any point of space in the zone of radar scanning using only a single Doppler radar. In this case the special method of interpretation the input information about radial velocities is suggested. Moreover, the assumption that the wind field in the zone of vector measuring appears to be a linear one is introduced. The zone dimensions are considered to extend from kilometres to some dozens of kilometres length.

REFERENCES

Browning K.A., Wexler R. A determination of kinematic properties of a wind field usng Doppler radar // J. Appl. Meteorol. -1968. -V. 7. - N 1. -P. 105-113.

Caton P.A.F. Wind measurement by Doppler radar // Meteorol. Mag. -1963. - V. 92. -N 1092. - P. 213-222.

Lhermitte R. M., Atlas D. Precipitation motion by pulse Doppler radar // Proc. 9th Weather Radar Conf. - 1961. - P. 218-223.

РАДИОЛОКАЦИОННОЕ ИССЛЕДОВАНИЕ ГРОЗОВЫХ ОБЛАКОВ И КАНАЛОВ МОЛНИЙ

Гальперин С.М., Щукин Г.Г.
ГГО им. А.И. Воейкова, С-Пб, Карбышева, 7 , Россия
Тел/Факс 812-2-47-86-81
E-mail shchukin@peterlink.ru

ABSTRACT

Thunderclouds were studied by meteorological radars with wavelengths λ = 3.2 cm, 10 cm, 35 cm, 200 cm and microwave radiometers (λ = 0.8 cm, 1.46 cm, 3.2 cm). The studies were carried out at MGO field laboratory located in Leningrad region. The results of studies are considered here. Clouds and lightnings parameters are presented including lightnings zones locations, locations of zones with different rainfall intensities, parameters of radar signals from lightnings and cloud water parameters in thunderstorm days.

В последние годы на полевой базе ГГО им. А.И. Воейкова особое внимание уделяется использованию дистанционных радиотехнических средств (РТС) при определении параметров грозовых облаков и возникающих в них разрядов.

С помощью РТС базы возможно проводить следующее:

- определять параметры грозовых облаков в процессе их эволюции, особенно вызывающих наибольший ущерб, в частности, измерять отражаемость облаков и осадков и водность облаков, а также измерять геометрические размеры эхо-сигналов метеообъектов, устанавливать влагозапас атмосферы в дни возникновения конвективных облаков. В этих целях использовались метеорологический локатор (МРЛ, λ=3,2 см) и радиометры, функционирующие на λ=0,8 см, λ=1,46 см и λ=3,2 см ;
- осуществлять радиолокационное обнаружение каналов молний типа облако-земля и облако-облако в радиусе до 170 км, определять координаты их радиоэха в поле эхо-сигналов облаков и осадков и измерять параметры радио-эха молний с помощью РЛС, излучающих на λ=10 см., λ=35 см и λ=200 см;
- устанавливать взаимное расположение в облаках зон различной отражаемости, водности, и молниевой активности, а также изменение их взаимного расположения при переходе облаков из одной стадии развития в другую.

Наблюдения за грозовыми облаками проводятся одновременно всеми РТС. Информация, получаемая пассивно-активными РТС комплекса, оперативно обрабатывается и документируется с помощью 3-х ПЭВМ. Четырехканальный блок аналого-цифрового преобразования позволяет проводить одновременную обработку данных с выходов 4-х различных РЛС и представлять эти данные на одном дисплее.

В результате экспериментальных исследований установлено:

1. Взаимное расположение в грозовых облаках зон молниевых разрядов, зон различной интенсивности осадков (**I**) и отражаемости облаков (**Z**). При этом рассматривались молнии, возникшие как в осадках, так и за их пределами. Интенсивность осадков оценивалась с учетом соотношения:

Z, мм^6 / м^3 = 200 $I^{1,6}$ мм/час.

Данные, полученные на основе наблюдений за 15-ти грозовыми облаками фронтального происхождения, находившимися в зрелой стадии развития, приводятся в табл.1

Таблица 1.

Количество грозовых разрядов (ГР), обнаруженных в осадках различной интенсивности и за их пределами

	I, мм/ч.					Вне зоны осадков	
	> 15	15-10,1	10-5,1	5-1	<1	Передняя зона	Тыловая зона
$\Sigma N_{гр}$	11	65	70	145	133	38	280
$\Sigma N_{гр}$= 424 (100 %)						$\Sigma N_{гр}$= 314 (100 %)	
%	2,6	15,3	16,5	34,2	31,4	11	89
Всего $\Sigma N_{гр}$= 738 (100 %)							
%	57,5					42,5	

Из табл.1 видно, что 82 % ГР обнаружены в осадках , где I < 10 мм/час, и только 18 % ГР - в зонах более интенсивных осадков (I > 10,1 мм/ час). Разряды вне зоны осадков распределены следующим образом: 11 % - в передней зоне осадков относительно их смещения, 89% - в тыловой их зоне. Не исключено, что взаимное расположение молний и осадков зависит от стадии развития грозового облака. Кроме того, могли иметь место случаи, когда ГР обнаруживались за пределами радиоэха осадков, фиксируемых МРЛ, что могло иметь место в тех случаях, когда на удалениях от 50 км до 100 км их интенсивность $I_{мин.} <\sim$ 0,015 - 0, 04 мм/ч. Исследование взаимного расположения зон молниевой активности и зон различной отражаемости облаков проводилось при определении Z выше уровня расположения нулевой изотермы на ~2 км. Размеры радиоэха облака на этом уровне сопоставлялись с размерами эхо-сигналов молний. Далее рассматривалось количество эхо-сигналов ГР в следующих градациях с различной отражаемостью: **$\lg Z_{макс.}$- п**, где **п**=0, 1, 2, 3, 4 и 5. Результаты обработки данных представлены в табл. 2.

Таблица 2

Результаты сопоставления координат 650 ГР с зонами эхо-сигналов грозовых облаков высотой 11-13 км, имеющих различную отражаемость

	Количество ГР в зонах $\lg Z_{макс.}$ -п					
$\lg Z_{макс.}$ -п	**п = 0**	**п =1**	**п =2**	**п =3**	**п =4**	**п =5**
Всего	120	64	231	116	92	27
% 18,5	18,5	9,8	35,5	17,8	14,2	4,2

Из данных, представленных в табл.2, следует:

- молнии в интенсивных грозовых облаках фронтального происхождения могут быть обнаружены как в зонах, где $\lg Z_{макс.}$, так и в зонах, где отражаемость на 4-5 порядков меньше максимальной;

- в зонах с отражаемостью в пределах ($\lg Z_{макс} + \lg Z_{макс} - 1$), то есть в непосредственной близости от $Z_{макс.}$, обнаружено ~28 % радиоэха ГР, остальные ~72 % ГР были зафиксированы в тех зонах облака, где $Z < \lg Z_{макс} - 1$.

2. Параметры радиоэха вспышек молний, [1]:

- эффективная площадь рассеяния - ЭПР (δ, м^2) каналов молний, обнаруженных на λ = 35 см и λ = 200 см при горизонтальной ($\lambda_Г$) и вертикальной ($\lambda_В$) поляризациях радиоволн (табл.3).

Таблица 3

ЭПР ($\bar{\delta}$, м^2) каналов молний, обнаруженных на λ=35см и λ=200см

λ, см	Поляризация	R, км.	$N_{общ.}$	$\bar{\delta}$, м^2
200	Горизонтальная	50-80	146	23
	Вертикальная		239	18,3
35	Горизонтальная	50-60	134	19,7
	Вертикальная		152	18,3

- время существования радиоэха вспышек молний (τ) на $\lambda_{Г,В}$=200 см и $\lambda_{Г,В}$= 35 см ($\tau_{200Г}$,$\tau_{200В}$, $\tau_{35Г}$ и $\tau_{35В}$) (табл.4).

Таблица 4

Значения $\bar{\tau}_{200Г}$ и $\bar{\tau}_{200В}$ в зависимости от R

R, км	$\bar{\tau}_{200Г}$, мс	$\bar{\tau}_{200В}$, мс	$N_{гр}$
30-40	320	280	47
70-90	270	230	333
115-120	250	170	135

Среднее время существования радиоэха каналов молний, обнаруженных при R=60-120 км на $\lambda_{Г,В}$= 35 см , составляет ~300 мс.

Сопоставление $\bar{\tau}_{200В}$ и $\bar{\tau}_{35В}$, а также $\bar{\tau}_{200Г}$ и $\bar{\tau}_{35Г}$ показывают их незначительное взаимное различие, что дает основание утверждать о равной вероятности обнаружения молний двумя типами РЛС $_{метр}$(λ = 200 см) и РЛС $_{дц}$ (λ = 35см), имеющими одинаковую поляризацию радиоволн.

При частоте посылок зондирующих импульсов РЛС, обнаруживающих молнии, равной 300 Гц (T=3,3 мс), с помощью таких РЛС при вертикальной и горизонтальной поляризации антенн можно зафиксировать ~50-90 эхо-сигналов одиночных вспышек молний, что обеспечивает высокую надежность обнаружения каждой вспышки молнии.

3. Определены с помощью РЛС $_{метр.}$ размеры радиоэха вспышек молний в радиальном направлении, в среднем равные 8,9 км при максимальных значениях до 20 км. Эти размеры совпадают с размерами радиоэха, установленными разностно-дальномерной системой [2].

4. Установлено, что в июне - июле в Ленинградской области могут возникать аномальные грозовые облака, в которых зафиксированы аномальные вспышки молний [3]. Такие облака имеют следующие характеристики:

-имеют верхнюю границу радиоэха $H_{в.г.}$ >10 км,

-в них фиксируются зоны с высокой отражаемостью (lg Z >3,0), имеющие вертикальную протяженность до 7 - 9 км.

Отличительной особенностью аномальных облаков является то, что при их возникновении в них можно обнаружить радиоэха вспышек молний, следующих через Δt=2,5 - 3,5 сек. Имели место случаи, когда молнии регистрировались через $\Delta t < 1$ сек.

Используемая в наблюдениях на базе РЛС $_{метр.}$ обычно не обнаруживает облаков и осадков. При появлении аномальных грозовых облаков эта РЛС фиксирует в них дискретные зоны постоянного отражения (ЗПО), площадь которых в 80% случаев не превышает 150 км^2 , что соответствует радиальной их протяженности R < 6,8 км. В отдельные дни наблюдений время существования радиоэха ЗПО на экранах РЛС $_{метр.}$ изменялось в пределах от 5 до 52 мин.

5. По результатам СВЧ-радиометрических измерений параметров атмосферы и облаков в период интенсификации электрической активности получены статистические данные о влагозапасе атмосферы (Q), содержащей конвективные облака на различных стадиях развития, в том числе на стадии грозовой активности. В периоды, когда конвективные облака достигали стадии грозового облака, отмечались наибольшие значения влагозапаса атмосферы (табл.5), мезомасштабные вариации влагозапаса атмосферы в области грозового облака в отдельных случаях превышали 50% среднего значения [4].

Таблица 5

Среднее значение и среднее квадратическое отклонение O_A в зените в дни развития конвективных облаков

Параметры	Cu	Cb, грозовые облака
СЗ (O_A), кг/м^2	19,73	29,65
СКО (Q), кг/м^2	3,17	2,93

На ограниченном количестве наблюдений установлено несовпадение координат зон ГР и максимальной водности в грозовом облаке.

Литература

1. Степаненко В.Д., Гальперин С.М. Радиотехнические методы исследования гроз. Гидрометеоиздат, Л. 1983, 204 с.

2. Proctor. D.E Lightning and Precipitation in a Small Multiceccular Thunderstorm. J.Geophys. Res. ,1983, v.88, NC9, pp.5421-5440.

3. S.M.Galperin, V.D.Stepanenko, V.I.Frolov. Study of features of very intensive thundarstorm clouds using simultaneous metres and centimetres radar observations. Proc.10-th International Conference on Atmospheric Electricity. Osaka, Japan, 1996, pp.220-223.

4. Щукин Г.Г., Степаненко В.Д., Егоров А.Д., Гальперин С.М., Караваев Д.М. Радиофизические исследования атмосферы и подстилающей поверхности. Современные исследования Главной геофизической обсерватории, т.1. Гидрометеоиздат, С-Пб, 1999, с.172-190.

1 MEASUREMENT TECHNOLOGY, PERFORMANCE, AND QUALITY ASSURANCE

1.4 Measurement of the Atmospheric Composition

Keynote Paper

Atmospheric Composition – A Challenge for the Observations

Wolfgang Fricke

Deutscher Wetterdienst
Meteorologisches Observatorium Hohenpeissenberg
Albin-Schwaiger-Weg 10
D-82383 Hohenpeissenberg
Germany
Fax +49 8805 9200 229
e-Mail: Wolfgang.Fricke@dwd.de

1 Introduction

When meteorological observations gradually started and first networks were established about 200 years ago, emphasis was put on the measurement of physical parameters in the atmosphere with the aim of analyzing and predicting weather and climate. Nowadays, data on the physical condition of the atmosphere are routinely collected by a world-wide network of synoptic, climatological and aerological observation stations. Data on the *chemical* condition of the atmosphere became increasingly important in the course of the 20th century; first for reducing the impact of air pollution on human health, then for protecting the environment against e.g. acidic rain, stratospheric ozone loss, increases in tropospheric ozone, and climate modification due to changes in the radiative balance of the earth-atmosphere system. The need for global atmospheric chemistry monitoring programs was first met by the World Meteorological Organization in the 1950's. These first and very important efforts were consolidated in 1989, when the Global Atmosphere Watch (GAW) Program was implemented.

2 The GAW Program

The objective of GAW as a worldwide coordinated network of observing stations is to monitor the long-term evolution of the atmospheric composition on a global and regional scale in order to assess this contribution to climate change and environmental issues. For this purpose it provides up-to-date information on the chemical composition of the atmosphere and related physical parameters and addresses specific issues related to changes in the global atmosphere (climate, ozone, pollution transport etc.). GAW is committed to deliver high-quality and long-term data in order to support scientific studies on the state of the atmosphere and its evolution in the past and future with respect to climate change. It represents an effort of exceptional complexity in the field of environmental measurement and assessment. The main elements of GAW are

- A network of 22 global and about 400 regional stations
- 3 Quality Assurance / Science Activity Centers (QA/SAC)
- World Calibration Centers (WCC)
- World Data Centers (WDC)

The parameters to be monitored in the GAW program are (Miller, 1998)

- Greenhouse gases (carbon dioxide, CFCs, methane, nitrous oxide, tropospheric ozone)
- Ozone (surface, total column, vertical profile by both ground-based and satellite)
- Solar radiation including ultra-violet
- Precipitation chemistry
- Chemical and physical properties of aerosol including optical depth
- Reactive gases (carbon monoxide, sulfur dioxide, nitrogen oxides, volatile organic compounds)
- Persistent organic pollutants and heavy metals
- Radionuclides (krypton-85, radon, beryllium-7, lead 210)
- Meteorological observations

The global stations are supposed to monitor as many of these components as possible, while regional stations may have a less extensive monitoring program. The actual map of GAW global stations is shown in Fig. 1.

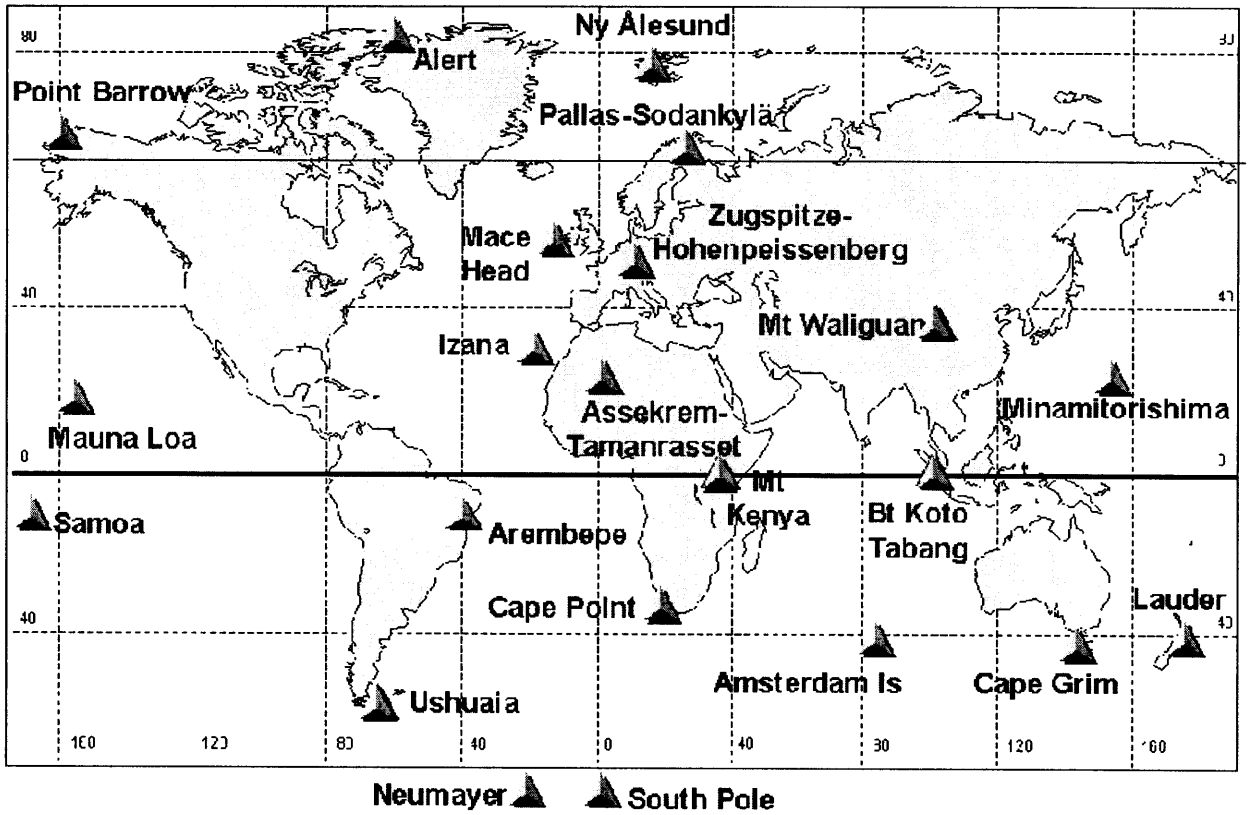

Fig. 1: Geographical distribution of GAW global stations (Source: WMO-AREP, 1999)

The Quality Assurance / Science Activity Centers (QA/SAC) give support to the stations by providing standard operating procedures for the measurements to ensure internationally comparable data quality, by organizing audits and instrument calibrations, by taking care of data quality control where necessary, by assisting with training, capacity building programs and by arranging

partnerships between GAW stations ("twinning"). They were established in Japan (for Asia and Oceania), the USA (for the Americas) and Germany (for Europe and Africa).

Most WCCs have global responsibility for performing station audits of selected parameters. The following WCCs are established: For precipitation chemistry (SUNY/USA), carbon dioxide (NOAA/USA), carbon monoxide, surface ozone and methane (EMPA/CH) (Hofer et al., 1998), radiation and optical depth (PMOD/CH), total ozone (Brewer: MSC/CDN, Dobson: NOAA/USA), and vertical ozone sondes (FZJ/D). The QA/SAC Americas at SUNY conducts annual intercomparisons of precipitation chemistry laboratories participating in the GAW program. There is still a need for a long-term funding of WCCs for aerosol physics and chemistry, UV radiation, radionuclides, CFCs, VOC, SO_2, NO_x, N_2O and radioactive tracers.

The quality controlled data are finally archived in the World Ozone and Ultraviolet Radiation Data Center (WOUDC) at MSC Toronto (Canada), in the World Data Center for Surface Ozone (WDCSO) at NILU, Kjeller (Norway), in the World Data Center for Greenhouse Gases (WDCGG) at Tokyo (Japan), in the World Radiation Center (WRDC) at St. Petersburg (Russian Federation), in the World Data Center for Aerosols (WDCA) at Ispra (Italy) in the World Data Center for Aerosol Optical Depth at Asheville (USA) and in the World Data Center for Precipitation Chemistry (WDCPC) at Asheville (USA). Maps of stratospheric ozone data are generated at the Ozone Mapping Center (WO_3DC) at Thessaloniki (Greece).

3 The technical challenge

Besides the large logistical and organizational effort associated with such a complex worldwide monitoring network there are numerous technical drawbacks that have to be known and considered. The three major components accounting for 99.96% of dry air - nitrogen, oxygen and argon – show no significant variation with time and are climatically not relevant. Concentrations of substances that affect climate are variable according to their atmospheric residence time and range from a few hundred ppm (CO_2) to some ppt. They require measurement techniques with low detection limits, especially at the remote GAW global stations. The GAW objective of creating "data of known quality, adequate for their intended use" mostly means a need for creating data of high quality with high accuracy and precision in order to enable early detection of trends in a time series strongly masked by meteorological noise. But even well established commercial instruments may cause problems - sometimes under certain conditions only - that demand experience since they are not described in the manuals. The following examples may serve as an illustration for interference causing misinterpretation of data.

The GFC/NDIR method for carbon monoxide allows continuous monitoring, requires little maintenance and is therefore a well established method. However, it shows interference with water vapor or other gases absorbing in the same IR range. Using synthetic air as zero gas or not determining the zero value within relatively short time intervals can lead to false measurements, as Fig. 2 illustrates. The black squares show the measured CO signal, corrected for the zero value at midnight only. If the zero signal (black circles) influenced by variable water vapor concentrations (like the CO signal itself) is measured every 20 minutes and subtracted from the measured CO signal, the resulting corrected mixing ratios (solid line) are significantly different from before. The price for the improved data quality is a discontinuous measurement with a reduced time resolution of 20 minutes.

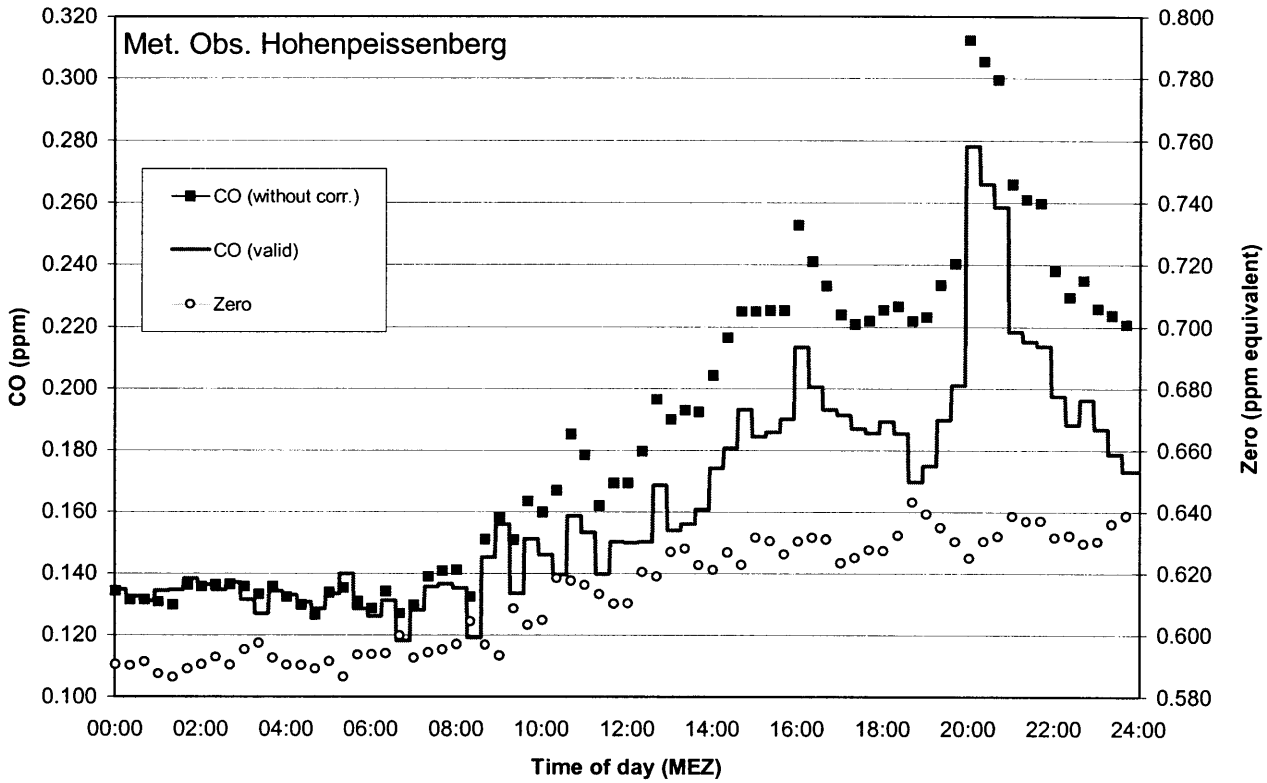

Fig. 2: *Mixing ratios of CO without (black squares) and with (solid line) correction for water vapor impact on zero line at Hohenpeissenberg on April 23, 2000*

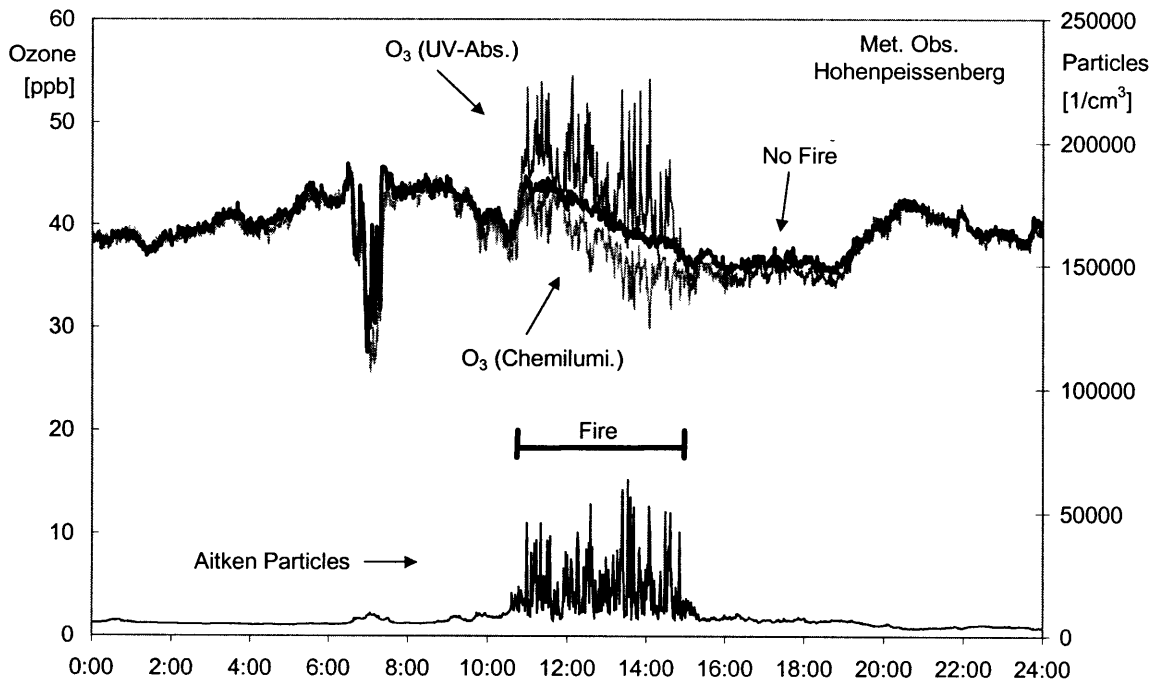

Fig. 3: *Different interference of two ozone monitors with aerosol in forest fire smoke on Feb 7, 2000 at the GAW station Hohenpeissenberg. Bold black curve: Ozone mixing ratio outside fire plume.*

Fig. 3 shows high concentrations of Aitken particles at Hohenpeissenberg between 11:00 and 15:00 CET on Feb 7, 2000, originating from a small local forest fire. They cause opposite interference in the ozone signal of two different monitors: While the instrument using UV absorption for ozone detection shows an increase in ozone, the chemiluminescence instrument suggests decreasing mixing ratios; both correlate resp. anticorrelate well with the Aitken particle concentration. These small particles obviously pass the 5 µm pore filter in the sampling lines of both instruments. In the UV absorption monitor they are then retained in the scrubber that creates the reference signal, causing an artificial *positive* ozone interference. In the other ozone monitor the chemiluminescence reaction between O_3 and ethene is quenched by the Aitken particles in the reaction chamber, causing an artificial *negative* ozone interference. The bold black curve was obtained with a nearby third ozone monitor not influenced by the forest fire plume. The interference did not appear during the event with reduced ozone mixing ratios around 7:00 CET, when Aitken particle concentrations were low.

These interference effects with Aitken particles are important and must be considered in areas with frequent biomass burning. They were only noticeable since ozone monitors with different detection techniques were operated parallel. This emphasizes the necessity for detailed comparison of instruments working with different detection principles. Standardization of instruments is desirable but not always feasible, especially when sampling methods have to be adjusted to very different climatological conditions. In this context it has to be stressed that, in addition to the monitoring instruments, the whole air inlet system has to be thoughtfully designed and taken into account for calibration. Wherever it is possible, measurements should be traceable back to a common standard.

4 The scientific challenge

A sound analysis of the meteorological and climatological conditions at the GAW station is a prerequisite for the scientific evaluation and interpretation of the chemical data. Trajectories are a very useful tool for relating concentrations measured at a receptor site to possible sources.

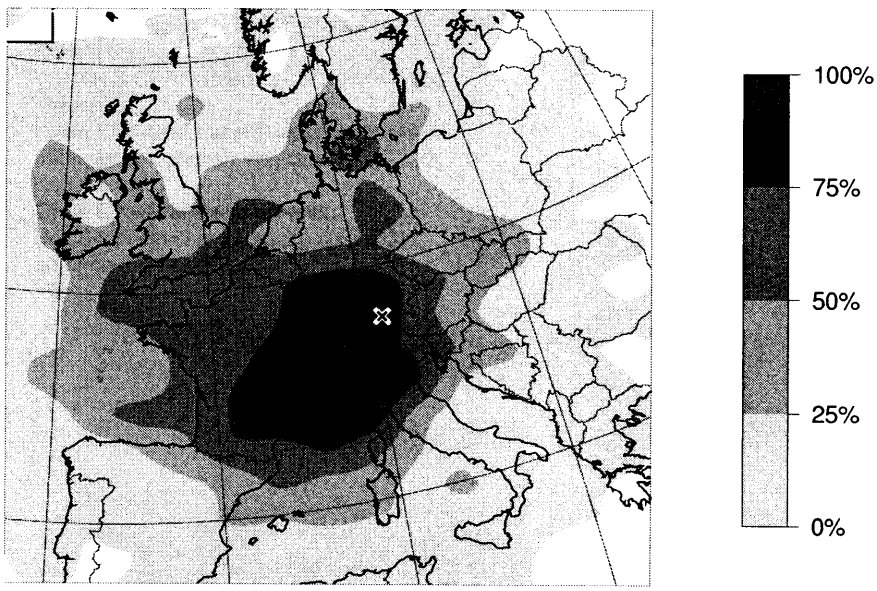

Fig. 4: *Probabilities for positions of air 24 hours before arrival at the GAW station Hohenpeissenberg at 3 km a.s.l. Daily trajectories (00 and 12 UT) 1992-1998.*

Trajectory climatologies give an impression of the distances from which the air can be transported to the respective GAW station within a given time interval. Fig. 4 shows an example of probabilities for positions of air 24 hours prior to arrival at the GAW station Hohenpeissenberg at 3 km a.s.l., calculated from trajectories twice a day in 1992 to 1998 with the TRAJEK model of the German Meteorological Service (Fay et al., 1995). The single trajectory positions were counted into grid elements whose size is shown in the upper left corner of the graph. Then, areas of equal cumulative frequency were plotted. The graph shows that there is a higher probability for the air to be southwest to west rather than east of Hohenpeissenberg 24 hours prior to arrival at the station. With a 50% probability it is within a circle of 600 km radius with center over eastern France. Graphs like these also allow for an assessment of the air-shed of a receptor site for trace substances with different atmospheric residence times.

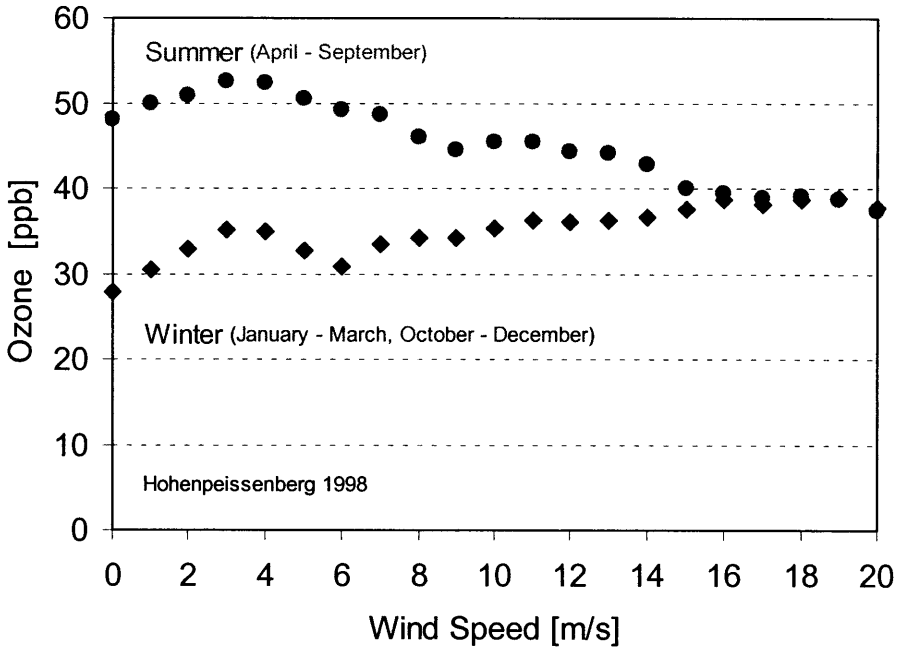

Fig. 5: *Ozone mixing ratios at Hohenpeissenberg in summer and winter 1998 as a function of wind speed for assessing its background value (Kaminski and Gilge, 2000).*

An example for the importance of combining atmospheric chemistry data with meteorological data is given in Fig. 5. The background mixing ratio of ozone can easily be derived, when it is plotted as a function of wind speed: While local effects on ozone like photochemical production in summer and chemical destruction or deposition in winter are mainly observable at low wind speed, mixing ratios converge with growing wind speed towards a value which can be interpreted as the background mixing ratio.

It is one of the scientific challenges to separate measured concentrations into a fraction due to transport and another due to local formation/destruction. Since most physical and chemical data in the atmosphere contain local, regional and large-scale information, whereas GAW is mainly interested in the early detection of large scale changes in the atmosphere (i.e. in data with high spatial representativeness), the GAW DACH project was initiated in 1996. It is a joint cooperation between the German, Austrian and Swiss (D-A-CH) Meteorological Agencies DWD, ZAMG and

SMI. The aim is to investigate the spatial representativeness of the GAW data at four alpine mountain sites and to develop filters for extracting data with extended spatial representativeness from the dataset. Filter functions which point out concentration fluctuations caused by local meteorological and chemical processes are expected to be an important tool for detecting trends earlier and more reliably. The flagging of data according to their representativeness in space increases the potential for their interpretation. Such a characterization of data should be implemented at all GAW stations. This requires the data bases in the GAW data centers to allow for storage of these flags. The DACH cooperation is a promising model of cooperation with and among other GAW stations. It serves for data quality, which is an inevitable pre-requisite for data evaluation and interpretation. The way of cooperation within the DACH project can therefore serve as a general model of linking stations with the aim of characterizing a whole region with respect to atmospheric chemistry. A first report from this project was recently published (Fricke et al., 2000).

A number of Scientific Advisory Groups (SAG) has been established by the WMO in order to elaborate recommendations for the measurement techniques within GAW and to give assistance to the stations with respect to scientific questions. Close cooperation between scientists at the GAW stations and research institutes as well as universities is very important for the success of the program.

5 The political challenge and benefit

A few words should be said about the political challenge of establishing a global, long-term network for atmospheric chemistry. The establishment of stations in the frame of GAW requires a long-term financial commitment and may therefore be difficult. The scientific community dealing with atmospheric research expects an increasing influence of human activity on the atmosphere with growing global population and related increasing energy production and industrial activities in the 21st century. National and international policy decisions affecting the environment in this century will strongly depend on reliable scientific data gathered through GAW. The mutual dependency of countries in global meteorology is obvious and has long been recognized. The same holds for data on the chemical condition of the atmosphere, although it might not yet be that obvious. The meteorological and chemical networks were often established independently from each other. It is time to merge them into a common network. Meteorological agencies in all countries should be encouraged to establish own stations or to make financial contributions to joint stations or routine measurement programs within GAW. Only national agencies with continuous funding can guarantee the necessary long-term commitment for a network like this. Climate protection is a global challenge, it can therefore only succeed in the frame of a global effort.

6 Outlook

A new focus within GAW will be on the GAW Urban Research Meteorology and Environment (GURME) project. It responds to the requests for assistance by many national meteorological services in dealing with urban issues, the management of which requires special attention. More emphasis will have to be put on capacity building, education and twinning, and the exchange of experience between the active GAW stations. Close cooperation with satellite programs measuring ozone and other trace components including aerosols (ground truthing) will be improved in order to

further develop GAW into a 3-dimensional network. The actual strategic plan for GAW (WMO, 1997) is being revised and actualized.

Acknowledgement

The support by Uwe Kaminski and Stefan Gilge in preparing this contribution is gratefully acknowledged.

7 References

Fay, B., H. Glaab, I. Jacobsen, R. Schrodin (1995): Evaluation of Eulerian and Lagrangian atmospheric transport models at the Deutscher Wetterdienst using ANATEX surface tracer data. Atmos. Environ., 18, 2485-2497.

Fricke, W., A. Fischer, J. Forrer, S. Gilge, P. Hofer, P. Jeannet, A. Kaiser, K. Kenndoff, R. Nemeth, L. Ries, P. Winkler (2000): Filterung luftchemischer Meßreihen im Alpenraum zur Charakterisierung ihrer Repräsentanz, GAW-DACH-Projekt. Berichte des Deutschen Wetterdienstes 211, Offenbach/Main.

Hofer, P., Buchmann, B., Herzog, A. (1998): The World Calibration Centre for Surface Ozone and Carbon Monoxide. In: SAEFL and SMI (Ed.), Global Atmosphere Watch (GAW) – International activities and Swiss contribution. Abstracts of the Conference, 14-15 October 1998, Swiss Federal Institute of Technology, Zurich, Switzerland.

Kaminski, U., S. Gilge (2000): Zum Trend der Hintergrundkonzentration von Ozon. Ozonbulletin des Deutschen Wetterdienstes Nr. 75, 6. Juni 2000.

Miller, J.M. (1998): WMO's Global Atmosphere Watch: An International Programme. In: SAEFL and SMI (Ed.), Global Atmosphere Watch (GAW) – International activities and Swiss contribution. Abstracts of the Conference, 14-15 October 1998, Swiss Federal Institute of Technology, Zurich, Switzerland.

WMO (1997): The Strategic Plan of the Global Atmosphere Watch (GAW). WMO-GAW Report No. 113. WMO-TD No. 802.

More information through the internet:

on the WMO GAW program:	http://www.wmo.ch/web/arep/gaw_home.html
on the Hohenpeissenberg Observatory:	http://www.dwd.de/research/mohp/hp2/gaw/gaw.htm

1 MEASUREMENT TECHNOLOGY, PERFORMANCE, AND QUALITY ASSURANCE

1.4 Measurement of the Atmospheric Composition

Measurement of Atmospheric Components by a Ground-based Remote Sensing Method

Wang Gengchen, Kong Qinxin, Liu Guangren, Gu Zhifang, Wan Xiaowei
Institute of Atmospheric physics, CAS, Beijing, 100029, China.
Tel.:86-10-62389420, Fax: 86-10-62028604 E-mail: wanggc@mimi.cnc.ac.cn

Grechko E.I ., Fokeeva E.V.
Institute of Atmospheric Physics, RAS, Moscow, 109017, Russia
Tel.: 07-095-9533695, Fax: 07-095-9531652 E-mail: igran@atm.phys.msu.su

1. INTRODUCTION

Study on minor gases components in the atmosphere, at present time, attracts more and more attention because of it's important role in the atmospheric chemistry processes in the troposphere. Increase of concentration of gases components in the atmosphere, especially in the city region is caused mainly by development of industry and transportation, so control of gases component at different geographical places has became a crucial problem both for the atmospheric chemistry and for air quality assessment[1, 2].

A ground-based spectroscopic method for monitoring gases components content in the atmosphere is developed in this paper, and some results of CO column content in Beijing district obtained by using solar spectroscopy are given and discussed.

2.METHOD AND APPARATUS

According to atmospheric molecular spectroscopy, most gases components in the atmosphere have their own characteristic spectrum in the infrared region, that gives a foundation for determination of their content in the atmosphere by using spectroscopic method, namely, content of a given component can be determined according to it's absorption at a selected wavelength. Some spectral parameters used for remote sensing of some gases constituents in the atmosphere are give in Tab 1.

Tab 1. Spectral parameters for some gases in the atmosphere

species	absorption band (μm)	absorption line (cm^{-1})	spectral resolution (cm^{-1})
CO_2	2.06	4854.40	0.25
CO	4.63	2158.30	0.20
CH_4	3.33	2998.91	0.20
C_2H_4	3.36	2976.8	0.07
N_2O	4.5	2469.10	0.20
O_3	9.6	1043.80	0.20
NO_2	0.44	22994.0	0.50
H_2O	6.3	2156.59	0.14

The used spectroscopic method for gases content measurement is based on absorption of solar radiation at by a given gas to be measured [3, 4].

For a selected wavenumber, solar radiation reached at earth's surface I(ν) is given by following equation:

$$I(\nu) = \int A(\nu - \nu')d\nu' \cdot I_O(\nu)\exp[-m\int C(z)k(\nu,p,T,)dz]$$

where: $I(\nu)$, $I_O(\nu)$ are solar radiation at surface and at top of the atmosphere, respectively, $A(\nu)$ is instrumentation function, m is atmospheric mass, k is absorption coefficient, C is concentration of gas to be measured, P, T are atmospheric pressure and temperature, respectively.

It can be seen, that gas column content can be written as

$$C = \frac{1}{m} \int_{z_l}^{\infty} C(z)dz$$

Generally speaking, determination of gas column content needs a set of data such as vertical profile of the measured gas, profile of pressure, profile of temperature, and overlap spectrum of various atmospheric components as well, that make the problem unresolvable in practice, for this reason, atmospheric gaseous components are measured by using spectroscopic method with high spectral resolution. that means the used spectroscopic instrument should have spectral resolution in order of one or two halfwilth of the selected absorption line. Besides, the selected absorption line should be as pure as possible in order to remove interference of other components in the atmosphere.

Since 1992, monitoring of CO, H_2O, CH_4, N_2O column contents by using above-mentioned solar spectroscopy have been made in Beijing district. For this purpose, a spectroscopic system with high spectral resolution of 0.2 cm^{-1} is used, the system consist mainly of sun tracking system, spectrometer with grating of 300 lines per 1 mm, head-cooled detector and data taking unit.

3. RESULTS AND DISCUSS

As a example, some results of CO column content measured in time period from 1992 to 1999 are given in Tab.2 for estimation of air quality and it's variation in Beijing district.

Tab. 2 CO column content in the atmosphere in Beijing (1992,1996-1999)

year	1992		1996			1997			1998		1999			
month	9	10	10	11	12	5	10	11	10	11	6	7	10	11
daily average	0.149	0.125	0.161	0.181	0.141	0.112	0.093	0.157	0.157	0.185	0.146	0.145	0.120	0.151
maximum	0.177	0.197	0.192	0.665	0.247	0.279	0.123	0.372	0.328	0.416	0.289	0.232	0.358	0.493
minimum	0.082	0.079		0.075	0.084	0.064	0.066	0.077	0.065	0.088	0.086	0.094	0.060	0.065
average Δc	0.067	0.046		0.106	0.057	0.048	0.027	0.080	0.092	0.097	0.060	0.051	0.060	0.086

Besides average CO content, the maximum and minimum CO contents are also given in Tab. 2 showing a large variation range. It is interest to compare the average CO contents, C with background CO content C_b for the days of measurement. Generally speaking, C_b represents unpolluted atmosphere. So, difference between C and C_b ($\Delta C = C - C_b$) can be considered as a mark of the atmospheric pollution level with CO. As it can be seen, for Beijing, the average ΔC ranges from 0.03 atm.cm to 0.10 atm.cm for the time period of measurements , while in very clear days and under appropriate meteorological condition, CO content of 0.070 atm.cm was observed as CO background content for Beijing area. The most lowest CO contents closing to it's background value were observed in Beijing when the wind direction is Northern and Northern-Western and average wind speed is about 6~7m/s in layer of 0~300m.

Further analysis of meteorological data obtained at meteorological tower shows that in the most case, the background CO content is observed under unstable stratification and rapid increase of wind speed with altitude in layer up to 300m. It is easy to understand that the CO background content and all

low CO contents are observed only under more appropriate meteorological conditions favorable to spreading pollutants in the atmosphere.

A typical example for measured daily variation of CO column content for some days is given in Fig. 1. It can be seen, that on 9 November, 1996, CO column content reaches it's maximum of 0.48 atm.cm, that is highest CO content for whole period of measurements. Wind direction on the day is 165~190, average wind speed ranges from 1.7 m/s to 2.5 m/s, and almost no variation of wind speed with altitude was observed, moreover, such wind structure lasted for 3 days. All these meteorological conditions lead to accumulation of pollutants in the boundary layer. On 7 October, 1992, the meteorological condition was the similar to that on 9 November, 1996, but CO content was obviously lower, that is explained by possible increase of atmospheric pollutants for last years in Beijing and also by working of heating equipment during the measuring period in 1996.

Dependence of CO increase ΔC on wind direction in the layer of 0~300m for various days in 1992 and 1996 is analyzed and is presented in Fig. 2. As Fig. 2 shows that the highest ΔC are observed under wind direction of 150~180 both for 1992 and 1996, that is understandable, because our observation site is located at Northern part of Beijing district, in case of 150~180 wind direction air mass reached observation site must pass whole Beijing city, that causes ΔC increase.

As for wind speed, a concept on stay time t of air mass over Beijing city before it reached field of observation is introduced to estimate influence of wind speed on variation of CO content in the atmosphere. It is proposed that we have $t = L/V$, where L is distance from city boundary in windward direction to observation site, V is average wind speed in 0~300m layer.

After we have time t, variation of CO column content C from day to day can be explained by using equation $C=Q \bullet t$, where Q is a specific intensity of CO source.

There from the CO emission intensity of Beijing city can be estimated easily if CO content and stay time of air mass over Beijing city are known.

4.CONCLUSION

1. Solar spectroscopic method is a more prospective way for determination of gases species column content in the atmosphere, especially for study on city pollution.
2. Selection of observation site at Northern side of Beijing for gases column content study is very reasonable, in case of Northern wind, the background content for Beijing district can be observed and in case of Southern wind, more high content of measured species representing serious air pollution in Beijing area is observed.
3. CO column content of 0.070 atm.cm can be considered as a background CO content C_b in the atmosphere in Beijing.
4. Under some appropriate meteorological conditions, CO column content over Beijing city can reach as high as 0.48 atm.cm, that exceeds it's background value in about 6 times.
5. Emission of measured species intensity in Beijing district can be estimated on base of measured column content and average wind speed in 0~300m layer.

REFERENCES

1. Dvoryashina et. al., On the carbon monoxide atmospheric abundance variation for 1970 1982. Izv. Akad. Nauk. SSSR, Ser. Fiz. Atmosfer i Okeana, 20, 40~47, 1984.
2. Dianov-Klokov V.I., Spectroscopic investigations of gaseous pollutants in the atmosphere above cities, Izv. Akad, SSSR, Ser. Fiz. Atmosfer i Okeana, 20, 883~900, 1984.
3. Fokeeva E. V., Peculiarities of a technique for determination of carbon oxide integral content over city, Izv. Akad. Nauk. SSSR, Ser. Fiz Atmosfer i Okeana, 17, 829~833, 1981.
4. Dianov-Klokov V.I. et. al., Spectroscopic measurements of atmospheric carbon monoxide and methane 1: Latitudinal distribution, J. of Atmospheric Chemistry, 8, 139~151, 1989.

Fig. 1 **Daily average CO column content (10.29-11.17,96)**

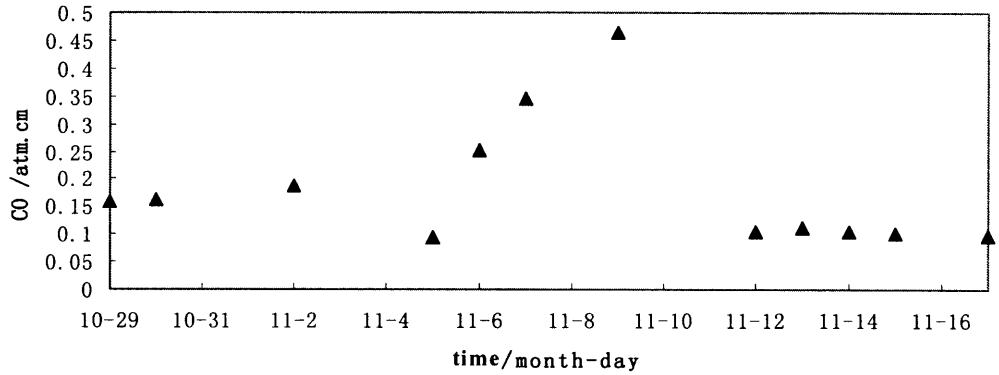

Fig.2 Dependence of CO variation on wind direction

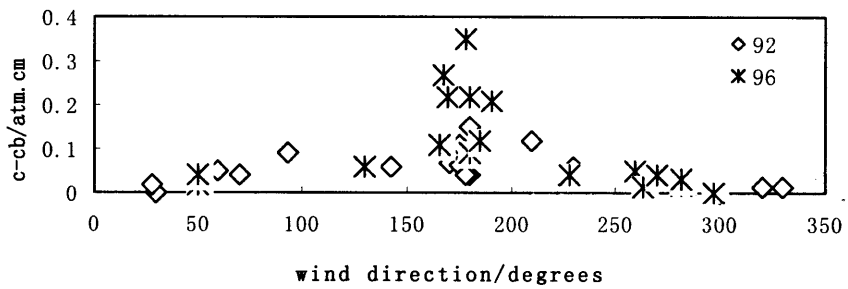

МАЛОЗАТРАТНЫЕ ТЕХНОЛОГИИ МЕТРОЛОГИЧЕСКОГО ОБЕСПЕЧЕНИЯ МОНИТОРИНГА ЗАГРЯЗНЕНИЯ АТМОСФЕРЫ

Вольберг Н.Ш., Гуревич И.Г, Кузьмина Т.А. и Павленко А.А.
Главная геофизическая обсерватория им. А.И. Воейкова,
ул. Карбышева, д.7, Санкт-Петербург, Россия
тел.247-86-70, факс 247-86-61, E-mail volberg @ main.mgo.rssi.ru

Results of studies are considered on development of low- cost technologies for metrological support of air pollution monitoring: solid - samples mini-set for external checking accuracy and precision of laboratory analysis; stable solid and liquid samples of unstable pollutants; non-cylinder portable equipment for external checking of calibration precision of CO- analyzers; portable generator of testing-gas mixtures; technique of error decreasing for network measurements using passive samplers.

Для обеспечения достоверности получаемой информации о загрязнении объектов природной среды необходим систематический внешний контроль точности проведения анализов проб в сетевых лабораториях. Ограниченность финансирования этих работ заставляет искать пути снижения их стоимости. Целью настоящей работы является краткое изложение результатов исследований, проводившихся в этом направлении в лаборатории методов мониторинга загрязнения атмосферного воздуха Главной геофизической обсерватории, являющейся в этой области базовой организацией по метрологии Федеральной службы России по гидрометеорологии и мониторингу окружающей среды.

Контроль точности анализа путём рассылки в лаборатории шифрованных проб является существенно более экономичным, чем инспекторский с выездом на место. Кроме того, его можно проводить практически одновременно во всех проверяемых лабораториях. Это даёт богатый материал для оценки правильности и воспроизводимости результатов анализа в сетевых лабораториях. Чаще всего в настоящее время такой контроль осуществляют путём рассылки ампул с растворами, содержащими определяемое вещество в концентрации, известной только проверяющей организации. Следует отметить, однако, что этот метод не позволяет надёжно контролировать погрешность измерений во всём диапазоне измеряемых концентраций. Из-за недостаточной устойчивости слабых растворов даже устойчивых веществ (что является следствием взаимодействия растворов со стенками ампулы) нижний предел концентраций в государственных стандартных образцах обычно составляет 1 мг/см^3. Вместе с тем, особый интерес при контроле представляют концентрации на два - три порядка меньшие, наиболее часто встречающиеся при анализе объектов окружающей среды. Кроме того, весьма желательно иметь целый набор образцов, охватывающий весь диапазон измеряемых концентраций без многоступенчатого разбавления исходного раствора.

Для обеспечения внешнего контроля точности анализов проб при мониторинге загрязнения атмосферного воздуха нами были разработаны способы изготовления твёрдых образцов, содержащих ион аммония, нитрит-, хлорид- и сульфат-ионы. Образцы готовятся путём точного дозирования в микроячейки из полимерной плёнки раствора нужного вещества точно известной достаточно большой концентрации с последующим высушиванием

нанесенной капли. Раствор содержит добавку соединения, обеспечивающего после испарения растворителя образование прочного конгломерата, приклеенного к полимеру.

Достоинствами твёрдых образцов веществ по сравнению с жидкими являются:

-неограниченный срок хранения даже микроколичеств устойчивых веществ из-за практически полного отсутствия их взаимодействия с полимерной подложкой как вследствие её инертности, чистоты и ничтожной скорости диффузии в твёрдом теле, так и из-за очень небольшой величины поверхности их контакта;

-отсутствие опасности разрушения из-за замерзания, компактность и малая масса значительно облегчающие и удешевляющие их пересылку по почте;

-возможность легко менять содержание дозируемого вещества в образце изменением величины высушиваемой капли раствора, что существенно облегчает изготовление комплектов образцов, охватывающих весь диапазон измеряемых методикой его количеств.

Воспроизводимость массы дозированного вещества в твёрдых образцах конечно ниже, чем воспроизводимость концентрации раствора, разлитого из одного сосуда. Среднеквадратическое отклонение для твёрдых образцов разных веществ находится в пределах от ± 3 до 7% . Однако, это частично компенсируется отсутствием погрешности от многоступенчатого разбавления , необходимого при использовании жидких образцов.

Особенно важной и существенно более трудной является задача создания хорошо сохраняющихся образцов нестойких веществ, прежде всего диоксида серы и сероводорода. Актуальность поблемы обусловлена тем, что из-за отсутствия государственных стандартных образцов нестойких веществ градуировку средств измерения приходится производить с помощью смесей, аттестация которых осуществляется на месте использования с применением другого метода. Очевидно, что при этом возможно появление больших систематических погрешностей. Ранее нами были разработаны способы изготовления устойчивых при хранении порошкообразных образцов, содержащих небольшую концентрацию таких легко окисляющихся веществ как сульфит- и сульфид-ионы. Стабильность при хранении обеспечивает возможность их аттестации и использования в качестве стандартных образцов не только для внешнего контроля, но для градуировки средств измерения. Их применение не только способствует повышению достоверности измерений, но и существенно сокращает трудовые и материальные затраты на градуировку приборов.

В последнее время разработаны также более простые в изготовлении устойчивые при хранении жидкие образцы микроколичеств этих же ионов и имитатора хлора.

Следует отметить, что контроль точности, выполняемый с использованием жидких и твёрдых образцов, охватывает лишь стадию анализа отобранной из воздуха пробы. Вместе с тем, значительная часть ошибок возникает на этапах отбора, транспортировки и хранения проб. Поэтому весьма актуальной является разработка газообразных образцов, содержащих известные микроколичества контролируемых веществ, - для внешнего контроля измерений, производимых с использованием лабораторных («ручных») методов анализа, и образцов, содержащих известные концентрации газов, - для внешнего контроля точности градуировки автоматических газоанализаторов.

В настоящее время такой контроль осуществляют с помощью баллонных газовых смесей в процессе инспекции, поскольку пересылка баллонов по почте затруднительна .

Для обеспечения возможности проведения внешнего контроля точности показаний автоматического газоанализатора монооксида углерода нами был использован способ приготовления поверочных смесей в проверяемой лаборатории без баллонов. Смеси готовятся путём разбавления дозированного (шифрованного) количества CO, содержащегося в присылаемой по почте стеклянной микроампуле, заданным объёмом воздуха. Для этой цели была разработана техника изготовления микроампул, содержащих дозированные количества CO – от 100 до 1000 мкг. Проверяемая лаборатория сообщает проверяющей следующие данные: результаты измерения концентраций CO в воздухе для разбавления, точный объём

разбавляющего воздуха и величину концентрации CO в приготовленной смеси газов. Описанный способ может быть использован также для градуировки газоанализаторов. В этом случае потребителю сообщается величина массы газа, находящегося в ампуле. Достоинствами описанного способа по сравнению с баллонными являются лёгкость пересылки ампул по почте и возможность приготовления из образцов с одинаковым содержанием CO газовых смесей с разной его концентрацией.

Для метрологического обеспечения автоматических газоанализаторов, включённых в состав станций контроля загрязнения атмосферы, наиболее удобны генераторы газовых смесей, основанные на использовании стабильных источников микропотока (СИМП) - проницаемых трубок, заполненных сжиженными газами или летучими жидкостями. С помощью таких генераторов можно приготавливать смеси, содержащие большую часть газовых примесей, контролируемых с помощью автоматических газоанализаторов: диоксиды серы и азота, сероводород, сероуглерод, аммиак, хлор и ряд других. Генераторы включают три основных блока: блок подачи разбавляющего воздуха, блок его очистки и термостатированную камеру, содержащую СИМП с дозируемым веществом. Для обеспечения постоянства продуцируемого СИМП микропотока вещества он должен предварительно выдерживаться при постоянной температуре в течение более или менее длительного времени. В зависимости от дозируемого вещества и толщины стенок трубки для стабилизации потока требуется время от нескольких десятков минут до суток. Поэтому для обеспечения возможности быстрого перехода от генерирования одной смеси к другой необходимо, чтобы все СИМП находились всё время при рабочей температуре.

Нами разработан переносный генератор газовых смесей, основанный на применении комплекта СИМП. Его особенностью является способность сохранять постоянную температуру всех проницаемых трубок в течение рабочего дня в автономном режиме за счёт теплоты фазового перехода термостатирующего вещества. Это даёт возможность переходить от дозирования одного вещества к дозированию другого за 5-15 минут и обслуживать одним генератором все автоматизированные станции, имеющиеся в населённом пункте.

Наиболее экономичными методами измерения средних концентраций примесей в воздухе являются методы с использованием пассивных пробоотборников.. Однако, их погрешность, вызванная влиянием изменений влажности и температуры анализируемого воздуха, существенно больше, чем при активном отборе проб. С целью снижения погрешности пассивных пробоотборников предлагается использование корректировочного коэффициента, который определяется путём одновременного параллельного измерения концентрации вещества в атмосферном воздухе при помощи автоматического газоанализатора и расположенного рядом пассивного пробоотборника. Способ позволяет с помощью одного газоанализатора уточнить результаты измерений, полученных при использовании многих пассивных пробоотборников, экспонированных одновременно с контрольным, расположенных в целом районе со сходными параметрами анализируемого воздуха.

АВТОМАТИЧЕСКАЯ УСТАНОВКА, ПРЕДНАЗНАЧЕННАЯ ДЛЯ ИНТЕГРАЛЬНЫХ СОДЕРЖАНИЙ CH_4 И CO_2 НА БАЗЕ ФУРЬЕ-СПЕКТРОМЕТРА

А.И. Решетников, С.П. Образцов, В.И. Привалов, Д.В. Румянцев
Tel. 8-812-2478671, Fax 8-812- 2478661, E-mail Reshal@infopro.spb.su

ABSTRACT

For some tasks connected to necessity of estimations of emission by large antropogenical sources of the greenhouse gases, the important addition to local methods of the analysis can become the remote spectroscopic method. In the report the brief description of high-speed installation on base of FTIR spectrometer of the moderate spectral resolution intended for continuous measurements of the integrated contents of the greenhouse gases (methane and carbon dioxide) in column of an atmosphere or its part is given. As a source of radiation the sun is used. The basic characteristics of installation are given. The way of retrieval of the contents of gases based on use of least-squares method and comparison of experimental and calculated spectra is stated. By results of real measurements the error of retrieval of the methane content is estimate at the analysis of a solar spectrum of gas in an interval of frequencies appropriate to the absorption band or one of its branches. The basic opportunity of improvement of quality of retrieval of the contents of gases is shown at improvement of the spectral resolution and decreasing of an instrument error of measurements.

Использование спектроскопических методов для наблюдения газовых составляющих атмосферы имеет достаточно длительную историю, хотя для задач мониторинга содержания парниковых газов в атмосфере применение этих методов ограничено, что связано с относительно высокими погрешностями восстановления. Для наблюдений содержания газов в атмосфере при использовании солнца в качестве источника излучения применяется широкая область инфракрасного диапазона длин волн 1.8 – 14.0 мкм. В этом спектральном диапазоне расположены полосы поглощения основных парниковых газов: диоксида углерода, метана, озона, закиси азота и водяного пара.

Применение спектроскопических методов, тем не менее, может быть оправдано, если за счет накопления спектров, полученных в идентичных условиях, удастся существенно снизить случайную составляющую погрешности. Их целесообразно использовать и в ситуациях, когда следует ожидать значительного возрастания содержания измеряемого газа, по крайней мере, в пограничном слое атмосферы. Как показали наши in-situ измерения под Санкт-Петербургом, в утренние часы (непосредственно после восхода солнца) при наличии инверсии и направлениях ветра со стороны города наблюдалось существенное увеличение концентрации метана (рост концентрации начинался перед заходом солнца). Значения наблюдаемых концентраций метана превышали региональный фоновый уровень на 20-30%, а в отдельных случаях и на 40-50%. Поскольку наблюдаемое увеличение концентрации имеет явное антропогенное происхождение, то возникает вопрос об использовании спектрометрических измерений (одновременно с контактными) для определения содержания или средневзвешенных концентраций газов в пограничном слое.

Для наблюдения содержаний парниковых газов в атмосфере (включая озон и водяной пар) была разработана быстродействующая автоматизированная установка на базе Фурье-спектрометра среднего спектрального разрешения, в которой в качестве источника излучения используется солнце. Основные технические характеристики установки приведены ниже:

1. Полуширина аподизированной аппаратной функции около 0.8 $см^{-1}$. Длина смещения подвижного зеркала – 6 мм.
2. Длина волны референтного канала - 0.6328 мкм
3. Время регистрации одной интерферограммы – 4 секунды.

4. Основной фотодетектор – термоохлаждаемый фоторезистор) – PbSe (с предусилителем), с удельной обнаружительной способностью $D^*=5.5\cdot10^9$ $Вт^{-1}\cdot см\cdot Гц^{1/2}$,
   постоянной времени – 100 мкс,
   интегральной вольтовой чувствительностью - $2\cdot10^6$ В/Вт,
   диапазон линейности приемно-усилительного тракта (ПУТ) □ 10^4
5. Спектральный диапазон (со светоделителем CaF_2) – 1.8 – 5.0 мкм,
   со светоделителем KCl: 3.0 – 14.0 мкм.
   (при смене светоделителя фотодетектор PbSe заменяется на КРТ или МГ-30).
6. Световой диаметр оптического пучка – 50 мм.
7. Отношение сигнал/шум в главном максимуме единичной интерферограммы □ 500.
8. Разрядность АЦП - 10^{12}

Одним из наиболее важных параметров Фурье-спектрометра, определяющих качество восстановливаемого спектра, является стабильность скорости движения подвижного зеркала в процессе регистрации интерферограммы. При ограниченной полосе пропускания ПУТ нестабильность скорости вызывает дополнительные искажения интерферограммы. Однако это явление возникает на начальном участке движения подвижного зеркала интерферометра до установления постоянной скорости. В виду того, что постоянная скорость движения устанавливается через определенный интервал времени, то условия регистрации односторонней интерферограммы (ОИФР) следует рассматривать как почти односторонней или квазиодносторонней. Нами применялся метод регистрации ОИФР, поскольку используемая длина разности хода здесь в 2 раза выше, чем для двусторонней интерферограммы. Недостатком ОИФР является наличие фазовых искажений, обусловленных неидеальностью юстировки интерферометра и конечностью ширины полосы пропускания ПУТ. Для коррекции фазовых искажений (ФИ) был использован метод Формана. По небольшой части ОИФР в районе нулевой разности хода (200 – 300 точек) определялась корректирующая функция. Затем выполнялась свертка исходной ОИФР с этой функцией. Скорректированные последовательно зарегистрированные интерферограммы затем суммировались и уже по суммарной интерферограмме восстанавливался конечный спектр. Спектрометрическая установка обеспечивает возможность непрерывной регистрации до 100 интерферограмм.

Для восстановления интегрального содержания (или средневзвешенной по высоте концентрации) измеряемого газа была разработана специальная программа с использованием которой предварительно вычислялся спектр пропускания атмосферы в заданном спектральном интервале с учетом известных параметров спектрометрической установки и условий наблюдений (в случаях, когда это было необходимо). При вычислении спектра пропускания атмосферы использовалась база данных вращательных линий HITRAN-92 и среднемесячная эмпирическая статистическая модель атмосферы или данные радиозондирования, преобразованные в соответствии с принятой в модели схемой разбиения на слои.

Расчет спектра пропускания ведется при использовании следующей формулы, часть параметров которой, полученных в процессе предварительных исследований, задается н не изменяется в течение серии или всего периода наблюдений. Другая часть параметров, характерных для конкретного времени наблюдений, вводится для каждой серии наблюдений:

$$U(\nu_i)=\int_{\Delta\nu} G(\nu)A(\nu-\nu_i)\left\{\left[\prod_{j=1}^{M}\exp\left(-mc_j\int_{z}^{H}K_j(T(z),P(z),\nu)dz\right]\right\}d\nu+U_0+\delta U, \quad (1)$$

Здесь: i = 1…N- номер точки в спектре,

j =1..M – индекс газа, поглощение которым учитывается при расчете пропускания рассматриваемом спектральном интервале,

$G(\nu)$ - линейная функция, учитывающая наклон нулевой линии (пиния, соответствующая 100%-ому пропусканию) в регистрируемом спектральном диапазоне ,

$A(\nu - \nu_i)$- аподизированная аппаратная функция спектрометра,

m – атмосферная воздушная масса,

c_j – средняя по высоте концентрация j-го газа в слое,

$K_j(T(z)P(z), \nu)$ – коэффициент поглощения j-го газа, зависящий от частоты ν, температуры слоя на высоте z - T(z) и давления на этой высоте - P(z),

U_0 – постоянная составляющая,

δU –случайный шум (в основном, это шум детектора излучения).

H – высота верхней границы атмосферы, начиная с которой вклад в поглощение газа, содержащегося выше, уже не влияет на формирование солнечного спектра пропускания столба атмосферы.

Значения температуры, давления и абсолютной влажности в соответствующих слоях атмосферы идентичной толщины для расчета коэффициента поглощения берутся из соответствующей модели атмосферы, полученной посредством обработки многолетних данных радиозондирования на аэрологической станции пос. Воейково или данных радиозондирования.

Рассчитанный т.о. спектр сравнивается с экспериментально измеренным. Посредством изменения наклона нулевой линии (соответствующей отсутствию селективного поглощения), сдвига характерных максимумов поглощения экспериментального спектра и изменения средневзвешенных по высоте концентраций газов (поглощение которыми в данном спектральном диапазоне существенно) добиваются минимального (используя метод наименьших квадратов) отличия экспериментального спектра от расчетного. Значения параметров, обеспечивающие минимум указанного различия, принимаются за значения искомых параметров. Количественной мерой сохранившегося отличия экспериментального спектра от расчетного является величина невязки, определяемая как:

$$\Psi = \sqrt{\sum_i (Uiex - Uipac)\text{^}2 \Big/ N-1} \qquad (2)$$

где: U_{iex} - спектральное пропускание (или спектральный поток, тогда величина невязки будет размерной) в i-ой точке экспериментального спектра, U_{ipac} – то же, но для расчетного спектра,

N – число спектров (интерферограмм), использованных для получения осредненного спектра пропускания атмосферы.

Была разработана программа обработки спектров, обеспечивающая возможность восстановления средневзвешенной по высоте концентрации газа по результатам измерений солнечных спектров. Программа является универсальной и пригодна для восстановления содержания газа в атмосфере, если его полоса поглощения находится в рабочем спектральном диапазоне Фурье-спектрометра.

Основными установками вводимыми в программу были следующие: - граничные частоты спектрального диапазона, полуширина аппаратной функции (АФ), относительная погрешность измерения спектральных потоков δU, путь данных ввода-вывода, по которым

программа осуществляет поиск данных радиозондирования, статистических моделей, проводит суммирование интерферограмм, выполняет преобразование осредненной интерферограммы в спектр.

Ниже на Рис.1 приведен результат восстановления общего содержания метана с использованием изложенного подхода по результатам наблюдений 5.05.99 г. Как следует из Рис.1, определенная т.о. величина средневзвешенной объемной концентрации метана, составляет C=2.03 ppm при величине невязки 1.4. Полученная величина невязки означает, что относительное различие в спектрах (расчетном и экспериментальном) не превышает 1.4%, из которого только 0.4% обусловлены погрешностями не связанными с шумом приемно-регистрирующей системы. Погрешность восстановления содержания CH_4 при этом не превышает 3%. Она может быть еще снижена, если удастся повысить соотношение сигнал/шум в главном максимуме единичной интерферограммы, либо увеличить число просуммированных интерферограмм.

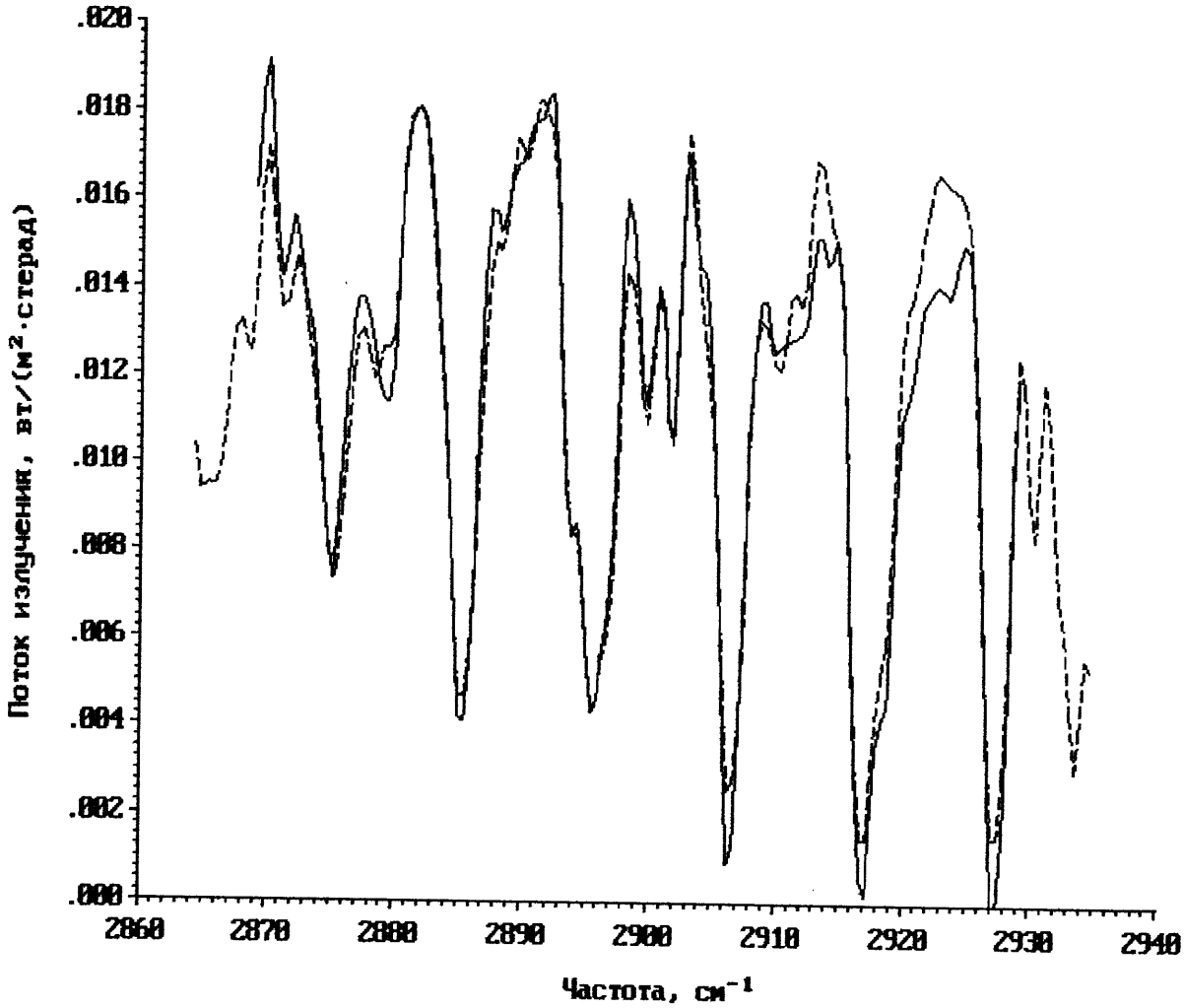

Рис.1

Результат сравнения расчетного (пунктир) и измеренного спектра (сплошная линия) пропускания атмосферы или расчетных и измеренных спектральных потоков. Измерение выполнено 5.05.99 г. при атмосферной массе m=1.38. Полуширина АФ равна 0.804 $см^{-1}$, сдвиг между максимумами поглощения расчетного и экспериментального спектров –0.98 $см^{-1}$. Восстановленная средневзвешенная концентрация метана составила 2.028 ppm, общее содержание водяного пара в столбе атмосферы – 3.77 $Кг/см^2$.

1 MEASUREMENT TECHNOLOGY, PERFORMANCE, AND QUALITY ASSURANCE

1.5 Instruments and Systems Operated under Harsh Environment Conditions

Operation of Automated Surface Observing Systems in Harsh Climatological Environments

M. Douglas Gifford, National Weather Service, OSO14X1
1325 East-West Highway, Room 4234, Silver Spring, MD 20910, U.S.A.
Phone: +1 301/713-2093 Fax: +1 301/713-2099
email: malcolm.gifford@noaa.gov

Garry M. Pearson, Meteorological Service Canada
Monitoring and Water Survey, 45 Alderney Drive, 16th Floor
Dartmouth, N.S., Canada
Phone: +1 902/426-9131 Fax: +1 902/426-9158
email: garry.pearson@ec.gc.ca

Kjell Hegg, Norwegian Meteorological Institute
P.O. Box 43, Blindern, N-0313 Oslo, Norway
Phone: +47 22/96-3227 Fax: +47 22/96-3050
email: kjell.hegg@dnmi.no

1. Introduction

There is a growing trend whereby manual observations of weather parameters are being replaced by the introduction of automated weather observing systems. Mature automated weather observing systems are capable of producing accurate results when operating under relatively benign climatological conditions. However, when designing and operating these systems for use in harsh climatological conditions, many challenges must be addressed.

This paper will summarize the experience gained by the United States, Canada, and Norway in developing and operating automated weather observing systems under extremely harsh climatological regimes ranging from tropical to arctic. Aspects of automated systems considered include effects on sensors, systems design, installation, maintenance, and robustness. It is hoped that lessons learned from these experiences will provide guidance to those operating in similar environments. These lessons learned may also provide insight into future directions to assist investigations addressing some of these issues.

2. Climatic Regimes

2.1 Mountain/Arctic Climate

Some of the most challenging problems are encountered when designing, installing, and operating automatic weather stations in mountain and arctic climatic regimes. In order to survive the environment and produce accurate output, these stations must be designed to withstand extremely cold temperatures, heavy snowfall, extreme snow depths, and excessive stresses caused by wet snow accretion and heavy icing.

During mild winter weather, the electronics components usually give off enough heat to maintain an acceptable operating temperature inside the electronics enclosures. However, in colder arctic environments, additional heaters must be provided in order to keep internal temperatures of electronics enclosures at an operational level. In the harshest of extreme arctic/mountain environments, special equipment shelters have to be installed to ensure proper operation of the electronic equipment and provide maintenance technicians with protection from the elements (see Figure 1).

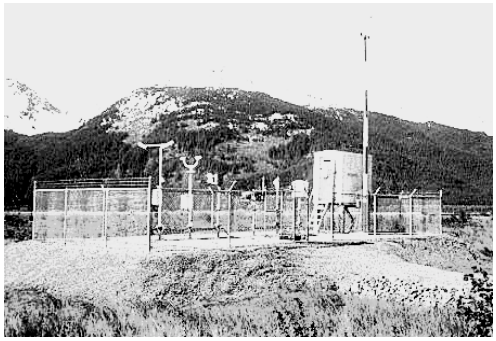

Figure 1. Haines, Alaska ASOS

To prevent blockage of the lenses and windows of optical sensors by snow and ice, lens heaters or window conditioners have to be employed. These may be contact heaters applied

directly to the surface of the lens or in the form of an external heat source. Some protection from lens blockage can be provided by the use of heated lens hoods. However, wind-driven wet snow has been shown to block the lenses of some instruments in spite of the added protection (see Figure 2). A recent EUMETNET project reported similar impacts to operations caused by ice and wet snow blocking sensors and instrument shelters [EUMETNET, 1999].

Special considerations have to be made when installing and maintaining stations in mountain and arctic climates. This is especially true when the sites are located on or near permafrost. For those stations, great care must be taken not to disturb the terrain. The installation at Haines, Alaska (see Figure 1) is an example of the steps taken to prevent damage to the underlying permafrost. The transmission of heat energy is minimized by thick layers of gravel and insulation both at the sensor suite and the access road.

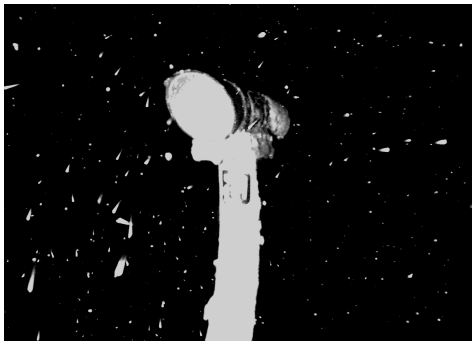

Figure 2. Lens Blockage

At some mountain/arctic sites, such as the Haines, Alaska site, the addition of a strong fence is required to prevent damage to the automatic weather station by large wildlife species such as bears and moose. In the Svalbard region of Norway, where fences are not permitted, all exposed cables must be protected with sturdy stainless steel tubing to avoid damage caused by polar bears.

At selected automatic weather stations, extreme snow depths may be encountered. In order to prevent deep snow from covering the sensor suite, some stations in the United States have been installed on elevated platforms. At Mullan Pass, Idaho, the sensor suite is mounted atop a fourteen-foot (4.3 meter) high platform (see Figure 3).

Figure 3. Mullan Pass, Idaho

2.2 Maritime Climate

Operation of automatic weather stations in coastal environments also presents many challenges. Installations along the coast are usually subjected to the effects of sea spray. The residual salt from the spray can coat the lenses of optical sensors, reducing sensor functionality while increasing the maintenance workload required to clean the lenses.

Sea spray can also contribute to a more rapid deterioration of materials used in the automatic weather station. At a minimum, the corrosion caused by salt air and sea spray increases the maintenance workload needed to prevent early failure of materials. Left unchecked, severe corrosion can cause weakened components to fail suddenly, resulting in a loss of support structures and sensors (see Figure 4).

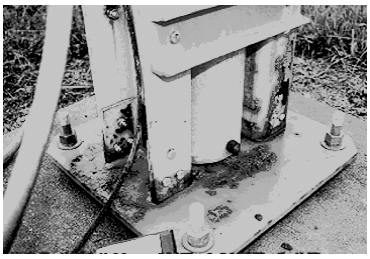

Figure 4. Extensive Corrosion

Salt corrosion is an incessant problem at maritime coastal stations, causing premature component failure. For example, metal junction boxes exposed to salt spray experience complete corrosion after 4 to 5 years of service. Figure 5 shows a typical case of such corrosion after less than 5 years service on Sable Island, Nova Scotia. Aluminum boxes fare somewhat better, lasting 8 to 9 years before replacement is necessary. Open wiring is usually clear coated where boxes are not completely sealed. Boxes, even if completely sealed, will have a small hole bored to ensure moisture drainage in the event of moisture formation. Desiccants are used in all Canadian applications. The service technicians are currently experimenting with various new rust inhibitors to further extend the life of these systems.

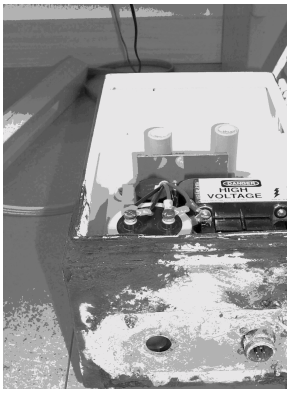

Figure 5. Corrosion

Sable Island also presents excellent examples of the deterioration caused by blowing sand and salt. The site is a small sand-covered island approximately 200 km east of Nova Scotia. Incidences of blowing sand result in a sandblasting effect, frosting over glass sensors such as the sunshine recorder. In addition, the sandblasting removes the anodized coating on aluminum surfaces, thus increasing the rate of salt corrosion.

Some coastal stations at high latitudes, such as St. John's, Newfoundland, are extremely susceptible to the problems caused by freezing precipitation and icing accompanied by high winds. These stations may experience ice accretion on the sensors rendering the output from the station unrepresentative. Figure 6 shows typical ice accretion on cup and vane wind equipment at St. John's.

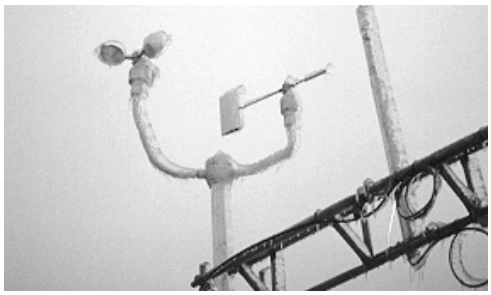
Figure 6. Ice Accretion

At coastal sites, electrical connectors and junctions are often replaced with aluminum parts, although conversion to PVC is preferred. Silicone grease is applied liberally to inhibit corrosion. A new formulation is currently being tested. This substance has the consistency of petroleum jelly when applied, and thickens to a flexible finish as it dries. It can easily be scraped off and has good potential for protecting connectors and seals.

Some coastal sites require unusual precautions when the automatic weather station must be sited very close to the water. The sensor suite at Sitka, Alaska is installed at the top of an abandoned seaplane ramp very close to the bay. During periods of high winds, the swells on the bay would heave large rocks up the ramp at the sensor suite. Thus, a substantial seawall had to be constructed to prevent damage to the equipment. Coastal stations may also be affected by extreme wind speeds during the passage of hurricanes and severe cyclonic storms. Therefore, automatic weather station equipment at these sites must be capable of withstanding wind speeds up to 75 m/sec [WMO, 1996].

Figure 7. Sitka, Alaska

2.3 Desert Climate

Automatic weather stations installed in desert environments are subjected to a combination of extremely high ambient temperatures, low relative humidity, and blowing dust and sand. As mentioned earlier, blowing sand and dust can have a sandblasting effect on surfaces such as glass covers, sensor lenses, anodized aluminum, and painted surfaces. Certain adhesives can also be modified by constant exposure to high temperatures and blowing dust and sand.

Exposure to these conditions, plus the effects of extremely high ultraviolet radiation, can result in early failure of insulation on exposed wiring and more frequent maintenance actions to repaint metal surfaces.

2.4 Tropical and Sub-Tropical Climates

With the exception of hurricane-force winds mentioned earlier, excessive rainfall is the primary concern at stations installed in tropical and sub-tropical climates. Sudden torrential rainfall can easily submerge equipment that has been installed in low-lying areas as shown in Figure 8. To minimize damage to equipment that must be installed in flood-prone areas, the sensors and communications equipment can be mounted on the same type of platforms that are used in mountainous regions. During the massive flooding of the Mississippi River valley in 1993, the Jefferson City, Missouri ASOS was spared any significant damage through the use of such a platform (see Figure 9).

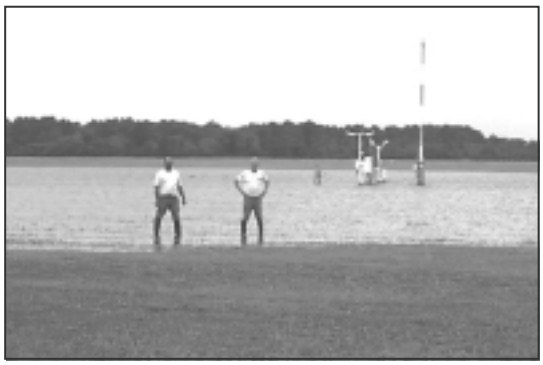

Figure 8. Flooded Sensor Suite

3. General Design Considerations

Power and communications are critical elements of all automatic weather stations, regardless of the severity of the environment. Some simple Norwegian stations - measuring temperature, humidity, pressure, and wind – have been designed to operate on battery power for up to two years. Such stations must necessarily have a very carefully calculated power budget without much need for heating. Remote sites are also prone to interruptions in commercial power. Therefore, these sites may be configured with uninterruptable power supplies to span the gaps in available AC power. Telecommunications may be unavailable or unreliable at some remote sites. In such cases, satellite communications or other backup means of communications needs to be provided in order to ensure a smooth flow of data.

Figure 9. Jefferson City, Missouri

4. References

Tammelin, B., Joss, J., and Haapalainen, J., “Specification of Severe Weather Sensors,” EUMETNET Contract EMN/C5 3/10/97

“Guide to Meteorological Instruments and Methods of Observation,” World Meteorological Organization (WMO) No. 8, Geneva, Switzerland, 1996

EXPLOITATION DES INSTRUMENTS METEOROLOGIQUES EN MILIEU TROPICAL

Par Mr. Facinet SOUMAH
Direction Nationale de la Météorologie BP : 566 Conakry - Rép. de GUINEE
Tél : (224) 45 48 15 e-mail : meteogui@leland-gn.org

Les interactions de plus en plus nombreuses de la société et de l'atmosphère conduisent à une croissance accrue des besoins en informations sur notre environnement ; d'où un plus grand nombre de demandes sur l'état de l'atmosphère . Ceci conduit à l'augmentation de la densité des réseaux et la fréquence des observations avec un nombre toujours croissant de paramètres météorologiques à mesurer. Comme conséquences, le matériel et les logiciels existants doivent ainsi être adaptés à de nouvelles exigences.

Des progrès apparaissent tous les jours :Certains améliorent les performances de capteurs existants alors que d'autres sont fondés sur de nouveaux principes physiques. Il n'est pas toujours satisfaisant de se fier aux fournisseurs de matériel pour déterminer les contraintes d'exploitation. C'est pourquoi, la Commission des Instruments et des Méthodes d'Observation (CIMO) donne les conseils suivants aux membres de l'Organisation Météorologique Mondiale (OMM) et conséquemment à tout service qui procède à des mesures météorologiques :

- une documentation suffisante pour bien comprendre les possibilités et caractéristiques des systèmes à mettre en service ainsi que les algorithmes éventuellement employés ;
- une compétence technique suffisante pour déterminer les prescriptions du système et évaluer la valeur de ses possibilités et caractéristiques ainsi que des algorithmes employés dans celui - ci.

Lorsqu'on planifie la mise en place et l'exploitation d'un réseau de stations, il est de la plus grande importance d'envisager les divers problèmes que posent les installations, la maintenance et l'étalonnage, en se souciant davantage de l'organisation, et de la formation du personnel technique.

C'est pourquoi, la CIMO vient en aide aux membres en organisant régulièrement des comparaisons internationales d'instruments. Les résultats de ces comparaisons peuvent être intéressants pour évaluer les diverses techniques de mesure.
Parmi les recommandations et conseils donnés aux membres par la CIMO on peut noter ceux ayant trait aux capteurs à savoir :

- robustesse des capteurs employés dans les stations ;
- absence de défauts intrinsèques générateurs d'erreurs systématiques.

En effet, la capacité des capteurs et systèmes d'observation à remplir les critères fixés se modifie constamment avec le perfectionnement des instruments et des techniques.

Toutefois, au cours des dernières années, de nombreux instruments météorologiques ont été dotés de circuits électriques et /ou électroniques et intégrés à des stations automatiques. En milieu tropical, l'exploitation de ces équipements se heurte à des conditions climatiques dont voici quelques effets :

- **Insolation** : les salissures s'accumulent sur les fenêtres des capteurs d'insolation en provoquant les modifications apparentes du seuil d'insolation.
- **Rayonnement** : la plupart des capteurs de rayonnement exploités dans les stations traditionnelles peuvent être reliés à un système automatique. Dans ce cas, en plus des interférences électromagnétiques dues aux câbles de transmission des signaux qui provoque la difficulté à établir des mesures correctes ; l'accumulation de salissures sur les fenêtres des instruments est encore plus critique pour la mesure du rayonnement. On considère que le dépôt de poussière sur le dôme des pyranomètres provoque une baisse d'exactitude de 2 %. C'est pourquoi, il est difficile d'envisager l'emploi de tels appareils à des endroits moins visités et pendant la saison sèche.
- **Hauteur des nuages**: Ceilomètre (laser) ; l'accumulation de poussière ou d'autres salissures sur les fenêtres par lesquelles s'effectuent l'entrée et la sortie du faisceau de lumière visible ou infrarouge peut nuire à leur fonctionnement.
- **Précipitation** : Le pluviographe à auget basculaire et le pluviomètre Association sont rapidement souillés par les feuilles d'arbres, le sable etc. .. Il faut donc les installer soigneusement.
- **Vent** : L'emploi d'anémomètres ordinaires à coupes ou à moulinet produisant des impulsions ou des fréquences est courant et ne pose pas de problèmes techniques particuliers autres que ceux imputables aux décharges électriques et aux intempéries.

Dans les régions orageuses comme la République de Guinée, de nombreux appareils sont endommagés suite aux intenses décharges électriques.
Ainsi, entre 1995 et 1998, à l'Aéroport de Conakry, plusieurs appareils à vent, de récepteur d'images satellitaires, de transmetteurs et des plates-formes de collecte de données (DCP), les calculateurs et les blocs d'alimentations n'ont pas été épargnés. Les anomalies sont enregistrées suite aux surtensions provoquées par les décharges.

Par ailleurs, dans les parties nord du pays où les températures atteignent 45° C à l'ombre, ce sont les coupelles des moulinets (appareil à vent) qui se déforment sous l'effet de l'humidité et de la forte chaleur. Les abris météo météorologiques dont les persiennes sont en bois se rongent, tandis que les supports métalliques se rouillent rapidement.

En période d'intenses précipitations (juillet - août), les communications par BLU entre les stations et le Centre Météorologique National (CMN) sont interrompues par des manifestations orageuses.

C'est pourquoi, pour remédier à la situation, il est crée au niveau de la Direction Nationale de la Météorologie et Services Associés / Agence de la Navigation

Aérienne (ANA), la Société Générale d'Electricité (SOGEL) une commission chargée d'étudier la réaction des systèmes face aux intempéries.

Actuellement, une étude est en train d'être menée pour la détermination des caractéristiques électriques des sols de la plupart des localités du pays. Ceci pour mieux inviter les fabricants et suggérer des modèles de paratonnerres et autres dispositifs à mettre en place en vue de sécuriser tous les équipements de mesures météorologiques et les autres systèmes exploités à travers le pays.

OPERATIONAL CONSIDERATIONS IN IMPLEMENTING A NETWORK OF AUTOMATED UPPER AIR STATIONS IN HARSH ENVIRONMENTS

R.P. Canterford, P.R. Smith, L.J. Braden and M.J. Joyce
Australian Bureau of Meteorology
PO Box 1289K, Melbourne, Vic, AUSTRALIA
Tel (+613) 9669 4225, Fax (+613) 9669 4168
E-mail R.Canterford@bom.gov.au

Abstract

This paper outlines the important aspects of implementing and running a network of ten automated upper air stations in remote and harsh environments. Points considered include reliability, staffing, remote balloon releases, adaptive observations, quality control and some engineering issues. The development and operational aspects required to achieve a mature, reliable operational network are discussed.

1. Introduction

In August 1995 the Australian Bureau of Meteorology (ABM) purchased a robotic automated upper air system, the Autosonde, manufactured by Vaisala Oyj. It was installed early in 1996 for full trials at the ABM's training centre. It proved to be an effective upper air system after adaption by the ABM and manufacturer engineers to satisfy Australian engineering and observations requirements. In particular the system had to be able to operate in harsh conditions in the Australian outback and on remote islands. After a system evaluation against set engineering and observations criteria, the ABM entered a contract with Vaisala to purchase up to 10 units (since extended to 12 units). Australia has a network of 50 upper air stations on the mainland, islands and in Antarctica, so the automated stations represent about 20% of the network. This paper outlines some of the operational problems encountered in establishing the network in a harsh environment, steps taken by the ABM and the manufacturer to overcome these difficulties and the use of a central ABM Help-Desk. It was found that operating the systems in harsh environments required monitoring and intervention by fully trained staff on duty (but reduced in number). This is a departure from them being operated autonomously with minimal or no staff on station.

Additionally, a number of ABM Autosonde locations are part of the Global Climate Observing System/ Global Upper Air Network (GCOS/GUAN) and successfully release 800 gm balloons which provide upper air soundings to the required 5 hPa level.

2. Integration into the Conventional Upper Air Network

Prior to purchase, an exhaustive analysis of all upper air systems technologies was undertaken and it was concluded that a network of ten Autosondes was the best mix of the new navaid systems and current radar wind find technology (Figure 1). An additional complication occurred in 1997 with the closure of the Omega navigation system. This forced the ABM to use GPS technology at its Antarctic stations and Cocos Island. A similar impact occurred at the Autosonde locations, which also need to run GPS radiosondes. At these stations there are increased costs of consumables (above standard radiosondes). Standard radiosondes were normally released only once per day at 00UTC with a further two per week (temporally staggered across the network of 50 stations) at 12UTC to provide a skeleton network.

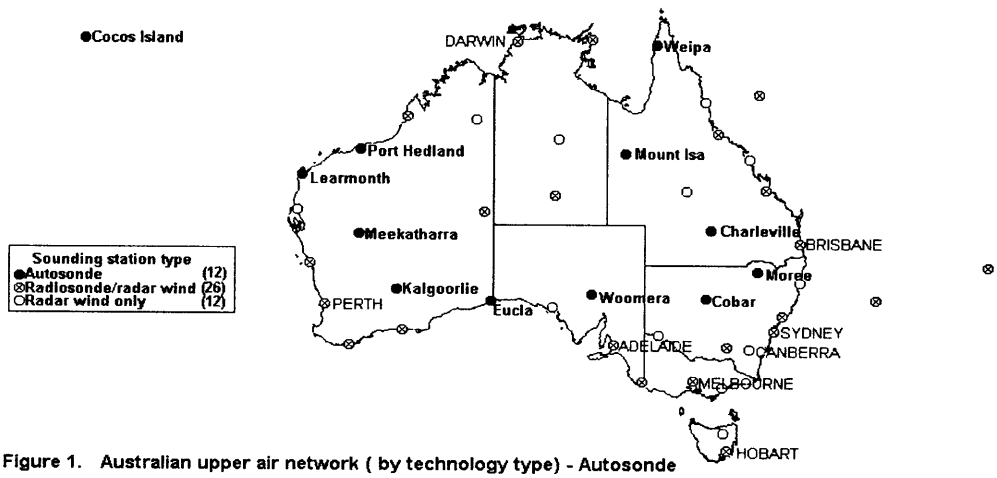

Figure 1. Australian upper air network (by technology type) - Autosonde
Note: Antarctic bases not shown - Macquarie Island, Mawson, Casey and Davis

With the introduction of the Autosondes, both 00 and 12 UTC radiosonde flights were required and this has also added considerably to the consumable costs. Balloon-based wind finding systems continue to provide the sole practical means of obtaining routine upper-wind data for the ABM's general network purposes on a day-to-day basis. Of the various systems available, wind finding radar has long been the backbone of the ABM's network, mainly because of the low cost of its passive balloon-borne package compared with the expensive active packages required by alternative systems such as GPS radiosondes and radio theodolites.

While performance and logistics issues have played some part in the choice of system for particular locations, such as the use of navaid sondes in the Antarctic, low consumables cost has been the predominant factor behind the choice of radar for most locations in the past. Additionally, the low-cost adaptation of Wind Find (WF) radars for dual-role operation has allowed a substantial expansion of Australian weather watch radar coverage in many areas where stand-alone Weather Watch (WW) radars would not have been economically justifiable.

One notable disadvantage of WF radar is the lack of a demonstrated capability for reliable unattended operation because of the target acquisition problem. In contrast, the Autosonde navaid sonde system has automated the balloon launch operation and requires no target acquisition, thereby allowing unattended operation for days at a time. (Note: When connected to an electrolytic hydrogen generator, daily visits are required due to safety considerations). This can have significant implications in regard to staff deployment and the need for buildings and other infrastructure. While the Autosonde has reduced requirements for staff in remote areas, experience has shown that an optimum of two staff are still required for unforeseen circumstances, performance of other surface observations and provision of meteorological information to the public. The complex nature of the Autosonde and associated computer operating systems requires a commensurate level of operator skill and computer literacy. A comprehensive training schedule is necessary for all staff that operate this equipment and thus the system does not readily lend itself to a system of cooperative or contract staffing. However, the Autosonde does allow the station to be unattended over periods of short-term staff absence such as a weekend, although this does not currently occur at ABM stations.

The uninstalled capital costs of WF radar and Autosondes are very broadly comparable, while further experience is needed to assess the longer-term differences in maintenance requirements. Both systems have their own peculiar mechanical complexities, but the Autosonde has an advantage in avoiding the expensive high-power components used in radar transmitters.

3. The Benefits and Costs of Introduction of the Automated Systems

A summary of the advantages and disadvantages of introducing these systems to remote harsh locations is given below:

Benefits:

- Occupational Health and Safety (OH&S) requirements considerably improved due to minimal hydrogen gas and balloon handling and nil high power transmitters.
- Alternative upper air technology added to overall network to avoid dependence on radar alone.
- Net running costs (staff and consumables) slightly less than original WF based systems.
- Maintenance costs less.
- World-wide move away from WF radar.
- Ability to initiate and quality control flights remotely from non-Autosonde locations.
- Ability to quality control climate data non-real-time.
- Ability to schedule additional flights at short notice (45 minutes): beneficial for severe weather and general adaptive observations.
- Technology should be able to be updated more readily (modular).

Costs:

- Consumable costs higher (but more than offset by reduced staffing requirements).
- Increased workload centrally to provide support for installation and on-going operation.
- Reduced capacity for intermediate (to 00 and 12 UTC) flights due to consumable costs.
- Autosonde computer technology can cause difficulty for some local staff.
- Risk associated with change in technology.
- Dependence on one supplier of technology at these particular locations in the network.

4. Technical Aspects - Installation

Implementation of the Autosonde network commenced in 1997 and has progressed as follows:

STATION	WMO NO.	INSTALLED	EXTREMES OF WEATHER AND ENVIRONMENT
Cobar	94711	May 1997	Dusty, +40°C summer temperature, 0°C minimum winter temperature
Cocos Island	96996	October 1997	Tropical cyclone prone, lightning prone, high humidity, maritime climate
Learmonth	94302	December 1997	Tropical cyclone prone, lightning prone, high humidity, maritime climate
Port Hedland	94312	May 1998	Tropical cyclone prone, lightning prone, high humidity, maritime climate
Meekatharra	94430	August 1998	Dusty, +40°C summer temperature
Mount Isa	94332	October 1998	Dusty, +40°C summer temperature
Weipa	94170	November 1998	Monsoonal rainfall tropical cyclone prone, lightning prone, +80% humidity, maritime climate
Eucla	94647	August 1999	Dusty, +40°C summer temperature, maritime climate
Charleville	94510	January 2000	Dusty, +40°C summer temperature, +70% humidity, -1°C minimum winter temperature.
Moree	95527	June 2000	Dusty, +40°C summer temperature, -1°C minimum winter temperature
Kalgoorlie	94637	Planned - 2000	Dusty, +40°C summer temperature
Woomera	94659	Planned - 2000	Dusty, +40°C summer temperature

Autosondes have been placed at radiosonde stations where, for various reasons, it had become difficult to guarantee continuity of upper air program. As noted above, the majority of these stations are in remote areas with fairly harsh climate extremes including both maritime and desert regimes. Autosondes located in the tropical cyclone prone areas of Northern Australia are installed to tropical cyclone ratings and have withstood (Learmonth, 1999) a Category 5 tropical cyclone, including a record wind gust for Australia of 267 kilometres per hour (Tropical Cyclone Vance, 1999)[1]. Minimal structural damage was sustained on this occasion and the unit was quickly returned to operational capability. (A.Valentine, 1999.)[2]

5. Technical Aspects - Operations

Implementation of the Autosonde network has seen a number of operational (and consumable) problems arise:

- Balloons not releasing due to adhesion during tropical downpours.
- Humidity affecting the GPS module and premature battery activation.
- Battery failure resulting in early cessation of soundings or failure of radiosonde to activate at release.
- Radiosonde inability to reach minimal signal strength resulting in sounding failure.
- Failure of gas valves and regulators when systems are connected to a hydrogen electrolyser
- Gas flow problems due to insect infestation in supply lines.
- Performance of air conditioning in extreme temperatures.
- Lightning strikes disabling fibre optic connection between the Autosonde and its automatic weather station.
- Poor GPS wind calculation. Causes including poor satellite geometry and intermediate frequency (IF) drift.

The Bureau has modified the fully automatic system to allow for manual quality control of soundings. This takes place in real-time by on-station staff or by staff at another nominated station. The ABM has been able to make a more effective utilisation of available staffing resources through the networking of Autosondes via remote terminals from capital city locations, where 24-hour operation is already maintained to meet aviation requirements. Networking also allows forecasting staff to remotely schedule ad hoc releases when stations are not staffed. This has been particularly useful during tropical cyclone seasons in northern Australia and for additional adaptive observations. Other ABM specific modifications (developed in cooperation with Vaisala Pty. Ltd.) and procedures include:

- A balloon bursting probe and water sprays are installed in the launch tank for safety reasons.
- Introduction of a central Help Desk which is available during sounding hours. This facility has retrieved (in real-time) over 200 soundings that would have been unrecoverable or greatly delayed without the service.
- Electrolytic hydrogen generators are used at several sites.
- A rain shield has been installed between the Autosonde container and the filling tank. The additional shielding now lessens the impact of monsoon rains on balloon release performance.
- Tie-downs for the Autosonde container and heavy-duty struts to support the launching tank have been installed for tropical cyclone proofing purposes.
- De-humidifiers are installed to prevent humidity affecting the transmitters and batteries of loaded radiosondes.
- Added optional wind shields to all systems.
- Most Autosondes are connected via a 64kb frame relay Wide Area Network (WAN). The standard modems are only used for backup. WAN facilities are unavailable at two stations. These stations use V32 modems which can impede successful completion of a sounding e.g. Weipa radio modem communications failure during wet weather.
- A remote Autosonde PC is located in the meteorological office of the site that the Autosonde is located. This PC is used to monitor and quality control soundings whenever the station is staffed.

- Another remote PC is based at a major capital city airport that always operates 24-hour rosters 365 days per year. The similarly trained staff quality control soundings and launch non-standard soundings whenever the meteorological office at the Autosonde site is not staffed.
- Extensive use is made of Windows NT scripting to automate a number of Australian-specific procedures.

6. Reliability/performance

Figure 2 shows the percentage of scheduled 12 and/or 00UTC soundings per month that reached at least 200 hPa. Not included are data relating to missing winds, non-supply of consumables or outages associated with maintenance policy. The lower percentages in May 1998 and May 1999 were mainly caused by consumable related problems.

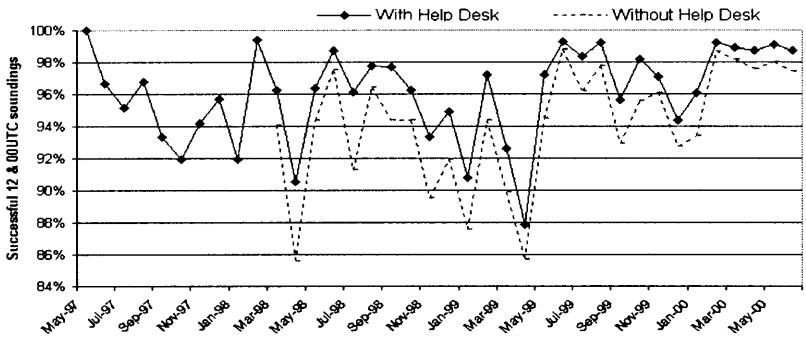

Figure 2. Historical Change in the Performance of the Autosonde Network

Typical reasons for sounding failure include:

- Balloon train snagging at release. This has been lessened by use of a Bureau designed parachute which is inserted into the balloon.
- Radiosonde activation failure. A reserve radiosonde is automatically released or, if this fails, a release is manually scheduled. Modifications to radiosonde design have lessened failure due to battery failure.
- Nil or missing winds. Modifications to the GPS module of the radiosonde as well as software changes (mainly for GPS IF drift) have seen a lessening of this problem. However, this problem still occurs with varying frequency due to use of consumable stock on hand.
- Frequency interference. This may be caused by a clash in radiosonde frequency during second releases.
- Non-delivery of messages and or data files. Usually recoverable by Help Desk.
- Operator error. The Autosonde is a highly complex system that requires a high level of operator training for both permanent and temporary staff.
- Gas flow problems caused by faults in either the hydrogen regulator attached to the gas supply or the gas flow control valve within the Autosonde. May be partly due to ABM use of electrolytic hydrogen generators.

7. Conclusions

Given that the ABM conventional systems could not be sustained at these particular stations in the network, the Autosonde network has made a very valuable contribution. However, continued support and ongoing development, especially for consumables, has been and is still required to maintain the satisfactory standard shown in recent months (Figure 2).

Acknowledgements

The authors would like to thank ABM engineering staff for their extensive work in adapting the system and for achieving many difficult installations, such as Weipa and Cocos Island. This included, in particular, Messrs Graham Jones, Ross Hibbins, Albert Houston and Laurence McBean.

Vaisala Pty. Ltd. (Australia) also provided excellent cooperation in solving the unique logistics and technical problems faced in the harsh conditions, in particular Messrs. Robert Caplikas and Richard Walsh.

---

1 *Tropical Cyclone Vance (1999): Meteorological Summary. Australian Bureau of Meteorology, Northern Territory Severe Weather Office.*

2 *A. Valentine (1999): Internal engineering report: Australian Bureau of Meteorology "Structural damage from TC Vance".*

****

UNATTENDED MICROWAVE REMOTE SENSING SYSTEM FOR WINTER CLOUDS PARAMETERS MONITORING

Koldaev A.V., Kadygrov V.E., Koloskov A.B., Miller E.A., Mironov A.F.

Central Aerological Observatory, Roshydromet,
#3 Pervomayskaya St. Dolgoprudny, Moscow Reg.,
141700 Russia, phone/fax +7 (095) 408-7758,
E-mail: attex@gin.global-one.ru

1. INTRODUCTION

It is well known that winter cloud at the middle and high latitudes of North Hemisphere are potentially dangerous for aircraft in-flight icing. During the last three winters at least one airplane crash within each season with many injured and killed were reported in the USA and Canada.
Although the problem of airplane in-flight icing is investigated within last 50 years in different countries, the development of the modern remote sensing technique for detection such a dangerous phenomena is still very actual. After FAA prognoses (USA Federal Aviation Administration) at least one icing induced crush per week will be observed within nearest 10 years due to increase of civil aviation flight intensity if no any new detection and protection technologies will be found.

The microwave remote sensing is one of the most developed and well applied technology for detection of supercooled liquid water zones, which are responsible for aircraft icing in winter clouds (E. Westwater, 1980). There are two basic restrictions of implementation of the microwave remote sensing into a practical use of civil airport service: 1. Ground based microwave radiometers can not distinguish the height of supercooled water location; 2. Ground based microwave systems are exposed to very harsh environmental conditions that are dramatically influenced not just on the accuracy, but on the reliability of the data also.

The theoretical possibility of the dangerous height determination - height of the supercooled water location was discussed in (Khaikine, 1994). In (Koldaev,1996) it was shown experimentally the ability of two wavelength microwave remote sensing to detect the height of supercooled liquid water into a winter clouds. Because of two references above, we will not discuss the theoretical background and experimental evidences of the method in the present article. Instead of that we will focus our attention on the description of the technical solutions of the second problem mentioned above. Thus the presented paper describes two approach for creation of commercial model of two wavelength ground based system capable of operating in an unattended mode with self calibration and data quality control provided.

2. TECHNICAL REQUIREMENTS TO UNATTENDED MICROWAVE SYSTEM

During the field experiments mentioned above, two wavelength ground-based microwave systems were used. The most advanced measuring system configuration had been designed for the Canadian Freezing Drizzle Experiment III which was carried out in Ottawa region during December 1997-February 1998. (Koldaev, 1998) It was a trailer housing with thermo-stabilizing system, in which two microwave radiometers with 85 GHz and 37 GHz working frequencies were installed. Atmospheric radiation was received through the radio-transparent window after its reflection by a flat metal sheet. The calibration was performed by using a "black body" and "clear sky" technique. For this purpose, an absorber was placed beneath the flat reflector. Then, the radiometers received signals from the absorber when the reflector was looking at the nadir direction. In fact, systems of

this kind mounted in a trailer to make long-term measurements are commonly used. The system was run by skilled personnel because almost all the procedures involved (such as calibration) required manual operation or at least supervision (data quality and radiometer operability control). The experience gained both from these operations and previously allows formulating basic limitations of most recent ground-based microwave systems and, therefore, developing technical requirements for an unattended system. The main problems and their possible solutions are presented in Table 1 in terms of comparison.

PROBLEM	SOLUTION
Precipitation problem for antenna system	Automated cleaning system adjusted for specific precipitation type
"Black body" quality control: thermal equilibrium with the environment, precipitation, direct sun and windshield factor	Black body in weatherproof housing
Thermo-stabilization of the microwave system's operation volume.	Automated control and maintaining the whole system's stable temperature
Manual calibration during "clear sky" conditions.	Automated regular calibration procedure under any weather conditions with a built-in "black body"
Expert control of environmental conditions acceptable for proper calibrations	Automated monitoring of "clear sky" conditions
Commonly, the systems are not portable	Portable, easy-to- installs system with a possibility of autonomous power supply and data transmission via radio modem.

Table 1. Problems, to be resolved for creating an unattended system

3.CONSTRUCTION OF THE ALPHA-SAMPLE SYSTEM

The alpha-sample of the system, which was aimed to meet the requirements above, was created in Russian Company ATTEX under supervision of the CAO specialists in 1999.
The drawing and the general view of the system are presented in Fig. 1.
The main features of the system were as follows:

I) Weather protection: each radiometer is installed in a separate housing. The housing has the shape of a tube 14" in diameter and 32" long. The tube consists of two parts - a stationary and a rotating one. The stationary part includes a microwave radiometer with an antenna, a thermo-stabilizing system, a stepping motor, two electromagnetic clicks, a microprocessor control board, and a set of sensors. The rotating part includes a turning flat metal reflector with one side used as a reflector and the other covered by an absorber. Atmospheric radiation is received through a radio-transparent window at the top of the rotating part. The connection between the rotating and stationary parts is waterproof.
II) All-weather operation: the shape of the weather protection housing prevents snow and water accumulation. The devices are installed in separate housings. To protect the radio-transparent window from water drops or snow, the rotating part is turned each 5-20 minutes and the windshield cleaners, who are solid with the stationary part of the housing, clean it. Two thermo-stabilizing systems are used to provide a $+40^0C/-40^0C$ range of operation. The first one is inside the radiometer. It maintains $+50^0C+/-0.5^0C$ temperature inside the radiometer box. The second one is in the stationary part of the housing. It does not provide such an accurate thermo-stabilization, but makes it possible to control the inner temperature by using a heating/cooling system.
III) Self-calibration: when the rotating part is turning to clean the window, one of the electromagnetic clicks releases the flat mirror for it to turn over and expose the absorber. The other

click fixes the mirror's position. The rotating part is not thermally insulated from the environment but has good thermal insulation from the stationary part and the absorber being at ambient temperature.
As the ambient temperature changes at least by 5^0C every 24 hours, one needs to get information about the recent temperature value and the output code of the radiometer to continuously update the calibration data set.
IV) Unattended operation: unattended mode of operation as well as "real-time" data processing and transmission via radio modem is performed by the in-built microprocessor board. A 12 V automobile accumulator is used as power supply.

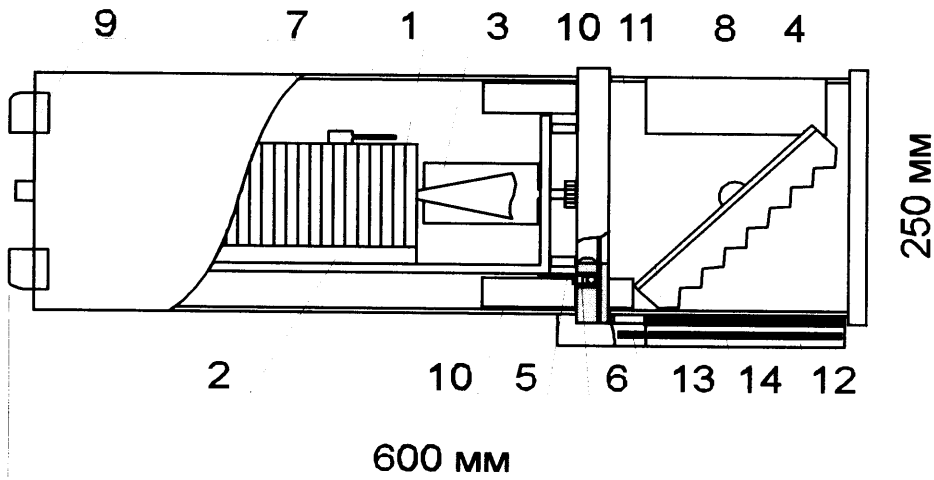

Figure 1. Drawings of the alpha-sample of unattended system

1.Radiometer 2.Microprocessor card 3.Stepping motor 4.Mirror 5.Sensor of antenna position 6.Magnet 7.Termistor 8. Teflon 9.Fans 10.Mirror control units 11."Black body" 12.Cleaning unit 13.Precipitation sensor with heater 14.Cleaning heater

4. THE BETTA-SAMPLE OF UNATTENDED SYSTEM

The first field-test with the unattended system described above were carried out in a frame the field project AIRS (Alliance Icing Research Study) conducted by Environment Canada with support of FAA within November 29, 1999- February 19,2000. The system was installed in Ottawa international airport during December and January and in Montreal international airport during February. Field-tests shown that the system can operate in unattended mode reliably within a long period of time. That means automatic mode of calibrations and real time data processing and transmitting were working well. But at the same time a number of disadvantageous were observed. Namely:
1.The calibration coefficients were strongly depends on the type of the surroundings -wet and dry earth surface as well as surface covered by snow led to different value of the coefficients.
2. Precipitation sensor based on the measurements of heat losses due to precipitation can not work properly under harsh conditions.
3. Even the maximum rate of the rotating can not provide proper cleaning of the Teflon window, which lead to accumulation of snow or freezing the window.
The analysis of these disadvantageous indicates that: 1. instability of calibration coefficients is the result of side lobes of antenna system; 2. precipitation sensor should work without direct contact with precipitation; 3. rotating of the teflon head should be done continuously to provide cleaning in all weather condition.
The beta-sample of the system was created in ATTEX recently and is accumulated all technical solutions to avoid the problems indicated during the test with the alpha-sample.

The picture of the beta-sample is presented at the Fig 2

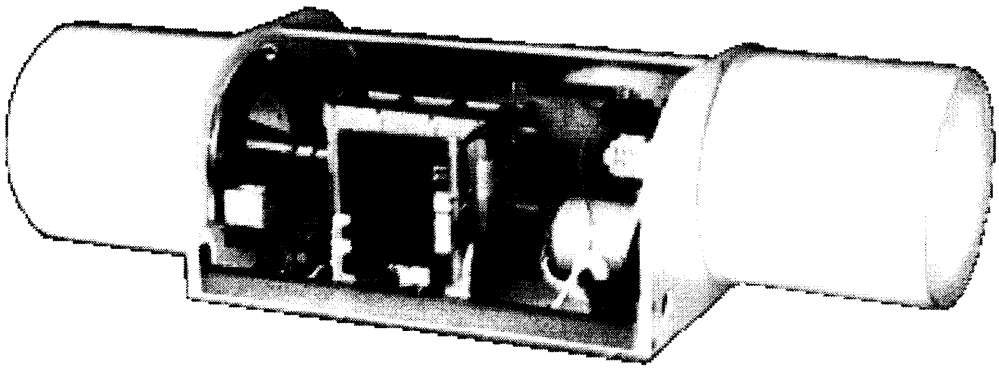

Figure 2. Overview of the beta-sample of ground based microwave unattended system

The principal difference of the beta-sample is that the rotating head is made with teflon in full. It means no any metal construction and details are not included. Such a feature allow to rotate the teflon head continuously during the receiving the signals from zenith direction. The rotation is provided by a regular 12 V DC motor. The flat mirror is not connected any how with the rotating part and is scanned by a special high accuracy stepping motor which is stationary installed inside the rotating head. The "black body" for inside calibrations is installed on the chase of the stepping motor beneath the mirror. So the calibrations are conducted when the mirror is turned to nadir direction. The complete teflon made rotating head in accompany with separately scanned mirror reduced the side lobe effects very much that provides stability of calibration coefficients despite on the environment. A new precipitation sensor is made on the "capacitor" principle and mounted separately from the cleaning unit.

5. ACKNOWLEDGEMENTS

The authors are very thankful to Walter Strapp for his kind assistance in the experimental work with alpha sample of unattended microwave systems during AIRS project and very useful recommendations.
We also thank Arkadi Troitsky for his permanent attention to this work.

6. REFERENCES

1. Westwater E.R., Guirand F.O., "Ground-based microwave radiometric retrieval of precipitable water vapour in the presence of clouds with high liquid content", *Rad.Sci.*, v15,No15, 947-957 (1980)
2. Khaikin M.N., Koldaev A.V., "Remote sensing of aircraft icing zones parameters", *TECO-94 WMO/TD-No 588 Report No 57*, 413-417 (1994)
3. Koldaev A.V., Troitsky A.V., Strapp J.W. and Sheppard B. Ground based microwave measurements of integral liquid water content of Arctic clouds during BASE. *Proc. Of 12-th International Conference on Clouds and Precipitation*, v.1 pp.442-445, Zurich, Swizerland, 1996.
4. Koldaev A.V., Kadygrov E.N., Troitsky A.V., "Remote sensing of average LWC layer height inn winter clouds", *Proceedings of the eighth atmospheric radiation measurement (ARM) science team meeting*, 381-384 (1998).

Static windsensor Quatro for harsh environmental conditions

Ernesto Burgos, Kurt Nemeth
Wilh. Lambrecht GmbH
Friedländer Weg 65-67
37085 Göttingen, Germany

Tel +49-(0)551-4958-0
Fax +49-(0)551-4958-312
E-Mail info@lambrecht.net
Internet www.lambrecht.net

1 GENERAL

The Lambrecht Static windsensor Quatro, rugged and reliable, all solid-state without moving parts, is dedicated for various meteorological purposes like meteorological service, air traffic control, vessels, air pollution control, environmental sciences and industry. The sensor features a high sophisticated instrument for severe environmental conditions like high mountain, industrial, offshore, navy and military applications.

The rugged mechanical construction of the instrument, the coated sensor elements and the electronics design perform a mean time between failure (MTBF) of 25.000 hours. A heated head keeps the instrument icefree up to -40 degrees despite of extreme wind-chill effects. The instrument fullfills all relevant regulations like WMO No6, VDI 3786 and is proofed for EMC, ESD, shock, vibration, salt spray and operates in all weather conditions like rain, fog, temperature, dust, industrial pollution and sand storms.

The high speed range of up to 80 m/s and the low starting threshold make the instruments suitable for windmeasurings from small breezes to force hurricanes in all climate conditions.

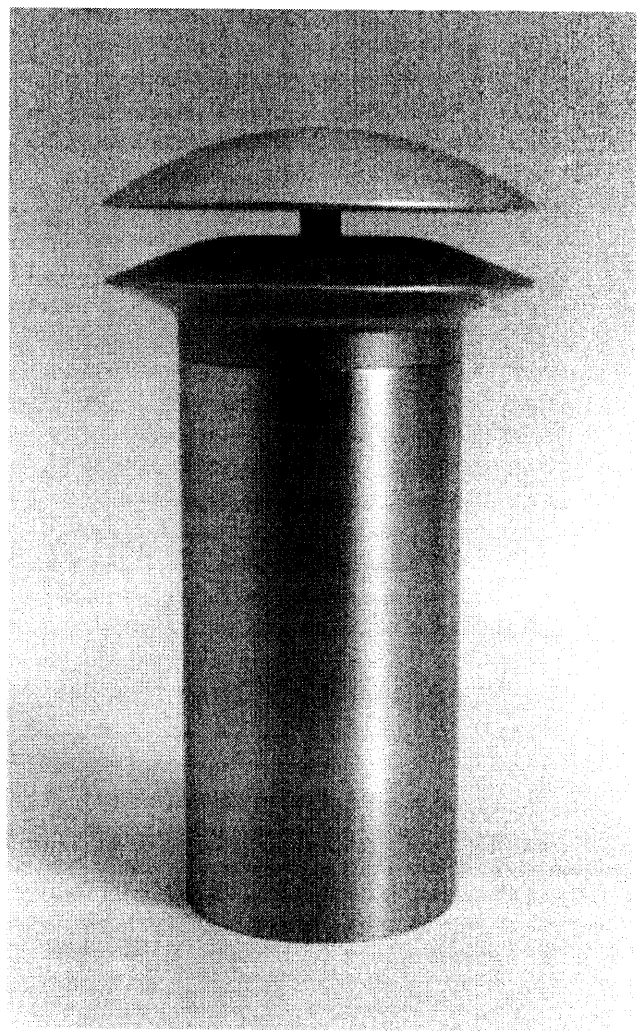

2 INTRODUCTION

The Lambrecht Static windsensor Quatro incorporates an innovative wind velocity and direction measurement system that detects thermal field variations (TFV) caused by the wind flowing past a heated cylinder.

The TFV technique is very accurate, responds rapidly to wind changes and has a low starting threshold of 0.1 m/s and a high speed range of 80 m/s. The instrument requires no calibration, no bearing replacement or any other periodic maintenance to keep its accurate performance and resists agressive chemical and salty environmental conditions.

The Static windsensor is a compact and completely self-contained meteorological instrument. All components are enclosed in a sealed, ice-free and weatherproof cylinder. The incorporated microprocessor determines weather parameters, performing self-diagnostic tests and transmitting data and status information. The system is an intelligent device capable of transmitting various data like instantaneous, gliding mean and extreme values over an RS-485 serial digital interface.

3 THEORY OF OPERATION

Unique for meteorological sensors is its patented Thermal Field Variation (TFV) technique for measuring wind speed and direction. As already explained, the station detects thermal field changes caused by wind passing by a heated cylinder exposed to the winds. This principle is easily demonstrated when using a wet finger to sense the wind speed and direction. The TFV-Sensor is a small, rugged cylinder with several plated vertical resistor/temperature sensors mounted symmetrically around its outer surface. The cylinder surface is heated to a controlled, constant temperature of 50 °C above the ambient temperature. At calm conditions, the thermal field radiation of the cylinder is homogeneous and all the vertical temperature sensors sense the same signal level.

TFV Principle

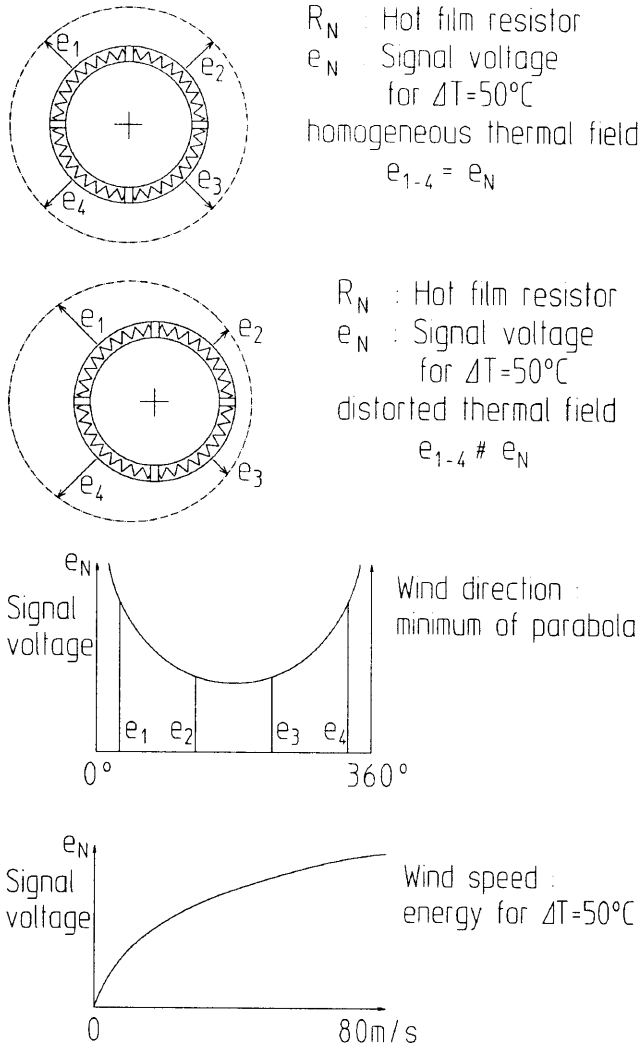

The thermal field is being influenced by passing air, which results in a symmetric, parabolic shape. The signals from the vertical sensors are used by the microprocessor to determine the parabolic form showing the related wind direction. The amount of energy required to maintain the surface at a constant temperature above ambient is used to determine the wind velocity. Because thermal radiation and convection depend on air density, the required balance energy is related to the ambient temperature and barometric pressure. The determination for the windspeed is performed by the derived algorithm from the King Formula with difference temperature control method.

$$U = C_R \cdot \frac{T}{P}(e^2 - e_0^2)^2$$

e_0	Reference Voltage	at U=0
e	Voltage	[V]
U	Wind speed	[m/s]
P	ambient Pressure	[hPa]
T	ambient Temperature	[K]
C_R	sensorspecific Constant	

4 TECHNICAL DESCRIPTION

The Lambrecht Static windsensor Quatro is an all solid-state design without moving parts, consisting of:

1) Hot film resistors, 2) Signal conditioning with temperature/pressure compensation, 3) Built-In test Equipment (BITE) and serial communications interface, 4) DC power supply and heating device and 5) Weatherproof housing.

1) The hot film resistors are controlled with constant resistor method by measuring the signal voltage and controlling the current via the microprocessor to keep the constant temperature difference of 50 degrees.

2) The microprocessor signal conditioner consisting of analog-digital-converter, digital controlled current source, temperature and pressure sensor for air density compensation, microprocessor with RAM, Flash-EPROM, watchdog and voltage control device.

3) BITE consisting of individual hot film resistor check, supply voltage range, heating control, internal reference and housekeeping data for status report via the serial interface. Data communication consisting of instantaneous, gliding means of 2 / 10 minutes and extreme values via ESD-protected RS 485 interface.

4) Galvanic isolated and overvoltage protected DC-DC-Converter for wide input range of 10 to 30 V_{DC}. Temperature controlled heating device for non-icing operation.

5) Weatherproof housing with heated head, TFV-Sensor, sealed electronic devices, temperature, pressure sensor and 12 pin connector for standardized 2"-tube installation with low weight and small dimensions. Rugged and reliable construction with non-corrosive materials and sensor with protective, teflon coated surface.

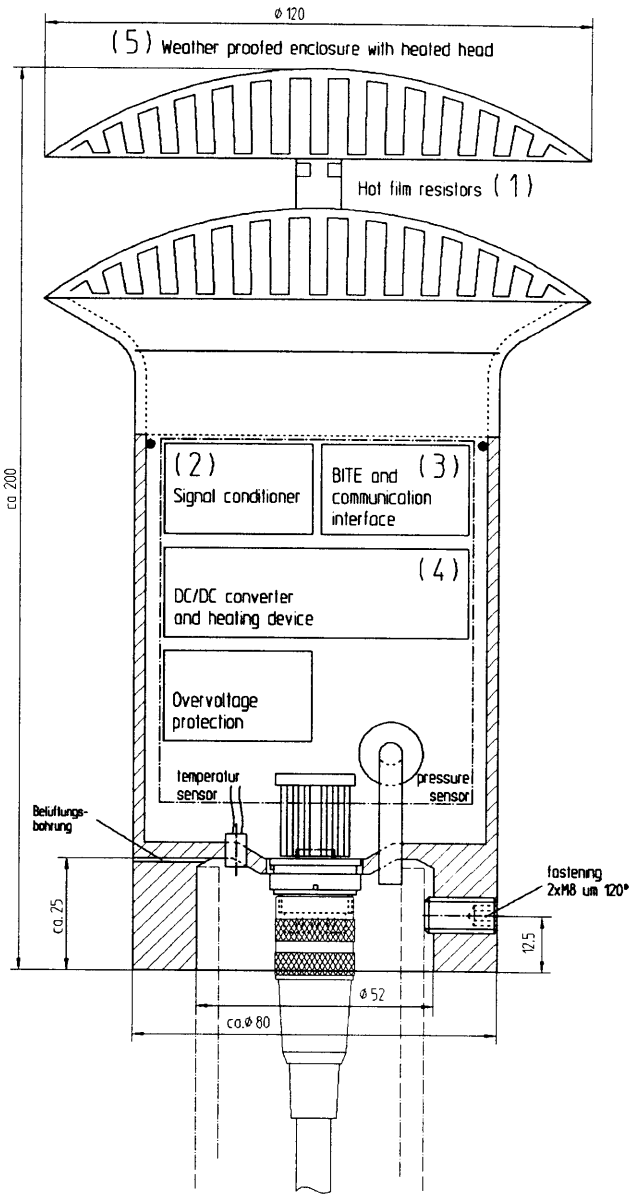

5 TECHNICAL DATA

Wind speed:	0.1 to 80 m/s
Resolution:	0.1 m/s
Accuracy:	±2% (0 to 35 m/s) ±4% (35 to 80 m/s)
Wind direction:	0 to 360 degrees
Resolution:	1 degree
Accuracy:	±2.5 degrees
Measuring interval:	100 msec
Operating range:	-40 to +60 degrees
Power supply: (Sensor)	10 to 30 V_{DC} / 15 VA
(Heating Device)	20 to 28 V_{DC} / 100 VA
Isolation voltage:	2.500 V_{DC}
Serial port:	RS 485, ASCII-Data-Output
Distance:	1.200 m (9600 Baud)
Data:	Instantaneous value Mean value 2/10 min Gust and variance Sensor status
Protection class:	IP 63
Dimensions:	height 200 mm
Diameter:	110 mm
Weight:	1.5 kg

6 REFERENCES AND APPROVALS

The Lambrecht Static windsensor Quatro is operating on the peak of the Klein Matterhorn in the Swiss alps on 3980 m above sea level since 1998. The windsensor has been installed with a complete weather station SYNMET with additional parameters like temperature, relative humidity, pressure, precipitation and sunshine duration and reports the SYNOP-Message continously. Extreme temperatures to -40 degrees and high windspeed of 70 m/s have been recorded and the extreme occurence of lightning strokes are regular operating conditions. The complete safety design consists of overvoltage protection elements for signal and power lines, galvanic isolated serial interfaces, shielded cables, glasfibre-mast, central earthing , AC mains with UPS and GSM-communication.

Technical improvements regarding lighting strokes and vertical upstreamed windforces to the head of the instrument have been made due to occured problems during the two year operation period.

At the time beeing this station is the highest installed automatic unattended weather station of the world.

An actual marine environmental test regarding navy vessel application will be performed this year at the official test authority of the German armed forces (Bundeswehr).

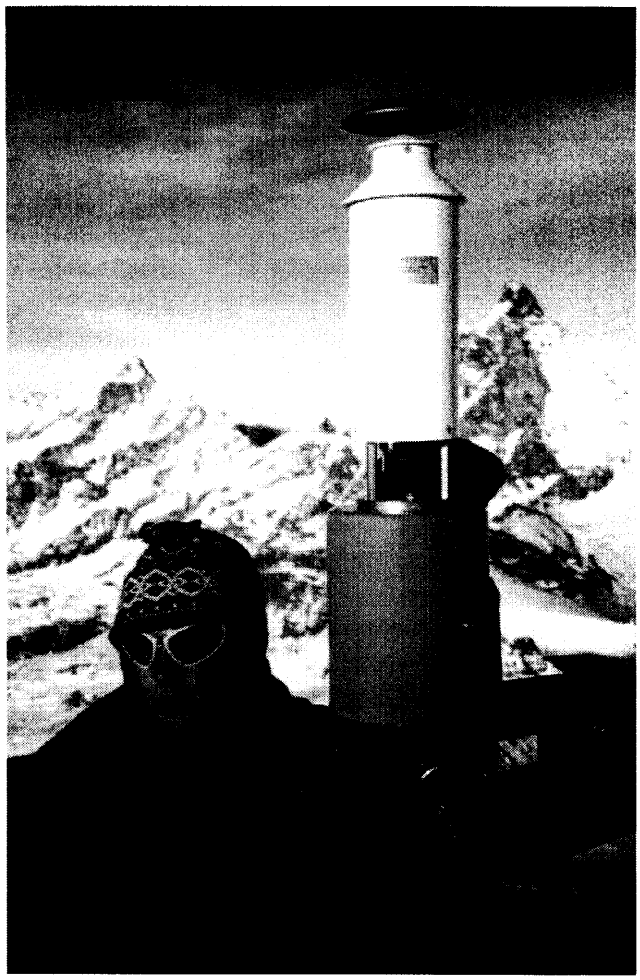

7 QUALITY CONTROL

All windsensors are tested in the Lambrecht windtunnel and the tolerances of the hot film resistors are compensated during the automated range simulation where the individual sensorspecific constant is stored in the EEPROM of the microprocessor signal conditioner. The Lambrecht quality management, certified according to ISO 9001 since 1995, assures the accuracy and performance of the instrument for the use in regular meteorological and harsh environmental conditions or where safety control is required.

8 STANDARDS AND REGULATIONS

EMC:	EN 50081/82, VG 95773
ESD:	IEC 1000-4-2
Electric safety:	VDE 100
Wind:	WMO-No.8 VDI 3786 Bl 2
Shock:	MIL-S-901C
Vibration:	MIL-STD-167
General:	MIL-STD-810B

1 MEASUREMENT TECHNOLOGY, PERFORMANCE, AND QUALITY ASSURANCE

1.6 Urban Meteorology

Keynote Paper

THE REQUIREMENTS OF URBAN METEOROLOGICAL MEASUREMENTS AND CIMO's ROLE

R.D. Vashistha
Instruments Division, India Meteorological Dept., Pune-5, India.
Fax: (91) (020) 5533201, Email: ramdhanv@hotmail.com or imdpune@pn3.vsnl.net.in

1. Introduction:

The science of meteorology heavily depends on the methodical and routine observations, experiments and analytical scientific methods. The observations enable a proper evaluation of the changes in each of the weather elements. The observations are made either using sensory parts of the observing personnel or instruments. Meteorological observations cater to different disciplines like synoptic, climatological, aeronautical, agricultural and marine meteorology. Meteorological observing stations are spaced depending on the purpose for which the measurements are required, the variability of the weather elements and the terrain of the area. A strict conformity exists on the parameters to be observed, siting and exposure conditions and the schedule of measurements. In almost all cases the recording site is expected to represent a large area of homogenous terrain and vegetation coverage. The parameters to be monitored and the accuracy requirements in their measurements, however, vary depending on the specific needs for the data. The instruments have accordingly different specifications and characteristics so as to provide quality of data required for the specific purposes. Instruments used for climatological purposes need to be rugged, even if they are slow in response while those needed for aviation purposes need to have very high resolving powers and fast in response to changing weather conditions.

Measurements made at a climatological or synoptic station located in near-rural conditions may represent a large area say 150 km around the station. This, however, is not true for a station located near an urban area. Such a representative site even inside the urban area becomes more difficult and in most of the cases, the site requirements are specific for the selected urban area depending on the peculiarities of the urban area. These, in all probability, will be in variance with those of WMO guidelines. Even if the site requirements were satisfied at the time of commissioning of the station, these do get seriously vitiated with time when the urban area expands and creeps all round the observing site.

There is no set pattern of layouts in urban areas. The spacing between and the size of individual buildings are neither uniform. Besides an urban area may have few industries at its centre or at its peripheries, resulting in high fluctuations in temperature regime and the pollutant deposits at different parts of the urban area. The buildings with their differing heights and girths pose obstacles to the general wind flow and cause serious eddy currents around them. Because of the disproportionate and varied distributions in the temperature and wind fields in such environments, monitoring the weather parameters in an urban area becomes more complex. Human interference by way of domestic and commercial activities, and vehicular traffic also lead to major perturbations in the general weather pattern of the area. The heat and moisture released by the human activities and the gaseous exhausts especially from vehicles and industries have effects on the urban weather to varying degrees.

Thus monitoring the changes in the weather elements in an urban location is a highly complicated task. The selection of sites for such measurements cannot conform to the general sites requirements as laid down by WMO. We may not also be able to lay down a generalised criteria for urban meteorology as the requirements will be different and peculiar for each urban location, depending on the spatial locations of housings - residential, business and industrial, open-air parks, vegetation, playgrounds etc. and also on the general weather pattern of the country side in which the individual town or city is located. The standard instruments, which are rugged and simple in design for use in a synoptic or climatological network system as per WMO norm, are not suitable for urban studies. They have their own limitations under such varying and typical exposure conditions of an urban location. Some areas may need a small network of observing stations because of the large variations in the settlement patterns. Conventional type of instruments in such cases, though economically viable, will need a large number of manpower, which is not otherwise cost-effective. Besides, such instruments will need periodical manual observations, which will disturb the otherwise highly fragile and continuously changing urban environment. This would then mean that a remote sensing type of instrumentation with minimum need for manual maintenance and operation has to be resorted to. This, however, imposes a constraint as the initial financial input will he higher, though it would be more efficient working system in the long run.

Thus organizing a measurement system in an urban environment requires careful consideration of the cost-effectiveness of operating each such station, the site selection depending on the peculiarity of each location and efficient instrumentation suitable for specific site.

2. The Urban Atmosphere:

Oke (1998) has illustrated a very lively idealized vertical structure of the urban atmosphere. Urbanization process activates many atmospheric anomalies. The change in the nature of the surface characteristics cannot be over stressed. The buildings, trees, roads etc. create their own microclimate and these repetitive structures and elements are recombined into larger microscale climate unit. When considering the picture as illustrated by Oke, a complicated picture emerges out. It is rather an uphill task for a meteorologist to locate a station in an Urban Terrain Zone (UTZ), which could be representing the whole city or town. Nevertheless, it may be possible to find out representative areas of suitable dimension where an urban climate station could be established.

3. The need of establishing guidelines for observations in urban areas:

Establishing guidelines for observations in urban areas is a complex issue and this need has been felt since very long. WMO tried to address this issue by circulating a questionnaire in 1975 for finding out the status of urban observations and the need for guidelines. Van Gysegem (1978) recognised the complexities of these issues from this report and recommended more research in the field before defining guidelines. He stressed mainly on two vital issues of exposure for representation of data and suitable sensors, which could respond to the turbulent atmosphere without errors. More than 20 years of time span has opened up the urban issue with a new vigor among climatologists. With the availability of state-of-the-art technology, the field of urban observations could be taken up in a more satisfying term when a climatologist may have to study the variations in temperatures at a micro scale level from 0.2 C to 0.5 C or so over a period of a decade or more. When a climatologist makes his study, he presumes that observing network provide him fairly accurate and error free data. He normally does not possess the details of measuring sites and goes by the established criterion for instrument exposure, siting, representation of measurements and homogeneity of data.

4. Siting and type of Meteorological Instruments:

As discussed in the preceding paragraphs, the decision making process that leads to the selection of a site and placements of instruments in urban area is a complex one and involves hard decisions many times deviating from the established WMO norms and national Guides. This flexibility is very essential while introducing the concept of requirement of urban measurements. For instance, in a densely populated urban location, there will not be any open area where a site satisfying the general requirements of conventional meteorological observing site could be found. If no location is suitable at the ground level, we may have no option to use an elevated location, such as a terrace of a building. In such thickly populated areas, the effective boundary layer also is lifted up. The orientation of rows of buildings also contribute to changes in the free flow of winds, giving rise to calm areas behind the buildings and eddy currents and whirls beyond that vicinity. They may also give rise to the tunneling effect, causing channelised strong wind flow if the prevailing wind direction is parallel to the rows of buildings. In such cases, the temperature regime is highly disturbed. Following paragraphs highlight the requirements, which are relevant for individual elements in urban areas.

4.1 Temperature and Humidity:

The measurement of temperature and humidity under a standard thermometer screen popularly called Stevenson's screen made from special type of wood or FRP at 2m above ground is appropriate. The distance to obstacles should be kept a minimum of 2 times of their height. However, some relaxation may have to be kept in mind while considering the safety, access and availability of infrastructure facilities for maintaining the site. The size of the screen, however, is to suit the type and size of sensors used.

A mercury-in-glass thermometer may appear very cost effective as they have the required accuracy and long-term stability. This would, however, need large size thermometer screen and manpower for making the periodic eye measurements. As mentioned earlier, it is not cost effective in long-term considerations. Besides, it is not desirable to frequently disturb the environment condition around the thermometers by regular opening and closing the screen door. A platinum resistance thermometer or a thermistor thermometer, having sufficient stability in calibration and larger resolving power will allow fairly maintenance-free measurements and also remote sensing of temperature. Being very small in size, the thermometer screens will also be unobtrusive and can be installed easily.

The best way of measuring humidity is to have a "wet-bulb" thermometer, with the sensor kept moist by conventional wick immersed in water. This, however, will again need frequent changing of the distilled water, which again call for sufficient manpower. It would, therefore, be necessary to go in for sensors whose characteristics change with water vapour content in the atmosphere. Lithium chloride hygroscopic resistors or similar sensors will ideally suit the remote sensing methods, though sufficient care steps have to be undertaken to overcome their deficiencies (ref.18) (WMO, 1986). The polymer dielectric capacitive type of

sensor, popularly known as HUMICAP could also be used for measurement of humidity in urban areas when dust and acidic pollution is less

4.2 Soil Temperature:

Soil temperature measurement does not form a part of a standard climate station. Nevertheless, this parameter needs to be considered while planning an urban station. The measurement of soil temperature at a depth of around 0.5m and more may provide a better understanding of urban thermal modification. Though this parameter will give good data, it is highly doubtful if one can get a suitable site, which no one will tread on. It is necessary that the site is not in a depression location where rainwater is likely to stagnate after a spell of rain. It also should not be too close to large water reservoirs, watered gardens etc. from which the soil may get additional moisture supply.

A resistance thermometer or a thermocouple thermometer would meet the measurement requirement with remote recording feasibility.

4.3 Wind Speed and direction:

While selecting a site in an urban area, the available standard procedures for installing wind instruments pose an uphill task and do not work. The presence of trees, buildings, streets make it rather impossible to take measurement at a distance of 10 times from the obstacle and at a height of 10m. A height of 10m for wind measurement will not give satisfactory results in urban area with taller obstacles. Minimum height for wind measurement is the top of the roughness sublayer and a method to predict its height should be evolved. In very crude terms, it is about 2½ to 4 times the ZH (typical height of building and trees) [Oke 1998]. It is desirable to place the wind instruments at another place nearby better exposed to the wind rather than installing them in the same enclosure where temperature and humidity measurements are observed. However, special care is required to be taken while selecting the supporting structure so that the airflow is not distorted and erroneous observations do not waste all the efforts. Installing the wind equipment on rooftops is not recommended as such sites may give distorted wind measurements.

There are quite a number of wind instruments available. Leaving out cup-counter anemometers, as they need manual observations, cup generator anemometers, propeller sensor anemometers and photosensitive anemometers are most suitable for the remote sensing wind measurements. The signal converter suitable for the remote indication of the wind speed though the commonly used rotation sensors is the electrical contact breaker. This may be a mechanical one or a permanent magnet reed-relay device. In either case, the electrical pulses, which are proportional to wind speed, are measured. Both suffer because of inherent inertia that have to be overcome, thus raising the minimum threshold of wind speed. The photosensitive type uses the optical light chopper device in which the rotational sensors cut off the light from an LED from illuminating a photodiode. The resistance of the reverse-biased photodiode falls in proportion to the illumination, which is masked by a rotating disk attached to the rotating sensor. The signal converter can also be achieved by the use of a brushless a.c. generator in which the rotating magnet induces a.c. voltage in the stationary stator winding. The use of sonic anemometers could also be a good alternative to cup anemometers but at present more experience is required to be gained in their long term reliability.

4.4 Precipitation:

The measurement of total precipitation and rate of precipitation are important for urban hydrological applications. As a standard practice the site of raingauge should be well away from trees and buildings, walls or other obstructions. The distance of any such obstacle from raingauge should not be less than twice the height of the object above the rim of the gauge and preferably four times the height. However, very open sites, though suitable for other instruments may pose difficulty in rainfall catch particularly in strong winds. This also makes a strong case for not siting the raingauge at a similar height of wind sensors. The exact layout of the buildings – domestic, industrial and commercial - has a great influence on the amount of rainfall that reaches the ground in a city, as they do affect the wind speed and directions. The terrain – a slopping surface as in the case of hilly terrain and a meadow shape – and the available open space for measurements at the ground level also decides on the site for the rain gauge. Unless the rainfall is due to a system like monsoon currents or low pressure phenomena like depressions or storms, the distribution of the precipitation over an area is not likely to be even and hence rainfall measured at an open space which may be at a given part of the city, is not likely to be representative of the area. In case spatial distribution is desired inside the city area, the site criteria laid down for a normal meteorological station will have to be breached and measurements may have to be made even on elevated locations, if no suitable site is available at the ground level. Windshields may then have to be provided for the precipitation gauge.

Since measurement of precipitation does not get vitiated much due to measurements being recorded by an observer, it is enough if a Simon raingauge or a siphon-recording rain gauge is used. However, this would need manpower for measuring the rainfall and for maintenance, especially an urban environment is

likely to produce large quantities of pollutants that may settle in to the precipitation gauge. For remote sensing, tipping bucket precipitation recorder in which each motion of a twin metallic vessel resting on a knife-edge support causes an electric pulse in an electrical circuit switched on by a permanent magnet – actuated reed-relay. The tipping bucket sensor and the recording mechanism are connected by a two-lead cable to a digital counting system. The system is highly suitable for automatic monitoring. However, it suffers on three important accounts, (i) discrete nature of the data, particularly with light rain and drizzle, (ii) loss in recording due to time lag in successive tipping motions and (iii) appreciable evaporation losses from the buckets. A volumetric-valve type sensor is another design that can be used. It is a small cylindrical vessel provided with an electric valve at the outlet, which is operated by an electric water-conductivity relay. The upper parts of the vessel hold the electrodes. The rainwater as it enters the vessel and reaches the electrodes, an electric current is passed to obtain an electric signal, which operates a magnetic valve to drain the water out. Each draining cycle is digitally counted. This system enables one to achieve improved sensitivity by smaller quantizing step, improved accuracy because of the small discharge time and reduces the evaporation losses.

Solid precipitation is best made using weighing balance precipitation recorders.

4.5 Radiation and bright sunshine:

The requirement of measurement of direct solar and global irradiance and duration of bright sunshine in the urban areas could be met by mounting the instruments on the roof of a tall building, which is free from the shadow of adjoining trees or other taller objects. Nevertheless the height above the ground and its surface are important if one has to measure the net radiant energy where albedo plays an important role.

Global solar radiant exposure is normally measured using blackened thermopile sensor, which is protected from, weather and dust by two concentrically mounted hemispherical glass covers. These glass covers also serve to filter off the terrestrial radiation from the atmosphere. The thermo e.m.f output can be measured using an integrator or a data acquisition system. Since we have to measure energy over a time, instantaneous recording of the value at specified times, as in the case of other weather elements will not be of any use. Only integrating system over known time intervals is needed so as to obtain the total energy received during the interval. Photo sensitive transducers like silicon photodiode are also being used, even though their response is not flat in the entire wavelength ranges of concern.

Direct solar irradiance is normally recorded using a thermopile pyrheliometer mounted on a solar tracker. Thermopile pyrheliometers have thermopiles mounted at one end of a long metallic tube whose other end is exposed to the sun. To minimize recording of diffuse irradiance, a series of diaphragms limit the view angle to not larger than 5o. A sighting device helps in keeping the sensor always perpendicular to the solar irradiation. The instrument is mounted on a good solar tracker to keep the sensor always oriented at the sun. Whenever the sun is obstructed by opaque clouds the output drops to zero. The amount of radiant energy also gets affected by dust and smoke particles that lie in the path of sun's irradiation. Thus it is possible to evaluate qualitatively the effect of clouds and the extent of atmospheric pollution.

Measuring net radiant energy in an urban area is a more difficult task, as the net pyrradiometer has to be installed near the surface, yet free from obstructions and even human movement in its vicinity. The buildings around also contribute to the energy level by their emissions at their own temperatures. Unless a very careful watch is maintained, the data collected will not be representative.

Measurement of sunshine can be made using conventional sunshine recorder or photoelectric recorders with chopping blades. In the case of pyranometers it is necessary to have temperature compensation provisions. The pyranometers should not have cosine error, spectral response and non-linear output. Similar characteristics should be ensured for pyrheliometers also. In addition the solar tracker should be precise in tracking the sun. It is necessary to have periodic checks on the proper performance of the solar tracker. In all cases, exact North-South alignment and exact horizontality (proper leveling) have to be ensured. In the cases of solar tracker and the sunshine recorder, they should be adjusted for latitudinal inclination. All radiation instruments need periodic check and regular cleaning is essential to ensure reasonably reliable data.

4.6 Atmospheric Pressure:

The measurement of atmospheric pressure in urban areas has not been considered by many experts. This parameter is important for an urban climatologist when the city is too large with hilly terrain, water bodies and surrounded by coastlines. Pressure anomalies in the UTZ may help weathermen in assessing the local extreme events, which have become a cause of concern to a city dweller.

The measurement of atmospheric pressure in the city does not pose significant problems. Exposure requirements are met by mounting the instruments along with the temperature sensor shield or

independently in a separate enclosure at the same height as temperature shield. However, it is stressed that most of the measuring devices for atmospheric pressure are quite expensive and proper care is required to be taken regarding the security. The instruments should be placed in an enclosure, which can be locked.

The basic instruments for the measurement of atmospheric pressure like mercury barometer and aneroid barometer, though reliable, need continuous presence of manpower for observation and maintenance. They need elaborate arrangement for installation including a robust enclosure. For urban measurements the sensors like silicon capacitive absolute pressure sensor with remote indicating facility will be more suitable. These sensors need microprocessor-based electronics for high order linearization and thermal compensation.

4.7 Evaporation:

Measurement of evaporation using the pan system will not give meaningful observations. The microscale advection of heat from buildings will make the observation unrealistic. It is also difficult to evolve a meaningful pan coefficient for urban surroundings.

4.8 Atmospheric Pollution:

A meteorological air pollution station will monitor the concentration of pollutants for the surrounding area. The pollution over an urban area is quite different. The types of pollutants will vary even over very short distances, depending on the industrial and urban activities within an urban area. It is therefore necessary that different types of sensors are used for different locations. The site selected should be in the downward direction in each case. Since the pollutants pose a definite hazard to the population and even to the vegetation around, a sense of urgency is to be shown on monitoring the pollution levels. However, this issue has not been taken up here and is required to be dealt with separately.

5. Requirement of Meteorological Instruments for Urban Measurements:

The requirement of meteorological instruments for measuring urban weather become some what stringent and specific when one has to monitor the microscale and local scale climate determined by the physical character of the surface and its close surroundings. There are several factors, which need to be considered while choosing meteorological instruments:

- Accuracy including resolution and response time
- Reliability (maximum MTBF and minimum MTBR), durability of repeatability and stability.
- Absence of hysterisis effect
- Convenience of operation and maintenance
- Robustness and stability
- Cost of operation and maintenance

Meteorological sensors, which have to be picked up for urban measurements, should meet the WMO requirements (WMO 1998, CIMO Guide) in general. The measuring device should be well established with proven accuracy and resolution. It should be certified by the experts in the field for sustainability, repeatability, calibration and maintenance. The air temperature and humidity measurement sensors should be protected from solar and other radiation exposures. The most widely used shelters, which are acceptable, are made of wood painted white or fiber reinforce plastic (FRP), which is a UV stabilized plastic construction. These enclosures, sometimes known as Stevenson's Screens are found to be very authenticated and proven shelters for housing temperature and humidity sensors.

Table 1, as reproduced at the end of the paper, provides a list of variables required for urban observations and gives an overview on their highly desirable specifications.

6. Automatic vis-à-vis Manual Observations:

When there is a growing need for meteorological data from urban areas, it is very relevant to give due consideration for automatic means of observations. Many National Meteorological Services including developing countries have gathered valuable experience in the operation of automatic weather stations (AWS) and a lot of data is available on their performance vis-à-vis manual observations. The use of automatic weather stations for urban areas will ensure the reduction in the requirement for manpower and associated supporting costs like housing, transport and utilizing these resources for increasing the density of observational network. Nevertheless, there is still a lack of will for acceptance of the data from AWS on the part of authorities in many Meteorological Services. This could be attributed mainly to the requirement of high level of standards for maintenance and servicing experts. These systems are complex and delicate and could lead to unreliable data if not handled properly and by qualified and trained personnel. If this requirement is given due consideration, the AWS could be widely used for collecting urban observation both in real time and delayed mode. Such stations give unattended operation for 12-16 months and could provide very reliable data through telephone line, wireless or through a satellite link. Semi automated weather

stations could also be considered for urban measurements while stations could provide the accuracy of manual observations and at the same time disseminate the data automatically to the user. The automatically measured data could be supplemented by manual input of visual observations on visibility, present and past weather.

7. Calibration, checking and quality control:

To ensure accuracy and reliability of urban observations, it is essential that the standard protocols for checking and calibrating the instruments be strictly followed. National Meteorological Services are required to extend their financial support to central facilities of checking and calibration, who maintain various standards in their Services for meeting the requirements of urban stations. As the stations work in urban areas, it may not be difficult to provide infrastructure support for meeting such requirements.

8. Location of Urban Data Dissemination Centres:

The Chiefs of National Meteorological Services have to consider this aspect and locate these centres where the synoptic and other data are routinely received, disseminated and stored. WMO is required to generate a separate code for recognising this data from other types of data. The personnel in the quality assurance checks have to ensure homogenous and reliable observations.

9. Metadata:

The importance of a detailed description of stations, instruments and site surroundings is very important and should form a part of the specifications while projecting a site. The information should be regularly updated. In general, the following may be taken up as broad guidelines while considering Metadata (data about data).

- Name of station
- Code number of station
- Latitude and longitude and height above mean sea level (elevation)
- Contact person with full address of the station including Tel No., Fax No. and e-mail address.
- Name of the installer
- Date of installation/commissioning.
- Topography of the station
- Nature of surroundings with a photograph
- Type of station – manual or automatic
- If automatic, complete wiring plan and type of communication on which data is available.
- Number of parameters being measured
- Nodal office where data is disseminated, processed and archived
- Access of station by road, land, air etc.

The above information looks very elementary, but for siting a station in urban terrain zones the information is very relevant as each site will have its own peculiarities and there is no way to standardize the station's description.

Concluding Remarks:

The preceding paragraphs give a very brief account of the requirement for measuring urban weather. The challenge really involves complexities and they further multiply if urban measurements have to include the urban pollutants in addition to the meteorological elements. Nevertheless, both the issues need to be handled independently though closely interrelated. The requirements of urban measurements may have to be augmented and optimized if WMO has to address to the specific need of urban measurements in developing countries. CIMO on its part has taken note of the need for codification on the measurements for monitoring urban climatology. It has appointed co-rapporteurs to go into the requirements for such measurements and bring out a possible guideline on site selection and instrumentation needed for such special urban requirements. The tasks involved are being attended to by them and a draft report is to be prepared incorporating their recommendations.

References:

1. WMO, 1970 — Urban Climates - WMO-technical note No.108.
2. Munn, R.E. 1973, — Urban Meteorology, some selected topics, Bull. Amer. Meteorological Soc., 54, 90-93.
3. Van Gysegem, A. 1978, Meteorological observations in urban environment, Institute Royal Meteorologique de Belgique, Bruxelles, Publications Serie B, No.93.
4. Munn, R.E. 1981, — The Design of Air Quality Networks McMillan Publishers, London.
5. WMO, 1982, — Report of the Meeting of Experts on Urban and Building Climatiology. WCP-37, WMO Geneva.
6. Hosker, R.P.Jr., 1985, Flow around isolated structures and building clusters, ASHRAE Trans, 91(2B), 1671-92.
7. Nakmura, Y and T.R.Oke, 1988 — Wind, Temperature and Stability Conditions in an East-West Oriented Urban Canyon, Atmos.Environ, 22, 2691-2700.
8. Oke, T.R. 1988, — The Urban energy balance, Phy.Geo, 12, 471-508.
9. Ellelen, R. 1990/91, — Mapping and Measuring buildings in the Canopy boundary layer in ten U.S. cities Energy, 15/16, 1025-1049.
10. Arnfield, J. et.al., 1991 Physical and boundary layer Climatology, Phy.Geo.12, 189-206.
11. WMO, 1992 — Measurement of Temperature and humidity, WMO-Technical No.194.
12. Rotach, M, 1995 — Profiles of turbulence statistics in and above an urban street Canyon, Atmos. Environ, 29, 1473-86.
13. WMO, 1996 — Guide to Meteorological Instruments and methods of observation, 6th edn, WMO, No.8 Geneva.
14. WMO, 1997 — Report of the Meeting of the Task force on TRUCE, WCA SP-40, WMO, Geneva.
15. WMO, 1997 — Instruments and Observing Method Part I and Part II, Report No.65.
16. WMO, 1998 — Instrument and Observing Method Report No.68.
17. Oke, TR, 1999 — "Observing Urban Weather and Climate using 'Standard' Stations", proceedings of the 15th International Congress of Biometeorology and International Conference on Urban Climatiology, Australia.
18. WMO, 1986 — Compendium of lecture notes on Meteorological Instruments for Class III and Class IV meteorological personnel, WMO – No.622.

****

Table 1: List of variables required for urban observations and desirable specifications

Sensors	Operating Range	Accuracy	Resolution	Response Time	Averaging Period	Threshold	Exposure Criteria	Type of Sensor
Temperature*	-50°C to +50°C	±0.2°C to ±0.3°C	0.1°C	30-60 s	1 minute	NA	1. Inside a radiation shelter at height of 1.5 to 2 m 2. 2-3 times of obstacle height.	PRT/ Thermistor
Humidity	0-100%	2-5%	1%	30-60 s	1 minute	NA		Hygristor/ Dewcell Humicap
Wind Speed	0-75ms^{-1}	±1 ms^{-1}	0.1 ms^{-1}	1-5 minutes	Sampling period of about 5 s to be integrated 2-10 minutes	0.5 ms^{-1} to 1 ms^{-1}	10 m above ground, 2-3 times of obstacle height.	CGA/ Propeller Photo-electric/ Sonic
Wind direction	0° to 360°	±5°	5°	1-2 minutes	Sampling period of about 5 s to be integrated 2-10 minutes	0.5 to 1 ms^{-1}	- do -	Vane
Precipitation	0-999 mm in a day	0.5 mm or 5% of reading	0.5 mm	1 mms^{-1}	Measured for 24 h from 3 UTC to 3 UTC of next day	0.5 mm	2-4 times height of obstacle	Tipping bucket/ valve volumetric weighing balance
Atmospheric Pressure	800-1080 hPa	0.3 hPa to 0.5 hPa	0.1 hPa	30 s	60 s average with 5 s sampling	NA (Normally defined by datum pressure of a place)	As stated for temperature & humidity measurements	Silicon Capacitance
Solar Radiation (Global/ direct)	0-1500 Wm^{-2}	±1%	1-2 Wm^{-2}	10 s	1 day	0.0 Wm^{-2}	No shadow should fall on the sensor and easy access.	Thermopile pyrheliometer / Pyranometer
Sunshine Duration	Sunshine "on" above threshold	±2%	0.1 h	10-15 s	1 day	120 Wm^{-2}	Unobstructed field of view along the direct solar path.	Photo-electric

* These specifications also hold good for the measurement of "soil temperature" except that the exposure criteria for the measurement of soil temperature is to be determined by the depth of soil at which the measurements are done. Normally the measurement of soil temperature at a depth of around 0.5m may provide a reasonably good understanding of urban thermal modification.

1 MEASUREMENT TECHNOLOGY, PERFORMANCE, AND QUALITY ASSURANCE

1.6 Urban Meteorology

AUTOMATIC WEATHER STATION FOR COLLECTING METEOROLOGICAL DATA FROM URBAN AREAS

R.D. Vashistha and S.K. Srivastav*
India Meteorological Department, Pune-411 005.
*India Meteorological Department, New Delhi - 110 003, India

Abstract

The accelerated rate of growth of cities in all parts of the world has offered a challenge to meteorological community to understand the complexities of urban climate. The first task in this direction is to establish meteorological observing network in urban areas, which is highly in adequate at present. India Meteorological Department has been trying for more than a decade for evolving a realistic and reliable automatic weather station, which could be utilized for multifunction tasks like urban climatic studies, cyclone warning, flood forecasting etc. The present paper highlights the salient features of an automatic weather station which is being utilized by India Meteorological Department for collecting data pertaining to air temperature, relative humidity, atmospheric pressure, precipitation, solar radiation, wind speed and direction etc. Efforts have also been made in the presentation to analyze the data collected from two typical sites in Pune (India) one located inside the city area and the other being in suburban area. Site layout plan and the exposure conditions for the instruments have also been discussed in the paper.

Introduction:

There is a growing need for meteorological community to study urban climate. This area has generated new demands for meteorological instruments which could be effectively utilized for collecting meteorological observations from urban Terrain Zones. This specific requirement could pose severe constraints both in infrastructure and resources especially for developing countries. The present paper highlights an "Automatic Weather Measuring System which could be utilized for collecting meteorological data from Urban Terrain Zone. As the system operates unattended for a period more than 200 days, the national meteorological services could effectively introduce this type of system for urban measurements without much financial implications on manpower. India Meteorological Department has been operating such type of systems in their national network and some of them are located in urban areas.

System Concept:

An automatic weather station consists of the following components:

- Sensors
- Signal conditioning unit
- Data Conversion, Storage and Transmission System (DCSTS)
- Power supply unit
- Satellite transponder (Data Relay Transponder)/Telephone Modem
- Central Data receiving, processing and disseminating system.

The signal conditioning unit converts the input signal from analog sensors to a conditioned output of required level and is given to Data Conversion and formatting unit. This unit also provides 10 bit binary output for digital sensors like precipitation and duration of bright sunshine. Calibration voltages for monitoring the linearity of A/D Converter are also generated in signal conditioning unit. System health bits indicating the status of critical voltage levels are also available from this unit. The DCSTS unit controls the functioning of AWS field station. It provides the required switched and continuous power supplies of required capacity to the sensors and conditioning units. It consists of a control logic unit, multiplexer cum A/D converter, health monitor circuit, memory module, pseudo random burst sequence generator and UHF transmitter or a telephone modem.

The AWS message consisting of data, station identification code, start and end signals are transmitted through a suitable antenna to a central receiving station via INSAT-Satellite. The length of the DCP message is in 422 bits in the following format:

Carrier and bit time recovery	Frame Synch	Station Identification	Data Frame	EOT Code
160 bits (100 0's, 60 1's	16 bits D8E2	31 bits	199 bits	16 bits (FADE)

The data from AWS could also be retrieved by using a telephone modem if a telephone line is available in the site. The following diagram gives the system concept

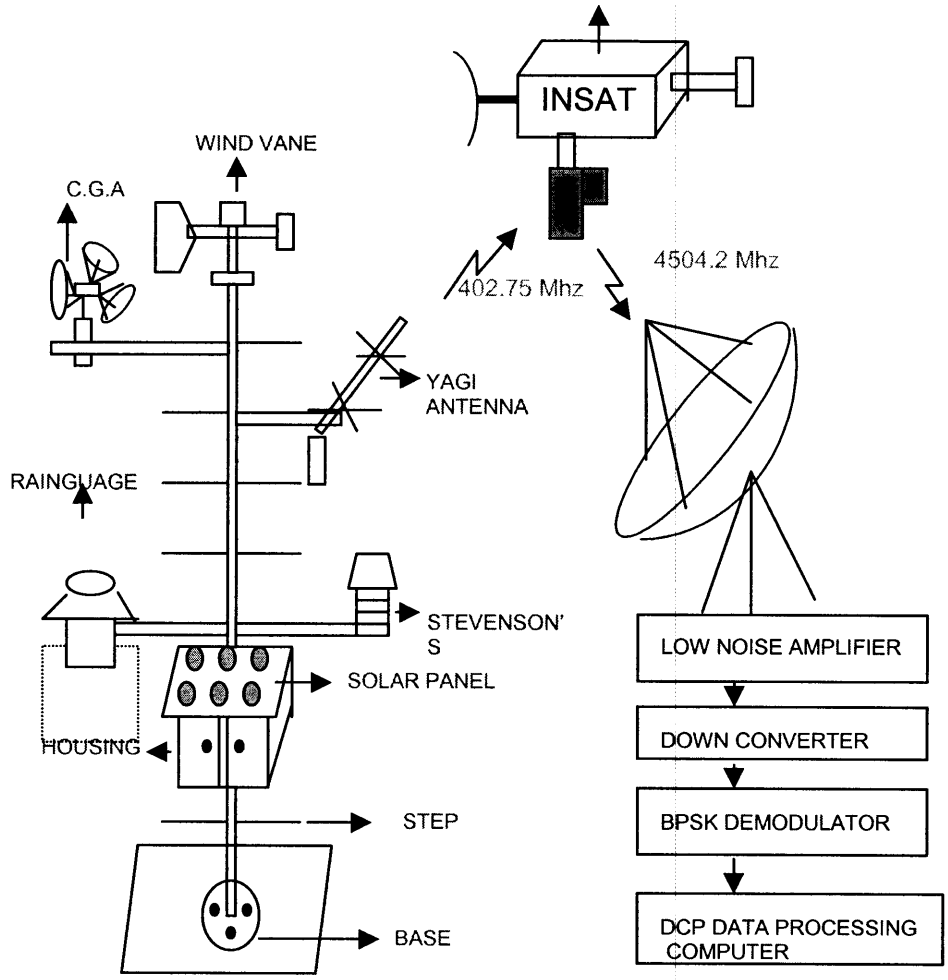

AUTOMATIC WEATHER STATION **RECEIVING EARTH STATION**

The Table below gives the list of sensors used for urban measurements:

Parameter	Sensor Used	Range	System accuracy
Temperature	Thermistor	0-50°C (or-20 to +30°C)	0.5°C
Wind speed	Cup Generator Anemometer	0-100 knots	1 knot
Wind direction	Potentiometric Windvane	0-360°	1°
Pressure	Aneroid	0-100 hPa above a fixed datum	0.5 hPa
Relative Humidity	Humicap	0 - 100%	5%
Rainfall	Tipping Bucket Raingauge	0 - 1023 mm	1 mm
Solar Radiation	Sunshine Switch	0 - 1023 minute.	1 minute

Site selection and instruments exposure:

At present there are no guidelines for siting a weather station in an urban terrain zone. The exposure conditions for individual elements have yet to be been defined by WMO. This task has been recently taken up by CIMO by appointing experts. The present sites which are located in urban areas in India are in close conformity to the siting conditions defined by WMO (WMO/TD No.862) for establishing Automatic Weather Stations.

Calibration of the system and Data Quality:

Most of the sensors employed for the measurement of various parameters are manufactured in IMD's workshop at Pune. Their calibration schedule is maintained by deputing technical personnel in the field site who carry the secondary standards for different elements. This is required to be done at least once in six months to sustain the quality of data. The data from the Automatic Weather Stations has been compared with the manual observations and it agrees fairly well with the manual observations if the manual observations are reliably taken. The following graphs give a comparison of AWS data from two urban locations at Pune (India).

Concluding Remarks:

The introduction of Automatic Weather Station for collecting meteorological data from urban areas at selected sites will give a new confidence to weathermen for studying the complexities of urban climate. The large expenditure for infrastructure and manpower could be saved by employing such type of system in Urban Terrain Zone. The data could be collected in a central processing and dissemination centre using a telephone modem. The extreme weather event like flash floods, storms, etc. which are not uncommon in urban areas could be studied in details if a network of such stations is established by selecting suitable site representation in urban terrain zones. It is noted from the graphs of fig.1 that the data of AWS from both the sites at Pune(India) city are in good agreement with the data from manual observation.

REFERENCES

1. WMO 1992 Measurement of temperature and humidity, WMO-technical No. 194
2. WMO 1996 Guide to Meteorological Instruments and methods of observation 6th Edition, WMO No. 8
3. WMO 1997 Instruments and observing method Part I and Part II, Report No. 65.
4. WMO 1998 Instruments and observing method Part I and Part II, Report No. 68.
5. Oke T.R. 1998 Observing Urban Weather and Climate stations TECO-1998.
6. Vashistha R.D., et.al. 1994 WMO Technical Conference of Instruments and methods of observations.

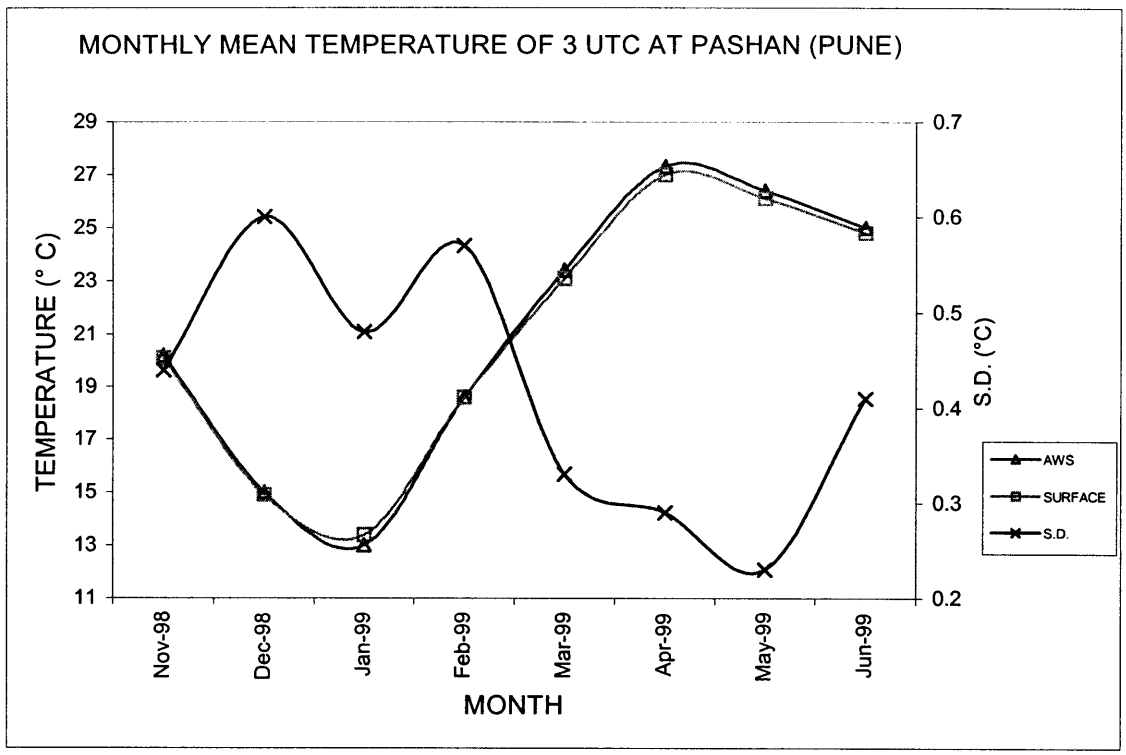
MONTHLY MEAN TEMPERATURE OF 3 UTC AT PASHAN (PUNE)
TEMPERATURE (° C)
S.D. (°C)
MONTH
Nov-98
Dec-98
Jan-99
Feb-99
Mar-99
Apr-99
May-99
Jun-99
AWS
SURFACE
S.D.

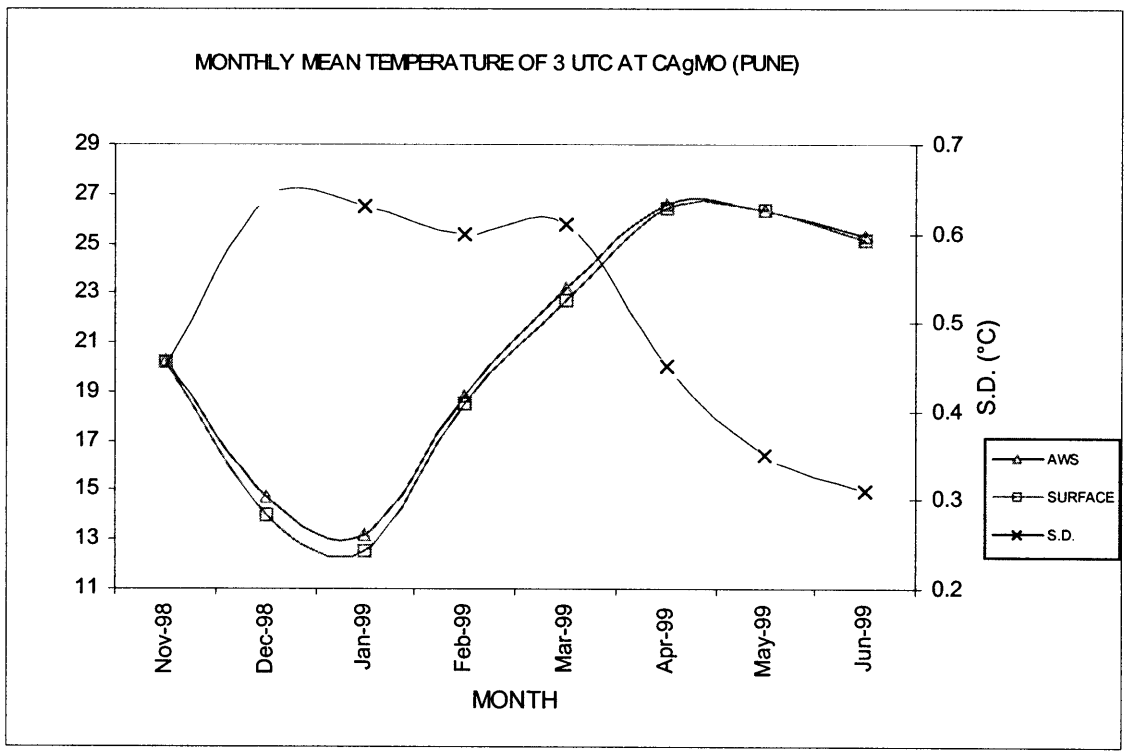
MONTHLY MEAN TEMPERATURE OF 3 UTC AT CAgMO (PUNE)
S.D. (°C)
MONTH
Nov-98
Dec-98
Jan-99
Feb-99
Mar-99
Apr-99
May-99
Jun-99
AWS
SURFACE
S.D.

2 MANAGEMENT OF INSTRUMENTS AND TECHNICAL SUPPORT FOR OPERATIONAL MEASUREMENTS

DEVELOPMENTS IN A MODERN QUALITY MANAGEMENT SYSTEM: OBSERVATIONS QUALITY CONTROL, NETWORK PERFORMANCE AND METADATA DATABASE

R.P. Canterford, D.K. Evans and L.C. Allan

Australian Bureau of Meteorology
PO Box 1289K Melbourne, Vic. AUSTRALIA
Tel (+613) 9669 4225, Fax (+613) 9669 4168
Email : R.Canterford@bom.gov.au

Abstract

The Australian Bureau of Meteorology Quality Management System (QMS) for its meteorological and environment measurement networks has undergone modernisation in several areas in recent years. These changes have included automated quality control modules in observations data entry equipment and automated instruments. In addition, performance monitoring systems are being upgraded to account for new instruments and sensors. Further, a computer based metadata database and associated tools is enhancing these developments and provides ready access for climate research and for managers and technicians to complete the feedback loop for necessary improvements to instruments and networks.

1 Introduction

Modern management of instruments and associated technical support for environmental measurement networks has created new challenges. These have arisen from the changes in the technology employed for the observational instruments, the often declining support resources and the standards that must be met for the Global Climate Observing System (GCOS) and the Global Observing System (GOS). The increasing complexity of modern sensors and equipment is placing additional demands on managers and technical staff. Therefore distributed quality control (QC) and performance monitoring procedures and systems must be established, utilising computer-based technology at the data source and the user interface. These quality management tools enhance the conventional QC and QM procedures undertaken by most National Meteorological and Hydrological Services (NMHS). This paper will outline developments within the Australian Bureau of Meteorology (ABM) that have occurred in recent years and which will provide a firm basis for the critical change necessary for its quality management system in the next decade. This will include an outline of how improved computer based tools, such as an Electronic Field Book (EFB), Automatic Weather Station (AWS) control systems and a metadata data base (SitesDb), assist with appropriate network management.

2 Requirements for Instrument Quality Management

The formal requirements for Quality Management are given in WMO (1981) with procedural guidance in WMO (1989). The CIMO Guide (WMO, 1996) provides good guidance for NMHSs on this topic. It points out that quality control must be performed at all stages, from raw sensor output through to archiving of the meteorological data, including reduction to Level II. With new technology, algorithms are becoming more detailed and QC in this regard is particularly important. With increasing communications for all measurements, QC must be carried out both in real time and in delayed mode. As highlighted by the CIMO Guide, this QC information must be followed up by observations managers at all levels. New technology tools to assist with these QC and performance monitoring processes will be described in the following sections. Changing instrument technology and resource constraints can make it difficult to achieve all the requirements of data quality management: prescribed uncertainty, resolution, continuity, homogeneity, etc. Therefore new tools based on modern technology assist greatly.

3 The Quality Management System

In order to support quality control and monitoring, the ABM's overall quality management system includes procedures and manuals on the requirements for instrument siting and exposure, inspections, maintenance etc. It also includes good documentation of these activities undertaken at all stations within a network. Additionally, key metadata is essential for users and network operators to assist in identifying data quality and homogeneity factors over the life of the observations. Another essential component is training in all facets of methods of observations, inspection, maintenance, installation at appropriate locations and metadata record keeping. The International Organisation for Standards (ISO) set of quality management standards, ISO 9000 series, is aimed at assuring quality and consistency and can provide a useful checklist or benchmark for an NMHS quality management system, but do not necessarily need to be formally adopted. The ABM, although not formally adopting them for its QMS, does satisfy all activities and

documentation that form part of the ISO standard. The ABM's QMS computer based tools are discussed in the following sections. These developments are essential for an efficient modern QMS.

Substantial documentation for local conditions is required for siting and exposure of instruments. This is obviously based on WMO guidelines (WMO No. 488, 1989). Any changes should follow more recent guidelines provided in various WMO documents, but particularly follow the Global Climate Observing System requirements, such as suitable overlap periods. In any event, changes to sensors and equipment should be recorded historically as part of the metadata record (see later).

Inspection of instruments is required to ensure correct observing practices, calibration against standards (which also have their own heirachy in any quality management system - traceable to national and Regional standards) and any changes to equipment or maintenance required. It should be noted that a feature of the more complex technological equipment being established by NMHSs, such as AWS, is that they can require inspections/calibration more often than conventional equipment. This frequency can be six monthly or more often depending on sensor drift and maintenance requirements. Management needs to be fully aware that resources possibly saved through network automation must be at least partially offset by additional resources for the inspection/calibration component of the quality management system. As discussed later in this paper, a computerised metadata database is essential to keep track of these more frequent calibrations and inspections and the performance of individual modern sensors. It also assists greatly the work practices of the inspection or instrument maintenance staff, as well as observations managers.

4 Developments for Improved Quality Control

The ABM operates a substantial upper air network of 50 stations (of which 10 are currently automated with minimum staffing) and over 800 synoptic stations. Approximately half the synoptic surface network is operated by contract staff (using the EFB) and the remaining consists of AWS. Modern instrumentation introduced into these networks is providing new demands on quality management systems. For the quality management system to be effective in an environment of reducing resources, quality control (and performance monitoring) must be an integral part of the observing instrument or system. To this end, the ABM has established comprehensive QC facilities at the source of the observation.

Electronic Field Book

The ABM in the past used a number of procedures to transmit observations to real-time users (eg. forecasters) and to the Australian National Climate Centre (NCC), where data are archived. When observers performed an observation, it was entered manually into a Field Book and transmitted by SYNOP. At the end of the month, all Field Books were returned to NCC for checking, data entry, and archiving. New technology has meant that much of the manual quality control and data entry can be automated and performed in real time. A laptop computer is used as the preferred platform, connected via a modem for transmission on the telephone line of the observer.

The EFB data entry system has been designed to largely mirror current practices of data entry into the Field Book. Once the Observer has performed the observation, data are entered using the computer keyboard and the menu-driven EFB software. Quality Control (QC) is performed automatically on elements entered. Once the observation has been entered, the EFB automatically stores the data, encodes the observation, and transmits the data to the Regional Office. The QC module of the EFB operates by ensuring:

(i) data entered for the various parameters observed are mutually consistent;
(ii) each value entered is checked against the extreme values (lowest and highest) recorded at the particular station. A file containing these extreme values for each element observed for each month and each synoptic hour at the station resides on the EFB terminal. If an entered value is either a record high or a record low, the Observer is advised and asked to confirm the value. Once confirmed, the value is accepted, but will not be written to the climate data file until it is reconfirmed at the central NCC;
(iii) entry for all parameters observed at the station is required before the message can be sent; and
(iv) the actual time of observation is recorded (via the computer clock) as well as the nominal time.

The EFB's QC module ensures that data entered are consistent, and will not allow the message to be sent until all inconsistencies are removed. Some QC checks are done immediately after the value has been entered. Other checks are not performed until the Observer attempts to finalise the observation. The EFB QC provides immediate feedback to the observer to correct problems, reduces or eliminates coding errors, and enables managers to quickly determine problems with measurements. This is an efficient use of resources for a widespread network and the laptop computers have proven quite reliable for use in remote areas by contract staff.

Automatic Rain Gauges

Another system for Australia's large remote automatic recording rain gauge network is a comprehensive QC computer module distributed to local observations managers for delayed QC (but much less delayed than older manual

systems): an efficient use of resources in the quality management system. Final QC is again carried out prior to archival.

Automatic Weather Stations

The increasing use of AWS networks is providing new problems for data quality, but automated QC is again essential in the quality management system. The EFB QC module, slightly modified, is being incorporated into the software of all automatic weather stations. In particular, it has already been incorporated into the manual entry console (required at some stations for visual parameter entry), and operates on both manual data and automatic data. To assist in the quality management system for all data, it is important that the instruments and sensors are of high quality. This can be established by analysis of metadata, which includes sensor type, calibration or maintenance requirements. The harsh environmental conditions and great distances required to travel to remote AWS installations has provided additional demands on the Australian AWS network of over 400 stations. State-of-the-art hardware and highly intelligent software are necessary.

The AWS were developed in conjunction with a private Australian company, Almos Systems (Almos Systems, 2000). A sophisticated console for data entry of manual elements, local network display, and sensor alerts is provided to assist the observer. The alerts are an important component of the QC. As well as a robust and reliable design suitable for harsh conditions (from desert to tropical to maritime), the network has remote software configuration and diagnostic tools. This is essential for modern quality management of new technology as it greatly reduces maintenance costs and allows efficient feedback in the QC process.

Upper Air Network

Quality Control for upper air data has its own special features, which are becoming more automated with modern technology. As conventional upper air observations are very expensive, every care is taken to properly QC data and provide feedback to operators. Over the last decade new software, graphical tools and communications technology have greatly reduced the resources required for manual QC. New automated upper air systems (Canterford et al, 2000) are being introduced to part of the Australian upper air network and the network has been especially set up to quality control the upper air data in near real time, from remote terminals in other stations that are operated around the clock.

5 Performance Monitoring with advanced technology

The technology associated with surface and upper air measurements, along with modern communications, allows efficient implementation of performance monitoring of networks. The impact of changes to observations practices can be determined quickly and efficiently. For example, Australia recently increased its balloon size for 00 UTC radiosonde flights at GCOS Upper Air Network (GUAN) stations. The impact of greater heights reached could be monitored closely as shown in Figure 1:

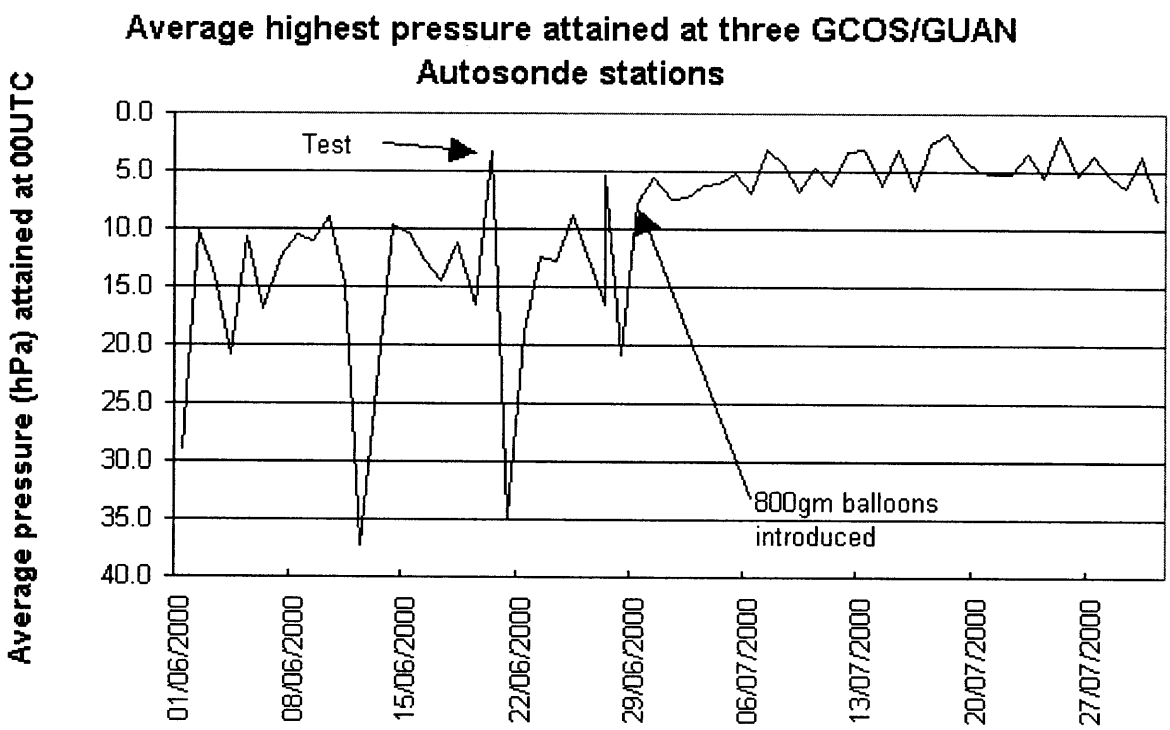

With the increased data volumes, the QMS must be able to alert the user of the data or the observations manager to data errors or inconsistencies and trends for network deficiencies. It can be near real time or delayed, depending on the level of use of the data. Because of the nature of the data's application, the ABM has several stakeholders undertaking this component of its quality management– the ABM operates the NCC climate archive as well as using the data for modelling, forecasting, private clients etc. Recent developments (Lockett and Plummer, 1998) have been undertaken to consolidate and further automate these procedures. They will be reported elsewhere.

6 Data Homogeneity: impacts of new instrument technology and the importance of modern metadata systems: SitesDb

As mentioned in earlier sections, new technology for sensors and instruments is having a marked impact on networks. To ensure data homogeneity, the QMS must encompass procedures to quickly record discontinuities, calibrations, new algorithms, etc., and enable managers to be alerted to deficiencies in maintenance and inspection procedures. As well as the QMS providing feedback on these changes and correcting poor choices or deficiencies, it should have adequate metadata or station histories. As pointed out in the CIMO Guide (WMO,1996) any modern QMS should have this in the form of a computer database for ease of access and updating. The ABM has developed such a web-based database. This comprehensive Oracle metadata database, known as SitesDb, allows restricted access to appropriate staff across the country to input observations and engineering metadata. In this way double handling of key information is avoided and the actual staff responsible for the metadata undertake on-site QC.

SitesDb allows access to all other users of the data so that appropriate decisions on the value of the data can be made. Inspection and calibration information are easily extracted and historical trends in metadata can be quickly accessed and assessed. In addition network performance statistics are readily available to managers for decision making on performance of instruments and sensors. It is being further developed to integrate all aspects of the ABM's QMS. It will also be linked directly to a financial database, allowing network managers and other managers to quickly assess the output costs of all elements of the network.

7 Conclusion

A modern comprehensive Quality Management System is essential. The increasing technology associated with observational instruments and systems is placing greater demands on efforts for data quality and homogeneity; but other technological advances are allowing greater automated QC and performance monitoring. EFB and AWS QC modules are supporting effective inspections and calibrations programmes. The new database SitesDb is providing essential accessible metadata, as well as information on the efficient use of resources in operating networks.

8 References

- Almos Systems (Aust). "Australian Bureau of Meteorology Automatic Weather Station Network". Manufacturer Report 2000.

- Canterford, R.P., Smith, P.R., Braden, L J. and Joyce, M. J. ""Operational Considerations in Implementing a Network of Automated Upper Air Stations in Harsh Environments. TECO 2000, Beijing.

- ISO 9001:1994 "Quality systems – Model for quality assurance in design, development, production, installation and servicing" International Organization for Standardization, Geneva.

- Lockett, D. and Plummer, N., "A Quality Assurance System to Improve Data Quality". Australian Bureau of Meteorology. Internal Report, 1998.

- Pannett, R. A.," Quality Data–Application of the ISO 9001 Quality Model" p123, TECO-1998, Casablanca, 1998.

- SitesDb Project Development Plan. Internal Australian Bureau of Meteorology document, 1995.

- World Meteorological Organization, 1981: Manual on the Global Observing System. Vol. 1 WMO- No. 544, Geneva.

- World Meteorological Organization, 1989: Guide on the Global Observing System. WMO- No 488, Geneva.

- WMO, 1996 : ***CIMO Guide***. "Guide to Meteorological Instruments and Methods of Observation". Sixth Edition. WMO No 8. 1996.

NEW APPROACH TO THE DEVELOPMENT OF CALIBRATION PROCEDURES AND DECISION SUPPORT SYSTEM REALIZED IN YUGOSLAVIA

Mladen B. MILINKOVIĆ, Jasmina KNEŽEVIĆ
Federal Hydrometeorological Institute of Yugoslavia,
Belgrade, Bircaninova 6, Yugoslavia
Phone: 645779, fax: 646369, e-mail: mmilinkovic@meteo.yu; jknezevic@meteo.yu

Dragan RADOJEVIĆ,
Institute "MIHAJLO PUPIN" Automation&Control Laboratory
Belgrade, Volgina 15,Yugoslavia
Phone: 772020, fax: 774265, e-mail: draganr@L100.imp.bg.ac.yu

1. Introduction

National Meteorological Laboratory (NML) has been formed and equipped within the Federal Hydrometeorological Institute of Yugoslavia (FHMI), more than 40 years ago. Within this period Laboratory has successfully solved different tasks connected to required accuracy and unification of observing and measuring methods within the Hydrometeorological Service of Yugoslavia.
NML disposes with set of standards for principal meteorological parameters such as atmospheric pressure air temperature, humidity, wind and solar radiation.
Testing equipment has been improved following the development of meteorological instruments and applied measuring techniques through automation of calibration process using PC platforms.
Namely, today's trends of introducing electrical sensors with electrical voltage, current, pulse, etc. outputs, as well as intelligent sensors with communication port, require adequate adjustment and automation of all components of standard measuring procedure which had analogous output, managing of those processes, collection, processing and archiving the obtained data.
This paper aims to present the level achieved in realization of the first phase of integrated semi-automatic system based on PC technology with use of standard and new equipment and our acquisition system for data processing.

2. Basic steps in calibration procedure improvement

- Maintenance and improvement of existing level of accuracy in sensor calibration;
- Selection of adequate acquisition system to ensure automation of calibration process without degradation of measurement accuracy and to keep it at the same or better level than that of the standard possess;
- Selection of relevant algorithms for processing of the data obtained by measurement according to CIMO recommendations;
- Producing the appropriate software for each calibration procedure.

3. Realization of integral calibration system

Automation of calibration process for sensors with electrical output is PC - based with adequate acquisition card and appropriate software aiming to achieve an equal or better accuracy than that of Laboratory physical standards. Accordingly, we have decided to make use of authentic domestic solution with acquisition PC slot card already applied at our first Automatic Weather Station.

The Figure shows the scheme of integrated system comprising the following: Calibration Laboratory (thermometry, hygrometry, anemometry, barometry), AWS within the field-testing area and the National Solar Radiation Center (NSCR).

3.1 Automatic Weather Station

The Automatic Weather Station (AWS) - FHMI-EKOLAB SPC06 being completely Yugoslav product represents a new generation of multipurpose AWS with improved characteristics, accuracy and reliability. It is composed of PC, PC slot acquisition card appropriately designed with all the sensors measuring meteorological parameters connected via connection box.

The System is open and can be easily upgraded with a set of basic meteorological sensors with electrical output, as well as a number of sensors with specific purpose up to total number of 16 analogue and 16 pulse inputs. This specific purpose software provides the user with the continuos data acquisition, as well as with visual representation of measured meteorological parameters, direct read-out of measured and computed quantities, printing and graphical representation of archived data. The selection of professional components and original solutions applied to hardware and software results in the best accuracy and reliability within a long time period of station correct functioning even in extreme weather conditions. This high quality AWS is used for field testing of other AWSs in the outdoor conditions. Since it is installed within the testing area the accuracy of its sensors' readings are continuously compared to NML standards. The AWS is connected into the LAN and through telecommunication hub its data are available for remote users via Intranet and Internet.

3.2 Acquisition PC slot card

Having in mind the importance of selection of appropriate acquisition system, we have chosen the reliable solution for homemade acquisition card* successfully applied in the first domestic AWS. The advantage of this acquisition card with respect to the others mostly used for application in industry, is its good resolution, which enables its use for laboratory purposes.

The acquisition card is made of reliable professional components so it keeps completely the accuracy of the calibrated sensors, and moreover its own accuracy is improved by two additional significant figures since it is connected to digital multimeter HP 34401A. Card parameters relay upon the accuracy of the HP multimeter attested at Yugoslav Federal Bureau of Standards. In this way each meteorological quantity which is connected to physical standards is obtained as an electronic one, becoming the substandard of higher accuracy, i.e. having a new measure of corrective value.

The use of this card enables the multipurpose application in different measuring structures being appropriately designed for each one of them particularly.

Basic characteristic of the acquisition card is as follows:

- to work with 16 analogous and 16 pulse inputs thus enabling the connection of electronic standard, sensors which are being calibrated together with voltage outputs to manage the work of chamber, thermo - baths and wind tunnel;
- 14 bit A/D conversion (20000 counts, 4 ½ significant figures) provides 0.01 resolution for all measured values obtained from standards and sensors;
- the use of this card doesn't require interface, thus eliminating the risk of possible reliability and defined accuracy degradations;
- the possibility of self calibration before the start of acquisition cycle is achieved by means of hardware;

4. Software

For each calibration procedure appropriate software written in C^{++} (Borland) ensures the following:

- collecting of measured values from sensor under calibration and standard, every second,
- testing the accuracy of the acquisition unit during the process of pre-calibration check by means of special calibrator for sensors with analogous read-out (resistance, current, voltage) and for sensors with pulse output check with quartz stabilized frequency,
- defining the range and steps which measuring-calibrating equipment has to gain during the sensor calibration,processing of direct and derived values,
- alarming and flagging at the occurrence of measured values exceeding the defined accuracy of measurement,
- graphical and numerical presentation of instantaneous and/or derived measured values,
- archiving of all measured and derived values obtained form standards and sensors under calibration.

*The authors of this card are electrical engineers Slavoljub & Miroslav PETROVIC (EKOLAB-Belgrade)

5. Realization of semi-automation in Calibration Laboratory

5.1 Pressure

Laboratory has large standard mercury barometer of R.Fuess type (system Wild-Pernet-Fuess) with readings improved by means of optical device (katetometer), and Digital pressure gauge MENSOR DPG II as transfer standard. These two standards are intercompared before and after each calibration process. The testing and calibration of sensors is performed in special baro-chamber by connecting them to a special input in the acquisition unit. In Laboratory there are two improved baro-chambers, as well as a special baro-chamber which is used for calibration of all station mercury barometer types over full range (800 – 1070 hPa) by means of given programmed pressure values. When stabilized measuring conditions are achieved through measuring and regulation devices controlled by PC, the acquisition of valid data starts.

5.2 Temperature

For thermometer calibration, depending on the type and other factors, two thermo-baths and a thermo-chamber HERAEUS VOTSCH are used. In Figure is schematically shown the thermo-bath used for calibration of classical glass thermometers which are compared to THERMOSCHNEIDER standard thermometer set having resolution 0.02°C. Programming of calibration within the range –30°C to +50°C is performed in predefined steps using the working substandard Pt100 (1/3 DIN 43760). For integrated sensors the calibration is performed in thermo-chamber.

5.3 Humidity

Automation of calibration process for humidity sensors is performed in thermo-hygro chamber (HERAEUS VOTSH) within the range 10-96 % RH using software predefined steps. As a working standard for electronic sensor is used a modified psychhrometer LAMBRECHT (Frekenberger type), with resolution of 0,01°C relaying on standard thermometer with HP 34401A and a working standard Pt100. This working standard is connected to the acquisition unit and it controls the thermo-hygro chamber functioning by means of output bits.

5.4 Wind

There is a Wind Tunnel (closed circuit type, semi-open, elliptic working space 0,8m x 0,6m, length 1,2m) in the Laboratory, with standard (E.SCHILTKNECHT-high precision micro-pressure gauge of measuring range 0-300mm$H_2$0, with accuracy 0,03 %F.S.). Calibration automation is performed by means of parallel connection of differential pressure sensor (range 0-20 hPa, resolution 0,01 hPa) to standard micromanometer. Measuring humidity, air temperature and pressure sensors having electrical output during the calibration, a set of continuous data of air density is obtained, i.e. the instantaneous speed of laminar flow in wind tunnel. Sensors (analogous or pulse) are connected to their corresponding entries on the connection box. This enables the measured data to be collected, processed, displayed, printed and archived. At the moment the system is semi-automatic because the wind tunnel is being operated manually.

6. Decision Support System

At this moment, the National Meteorological Laboratory of the FHMI is undergoing the first stage of the Decision Support System (DSS) Project, aiming to the improvement of calibration components, as well as maintenance and supervision of the functioning of the entire system.
The focus of this stage is the identification of the expert system's functions and the selection of adequate computing techniques. Having in mind the complexity of the nature of this problem on one hand, and the accuracy requirements on the other hand, it was decided to make use of computational intelligence-soft computing techniques.
Soft computing comprises a number of computing techniques having a common property of tolerance towards ambiguities, imprecision and understatements characterizing the real problems.

The soft computing principal techniques are: fuzzy sets and fuzzy logic theories, neural-computation with artificial neural nets, evolutionary computation with genetic algorithms, a part of probability theory, and machine learning theory, etc. The planned system for decision making support is based on two groups of soft computing techniques:

(a). Fuzzy techniques: for acquisition of relevant qualitative knowledge linguistically described and approximate decision making; and

(b). Neural-computing techniques: for identification of cause-consequence relations between relevant quantitative data (as a general functions' aproximator). DSS will dispose with the possibility of combining of these two principal groups of technique within a so-called hybrid-techniques approach. It is to be emphasized that the new consistent [0,1]-valued logic [1] will be used here. Comparing to other fuzzy logic, this new logic is consistent in the sense of classical Boolean logic. This new approach is based on fuzzy measures and fuzzy integrals, which have been introduced into fuzzy techniques by Japanese Prof. Michio SUGENO from Tokyo Institute of Technology [2].

7. Conclusions

In our opinion we succeeded to realize the first stage of the integrated system for calibration of sensors with electrical output in a rational way using our own acquisition card and adequately written software. By use of physical standards the transition to working electronic and process standards has been realized and the adequate use of PC platform with all its advantages and possibilities of system upgrading.

So, our specialists can fully control the maintenance of this integrated system.

Since this system is of the modular type, i.e. open it gives us the possibility to continue the automation of the calibration processes, as well as of solar radiation sensors and all other sensors for hydrometeorological and environmental measurements.

We expect that we shall, in near future, achieve a new quality and consistent approach by use of DSS and its incorporated tools, both in the control of the integrated calibration system functioning in NML, and solving some data quality analysis problems, in Hydrometeorological Service of Yugoslavia.

8. References

1. Dragan. RADOJEVIC; [0,1]-valued logic: A natural generalization of Boolean logic, YUJOR- Yugoslav Journal of Operations Research, Belgrade, Yugoslavia, (2000), Vol. 10. No.2

2. Michio SUGENO; Theory of fuzzy integrals and its applications, Thesis, Tokyo Institute of Technology, 1974

INTEGRATED SYSTEM FOR CALIBRATION

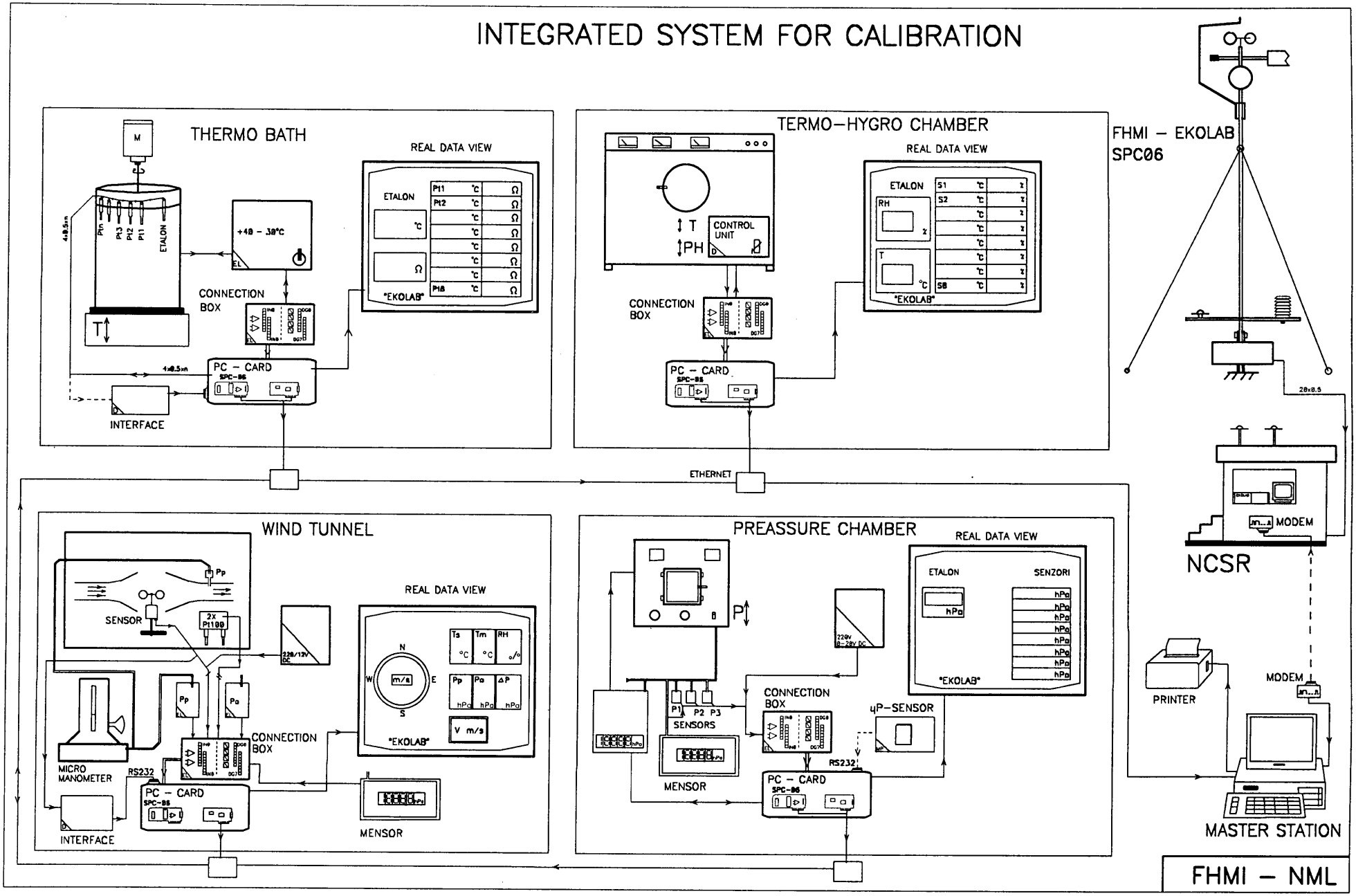

SOME ASPECTS OF QUALITY ASSURANCE PROCESS AT THE SLOVAK HYDROMETEOROLOGICAL INSTITUTE

Miroslav Ondráš, Oľga Novanská
Slovak Hydrometeorological Institute, Jeséniova 17, 833 15 Bratislava, Slovakia
Tel: +421 7 5477 4052 ; Fax: +421 7 5477 3620; E-mail: Miroslav.Ondras@mail.shmu.sk

Guarantee of quality products and services requires implementation of the Quality Assurance System. From the point of view of application of STN EN ISO 9001 the Slovak Hydrometeorological Institute (SHMI) represents wide spectrum of processes where inputs and outputs are both data and information.

The strategy of the SHMI is aimed at the provision of continuously increasing reliability of provided services by means of controlled processes based on the internationally approved agreements, methods, procedures and recommendations with respect to the quality, user benefit, cost and risks. To achieve the objective controlled processes are used as they only can find errors and guarantee their corrections.

The Quality Assurance covers both the Quality Management Systems as well as the Quality Measurement System. Implementation of both systems is a longer-lasting process currently affecting most of the SHMI activities.

The SHMI comprises Meteorological Service and Hydrological Service. The main task of the SHMI is to monitor both quantitative and qualitative parameters of the atmosphere (including air quality) and hydrosphere; to collect, check and validate, process and evaluate, interpret and archive of data and information; to provide data and information on the past, present and future state of atmosphere and hydrosphere; to study atmospheric and hydrospheric processes. The basic mission of the SHMI in observing and understanding weather and climate and providing services in support of national (and international) needs being extended into nearly all field of human activities.

The National Meteorological Observing Network has 13 subsystems that are continuously transforming into an integrated (and composite) National Observing System. The composition of the Meteorological Observing Network is in Table 1.

Table 1 Composition of the National Meteorological Observing Network

SUBSYSTEMS		NUMBER OF STATIONS		MESURED VARIABLES
		Present	Target	
1	Automatic Weather Stations	27	87	16
2	Weather Radars	2	4	3
3	Satellite PDUS	1	2	2
4	Lightning detection stations	3	4	3
5	Climatological stations - manual	86	30	28
6	Precipitation stations – manual	568	150	8
	Precipitation stations – automatic	0	500	1
7	Solar radiation	5	8	5
	Stratospheric ozone	1	1	4
8	Phenological stations	225	225	10
9	Soil moisture and temperature stations	8	8	2
10	Boundary layer measurement stations	2	2	6
11	Upper-air stations	1	2	5
12	Gamma dose radiation stations – automatic	14	26	1
	Gamma dose radiation stations - manual	2	4	2
13	Ambient air quality stations – local	14	33	5
	Ambient air quality stations – regional	4	7	8
	Surface ozone stations	17	21	1

As far as the Quality Measurement System is concerned the following aspects are taken into account and became a part of controlled processes (full implementation of which being at the time of ISO 9001 is administered):

- Revision of conformity of observing, communication, data processing, data management systems;
- Revision of equipment records and revision of meteorological confirmation;
- Validation of calibration methods and procedures;

- Sustainable revision of conformity of Instrumentation, Facility and Staff;
- Continuous integration with ISO System;
- Sustainable revision of conformity of Management Strategy on Quality (Quality Policy);
- Periodic certified training for observers, technicians, supervisors, meteorologists;
- Periodic revision of QC/QA implementation and conformity on Management level;
- Periodic revision of Preventive measures;
- Periodic revision of Complaints and Corrective action (Management review);
- Periodic internal and external Audits;
- Periodic review of Contracts;
- System of controlled documentation;
- Sustainable validation of conformity of Quality Guide;
- Filing system.

How the Quality Management System and Quality Measurement System interact is presented on Figure 1.

Figure 1 Quality Assurance System at SHMI

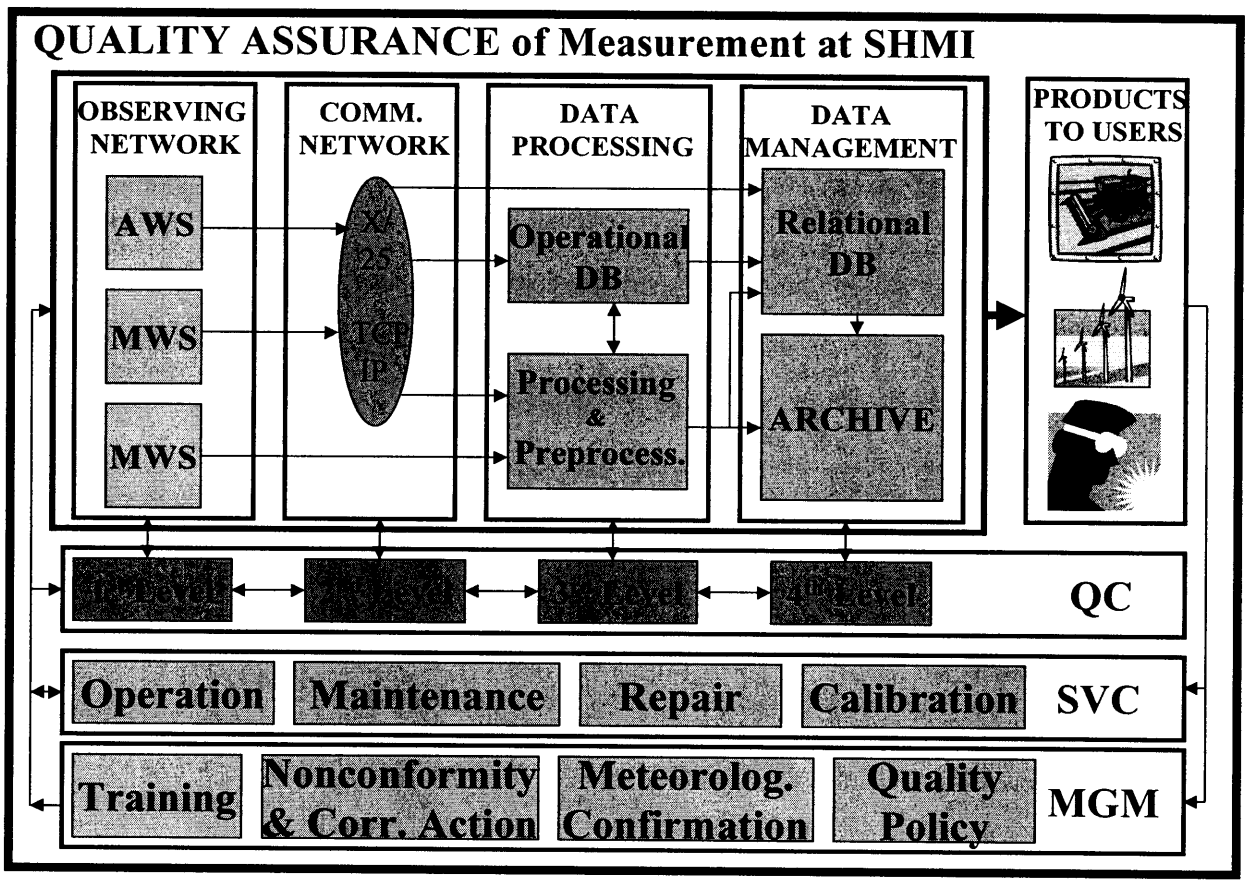

Notes: AWS – Automatic Weather Station, MWS – Manual Weather Station, QC – Quality Control, SVC - Services, MGM - Management

Within the Quality Measurement System it is necessary for the sake of confidence in the products and decisions, based on the measured data, to control all measurement processes. Control procedure of measurement process provides fast nonconformity findings, their analysis and remedial corrective action.

Measurement process begins with traceability of measuring instruments to appropriate standards continue through the meteorological confirmation and ends with direct data measurement either manually or automatically. Methods of control of measurement processes are based on regular data quality control by means of monitoring, testing and analysis of measured data.

Within the monitoring there are four levels of data Quality Control as seen on Figure 1. Many steps are fully automated and in this case corrective measure is done automatically. Some steps that are still manual (and will be) are mostly applied in non-real time with the corrective measure done manually as well.

The third group of steps are semi-automated applied in near real-time with mostly manual corrective measure.

The data Quality Control within the third group is based mostly on comparison of data measured automatically and data measured manually. At most observing sites an observer comes to make manual climatological observation using different instrumentation, with the same exposure as AWS' sensor, three times a day (07,14,21 h). This routine originally prepared for long-term data comparison proved to be an essential tool for near real-time data Quality Control. Its modules for Detection of faulty sensors and for Detection of gross errors provide text messages to System manager as well as to the observing site for possible corrective action.

The important element of control of the measurement process is the guarantee of quality of measuring equipment – meteorological confirmation. The basis for the meteorological confirmation is the calibration of measuring instruments. Through the calibration of measuring instruments the traceability to appropriate national standards is done.

Calibration of measuring instruments is done by Calibration Laboratory. Its history at SHMI is dated back to early 60th. New requirements for quality measurements aimed at rehabilitation of Calibration Laboratory in 1997. Together with implementation of new calibration equipment quality system was established upon the STN EN 45 001 and methodical guidelines for accreditation of the Slovak National Accreditation Service.

SHMI's Calibration Laboratory for meteorological instruments provides at present calibration of the instruments as seen in Table 2.

Table 2 Calibrated Meteorological Instruments

Instruments	Measuring Range	Best Measured Capability
Liquid in glass thermometers (all kind)	-30 to +40 ^{o}C	0,11 ^{o}C
Temperature sensors (PT100)	-40 to +60 ^{o}C	0,02 ^{o}C
Thermographs	-35 to +45 ^{o}C	0,3 ^{o}C
Psychrometers	10 to 90 % RH	1,5 % RH
Mechanical hygrometers	10 to 90 % RH	3,0 % RH
Capacitance hygrometers	10 to 90 % RH	1,5 % RH
Hygrographs	20 to 90 % RH	1,5 % RH
Digital barometers	650 to 1050 hPa	0,12 hPa
Mechanical barometers	650 to 1050 hPa	0,01 % MR
Mercurial barometers	650 to 1050 hPa	0,12 hPa
Anemometers	0,15 to 50 m.s^{-1}	0,1 m.s^{-1}
Anemographs	0,15 to 50 m.s^{-1}	0,1 m.s^{-1}

The calibration of other meteorological instruments is done upon subcontracts with the National Metrology Authority and in some cases (solar radiation) international comparison is used.

SHMI's Calibration Laboratory for meteorological instruments uses at present calibration equipment as seen in Table 3.

Table 3 Calibration Equipment

Parameter	Equipment	Reference Standard
Temperature	JULABO Ultracryostat FP 40 HP	Set of TWG Mercurial Thermometers;
	MLW Ultracryostats MK70	ROSEMOUNT SPRT 162CE;
	Fully automated HART SCIENTIFIC 1560 and HS 2562	VAISALA DTS 12A
	PC controlled FEUTRON Chamber KPK 600	
Humidity		VAISALA HMP 35
	VAISALA HMK 13B	KRONEIS Dew Point Meters 630
Pressure	DH INSTRUMENTS Calibrator PPC2+ A0023-R; Pressure Generators	DH INSTRUMENTS Calibrator PPC2+ PAROSCIENTIFIC Digital Barometer
Wind	THEODOR FRIDRICHS Aerodynamic Tunnel	Set of TESTO 400

To assure the quality of the measurement process the regular maintenance and repair is done by the authorized sub-contractor of the producer. Repair is done upon the priorities in one of three limits – 1 day, 3 days and 5 days respectively.

The training of staff is done by specialized and refreshment courses or self-study and selected personnel should pass through the certification process, depending on education, every two or five years respectively.

At present the following documents within the Quality Measurements System are introduced:

- Quality Policy Document
- Quality System Documents
- Control Quality System Documents
- Calibration Methods Documents with measurement uncertainty
- Procedures for Equipment and Measuring Instruments' Usage, Handling and Maintenance
- Traceability Assurance Documents

Above Documents are subjects of basic chapters in the Quality Manual established upon the General requirements for the competence of testing and calibration laboratories. The other chapters of the manual provide procedures on:

- Internal and external Audits
- Staff, Staff and Equipment rooms
- Filing System
- Validity System
- Complaints
- Subcontracts
- Security

After a number of Internal Audits the first International External Audit was done upon the ISO 17 025 (July 2000). This was done within the PHARE/PRAQ III Project "Preparing conformity assessment bodies for accreditation for calibration laboratory". The accreditation of SHMI's Calibration Laboratory for meteorological instruments is expected by the end 2000/beginning 2001.

****

USA National Weather Service Radiosonde Upper Air Excellence Award Program

Carl A Bower, Jr. and William H. Blackmore

National Oceanic and Atmospheric Administration, National Weather Service

1325 East-West Highway
Silver Spring, Maryland 20910 USA

1. Introduction

The National Weather Service (NWS) has implemented an annual awards program for Upper air observations. Each year, the outstanding upper air observing station is recognized for excellence. Measures of excellence are determined for providing verified, consistent, and high-quality upper air observations supporting numerical weather predictions for regional and global forecast guidance products. Three elements are used to measure station performance. Fifty percent of the weight for upper-air data quality and availability is determined according to a scoring system derived from the NWS National Centers for Environmental Prediction (NCEP) computer generated statistics. Thirty percent of the weight is allocated to adherence to national policies, procedures, and initiatives to improve upper air programs. The third area with twenty percent of the weight is station operational performance including logistics management, quality assurance, and timeliness.

2. NCEP Statistics Generation

Statistics for all radiosonde flights for each station in the National Weather Service supported network are generated monthly by the NCEP. The statistics summaries are generated for height, temperature and wind categories and provide an excellent opportunity to monitor the radiosonde network performance in a non-labor intensive manner. Table 1 depicts the format NCEP uses and the category definitions. All stations in the network are included in the monthly statistics.

Table 1. Basic table format for height, temperature and wind.

						Atmospheric Pressure Level									Termination Category					
						> 400 hPa			399 - 100 hPa			< 99 hPa			Soundings Number					
STA	ID	NS	NB	SR	SA	CR	NT	NR	CR	NT	NR	CR	NT	NR	A	B	C	D	E	F
70026	BRW	59	59	0	0	0	427	0	0	303	0	0	210	0	61	60	54	44	0	0

STA = WMO international station index number

ID = Station call letters

NS = Number of soundings with data received on time (by NCEP) for the month

NB = Number of soundings with bulletins received on time (by NCEP) for the month

SR = Number of soundings with significant rejections (more than 10% total)

SA = Number of soundings with any data rejections

CR = Number of soundings in that data reports category with any rejections

NT = Number of heights in that data reports category for the month total

NR = Number of heights rejected in that data reports category for the month

A = > 400 hPa -- Region IV (see Manual on Codes, WMO-No. 306). A sounding that fails to reach 400 hPa is deemed a failed flight and a second release may be authorized.

B = > 100 hPa -- level that separates the TTAA and TTBB messages from the TTDD and TTCC.

C = > 50 hPa.

D = > 20 hPa -- level for 80% radiosonde balloons are expected to achieve (about 26 km).

E = > 10 hPa level that should be achieved by 60% of the launches to satisfy NCEP requirements.

F = > 5 hPa -- WMO goal for GCOS Upper-air Network altitude performance.

NOTE: Elements A through F are compiled 6 hours or more after balloon release (11:00 or 23:00 UTC) and before NCEP data deletions are applied to the soundings. These statistics provide grounds to examine station staff performance, equipment and communications failures, maintenance, personnel performance, and support from headquarters and regional management.

Tables 2 through 4 for upper-air observations covering height, wind, and temperature performance statistics demonstrate the usefulness of such statistics for getting an overview on the performance. In Table 2, station 72518 shows height error problems in the 399-400 hPa and less than 99 hPa pressure categories. The soundings in these categories with data rejections are related to the problems in Table 4 for the same station showing soundings with rejected temperatures. This station lacks a solar correction for the temperature sensor. Table 3 for station 78486 is a station launching one sounding per day. Of note in this table is the low rate of on-time soundings to NCEP and the total rejection of wind data for the three pressure level categories. The rejection of the wind data was traced to faulty system alignment.

Table 2: Summary of height performance June, 2000.

						Atmospheric Pressure Level									Termination Category Soundings Number					
						> 400 hPa			399 - 100 hPa			< 99 hPa								
STA	ID	NS	NB	SR	SA	CR	NT	NR	CR	NT	NR	CR	NT	NR	A	B	C	D	E	F
70026	BRW	56	56	2	2	0	419	0	2	301	8	2	225	7	60	60	60	58	49	0
72518	ALY	52	52	28	28	0	402	0	27	281	50	28	283	140	59	57	55	53	50	44
72681	BOI	56	57	0	0	0	350	0	0	290	0	0	274	0	58	58	58	57	52	40

Table 3: Summary of wind performance March, 2000.

						Atmospheric Pressure Level									Termination Category Soundings Number					
						> 400 hPa			399 - 100 hPa			< 99 hPa								
STA	ID	NS	NB	SR	SA	CR	NT	NR	CR	NT	NR	CR	NT	NR	A	B	C	D	E	F
70026	BRW	58	58	0	10	0	1238	0	4	865	4	6	574	6	62	60	58	38	0	0
78486	DSD	6	6	28	28	28	645	645	26	379	379	20	242	242	27	21	19	13	0	0
72681	BOI	62	62	0	11	3	1065	5	3	951	5	7	967	7	62	59	59	58	46	0

Table 4: Summary of temperature performance June, 2000.

						Atmospheric Pressure Level									Termination Category Soundings Number					
						> 400 hPa			399 - 100 hPa			< 99 hPa								
STA	ID	NS	NB	SR	SA	CR	NT	NR	CR	NT	NR	CR	NT	NR	A	B	C	D	E	F
70026	BRW	56	56	2	3	1	1250	1	2	531	12	2	435	13	61	60	60	58	50	0
72518	ALY	52	52	25	30	9	1098	15	24	792	102	25	917	416	59	57	56	54	51	44
72681	BOI	56	57	0	14	14	824	15	0	646	0	0	806	0	59	59	59	57	52	42

3. National Upper-air Station Performance Ranking Program

From the above statistics, it is possible to compute the terms for equation (1). To evaluate NWS upper-air station performance and help improve data availability, quantity and quality, the following equation (including appropriate weighting factors) is used to rank station performance:

$$\text{Score} = A/2 + B + C + D/2 - E/5 - F/5 \quad \text{where,} \qquad (1)$$

A = Percent of monthly soundings arriving at NCEP by 0200 or 1400 UTC. To score in this category, all coded messages (with or without data) must be received.
B = Percent of monthly soundings achieving the minimum 400 hPa requirement.
C = Percent of monthly soundings achieving 50 hPa.
D = Percent of monthly soundings achieving 20 hPa.
E = Percent of monthly temperature levels between surface and 400 hPa rejected by NCEP.
F = Percent of monthly wind levels between 400 and 100 hPa rejected by NCEP.

Elements B through F are compiled 6 hours or more after balloon release (11:00 or 23:00 UTC) and before NCEP data deletions are applied to the soundings. The maximum score a station can achieve with this equation is 300. It is important to note that a station's ranking does not solely reflect station staff performance. Factors such as equipment and communication failures, maintenance personnel performance, and support from NWS Regional office and Headquarters management, are also taken into consideration when evaluating station scores.

4. NWS upper-air station rankings for 3 months:

A perfect score based on the above equation is 300. Table 5 shows sample scores for four different rankings. The 92 stations in the NWS upper air network are ranked and scored each month. The range of scores from a top station to a bottom ranked station can exceed 100 points.

Table 5. Sample Station Scores and Rankings

Rank	Station	March Score	Station	April Score	Station	May Score
1	72364	298.4	72403	299.56	72597	299.63
2	72274	297.93	72597	296.93	91285	298.24
46	72365	283.03	72681	284.13	70326	287.77
90	74494	239.37	72426	240.48	72659	248.38

5. Key network performance indicators since the inception of the awards program

Since the start of the upper air performance program, the trend in station performance has shown continued improvement as shown in Figure 1. The improvement is mostly a function of human factors. Except for the data processing software, the ground systems, radiosondes, and balloons have remained nearly unchanged. Figure 2 is noteworthy, particularly in the improvement in radiosondes reaching the 10 hPa level. The NWS requirement is for 60 percent of the flights over the network to reach 10 hPa. Figure 3 shows the timeliness of upper air data arriving at the NCEP in time for the early forecast model runs. The trend is upward over the period.

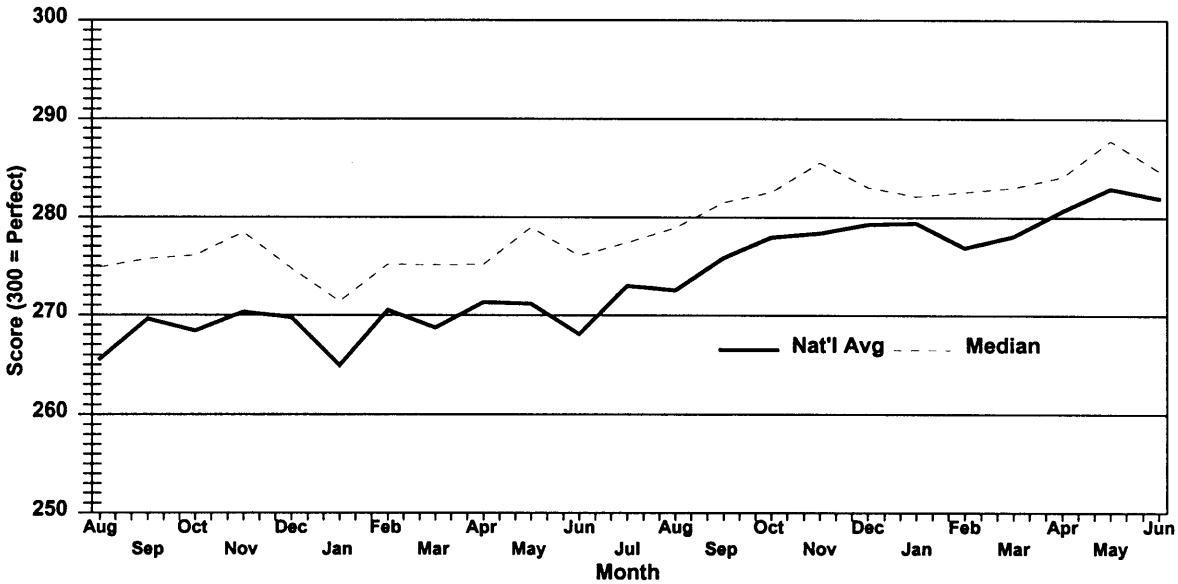

Figure 1. Average and Median Performance Scores from August, 1998 to June, 2000

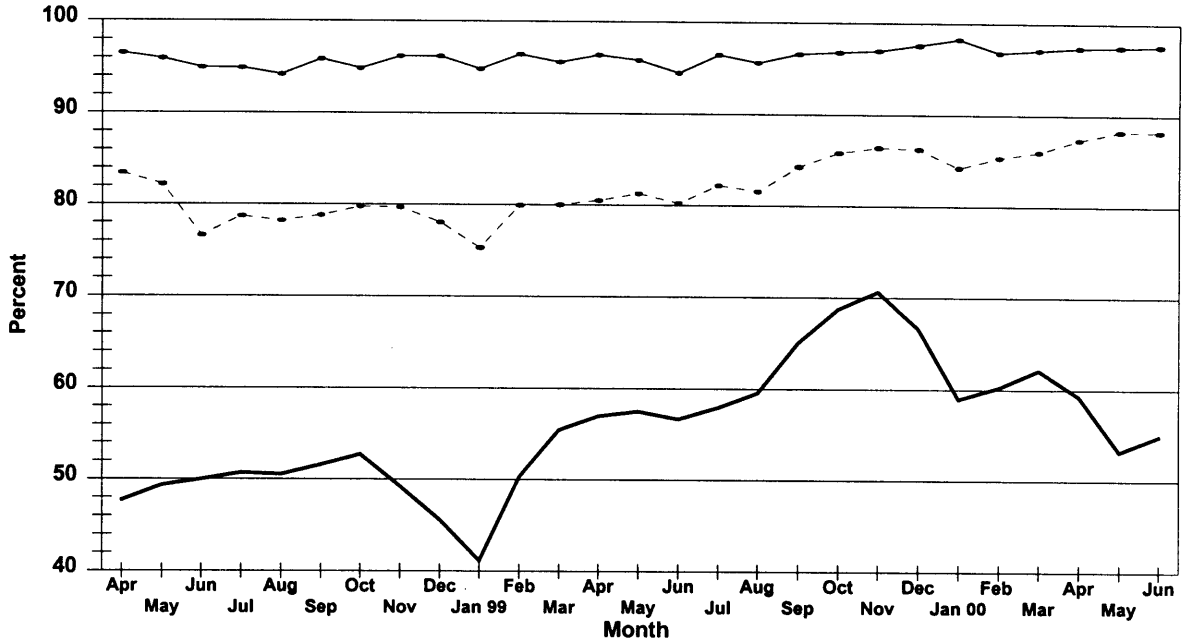

Figure 2. Percentage of upper air observations reaching or exceeding 400 hPa (thin line), 20 hPa (thin dashed line), and 10400 hPa (thick line) from April, 1998 to June, 2000.

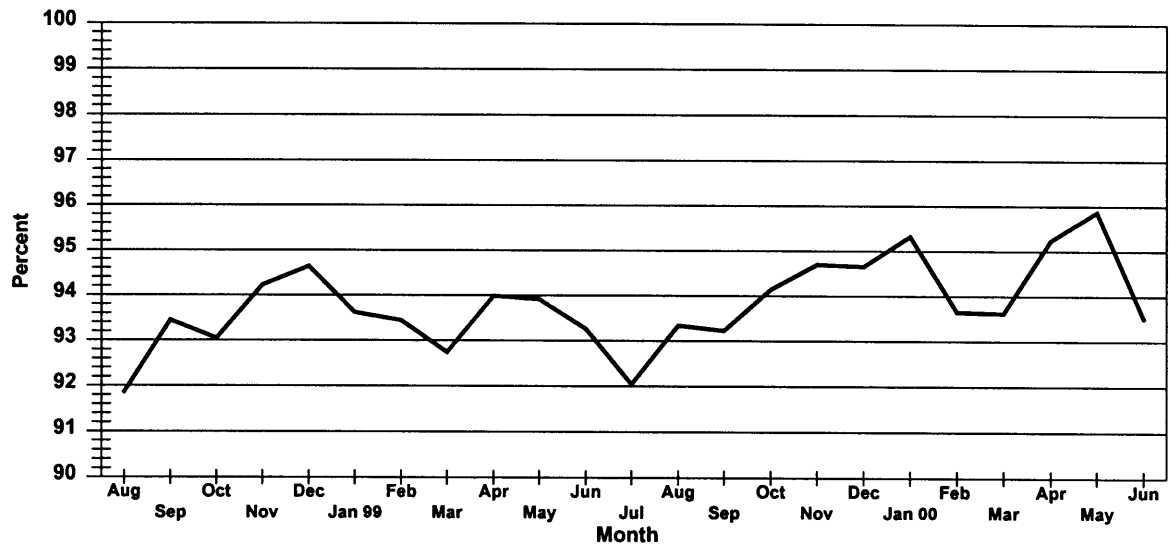

Figure 3. Percentage of upper air observations (with data) on time (by 0200 or 1400 UTC) to NCEP from August, 1998 to June, 2000.

6. Conclusions:

Since the beginning of the performance recognition program and the publication of monthly station rankings, the upper air network performance has improved through greater attention to optimal operational procedures, fault isolation and correction, and improved provisioning of appropriate expendable items. Senior NWS management are now able to monitor network performance against performance goals. The ability to manage this quality assurance activity is enabled by the NCEP automation of the radiosonde flight performance statistics for each 0000 and 1200 UTC flight for each site in the 102 NWS station network.

METEOROUTES :

The Walloon meteorological observation programme which aims at improving climatic forecasts

Thierry LEDENT
Attaché
Walloon Ministry of Equipment and Transport
Motorway District of CHARLEROI
Rue de la Tombe, 110 - Marcinelle
phone: +32 71 60 10 71
fax: +32 71 60 10 89
E-Mail : tledent@met.wallonie.be

ABSTRACT

Numerous investments have been made to carry out the "Météoroutes" programme which strives to offer a better service to the Walloon citizen during wintertime.

The Walloon territory is covered by fifty automatic weather stations. These stations permanently pick up parameters related to atmospheric conditions and road climatology. The network systematically sends these parameters to the PEREX centre (permanent station for network operation) and to the Air Force METEO WING which make short-term climatic forecasts for each of the main stations.

Although the measures are not carried out in compliance with W.M.O. specifications, their multiplicity enables the forecasters to fine-tune their predictions.

Taking account of a data exchange possibility, it is obvious that the automatic measurements carried out by the road managers of numerous countries can be of great benefit to meteorological observation services.

Presentation of "Météoroutes"

Each country, each region is aware of the difficulty to maintain minimum traffic conditions on its own road and motorway network. Road managers pour considerable energy as regards human and financial resources into the territory's winter serviceability.

In winter, the climate of the Walloon Region is often characterized by alternate cycles of night frost and positive day temperatures.

Wallonia has variable geographic features which only benefit little from maritime influence and are subjected to south-west prevailing winds.

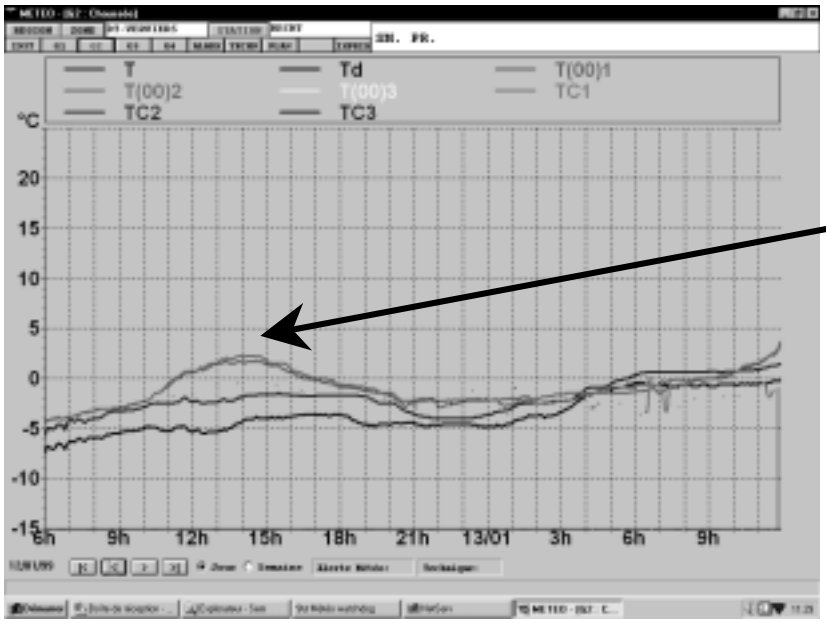

Example of frost and defrost

On upper curves (road surf. Temp.) there is a gap between –4°C and +3°C.

Example of road temperatures graphic

The "Météoroutes" project was set up to make up for all the inaccuracies related to pavement temperature forecasting. The project consists in centralizing all the climatic data at one permanent station for network operation called PEREX.

To achieve this, the M.E.T. invested in the installation of 15 main weather stations and 33 secondary stations.

With the help of our consultant, professor ERPICUM, specialist in climatology of the Liège University, the main stations have been set up so as to cover the region and to warn of the arrival of cold fronts wherever they come from.

Nearly all of the stations are located alongside the motorway network so that we can use our own electricity power supply system and communication network.

The aim pursued is to create a system for pavement surface temperature forecasting nearby each main station – which means that 15 different forecasts are made.

The stations measure relative air humidity, temperature, wind speed and direction, global radiation (pyranometer), atmospheric radiation (pyrgeometer). A rainfall detector indicates the nature (rain or snow) and the intensity (high, low, nil) of precipitation and a pluviograph has also been placed to determine its quantity. This recording raingauge measures the amount of precipitation averaged over periods of 6, 30 or 60 minutes.

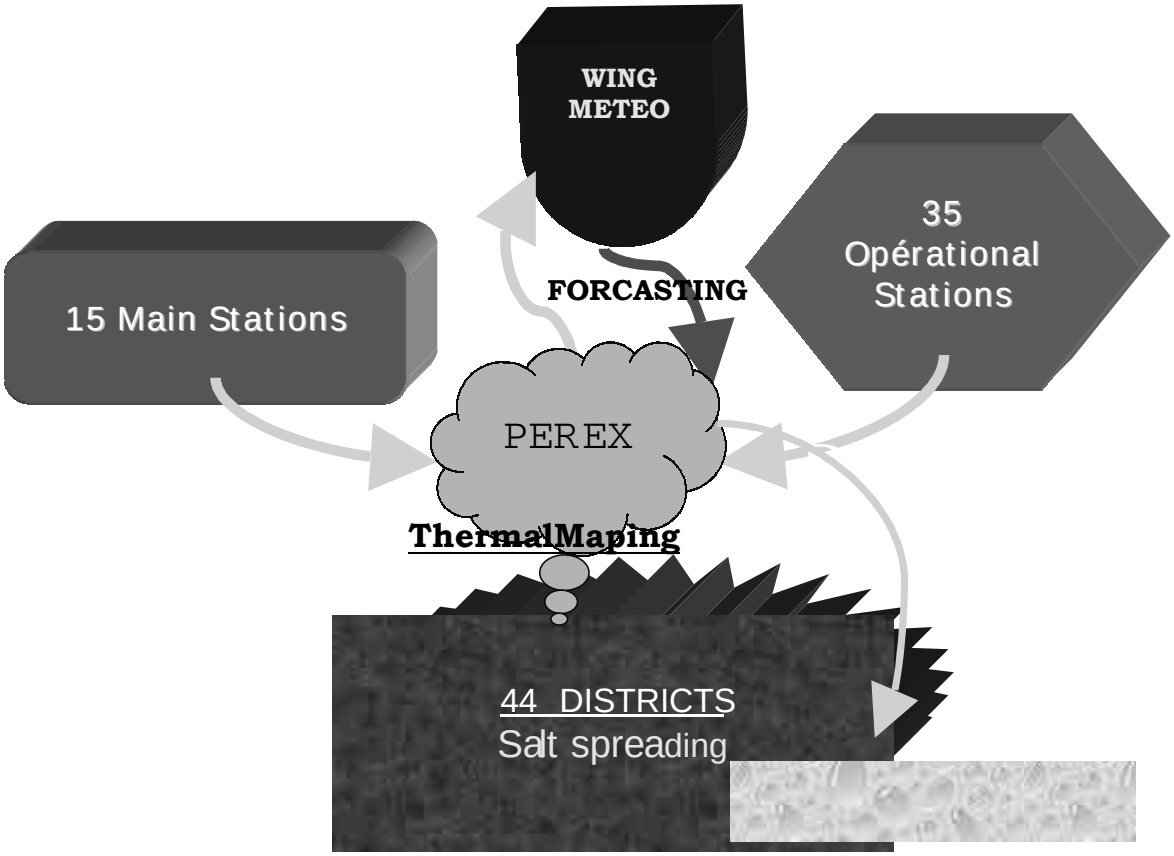

Ground based sensors which are of prime importance to our services measure the temperatures at pavement surface as well as at 5, 10 and 20 cm below pavement surface in order to take account of the thermal inertia of the road foundation. Moreover, these sensors indicate the condition of the pavement surface – dry, moist or wet.

The secondary operational stations situated in each road district are less sophisticated and are equipped neither with wind and radiation sensors nor with pluviographs. Temperature sensors are installed at pavement surface and at 5 and 10 cm below. They are very useful to the local managers who refer to them in real time.

All the stations gather the measure data. They process them and send them every 6 minutes to a central unit of the PEREX centre and to the METEO WING. More than 78000 climatic measures as well as more than 43000 measures coming from the road sensors are processed automatically each day.

Although some measures do not comply entirely with W.M.O. standards, it would be a pity if they would not be taken into consideration by meteorologists.

To endow these data with characteristics ensuring their validity and reliability in time, a certain number of conditions must be satisfied. As far as the Walloon Region is concerned, a maintenance programme was developed for the weather stations and ensures

that repairs of the sensors will be carried out at short notice. This means that, in winter, a temperature sensor should be replaced within 5 hours from the moment that the failure was detected.

The METEOROUTES programme fits in with a traffic management scheme operational night and day. In case of malfunction, this system makes quick action possible by analysing the failure detection software as well as data from video images or additional information provided by the managers.

Data are centralized and archived at the Perex Centre (which stands for **Per**manence d'**Ex**ploitation) and are redistributed to the managing road districts, the territorial directorates, particular users of the Walloon Region as well as to the Liège University.

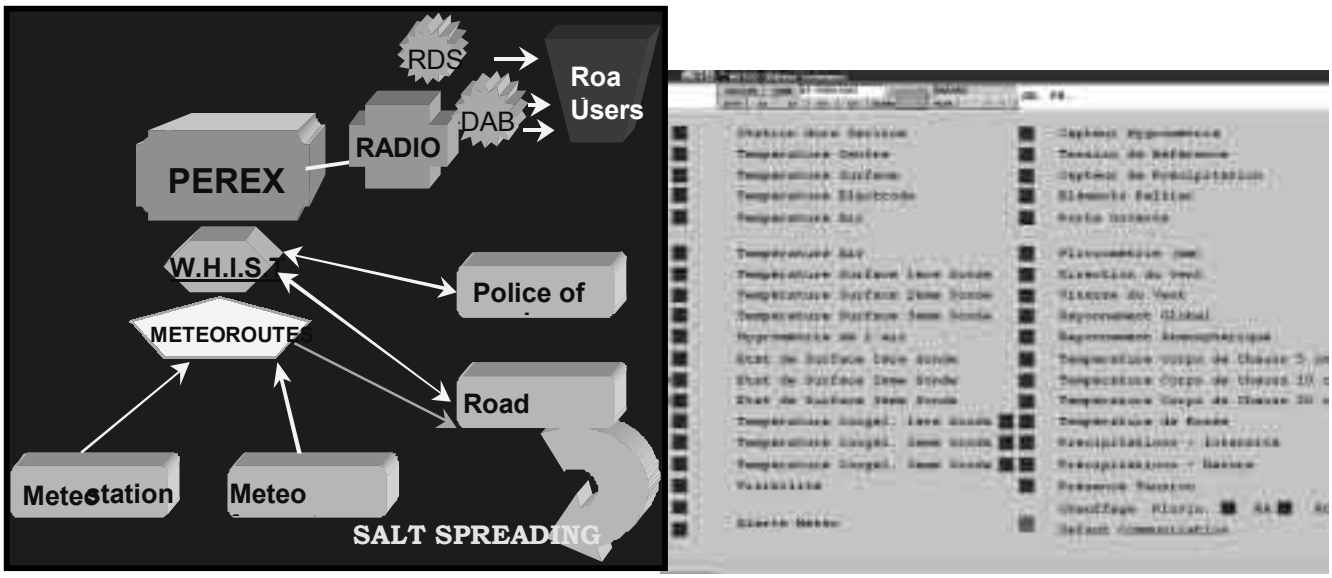

The network architecture is based on advanced technological elements such as automatic data acquisition stations, a specific X.25 network, Unix computers, AIX work stations, an IP WIN network, and also local user NT terminals.

The thoroughness of the whole system follow-up enables to guarantee the credibility of the measured meteorological data. Weather forecasters can process these measures in order to confirm their data, to refine their forecasting application and to conduct climatology studies.

At present, a complete counting of this type of weather stations is being carried out within the framework of the CIMO.

****

A Lifecycle Management System for National Monitoring Networks in Canada

Garry M. Pearson [1], Meteorological Service of Canada, Dartmouth, NS, Canada
Dave Dockendorff, Meteorological Service of Canada, Downsview, ON, Canada
Darryl Lynch, Meteorological Service of Canada, Downsview, ON, Canada

Introduction

The management of national atmospheric monitoring networks contains many challenges in terms of standards, quality, and maintenance. Users of data from these systems want assurances of accuracy, reliability and timeliness. To respond to these demands and to ensure a sustainable network, Canada is implementing a series of measures in the management of its national meteorological and hydrological monitoring programs. Collectively, these measures encompass a lifecycle approach to the management of these systems and is comprised of a quality management system, real time data quality monitoring, and a lifecycle procurement management system. In fact, the goal of this approach is to make life cycle considerations an integral part of the decision making process at all levels of the organization.

This framework is intended

- To provide a sound decision making structure for the investment in new systems or technologies based on scientific, operational, and policy requirements.
- To provide sound engineering management practices for the operation and maintenance of the operational observing systems to minimize costs and maintain performance standards.
- To ensure sustainability of observing systems through life-extension, re-investment and decommissioning strategies.

This paper will describe these systems and present Canada's experiences in implementing these management tools in the operation of its national atmospheric monitoring networks.

Components of the Life Cycle Management System

The national monitoring networks in use in Canada comprise of a complex system characterized by a mixture of in-house and commercial systems. With global markets opening up to technology providers, national meteorological organizations have been gradually devolving themselves of in-house development. This trend is not without its pitfalls, and has lead to interesting challenges in the management of complex observing networks comprised of mixtures of commercially available and in-house systems. In Canada this is further complicated by the respective roles of Environment Canada -Meteorological Service of Canada (MSC), Transport Canada (regulator), and NAV CANADA. (national aviation navigation services provider).

Increased levels of accountability and fewer resources within government means that it is important to manage the investment decision-making carefully. This framework is meant to be a guide to this decision making and management process.

The Life Cycle Management System (LCMS) is comprised of processes and tools to achieve its goals. It was developed based on best practices in industries with similar management issues. The primary components of the LCMS are: strategic direction analysis, requirements definition, engineering and investment analysis, Investment decision making process, implementation into operations, in-service management, performance measurement, life extension, decommissioning.

1. Strategic Direction Analysis

Strategic direction analysis provides the overall program direction for the monitoring systems within the MSC. It is here where the purpose, present and future activities for these networks are defined in terms of scientific, operational, and policy requirements. The strategy encompasses scientific direction, anticipated user needs, and advances in technology. There is a direct link between this strategic direction and the department's business lines, program priorities and requirements, and international obligations.

The Strategic Direction:

1) Provides a brief overview of what technological changes have been implemented in each network over the past year.

2) Identifies strategic directions and associated R&D that should be pursued and that will improve or enhance a particular program delivery.

3) Links the capital projects to the specific network(s) they support and thus provides a historical perspective as to capital allocations.

Figure 1 **Long-term Capital Investment Strategy**

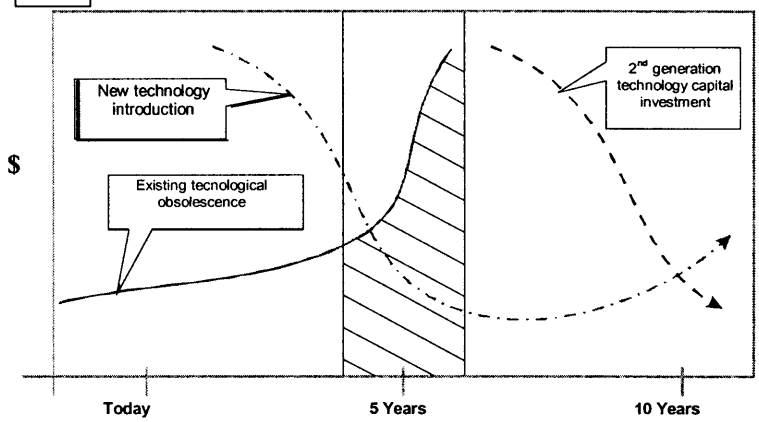

Changes to monitoring systems can be triggered by a number of factors such as changes in informational requirements, technological advances, rust out, health and safety or funding pressures.

Therefore, the Strategic Direction forms a fundamental basis for major capital decision making by ensuring that proposed changes to monitoring systems adhere to overall strategic directions of the MSC.

2. Definition of Requirements

The definition of requirements for new or changing monitoring systems is an iterative process between the needs of the users and potential engineering solutions. Requirements are driven from a combination of operational, scientific and policy needs. It is important that system requirements are formalized so that investment decision making has a rational basis. Formalized requirements are documented in a manner which does not assume an engineering solution, but merely states what is needed, not how it is to be accomplished. Requirements are defined using the following elements: Overview, Operational Requirements, Technical Performance Specifications, Physical Integration, Functional Integration, Health and Safety, In-Service Support, and Test and Evaluation

3. Engineering and Investment analysis

Engineering and Investment analysis provides a comprehensive analysis of the total lifecycle implications of implementing a new or revised monitoring system. The goal is to ensure that a solution strikes an optimum balance between meeting requirements and affordability. This analysis provides input into the Investment Decision Process. The following factors comprise this analysis: Strategic Direction Analysis (does the proposed solution fit into the overall strategic direction?), requirements (does the proposed solution meet stated requirements?), Engineering Analysis (i.e. engineering impacts), market analysis (commercial possibilities), alternatives analysis (other methodologies or partnerships), factors analysis (cost/benefit, effectiveness, supportability issues, etc.), service life extension analysis.

4. Funding Decision Making

Capital allocations for investment into monitoring systems takes place through a committee structure involving a challenge process. Those responsible for decision-making require assurances that priorities are relevant, requirements will be met, alternatives considered, solutions are affordable, and long term cost implications are considered. In essence, to ensure that complete life cycle costs are considered in the capital Investment decision making process. All of the previous steps are to ensure that sufficient consideration for all of these factors have been analysed in preparation for application for funding decisions.

5. Implementation into Operations

Commissioning protocols are used when new equipment is introduced into operational networks. An example would be the AWOS Commissioning Protocol which involves standards and procedures used by the Meteorological Service of Canada (MSC) to ensure that each Automated Weather Observing Station (AWOS) used for aviation programs is verified before being approved for operational use. The process is a very rigorous one which includes verification of components and installation procedures, end to end proof of performance testing, (including the communications networks), message processing software, training, user notification and formal sign-off procedures. This Commissioning Protocol also comprises part of the MSC's quality management system for METAR's.

Whenever new equipment is purchased it is also necessary to comply with a: Contract and regulatory system for procurement administered by Public Works and Government Services Canada. These regulations help ensure that companies have a fair opportunity to compete, that the Canadian Government gets good value and that conditions under the North American Free Trade Agreement (NAFTA) and the General Agreement on Tariffs and Trade (GATT) are followed.

6. In-Service Management

Maintenance policies and procedures must be established for all operational equipment. This includes documentation on the installation and operation of the equipment along with related training material and special diagnostic equipment and software. In the field and depot maintenance by both Regional Maintenance and contracted out repair and overhaul must also be considered.

Formal quality management practices ensure that standards, procedures, and practices are clearly defined, documented, and followed in all aspects of operations. Key elements include controlled documentation sets, qualification criteria for critical tasks, and clear processes for problem identification, performance measurement, auditing, and management review. The ISO 9002 standard has served as a model for developing a quality management system for the aviation observing component of the network. This system is scheduled for implementation in the fall of 2001. It is expected that the system will expand to encompass other observing networks over a period of time. Formal registration to the ISO standard however, is not an immediate objective

7. Performance Measurement

Performance measurement has become as an essential component in modern comptrollership. It can be as a powerful tool for strengthening an organization's relationships and accountability, and for improving its capacity to effectively manage scarce resources. It is important for both the improved management of information to appropriately lead and co-ordinate information, and for stronger accountability (parliamentary reporting).

Among items of primary importance for performance measurement are data availability to meet requirements of scientific, service and policy components in terms of data density, frequency, availability, quality and adherence to standards.

8. Change Management

The Change Management Board (CMB) ensures the orderly management of change to instruments, systems and algorithms employed in national meteorological and climatological networks. It ensures that the introduction of changes (either hardware, software, or procedural) will not adversely affect the integrity of existing networks with regard to quality or purpose. The board is comprised of a process whereby proposed changes are reviewed by experts in areas that may be affected by changes, to provide analysis of the impacts of these changes on the networks as a whole.

9. Life Extension

As equipment ages, systems may reach a decision point - Is it better to reinvest in new technology, or, for a relatively small investment, extend the life of the equipment a few more years ? The question is often complex and involves an engineering and costing analysis. The decision will be influenced by the overall operational state of the system, the potential engineering solutions available (or soon to be available), and incremental cost.

10. Decommissioning

The cost of decommissioning equipment is a factor that should be included in the life-cycle plan. This often-ignored factor can be significant and may be driven by health and safety or environmental concerns. In northern remote sites, the cost of removal or disposal of environmentally hazardous materials can be significant.

11. Implementation of LCMS in the Meteorological Service of Canada

The total life cycle management approach to national monitoring networks is being implemented in stages within the MSC. This requires changes to both organizational culture, procedures, and the development of management tools.

A number of tools are under development for the management of these systems. Briefly, they comprise of:

LCMS Analysis Web site: National Archive System meta-data information links, site configuration, asset information, costs, depreciation, component age analysis (i.e. Are system components nearing the end of their operational life ?), See Figure 2.

Action Request System: A national maintenance tracking system to follow maintenance issues on automatic stations and the lightning network. This system allows for the tracking of "trouble tickets", maintenance performed, site down-times, and ultimately, analysis of component failure issues. This type of system will be expanded to include other networks in the near future.

In terms of procedures, recent changes include the formal introduction of change management boards, the shift (within government) to full accrual accounting of assets and depreciation, improved engineering processes, and an improved challenge process in major funding decisions involving full life-cycle cost considerations.

12. Conclusion

The introduction a life-cycle management approach in the Meteorological Service of Canada is proceeding. It is anticipated that improved management tools and procedures will lead to better managed networks meeting the needs of users and clients.

Figure 2

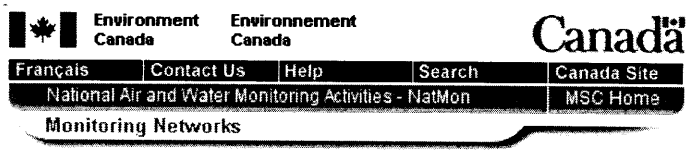

UA Network Queries and Mapping

Network Query

(From server database)

Province/Region:
Canada
Alberta

Station ID, Station Name:
any
any

Measured Parameters:
any
Temperature
Humidity
Preassure
Wind speed and direction
Upper Air Winds
Upper Air Temp/Moisture

Instrument Component:
any
AES, battery eliminator
Aqua Fountain, water conditioner,

Observations Frequency:
any

Last Updated:
May, 2000

Latitude, Longitude:
any
any

Submit!
Go!

Interactive Mapping

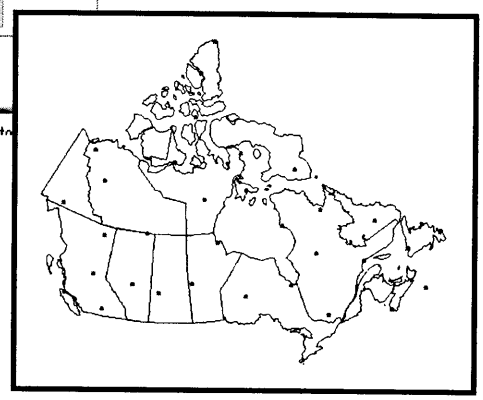

Site Information

Station ID	Station Name	Climate ID	Province	Station Type	Elevation (m)	Latitude	Longitude
10744.0	ALERT UA	2400306	NU	WS2	65.40	82.50	-62.33
7340.0	BAKER LAKE UA	2300505	NU	CON, WS2	50.80	64.32	-96.00
10754.0	CAMBRIDGE BAY UA	2400604	NU	WS2	25.10	69.13	-105.07
10745.0	CHURCHILL UA	5060606	MAN	CON, WS2	28.50	58.73	-94.07

Component Age Analysis

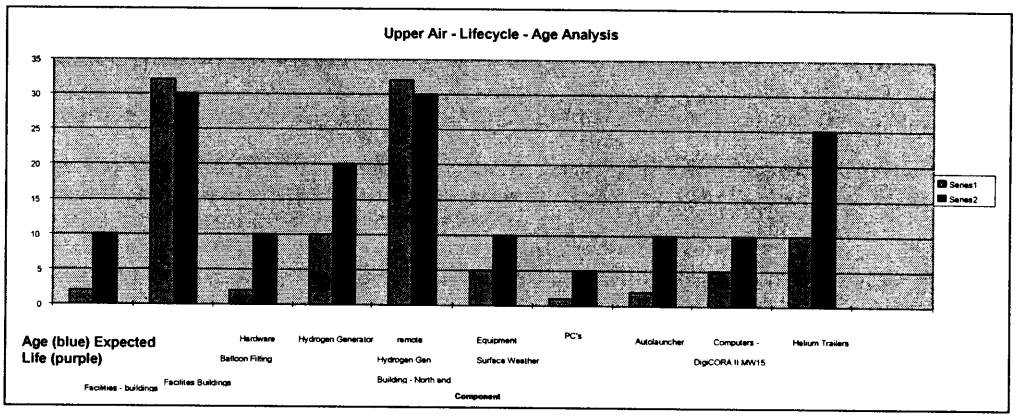

NUEVAS TECNOLOGIAS PARA LA MEDICION DE PRECIPITACION Y SU IMPACTO TECNOLOGICO

(New Technologies for Precipitation Gauging and their Impact)

Ing. Marielba Guillén Orellana
Institución: Ministerio del Ambiente y de los Recursos Naturales
Centro Simón Bolívar. Torre Sur. Piso 6. Oficina Nº606
Dirección de Hidrología Y Meteorologia. MARN. Caracas, Venezuela
Teléfono: 58-2-408-1445/408-1257 Fax: 58-2-4811947 E-mail: marielbag@yahoo.com

ABSTRACT

This paper tries to present a diagnosis of the Technologies Assessment, generated by the use of new technologies in rain measure instruments. It analyses for instance, how changing Clock systems for Litio bateries in automatic stations, to register rain, would affect economics, enviroment and the operator of the Automatic Rain Gauge; the use of the technology itself produce impacts. This paper will study the effects on society, when a technology is introduced, extended or modified. To evaluate new technologies for measuring rain, would be equivalent to value their uses.

La evaluación tecnológica es definida como la evaluación del impacto a corto y largo plazo de una tecnología de tal forma que se logre un uso optimo de los recursos y se alcance el desarrollo social y económico de una región, dentro de un marco de recursos disponibles y una visión de desarrollo.

Para algunos autores (José San Martín, 1992), evaluar una tecnología equivale a valorar sus usos, lo cual a su vez supone identificar y analizar los efectos directos e indirectos que se derivan del uso de una tecnología y de la tecnología misma.

Una de las definiciones de Impacto Tecnológico (Technology Assesment) más comúnmente usadas examina los efectos en la sociedad que ocurren cuando una tecnología es introducida, extendida o modificada con especial énfasis en aquellas consecuencias indirectas retardadas o aquellas que no sean intencionales (Joseph F. Coates, 1971).

En la presente evaluación de Impacto Tecnológico se utilizo como técnica la tormenta de ideas ("brainstorming") que es una técnica asociada con el enfoque global o individual sobre un problema no estructurado, que requiere un razonamiento reflexivo, y cuya característica descriptiva primordial es el cuestionamiento de enfoques y supuestos a nivel global (Ramos 2000). Después de la tormenta de ideas fue realizado un análisis critico personal.

Para Venezuela que es el caso que nos ocupa se va a realizar un diagnostico del impacto tecnológico que produjo el cambio de la tecnología para registrar la lluvia. La medición de la lluvia comienza en el año 1891 en la estación Cagigal y a través de mas de 100 años que han transcurrido hasta el presente de ha observado el cambio de los diferentes instrumentos utilizados para la medición de la lluvia desde el pluviómetro de cántaro pasando por los registradores que usan sistema de relojería como los pluviografos de sifón y de balancín hasta que a principios de la década de 1990 el Ministerio del Ambiente y de los Recursos Naturales decide debido al avance a nivel mundial de nuevas tecnologías para el registro de lluvia automatizar como primera fase la red de pluviografos en todo el territorio nacional.

Para la automatización se están utilizando sensores tipo balancín y datalogger que utilizan baterías de litio como fuentes de poder, como podemos observar se cambia el sistema de relojería por un datalogger que requiere para funcionar una batería de litio, cuya duración se estima en 5 años al final de los cuales la batería debe ser desechada y para lo cual en Venezuela no existe actualmente lugares adecuados para deshacerse de ellas, con lo cual quedaran expuestas al ambiente creando en un futuro focos de contaminación ambiental.

Otro de los impactos es el cambio de perfil académico que requiere el operador de la estación automática, ya que necesita conocimientos en electrónica y computación para instalar, mantener, procesar y analizar los datos de lluvia recabados automáticamente por el sensor, con lo cual muchos de los operadores con largos años de experiencia en estaciones con sistemas de relojería experimentan lo que se denomina resistencia al cambio y lo cual trae como consecuencia que deban ser relevados de sus cargos por personal mas joven con los conocimientos requeridos en las áreas antes mencionadas, pero con poca experiencia en la determinación de la calidad de la información que generan las estaciones automáticas.

Desde el punto de vista de la institución el impacto es económico ya que tiene que ofrecer una mayor remuneración al personal que opera las estaciones automáticas, esto debido a que aumenta la exigencia de conocimientos. El sistema tradicional de relojería tiene una vida útil de mas de 20 años en cambio las partes y repuestos de las estaciones automáticas se estima su vida útil en cinco años, con lo cual aumenta la frecuencia de adquisición de partes y repuestos y lo cual conlleva un aumento en el gasto para operar las estaciones automáticas.

Pero tambien hay que mencionar que debido a que se elimina el laborioso trabajo de evaluación de las bandas, se dispone en menor tiempo de un mayor volumen de datos en medios magnéticos con lo cual se agilizan los trabajos de investigación y de aplicaciones practicas en el campo de la meteorología

Toda tecnología requiere de una evaluación de los costos y beneficios. Para ello, se deben considerar todos los efectos directos e indirectos, sobre los actores sociales, que utilizarla tecnología, mediante el uso de la "matriz de apoyos y resistencias" (Hetman, 1975) ver Cuadro Nº 1.

****

Matriz de Apoyos y Resistencia del Proyecto Automatización de la Red de Pluviógrafos

Resistencias / Apoyos	Efectos Primarios: Cambios.	Efectos Secundarios: Adiestramiento	Efectos terciarios Costos	Ventajas atribuidas a la tecnología existente Comodidad, técnicas conocidas	Sugerencia de modificaciones de la tecnología existente Complementariedad
Beneficios primarios Especificidad	4 5				
Beneficios secundarios Sensibilidad		3 4			
Beneficios terciarios Precisión			4 5		
Beneficios generales atribuidos a la tecnología Celeridad en la obtención de los datos				4 5	
Alternativas propuestas a la tecnología deseada Fabricación de dataloger nacional					4 4

Escala :0 (ninguno), 1 (muy poco), 3 (neutro), 4 (mucho), 5 (mucho mas)
Fuente: elaboración propia (adaptado de Hetman, 1975).

Hetman, F.(1975). Evaluación Tecnológica y Sociedad. Madrid, España. OCDE, Ministerio de Relaciones Exteriores de España.

Effect of Data Collection Instruments on the Quality of Data: The Case of Ethiopia

Alemtsehay Estifanos
National Meteorological Services Agency
P.O. Box 3560
Addis Ababa, Ethiopia
Tel.: +251-1-615 779 (Off.); -158 326 (Res.) Fax: +251-1-517066
E-mail: Alemtsehaye@hotmail.com

Abstract

Meteorological data observing stations are scarcely distributed in Ethiopia. Besides, most of the stations are located near the main roads since communication and observing systems are still at early stage in the rural areas. Among the available stations, only 8% are equipped with single side band radios for the transmission and reception of meteorological data. On the other hand, there are only two upper air stations throughout the country. And, there is one Meteosat and NOAA data receiver at the head quarter that receives information daily. As a result of the inadequate distribution of stations, lack of good communication system, poor quality of instruments and lack of skilled manpower, the data collected for meteorological uses are not sufficient.

This study explores the data collection system and investigates the problem of measuring instruments, and suggests a remedy for it. Generally, the study focuses on the instruments used and the problems faced.

Introduction

Ethiopia has multiple types of climate, ranging from arid to humid types. More than 80% of the labor force are engaged in agriculture. Agriculture, mostly rain-fed, is highly sensitive to variations in weather and climate. The country has experienced recurrent droughts, a high rate of deforestation, soil degradation and loss, and severe over-grazing. It is of vital importance that Ethiopia should give due consideration for meteorological observation. Therefore, quality data should be collected for use in agricultural and allied planning activities. Hence, rehabilitation of destroyed observatories, maintenance and upgrading of observatories should be given a priority.

Meteorological Observation and Data Collection

In Ethiopia, meteorological observation and data collection started in the late 1930s at Addis Ababa (Fantolli 1965). In the early fifties a meteorological unit was established under the aegis of the Civil Aviation Department to meet the requirements of the growing aviation industry. Thereafter meteorological observations and data collection systems were promoted and stations have been established one after the other (NMSA 1992). An increased awareness of the importance and the need for application of meteorological information to various socio-economic activities led to the establishment of the National Meteorological Services Agency (NMSA) in 1980. At the NMSA Meteorological Instruments Laboratory and Calibration Workshop is established for routine check of the instruments. There are about five automatic stations, which are not currently working due to lack of skilled manpower. Also estimated rainfall and vegetation index maps are produced using the METEOSAT and NOAA facilities.

Satellite-based data collection and distribution systems are also integrated in the GTS system.

i) The METEOSAT and NOAA Data Capture System

At the NMSA, there is remotely sensed data collection site equipped with the METEOSAT /PDUS and NOAA/HRPT ground receiving facilities. The NOAA/HRPT hardware facilities including an HRPT antenna, HRPT frame synchronizer, buffer and hardware interface with PC attached to a printer. Using the NOAA /HRPT facility the Normalized Difference Vegetation Index (NDVI) maps are produced every ten days to serve the purposes of vegetation monitoring. For tracking the NOAA satellites and facilitate data acquisition, information called TBUS is collected through GTS network.

The METEOSAT/PDUS reception system consists of a receiving antenna driven by a PC-AT attached to a printer. The system is used to produce Cold Cloud Duration and Estimated Rainfall maps. As the techniques of estimating rainfall are associated with the temperature of cloud tops, the process requires certain temperature thresholds to be fed to the computer prior to capture. At present, calibration at temperature thresholds of -40°C, -50°C and -60°C are used for different Zones of the country. Although estimated rainfall products are used for current rainfall monitoring purposes, the calibration process is still in progress.

ii) The Meteorological Data Distribution (MDD) Capture system

In the MDD system, pictorial, text and binary data are transmitted for the ground stations to the satellite and made available to all ground users. Pictorial data are transmitted from Bracknell text bulletins and reports from Rome. The Toulouse center also sends different outputs of numerical weather prediction from the Meteo-France. The MDD data capture system was installed at NMSA in November 1992 and processed maps (actual and prognosis maps, NDVI, etc) and alpha numerical data are received. The MDD system is upgraded with new operating system and displaying package after the year 2000.

iii) Data Collection Platforms (DCPs) and Data Reception System (DRS)

The DCP system is designed to make unattended operation over an extended period. Meteorological observation from remote and inaccessible areas can be made using the DCP system. Data collected from stations is transmitted via METEOSAT and reception is made using the DRS system. There were about 8 DCP stations, but at present none of the stations are operational due to lack of spare parts.

Measuring instruments and problems

Most of the measuring instruments and device have been installed at the time the expansion of networks during the early 1950s. Major problem experienced has been lack of spare parts. Supervision has also been poor. This is due to financial constraints and skilled manpower. For example, some of the thermohygro-graphs need sensors and maintenance of the mechanical part. The standard orientation for sunshine recording instruments is North-South. However, due to occasion cracking of the land on which the instrument rests, the orientation slightly changes. This gives erroneous results.

In our country we have Meteorological Instruments Laboratory and Calibration Workshop. Instruments are usually checked for standard and calibration and maintenance are done at the laboratory. However, calibration and standardizing equipment are scarce. Calibration and standardization equipment in scare include:

1. **Pressure chamber:** We calibrate pressure-measuring devices such as aneroid barometers, barographs and mercury barometers. These instruments should be calibrated at regular intervals using the calibration apparatus. Also our national standard barometer needs to be calibrated at regular intervals at the Regional Calibration Centre in Nairobi,

Kenya. However, due to financial constraints, we are not able to send instrument to get it calibrated. As a result error in measurements could occur.

2. **Humidity Sensor calibration Equipment**. We have this instrument but the instrument has not been functional for a long time due to the inlet water pipe has a leakage problem. As a result the drainage facility has been failed. Therefore, we have to go for the zero adjustment system.

3. **Wind tunnel calibration instrument**: There is no wind tunnel calibration instrument. We have electrical wind system and wild type wind system. Cleaning and lubricating is usually done, but due to unavailability of the calibration equipment, error in measurement could creep in.

Problem encountered in the present network System

1. Although the meteorological stations do not well represent the various climatic and agro-ecological conditions of the country, maintenance has been a problem since we do not have adequate transport facilities and lack of spare parts.
2. The available few automatic and semi-automatic stations are not operational due to lack of skilled manpower and spare parts.
3. Problem of communication system due to noise interference and problems in getting a high speed and leased telephone line from the Ethiopian Telecommunication Authority.
4. Lack of skilled manpower to operate and maintain the new systems of MDD and *Messir*.
5. The DCP is not working due to lack of spare parts.

RECOMMENDATION AND CONCLUSION

1. Public awareness programmes should be enhanced so that people may protect the instruments from damage.
2. The available few automatic and semi-automatic stations have to be operational in order to use them at remote areas. There is also a need to expand observatories by automatic stations as they have advantages over the manned station at remote locations. The observing stations at the airports have to be replaced by automatic and semi-automatic stations to get a reliable and real time data for aeronautical services.
3. Most of the observatories send their data by hand and post. This system of communication has to be complemented by other means in order to get the information on real time basis. The present System of communication is mainly by Voice (SSB). So, in order to avoid traffic and ease the frequent maintenance demand, the communication system at some of the stations in the regional meteorological centers has to be changed by data and voice communication system.
4. Training of manpower to properly operate and maintain the automatic stations, the MDD and *Messir* system, and the data communication system has become a necessity.

References

Ademe Mekonnen, 1993. Meteorological observation and data collection system in Ethiopia. Proceedings of the Environmental Monitoring and Natural Resources Protection. Sahel and Sahara Observatory (French Govt.) and Ministry of Natural Resources Environmental Protection.

Fantolli, A.1965.Contributo Alla Climatologia Dell'Ethiopia organizazione Poligrafic Industrials .Roma ,Italy.

Seyoum yami. 1993 Data collection in Ethiopia: Achievement and problems paper presented at the Second DCP-users conference Athens Greece ,14-17 Sept 1993

3 CAPACITY BUILDING AND TECHNOLOGY TRANSFER

DEVELOPPEMENT ET PERSPECTIVES DE L'ENSEIGNEMENT DES INSTRUMENTS METEOROLOGIQUES

Hamza Abderrahim

Institut Hydrométéorologique de Formation et de Recherche
BP 7019 Es Seddikia 31025 Oran (Algérie)

Tel (+213) 6 42 12 10 – Fax : (+213) 6 42 13 12 – E-mail : abhamza@multimania.com

L'élaboration de renseignements météorologiques, nécessite un travail de base considérable. La collecte de données doit se faire à partir d'instruments justes et fiables. En conséquence un personnel de qualité est nécessaire pour assurer la maintenance des équipements.

La formation professionnelle en instrumentation météorologique relevant de la compétence des organismes concernés doit être pensée de manière à ce que le personnel technique soit correctement formé et puisse offrir des services multidisciplinaires et répondre aux aspirations des usagers de plus en plus nombreux.

Les formateurs et instructeurs en instruments météorologiques, doivent suivre de près les nouvelles tendances, afin de mieux percevoir les besoins des usagers, et améliorer les prestations pédagogiques.

Devant la montée des préoccupations nationales et globales, les services météorologiques devraient adopter une stratégie dont les missions et les responsabilités montreront les orientations et les changements à apporter dans l'enseignement et la formation d'un personnel hautement qualifié.

L'intensification de cet enseignement serait d'autant plus utile que les générations futures seraient à même de saisir de manière plus probante les liens étroits existants entre l'instrument de mesure et la donnée qu'il fournit, et son utilité pour la connaissance du temps.

L'Institut Hydrométéorologique de Formation et de Recherche (IHFR), agréé depuis 1974 comme Centre Régional de Formation Professionnelle (CRFPM) de l'Organisation Météorologique Mondiale (OMM), a la charge de former les météorologistes des pays africains francophones. Près de 25 pays africains ont bénéficié d'une formation au sein de cet établissement.

Le CRFPM d'Oran (Algérie), outre la formation de techniciens (classe III OMM) et ingénieurs (classe II OMM) en météorologie, offre également la possibilité de former des Techniciens en instruments météorologiques. Cette catégorie de personnel, à l'issue de leur formation a la charge de l'installation et de la maintenance du réseau instrumental et des équipements météorologiques des télécommunications météorologiques.

Le cursus de cette filière, existe déjà depuis 1974 et s'étale une période de 24 mois. Les programmes de formation ont été établis selon les attentes des pays africains faisant appel à nos services d'une part, et conformément aux recommandations de l'OMM en matière de formation de spécialistes en instruments d'autre part.

La répartition des divers modules composant cette filière reposait essentiellement sur des enseignements dans une première phase de matières fondamentales (mathématiques, physique, thermodynamique....) et de matières de spécialisation (instruments météorologiques, équipements de transmission....), dans une deuxième phase.

Devant les exigences de plus en plus accrues des utilisateurs de produits météorologiques, et compte tenu de l'évolution croissante des techniques instrumentales, une révision de fond de l'enseignement de cette formation spécialisée a été initiée et a donnée naissance en 1995 à la création d'un nouveau cycle de formation, celui de Technicien Supérieur en Instruments Météorologiques.

De durée sensiblement plus longue que la précédente filière, cette dernière s'étale sur une période de 30 mois.

C'est dans l'optique d'une meilleure approche des connaissances techniques récentes que des modules de formation portent en partie tout au moins sur l'initiation des techniques de réception par satellite, radar à effet Doppler, stations automatiques, radiosondage...etc.

La formation de ces spécialistes en instruments météorologiques se divise en trois phases :

- phase 1 : acquisition de connaissances de base
- phase 2 : compléments et spécialisation
- phase 3 : projets de fin d'études et stages en lieu de travail

La répartition des volumes horaires, sur un total de 2286 heures, des divers modules de formation a été établie comme suit :

	VOLUME HORAIRE	POURCENTAGE
PHASE 1	864	38 %
PHASE 2	894	39 %
PHASE 3	528	23 %

De par notre expérience, en tant que centre régional de formation, et de par les objectifs auxquels nous aspirons, nous pensons qu'une réflexion régulière avec les services du réseau instrumental et autres utilisateurs paraît nécessaire pour élaborer de meilleures stratégies de formation.

L'objectif d'une formation quelconque ne doit pas se borner à un enseignement académique de disciplines variées, mais à inculquer une nouvelle perception de l'utilité des connaissances acquises. Ce qui laisse supposer une prise de conscience de la nécessité d'une utilisation accrue des techniques instrumentales modernes, pour améliorer les prestations et participer de manière conséquente au développement en général.

En effet, il nous est apparu indispensable au cours de notre expérience de formation de ce cycle, d'avoir recours à tout procédé d'information pouvant apporter un complément bénéfique à nos étudiants.

Face à l'évolution incessante des techniques de l'environnement informatique et des moyens de télécommunications, le recours à des méthodes et moyens pédagogiques nouveaux, tels que

l'enseignement assisté par ordinateur et le télé-enseignement, seraient sans aucun doute d'un apport certain et bénéfique.

Le télé-enseignement mériterait une attention particulière, en égard à sa haute technicité, sans toutefois se substituer à l'enseignement dit classique. Le télé-enseignement, quelque peu inapproprié actuellement pour un enseignement spécialisé ou une formation impliquant des expériences pratiques, trouverait quand même des applications intéressantes dans la formation professionnelle destinée à des spécialistes pour s'enquérir des nouvelles techniques.

Il faudrait néanmoins souligner que le télé-enseignement trouverait principalement sa place dans l'enseignement des techniques que les professeurs de métier ne sauraient assurer pleinement et de meilleure façon que les experts de la dite technique, parfois complexe et surtout récente.

En outre, l'avènement d'Internet peut nous conduire à un remaniement des méthodes pédagogiques et des innovations didactiques, et ce par un recours à des logiciels performants de télé-enseignement, élaborés de préférence conjointement avec les concepteurs (ou industriels) d'une part et les utilisateurs potentiels d'autre part.

Le nombre insuffisant de CD-ROM mis à notre disposition, dans le domaine des instruments météorologiques, a fait que le World Wide Web, comme complément d'information, trouve de plus en plus d'écho chez nos étudiants.

La prise de conscience d'une évolution des programmes de formation est certes comprise et partagée par tous. Cependant, devant les changements technologiques rapides survenus au cours de cette dernière décennie, un retard de plus en plus profond pourrait être occasionné par ceux dont le renouvellement des équipements et infrastructures s'avérerait difficile et onéreux.

Les propositions ou recommandations retenues permettront d'identifier les besoins de la formation, d'actualiser et d'enrichir les programmes, de choisir les méthodes de formation appropriée, et d'évaluer les ressources nécessaires au type de formation prédéfinie.

La météorologie, une science sans frontières, au service du bien-être de l'homme, du fait de l'élargissement des ses applications, s'intéresse de plus en plus fortement à l'évolution du climat et à l'environnement terrestre. Les implications diverses font qu'une logistique adéquate est primordiale pour permettre aux services météorologiques d'évoluer dans le contexte d'une communauté scientifique et technique qui progresse rapidement. Nous nous ne lasserons pas d'évoquer à nouveau la nécessité d'un développement des ressources humaines, l'amélioration des structures et un financement approprié, pour pouvoir se conformer aux nouvelles normes imposées par la technologie.

Ceci nous mène à penser qu'un renforcement de la coopération entre les constructeurs, les utilisateurs et les centres de formation, mènerait sans aucun doute à une formation pertinente des générations futures déjà en phase avec le monde de demain.

Aussi dans le cadre de notre mission au sein de l'Afrique, en tant que CRFPM, chargé de la formation de générations du troisième millénaire, nous estimons que nous devons contribuer au développement de l'enseignement des instruments par des opérations pédagogiques portant notamment sur :

- l'élaboration de CD-ROM sur les instruments météorologiques

- l'ouverture de sites sur le Web ,en particulier sur les instruments classiques, toujours utilisés dans nos régions

- conforter la formation continue, par des modules de spécialisation de courte durée , en particulier sur l'observation par satellite ,le radar, les stations automatiques, la mesure du rayonnement solaire....

Capacity Building for Instrumentation

Kruus, Jaan and Angle, Bruce***
* 1512 - 39 Pemberton Ave., North York, ON M2M 4L6, Canada; jaankruus@attcanada.net
** Senior Advisor, International Affairs, Meteorological Service of Canada, Environment Canada; Bruce.Angle@ec.gc.ca

Capacity Building Defined

In a global context, "capacity" refers to the ability of individuals and institutions to make and implement decisions and perform functions in an effective, efficient and sustainable manner. At the individual level, capacity building refers to the process of changing attitudes and behaviors — developing skills and imparting and acquiring knowledge while maximizing the benefits to society of knowledge exchange, participation and ownership. At the institutional level it focuses on the overall organizational performance and functioning capabilities, as well as the ability of an organization to adapt to change.

The National Meteorological and Hydrological Service (NMHS) in Society

Beginning with the assumption that a base of meteorological activity is necessary to sustain and develop any nation's economy and to provide for the safety of its people, it is self-evident that the need for an effective infrastructure of an NMHS should be considered an essential element of national plans. The necessary components are instrumentation, data processing and telecommunications. Such a base is seriously deficient in many countries, yet does not command the attention of national governments to allocate resources for its full development. The authors recognize that often the most difficult problems to overcome, other than a lack of national financial resources, are not technical but political and bureaucratic. Four such obstacles could be:

- over-identification of many NMHSs with a single economic sector (e.g. aviation);
- inefficiencies resulting from duplication of effort when specific roles (e.g. flood forecasting, media broadcasts) are assumed by other government departments or private organizations;
- lack of scientific and technical knowledge and awareness in decision-makers;
- restrictions on importation and international transportation of equipment and materiel.

Capacity Building in NMHSs

Plans to build capacity in an NMHS must be seen as an integral component of the national plan for development. We should avoid presenting the needs for improved infrastructure and training on the basis of fulfilling the NMHS mission. Rather, they contribute to the NMHS's multi-faceted approach to assisting economic development and meeting human needs to achieve improved productivity and long-term environmental quality. Improved early warning systems for floods, long term data sets of good quality to better understand climatic influences and improved telecommunication to warn and inform the citizens are just a few of the benefits of an improved infrastructure in an NMHS. Our collective message must be that improved data will assist in the economic potential of the nation, the health and safety of its population and in development of environmental policy and enforcement mechanisms. Such data will also support the private sector and governments in their endeavors to incorporate environmental considerations into their decision-making.

To improve success in achieving national support in acquiring scarce financial resources from governments and external sources, the authors propose that one must increase the visibility of the NMHS. To this end the following principles need be considered when developing project proposals:

The big picture	Focus the strategy on long-term capacity building, not immediate short-term performance improvement. There may be additional benefits derived beyond the project.
National control	Highlight central role of the NMHS to plan, design and manage the process.
Collaborative framework	Encourage broad "ownership" including local non-governmental organizations, academia and the private sector.
The Business Case	Explore all options (e.g. make or buy, skills development, engaging partners) and pay greater attention to the cost benefits of decisions.
Outcomes	Articulate outcomes such as improved products and services based on national objectives rather than inputs to be provided.
Sustainability	Emphasize self-reliance and ability to maintain systems.

An Illustrative Study

To make the discussion more concrete, let us consider a simple example of instrumentation for wind measurement. A similar methodology and principles can be applied to larger, more complex cases. Assume that one must refurbish or replace a number of anemometers in order to maintain or improve the climatological record and services to the public. Let us first enumerate three possible strategies that should be evaluated:

- Replace with commercially available instruments;
- Design and build new anemometers using technology appropriate to national capabilities and requirements:
- Refurbish existing anemometers.

For each of these potential strategies, we must identify the requirements for both the human and financial resources and the time when they will be required. The analysis must consider not only what is needed for the replacement or upgrade but also the requirements for future calibration and maintenance of the new equipment throughout its lifetime. We should also consider how new skills and facilities will add to and complement those already in place, how they may assist in meeting other requirements and how they fit into any national technology programmes or policies.

Each of the three examples of strategies – procurement, redesign or refurbishment – requires a different set of skills in the personnel.

Replacement with commercially available equipment

In the case of procurement of internationally available equipment, skills are required to specify and assure the quality of equipment procured. This does not generally need ability to understand the details of the internal operation to the level of being able to design modifications to the equipment. It does require the communication in procurement documentation of the operational requirements and environment in which the equipment will operate. It is also important to understand the limitations of the technology and the equipment being offered. There will be the need to assure that on delivery the equipment is adequately calibrated and otherwise meets the specifications. Additionally, there must be adequately trained personnel to install and maintain the equipment for its projected lifetime.

Design and build using appropriate technology

The option of designing and building an anemometer using technology appropriate to national capabilities and requirements presents a different type of challenge. Initially one would have to review the various scientific principles on which anemometry is based. These will suggest the technologies for their expression in working instruments. A review of current state of the art is useful here to establish what has been possible in other countries with the requirement of producing commercially viable equipment. This may also suggest how to implement the various possible designs by substitution of more appropriate or available technologies. It is important at this stage to consider not only traditional skills but also those at the leading edge of technology. Over the long term, substitution of software for hardware, for example, could lead to less expense when changes to the observational programme or to data processing will be required.

In parallel, there needs to be an inventory of nationally available skills and technologies. This may usefully be extended to consideration of regional capabilities if a group of countries is able to combine to execute the project, each perhaps contributing to some specific part of the final design and manufacture.

Finally, for each of the potential technically feasible approaches there needs to be a realistic cost estimate. This must include not only the immediate costs of the design and construction effort but also the cost of acquisition of the required skills and technical facilities. On the other side of the ledger, one must consider the sometimes unquantifiable benefits of being able to use the capacity for other projects in the national interest.

Refurbish existing anemometers

This may be an effective option when the instruments are generally operational but require the replacement of some component that is no longer available, or that can be procured or produced locally at lower cost. For the anemometer example it might be replacement of the bearings, with possible modifications to the shaft or housing. When considering this approach, the various costs and benefits must again be analyzed carefully. Some of these may be difficult to quantify but, nevertheless, could lead to significant benefits. An example may be the initiation of building up a capability to take on more challenging design tasks.

The refurbishment project will require planning that is similar to that of the designing and building project. A careful analysis is needed of any impacts at the interfaces of the new equipment or software to ensure that the changes are compatible and do not degrade performance. However, the undertaking may be simpler than building an entirely new instrument in that it should be possible to limit the need to a smaller set of

technical skills and facilities. In the example of the bearing replacement these would be mechanical engineering and a good machine shop capability.

Opportunities for Partnerships

In the past few years the world has witnessed a historic transformation. Political alliances have altered, market economies have flourished, the global information village is nearing a reality and technology advances at an unprecedented rate. Multilateral Environmental Agreements attest to the fact that every nation is concerned about humankind's impact on the global as well as on the local environments. Nevertheless, humankind's ability to systematically observe, record and analyze environmental change has been compromised by economic forces beyond the control of NMHSs. How an NMHS maintains or furthers its mission in protecting humans from the environment and in continuing to contribute to the socio-economic well-being of their citizens is a real dilemma.

As Table 1 illustrates, this complex landscape presents enormous opportunities for partnerships of existing and emerging programmes, actors and events that could assist NMHSs in building infrastructure useful in fulfilling their mission. The list is not exhaustive: much additional information can be obtained by searching the World Wide Web and working directly with regional institutions and programmes.

Conclusions

Capacity building activities are based on many different drivers: a national policy on technology, a global programme of action or a project to address specific NMHS requirements. A considerable part of capacity building may be more appropriately referred to as "capacity acquisition", which requires planning and sustained effort on the part of the recipient. To maximize the potential for success, capacity building must be designed to meet some clearly defined national requirement articulated in a way that engenders broad support from government and other sectors. Once this support is acquired, assistance from, *inter alia*, international institutions or neighbouring countries may reduce the requirements for national capacity.

Capacity building starts with an initiative supported by commitment at individual and national levels. Continuous motivation and innovation on the part of the individuals within the NMHS underpin success. Partnerships and mutual benefits must be identified and exploited and the ensuing improvements to infrastructure of acquisition of skills and knowledge must be sustainable.

In order to improve success, the following actions should be included in the overall plan:

- Access and make extensive use of the material and human resources of technical support units, training centres and other expertise in developed countries;
- Engage International Organizations and, in particular, WMO;
- Acquire a "critical mass" though partnering with industry and other neighbouring NMHSs.

Implementation may take several years while a gradual increase in national capacity is realized. Focused effort and a national champion will be needed to bring the project to a successful conclusion. It will be necessary to review progress from time to time in order to verify that targets, tactics, goals and process remain realistic and relevant to current technology and policies.

Bibliography

Griggs, David; *What donors think about when assessing VCP requests;* in WMO Bulletin Volume 45, No 3 (July 1996); pp. 241 – 245.

García-Legaz, Carlos, and Valero, Francisco; *Institutional Capacity Building For Training In Meteorology*; in WMO Bulletin Volume 48, No. 2 (April 1999); pp. 169 – 175.

Yerg, Martin; *New Approaches to Technical Cooperation*; in WMO Bulletin Volume 45, No 3 (July 1996); pp. 250 – 253.

Organization for Economic Co-operation and Development (OECD); *Donor Assistance To Capacity Development In Environment Development Co-Operation*; in Guidelines Series.

Table 1: Capacity Building; Opportunities for Partnerships

Activity	Mechanisms	Opportunities
Multilateral Environmental Agreements	- Montreal Protocol - Framework Convention on Climate Change - Convention on Biological Diversity - Convention to Combat Desertification	Various articles within these instruments promote the need for institutional and technical capacity building activities to enable all signatories to achieve their aims
United Nations Programmes and UN Specialized Agencies	- United Nations Development Programme, United Nations Environment Programme	The UNDP is the key UN instrument for development. Although its focus is on poverty alleviation, it does assist with technical cooperation activities.
	- **WMO and its various programmes and Constituent Bodies, e.g.** Regional and Sub Regional Offices, Education and Training Programme and RMTCs, Technical Cooperation Programme, Executive Council Advisory Group on Technical Cooperation - Regional Programme.	The strength of WMO lies in bringing like-minded mission oriented players together. It can provide technical and administrative assistance to project definition, location of potential donors, negotiations for assistance, project management and evaluation of results. Some services may be delivered through Regional Meteorological Training Centres, Regional Instrument Centres, Fellowships, Voluntary Cooperation Programme etc. Regional fora can help articulate national plans into an integrated regional perspective.
	- UNESCO - IOC; Training, Education and Mutual Assistance in Marine Science (TEMA)	IOC - TEMA has been effective in facilitating the exchange of initiatives in marine science between UN family agencies
UN Conference on Environment and Development (UNCED)	- Commission on Sustainable Development (CSD) and Agenda 21	CSD meeting 9 (2001) will emphasize Chapter 9: Protection of the Atmosphere. 2002 is the tenth anniversary of UNCED with increasing focus on development of capacity for environmental projects.
Implementation of global networks and large scale science experiments and assessments	- World Weather Watch - Hydrology and Water Resource Programme - Global Climate Observing System, - Global Ocean Observing System - World Climate Research Programme - Inter-governmental Panel on Climate Change - ARGO Project	Joint efforts amongst UN, academic, private sector and national institutions are growing. These present opportunities for infrastructure and other needs to build capacity. The implementation of the Global Climate Observing System (GCOS) is an emerging example.
International Funding Institutions	- World Bank – Global environment Facility (GEF) *Capacity Development Initiative* (CDI)	The World Bank is trustee of the Global Environment Facility Trust Fund and a GEF Implementing Agency. The portfolio of projects under implementation includes projects directly managed by the Bank as well as those managed by the International Finance Corporation, the Inter-American Development Bank, and the Asian Development Bank. GEF has recently taken keener interest in improving technical infrastructure.
Organization for Economic Cooperation and Development	- Capacity Development in Environment	OECD brings together the more technologically advance nations.
Regional Banks	- Inter-American Development Bank (IDB) - African Development Bank - Asian Development Bank - others	As example, the Ibero-American Climate Project Feasibility Study funded by the IDB will be used as an implementation plan for technical infrastructure in four South American countries.
Regional organizations	- Organization of American States (OAS), - Agency of Air Safety in Africa and Madagascar (ASECNA) - Asia Pacific Network - Inter-American Institute for Global Change Research (IAI) - Commonwealth - European Union	There are numerous national affiliations on a regional scale, some economic, some scientific. Each presents opportunities to advance the aims of an NMHS in technical endeavours including training.
Bilateral Assistance	- Official Development Assistance (ODA)	There is growing interest amongst donors to support national plans that improve early warning systems to mitigate the effects of natural disasters. WMO Members are often well connected to their international development agencies.
Private sector	- Instrument manufacturers - the media, with emphasis on international broadcasters - Insurance industry - Tourism and trade - various other economic sectors	Strong partnerships can be forged with the private sector, ranging from negotiation of fair pricing for consumables to improving relations with other sectors such as media outlets who require timely, accurate information for the delivery of their products and services.

****

APPENDICES

- List of members of the International Programme Committee for the preparation of TECO-2000

- List of publications in the Instruments and Observing Methods Report series

LIST OF MEMBERS OF THE INTERNATIONAL PROGRAMME COMMITTEE

set up for the

WMO TECHNICAL CONFERENCE ON METEOROLOGICAL AND INVIRONMENTAL INSTRUMENTS AND METHODS OF OBSERVATION

TECO-2000

R.P. Canterford	Scientific Director	Australia
Baoxiang XU		China
J. Kruus		Canada
A. Belhouji		Morocco
A. Gusev		Russian Federation
J. Nash		UK
K. Schulze	Co-ordinator	WMO Secretariat

LIST OF PUBLICATION

published within the

INSTRUMENTS AND OBSERVING METHODS REPORTS SERIES

(IOM-Report Series)

(with WMO/IOM-No. and WMO/TD-No.)

IOM-No. *(TD-No)*	Title	Remark
IOM 1	Automated Meteorological Systems Papers presented at the Technical Conference on Evolution and Standardization of Observing Techniques in Light of Automation, Norrköping, Sweden, 1980	***out of print***
IOM 2	Instrument Development Inquiry (Third Edition), 1980	***out of print***
IOM 3	Lower Tropospheric Data Compatibility. Low-level Intercomparison Experiment, USA, 1979	***out of print***
IOM 4	WMO Equipment Survey – Meteorological Satellite Ground-based Receiving Equipment, 1980	***out of print***
IOM 5	WMO Catalogue of Radiosondes in Use by Members, 1981	***out of print***
IOM 6	Preliminary Analysis of a Questionnaire on Aerodrome Meteorological Measurements By M. M. Etienne (Belgium), 1981	
IOM 7	The Meteorological Use of Navaid Systems - A brief technical assessment By A. Lange (Finland), 1981	
IOM 8	Report on Meteorological Radars By G. A. Clift, 1981	
IOM 9	Papers presented at the Second WMO Technical Conference on Instruments and Methods of Observation (TECIMO-II), Mexico City, Mexico, 1981	
IOM 10	Radiation Effects on the WMO Reference Psychrometer in the Field By R. G. Wylie and T. Lalas (Australia), 1981	
IOM 11	WMO Catalogue of Radiosondes in Use by Members, 1982	
IOM 12	Meteorological Observations by Laser Indirect Sensing Techniques By A. O. van Gysegem (Belgium), 1982	
IOM 13	The Use of Hydrogen for Inflation of Meteorological Balloons, 1982	
IOM 14	Summary Results of a 1978 Survey of Calibration Facilities and of Tests and Evaluation of Instruments	***out of print***
IOM 15	Papers presented at the WMO Technical Conference on Instruments and Cost-effective Meteorological Observations (TECEMO), Noordwijkerhout, Netherlands, 1984	
IOM 16 *(TD 146)*	Comparison of Pyranometers and Electronic Sunshine Duration Recorders of RA VI, Budapest, Hungary, 1984 By G. Major (Hungary), 1986	
IOM 17 *(TD 38)*	International Comparison of National Precipitation Gauges with a Reference Pit Gauge By B. Sevruk and W. R. Hamon, 1984	
IOM 18 *(TD 112)*	Guidance Material on Meteorological Instruments Suitable for Use in Developing Countries By E. S. Engawi (Saudi Arabia), 1986	
IOM 19 *(TD 230)*	Some General Considerations and Specific Examples in the Design of Algorithms for Synoptic Automatic Weather Stations By D. T. Acheson (USA), 1987	
IOM 20 *(TD 177)*	Stations Automatiques à Faible Coût By P. Viton (France), 1986	
IOM 21 *(TD 175)*	Algorithms for Automatic Aerological Soundings By A. H. Hooper (United Kingdom), 1986	
IOM 22 *(TD 50)*	Papers presented at the WMO Technical Conference on Instruments and Methods of Observation (TECIMO-III), Ottawa, Canada, 1985	
IOM 23 *(TD 51)*	Keynote papers presented at the Third WMO Technical Conference on Instruments and Methods of Observation (TECIMO-III), Ottawa, Canada, 1995	

IOM-No. (TD-No)	Title	Remark
IOM 24 (TD 231)	Instruments Development Inquiry (Fourth Edition) By E. Prokhorov (USSR), 1987	
IOM 25	Papers presented at the Workshop on the Correction of Precipitation Measurements, Zürich, Switzerland, 1985	
IOM 26	Lectures presented at the Workshop for Instrument Specialists (Buenos Aires 1984) (in Spanish)	***out of print***
IOM 27 (TD 176)	WMO Catalogue of Radiosondes and Upper-Air Wind Systems in Use by Members (1986)	
IOM 28 (TD 174)	WMO International Radiosonde Comparison - Phase I, Beaufort Park, UK, 1984 By A. H. Hooper (United Kingdom), 1986	***out of print***
IOM 29 (TD 312)	WMO International Radiosonde Intercomparison - Phase II, Wallops Island, USA, 1985 By F. Schmidlin (USA)	***out of print***
IOM 30 (TD 195)	WMO International Radiosonde Comparison, UK, 1984 & USA, 1985 By J. Nash (United Kingdom) and F. Schmidlin (USA), 1987	***out of print***
IOM 31	The Measurement of Gustiness at Routine Wind Stations - A Review By A. C. M. Beljaars (Netherlands), 1987	
IOM 32 (TD 217)	WMO International Ceilometer Intercomparison, UK, 1986 By D. W. Jones, M. Ouldridge and D. J. Painting (all United Kingdom), 1988	
IOM 33 (TD 222)	Papers presented at the WMO Technical Conference on Instruments and Methods of Observation (TECO-1988), Leipzig, German Democratic Republic, 1988	***out of print***
IOM 34 (TD 289)	WMO Assmann Aspiration Psychrometer Intercomparison, Potsdam, German Democratic Republic, 1987 By D. Sonntag (Germany), 1989	
IOM 35 (TD 303)	Papers presented at the Fourth WMO Technical Conference on Instruments and Methods of Observation (TECIMO-IV), Brussels, 1989	***out of print***
IOM 36 (TD 344)	Compatibility of Radiosonde Geopotential Measurements By M. Kitchen (United Kingdom), 1988	
IOM 37 (TD 309)	Information on Weather Radars used by WMO Members By M. Gilet (France), 1989	
IOM 38 (TD 316)	WMO International Hygrometer Intercomparison, Oslo, Norway, 1989 By J. Skaar, K. Hegg, T. Moe, K. Smedstud (all Norway)	
IOM 39 (TD 313)	Catalogue of National Standard Precipitation Gauges By B. Sevruk (Switzerland) and S. Klemm (Germany), 1989	***out of print***
IOM 40 (TD 451)	WMO International Radiosonde Comparison - Phase III, Dzhambul, USSR, 1989 By A. Ivanov, A. Kats, S. Kurnosenko, N. Zaitseva, (all Russian Federation) and J. Nash (UK)	***out of print***
IOM 41 (TD 401)	First WMO International Intercomparison of Visibility Measurements, UK, 1989 By D. J. Griggs, D. W. Jones, M. Ouldridge, W. R. Sparks (all United Kingdom)	***out of print***
IOM 42	WMO Automatic Sunshine Duration Measurement Comparison, Hamburg, Germany, 1989	*not published*
IOM 43 (TD 308)	First WMO Regional Pyrheliometer Comparison of RA II/RA V, Tokyo, Japan, 1989	
IOM 44 (TD 345)	First WMO Regional Pyrheliometer Comparison of RA IV, Ensenada, Mexico, 1989 By I. Galindo (Mexico)	
IOM 45 (TD 310)	Analysis of Instrument Calibration Methods used by Members By H. Döring (Germany), 1989	
IOM 46 (TD 474)	The WMO Automatic Digital Barometer Intercomparison, De Bilt, Netherlands, 1989 By J.P. van der Meulen (Netherlands), 1992	

IOM-No. (TD-No)	Title	Remark
IOM 47 (TD 452)	Reports of the CIMO Working Group on Surface Measurements Guidance on the Establishment of Algorithms for Use in Synoptic Automatic Weather Stations - Processing of Surface Wind Data By D. Painting (United Kingdom), 1991	
IOM 48 (TD 328)	International Workshop on Precipitation Measurements St. Moritz, Switzerland, 1989	***out of print***
IOM 49 (TD 462)	Papers presented at the WMO Technical Conference on Instruments and Methods of Observation (TECO-92), Vienna, Austria, 1992	***out of print***
IOM 50 (TD 541)	Historical Changes in Radiosonde Instruments and Practices By D. J. Gaffen (USA), 1993	***out of print***
IOM 51 (TD 570)	Overview of Real-time Lightning Detection Systems for use by Meteorological Services By R.L. Holle and R.E. López (both USA), 1993	
IOM 52 (TD 571)	Results of the Working Group on Weather Radars Part I: Severe Weather Recognition, By G. G. Shchukin (Russian Federation) Part II: Utilization of Doppler Radars for Monitoring Tropical Cyclones as one Element of the Global Monitoring System, By Hisao Ohno (Japan), 1993	***out of print***
IOM 53 (TD 572)	Segunda Compariación de la OMM de Pirheliómetros Patrones Nacionales AR III, Buenos Aires, 1991 By M. Ginzburg (Argentina), 1992	***out of print***
IOM 54 (TD 578)	Instruments Development Inquiry (fifth edition) By J.P. van der Meulen (Netherlands), 1993	***out of print***
IOM 55 (TD 589)	Siting and Exposure of Meteorological Instruments L'emplacement des sites et l'exposition des instruments météorologiques By J. Ehinger (Switzerland), 1993	
IOM 56 (TD 587)	Report by the Rapporteur on Radiosonde Compatibility Monitoring Part A - WMO Catalogue of Radiosondes and Upper-air Wind Systems in Use by Members Part B - Compatibility of Radiosonde Geopotential Measurements 1990, 1991 and 1992 By T. Oakley (United Kingdom), 1993	
IOM 57 (TD 588)	Papers presented at the WMO Technical Conference on Instruments and Methods of Observation (TECO-94), Geneva, Switzerland, 1994	***out of print***
IOM 58 (TD 670)	Papers presented at the International Workshop on Experiences with Automatic Weather Stations on Operational Use within National Weather Services, Vienna, Austria, 1995)	***out of print***
IOM 59 (TD 742)	WMO International Radiosonde Comparison - Phase IV; Final Report. Tsukuba, Japan, 1993 By S. Yagi, A. Mita and N. Inoue (all Japan), 1996	***out of print***
IOM 60 (TD 771)	Description and User Guide for the Radiosonde Comparison and Evaluation Software Package *(RSKOMP - Version 3/Version 4)* By S. Kurnosenko (Russian Federation) and T. Oakley (United Kingdom), 1996	
IOM 61 (TD 842)	Road Meteorological Observations By R.E.W. Pettifer (United Kingdom) and J. Terpstra (The Netherlands), 1997	
IOM 62 (TD 859)	WMO Wind Instrument Intercomparison By P. Gregoire and G. Oualid (both France), 1997	
IOM 63 (TD 860)	Operational Use of Ground-based Remote Sensors: A Review By D.W. Beran (USA), 1997	
IOM 64 (TD 861)	Tercera Comparación Regional de la OMM de Pirheliómetros Patrones Nacionales De la AR III Informe Final, Centro Regional de Radiación, Santiago de Chile, 24 de Febrero al 7 Marzo de 1997 Preparado por Manuel Vargas Muñoz (Chile), 1997	
IOM 65 (TD 862)	Guidance on Automatic Weather Systems and their Implementation Part I: Guidance Specifications (Functional) for a General Purpose Automatic Weather Station Part II: Implementation and User Training Considerations By Observation & Engineering Branch, Australian Bureau of Meteorology, 1997	

IOM-No. *(TD-No)*	Title	Remark
IOM 66 *(TD 871)*	Recent Changes in Thermometer Screen Designs and their Impact By A. Barnett, D.B. Hatton and D.W. Jones (all United Kingdom), 1998	
IOM 67 *(TD 872)*	WMO Solid Precipitation Measurement Intercomparison - Final Report By B.E. Goodison, P.Y.T. Louie (both Canada) and D. Yang (China), 1998	*Accessible through WMO's Web Page*
IOM 68 *(TD 873)*	Guidance Material on the Choice of Meteorological Instruments for Surface Observations Suitable for Use in Developing Countries By J.B. Odero (Kenya), 1998	
IOM 69 *(TD 874)*	Weather Radars used by Members By T. Mammen (Germany), 1998	
IOM 70 *(TD 877)*	Papers Presented at the WMO Technical Conference on Meteorological and Environmental Instruments and Methods of Observation (TECO-98), Casablanca, Morocco, 1998	***out of print***
IOM 71 *(TD 878)*	Instrument Development Inquiry (Sixth edition) By J.P. van der Meulen (Netherlands), 1998	-
IOM 72 *(TD 886)*	Report by the Rapporteur on Radiosonde Compatibility Monitoring Part A: WMO Catalogue of Radiosondes and Upper-air Wind Systems in Use by Members (1998) Part B: Compatibility of Radiosonde Geopotential Measurements 1995, 1996 and 1997 By T. Oakley (United Kingdom), 1998	
IOM 73 *(TD 887)*	WMO Intercomparison of Present Weather Sensors/Systems - Final Report, Canada and France, 1993 - 1995 By M. Leroy, C. Bellevaux, and J.P. Jacob (all France), 1998	

****